



Styliani Fragki

**PAVING THE WAY TOWARDS
THE NEXT GENERATION
RISK ASSESSMENT**

Quantitative *in vitro* to *in vivo* extrapolations
for the prediction of human toxicity
based on alternative testing

**PAVING THE WAY TOWARDS
THE NEXT GENERATION RISK ASSESSMENT**

*Quantitative in vitro to in vivo extrapolations for the prediction of
human toxicity based on alternative testing*

Styliani Fragki

Paving the way towards the next generation risk assessment- Quantitative in vitro to in vivo extrapolations for the prediction of human toxicity based on alternative testing

ISBN: 978-94-6483-001-9

DOI: <https://doi.org/10.33540/1679>

Cover & Layout design: Iliana Boshoven-Gkini | AgileColor.com

Print: Ridderprint | www.ridderprint.nl

All rights reserved. No part of this publication may be reproduced, stored in a retrieval system, or transmitted in any form or by any means, electronic, mechanical, by photocopying, recording, or otherwise, without the prior written permission of the author.

PAVING THE WAY TOWARDS THE NEXT GENERATION
RISK ASSESSMENT

*Quantitative in vitro to in vivo extrapolations for the prediction
of human toxicity based on alternative testing*

DE WEG VRIJMAKEN VOOR VERNIEUWDE
TOXICOLOGISCHE RISICOBEOORDELING

*Voorspelling van humane toxiciteit op basis van alternatieve testsystemen
en in vitro naar in vivo extrapolatie*

(met een samenvatting in het Nederlands)

Proefschrift

ter verkrijging van de graad van doctor aan de Universiteit Utrecht op gezag van de rector magnificus, prof. dr. H.R.B.M. Kummeling, ingevolge het besluit van het college voor promoties in het openbaar te verdedigen op dinsdag 14 maart 2023 des middags te 14.15 uur

door

Styliani Fragki

geboren op 1^{ste} september 1983 Thessaloniki, Greece

Promotoren

Prof. dr. Aldert H. Piersma

Prof. dr. ir. R.C.H. (Roel) Vermeulen

Copromotoren

Dr. Marco J. Zeilmaker

Dr. Mirjam Luijten

Assessment Committee

Prof. dr. ir. IMCM (Ivonne) Rietjens

Prof. dr. ir. J. (Juliette) Legler

Prof. dr. Frans Russel

Prof. dr. Ronette Gehring

Prof. dr. Martin van den Berg

This research was financially supported by the European Union's Horizon 2020 research and innovation programme under Grant agreement No 733032 HBM4EU (www.HBM4EU.eu).

Contents

Table of Contents	5
Abbreviations	8
CHAPTER 1 General introduction	11
The use of chemicals in the society and traditional toxicity testing	12
The Next Generation Risk Assessment (NGRA)	14
Quantitative In vitro to In vivo extrapolation: QIVIVE	15
Problem Definition	19
Outline of the thesis	19
References	21
SECTION I	26
CHAPTER 2 Applicability of generic PBK modelling in chemical hazard assessment: A case study with IndusChemFate	27
Abstract	28
Introduction	29
Methodology	31
Results	35
Discussion	48
Acknowledgements	52
Funding	52
Disclosures of interest	52
References	53
Supplementary Material	59
References-Supplementary Material	74
SECTION II	76
CHAPTER 3 <i>In vitro</i> to <i>in vivo</i> extrapolation of effective dosimetry in developmental toxicity testing: Application of a generic PBK modelling approach	77
Abstract	78
Introduction	79
Materials and Methods	81
Results	87
Discussion	96
References	100
Supplementary Material	105
References-Supplementary Material	107

CHAPTER 4 Integrating *in vitro* chemical transplacental passage into a generic PBK model: A QIVIVE approach 109

Abstract	110
Introduction	111
Materials and methods	113
Results	120
Discussion	129
Acknowledgement	135
Funding	135
References	136
Supplementary Material	141
References-Supplementary Material	152

SECTION III 154

CHAPTER 5 Systemic PFOS and PFOA exposure and disturbed lipid homeostasis in humans: what do we know and what not? 155

Abstract	156
Introduction	157
PFOS and PFOA: lipid homeostasis perturbations	159
Mechanistic pathways involved in PFAS-induced lipid perturbations	167
Species differences in toxicokinetic properties of PFOS and PFOA	180
Conclusions and recommendations	184
Acknowledgements	187
Funding	188
Disclosures of interest	188
References	189

CHAPTER 6 Determination of *in vitro* relative potencies for a series of perfluoroalkyl substances (PFASs) based on gene expression changes in HepaRG liver cells 201

Abstract	202
Introduction	203
Materials and methods	205
Results	210
Discussion	221
Acknowledgements	224
Conflict of interest statement	224
References	225
Supplementary Material	229
References-Supplementary Material	244

CHAPTER 7 New Approach Methodologies: A Quantitative <i>In vitro</i> to <i>In vivo</i> Extrapolation case study with PFASs	247
Abstract	248
Introduction	249
Materials and Methods	251
Results	259
Discussion	267
Acknowledgements	273
Conflict of interest statement	273
References	274
Supplementary Material	279
References-Supplementary Material	311
CHAPTER 8 Summary and General Discussion	313
Summary	314
General discussion	317
The procedure for QIVIVE with PBK model reverse dosimetry	317
In vitro test system and biomarkers: what is a meaningful readout?	318
Consideration of in vitro biokinetics	319
Exposure dose metrics and dependency on time	321
How is the appropriate PBK model selected?	322
PBK model parameterization with in vitro and in silico data	325
Predicted equivalent effect doses	325
Final remarks and conclusions	326
References	328
APPENDIX	357
Nederlandse samenvatting	357
List of publications	360
Curriculum Vitae	361
Acknowledgements	362

Abbreviations

3R	Replacement, Reduction, Refinement
ADME	Absorption, distribution, metabolism and excretion
AOP	Adverse outcome pathway
BMDL	Benchmark dose lower bound
BMR	Benchmark response
BMDLU	Benchmark dose upper bound
LOAEL	Low observed adverse effect level
EST	Embryonic stem cell test
mESTc	Murine/mouse cardiac embryonic stem cell test
mESTn	Murine/mouse neural embryonic stem cell test
NAMs	New Approach Methodologies
NOAEL	No observed adverse effect level
NGRA	Next generation risk assessment
PBK model	Physiologically based kinetic model
PFASs	Per- and polyfluoroalkyl substances
QIVIVE	Quantitative in vitro to in vivo extrapolations
QSAR	Quantitative Structure Activity Relationship
WEC	Whole embryo culture
ZET	Zebrafish embryo test

'If you want to end the war then instead of sending guns send books,
instead of sending tanks send pens,
instead of sending soldiers send teachers'

Malala Yousafzai

Chapter 1

General introduction



The use of chemicals in the society and traditional toxicity testing

Once upon a time most human needs were met with the use of materials directly available in the wild nature. People depended mainly on natural resources from where they extracted and used primary materials, such as wood, stone, metals etc. Nowadays, the scenery has changed completely, where nearly everything in developed human societies is in one way or another involving the use of manmade chemicals. As such, the local supermarket, garden and pharmacy store trade a vast array of products containing chemicals, like shampoos, vitamin supplements, detergents, pesticides, medicine and many more. In the 20th century with the birth of the ‘*the Chemical Age*’, the volume of chemicals that are commercially available on a global scale, and in particular after the 1970s, have increased dramatically. As such, it is a recognized fact that chemicals play an important role in our lives, but at the same time, they may pose risks for human health and the environment (Institute of Medicine’s Roundtable on Environmental Health Sciences 2014; van Leeuwen CJ 2007).

The science of toxicology has served society by protecting humans and ecosystems from potential dangers due to harmful effects of chemicals. The main methodological tool used by toxicologists for the control of chemicals and their potential risks is known as *risk assessment* (Henry 2003; National Research Council Committee on the Institutional Means for Assessment of Risks to Public 1983; WHO 1999). Risk assessment is in fact a conceptual framework with which scientists are able to determine the adverse effects of a chemical, as well as dose-response and exposure relationships, thereby enabling the characterization of the potential risk (Institute of Medicine’s Roundtable on Environmental Health Sciences 2014) (Figure 1). In other words, the primary goal of risk assessment is to define, with as low uncertainty possible, the risk related to exposure to hazardous chemicals and establish acceptable exposure limits for humans and the environment (WHO 1999).

From a regulatory perspective, chemical risk assessment is regulated by various legislative frameworks within the European Union, which has started back in the 1960’s (Henry 2003). Many different categories of chemicals can be identified for which a separate regulation has been developed (see examples in Table 1). Traditionally, toxicity testing is relying primarily on animal bioassays, which have been so far a cornerstone of chemical safety evaluation. In essence, adverse biological responses are monitored after dosing homogenous groups of animals with toxicants at high levels (Krewski et al. 2009). The main objective is to identify exposure levels to the chemicals below which no adverse effects shall be expected. For the derivation of safety limits for humans, a point of departure (PoD) is defined from the animal data, which may be a NOAEL (no observed adverse effect level) or a BMD (benchmark dose) (Judson et al. 2011; Sand et al. 2017). PoDs are thereafter, divided by assessment factors in order to account for any uncertainties pertaining to intra- and interspecies variability, or more susceptible human subpopulations (ECETOC 2003; Falk-Filipsson et al. 2007; WHO 1999).

Chemical Risk Assessment

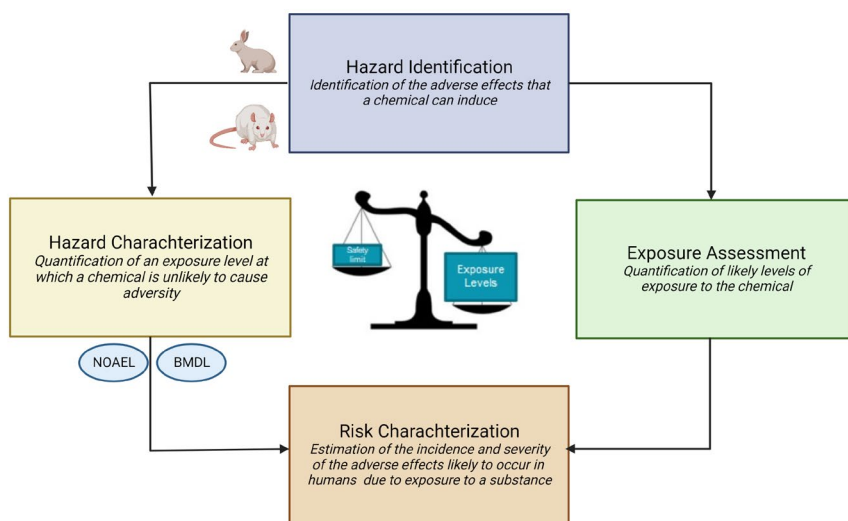


FIGURE 1 An overview of the current Chemical Risk Assessment process, as based on animal data for most of the EU regulatory frameworks. Risk is a function of hazard and exposure. The main elements of the process are the: hazard identification, hazard characterization, exposure assessment and risk characterization. NOAEL: no observed adverse effect level, BMDL: benchmark dose lower bound; both determined based on the animal toxicity data in most of the cases (Created with Biorender.com).

TABLE 1 Examples of EU Regulations for chemical substances.

Chemical Categories	Regulation
Pesticides, plant protection products	Regulation (EC) No 1107/2009
Biocides	BPR Regulation (EU) No 528/2012
Industrial Chemicals	REACH Regulation (EU) No 1907/2006
Food additives	Regulation (EC) No 1333/200
Feed additives	Regulation (EC) No 1831/2003
Veterinary Medicinal Products	Regulation (EU) 2019/6

This approach is based on the notion that fundamental biological processes are similar across species to a satisfying extent, thereby allowing for such extrapolations (Varga et al. 2010). The inference that observations in animal experiments are relevant for human health has been so far fundamental not only to toxicology, but also to experimental biology and medicine (National Research Council Committee on the Institutional Means for Assessment of Risks to Public 1983). However, although hitherto animal studies have undoubtedly facilitated the understanding of such sciences and the toxic potential of chemicals, their relevance for human health risk assessment has been questioned (Krewski et al. 2010; Van Norman 2019a). On one hand, the animal-based observations are extrapolated to expected human responses at considerably lower exposure levels, let alone the very heterogeneous genetically diverse human population compared to the inbred strains commonly used in these studies. Additionally, these standard toxicity tests

used widely within regulatory contexts provide only limited information on the mechanism of action, which is important for clarifying interspecies differences (NRC 2007). Despite this deeply rooted belief that animal models are the golden standard for predicting human toxicity (Ferreira et al. 2019; Gad ; Huff et al. 2008), several data illustrate otherwise (Bailey et al. 2014; 2015; Hackam and Redelmeier 2006; Olson et al. 2000; van Meer et al. 2012; Wang and Gray 2015) and hence, resulted in increasing scientific criticism within the community. A clear example comes from the pharmaceutical sphere, where ~45% of new drugs fail in human clinical trials, because of unexpected human toxicity (Van Norman 2019b).

Next to the above, animal studies are extremely expensive and time-consuming, whereas the continued use of large numbers of animals for toxicity testing also raises serious ethical considerations. For example, only for the REACH Regulation on industrial chemicals, the initial estimate on required test animals was 3.9 million, if alternative methods would not have been accepted (Katinka van der Jagt 2004). In line, with the 3Rs principles on *Replacement, Reduction and Refinement* of animal use as defined by Russel and Burch in 1959 (Tannenbaum and Bennett 2015), and considering the overall limitations of animal models as mentioned above, there is a clear requirement for implementing New Approach Methodologies (NAMs) in chemical safety evaluations.

The Next Generation Risk Assessment (NGRA)

An alternative paradigm for the chemical safety assessment was first presented in 2007 by the U.S. National Research Council (NRC) with its ground-breaking report 'Toxicity Testing in the 21st Century: A Vision and a Strategy' (Krewski et al. 2010). According to NRC, modern toxicology should be based on well-designed *in vitro* assays that unravel perturbation of cellular responses and move away from using black box animal models. Many initiatives thereon, embraced this vision and joined forces in transforming toxicity testing: from apical endpoints at an organism level in animal assays to mechanistic endpoints, via understanding the underlying toxicity pathways in human cells and cell lines, or tissue surrogates (Basketter et al. 2012; Rovida et al. 2015). Eventually, the goal would be to maintain the exposure levels to toxic agents below the levels at which the cellular pathways could be substantially disturbed (Krewski et al. 2009). This use of mechanistically based and high-throughput tests performed in such systems can cover a wide range of toxicity pathways and modes of action, and large concentration regimens can be applied. As such, they may provide adequate sensitivity for the detection of effects at human-relevant exposure levels, which cannot be obtained with the high-dose animal toxicity studies (Bhattacharya et al. 2011; Krewski et al. 2009).

The complexity of the *in vitro* cell-based models can vary significantly. For example, within ToxCast and Tox21, US EPA focuses on toxicity predictions based on high-throughput screening with bioactivity profiling, aiming at identifying cellular pathways of toxicity and underlying mechanisms (Judson et al. 2011; Wambaugh et al. 2013). On the other hand, the more sophisticated models are the three dimensional cell cultures with more than one cell

line and the organ-on-a-chip technology, mimicking the *in vivo* microenvironment (Rim 2019). In general, *in vitro* studies are not capable of detecting an adverse effect but rather biomarkers of effects, that will be indicators of pathology.

As part of facilitating the move towards mechanistic toxicology the concept of Adverse Outcome Pathways (AOPs) emerged (OECD 2012). An AOP is conceptually a series of biological key events occurring sequentially: starting from a molecular initiating event, and resulting in an adverse outcome at higher levels of biological organization, such as a whole organism or even a population (Ankley et al. 2010; Bal-Price and Meek 2017; Vinken 2013). In this sense, the AOP broadens the idea of ‘mode of action’ since it starts with a molecular event at a cellular level and can go up to the population level (Vinken 2013).

During the last decades, scientists have made a noteworthy progress in developing alternative tests for the realization of this vision and towards the elimination of animal testing (Carmichael et al. 2022a; Knudsen et al. 2015). Next to this, advances in *in silico* toxicology lead to the creation of a wide variety of computational tools that can complement *in vitro* toxicity assays. Important examples are techniques and models like read-across, structural alerts, QSARs (Quantitative Structure Activity Relationships) and machine learning. The main underlying assumption of such approaches is the relationship between a compound’s structure and its biological activity. As such, *in silico* predictions may relate to chemical toxicity, mechanisms or exposure (Myatt et al. 2018; Pawar et al. 2019; Raies and Bajic 2016). Other computation tools are toxicokinetic models that are used for the quantitative extrapolations of the *in vitro* data to the human situation (Basketter et al. 2012; Krewski et al. 2009).

As a result of this concentrated effort to change chemical toxicity testing, the terms New Approach Methodologies (NAMs) and Next Generation Risk Assessment (NGRA) have emerged (ECHA 2017). On one hand NAMs represent the *in vitro*, *in silico*, and overall computational tools, which can be used in combination for the prediction of chemical hazard and risk assessment, whereas the term NGRA encompasses the overall vision of integrating this new type of information into chemical safety decision-making towards a human-focused testing paradigm (Ball et al. 2022; Carmichael et al. 2022a; Dent et al. 2018; Dent et al. 2021a).

Quantitative *In vitro* to *In vivo* extrapolation: QIVIVE

The concept of QIVIVE with PB(P)K modelling

An essential component of NAMs is quantitative *in vitro* to *in vivo* extrapolation, a process known as QIVIVE (Adler et al. 2011; Bell et al. 2018; Chang et al. 2022; Henneberger et al. 2021; Yoon et al. 2012). With QIVIVE the *in vitro* concentration-effect relationships are linked to *in vivo* organ exposure, and thereafter, to equivalent human exposure, a process determined by the chemical’s toxicokinetic characteristics (Adler et al. 2011; Kramer et al. 2015; Punt

et al. 2011). Given that *in vitro* and *in vivo* exposure situations differ fundamentally, such extrapolations are complex and require the integration of toxicokinetics. For example, in the *in vitro* assays, the compound of interest is directly added to the assay medium, thereby allowing an apparently simpler exposure situation when compared to the *in vivo* situation. On the other hand, in a complete living organism the absorption, distribution, metabolism and excretion (ADME, or else toxicokinetics) processes determine the route from external exposure to the target organ (Jones and Rowland-Yeo 2013), whereas they are absent (or different) in an *in vitro* cell culture (Groothuis et al. 2015). As such, integration of toxicokinetics is a necessary element to complement the *in vitro* toxicity approaches, allowing for linking the concentrations tested to respectful doses, in a reverse dosimetry approach (Hartung 2018; Louise et al. 2017; Punt et al. 2021a).

For the incorporation of toxicokinetics, the most advanced approach dictates the application of Physiologically Based (Pharmaco)Kinetic (PB(P)K) models (Figure 2). PBK models are sophisticated dosimetry models, simulating the ADME processes in the human body (or other organisms) (Jones and Rowland-Yeo 2013). Thus, they can be used to predict the systemic effective doses of substances at a specific target site, but also *vice versa*, with reverse dosimetry, for the prediction of external dose-responses *in vivo* starting from the *in vitro* concentration-response curves. In such models the body is described by compartments each of which represents a specific organ or tissue (e.g. liver, heart, kidney, muscle, spleen etc.), while blood flow governs the mass transfer across the body (Bois et al. 2010; Clewell and Clewell 2008; Kuepfer et al. 2016). They are constructed on the basis of four types of parameters: (a) physiological (e.g. cardiac output, blood perfusion rates, respiratory rate), (b) anatomical (e.g. body size, organ weights) parameters, which are species' specific; (c) biochemical (metabolic rates), and (d) substance-specific physicochemical parameters (e.g. Kow, vapour pressure, molecular weight). The mathematical description is comprised of a set of differential equations, which can be numerically integrated by different software packages¹ (Jongeneelen and Berge 2011).

PBK models are mostly designed for a single (or a small group of) compound(s), and are tailored for the kinetics of these chemicals *per se* (OECD 2021a; WHO 2010). They are commonly considered quite demanding with respect to experimental data needed for their parameterization, accurate calibration and verification (Jamei 2016b; Lu et al. 2016a; Yang 2011). Such comprehensive data are often not available for non-drug (environmental and in commerce) chemicals (Breen et al. 2021), hampering as such the PBK application to data-poor substances. In addition, due to their complexity they often require mathematical and programming expertise (Bessemers et al. 2014) and hence, their broader application and use from non-modelers is cumbersome. For instance, PBK modelling, is not applied for risk assessment purposes during the regulatory dossier evaluation of several chemical families (e.g. pesticides, biocides etc.) (Punt et al. 2017).

1 Commonly used computer languages (differential equation solving): Berkeley Madonna, R, MATLAB, acsIX Painsi, 2017 #127

Alternatively, a more *generic* approach with the use of, user-friendly, ready-to-use PBK models (or platforms), which can be applied for many compounds, would facilitate to overcome these barriers. A *generic* PBK model shall be designed in such a way so as to be intuitive to the user, and able to predict toxicokinetics with a minimum parameterization (Basketter et al. 2012; Leist et al. 2014). Generic PBK models contain a pre-defined compartmental structure incorporating species-specific physiological parametrization, whereas chemical-specific parameters may be derived from animal/human-based *in vitro* biokinetic assays combined with *in silico* models (e.g. QSARs²) (Louisse et al. 2020a; Paini et al. 2019; Punt et al. 2021b). Enclosed QSARs predict model parameters based on the molecular structure and physicochemical properties of the compounds (Peyret et al. 2010; Rodgers and Rowland 2007), overcoming the issue of *in vivo* kinetic data paucity for parameterization.

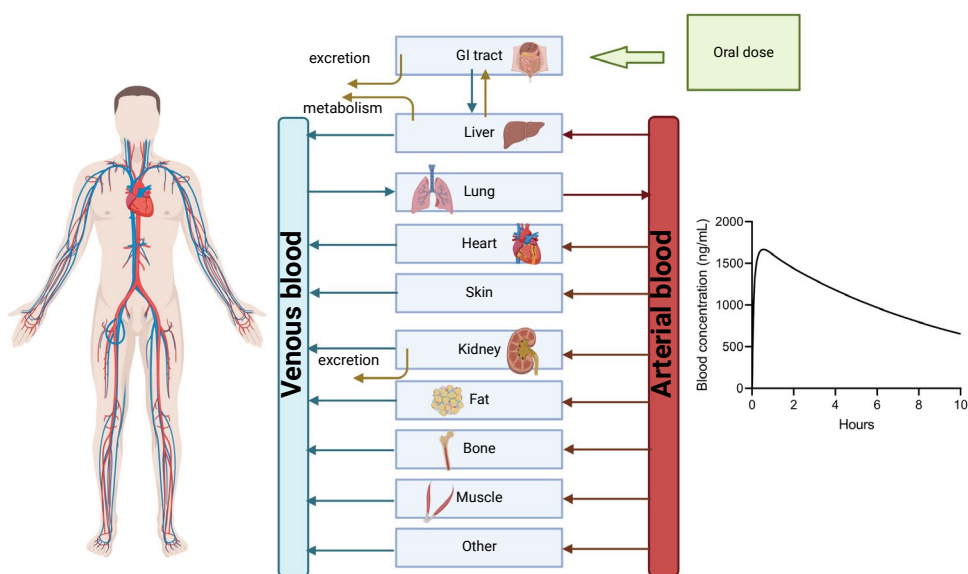


FIGURE 2 Schematic representation and example simulation of a PBK model (Created with Biorender.com).

A series of commercially available software packages or platforms, with at least some of these generic characteristics, are already developed and are widely used especially in the pharmaceutical field during the process of drug development. Typical examples are the commercial PBK platforms *SimCyp*, as well as *GastroPlus*, able to predict *in vivo* kinetics with *in vitro* and *in silico* (QSARs) information. The QSARs are used for the prediction of processes such as metabolism, blood protein binding and lipophilicity (Creton et al. 2009). These software packages are applied in the regulatory processes for the prediction of drug kinetics in populations (Punt et al. 2018). However, these models are rather complex and the model structure and use are not always directly accessible to the user (Bessemers et al. 2014). Other examples of generalized PBK models for pharmaceutical agents are Poulin and Theil (2002), focused on drug discovery prior to *in vivo* studies and *PKSim* by Willmann et al. (2005).

Initiatives to develop generic models for non-pharmaceutical, and data-poor compounds in terms of toxicokinetic data availability, have also been taken. Important examples of generic models/platforms are CEFIC LRI IndusChemFate³, *MegGen* and US-EPA High-Throughput Toxicokinetics (httk)-R package⁴, PLETHEM⁵, the web-based toolbox from Wageningen University, The Netherlands⁶ (Punt et al. 2021b) and the MCRA9 (implemented in the EuroMix toolbox) (Tebby et al. 2020).

IndusChemFate is a generic, freely available PBK model, written in Visual basic and distributed as an MS Excel spreadsheet-file. It incorporates QSARs, developed to predict partitioning model parameters of a substance solely from physicochemical characteristics (Jongeneelen and Berge 2011), overcoming in this way the problem pertaining to availability of such parameters. *IndusChemFate* was developed for screening purposes of new data-poor industrial chemicals (volatile & semi-volatile organic substances) following three potential exposure routes: inhalation, oral and dermal. The implementation of the model in Excel makes it relatively easy and intuitive to users. *MEGen* is a web application for the rapid construction and documentation of custom-built deterministic PBK model code. *MEGen* comprises a parameter database and a model code generator that produces code for use in several commercial software packages and one that is freely available (Bessemers et al. 2014). *Httk* is in practice an R- package for PBK modelling developed by the US EPA, which may be used to calculate steady-state blood levels of substances (Pearce et al. 2017). The package contains a one-compartment and a 4-compartment model. *PLETHEM* stands for Population Lifecourse Exposure-To-Health-Effects Model Suite. This computational platform is currently being developed by ScitoVation scientists in collaboration with US EPA. *PLETHEM* will provide a freely available, open-source, user-friendly platform for rapid modelling across the source-to-outcome continuum using only *in silico* and *in vitro* data.

Nevertheless, many of these modelling strategies have not been evaluated on their aspect of simulating chemical kinetics over a wide span of chemical physicochemical properties, a *fundamental pre-condition* for the employment of generic PBK models in hazard identification (OECD, 2021).

QIVIVE examples with PBK model-based reverse dosimetry

Several examples of QIVIVE with PBK model-based reverse dosimetry have been so far published for different toxicity endpoints and various compounds, like for example: neurotoxicity (Forsby and Blaauboer, 2007 (Kasteel et al. 2021; Noorlander et al. 2022; Zhao et al. 2019), cardiotoxicity (Li et al. 2021), nephrotoxicity (Abdullah et al., 2016), hepatotoxicity (Chen et al. 2018b; Yu et al. 2020) Klein et al., 2016), and developmental toxicity (Li et al. 2017a; Louisse et al. 2015; Louisse et al. 2010; Scholze et al. 2020; Strikwold et al. 2017; Strikwold et al. 2013). These studies aimed at deriving a predicted human toxicity

3 <http://cefic-lri.org/toolbox/induschemfate/>

4 <https://cran.r-project.org/web/packages/httk/index.html>

5 <http://www.scitovation.com/plethem.html>

6 <https://www.qivivetools.wur.nl/>

dose-response curve and/or a PoD to be used for risk assessment and illustrated the potential of combining *in vitro* results and PBK modelling in deriving human toxicity standards.

Reverse-dosimetry PBK modelling has been also applied on high-throughput toxicity screening of chemicals in the chemical prioritization program of US EPA ToxCast, on the basis of *in vitro* assays on metabolism and protein binding and QSAR physical-chemical properties (Rotroff et al. 2010; Wambaugh et al. 2018; Wambaugh et al. 2015; Wetmore et al. 2013; Wetmore et al. 2012). The tool specifically used and developed for the prediction of kinetics was the *httk* model (see above for more information).

Problem Definition

Notwithstanding the major efforts to eliminate, or at least reduce, animal experiments for toxicity testing, most of the regulatory frameworks within the EU still require a considerable amount of animal data for chemical safety assessment (Fentem et al. 2021). Exception is the Cosmetics Regulation where since 2013, testing cosmetic products or their ingredients on animals is banned. On the contrary, for industrial chemicals, the European competent authority ECHA (European Chemicals Agency), following for example compliance checks of chemical registration dossiers, is requesting companies to perform additional animal studies, even if initially it has been considered scientifically acceptable to apply NAMs. Before regulatory authorities accept NAMs, they have to be convinced that they can provide equivalent or maybe improved protection of human health than the animal tests replaced. As such, it is essential to gain confidence with experience and consequently, more published examples on how NAMs may be used in risk assessment would facilitate their acceptance (Knight et al. 2021). Accordingly, gaining more experience on QIVIVE with PBK modelling, as an essential component of NAMs, with the creation of case studies and proof-of-principle approaches is pivotal for moving towards the Next Generation Risk Assessment.

Outline of the thesis

The overall purpose of this thesis was to explore the application of PBK models for QIVIVE purposes. The first goal, described in **Section I**, was to evaluate the performance of generic PBK models with incorporated QSAR model parameterization, in terms of their capacity to predict toxicokinetics of a wide span of chemicals, regarding certain physicochemical and biological properties (**Chapter 2**). This Chapter compares the capacity of two generic PBK models, a simpler *versus* a more complex model, to predict the toxicokinetics of chemicals with a wide span of chemical and biological properties.

The goal of **Section II** was to investigate QIVIVE for the endpoint of developmental toxicity with the use of data from alternative embryotoxicity assays. This requires the scaling of *in vitro* observed dose-response characteristics to *in vivo* fetal exposure. In **Chapter 3**, three different classes of developmentally toxic chemicals were chosen as model compounds.

QIVIVE was performed with the use of a generic PBK model (IndusChemFate), whereas chemical maternal blood concentrations were used as a proxy for fetal exposure. In **Chapter 4**, the approach was extended with the incorporation of physiological alterations occurring in the maternal body during gestation, placental transfer, and fetal growth. Placental transfer was studied *in vitro* with the BeWo assay. The application of the new PBK model for predicting *in vivo* effective dose levels from *in vitro* studies was illustrated with *in vitro*-based PBK modelling reverse dosimetry.

In **Section III**, a NAMs case study is presented for the ‘forever chemicals’, per- and polyfluoroalkyl substances (PFASs). **Chapter 5** introduces the reader to the ‘PFASs problem’ and reviews the main issues related to modulation of lipid homeostasis by the two most common congeners PFOA and PFOS. The number of existing PFASs is estimated to be around a few thousands, and for many of these *in vivo* toxicity data are lacking. For this reason, application of NAMs can be useful for the screening of PFASs and the identification of compounds to be prioritized for a more comprehensive hazard characterization. This is explored in **Chapter 6**, where the effects of 18 PFASs on triglyceride levels and expression of selected genes was studied in human HepaRG cells. Based on these *in vitro* readouts, used as biomarkers for liver toxicity and lipid perturbations, Relative Potency Factors (RPFs) are derived. As a next step in **Chapter 7**, the feasibility of predicting PFAS-induced lipid disturbances and hepatotoxicity, by a combined *in vitro-in silico* approach, is assessed. In this QIVIVE case study, *in vitro* concentration-response data obtained in HepaRG cells are converted into dose-response curves, with physiologically based kinetic (PBK) model-facilitated reverse dosimetry.

Chapter 8 summarizes the results of the previous chapters of the thesis and provides a discussion on its contribution to QIVIVE, NAMs and NGRA. In addition, future perspectives on how to take the field forward are provided.

References

- Adler S, Basketter D, Creton S, Pelkonen O, van Benthem J, Zuang V, Andersen KE, Angers-Loustau A, Aptula A, Bal-Price A et al. 2011. Alternative (non-animal) methods for cosmetics testing: Current status and future prospects-2010. *Archives of toxicology*. 85(5):367-485.
- Ankley GT, Bennett RS, Erickson RJ, Hoff DJ, Hornung MW, Johnson RD, Mount DR, Nichols JW, Russom CL, Schmieder PK et al. 2010. Adverse outcome pathways: A conceptual framework to support ecotoxicology research and risk assessment. *Environ Toxicol Chem*. 29(3):730-741.
- Bailey J, Thew M, Balls M. 2014. An analysis of the use of animal models in predicting human toxicology and drug safety. *Altern Lab Anim*. 42(3):181-199.
- Bailey J, Thew M, Balls M. 2015. Predicting human drug toxicity and safety via animal tests: Can any one species predict drug toxicity in any other, and do monkeys help? *Altern Lab Anim*. 43(6):393-403.
- Bal-Price A, Meek MEB. 2017. Adverse outcome pathways: Application to enhance mechanistic understanding of neurotoxicity. *Pharmacology & therapeutics*. 179:84-95.
- Ball N, Bars R, Botham PA, Cuciureanu A, Cronin MTD, Doe JE, Dudzina T, Gant TW, Leist M, van Ravenzwaay B. 2022. A framework for chemical safety assessment incorporating new approach methodologies within reach. *Archives of toxicology*. 96(3):743-766.
- Basketter DA, Clewell H, Kimber I, Rossi A, Blaauboer B, Burrier R, Daneshian M, Eskes C, Goldberg A, Hasiwa N et al. 2012. A roadmap for the development of alternative (non-animal) methods for systemic toxicity testing. *Altex*. 29(1):3-91.
- Bell SM, Chang X, Wambaugh JF, Allen DG, Bartels M, Brouwer KLR, Casey WM, Choksi N, Ferguson SS, Fraczkiwicz G et al. 2018. *In vitro* to *in vivo* extrapolation for high throughput prioritization and decision making. *Toxicol In vitro*. 47:213-227.
- Bessemers JG, Loizou G, Krishnan K, Clewell HJ, 3rd, Bernasconi C, Bois F, Coecke S, Collnot EM, Diembeck W, Farcal LR et al. 2014. Pbtik modelling platforms and parameter estimation tools to enable animal-free risk assessment: Recommendations from a joint epaa--eurl ecvam adme workshop. *Regulatory toxicology and pharmacology : RTP*. 68(1):119-139.
- Bhattacharya S, Zhang Q, Carmichael PL, Boekelheide K, Andersen ME. 2011. Toxicity testing in the 21 century: Defining new risk assessment approaches based on perturbation of intracellular toxicity pathways. *PLoS One*. 6(6):e20887.
- Bois FY, Jamei M, Clewell HJ. 2010. Pbpk modelling of inter-individual variability in the pharmacokinetics of environmental chemicals. *Toxicology*. 278(3):256-267.
- Breen M, Ring CL, Kreutz A, Goldsmith MR, Wambaugh JF. 2021. High-throughput pbtk models for *in vitro* to *in vivo* extrapolation. *Expert Opin Drug Metab Toxicol*. 17(8):903-921.
- Carmichael PL, Baltazar MT, Cable S, Cochrane S, Dent M, Li H, Middleton A, Muller I, Reynolds G, Westmoreland C et al. 2022. Ready for regulatory use: Nams and ngra for chemical safety assurance. *Altex*.
- Chang X, Tan YM, Allen DG, Bell S, Brown PC, Browning L, Ceger P, Gearhart J, Hakkinen PJ, Kabadi SV et al. 2022. Ivive: Facilitating the use of *in vitro* toxicity data in risk assessment and decision making. *Toxics*. 10(5).
- Chen L, Ning J, Louise J, Wesseling S, Rietjens IMCM. 2018. Use of physiologically based kinetic modelling-facilitated reverse dosimetry to convert *in vitro* cytotoxicity data to predicted *in vivo* liver toxicity of lasiocarpine and riddelliine in rat. *Food and Chemical Toxicology*. 116:216-226.
- Clewell RA, Clewell HJ, 3rd. 2008. Development and specification of physiologically based pharmacokinetic models for use in risk assessment. *Regulatory toxicology and pharmacology : RTP*. 50(1):129-143.
- Creton S, Billington R, Davies W, Dent MP, Hawksworth GM, Parry S, Travis KZ. 2009. Application of toxicokinetics to improve chemical risk assessment: Implications for the use of animals. *Regulatory toxicology and pharmacology : RTP*. 55(3):291-299.
- Dent M, Amaral RT, Da Silva PA, Ansell J, Boisleve F, Hatao M, Hirose A, Kasai Y, Kern P, Kreiling R et al. 2018. Principles underpinning the use of new methodologies in the risk assessment of cosmetic ingredients. *Computational Toxicology*. 7:20-26.
- Dent MP, Vaillancourt E, Thomas RS, Carmichael PL, Ouedraogo G, Kojima H, Barroso J, Ansell J, Barton-Maclaren TS, Bennekou SH et al. 2021. Paving the way for application of next generation risk assessment to safety decision-making for cosmetic ingredients. *Regulatory Toxicology and Pharmacology*. 125:105026.

- ECETOC. 2003. European centre for ecotoxicology and toxicology of chemicals. Derivation of assessment factors for human health risk assessment. Tr086.
- ECHA. 2017. Non-animal approaches—current status of regulatory applicability under the reach, clp and biocidal products regulations. ECHA Helsinki, Finland.
- Falk-Filipsson A, Hanberg A, Victorin K, Warholm M, Wallén M. 2007. Assessment factors—applications in health risk assessment of chemicals. *Environmental Research*. 104(1):108-127.
- Fentem J, Malcomber I, Maxwell G, Westmoreland C. 2021. Upholding the eu's commitment to 'animal testing as a last resort' under reach requires a paradigm shift in how we assess chemical safety to close the gap between regulatory testing and modern safety science. *Alternatives to Laboratory Animals*. 49(4):122-132.
- Ferreira GS, Veening-Griffioen DH, Boon WPC, Moors EHM, Gispens-de Wied CC, Schellekens H, van Meer PJK. 2019. A standardised framework to identify optimal animal models for efficacy assessment in drug development. *PLoS One*. 14(6):e0218014.
- Gad S. *Animal models in toxicology* (2nd ed.). Crc press. .
- Groothuis FA, Heringa MB, Nicol B, Hermens JL, Blaauboer BJ, Kramer NI. 2015. Dose metric considerations in *in vitro* assays to improve quantitative *in vitro-in vivo* dose extrapolations. *Toxicology*. 332:30-40.
- Hackam DG, Redelmeier DA. 2006. Translation of research evidence from animals to humans. *JAMA*. 296(14):1727-1732.
- Hartung T. 2018. Perspectives on *in vitro* to *in vivo* extrapolations. *Appl In vitro Toxicol*. 4(4):305-316.
- Henneberger L, Huchthausen J, Wojtysiak N, Escher BI. 2021. Quantitative *in vitro*-to-*in vivo* extrapolation: Nominal versus freely dissolved concentration. *Chemical research in toxicology*. 34(4):1175-1182.
- Henry CJ. 2003. Distinguished service award: Evolution of toxicology for risk assessment. *International Journal of Toxicology*. 22(1):3-7.
- Huff J, Jacobson MF, Davis DL. 2008. The limits of two-year bioassay exposure regimens for identifying chemical carcinogens. *Environ Health Perspect*. 116(11):1439-1442.
- Institute of Medicine's Roundtable on Environmental Health Sciences R, and Medicine 2014. Roundtable on environmental health sciences, research, and medicine; board on population health and public health practice; institute of medicine. Identifying and reducing environmental health risks of chemicals in our society: Workshop summary. Washington (dc): National academies press (us); 2014 oct 2. 2, the challenge: Chemicals in today's society. Available from: <https://www.Ncbi.Nlm.Nih.Gov/books/nbk268889/>.
- Jamei M. 2016. Recent advances in development and application of physiologically-based pharmacokinetic (pbpk) models: A transition from academic curiosity to regulatory acceptance. *Current pharmacology reports*. 2:161-169.
- Jones H, Rowland-Yeo K. 2013. Basic concepts in physiologically based pharmacokinetic modeling in drug discovery and development. *CPT Pharmacometrics Syst Pharmacol*. 2(8):e63.
- Jongeneelen FJ, Berge WF. 2011. A generic, cross-chemical predictive pbtk model with multiple entry routes running as application in ms excel; design of the model and comparison of predictions with experimental results. *The Annals of occupational hygiene*. 55(8):841-864.
- Judson RS, Kavlock RJ, Setzer RW, Hubal EA, Martin MT, Knudsen TB, Houck KA, Thomas RS, Wetmore BA, Dix DJ. 2011. Estimating toxicity-related biological pathway altering doses for high-throughput chemical risk assessment. *Chemical research in toxicology*. 24(4):451-462.
- Kasteel EEJ, Lautz LS, Culot M, Kramer NI, Zwartsen A. 2021. Application of *in vitro* data in physiologically-based kinetic models for quantitative *in vitro-in vivo* extrapolation: A case-study for baclofen. *Toxicol In vitro*. 76:105223.
- Katinka van der Jagt SM, Jens Tørslov & Jack de Bruijn. 2004. Assessment of additional testing needs under reach. Effects of (q)sars, risk based testing and voluntary industry initiatives. File:///c:/users/fragkis/downloads/eur%2021405%20en.Pdf.
- Knight DJ, Deluyker H, Chaudhry Q, Vidal JM, de Boer A. 2021. A call for action on the development and implementation of new methodologies for safety assessment of chemical-based products in the eu - a short communication. *Regulatory toxicology and pharmacology* : RTP. 119:104837.
- Knudsen TB, Keller DA, Sander M, Carney EW, Doerrner NG, Eaton DL, Fitzpatrick SC, Hastings KL, Mendrick DL, Tice RR et al. 2015. Futuretox ii: *In vitro* data and *in silico* models for predictive toxicology. *Toxicological sciences* : an official journal of the Society of Toxicology. 143(2):256-267.

- Kramer NI, Di Consiglio E, Blaauboer BJ, Testai E. 2015. Biokinetics in repeated-dosing *in vitro* drug toxicity studies. *Toxicol In vitro*. 30(1 Pt A):217-224.
- Krewski D, Acosta D, Jr., Andersen M, Anderson H, Bailar JC, 3rd, Boekelheide K, Brent R, Charnley G, Cheung VG, Green S, Jr. et al. 2010. Toxicity testing in the 21st century: A vision and a strategy. *J Toxicol Environ Health B Crit Rev*. 13(2-4):51-138.
- Krewski D, Andersen ME, Mantus E, Zeise L. 2009. Toxicity testing in the 21st century: Implications for human health risk assessment. *Risk Anal*. 29(4):474-479.
- Kuepfer L, Niederalt C, Wendl T, Schlender JF, Willmann S, Lippert J, Block M, Eissing T, Teutonico D. 2016. Applied concepts in pbpk modeling: How to build a pbpk/pd model. *CPT Pharmacometrics Syst Pharmacol*. 5(10):516-531.
- Leist M, Hasiwa N, Rovida C, Daneshian M, Basketter D, Kimber I, Clewell H, Gocht T, Goldberg A, Busquet F et al. 2014. Consensus report on the future of animal-free systemic toxicity testing. *Altex*. 31(3):341-356.
- Li H, Yuan H, Middleton A, Li J, Nicol B, Carmichael P, Guo J, Peng S, Zhang Q. 2021. Next generation risk assessment (ngra): Bridging *in vitro* points-of-departure to human safety assessment using physiologically-based kinetic (pbk) modelling - a case study of doxorubicin with dose metrics considerations. *Toxicol In vitro*. 74:105171.
- Li H, Zhang M, Vervoort J, Rietjens IM, van Ravenzwaay B, Lousse J. 2017. Use of physiologically based kinetic modeling-facilitated reverse dosimetry of *in vitro* toxicity data for prediction of *in vivo* developmental toxicity of tebuconazole in rats. *Toxicology letters*. 266:85-93.
- Louisse J, Alewijn M, Peijnenburg A, Cnubben NHP, Heringa MB, Coecke S, Punt A. 2020. Towards harmonization of test methods for *in vitro* hepatic clearance studies. *Toxicol In vitro*. 63:104722.
- Louisse J, Beekmann K, Rietjens IM. 2017. Use of physiologically based kinetic modeling-based reverse dosimetry to predict *in vivo* toxicity from *in vitro* data. *Chemical research in toxicology*. 30(1):114-125.
- Louisse J, Bosgra S, Blaauboer BJ, Rietjens IM, Verwei M. 2015. Prediction of *in vivo* developmental toxicity of all-trans-retinoic acid based on *in vitro* toxicity data and *in silico* physiologically based kinetic modeling. *Archives of toxicology*. 89(7):1135-1148.
- Louisse J, de Jong E, van de Sandt JJ, Blaauboer BJ, Woutersen RA, Piersma AH, Rietjens IM, Verwei M. 2010. The use of *in vitro* toxicity data and physiologically based kinetic modeling to predict dose-response curves for *in vivo* developmental toxicity of glycol ethers in rat and man. *Toxicological sciences : an official journal of the Society of Toxicology*. 118(2):470-484.
- Lu J, Goldsmith MR, Grulke CM, Chang DT, Brooks RD, Leonard JA, Phillips MB, Hypes ED, Fair MJ, Tornero-Velez R et al. 2016. Developing a physiologically-based pharmacokinetic model knowledgebase in support of provisional model construction. *PLoS Comput Biol*. 12(2):e1004495.
- Myatt GJ, Ahlberg E, Akahori Y, Allen D, Amberg A, Anger LT, Aptula A, Auerbach S, Beilke L, Bellion P et al. 2018. *In silico* toxicology protocols. *Regulatory Toxicology and Pharmacology*. 96:1-17.
- National Research Council Committee on the Institutional Means for Assessment of Risks to Public H. 1983. Risk assessment in the federal government: Managing the process. Washington (DC): National Academies Press (US)
- Copyright © National Academy of Sciences.
- Noorlander A, Zhang M, van Ravenzwaay B, Rietjens I. 2022. Use of physiologically based kinetic modeling-facilitated reverse dosimetry to predict *in vivo* acute toxicity of tetrodotoxin in rodents. *Toxicological sciences : an official journal of the Society of Toxicology*. 187(1):127-138.
- OECD. 2012. Proposal for a template, and guidance on developing and assessing the completeness of adverse outcome pathways. OECD Publishing Paris.
- OECD. 2021.
- Olson H, Betton G, Robinson D, Thomas K, Monro A, Kolaja G, Lilly P, Sanders J, Sipes G, Bracken W et al. 2000. Concordance of the toxicity of pharmaceuticals in humans and in animals. *Regulatory toxicology and pharmacology : RTP*. 32(1):56-67.
- Paini A, Leonard JA, Joossens E, Bessems JGM, Desalegn A, Dorne JL, Gosling JP, Heringa MB, Klaric M, Kliment T et al. 2019. Next generation physiologically based kinetic (ng-pbk) models in support of regulatory decision making. *Comput Toxicol*. 9:61-72.

- Paini A, Leonard JA, Kliment T, Tan YM, Worth A. 2017. Investigating the state of physiologically based kinetic modelling practices and challenges associated with gaining regulatory acceptance of model applications. *Regulatory toxicology and pharmacology* : RTP. 90:104-115.
- Pawar G, Madden JC, Ebbrell D, Firman JW, Cronin MTD. 2019. *In silico* toxicology data resources to support read-across and (q)sar. *Frontiers in Pharmacology*. 10.
- Peyret T, Poulin P, Krishnan K. 2010. A unified algorithm for predicting partition coefficients for pbpk modeling of drugs and environmental chemicals. *Toxicol Appl Pharmacol*. 249(3):197-207.
- Punt A, Bouwmeester H, Schiffelers MWA, Peijnenburg A. 2018. Expert opinions on the acceptance of alternative methods in food safety evaluations: Formulating recommendations to increase acceptance of non-animal methods for kinetics. *Regulatory toxicology and pharmacology* : RTP. 92:145-151.
- Punt A, Louise J, Pinckaers N, Fabian E, van Ravenzwaay B. 2021a. Predictive performance of next generation physiologically based kinetic (pbk) model predictions in rats based on *in vitro* and *in silico* input data. *Toxicological Sciences*. 186(1):18-28.
- Punt A, Peijnenburg A, Hoogenboom R, Bouwmeester H. 2017. Non-animal approaches for toxicokinetics in risk evaluations of food chemicals. *Altex*. 34(4):501-514.
- Punt A, Pinckaers N, Peijnenburg A, Louise J. 2021b. Development of a web-based toolbox to support quantitative in-vitro-to-in-vivo extrapolations (qivive) within nonanimal testing strategies. *Chemical research in toxicology*. 34(2):460-472.
- Punt A, Schiffelers MJ, Jean Horbach G, van de Sandt JJ, Groothuis GM, Rietjens IM, Blaauboer BJ. 2011. Evaluation of research activities and research needs to increase the impact and applicability of alternative testing strategies in risk assessment practice. *Regulatory toxicology and pharmacology* : RTP. 61(1):105-114.
- Raies AB, Bajic VB. 2016. *In silico* toxicology: Computational methods for the prediction of chemical toxicity. *Wiley Interdiscip Rev Comput Mol Sci*. 6(2):147-172.
- Rim K-T. 2019. *In vitro* models for chemical toxicity: Review of their applications and prospects. *Toxicology and Environmental Health Sciences*. 11:94-103.
- Rodgers T, Rowland M. 2007. Mechanistic approaches to volume of distribution predictions: Understanding the processes. *Pharm Res*. 24(5):918-933.
- Rotroff DM, Wetmore BA, Dix DJ, Ferguson SS, Clewell HJ, Houck KA, Lecluyse EL, Andersen ME, Judson RS, Smith CM et al. 2010. Incorporating human dosimetry and exposure into high-throughput *in vitro* toxicity screening. *Toxicological sciences : an official journal of the Society of Toxicology*. 117(2):348-358.
- Rovida C, Asakura S, Daneshian M, Hofman-Huether H, Leist M, Meunier L, Reif D, Rossi A, Schmutz M, Valentin JP et al. 2015. Toxicity testing in the 21st century beyond environmental chemicals. *Altex*. 32(3):171-181.
- Sand S, Parham F, Portier CJ, Tice RR, Krewski D. 2017. Comparison of points of departure for health risk assessment based on high-throughput screening data. *Environ Health Perspect*. 125(4):623-633.
- Scholze M, Taxvig C, Kortenkamp A, Boberg J, Christiansen S, Svingen T, Lauschke K, Frandsen H, Ermler S, Hermann SS et al. 2020. Quantitative *in vitro* to *in vivo* extrapolation (qivive) for predicting reduced anogenital distance produced by anti-androgenic pesticides in a rodent model for male reproductive disorders. *Environ Health Perspect*. 128(11):117005.
- Strikwold M, Spenkelink B, de Haan LHJ, Woutersen RA, Punt A, Rietjens I. 2017. Integrating *in vitro* data and physiologically based kinetic (pbk) modelling to assess the *in vivo* potential developmental toxicity of a series of phenols. *Archives of toxicology*. 91(5):2119-2133.
- Strikwold M, Spenkelink B, Woutersen RA, Rietjens IM, Punt A. 2013. Combining *in vitro* embryotoxicity data with physiologically based kinetic (pbk) modelling to define *in vivo* dose-response curves for developmental toxicity of phenol in rat and human. *Archives of toxicology*. 87(9):1709-1723.
- Tannenbaum J, Bennett BT. 2015. Russell and burch's 3rs then and now: The need for clarity in definition and purpose. *J Am Assoc Lab Anim Sci*. 54(2):120-132.
- Tebby C, van der Voet H, de Sousa G, Rorije E, Kumar V, de Boer W, Kruijselbrink JW, Bois FY, Faniband M, Moretto A et al. 2020. A generic pbtk model implemented in the mcra platform: Predictive performance and uses in risk assessment of chemicals. *Food Chem Toxicol*. 142:111440.
- van Leeuwen CJ VT. 2007. Risk assessment of chemicals: An introduction. Second edition. European commission, joint research centre, ispra, italy. Netherlands organization for applied scientific research tno, zeist, the netherlands. National institute for public health and the environment, bilthoven, the netherlands. Isbn 978-1-4020-6102-8 (e-book).

- van Meer PJ, Kooijman M, Gispens-de Wied CC, Moors EH, Schellekens H. 2012. The ability of animal studies to detect serious post marketing adverse events is limited. *Regulatory toxicology and pharmacology* : RTP. 64(3):345-349.
- Van Norman GA. 2019a. Limitations of animal studies for predicting toxicity in clinical trials: Is it time to rethink our current approach? *JACC Basic Transl Sci*. 4(7):845-854.
- Van Norman GA. 2019b. Phase ii trials in drug development and adaptive trial design. *JACC Basic Transl Sci*. 4(3):428-437.
- Varga OE, Hansen AK, Sandøe P, Olsson IA. 2010. Validating animal models for preclinical research: A scientific and ethical discussion. *Altern Lab Anim*. 38(3):245-248.
- Vinken M. 2013. The adverse outcome pathway concept: A pragmatic tool in toxicology. *Toxicology*. 312:158-165.
- Wambaugh JF, Hughes MF, Ring CL, MacMillan DK, Ford J, Fennell TR, Black SR, Snyder RW, Sipes NS, Wetmore BA et al. 2018. Evaluating *in vitro-in vivo* extrapolation of toxicokinetics. *Toxicological sciences : an official journal of the Society of Toxicology*. 163(1):152-169.
- Wambaugh JF, Setzer RW, Pitruzzello AM, Liu J, Reif DM, Kleinstreuer NC, Wang NC, Sipes N, Martin M, Das K et al. 2013. Dosimetric anchoring of *in vivo* and *in vitro* studies for perfluorooctanoate and perfluorooctanesulfonate. *Toxicological sciences : an official journal of the Society of Toxicology*. 136(2):308-327.
- Wambaugh JF, Wetmore BA, Pearce R, Strobe C, Goldsmith R, Sluka JP, Sedykh A, Tropsha A, Bosgra S, Shah I et al. 2015. Toxicokinetic triage for environmental chemicals. *Toxicological sciences : an official journal of the Society of Toxicology*. 147(1):55-67.
- Wang B, Gray G. 2015. Concordance of noncarcinogenic endpoints in rodent chemical bioassays. *Risk Anal*. 35(6):1154-1166.
- Wetmore BA, Wambaugh JF, Ferguson SS, Li L, Clewell HJ, 3rd, Judson RS, Freeman K, Bao W, Sochaski MA, Chu TM et al. 2013. Relative impact of incorporating pharmacokinetics on predicting *in vivo* hazard and mode of action from high-throughput *in vitro* toxicity assays. *Toxicological sciences : an official journal of the Society of Toxicology*. 132(2):327-346.
- Wetmore BA, Wambaugh JF, Ferguson SS, Sochaski MA, Rotroff DM, Freeman K, Clewell HJ, 3rd, Dix DJ, Andersen ME, Houck KA et al. 2012. Integration of dosimetry, exposure, and high-throughput screening data in chemical toxicity assessment. *Toxicological sciences : an official journal of the Society of Toxicology*. 125(1):157-174.
- WHO. 1999. World health organization. Environmental health criteria 210. Principles for assessment of risks to human health from exposures to chemicals. Who, geneva.
- WHO. 2010. World health organization. International programme on chemical safety. Characterization and application of physiologically based pharmacokinetic models in risk assessment. Harmonization project document no. 9
- Yang R. 2011. The application of physiologically based pharmacokinetic (pbpk) modeling to risk assessment.
- Yoon M, Campbell JL, Andersen ME, Clewell HJ. 2012. Quantitative *in vitro* to *in vivo* extrapolation of cell-based toxicity assay results. *Critical reviews in toxicology*. 42(8):633-652.
- Yu L, Li H, Zhang C, Zhang Q, Guo J, Li J, Yuan H, Li L, Carmichael P, Peng S. 2020. Integrating *in vitro* testing and physiologically-based pharmacokinetic (pbpk) modelling for chemical liver toxicity assessment-a case study of troglitazone. *Environ Toxicol Pharmacol*. 74:103296.
- Zhao S, Kamelia L, Boonpawa R, Wesseling S, Spenkelink B, Rietjens IMCM. 2019. Physiologically based kinetic modeling-facilitated reverse dosimetry to predict *in vivo* red blood cell acetylcholinesterase inhibition following exposure to chlorpyrifos in the caucasian and chinese population. *Toxicological Sciences*. 171(1):69-83.

Section I



Chapter 2

Applicability of generic PBK modelling in chemical hazard assessment: A case study with IndusChemFate

Regulatory Toxicology and Pharmacology, 2022. Dec; 136:105267

DOI 10.1016/j.yrtph.2022.105267

Styliani Fragki¹

Aldert H. Piersma^{1,2}

Joost Westerhout³

Anne Kienhuis¹

Nynke I. Kramer^{2,4}

Marco J. Zeilmaker⁵

¹Center for Health Protection, RIVM, National Institute for Public Health and the Environment, P.O. Box 1, 3720 BA Bilthoven, The Netherlands

²Institute for Risk Assessment Sciences, Utrecht University, P.O. Box 80178, 3508 TD Utrecht, The Netherlands

³TNO Innovation for life, Princetonlaan 6 + 8, 3584 CB Utrecht, The Netherlands

⁴Toxicology Division, Wageningen University, PO Box 8000, 6700 EA Wageningen, The Netherlands

⁵Centre for Nutrition, Prevention and Health Services, National Institute for Public Health and the Environment (RIVM), Bilthoven, the Netherlands

Abstract

Toxicology is moving away from animal testing towards *in vitro* tools to assess chemical safety. This new testing framework requires a quantitative method, i.e. kinetic modelling, which extrapolates effective concentrations *in vitro* to a bioequivalent human dose *in vivo* and which can be applied on “high throughput screening” of a wide variety of chemicals. Generic physiologically based kinetic (PBK) models help account for the role of toxicokinetics in setting human toxic exposure levels. Furthermore these models may be parameterized based only on *in silico* QSARs and *in vitro* metabolism assays, thereby circumventing the use of *in vivo* toxicokinetics for this purpose. Though several such models exist their applicability domains have yet to be comprehensively assessed. This study extends previous evaluations of the PBK model IndusChemFate and compares it with its more complex biological complement (“TNO Model”). Both models were evaluated with a broad span of chemicals, varying regarding physicochemical properties. The results reveal that the “simpler” performed best, illustrating that IndusChemFate can be a useful first-tier for simulating toxicokinetics based on QSARs and *in vitro* parameters. Finally, proper quantitative *in vitro* to *in vivo* extrapolation conditions were illustrated starting with acetaminophen induced *in vitro* cytotoxicity in human HepaRG cells.

Introduction

Chemical toxicity testing for the prediction of human safety is currently going through an important transformation. The testing system, which is traditionally based on high-dose animal experiments, is shifting towards a system using primarily *in vitro* cell-based assays combined with computational methods (Carmichael et al. 2022a; Dent et al. 2018; Dent et al. 2021a; Fentem et al. 2021). In practice, applying *in vitro* assays in chemical safety assessment pre-supposes their quantitative *in vitro* to *in vivo* extrapolation (QIVIVE), in order to allow for the derivation of a ‘point of departure’ (Adler et al. 2011; Blaauboer 2008; Yoon et al. 2012). Inevitably this requires linking of *in vitro* observed concentration-effect levels to *in vivo* organ exposure, determined by the chemical’s physicochemical and toxicokinetic characteristics (Adler et al. 2011; Kramer et al. 2015; Punt et al. 2011).

The integration of toxicokinetics in QIVIVE can be facilitated by the use of physiologically based (pharmaco-)kinetic (PBK or PBPK) models (Adler et al. 2011; Bessems et al. 2014; Bouvier d’Yvoire et al. 2007; Hartung et al. 2011; Louisse et al. 2017; Punt et al. 2021b; Punt et al. 2011). PBK models provide biologically realistic organ dosimetry models, simulating ADME⁷ processes within the physiological concept of a whole organism, i.e. the blood flow, organ specific metabolism, growth, etc., and therefore predict a chemical’s internal dose at target organs. Such models require two types of parameters: species-specific physiological (e.g. cardiac output, blood perfusion rates organ weights) and substance-specific (e.g. uptake and metabolic rates, distribution partition coefficients) (Bois et al. 2010; OECD 2021b; Paini et al. 2021b; Peyret and Krishnan 2011; WHO 2010).

Usually *specific* PBK models are fine-tuned to the kinetics of individual compounds. Developing such models requires sufficient kinetic data enabling detailed parameterization and accurate calibration and verification (Jongeneelen and Berge 2011; Lu et al. 2016a; Yang 2011). Commonly, such data are not available for most non-drug chemicals, thereby hampering PBK application to data-poor chemicals. Alternatively, a *generic* PBK approach may be applied instead. Generic PBK models have a pre-defined generic compartmental structure incorporating species-specific physiological parametrization, whereas chemical-specific parameters may be derived from animal/human-based *in vitro* biokinetic metabolism assays combined with *in silico* models (QSARs⁸) (Paini et al. 2019; Punt et al. 2021a; Punt et al. 2021b). Here the enclosed QSARs predict partitioning model parameters based on the molecular structure and physicochemical properties of the compounds (Peyret et al. 2010; Rodgers and Rowland 2007), overcoming the issue of *in vivo* kinetic deposition data paucity for parameterization.

Previously, we explored the capacity of the generic PBK model IndusChemFate (Jongeneelen and Berge 2011), to simulate the toxicokinetics of developmental toxicants and their metabolites for QIVIVE with promising results (Fragki et al. 2022; Fragki et al. 2017). IndusChemFate was selected as being a simple-to-parameterize model, i.e. only

7 ADME: Absorption, Distribution, Metabolism and Excretion

8 QSAR: Quantitative Structure Activity Relationship

2

needing chemical specific physicochemical properties (QSAR-predicted) in combination with *in vitro* metabolism parameters, to describe chemical toxicokinetics. IndusChemFate's kinetic model structure and parameterisation was taken as the starting point for the Population Life-course Exposure To Health Effects Model (PLETHEM, Pendse et al. 2020) and MCRA-9 (Tebby et al. 2020; van der Voet et al. 2020) PBK models. Additionally, during an evaluation of various generic modelling approaches (Pletz et al. 2020), IndusChemFate was classified, next to US EPA's Httk (Pearce et al. 2017) to comply to WHO (2010) and OECD (2021b) criteria for Good Modelling PBK Practice for regulatory purposes. Nevertheless, IndusChemFate has not yet been evaluated on its aspect of simulating chemical kinetics over a wide span of chemical physicochemical properties, a *fundamental pre-condition* for the employment of generic PBK models in hazard identification (OECD 2021b).

In this work the performance evaluation of IndusChemFate was extended with a wider span of chemicals regarding certain physicochemical properties, and a QIVIVE case-study based on hepatotoxicity is presented. In parallel, it was studied whether IndusChemFate's model concept needs further refinement by comparing its performance with a more complex, generic PBK model (TNO Model, developed by the TNO⁹ authors). The TNO model was chosen because of its similar multi-compartment (perfusion limited) PBK structure and complementation to IndusChemFate's alleged physiological-kinetic limitations, with regards to 1. absorption kinetics (IndusChemFate: empirical one-compartmental absorption kinetics *vs.* TNO model: experimental stomach → colon transport with concomitant absorption from the gastrointestinal lumen into the small and large intestines), 2. organ: blood distribution (IndusChemFate: bound to lipid/water partitioning *vs.* TNO model: more complex lipid/water/protein organ: blood partitioning on the basis of a chemical's unbound blood concentration) and 3. intra-hepatic distribution (IndusChemFate: well-stirred perfusion limitation *vs.* TNO model: more refined dispersion modelling). Both models were run in parallel for single *per os* gavage exposure to substances. In order to allow for a meaningful comparison, selected chemicals differed over a wide range of physicochemical properties, i.e. lipophilicity (being the main determinant for the kinetics of lipophilic compounds), ionization at blood pH (as determinant of organ: blood partitioning) and plasma protein binding (as determinant for renal clearance). Their predictive capability was evaluated by a comparison with existing *in vivo* experimental data, as it is traditionally done for PBK models (OECD 2021b; Pains et al. 2019). Finally, to illustrate the application of both models to calculate a human equivalent dose, a proof-of-principle hepatotoxicity QIVIVE was applied for one of the chemicals with data from the human hepatoma cell line, HepaRG. To this end, both generic models were run in order to translate the *in vitro* concentration-response curves and corresponding thresholds for liver toxicity into *in vivo* dose-response curves and BDM(L)s for hepatotoxicity. The respective thresholds were compared with existing information on liver toxicity. In the end, the surplus value of generic PBK models for data-poor chemicals is discussed.

9 TNO: Netherlands Organization for Applied Scientific Research

Methodology

IndusChemFate basic concepts

IndusChemFate is a freely available multi-route PBK model developed under the CEFIC LRI umbrella, specifically for data poor volatile and semi-volatile industrial chemicals. It is written in Visual basic and it is distributed as an MS Excel spreadsheet-file. The model details have been specifically described earlier and hence, for detailed information the reader is referred to the original user manual of the model (<http://cefic-lri.org/wp-content/uploads/2014/03/User-manual-IndusChemFate-version-2.00-final21-11-2011.pdf>), (Jongeneelen and Berge 2011) and to Fragki et al. (2017).

In short, regarding the absorption of a gavage bolus IndusChemFate contains as empirical defaults 100% absorption (fraction absorbed: 1) and an absorption rate constant of 3 hr^{-1} . Organ:blood partitioning is perfusion based with organ:blood partition coefficient being QSAR calculated based on water/lipid content. As a default IndusChemFate only takes hepatic metabolism into account, with biotransformation being described by Michaelis-Menten saturable metabolism according to Ramsey and Andersen (1984), close to the well-stirred model for hepatic elimination (Rowland et al. 1973), with a substance exhibiting a flow-limited distribution and the liver being effectively a homogenous compartment (Pang et al. 2019). Chemical metabolism to specific metabolites is implemented in a sequential way: the parent compound is metabolized into a primary metabolite, followed by metabolism of the primary metabolite into a secondary metabolite, up to four subsequent metabolites. For each of the formed metabolites IndusChemFate contains a PBK sub-model. Default renal excretion depends on Glomerular Filtration Rate (GFR), water solubility and user defined re-absorption. Enterohepatic circulation is adopted by means of a bypass from the liver to the intestines by biliary excretion followed by re-absorption at a user defined rate. IndusChemFate does not take plasma protein binding specifically into account, but it is considered included to some extent in the QSAR algorithms for blood:air and blood:tissue partitioning, given that these are derived from experimental observations.

TNO model basic concepts

The TNO model consists of 15 tissue compartments: adipose, blood, bone, brain, colon, kidney, liver, muscle, pancreas, skin, small intestine, spleen, stomach and “remaining” organs. It was developed by TNO using R software to allow prediction of blood, (target) organ, urine and exhaled air concentrations of a range of chemicals and their primary metabolites on the basis of physicochemical properties and *in vitro* data. The TNO Model is an interactive R shiny application that is available upon request. This interactive tool allows simulating single or multiple exposure routes, short or long duration, single or daily exposure. The underlying PBK model structure (Figure 1) includes children and adults of all ages (Edginton et al. 2006; Haddad et al. 2001; ICRP 2002; Levitt et al. 2007). Though, as IndusChemFate, the TNO model allows for dermal and inhalatory absorption, only its oral route of exposure is of relevance here.

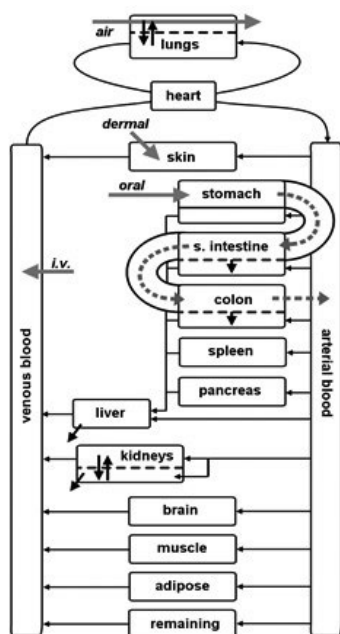


FIGURE 1 Schematic representation of the PBK model that is used in the TNO Model.

In the TNO model the oral absorption is based on a *per os* bolus administered in the stomach followed by transport further down the gastrointestinal (GI) tract from the stomach into the lumen of the duodenum, jejunum, ileum and colon as modelled by Thelen et al. (2011); (2012), using physiological parameters as presented by Wilson (1967), Jönsson et al. (2002) and Willmann et al. (2004). Throughout this transport, absorption from the lumen into the GI tract tissues takes place with the specific rate constant being determined by the lumen surface and a substance-specific, experimentally determined, permeability transport (P_{app}) coefficient.

In the TNO Model intrahepatic distribution is represented by means of a the more complex hepatic dispersion model, as previously described by Roberts and Rowland (1986), which is considered to more adequately reflect physiologic reality of the organ (Sodhi et al. 2020). Renal clearance is determined by the GFR (Schwartz et al. 1987) and the unbound concentration in blood. Enterohepatic circulation is not considered in the TNO Model. The TNO model is limited to the simulation of the parent compound only, i.e. it does not incorporate metabolite PBK sub-models.

The distribution into different tissues is predicted based on the calculations as presented by Peyret et al. (2010), with organ: blood partition coefficients being QSAR calculated based on water/neutral lipid/phospholipid/protein binding content.

In the TNO Model protein binding is considered for the calculation of the tissue: blood partition coefficient, hepatic and renal clearance. Corresponding model equations are provided in the Supplementary Material SM1. Table 1 illustrates the main differences and commonalities of IndusChemFate and the TNO model.

TABLE 1 Comparison of the two PBK models.

	IndusChemFate	TNO Model
Format & model language	Visual Basic, application in MS EXCEL	interactive R shiny application
Exposure routes	oral (bolus), inhalation, dermal	oral (bolus), intravenous (IV) inhalation, dermal
Species	human, rat, mouse	human, rat, mouse, guinea pig
Compartments	12: Blood, Lung, Heart, Brain, Skin, Adipose, Muscles, Bone, Bone marrow, Stomach & Intestines (lumped), Liver and Kidney	15: Blood, Lung, Heart, Brain, Skin, Adipose, Muscles, Bone, Bone marrow, Stomach, Intestines, Liver, Kidney, Spleen and Pancreas
Oral absorption	Default: 100% (option: user defined chemical specific value)	<i>In vitro</i> measure permeability coefficient (Papp, chemical specific)
Absorption rate constant	Default: 3 hr ⁻¹ (option: user defined chemical specific value)	Default: Generic transport of food bolus throughout the GI tract lumen compartments (stomach duodenum ileum colon, according to transport rates (Thelen et al. 2011; Thelen et al. 2012)(all chemicals, in combination with chemical specific uptake from the lumen into the GI tract compartments as determined by a permeability coefficient, see above)
Organ: blood distribution	QSAR (DeJongh et al. 1997); based on water & lipid content in tissues & the logKow (chemical specific)	QSAR (Peyret et al. 2010); each matrix: cell tissue, interstitial fluid, plasma, erythrocytes, consists of water, neutral lipids, phospholipids (neutral and charged) and proteins (chemical specific).
Metabolism	Sequential, saturable Michaelis-Menten metabolism, according to Ramsey and Andersen (1984), based on the well-stirred model (Rowland et al. 1973); hepatic, but possible for various organs (chemical specific)	Sequential & serial, saturable Michaelis-Menten metabolism, according to dispersion model of Roberts and Rowland (1986), hepatic (chemical specific)
Renal excretion	QSAR (Jongeneelen and Berge 2011) based GFR, depending on logKow (pH 7.4) water solubility resp. tubular re-absorption (chemical specific). (option: user defined value for the fraction tubular reabsorption)	Based on GFR, depending on the plasma fraction unbound (F _{up})(chemical specific)
Enterohepatic circulation	Optional: Excretion from the liver to the intestines via biliary excretion, followed by reabsorption	Not considered
Plasma protein binding	Not specifically considered.	Considered for the calculation of the tissue: blood partition coefficients, hepatic and renal clearance (chemical specific)

PBK model input parameters

Given the generic structure of the models the set of parameters required for their application are only chemical-specific and pertain to their physico-chemical characteristics and metabolism. Physicochemical parameters (octanol-water partition coefficients, vapor pressure, water solubility etc.) were obtained from QSARs or open databases (Supplementary Material SM2). If an experimental value was available this was

preferred over the estimated value. In both models, physicochemical properties are used for the calculation of organ:blood partition coefficients, as well as the renal clearance.

Required biochemical parameters (V_{\max} and K_M), were obtained in most of the cases from the open literature or derived from *in vitro* measured clearance (ratio V_{\max}/K_M) (Supplementary Material SM2). The values selected from *in vitro* biokinetic assays were scaled to the relevant *in vivo* units for both models in accordance to Barter et al. (2007). In the absence of *in vitro* measured hepatic clearance of the parent compound, respective parameter estimation was performed by fitting the hepatic ratio V_{\max}/K_M as a first order metabolic rate constant to *in vivo* kinetic data, separately for each PBK model.

PBK model simulations and substance selection

For the purpose of this research, 12 substances were selected (see Results) belonging to different chemical groups (e.g. medicine, cosmetics, pesticides etc.). Given the differences of the two models, compounds with a range in lipophilicity (corrected for ionization, i.e. $\log D$ -2 to 6.53), ionization at blood pH (0 to 1), and plasma protein binding (0 to 1) were employed, in order to allow for a meaningful comparison. These three physicochemical characteristics are expected to have a significant influence on the kinetic properties of most chemicals. It should be noted here that all the elements considered for the substance selection are referring only to the parent compounds and not to their metabolites (with the exception of parabens).

Both PBK models were used to simulate the time-course toxicokinetics of the selected chemicals. The models were applied for oral single exposures, primarily for humans, with the exception of the parabens where no oral toxicokinetic data were available; thus, information from rat toxicokinetic studies were used. Model performance was evaluated based on the model's capability to predict the following toxicokinetic parameters in the blood after a single exposure: maximum concentration (C_{\max}), time needed for reaching the C_{\max} , i.e. T_{\max} , and the area under the concentration time curve (AUC), after comparison with experimentally derived data. Experimental data from two different studies per chemical were used, when available. The simulations were performed here only for the parent substance, with the exception of parabens, where the primary metabolite was taken into consideration. Predicted chemical specific tissue:blood partition coefficients (PCs) were compared to experimentally derived PCs from rat studies, given the lack of data from humans.

Local sensitivity analysis

A local sensitivity analysis was performed to assess the influence of the model parameter variation on the model output (C_{\max} blood, AUC blood, C_{\max} liver, AUC liver). The parameters selected were those expected to markedly affect the outcome of the predicted toxicokinetics and they were chemical-specific. Each parameter was step-wise decreased by 5% to the original parameter value (Li et al. 2017b). The corresponding chemical concentrations were simulated over a single oral dose. The sensitivity analysis was

performed by calculating the sensitivity coefficients according to Evans and Andersen (2000), using the following equation:

$$SC = \left(\frac{\Delta m}{\Delta p} \right) \times \frac{p}{m}$$

where SC is the sensitivity coefficient, m is the model output (e.g., AUC), Δm is the change of the model output (chosen here a 5% decrease), p is the value of the parameter of interest (e.g., logP), and Δp is the change of the parameter value of interest. Each sensitivity coefficient was categorized according to the relative influence of each parameter and subdivided in three impact levels according to Yoon et al. (2009): low: $|SC| < 0.2$; moderate: $0.2 \leq |SC| < 0.5$; high: $0.5 \leq |SC|$.

PBK model-based reverse dosimetry for liver toxicity

In vitro hepatotoxicity of one of the selected compounds (acetaminophen: APAP) on human HepaRG (mainly hepatocyte like) cells (Pery et al. 2013) was used as a starting point for the QIVIVE illustrative example. Both IndusChemFate and the TNO Model were applied in a reverse-dosimetry approach so as to convert the *in vitro* hepatotoxicity concentration-response curve of acetaminophen to an equivalent *in vivo* dose-response curve. The *in vivo* dose metric selected for relating exposure to toxicity was the maximal concentration in the liver tissue (C_{max}), since acetaminophen hepatotoxicity is a result of acute poisoning (Bunchorntavakul and Reddy 2013). An *in vitro* biokinetic distribution model was applied for the estimation of the chemical's free concentration in the culture medium (Kramer 2010; Kramer et al. 2012). The model uses physicochemical properties of the compound to predict its *in vitro* distribution. Subsequently, all calculated free concentrations, instead of the nominal concentrations, were considered equal to the hepatic C_{max} levels and transformed to the corresponding external exposure using the two PBK models. The calculated equivalent external doses were analysed using the Benchmark Dose (BMD) approach, with the software PROAST (Slob 2002), so as to obtain the predicted *in vivo* dose-response curves. For a quantitative comparison with the usual range of acetaminophen human overdose, leading to hepatotoxicity (Bunchorntavakul and Reddy 2013; Jaeschke et al. 2011), 90% confidence intervals were estimated for the underlying BMD at 10% effect size (BMD₁₀) and at 20% effect size (BMD₂₀) (EFSA 2017). The confidence intervals are denoted by the lower (BMDL) and upper (BMDU) limits. As a benchmark response HepaRG cell viability was used as recorded with the *in vitro* assay (Pery et al. 2013).

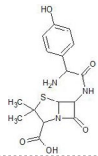
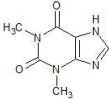
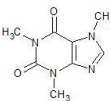
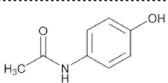
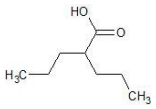
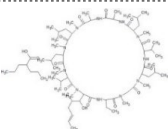
Results

Chemical selection

The twelve selected substances are presented in Table 2 whereas Figure 2 illustrates the range in lipophilicity (logD -2 to 6.5), ionization at blood pH (0 to 1), and plasma protein binding (0 to 1) taken into account in evaluating IndusChemFate's applicability domain.

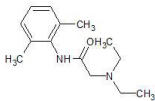
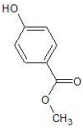
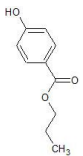
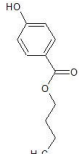
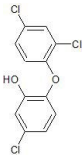
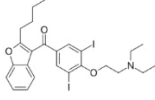
Hepatic metabolism is the main elimination route for most of the chosen compounds (Table 2) with the exception of amoxicillin (AMOX) with low hepatic metabolism (~30%), excreted renally mainly as a parent substance (Arancibia et al. 1980). Next to hepatic metabolism urinary excretion is the prime excretion route (for the parent or metabolites), apart from two compounds amiodarone (AMD) (Deng et al. 2011) and cyclosporin A (CyA) (Schwinghammer et al. 1991), which undergo enterohepatic removal and (partly) excretion via the faeces. Nevertheless, these two processes refer to the metabolites, since the parent compounds are extensively metabolized prior to excretion. Amongst these, five substances were included based also on specific toxicity to the liver: acetaminophen (APAP) (Mutlib et al. 2006), valproic acid (VPA) (Jawien et al. 2017), triclosan (TCS) (Wang et al. 2019), cyclosporin A (CyA) (Klintmalm et al. 1981) and amiodarone (AMD) (Buggey et al. 2015).

TABLE 2 Selected substances: chemical structure, physicochemical and biological properties, metabolism and excretion pathways.

Substance	Chemical Structure	MW ¹	Fraction ionized pH 7.4 ²	F _{up} ³	LogD ⁴
Amoxicillin (AMOX)		365.4	0.6	0.8	-2
Theophylline (THEO)		180.2	0.3	0.6	-0.16
Caffeine (CAF)		194.2	0	0.64	-0.07
Acetaminophen (APAP)		151.2	0.01	1	0.46
Valproic acid (VPA)		144.2	1	0.8	0.49
Cyclosporin A (CyA)		1202.6	0	0.062	1

10 NAPQI: N-acetyl-p-benzoquinone imine; Unconjugated NAPQI: binds covalently to proteins (cysteine groups), induces cell death & necrosis, liver failure

Metabolism ⁵	Excretion ⁵	Modelled Pathways
Hepatic, <30%. Main metabolites: Amoxicilloic acid and Amoxicillin piperazine-2,5-dione.	Renal, mostly excreted as parent in urine, <30% as metabolites	AMOX → all metabolites
Hepatic, main elimination route, complex metabolism.	Renal, as metabolites, ~ 10% unchanged in urine.	THEO → all metabolites
Hepatic, main elimination route; primarily xanthil (CYPs- paraxanthine ~80%, theobromine ~12%, theophylline ~ 4%) & after, uracil derivatives. More than 25 metabolites identified in humans.	Renal, as metabolites, <1% unchanged in urine.	CAF → all metabolites
Hepatic, main elimination route; glucuronidation (APAP G) & sulfonation (APAP S). Small fraction: NAPQI ¹⁰ <5%, toxic highly reactive metabolite, excreted as APAP mercapurate & APAP cysteine (APAP cys), detoxification with GSH.	Renal, as metabolites, <5% unchanged in urine	APAP → all metabolites
Hepatic, main elimination route; glucuronidation (VPA G, 30-50%), β -oxidation (~30%). Hepatotoxic reactive metabolite is the VPA- 4-ene (4-ene-valproic acid)	Renal, as metabolites, <3% unchanged in urine.	VPA → all metabolites
Hepatic (also some intestinal), main elimination route; over 30 metabolites.	Biliary (feces) excretion of metabolites (90% of dose, excreted mainly as metabolite); enterohepatic re-absorption. Only 6% of dose in urine. Total parent excretion: <1%	CyA → all metabolites

Substance	Chemical Structure	MW ¹	Fraction ionized pH 7.4 ²	F _{up} ³	LogD ⁴
Lidocaine (LID)		234.3	0.7	0.2	1.93
Methylparaben (MePa)		152.1	0.1	na	1.96
Propylparaben (ProPa)		180.2	0.1	na	3.04
Butylparaben (ButPa)		194.2	0.1	na	3.57
Triclosan (TCS)		289.6	0.35	0.01	4.58
Amiodarone (AMD)		645.3	0.92	0.04	6.53

¹ MW: Molecular weight taken from PubChem <https://pubchem.ncbi.nlm.nih.gov/>

² Calculated based on pKa/pKb values as predicted with MarvinSketch (ChemAxon) and logP from EpiSuite.

³ Fraction Unbound, information for each individual source for every chemical provided in the Supplementary Material

⁴ Data taken from EPI (Estimation Programs Interface) Suite™ <https://www.epa.gov/tsca-screening-tools/epi-suitetm-estimation-program-interface>

⁵ Information take as follows APAP: Mutlib et al. (2006); Pery et al. (2013), AMOX: Arancibia et al. (1980); Szultka et al. (2014), LID: Alexson et al. (2002); FDA (2010), VPA: Argikar and Rimmel (2009); Conner et al. (2018); Johannessen and Johannessen (2003), CAF: Arnaud (2011), THEO: Arnaud (2011), AMD: (Chen et al. 2015; Deng et al. 2011; Trivier et al. 1993), CyA: Pichard et al. (1996); Schwinghammer et al. (1991), Parabens: Aubert et al. (2012), TCS: Sandborgh-Englund et al. (2006).

Metabolism ⁵	Excretion ⁵	Modelled Pathways
Hepatic, main elimination route, complex metabolism.	Renal, as metabolites, <10% unchanged in urine. Renal excretion is believed to be via non-ionic diffusion.	LID→ all metabolites
Hepatic, main elimination route; main metabolite is the hydrolysis product <i>p</i> -hydroxybenzoic acid (PHBA). Minor metabolite the glucuronide conjugate of the parent & PHBA.	Renal, mainly as PHBA.	MePa→ primary metabolite PHBA
Hepatic, main elimination route; main metabolite is the hydrolysis product <i>p</i> -hydroxybenzoic acid (PHBA). Minor metabolite the glucuronide conjugate of the parent & PHBA.	Renal, mainly as PHBA.	ProPa→ primary metabolite PHBA
Hepatic, main elimination route; main metabolite is the hydrolysis product <i>p</i> -hydroxybenzoic acid (PHBA). Minor metabolite the glucuronide conjugate of the parent & PHBA.	Renal, mainly as PHBA.	ButPa → primary metabolite PHBA
Hepatic, main elimination route. Predominant metabolites are glucuronide & sulphate conjugates.	Renal, mainly as metabolites; feces (10%), as parent.	TCS→ all metabolites
Hepatic, main elimination route; one main metabolite, desethyl-amiodarone (DEA), equally toxic to the parent.	Biliary (feces) excretion of metabolites; only 1% unchanged in urine, negligible renal excretion of metabolite, only metabolites identified in bile.	AMD→ DEA (major metabolite)

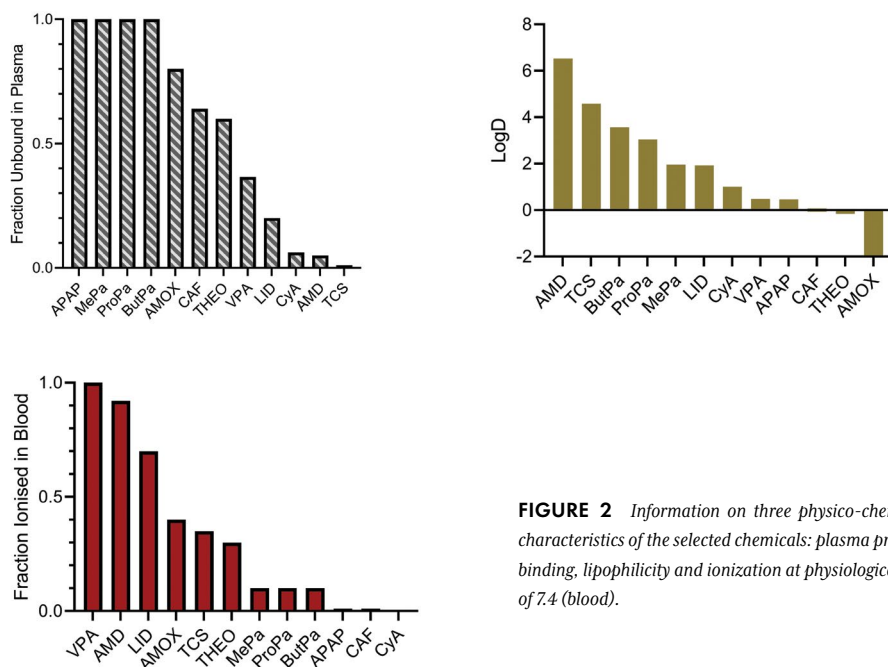


FIGURE 2 Information on three physico-chemical characteristics of the selected chemicals: plasma protein binding, lipophilicity and ionization at physiological pH of 7.4 (blood).

Estimation of tissue:blood partition coefficients

For the distribution of substances between the blood and organs, both models incorporate QSARs than can perform predictions based solely on the chemical's molecular structure. In the simpler IndusChemFate's QSAR the distribution between the blood and tissues is described as a function of water and lipid content of tissues, with the *n*-octanol:water partition coefficient ($\log K_{ow}$) and the acid:base dissociation constant (pKa) as input parameters. Ionization is taken partly into account, since the $\log K_{ow}$ at different pHs (blood & skin) (or else logD) is applied (Jongeneelen and Berge 2011). Hence, based on this model concept only the non-ionized fraction of the chemical will diffuse into the tissues. On the other hand, the TNO Model has implemented a more sophisticated QSAR (Peyret et al. 2010), previously designed for environmental chemicals and pharmaceuticals, which takes into consideration the role of more tissue components other than lipid and water. This unified algorithm is based on the principle that the concentration of a chemical in a 'biological matrix' is equal to the sum of its concentration in all respective compartments of the matrix. Each matrix (cell tissue, interstitial fluid, plasma, erythrocytes) consists of water, neutral lipids, phospholipids (neutral and charged) and proteins, with ionizable substances existing in an equilibrium between the ionized and non-ionized species (for details see Supplementary Material SM 1.5).

For six of the selected chemicals, experimental PC rat adipose tissue data were available. IndusChemFate-predicted rat PCs for the adipose tissue clearly were in better accordance with the *in vivo* measured experimental data compared to the TNO model-predicted

PCs (Figure 3), the TNO model calculating much lower PCs (min/max IndusChemFate/TNO ratio: 1.5 – 178, for details, see Supplementary Material SM3, Table 1). As in the rat calculated human adipose PCs were much higher in IndusChemFate than in the TNO model (for details, see Supplementary Material SM3, Table 1).

With regard to the other tissues, PC-predictions of both models were comparable (ratio <5-fold in most cases) and in line with experimentally observed values (see Figure 4), CyA being a clear exception to the rule. The TNO model highly underpredicted the PCs for CyA, which is also reflected in the overall estimates for this substance (see next section). In concordance with the rat IndusChemFate calculated human PCs were significantly higher than those of the TNO model (see Supplementary Material SM3, Figure 1).

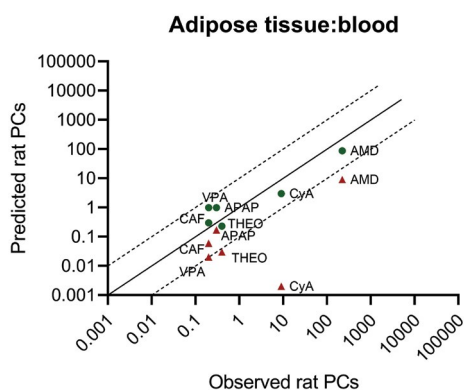


FIGURE 3 Comparison of the PBK model adipose tissue: blood partition coefficients (PCs) (green circles: IndusChemFate, red triangles: TNO Model) with data from experimental observations in the rat. The line of identity (slope equal to 1) is drawn, in order to depict the absolute differences between model predicted and experimentally determined PCs. Experimental results are taken as follows; CAF: Yun and Edginton (2013), APAP: Pery et al. (2013), VPA: Kobayashi et al. (1991), CyA: Kawai et al. (1998), AMD: Plomp et al. (1985).

Evaluation of the PBK-model predictions

Time-course kinetics

Except for metabolism both IndusChemFate and the TNO model can fully be calibrated on the basis of literature values (physiology), *in silico* (QSAR-based partition coefficients: PCs), experimentally determined absorption (TNO model) or default absorption kinetics (IndusChemFate: fraction absorbed and the absorption rate constant) and renal clearance. Given these constraints the hepatic Michaelis Menten metabolism parameters V_{\max} and K_M may (preferably) be obtained from of *in vitro* → *in vivo* scaling or by fitting the model to (the time-course) of *in vivo* kinetics. Of course the latter procedure is to be considered as conditional given the constraints mentioned above, i.e. all other parameters assumed to be known. In addition in the case of IndusChemFate re-parametrisation of the default absorption parameters remains optional.

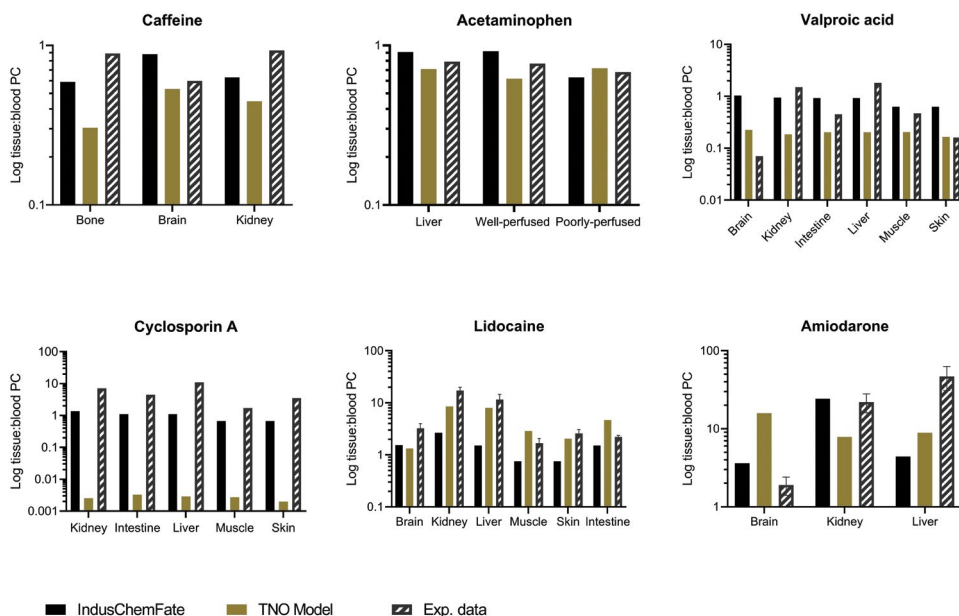


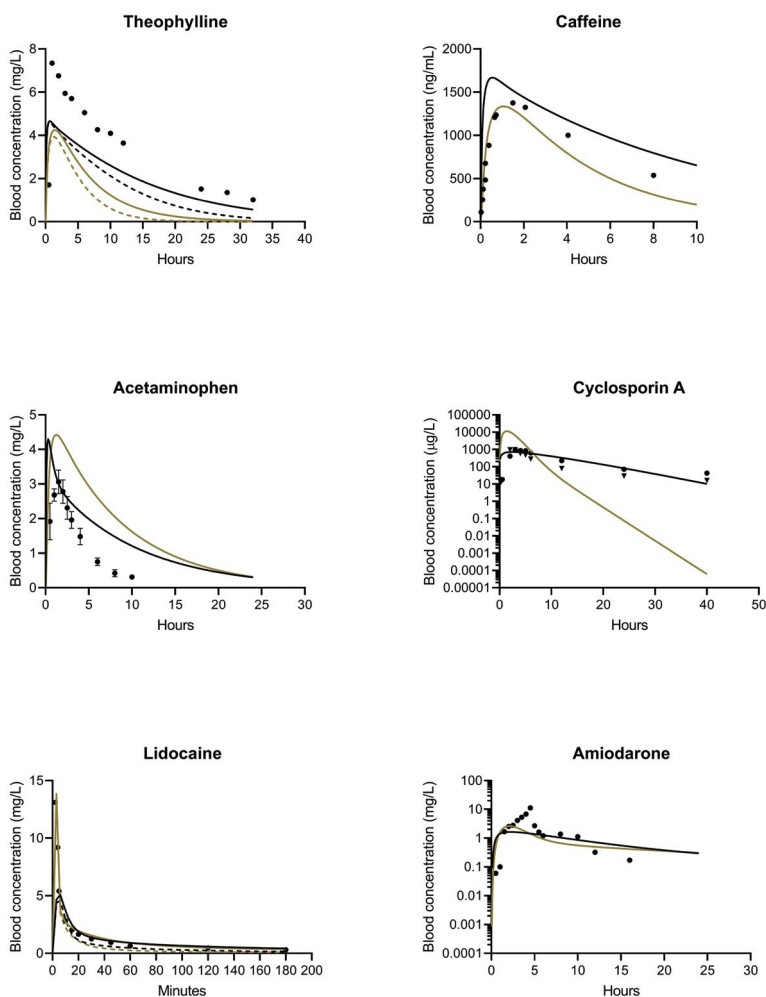
FIGURE 4 PBK-predicted and *in vivo* measured tissue:blood partition coefficients in the rat. Substances presented in the order of increasing lipophilicity ($\log D$: -2 to 6.5). Experimental results taken from the following sources; CAF: Yun and Edginton (2013), APAP: Pery et al. (2013), VPA: Kobayashi et al. (1991), CyA: Kawai et al. (1998), LID: Rodgers et al. (2005), AMD: Plomp et al. (1985).

For eight of the twelve selected chemicals metabolism parameters could be obtained from the literature, i.e. THEO, CAF, APAP, VPA, CyA, LID, TCS and AMD, leaving the parameters of AMOX and the parabens, MePa, ProPa and ButPa to be fitted on the *in vivo* kinetic data. Furthermore, for all chemicals human *in vivo* kinetic verification data were available, with the exception of the rat data for parabens. Simulations were made for the parent substance and not for their metabolites, except for the family of parabens where the sum of parent and primary metabolite (p-hydroxybenzoic acid, PHBA) was also modelled (because of toxicokinetic studies reporting on the total radioactive dose, thereby not discriminating between the parent paraben and the metabolite (Aubert et al. 2012).

The modelling was conducted by using *in vitro* measured intrinsic clearance after appropriate scaling (Barter et al. 2007). In the absence of *in vitro* measured hepatic elimination of the parent compound, respective parameter estimation was performed by fitting the hepatic ratio V_{\max}/K_M as a first order metabolic rate constant to *in vivo* data (AMOX and parabens).

Figure 5 shows the applicability of both the IndusChemFate and the TNO model for the time course of single-dose gavage kinetics of the chemicals (one of the kinetic studies per chemical). Graphs of the additional simulations (second kinetic study per example chemicals) are presented in the Supplementary Material (Supplementary Material SM4). With regard to the chemicals for which metabolism parameters could be obtained from the literature, IndusChemFate simulated the *in vivo* human THEO, CAF, APAP, CyA, and LID kinetics reasonably well for a generic PBK model. For comparison, the TNO model

simulated THEO, CAF, APAP, and LID, kinetics, as well as failing, however, in describing CyA kinetics. In more detail, in the case of APAP, IndusChemFate to some extent overestimated absorption kinetics, while slightly underestimating clearance from the blood. Here the TNO model described better the absorption kinetics, however, also underestimated the clearance from the blood. Both models slightly underestimated THEO kinetics. AMD kinetic profile was not so well predicted by both models. Neither IndusChemFate nor the TNO model were able to describe the kinetics of VPA and TCS, even after recalibration of the metabolism parameters, indicating the limitations of both model concepts to describe the human kinetics of these chemicals. In the case of AMOX and parabens calibrating the unknown (ratio) of the model parameters V_{max} and K_M led to a good description of human kinetics in the case of IndusChemFate, but (as expected because of a lack of metabolite PBK sub-models) not the TNO model.



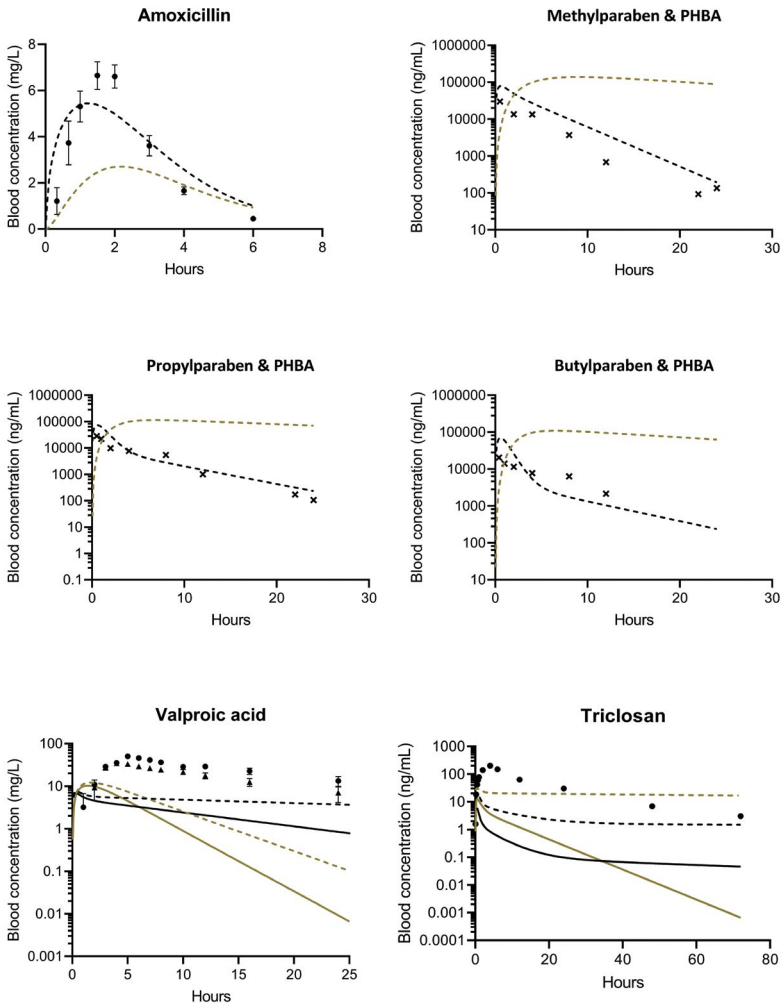


FIGURE 5 Blood time-course PBK simulations. Smooth lines: models calibrated on measured intrinsic clearance *in vitro* and human data (circle, triangle symbols). Dashed lines: models calibrated on *in vivo* kinetic data; Amoxicillin: human data, Parabens: rat data). Black lines represent IndusChemFate simulations and golden lines TNO Model simulations. *In vivo* data represent mean values and the bars indicate the standard errors of mean (AMOX, VPA) or standard deviation (APAP). Theophylline (THEO): 250 mg, single oral dose, two healthy volunteers (Dadashzadeh and Tajerzaden 2001). Caffeine (CAF): 100 mg, single oral dose (Zandvliet et al. 2005). Acetaminophen (APAP): 325 mg, single oral dose, eight healthy volunteers (Volak et al. 2013). Cyclosporin A (CyA): 875 mg, single oral dose, two bone marrow transplantation patients (Bertault-Pères et al. 1985). Lidocaine (LID): single dose given as a 3-min intravenous infusion of 3 mg/kg bw, five healthy volunteers (Grillo et al. 2001). Amiodarone (AMD): 1400 mg, single oral dose, one patient with cardiac arrhythmias (Kannan et al. 1982). Amoxicillin (AMOX), 500 mg, single oral dose, four healthy volunteers (Adam et al. 1982). Parabens: three parabens and their primary metabolite *p*-hydroxybenzoic acid (PHBA), 100 mg/kg bw, single gavage dose, rat experimental data (Campbell et al. 2015) (original data from Aubert et al. 2012). Valproic acid (VPA): 500 mg, single oral dose, 14 healthy volunteers (Ibarra et al. 2013). Triclosan (TCS): 3.75 mg, single oral dose, healthy volunteers. Substances presented in the order of increasing lipophilicity (logD: -2 to 1).

Toxicokinetic parameters' comparison: C_{max}, T_{max} and AUC

Figure 6 shows the C_{max} and AUC values as calculated from the two PBK-models (for actual values: see Supplementary Material SM5) together with respective values from the *in vivo* studies (per toxicokinetic study per chemical). Adequate predictions of the C_{max}, T_{max} and AUC parameters were performed by both models for THEO, CAF, APAP, AMOX (ratio <3-fold). IndusChemFate underpredicted the C_{max} for LID, when administered via an intravenous route, as it is not fit for this administration¹¹. For CyA, as already shown with the PCs, the TNO Model overpredicted the C_{max} values and the substance's clearance (faster than experimentally recorded). For the highly lipophilic AMD, predicted blood C_{max} values were 3-fold and 4-fold lower with the TNO Model and IndusChemFate, respectively, when compared to the *in vivo* data (Kannan et al. 1982), and both models illustrated an earlier T_{max}. The peak concentration in the blood was reached somewhat later *in vivo* (T_{max} ~4.5 hours) than with the PBK model estimations (T_{max}: IndusChemFate 2.5 hrs, TNO Model 2 hrs).

As expected (see above) for the highly ionized VPA in blood pH, IndusChemFate's C_{max} calculations do not fit well the experimental data, being larger by approximately a factor of 10. Peak blood estimates by the TNO model were closer to the observed data, but the model overpredicted the chemical's clearance. TCS's blood C_{max} was also more than an order of magnitude underpredicted by both PBK models. For VPA, additional simulations were performed this time with *in vivo* data on the hepatic elimination clearance (Ibarra et al. 2013). Nevertheless, only a slightly better fit to the data could be achieved for the AUC, with the blood peak concentrations being underestimated by 7- and 5-fold with IndusChemFate and the TNO Model, respectively. Similarly, adaptations of the enterohepatic circulation rate (with IndusChemFate) did not seem to improve the model predictions (data not shown). The same was seen for TCS, with no substantial improvements of the model calculations, after adaptation of the hepatic clearance.

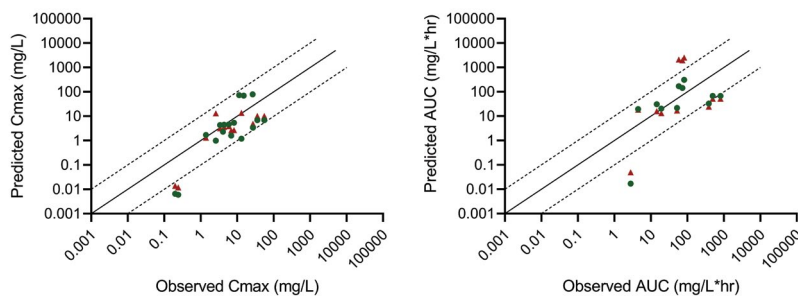


FIGURE 6 Comparison of the PBK model predicted blood peak concentrations (C_{max}) and Area Under the Curve (AUC) with experimental observations from different toxicokinetic studies for the selected chemicals (green circles: IndusChemFate, red triangles: TNO Model). Each circle or triangle represents a C_{max} or AUC from a kinetic study and the respective PBK-model prediction (one or two measurements for each chemical depending on the number of available studies; for the numerical values see Supplementary Material SM5).

¹¹ IndusChemFate was forced into IV predictions by increasing maximally the absorption rate of LID.

For the family of parabens rat toxicokinetic data were used in order to optimize PBK model performance, since human data were not available. Parabens are rapidly hydrolysed in mammals to their primary metabolite PHBA which was also modelled here together with the parent substance. IndusChemFate-predicted C_{max} values were 3-, 7- and 5-fold higher than *in vivo* measurements, for MePa, ProPa, and ButPa, respectively.

Sensitivity analysis

A sensitivity analysis was performed for one of the tested chemicals (APAP), which was chosen for the QIVIVE hepatotoxicity case study (see below). The most sensitive parameters for the AUC predictions (blood and liver) and for both PBK models appear to be the V_{\max} and K_M of the hepatic metabolism as indicated in Figure 7. In addition, in the case of IndusChemFate, AUC estimations also largely influenced by the renal re-absorption, which is in essence determined by the logD and water solubility of the chemical. With the TNO Model, plasma protein binding seems also to have a high impact on blood AUC values. For the prediction of the C_{max} in both compartments the absorption rate seems to have the highest influence in IndusChemFate, whereas for the TNO model parameters V_{\max} , K_M , logP, Fup were categorized as ‘moderate impact level’.

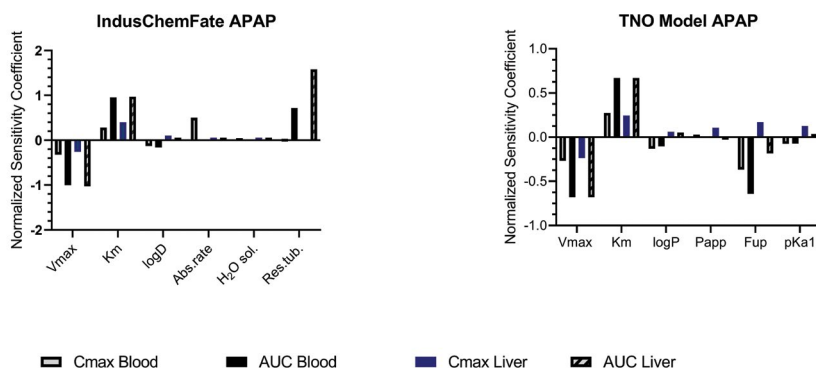


FIGURE 7 Normalized sensitivity coefficients of the two PBK models for the predicted C_{max} and AUC of acetaminophen (APAP) in both blood and liver.

QIVIVE for hepatotoxicity of acetaminophen

For the QIVIVE example the liver toxicant APAP was selected because of the availability of 1. a well defined dose-response relationship for *in vitro* cytotoxicity, being a relevant proxy for *in vivo* hepatic toxicity and 2. an adequate human PBK model. HepaRG cells (Pery et al. 2013) were used as a starting point for the derivation of human equivalent dose-response curves with PBK model-based reverse dosimetry (Figure 8). Results with the *in vitro* biokinetics model revealed that APAP is expected to be almost 100% free in the *in vitro* medium, and hence no further corrections were considered necessary; as such the nominal levels were used for the reverse dosimetry approach. The PBK-estimated oral human equivalent 90% confidence intervals for the BMD₁₀ and BMD₂₀ were compared with

the data from APAP acute poisoning. The results were found to be very close to the reported range of human overdose with APAP, which is between 150 and 500 mg/kg bw (Jaeschke et al. 2011) (Table 3).

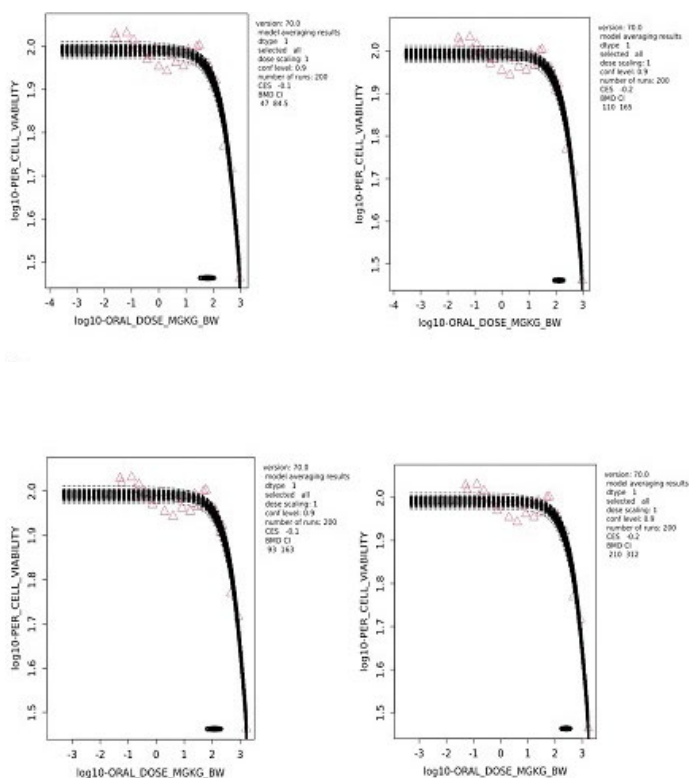


FIGURE 8 Predicted human dose-response curves for the hepatotoxicity of acetaminophen (APAP) and corresponding BMD analysis. Predicted curves were obtained from HepaRG *in vitro* concentration-response data with PBK modelling reverse dosimetry. The liver C_{max} was chosen as dose metric for relating exposure to hepatotoxicity. BMD analysis was performed by model averaging for the 10 and 20% (left and right graph, respectively) effect size. A. Application of IndusChemFate. B. Application of the TNO Model.

TABLE 3 Model averaged 90% confidence intervals (BMDL-BMDU) at a 10% and 20% effect size for hepatotoxicity, as determined by a BMD analysis of the *in vitro*-based PBK modelling reverse dosimetry predictions. BMD analysis performed with PROAST software. Acetaminophen human overdose data are taken from Jaeschke et al. (2011). *In vitro* toxicity data on HepaRG cells are taken from Pery et al. (2013).

IndusChemFate				TNO Model				Human overdose range (mg/kg bw)
Oral equivalent 90% confidence intervals for the underlying human BMD ₁₀ and BMD ₂₀ (mg/kg bw)								
BMDL ₁₀	BMDU ₁₀	BMDL ₂₀	BMDU ₂₀	BMDL ₁₀	BMDU ₁₀	BMDL ₂₀	BMDU ₂₀	
47	85	110	165	93	163	210	312	150-500

Discussion

The aim of this work was to extend a previous evaluation of the applicability domain of the generic PBK mode IndusChemFate and to compare this with that of a more complex model, i.e. a model incorporating more detailed organ:blood partition, liver metabolism and absorption kinetics (TNO model). Finally, the objective was to illustrate the potential application of IndusChemFate for QIVIVE purposes. Both models run with incorporated organ:blood and renal excretion QSARs and require minimum parameterization, stemming from *in silico* and *in vitro* sources. Substances selected for the simulations had a broad span in lipophilicity, blood ionization and blood protein binding, and were in parallel eliminated primarily via the liver. Together with findings reported elsewhere, this paper clearly shows the pros and cons in using generic PBK models in simulating chemical toxicokinetics in a data-limited environment. Furthermore, a PBK model-based reverse dosimetry for the hepatotoxicity of APAP is presented as a case study on QIVIVE with the use of such PBK models.

Both IndusChemFate and the TNO model consist of multiple compartments and contain a pre-defined structure with incorporated physiological and anatomical parameters for various species. Generated concentration-time curves (blood or organs) are perfusion-limited. Incorporated QSARs predict the distribution partition coefficients based on compound-specific physicochemical characteristics. Their most fundamental model-structure differences pertain to the distribution QSARs, hepatic metabolism, and blood protein binding consideration, which *a priori* were expected to be advantageous for the TNO Model, in terms of toxicokinetic predictions. Yet, the results demonstrate that in nine (AMOX, THEO, CAF, APAP, CyA, MePA, ProPa, ButPA, LID) out of twelve cases, IndusChemFate could straightaway be calibrated on literature data, to give a satisfactory description of available kinetic (time-course) data. However, IndusChemFate was not able to describe VPA, TCS and AMD kinetics. The more complex TNO model gave a satisfactory description of AMOX, THEO, CAF, APAP and LID kinetics. Comparison of the predictions with *in vivo* human data illustrated less than 3-fold differences with respect to the C_{max}, T_{max} and AUC parameters for AMOX, THEO, CAF, and APAP. Simulations of the three parabens and their primary metabolite by IndusChemFate, for the rat, also showed reasonable predictions. This was not the case for the TNO Model, but this can be explained by the fact that (as other generic PBK models) this model is not fit for the metabolite's PBK predictions given the lack of metabolite kinetics and renal clearance for the metabolite, placing the IndusChemFate in a more advantageous position.

For the very lipophilic AMD, C_{max} calculations were with a small underestimation by both models, whereas visual inspection of the whole predicted and observed blood time-course curves did not suggest a good overlay. This could possibly be the result of the known extensive tissue distribution of AMD, that warrants a substance-specific permeability-limited PBK model (Algharably et al. 2019; Lu et al. 2016b), which does not fit the current PBK model concept. PBK estimates of lower accuracy were recorded for VPA and TCS,

with both C_{max} and AUC underpredicted. Both models failed to provide a better fit to the empirical values, even after adaptation of the hepatic clearance, suggesting that both generic model concepts cannot describe the toxicokinetics of these chemicals, probably because of a lack of specific elements within the models, like active organ: blood transport processes. Another explanation for the failed predictions could be the incorporated QSARs for the calculation of the tissue: blood partition coefficients. For example, in the case of VPA both models predict much more chemical entering the tissues compared to what is recorded *in vivo*. As such, it cannot be excluded that the use of other distribution QSARs, for example Schmitt (2008b) or Rodgers et al. (2005); Rodgers and Rowland (2006), may have been more appropriate here. Nevertheless, the evaluation of other available distribution QSARs is beyond the scope of this paper and the default calculators were used as currently incorporated in the PBK models. It is acknowledged, however, that for the continuation of this work specific attention on the applied distribution QSARs shall be given when such generic PBK models are employed. In particular, their selection may be decided on a case-by-case basis, in accordance with the physicochemical characteristics of the substance of interest and the applicability domain of the respective QSAR, when this is defined (see for example the recent paper by Punt et al. 2022). It shall also be noted again that the experimental PCs shown here are from rat and not from human data.

Overall, it seems that, within the applicability domain of the investigated compounds and the available data (blood concentrations) the use of a model structure beyond that of IndusChemFate does not offer added value.

Regarding the chemical-specific parameterization, both models are solely based on *in silico* and *in vitro* data. Mainly QSARs are used for deriving physicochemical properties, whereas *in vitro* data provide for example information on hepatic metabolism (Louisse et al. 2020a). For *in vitro* hepatic clearance, although several methods are currently available, guidance for performing such studies is lagging behind, hampering as such their systematic characterization and harmonization (Gouliarmou et al. 2018). Intrinsic clearance values for the same chemical, determined in different hepatocyte studies, were recently found to have a very high variation, ranging by more than one order of magnitude for most substances included in that study (Louisse et al. 2020a). Parameterization with high variation would substantially affect the toxicokinetics predictions of the PBK models, underpinning the importance for the standardization of the *in vitro* biokinetic assays.

With respect to the derivation of QIVIVE based (chronic) Human Equivalent Doses (HED) the extrapolation of (preferably human) organ specific *in vitro* toxicity to “steady state” human organ kinetics is mandatory. Clearly, a priori, PBK models comply here, however classical 1- and 2-compartment models also may apply here (when combined with organ specific partitioning within the “steady state” central compartment). In this context, when calibrated solely on *in silico* and *in vitro* metabolism data, both approaches have been shown to be able to describe basic *in vivo* kinetics. In this context Wambaugh et al. (2018) describe the applicability of *in silico/in vitro* calibrated rodent 1- and 2-compartment modelling in

2

estimating *in vivo* observed the C_{\max}/AUC for 48 compounds (pharmaceuticals and others) after single dose administration. Similar findings have been reported for 2- and 3-compartment PBK models for example by Wambaugh et al. (2015) (PBK model consisting of the gastrointestinal tract, liver and rest of the body, calibrated on 74 pharmaceuticals and 11 other compounds in the rat), and Kamiya et al. (2021); (2019; 2020) (PBK model consisting of gastro-intestinal tract, liver, kidney and rest of the body, calibrated on 246 industrial chemicals in the rat) and for multi-compartment PBK models like for example by Punt et al. (2021a); (2022) (calibrated on 44 chemicals in the rat) and Fragki et al. (2017) (calibrated on 12 compounds in the rat). However, the modelling of human kinetics as shown in this manuscript only was presented in Wambaugh et al. (2015) (11 compounds). This stresses the need for additional analyses using human kinetic data as proposed by Breen et al. (2021) and (Sayre et al. 2020), using the above mentioned PBK models.

An important topic to be mentioned is the expected accuracy of the PBK model predictions (Shebley et al. 2018). Naturally, generic models cannot be expected to predict toxicokinetics as precisely as specific PBK models, fulfilling the commonly applied acceptability criterion for predicted values to be within two-fold of the observed values (WHO 2010). This criterion is prescribed for PBK models designed for a single or small group of chemicals, usually in a data-rich environment, where they can be properly evaluated and calibrated to fit experimental data. Generic PBK models by definition, may have lower accuracy, but a much larger applicability domain, and can be run with low parameterization. Although currently no consensus exists on how to evaluate the 'goodness of fit' for such generic models, a difference of up to a 10-fold in PBK-estimated dose metrics, compared to the *in vivo* observations, has often been recorded (Abdullah et al. 2016; Breen et al. 2021; Pletz et al. 2020; Punt et al. 2021b). Differences of such degree are within the intervals of biological variation (Janer et al. 2008a). Though it might be argued that IndusChemFate simulations in nine out of twelve compounds are within accepted variability of data underlying current chemical safety assessment additional analyses are needed to confirm this result, as well as to define the specific modifications needed to satisfactorily describe the kinetics of compounds like VPA and TCS. It shall be mentioned that in a recent evaluation of predictive performance of such generic PBK models for a large number of chemicals, Punt et al. (2022) proposes a quantitative criterion for the C_{\max} parameter: a 5-fold difference (predicted *vs* observed) is considered adequate, whereas a 10-fold difference, although less precise, is still seen as relevant.

The final part of this work was to illustrate the potential application of generic PBK models for QIVIVE. For this end, an *in vitro* concentration response curve for cytotoxicity of HepaRG cells was transformed into an equivalent dose-response curve by PBK model-based reverse dosimetry. APAP was selected as model compound since its toxicokinetics were well-predicted by both PBK models. The predicted BMDL-BMDU intervals based on data from HepaRG cells were in line with the reported ranges for human overdose (150-500 mg/kg bw) (Jaeschke et al. 2011), associated with severe hepatotoxicity. It is acknowledged

that *in vivo* cell viability may not be the immediate endpoint for predicting human hepatic toxicity or failure. Nevertheless, cytotoxicity is often considered the main hepatotoxicity readout (Albrecht et al. 2019), and has been employed in several other PBK-facilitated reverse dosimetry examples (Chen et al. 2018a; Gilbert-Sandoval et al. 2020; Ning et al. 2019a). It shall be mentioned though that prior to QIVIVE, the *in vitro* endpoints adequately reflecting the expected *in vivo* toxicity, as well as the appropriateness of the *in vitro* model shall be carefully considered (Knudsen et al. 2015). The HepaRG cell line chosen here is a unique model for studying hepatotoxicity, cause it retains important liver features, like the expression of many metabolizing enzymes (Andersson et al. 2012). APAP exhibits this toxicity due to a highly reactive metabolite, NAPQI (Mutlib et al. 2006). Since the HepaRG cell model contains a metabolizing system, it is possible that the observed *in vitro* cytotoxicity, is at least partly due to the formation of NAPQI in the system. It is, however, acknowledged that this remains a hypothesis that needs to be verified with experimental data.

In conclusion, the results of this study suggest that generic PBK models with a basic pre-defined structure are a useful tool for simulating first tier toxicokinetics of chemicals, with minimum parameterization, stemming from *in vitro* and *in silico* sources, whereas the development of bespoke probabilistic PBK models for use in a thorough *in vitro/in silico*-based risk assessment could be justified only for high priority chemicals. Nevertheless, the amount of chemicals applied was limited, and hence, more substances shall be evaluated according to the format laid down in this manuscript.

Future research should focus on defining better the applicability domain of such models, and developing guidance criteria for their performance capacity. This could lead, for example, in the establishment of a QSAR algorithm that will define their prediction potential, based on substance' physicochemical and biological properties. For start, in a data-poor environment, a minimal PBK model may suffice as a first-tier tool to simulate mammalian toxicokinetics. Additional processes for any chemical of interest, like enterohepatic circulation or active-transport uptake mechanisms, may be added only when biologically plausible and experimental data allow their numeric identification. Generic PBK model testing may initially be based on the average kinetics, integrating inter-individual variability at a later stage.

Acknowledgements

The authors acknowledge Yvonne Staal, National Institute for Public Health and the Environment (RIVM), Bilthoven, The Netherlands, for the critical reading of the paper and valuable comments.

Funding

This work was supported by Cosmetics Europe as part of the Long Range Science Strategy programme and the European Chemical Industry Council.

Disclosures of interest

The authors report no conflicts of interest.

References

- Abdullah R, Alhusainy W, Woutersen J, Rietjens IM, Punt A. 2016. Predicting points of departure for risk assessment based on *in vitro* cytotoxicity data and physiologically based kinetic (pbk) modeling: The case of kidney toxicity induced by aristolochic acid i. *Food and chemical toxicology : an international journal published for the British Industrial Biological Research Association*. 92:104-116.
- Adam D, de Visser I, Koeppe P. 1982. Pharmacokinetics of amoxicillin and clavulanic acid administered alone and in combination. *Antimicrob Agents Chemother*. 22(3):353-357.
- Adler S, Basketter D, Creton S, Pelkonen O, van Benthem J, Zuang V, Andersen KE, Angers-Loustau A, Aptula A, Bal-Price A et al. 2011. Alternative (non-animal) methods for cosmetics testing: Current status and future prospects-2010. *Archives of toxicology*. 85(5):367-485.
- Albrecht W, Kappenberg F, Brecklinghaus T, Stoerber R, Marchan R, Zhang M, Ebbert K, Kirschner H, Grinberg M, Leist M et al. 2019. Prediction of human drug-induced liver injury (dili) in relation to oral doses and blood concentrations. *Archives of toxicology*. 93(6):1609-1637.
- Alexson SE, Diczfalusy M, Halldin M, Swedmark S. 2002. Involvement of liver carboxylesterases in the *in vitro* metabolism of lidocaine. *Drug metabolism and disposition: the biological fate of chemicals*. 30(6):643-647.
- Algharably EAH, Kreutz R, Gundert-Remy U. 2019. Importance of *in vitro* conditions for modeling the *in vivo* dose in humans by *in vitro-in vivo* extrapolation (ivive). *Archives of toxicology*. 93(3):615-621.
- Andersson TB, Kanebratt KP, Kenna JG. 2012. The heparg cell line: A unique *in vitro* tool for understanding drug metabolism and toxicology in human. *Expert Opin Drug Metab Toxicol*. 8(7):909-920.
- Arancibia A, Guttman J, González G, González C. 1980. Absorption and disposition kinetics of amoxicillin in normal human subjects. *Antimicrob Agents Chemother*. 17(2):199-202.
- Argikar UA, Remmel RP. 2009. Effect of aging on glucuronidation of valproic acid in human liver microsomes and the role of udp-glucuronosyltransferase ugt1a4, ugt1a8, and ugt1a10. *Drug metabolism and disposition: the biological fate of chemicals*. 37(1):229-236.
- Arnaud MJ. 2011. Pharmacokinetics and metabolism of natural methylxanthines in animal and man. *Handb Exp Pharmacol*. (200):33-91.
- Aubert N, Ameller T, Legrand JJ. 2012. Systemic exposure to parabens: Pharmacokinetics, tissue distribution, excretion balance and plasma metabolites of [14c]-methyl-, propyl- and butylparaben in rats after oral, topical or subcutaneous administration. *Food and chemical toxicology : an international journal published for the British Industrial Biological Research Association*. 50(3-4):445-454.
- Barter ZE, Bayliss MK, Beaune PH, Boobis AR, Carlile DJ, Edwards RJ, Houston JB, Lake BG, Lipscomb JC, Pelkonen OR et al. 2007. Scaling factors for the extrapolation of *in vivo* metabolic drug clearance from *in vitro* data: Reaching a consensus on values of human microsomal protein and hepatocellularity per gram of liver. *Curr Drug Metab*. 8(1):33-45.
- Bertault-Pères P, Maraninchi D, Carcassonne Y, Cano JP, Barbet J. 1985. Clinical pharmacokinetics of ciclosporin a in bone marrow transplantation patients. *Cancer Chemother Pharmacol*. 15(1):76-81.
- Bessems JG, Loizou G, Krishnan K, Clewell HJ, 3rd, Bernasconi C, Bois F, Coecke S, Collnot EM, Diembeck W, Farcial LR et al. 2014. Pbt modelling platforms and parameter estimation tools to enable animal-free risk assessment: Recommendations from a joint epaa--eurl ecvam adme workshop. *Regulatory toxicology and pharmacology : RTP*. 68(1):119-139.
- Blaauboer BJ. 2008. The contribution of *in vitro* toxicity data in hazard and risk assessment: Current limitations and future perspectives. *Toxicology letters*. 180(2):81-84.
- Bois FY, Jamei M, Clewell HJ. 2010. Pbpk modelling of inter-individual variability in the pharmacokinetics of environmental chemicals. *Toxicology*. 278(3):256-267.
- Bouvier d'Yvoire M, Prieto P, Blaauboer BJ, Bois FY, Boobis A, Brochot C, Coecke S, Freidig A, Gundert-Remy U, Hartung T et al. 2007. Physiologically-based kinetic modelling (pbk modelling): Meeting the 3rs agenda. The report and recommendations of ecvam workshop 63. *Altern Lab Anim*. 35(6):661-671.
- Breen M, Ring CL, Kreutz A, Goldsmith MR, Wambaugh JF. 2021. High-throughput pbt models for *in vitro* to *in vivo* extrapolation. *Expert Opin Drug Metab Toxicol*. 17(8):903-921.
- Buggey J, Kappus M, Lagoos AS, Brady CW. 2015. Amiodarone-induced liver injury and cirrhosis. *ACG Case Rep J*. 2(2):116-118.

- Bunchorntavakul C, Reddy KR. 2013. Acetaminophen-related hepatotoxicity. *Clin Liver Dis.* 17(4):587-607, viii.
- Campbell JL, Yoon M, Clewell HJ. 2015. A case study on quantitative *in vitro* to *in vivo* extrapolation for environmental esters: Methyl-, propyl- and butylparaben. *Toxicology.* 332:67-76.
- Carmichael PL, Baltazar MT, Cable S, Cochrane S, Dent M, Li H, Middleton A, Muller I, Reynolds G, Westmoreland C et al. 2022. Ready for regulatory use: Nams and ngra for chemical safety assurance. *Altex.*
- Chen L, Ning J, Louise J, Wesseling S, Rietjens I. 2018. Use of physiologically based kinetic modelling-facilitated reverse dosimetry to convert *in vitro* cytotoxicity data to predicted *in vivo* liver toxicity of lasiocarpine and riddelliine in rat. *Food and chemical toxicology : an international journal published for the British Industrial Biological Research Association.* 116(Pt B):216-226.
- Chen Y, Mao J, Hop CE. 2015. Physiologically based pharmacokinetic modeling to predict drug-drug interactions involving inhibitory metabolite: A case study of amiodarone. *Drug metabolism and disposition: the biological fate of chemicals.* 43(2):182-189.
- Conner TM, Nikolian VC, Georgoff PE, Pai MP, Alam HB, Sun D, Reed RC, Zhang T. 2018. Physiologically based pharmacokinetic modeling of disposition and drug-drug interactions for valproic acid and divalproex. *European journal of pharmaceutical sciences : official journal of the European Federation for Pharmaceutical Sciences.* 111:465-481.
- Dadashzadeh S, Tajerzaden H. 2001. Dose dependent pharmacokinetics of theophylline: Michaelis-menten parameters for its major metabolic pathways. *European journal of drug metabolism and pharmacokinetics.* 26(1-2):77-83.
- DeJongh J, Verhaar HJ, Hermens JL. 1997. A quantitative property-property relationship (qppr) approach to estimate *in vitro* tissue-blood partition coefficients of organic chemicals in rats and humans. *Archives of toxicology.* 72(1):17-25.
- Deng P, You T, Chen X, Yuan T, Huang H, Zhong D. 2011. Identification of amiodarone metabolites in human bile by ultraperformance liquid chromatography/quadrupole time-of-flight mass spectrometry. *Drug metabolism and disposition: the biological fate of chemicals.* 39(6):1058-1069.
- Dent M, Amaral RT, Da Silva PA, Ansell J, Boislevé F, Hatao M, Hirose A, Kasai Y, Kern P, Kreiling R et al. 2018. Principles underpinning the use of new methodologies in the risk assessment of cosmetic ingredients. *Computational Toxicology.* 7:20-26.
- Dent MP, Vaillancourt E, Thomas RS, Carmichael PL, Ouedraogo G, Kojima H, Barroso J, Ansell J, Barton-Maclaren TS, Bennekou SH et al. 2021. Paving the way for application of next generation risk assessment to safety decision-making for cosmetic ingredients. *Regulatory Toxicology and Pharmacology.* 125:105026.
- Edginton AN, Schmitt W, Willmann S. 2006. Development and evaluation of a generic physiologically based pharmacokinetic model for children. *Clinical pharmacokinetics.* 45(10):1013-1034.
- EFSA. 2017. Update: Guidance on the use of the benchmark dose approach in risk assessment. *Efsa journal* 2017;15(1):4658.
- Evans MV, Andersen ME. 2000. Sensitivity analysis of a physiological model for 2,3,7,8-tetrachlorodibenzo-p-dioxin (tcdd): Assessing the impact of specific model parameters on sequestration in liver and fat in the rat. *Toxicol Sci.* 54(1):71-80.
- FDA. 2010. *Fda report on lidocaine.*
- Fentem J, Malcomber I, Maxwell G, Westmoreland C. 2021. Upholding the eu's commitment to 'animal testing as a last resort' under reach requires a paradigm shift in how we assess chemical safety to close the gap between regulatory testing and modern safety science. *Alternatives to Laboratory Animals.* 49(4):122-132.
- Fragki S, Hoogenveen R, van Oostrom C, Schwillens P, Piersma AH, Zeilmaker MJ. 2022. Integrating *in vitro* chemical transplacental passage into a generic pbk model: A qivive approach. *Toxicology.* 465:153060.
- Fragki S, Piersma AH, Rorije E, Zeilmaker MJ. 2017. *In vitro* to *in vivo* extrapolation of effective dosimetry in developmental toxicity testing: Application of a generic pbk modelling approach. *Toxicol Appl Pharmacol.* 332:109-120.
- Gilbert-Sandoval I, Wesseling S, Rietjens I. 2020. Predicting the acute liver toxicity of aflatoxin bl in rats and humans by an *in vitro-in silico* testing strategy. *Mol Nutr Food Res.* 64(13):e2000063.
- Gouliarmou V, Lostia AM, Coecke S, Bernasconi C, Bessems J, Dorne JL, Ferguson S, Testai E, Remy UG, Brian Houston J et al. 2018. Establishing a systematic framework to characterise *in vitro* methods for human hepatic metabolic clearance. *Toxicol In vitro.* 53:233-244.

- Grillo JA, Venitz J, Ornato JP. 2001. Prediction of lidocaine tissue concentrations following different dose regimes during cardiac arrest using a physiologically based pharmacokinetic model. *Resuscitation*. 50(3):331-340.
- Haddad S, Restieri C, Krishnan K. 2001. Characterization of age-related changes in body weight and organ weights from birth to adolescence in humans. *J Toxicol Environ Health A*. 64(6):453-464.
- Hartung T, Blaauw BJ, Bosgra S, Carney E, Coenen J, Conolly RB, Corsini E, Green S, Faustman EM, Gaspari A et al. 2011. An expert consortium review of the ec-commissioned report "alternative (non-animal) methods for cosmetics testing: Current status and future prospects - 2010". *Altex*. 28(3):183-209.
- Ibarra M, Vázquez M, Fagiolino P, Derendorf H. 2013. Sex related differences on valproic acid pharmacokinetics after oral single dose. *J Pharmacokinetic Pharmacodyn*. 40(4):479-486.
- ICRP. 2002. Basic anatomical and physiological data for use in radiological protection: Reference values. A report of age- and gender-related differences in the anatomical and physiological characteristics of reference individuals. Icrp publication 89. *Ann ICRP*. 32(3-4):5-265.
- Jaeschke H, McGill MR, Williams CD, Ramachandran A. 2011. Current issues with acetaminophen hepatotoxicity - a clinically relevant model to test the efficacy of natural products. *Life Sci*. 88(17-18):737-745.
- Janer G, Slob W, Hakkert BC, Vermeire T, Piersma AH. 2008. A retrospective analysis of developmental toxicity studies in rat and rabbit: What is the added value of the rabbit as an additional test species? *Regulatory toxicology and pharmacology : RTP*. 50(2):206-217.
- Jawien W, Wilimowska J, Klys M, Piekoszewski W. 2017. Population pharmacokinetic modelling of valproic acid and its selected metabolites in acute vpa poisoning. *Pharmacological reports : PR*. 69(2):340-349.
- Johannessen CU, Johannessen SI. 2003. Valproate: Past, present, and future. *CNS Drug Rev*. 9(2):199-216.
- Jongeneelen FJ, Berge WF. 2011. A generic, cross-chemical predictive pbtk model with multiple entry routes running as application in ms excel; design of the model and comparison of predictions with experimental results. *The Annals of occupational hygiene*. 55(8):841-864.
- Jönsson L, Liu X, Jönsson BA, Ljungberg M, Strand SE. 2002. A dosimetry model for the small intestine incorporating intestinal wall activity and cross-doses. *J Nucl Med*. 43(12):1657-1664.
- Kamiya Y, Handa K, Miura T, Yanagi M, Shigeta K, Hina S, Shimizu M, Kitajima M, Shono F, Funatsu K et al. 2021. *In silico* prediction of input parameters for simplified physiologically based pharmacokinetic models for estimating plasma, liver, and kidney exposures in rats after oral doses of 246 disparate chemicals. *Chemical research in toxicology*. 34(2):507-513.
- Kamiya Y, Otsuka S, Miura T, Takaku H, Yamada R, Nakazato M, Nakamura H, Mizuno S, Shono F, Funatsu K et al. 2019. Plasma and hepatic concentrations of chemicals after virtual oral administrations extrapolated using rat plasma data and simple physiologically based pharmacokinetic models. *Chemical research in toxicology*. 32(1):211-218.
- Kamiya Y, Otsuka S, Miura T, Yoshizawa M, Nakano A, Iwasaki M, Kobayashi Y, Shimizu M, Kitajima M, Shono F et al. 2020. Physiologically based pharmacokinetic models predicting renal and hepatic concentrations of industrial chemicals after virtual oral doses in rats. *Chemical research in toxicology*. 33(7):1736-1751.
- Kannan R, Nademanee K, Hendrickson JA, Rostami HJ, Singh BN. 1982. Amiodarone kinetics after oral doses. *Clinical pharmacology and therapeutics*. 31(4):438-444.
- Kawai R, Mathew D, Tanaka C, Rowland M. 1998. Physiologically based pharmacokinetics of cyclosporine a: Extension to tissue distribution kinetics in rats and scale-up to human. *The Journal of pharmacology and experimental therapeutics*. 287(2):457-468.
- Klintmalm GB, Iwatsuki S, Starzl TE. 1981. Cyclosporin a hepatotoxicity in 66 renal allograft recipients. *Transplantation*. 32(6):488-489.
- Knudsen TB, Keller DA, Sander M, Carney EW, Doerr NG, Eaton DL, Fitzpatrick SC, Hastings KL, Mendrick DL, Tice RR et al. 2015. Futuretox ii: *In vitro* data and *in silico* models for predictive toxicology. *Toxicological sciences : an official journal of the Society of Toxicology*. 143(2):256-267.
- Kobayashi S, Takai K, Iga T, Hanano M. 1991. Pharmacokinetic analysis of the disposition of valproate in pregnant rats. *Drug metabolism and disposition: the biological fate of chemicals*. 19(5):972-976.
- Kramer N. 2010. Measuring, modeling, and increasing the free concentration of test chemicals in cell assays. Utrecht.
- Kramer NI, Di Consiglio E, Blaauw BJ, Testai E. 2015. Biokinetics in repeated-dosing *in vitro* drug toxicity studies. *Toxicol In vitro*. 30(1 Pt A):217-224.

- Kramer NI, Krismartina M, Rico-Rico A, Blaauboer BJ, Hermens JL. 2012. Quantifying processes determining the free concentration of phenanthrene in basal cytotoxicity assays. *Chemical research in toxicology*. 25(2):436-445.
- Levitt DG, Heymsfield SB, Pierson RN, Jr., Shapses SA, Kral JG. 2007. Physiological models of body composition and human obesity. *Nutr Metab (Lond)*. 4:19.
- Li M, Gehring R, Riviere JE, Lin Z. 2017. Development and application of a population physiologically based pharmacokinetic model for penicillin g in swine and cattle for food safety assessment. *Food and Chemical Toxicology*. 107:74-87.
- Louisse J, Alewijn M, Peijnenburg A, Cnubben NHP, Heringa MB, Coecke S, Punt A. 2020. Towards harmonization of test methods for *in vitro* hepatic clearance studies. *Toxicol In vitro*. 63:104722.
- Louisse J, Beekmann K, Rietjens IM. 2017. Use of physiologically based kinetic modeling-based reverse dosimetry to predict *in vivo* toxicity from *in vitro* data. *Chemical research in toxicology*. 30(1):114-125.
- Lu J, Goldsmith MR, Grulke CM, Chang DT, Brooks RD, Leonard JA, Phillips MB, Hypes ED, Fair MJ, Tornero-Velez R et al. 2016a. Developing a physiologically-based pharmacokinetic model knowledgebase in support of provisional model construction. *PLoS Comput Biol*. 12(2):e1004495.
- Lu JT, Cai Y, Chen F, Jia WW, Hu ZY, Zhao YS. 2016b. A physiologically based pharmacokinetic model of amiodarone and its metabolite desethylamiodarone in rats: Pooled analysis of published data. *European journal of drug metabolism and pharmacokinetics*. 41(6):689-703.
- Mutlib AE, Goosen TC, Bauman JN, Williams JA, Kulkarni S, Kostrubsky S. 2006. Kinetics of acetaminophen glucuronidation by udp-glucuronosyltransferases 1a1, 1a6, 1a9 and 2b15. Potential implications in acetaminophen-induced hepatotoxicity. *Chemical research in toxicology*. 19(5):701-709.
- Ning J, Chen L, Rietjens I. 2019. Role of toxicokinetics and alternative testing strategies in pyrrolizidine alkaloid toxicity and risk assessment; state-of-the-art and future perspectives. *Food and chemical toxicology : an international journal published for the British Industrial Biological Research Association*. 131:110572.
- OECD. 2021. Guidance document on the characterisation, validation and reporting of physiologically based kinetic (pbk) models for regulatory purposes, oecd series on testing and assessment, no. 331, environment, health and safety, environment directorate, oecd.
- Paini A, Leonard JA, Joossens E, Bessems JGM, Desalegn A, Dorne JL, Gosling JP, Heringa MB, Klaric M, Kliment T et al. 2019. Next generation physiologically based kinetic (ng-pbk) models in support of regulatory decision making. *Comput Toxicol*. 9:61-72.
- Paini A, Tan YM, Sachana M, Worth A. 2021. Gaining acceptance in next generation pbk modelling approaches for regulatory assessments - an oecd international effort. *Comput Toxicol*. 18:100163.
- Pang KS, Han YR, Noh K, Lee PI, Rowland M. 2019. Hepatic clearance concepts and misconceptions: Why the well-stirred model is still used even though it is not physiologic reality? *Biochem Pharmacol*. 169:113596.
- Pearce RG, Setzer RW, Strobe CL, Wambaugh JF, Sipes NS. 2017. Httk: R package for high-throughput toxicokinetics. *J Stat Softw*. 79(4):1-26.
- Pendse SN, Efrementko A, Hack CE, Moreau M, Mallick P, Dzierlenga M, Nicolas CI, Yoon M, Clewell HJ, McMullen PD. 2020. Population life-course exposure to health effects model (plethem): An r package for pbpk modeling. *Computational Toxicology*. 13:100115.
- Pery AR, Brochot C, Zeman FA, Mombelli E, Desmots S, Pavan M, Fioravanzo E, Zaldivar JM. 2013. Prediction of dose-hepatotoxic response in humans based on toxicokinetic/toxicodynamic modeling with or without *in vivo* data: A case study with acetaminophen. *Toxicology letters*. 220(1):26-34.
- Peyret T, Krishnan K. 2011. Qsars for pbpk modelling of environmental contaminants. *SAR QSAR Environ Res*. 22(1-2):129-169.
- Peyret T, Poulin P, Krishnan K. 2010. A unified algorithm for predicting partition coefficients for pbpk modeling of drugs and environmental chemicals. *Toxicol Appl Pharmacol*. 249(3):197-207.
- Pichard L, Domergue J, Fourtanier G, Koch P, Schran HF, Maurel P. 1996. Metabolism of the new immunosuppressor cyclosporin g by human liver cytochromes p450. *Biochem Pharmacol*. 51(5):591-598.
- Pletz J, Blakeman S, Paini A, Parissis N, Worth A, Andersson AM, Frederiksen H, Sakhi AK, Thomsen C, Bopp SK. 2020. Physiologically based kinetic (pbk) modelling and human biomonitoring data for mixture risk assessment. *Environ Int*. 143:105978.

- Plomp TA, Wiersinga WM, Maes RA. 1985. Tissue distribution of amiodarone and desethylamiodarone in rats after repeated oral administration of various amiodarone dosages. *Arzneimittelforschung*. 35(12):1805-1810.
- Punt A, Louisse J, Pinckaers N, Fabian E, van Ravenzwaay B. 2021a. Predictive performance of next generation physiologically based kinetic (pbk) model predictions in rats based on *in vitro* and *in silico* input data. *Toxicological Sciences*. 186(1):18-28.
- Punt A, Louisse J, Pinckaers N, Fabian E, van Ravenzwaay B. 2022. Predictive performance of next generation physiologically based kinetic (pbk) model predictions in rats based on *in vitro* and *in silico* input data. *Toxicol Sci*. 186(1):18-28.
- Punt A, Pinckaers N, Peijnenburg A, Louisse J. 2021b. Development of a web-based toolbox to support quantitative in-vitro-to-in-vivo extrapolations (qivive) within nonanimal testing strategies. *Chemical research in toxicology*. 34(2):460-472.
- Punt A, Schiffelers MJ, Jean Horbach G, van de Sandt JJ, Groothuis GM, Rietjens IM, Blaauboer BJ. 2011. Evaluation of research activities and research needs to increase the impact and applicability of alternative testing strategies in risk assessment practice. *Regulatory toxicology and pharmacology : RTP*. 61(1):105-114.
- Ramsey JC, Andersen ME. 1984. A physiologically based description of the inhalation pharmacokinetics of styrene in rats and humans. *Toxicol Appl Pharmacol*. 73(1):159-175.
- Roberts MS, Rowland M. 1986. A dispersion model of hepatic elimination: 3. Application to metabolite formation and elimination kinetics. *Journal of pharmacokinetics and biopharmaceutics*. 14(3):289-308.
- Rodgers T, Leahy D, Rowland M. 2005. Physiologically based pharmacokinetic modeling 1: Predicting the tissue distribution of moderate-to-strong bases. *J Pharm Sci*. 94(6):1259-1276.
- Rodgers T, Rowland M. 2006. Physiologically based pharmacokinetic modelling 2: Predicting the tissue distribution of acids, very weak bases, neutrals and zwitterions. *J Pharm Sci*. 95(6):1238-1257.
- Rodgers T, Rowland M. 2007. Mechanistic approaches to volume of distribution predictions: Understanding the processes. *Pharm Res*. 24(5):918-933.
- Rowland M, Benet LZ, Graham GG. 1973. Clearance concepts in pharmacokinetics. *Journal of pharmacokinetics and biopharmaceutics*. 1(2):123-136.
- Sandborgh-Englund G, Adolfsson-Erici M, Odham G, Ekstrand J. 2006. Pharmacokinetics of triclosan following oral ingestion in humans. *Journal of Toxicology and Environmental Health, Part A*. 69(20):1861-1873.
- Sayre RR, Wambaugh JF, Grulke CM. 2020. Database of pharmacokinetic time-series data and parameters for 144 environmental chemicals. *Scientific Data*. 7(1):122.
- Schmitt W. 2008. General approach for the calculation of tissue to plasma partition coefficients. *Toxicology in vitro*. 22(2):457-467.
- Schwartz GJ, Brion LP, Spitzer A. 1987. The use of plasma creatinine concentration for estimating glomerular filtration rate in infants, children, and adolescents. *Pediatr Clin North Am*. 34(3):571-590.
- Schwinghammer TL, Przepiorka D, Venkataramanan R, Wang CP, Burckart GJ, Rosenfeld CS, Shaddock RK. 1991. The kinetics of cyclosporine and its metabolites in bone marrow transplant patients. *British journal of clinical pharmacology*. 32(3):323-328.
- Shebley M, Sandhu P, Emami Riedmaier A, Jamei M, Narayanan R, Patel A, Peters SA, Reddy VP, Zheng M, de Zwart L et al. 2018. Physiologically based pharmacokinetic model qualification and reporting procedures for regulatory submissions: A consortium perspective. *Clinical pharmacology and therapeutics*. 104(1):88-110.
- Slob W. 2002. Dose-response modeling of continuous endpoints. *Toxicological Sciences*. 66(2):298-312.
- Sodhi JK, Wang HJ, Benet LZ. 2020. Are there any experimental perfusion data that preferentially support the dispersion and parallel-tube models over the well-stirred model of organ elimination? *Drug metabolism and disposition: the biological fate of chemicals*. 48(7):537-543.
- Szultka M, Krzeminski R, Jackowski M, Buszewski B. 2014. Identification of *in vitro* metabolites of amoxicillin in human liver microsomes by lc-esi/ms. *Chromatographia*. 77(15):1027-1035.
- Tebby C, van der Voet H, de Sousa G, Rorije E, Kumar V, de Boer W, Kruiesselbrink JW, Bois FY, Faniband M, Moretto A et al. 2020. A generic pbtk model implemented in the mcra platform: Predictive performance and uses in risk assessment of chemicals. *Food Chem Toxicol*. 142:111440.
- Thelen K, Coboeken K, Willmann S, Burghaus R, Dressman JB, Lippert J. 2011. Evolution of a detailed physiological model to simulate the gastrointestinal transit and absorption process in humans, part 1: Oral solutions. *J Pharm Sci*. 100(12):5324-5345.

- Thelen K, Coboeken K, Willmann S, Dressman JB, Lippert J. 2012. Evolution of a detailed physiological model to simulate the gastrointestinal transit and absorption process in humans, part ii: Extension to describe performance of solid dosage forms. *J Pharm Sci.* 101(3):1267-1280.
- Trivier JM, Libersa C, Belloc C, Lhermitte M. 1993. Amiodarone n-deethylation in human liver microsomes: Involvement of cytochrome p450 3a enzymes (first report). *Life Sci.* 52(10):PL91-96.
- van der Voet H, Kruisselbrink JW, de Boer WJ, van Lenthe MS, van den Heuvel J, Crépet A, Kennedy MC, Zilliacus J, Beronius A, Tebby C et al. 2020. The mcra toolbox of models and data to support chemical mixture risk assessment. *Food and chemical toxicology : an international journal published for the British Industrial Biological Research Association.* 138:111185.
- Volak LP, Hanley MJ, Masse G, Hazarika S, Harmatz JS, Badmaev V, Majeed M, Greenblatt DJ, Court MH. 2013. Effect of a herbal extract containing curcumin and piperine on midazolam, flurbiprofen and paracetamol (acetaminophen) pharmacokinetics in healthy volunteers. *British journal of clinical pharmacology.* 75(2):450-462.
- Wambaugh JF, Hughes MF, Ring CL, MacMillan DK, Ford J, Fennell TR, Black SR, Snyder RW, Sipes NS, Wetmore BA et al. 2018. Evaluating *in vitro-in vivo* extrapolation of toxicokinetics. *Toxicological sciences : an official journal of the Society of Toxicology.* 163(1):152-169.
- Wambaugh JF, Wetmore BA, Pearce R, Strobe C, Goldsmith R, Sluka JP, Sedykh A, Tropsha A, Bosgra S, Shah I et al. 2015. Toxicokinetic triage for environmental chemicals. *Toxicological sciences : an official journal of the Society of Toxicology.* 147(1):55-67.
- Wang L, Mao B, He H, Shang Y, Zhong Y, Yu Z, Yang Y, Li H, An J. 2019. Comparison of hepatotoxicity and mechanisms induced by triclosan (tcs) and methyl-triclosan (mtcs) in human liver hepatocellular hepg2 cells. *Toxicol Res (Camb).* 8(1):38-45.
- WHO. 2010. World health organization. International programme on chemical safety. Characterization and application of physiologically based pharmacokinetic models in risk assessment. Harmonization project document no. 9
- Willmann S, Schmitt W, Keldenich J, Lippert J, Dressman JB. 2004. A physiological model for the estimation of the fraction dose absorbed in humans. *J Med Chem.* 47(16):4022-4031.
- Wilson JP. 1967. Surface area of the small intestine in man. *Gut.* 8(6):618-621.
- Yang R. 2011. The application of physiologically based pharmacokinetic (pbpk) modeling to risk assessment.
- Yoon M, Campbell JL, Andersen ME, Clewell HJ. 2012. Quantitative *in vitro* to *in vivo* extrapolation of cell-based toxicity assay results. *Critical reviews in toxicology.* 42(8):633-652.
- Yoon M, Nong A, Clewell HJ, 3rd, Taylor MD, Dorman DC, Andersen ME. 2009. Evaluating placental transfer and tissue concentrations of manganese in the pregnant rat and fetuses after inhalation exposures with a pbpk model. *Toxicol Sci.* 112(1):44-58.
- Yun YE, Edginton AN. 2013. Correlation-based prediction of tissue-to-plasma partition coefficients using readily available input parameters. *Xenobiotica.* 43(10):839-852.
- Zandvliet AS, Huitema AD, de Jonge ME, den Hoed R, Sparidans RW, Hendriks VM, van den Brink W, van Ree JM, Beijnen JH. 2005. Population pharmacokinetics of caffeine and its metabolites theobromine, paraxanthine and theophylline after inhalation in combination with diacetylmorphine. *Basic Clin Pharmacol Toxicol.* 96(1):71-79.

Supplementary Material

SM1. TNO Model description

SM 1.1 Non-eliminating tissues

In all non-eliminating tissues (adipose, bone, brain, muscle, pancreas, spleen, kidney and remaining) the mass-balance is perfusion limited:

$$\frac{dA_{\text{tissue}}}{dt} = Q_{\text{tissue}} \times C_{\text{arterial}} - Q_{\text{tissue}} \times \frac{C_{\text{tissue}}}{P_{\text{tissue:blood}}}$$

Here, A_{tissue} is the amount in the tissue, Q_{tissue} is the blood flow to the tissue, C_{arterial} is the arterial blood concentration, C_{tissue} is the tissue concentration and $P_{\text{tissue:blood}}$ is the tissue to blood partition coefficient.

SM 1.2 GI-tract

The GI tract is based on the model as presented by Thelen et al. (2011), in which the small intestine is divided into one duodenum compartment, three jejunum compartments and three ileum compartments. In addition, we distinguish between the luminal part of the organ and the actual tissue. As a result, we have $A_{\text{sto,lumen}}$ and A_{sto} to represent the amount in stomach lumen and stomach tissue, respectively, $A_{\text{duo,lumen}}$ and A_{duo} to represent the amount in duodenal lumen and duodenal tissue, respectively, $A_{\text{jej,lumen}}$ (compartments 1 to 3) and A_{jej} (compartments 1 to 3) to represent the amount in jejunal lumen and jejunal tissue, respectively, $A_{\text{il,lumen}}$ (compartments 1 to 3) and A_{il} (compartments 1 to 3) to represent the amount in ileal lumen and ileal tissue, respectively and $A_{\text{col,lumen}}$ and A_{col} to represent the amount in colon lumen and colon tissue, respectively.

$$\begin{aligned} \frac{dA_{\text{sto,lumen}}}{dt} &= -K_{\text{sto_duo}} \times A_{\text{sto,lumen}} \\ \frac{dA_{\text{duo,lumen}}}{dt} &= K_{\text{sto_duo}} \times A_{\text{sto,lumen}} - K_{\text{duo_jej1}} \times A_{\text{duo,lumen}} - CL_{\text{abs,duo}} \times A_{\text{duo,lumen}} \\ \frac{dA_{\text{jej1,lumen}}}{dt} &= K_{\text{duo_jej1}} \times A_{\text{duo,lumen}} - K_{\text{jej1_jej2}} \times A_{\text{jej1,lumen}} - CL_{\text{abs,jej1}} \times A_{\text{jej1,lumen}} \\ \frac{dA_{\text{jej2,lumen}}}{dt} &= K_{\text{jej1_jej2}} \times A_{\text{jej1,lumen}} - K_{\text{jej2_jej3}} \times A_{\text{jej2,lumen}} - CL_{\text{abs,jej2}} \times A_{\text{jej2,lumen}} \\ \frac{dA_{\text{jej3,lumen}}}{dt} &= K_{\text{jej2_jej3}} \times A_{\text{jej2,lumen}} - K_{\text{jej3_il1}} \times A_{\text{jej3,lumen}} - CL_{\text{abs,jej3}} \times A_{\text{jej3,lumen}} \\ \frac{dA_{\text{il1,lumen}}}{dt} &= K_{\text{jej3_il1}} \times A_{\text{jej3,lumen}} - K_{\text{il1_il2}} \times A_{\text{il1,lumen}} - CL_{\text{abs,il1}} \times A_{\text{il1,lumen}} \\ \frac{dA_{\text{il2,lumen}}}{dt} &= K_{\text{il1_il2}} \times A_{\text{il1,lumen}} - K_{\text{il2_il3}} \times A_{\text{il2,lumen}} - CL_{\text{abs,il2}} \times A_{\text{il2,lumen}} \end{aligned}$$

$$\frac{dA_{il3,lumen}}{dt} = K_{il2_il3} \times A_{il2,lumen} - K_{il3_col} \times A_{il3,lumen} - CL_{abs,il3} \times A_{il3,lumen}$$

$$\frac{dA_{col,lumen}}{dt} = K_{il3_col} \times A_{il3,lumen} - K_{col_out} \times A_{col,lumen} - CL_{abs,col} \times A_{col,lumen}$$

Here, $K_{tissue1,tissue2}$ is the transfer rate of mass from one luminal compartment to the next and $CL_{abs,tissue}$ is the absorption clearance from the luminal compartment. The absorption clearance is calculated based on the *in vitro* apparent permeability (Papp), multiplied with the effective luminal surface area (taking into account the presence of macro- and microvilli, as presented by Wilson (1967)). After absorption, the compound distributes into the different GI tissues connected to the systemic circulation.

$$\frac{dA_{sto}}{dt} = Q_{sto} \times C_{arterial} - Q_{sto} \times \frac{C_{sto}}{P_{stomach:blood}}$$

$$\frac{dA_{duo}}{dt} = CL_{abs,duo} \times A_{duo,lumen} + Q_{duo} \times C_{arterial} - Q_{duo} \times \frac{C_{duo}}{P_{small\ intestine:blood}}$$

$$\frac{dA_{jej1}}{dt} = CL_{abs,jej1} \times A_{jej1,lumen} + Q_{jej1} \times C_{arterial} - Q_{jej1} \times \frac{C_{jej1}}{P_{small\ intestine:blood}}$$

$$\frac{dA_{jej2}}{dt} = CL_{abs,jej2} \times A_{jej2,lumen} + Q_{jej2} \times C_{arterial} - Q_{jej2} \times \frac{C_{jej2}}{P_{small\ intestine:blood}}$$

$$\frac{dA_{jej3}}{dt} = CL_{abs,jej3} \times A_{jej3,lumen} + Q_{jej3} \times C_{arterial} - Q_{jej3} \times \frac{C_{jej3}}{P_{small\ intestine:blood}}$$

$$\frac{dA_{il1}}{dt} = CL_{abs,il1} \times A_{il1,lumen} + Q_{il1} \times C_{arterial} - Q_{il1} \times \frac{C_{il1}}{P_{small\ intestine:blood}}$$

$$\frac{dA_{il2}}{dt} = CL_{abs,il2} \times A_{il2,lumen} + Q_{il2} \times C_{arterial} - Q_{il2} \times \frac{C_{il2}}{P_{small\ intestine:blood}}$$

$$\frac{dA_{il3}}{dt} = CL_{abs,il3} \times A_{il3,lumen} + Q_{il3} \times C_{arterial} - Q_{il3} \times \frac{C_{il3}}{P_{small\ intestine:blood}}$$

$$\frac{dA_{col}}{dt} = CL_{abs,col} \times A_{col,lumen} + Q_{col} \times C_{arterial} - Q_{col} \times \frac{C_{col}}{P_{large\ intestine:blood}}$$

SM1.3 Liver

The majority of the liver's blood supply comes from the portal vein, which contains venous blood from the intestinal compartments and the spleen and pancreas. Metabolic clearance in the liver is represented by Michaelis-Menten kinetics with a maximum rate (V_{max}) and Michaelis-Menten constant (K_m).

$$\begin{aligned}
 \frac{dA_{liver}}{dt} = & Q_{liver} \times C_{arterial} + Q_{sto} \times \frac{C_{sto}}{P_{stomach: blood}} + Q_{duo} \times \frac{C_{duo}}{P_{small\ intestine: blood}} \\
 & + Q_{jej1} \times \frac{C_{jej1}}{P_{small\ intestine: blood}} + Q_{jej2} \times \frac{C_{jej2}}{P_{small\ intestine: blood}} + Q_{jej3} \times \frac{C_{jej3}}{P_{small\ intestine: blood}} \\
 & + Q_{il1} \times \frac{C_{il1}}{P_{small\ intestine: blood}} + Q_{il2} \times \frac{C_{il2}}{P_{small\ intestine: blood}} + Q_{il3} \times \frac{C_{il3}}{P_{small\ intestine: blood}} \\
 & + Q_{col} \times \frac{C_{col}}{P_{large\ intestine: blood}} + Q_{pancreas} \times \frac{C_{pancreas}}{P_{pancreas: blood}} + Q_{spleen} \times \frac{C_{spleen}}{P_{spleen: blood}} \\
 & - Q_{liver, total} \times \frac{C_{liver}}{P_{liver: blood}} - \frac{V_{max} \times C_{liv}}{K_m + C_{liv}}
 \end{aligned}$$

Here, A_{liver} is the amount in liver tissue, Q_{tissue} is the blood flow to the tissue, $Q_{liver, total}$ is the sum of blood flows entering the liver, $C_{arterial}$ is the arterial blood concentration, C_{tissue} is the tissue concentration and $P_{tissue: blood}$ is the tissue to blood partition coefficient.

SM1.4 Blood

The removal of compounds from arterial blood is based on the glomerular filtration rate (GFR), the fraction unbound in plasma ($f_{unbound, plasma}$) and the blood-to-plasma partition coefficient ($P_{blood: plasma}$)

$$\begin{aligned}
 \frac{dA_{arterial}}{dt} = & Q_c \times C_{lung, blood} - Q_c \times C_{arterial} - GFR \times \frac{C_{arterial} \times f_{unbound, plasma}}{P_{blood: plasma}} \\
 \frac{dA_{venous}}{dt} = & Q_{adipose} \times \frac{C_{adipose}}{P_{adipose: plasma}} + Q_{bone} \times \frac{C_{bone}}{P_{bone: plasma}} + Q_{brain} \times \frac{C_{brain}}{P_{brain: plasma}} \\
 & + Q_{muscle} \times \frac{C_{muscle}}{P_{muscle: plasma}} + Q_{skin} \times \frac{C_{skin}}{P_{skin: plasma}} + Q_{liver, total} \times \frac{C_{liver}}{P_{liver: plasma}} \\
 & + Q_{kidney} \times \frac{C_{kidney}}{P_{kidney: plasma}} + Q_{remaining} \times \frac{C_{remaining}}{P_{remaining: plasma}} - Q_c \times C_{venous}
 \end{aligned}$$

Here, $A_{arterial}$ and A_{venous} are the amounts in arterial and venous blood, respectively, Q_c is the cardiac output, Q_{tissue} is the blood flow to the tissue, $C_{arterial}$ is the arterial blood concentration, C_{venous} is the venous blood concentration, C_{tissue} is the tissue concentration and $P_{tissue: blood}$ is the tissue to blood partition coefficient.

SM1.5 Partitioning to the organs

The TNO Model has implemented the Peyret QSAR (Peyret et al. 2010), for environmental chemicals and pharmaceuticals, which takes into consideration the role of more tissue components other than lipid and water. This unified algorithm is based on the principle that the concentration of a chemical in a 'biological matrix' is equal to the sum of its concentration in all respective compartments of the matrix:

$$P_{tb} = \frac{P_{ct} \times F_{ct} + P_{it} \times F_{it}}{P_p \times F_p + P_e \times F_e} \quad (1)$$

where P_{tb} = tissue: blood partition coefficient (PC), P_{ct} = cell tissue: water PC, F_{ct} = fractional content of cells in tissue, P_{it} = interstitial fluid: water PC, F_{it} = fractional content of interstitial fluid in tissue, P_p = plasma: water PC, P_e = erythrocyte:water PC, F_e = fractional content of erythrocytes in blood.

Each matrix (cell tissue, interstitial fluid, plasma, erythrocytes) consists of water, neutral lipids, phospholipids (neutral and charged) and proteins, with ionizable substances existing in an equilibrium between the ionized and non-ionized species.

Each matrix:water partition coefficient of Eq. (1) (i.e. P_{ct} , P_{it} , P_e and P_p) can be computed as follows:

$$P_{mw} = \frac{(1 + I_m) \times F_{wm} + P_{ow} \times F_{nlm} + I_m \times P_{aplw} \times F_{apl m} + (1 + I_m) \times P_{prw} \times F_{prm}}{1 + I_w} \quad (2)$$

where P_{mw} : matrix:water partition coefficient; I_m : ionization term for the aqueous phase of the matrix m; F_{wm} : fractional volume of water equivalent in the matrix; P_{ow} : vegetable oil:water partition coefficient or n-octanol:water partition coefficient; F_{nlm} : fractional volume of neutral lipids equivalent in the matrix; P_{aplw} : acidic phospholipids:water partition coefficient; $F_{apl m}$: fractional volume of acidic phospholipids in the matrix; P_{prw} : protein:water PC; F_{prm} : fractional volume of binding proteins in the matrix; I_w : ionization term for water.

In Eq. (2), the term F_{wm} equals the sum of the fractional volume of water plus 70% of the content of neutral phospholipids, whereas the term F_{nlm} corresponds to the fractional volume of neutral lipids plus 30% of the content of neutral phospholipids (Poulin and Krishnan 1995a; 1995b). The ionization term of the matrix I_m was calculated using the Henderson–Hasselbach equation as follows (Rodgers and Rowland 2007):

$$I_m = 0 \text{ for neutrals}$$

$$I_m = 10^{pKa - pH} \text{ for monoprotic bases}$$

$$I_m = 10^{pH - pKa} \text{ for monoprotic acids}$$

$$I_m = 10^{pKa2 - pH} + 10^{pKa1 + pKa2 - 2pH} \text{ for diprotic bases}$$

$$I_m = 10^{pH - pKa1} + 10^{2pH - pKa1 - pKa2} \text{ for diprotic acids}$$

$$I_m = 10^{pKabase - pH} + 10^{pH - pKaacid} \text{ for zwitterions}$$

The implementation of these equations in the TNO model is presented below:

$$P_{prw} = (1/f_{up} - 1 - (10^{\log P}) * NL_p / (1 + \text{ionization.p})) / P_p$$

$$P_{plw} = (((P_{bp} - F_p) / (f_{up} * Fe)) - ((1 + \text{ionization.e}) * W_e + (10^{\log P}) * NL_e) / (1 + \text{ionization.p})) * ((1 + \text{ionization.p}) / (\text{ionization.e} * APL_e))$$

$$P_{ct} = (((1 + \text{ionization.ct}) * (W_{ct} + 0.7 * NPL_{ct}) + ((10^{\log P}) * (NL_{ct} + 0.3 * NPL_{ct})) + (\text{ionization.ct} * P_{plw} * APL_{ct})) / (1 + \text{ionization.w}))$$

$$P_{it} = (((1 + \text{ionization.it}) * (W_{it} + 0.7 * NPL_{it}) + ((10^{\log P}) * (NL_{it} + 0.3 * NPL_{it})) + ((1 + \text{ionization.it}) * P_{prw} * P_{it})) / (1 + \text{ionization.w}))$$

$$P_e = (((1 + \text{ionization.e}) * (W_e + 0.7 * NPL_e) + ((10^{\log P}) * (NL_e + 0.3 * NPL_e)) + (\text{ionization.e} * P_{plw} * APL_e)) / (1 + \text{ionization.w}))$$

$$P_p = (((1 + \text{ionization.p}) * (W_p + 0.7 * NPL_p) + ((10^{\log P}) * (NL_p + 0.3 * NPL_p)) + ((1 + \text{ionization.p}) * P_{prw} * P_p)) / (1 + \text{ionization.w}))$$

SM 2 Input parameters for IndusChemFate and the TNO Model

IndusChemFate		
Input Parameters	Value	Data source
Substance: Amoxicillin (AMOX)		
Fraction absorbed from the GI tract	default: 1	-
Density (mg/cm ³ or g/L)	1540	ChemSketch v.11 ¹
Molecular weight	365.4	PubChem
Vapour pressure (Pa) ²	1.7732E-11	⁵ EPI Suite™
Log(Kow) at skin pH 5.5 ³	-2	-EPI Suite™, MarvinSketch ⁶
Log(Kow) at blood pH 7.4 ³	-2	
Water solubility (mg/L) ⁴	4000	EPI Suite™
Resorption tubuli	default: ?	-
Enterohepatic removal (relative to liver venous blood)	default: 0	-
Vmax Liver (umol/kg tissue/h)	250	Calibrated
Km Liver (umol/L)	5	Calibrated
Substance: Lidocaine (LID)		
Absorption rate into intestinal tissue (l/h)	default: 3	-
Density (mg/cm ³ or g/L)	1026	ChemSketch v.11 ¹
Molecular weight	234.3	PubChem
Vapour pressure (Pa) ²	0.0023065	⁵ EPI Suite™
Log(Kow) at skin pH 5.5 ³	0.19	-EPI Suite™, MarvinSketch ⁶
Log(Kow) at blood pH 7.4 ³	1.93	
Water solubility (mg/L) ⁴	4100	EPI Suite™
Resorption tubuli	default: ?	-
Enterohepatic removal (relative to liver venous blood)	default: 0	-
Vmax Liver (umol/kg tissue/h)	1000	Calculation based on CLint
Km Liver (umol/L)	21.7	(Louisse et al. 2020a)
Substance: Caffeine (CAF)		
Absorption rate into intestinal tissue (l/h)	default: 3	-
Density (mg/cm ³ or g/L)	1450	ChemSketch v.11 ¹
Molecular weight	194.191	PubChem
Vapour pressure (Pa) ²	9.77E-07	⁵ EPI Suite™
Log(Kow) at skin pH 5.5 ³	-0.07	-EPI Suite™, MarvinSketch ⁶
Log(Kow) at blood pH 7.4 ³	-0.07	
Water solubility (mg/L) ⁴	21600	EPI Suite™
Resorption tubuli	default: ?	-
Enterohepatic removal (relative to liver venous blood)	default: 0	-
Vmax Liver (umol/kg tissue/h)	1239	Calculation based on CLint
Km Liver (umol/L)	245	(Louisse et al. 2020a)
Substance: Theophylline (THEO)		
Absorption rate into intestinal tissue (l/h)	default: 3	NR
Density (mg/cm ³ or g/L)	1465	ChemSketch v.11 ¹
Molecular weight	180.167	PubChem
Vapour pressure (Pa) ²	1.51E-09	⁵ EPI Suite™
Log(Kow) at skin pH 5.5 ³	-0.02	-EPI Suite™, MarvinSketch ⁶
Log(Kow) at blood pH 7.4 ³	-0.16	
Water solubility (mg/L) ⁴	7360	EPI Suite™
Resorption tubuli	default: ?	-
Enterohepatic removal (relative to liver venous blood)	default: 0	-
Vmax Liver (umol/kg tissue/h)	54	Calculation based on CLint
Km Liver (umol/L)	7.5	(Sohlenius-Sternbeck et al. 2012)
Substance: Acetaminophen (APAP)		
Absorption rate into intestinal tissue (l/h)	default	-
Density (mg/cm ³ or g/L)	1249	ChemSketch v.11 ¹
Molecular weight	151.2	PubChem
Vapour Pressure (Pa)	0.000259	⁵ EPI Suite™
Log(Kow) at skin pH 5.5	0.46	-EPI Suite™, MarvinSketch ⁶
Log(Kow) at blood pH 7.4	0.46	

TNO Model		
Input Parameters	Value	Data source
Molecular weight	365.4	PubChem
logP ³	0.87	EPI Suite™
Fraction unbound in plasma	0.8	CompTox Chemicals Dashboard ⁷
Blood:plasma partition coefficient	default:1	-
Ionization	zwitterion	MarvinSketch
pKa1	3.23	MarvinSketch
pKa2	7.22	MarvinSketch
Papp>(*10E-6 cm/s)	1.63	Alsenz and Haenel (2003)
Vapour pressure (mmHg)	1.3E-13	EPI Suite™
Vmax (nmol/min/g liver)	4.18	Calibrated
Km (mg/L)	5.48	Calibrated
Molecular weight	234.3	PubChem
logP ³	2.44	EPI Suite™
Fraction unbound in plasma	0.2	Poulin and Theil (2002)
Blood:plasma partition coefficient	default: 1	-
Ionization	zwitterion	MarvinSketch
pKa1	13.78	MarvinSketch
pKa2	7.75	MarvinSketch
Papp>(*10E-6 cm/s)	61.7	
Vapour pressure (mmHg)	0.0000173	EPI Suite™
Vmax (nmol/min/g liver)	16.67	Calculation based on CLint
Km (mg/L)	5	(Louisse et al. 2020a)
Molecular weight	194.191	PubChem
logP ³	-0.07	EPI Suite™
Fraction unbound in plasma	0.64	drugbank ⁸
Blood:plasma partition coefficient	default:1	-
Ionization	monoprotic base	MarvinSketch
pKa1	-1.16	MarvinSketch
pKa2	-	MarvinSketch
Papp>(*10E-6 cm/s)	81.1	Matsuzaki et al. (2019)
Vapour pressure (mmHg)	7.33E-09	EPI Suite™
Vmax (nmol/min/g liver)	20.65	Calculation based on CLint
Km (mg/L)	48	(Louisse et al. 2020a)
Molecular weight	180.167	PubChem
logP ³	-0.02	EPI Suite™
Fraction unbound in plasma	0.6	drugbank
Blood:plasma partition coefficient	default:1	-
Ionization	zwitterion	MarvinSketch
pKa1	7.82	MarvinSketch
pKa2	-0.78	MarvinSketch
Papp>(*10E-6 cm/s)	65.1	Matsuzaki et al. (2019)
Vapour pressure (mmHg)	1.13E-11	EPI Suite™
Vmax (nmol/min/g liver)	0.9	Calculation based on CLint
Km (mg/L)	1.4	(Sohlenius-Sternbeck et al. 2012)
Molecular weight	151.2	PubChem
logP ³	0.46	EPI Suite™
Fraction unbound in plasma	1	Poulin and Theil (2002)
Blood:plasma partition coefficient	1.56	Taylor et al. (2013)
Ionization	monoprotic acid	MarvinSketch
pKa1	9.38	MarvinSketch

IndusChemFate

Input Parameters	Value	Data source
Water solubility (mg/L)	14000	EPI Suite™
Resorption tubuli (?/estimated fraction)	default: ?	-
Enterohepatic removal (relative to liver venous blood)	default: 0	-
Vmax Liver (umol/kg tissue/h)	44400	Calculation based on CLint
Km Liver (umol/L)	4744	(Sohlenius-Sternbeck et al. 2012)
Substance: Triclosane (TCS)		
Absorption rate into intestinal tissue (l/h)	default: 3	-
Density (mg/cm ³ or g/L)	1490	ChemSketch v.11 ¹
Molecular weight	289.6	PubChem
Vapour pressure (Pa) ²	0.00062	⁵ EPI Suite™
Log(Kow) at skin pH 5.5 ³	4.76	-
Log(Kow) at blood pH 7.4 ³	4.58	EPI Suite™, MarvinSketch ⁶
Water solubility (mg/L) ⁴	10	EPI Suite™
Resorption tubuli	default: ?	-
Enterohepatic removal (relative to liver venous blood)	default: 0	-
Vmax Liver (umol/kg tissue/h)	1649	Ashrap et al. (2017)
Km Liver (umol/L)	123	
Substance: Amiodarone (AMD)		
Absorption rate into intestinal tissue (l/h)	0.3	Kannan et al. (1982)
Density (mg/cm ³ or g/L)	1580	ChemSketch v.11 ¹
Molecular weight	645.32	PubChem
Vapour pressure (Pa) ²	4.54E-11	⁵ EPI Suite™
Log(Kow) at skin pH 5.5 ³	4.78	-
Log(Kow) at blood pH 7.4 ³	6.53	EPI Suite™, MarvinSketch ⁶
Water solubility (mg/L) ⁴	0.000061	EPI Suite™
Resorption tubuli	default: ?	-
Enterohepatic removal (relative to liver venous blood)	default: 0	-
Vmax Liver (umol/kg tissue/h)	131.8	
Km Liver (umol/L)	38.6	Algharably et al. (2019)
Substance: Cyclosporin A (CyA)		
Absorption rate into intestinal tissue (l/h)	default: 3	-
Density (mg/cm ³ or g/L)	1016	ChemSketch v.11 ¹
Molecular weight	1202.6	PubChem
Vapour pressure (Pa) ²	1.00E-15	⁵ EPI Suite™
Log(Kow) at skin pH 5.5 ³	1	-
Log(Kow) at blood pH 7.4 ³	1	EPI Suite™, MarvinSketch ⁶
Water solubility (mg/L) ⁴	1000000	EPI Suite™
Resorption tubuli	default: ?	-
Enterohepatic removal (relative to liver venous blood)	default: 0	-
Vmax Liver (umol/kg tissue/h)	384	
Km Liver (umol/L)	5	Pichard et al. (1996)
Substance: Valproic acid (VPA)		
Absorption rate into intestinal tissue (l/h)	default: 3	-
Density (mg/cm ³ or g/L)	950	ChemSketch v.11 ¹
Molecular weight	144.214	PubChem
Vapour pressure (Pa) ²	11.3	⁵ EPI Suite™
Log(Kow) at skin pH 5.5 ³	2.23	-
Log(Kow) at blood pH 7.4 ³	0.49	EPI Suite™, MarvinSketch ⁶
Water solubility (mg/L) ⁴	2000	EPI Suite™
Resorption tubuli	default: ?	-
Enterohepatic removal (relative to liver venous blood)	default: 0	-
Vmax Liver (umol/kg tissue/h)	101400	Calculation based on CLint
Km Liver (umol/L)	15648	Fortaner et al. (2021)

TNO Model		
Input Parameters	Value	Data source
pKa2	-	-
Papp>(*10E-6 cm/s)	36.3	Paixão et al. (2012)
Vapour pressure (mmHg)	0.0000629	EPI Suite™
Vmax (nmol/min/g liver)	740	Calculation based on CLint
Km (mg/L)	717	(Sohlenius-Sternbeck et al. 2012)
Molecular weight	289.6	PubChem
logP ³	4.76	EPI Suite™
Fraction unbound in plasma	0.01	CompTox Chemicals Dashboard
Blood:plasma partition coefficient	default: 1	-
Ionization	monoprotic acid	MarvinSketch
pKa1	7.68	MarvinSketch
pKa2	-	-
Papp>(*10E-6 cm/s)	184	Stec et al. (2013)
Vapour pressure (mmHg)	4.65E-06	EPI Suite™
Vmax (nmol/min/g liver)	27.5	Ashrap et al. (2017)
Km (mg/L)	35.6	
Molecular weight	645.32	PubChem
logP ³	6.66	EPI Suite™
Fraction unbound in plasma	0.05	Poulin and Theil (2002)
Blood:plasma partition coefficient	1.1	Poulin and Theil (2002)
Ionization	monoprotic base	MarvinSketch
pKa1	8.47	MarvinSketch
pKa2	-	-
Papp>(*10E-6 cm/s)	4	Sevin et al. (2013)
Vapour pressure (mmHg)	3.41E-13	EPI Suite™
Vmax (nmol/min/g liver)	2	Algharably et al. (2019)
Km (mg/L)	25.1	
Molecular weight	1202.6	PubChem
logP ³	1	EPI Suite™
Fraction unbound in plasma	0.062	Poulin and Theil (2002)
Blood:plasma partition coefficient	1.283	Poulin and Theil (2002)
Ionization	neutral	MarvinSketch
pKa1	11.83	MarvinSketch
pKa2	-	-
Papp>(*10E-6 cm/s)	8	Chiu et al. (2003)
Vapour pressure (mmHg)	7.50E-18	EPI Suite™
Vmax (nmol/min/g liver)	6.4	Pichard et al. (1996)
Km (mg/L)	6	
Molecular weight	144.214	PubChem
logP ³	2.75	EPI Suite™
Fraction unbound in plasma	0.4	ChemScreen
Blood:plasma partition coefficient	0.74	ChemScreen
Ionization	monoprotic acid	MarvinSketch
pKa1	5	MarvinSketch
pKa2	-	-
Papp>(*10E-6 cm/s)	48	Yee (1997)
Vapour pressure (mmHg)	0.08475	EPI Suite™
Vmax (nmol/min/g liver)	1690	Calculation based on CLint
Km (mg/L)	2256	Fortaner et al. (2021)

IndusChemFate

Input Parameters	Value	Data source
Substance: Methylparaben (MePa)		
Absorption rate into intestinal tissue (l/h)	default: 3	-
Density (mg/cm ³ or g/L)	1209	ChemSketch v.11 ¹
Molecular weight	152.149	PubChem
Vapour pressure (Pa) ²	0.1139903	⁵ EPI Suite™
Log(Kow) at skin pH 5.5 ³	1.96	EPI Suite™, MarvinSketch ⁶
Log(Kow) at blood pH 7.4 ³	1.96	
Water solubility (mg/L) ⁴	4250.6	EPI Suite™
Resorption tubuli	default: ?	-
Enterohepatic removal (relative to liver venous blood)	default: 0	-
Vmax Liver (umol/kg tissue/h)	65709	Calibrated
Km Liver (umol/L)	4000	Calibrated
Substance: Propylparaben (ProPa)		
Absorption rate into intestinal tissue (l/h)	default: 3	-
Density (mg/cm ³ or g/L)	1134	ChemSketch v.11 ¹
Molecular weight	180.2	PubChem
Vapour pressure (Pa) ²	0.049	⁵ EPI Suite™
Log(Kow) at skin pH 5.5 ³	3.04	EPI Suite™, MarvinSketch ⁶
Log(Kow) at blood pH 7.4 ³	3.04	
Water solubility (mg/L) ⁴	500	EPI Suite™
Resorption tubuli	default: ?	-
Enterohepatic removal (relative to liver venous blood)	default: 0	-
Vmax Liver (umol/kg tissue/h)	180090	Calibrated
Km Liver (umol/L)	6000	Calibrated
Substance: Butylparaben (ButPa)		
Absorption rate into intestinal tissue (l/h)	default: 3	-
Density (mg/cm ³ or g/L)	1108	ChemSketch v.11 ¹
Molecular weight	194.2	PubChem
Vapour pressure (Pa) ²	0.033	⁵ EPI Suite™
Log(Kow) at skin pH 5.5 ³	3.57	EPI Suite™, MarvinSketch ⁶
Log(Kow) at blood pH 7.4 ³	3.57	
Water solubility (mg/L) ⁴	207	EPI Suite™
Resorption tubuli	default: ?	NR
Enterohepatic removal (relative to liver venous blood)	default: 0	NR
Vmax Liver (umol/kg tissue/h)	76950	Calibrated
Km Liver (umol/L)	1900	Calibrated

CLint: Clearance intrinsic; ¹ ChemSketch v.11: (ACD/ChemSketch 2011); ² QSAR (MPBPWIN v1.43) or experimental value; ³ QSAR (KOWWIN v1.68) or experimental value for logP, ionisation information from MarvinSketch (ChemAxon); ⁴ QSAR (WSKOW v1.42) or experimental value; ⁵ EPI Suite™, US EPA: <https://www.epa.gov/tsca-screening-tools/epi-suite-estimation-program-interface>; ⁶ MarvinSketch: ChemAxon; ⁷ CompTox Chemicals Dashboard; ⁸ Drugbank: <https://go.drugbank.com/drugs/DB00281>; Papp: Apparent permeability coefficient; CompTox Chemicals Dashboard: <https://comptox.epa.gov/dashboard/>

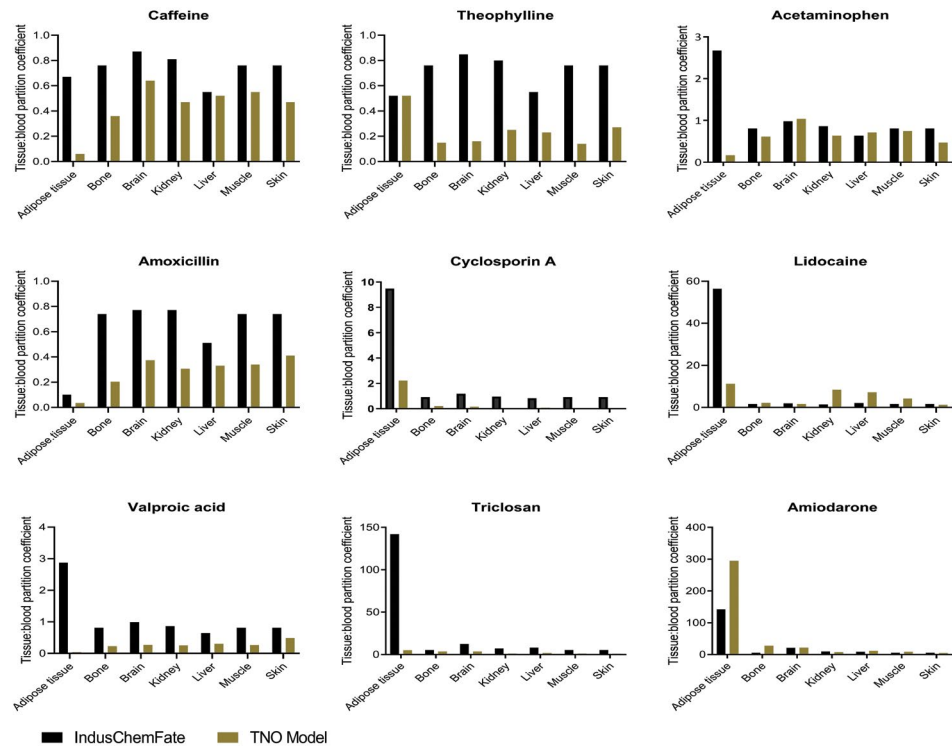
TNO Model		
Input Parameters	Value	Data source
Molecular weight	152.149	PubChem
logP ³	1.96	EPI Suite™
Fraction unbound in plasma	default:1	-
Blood:plasma partition coefficient	default: 1	-
Ionization	monoprotic acid	MarvinSketch
pKa1	8.5	MarvinSketch
pKa2	-	-
Papp>(*10E-6 cm/s)	40	Lakeram et al. (2008)
Vapour pressure (mmHg)	3.07E-04	EPI Suite™
Vmax (nmol/min/g liver)	1095	Calibrated
Km (mg/L)	608	Calibrated
Molecular weight	180.2	PubChem
logP ³	3	EPI Suite™
Fraction unbound in plasma	default:1	CompTox Chemicals Dashboard
Blood:plasma partition coefficient	default:1	-
Ionization	monoprotic acid	MarvinSketch
pKa1(acid)	8.5	MarvinSketch
pKa2(base)	-	-
Papp>(*10E-6 cm/s)	40	Lakeram et al. (2008)
Vapour pressure (mmHg)	3.07E-04	EPI Suite™
Vmax (nmol/min/g liver)	3001	Calibrated
Km (mg/L)	1081	Calibrated
Molecular weight	194.2	PubChem
logP ³	3.57	EPI Suite™
Fraction unbound in plasma	default: 1	CompTox Chemicals Dashboard
Blood:plasma partition coefficient	default: 1	-
Ionization	monoprotic acid	MarvinSketch
pKa1	8.5	MarvinSketch
pKa2	-	MarvinSketch
Papp>(*10E-6 cm/s)	40	Lakeram et al. (2008)
Vapour pressure (mmHg)	2.51E-04	EPI Suite™
Vmax (nmol/min/g liver)	1283	Calibrated
Km (mg/L)	369	Calibrated

SM3PBK-predicted tissue:blood partition coefficients by ICF and the TNO model

SUPPLEMENTARY TABLE 1 PBK-predicted and *in vivo* measured adipose tissue:blood partition coefficients in the human and rat. Substances presented in the order of increasing lipophilicity (logD: -2 to 6.5).

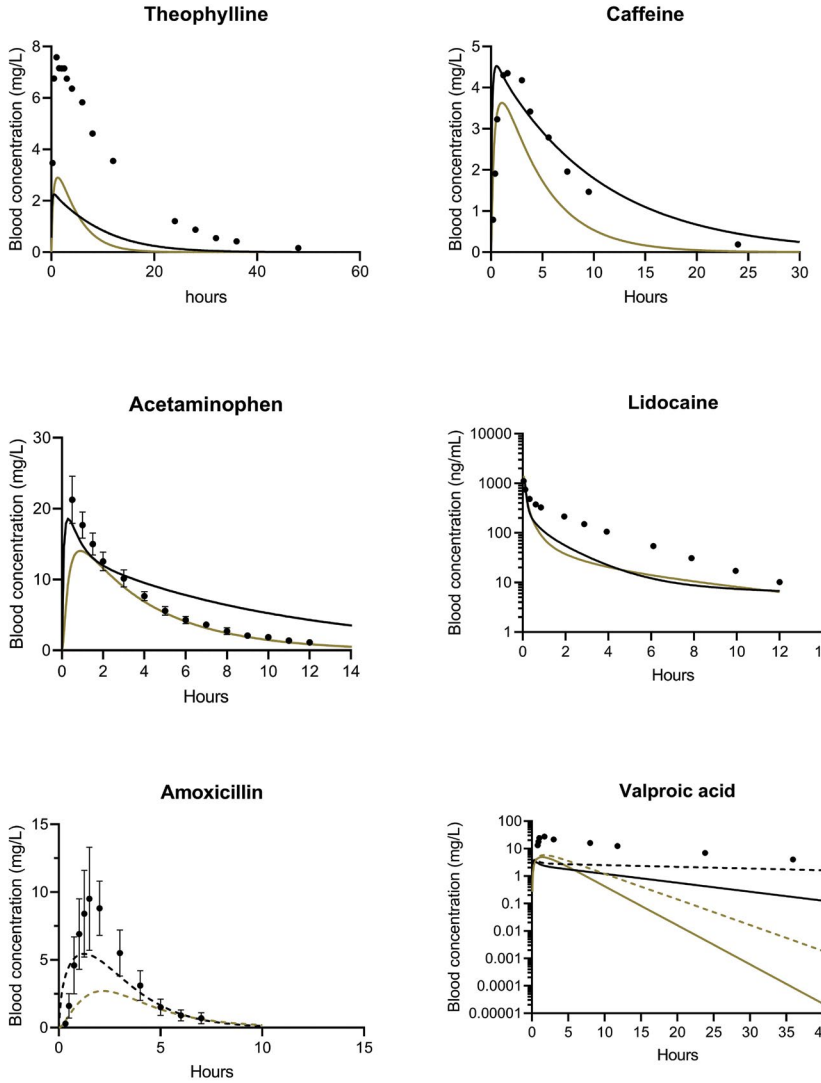
Substance	Human partition coefficients			Rat partition coefficients					
	ICF	TNO Model	Ratio two models	ICF	TNO Model	Ratio two models	Exp. data	Ratio ^a ICF/exp.data	Ratio TNO ^a Model/exp.data
AMOX	0.1	0.04	2.8	0.05	0.03	1.6	na	-	-
THEO	0.5	0.52	1.0	0.23	0.03	7.9	0.4	1.5	12.2
CAF	0.7	0.06	10.6	0.30	0.06	5.1	0.2	1.3	4.0
APAP	3	0.16	16.3	1	0.17	6.3	0.3	4.3	1.5
VPA	3	0.10	28.7	1	0.02	64.3	0.2	7.7	8.4
CyA	9	2	4.3	3	0.002	1782.2	9.1	2.7	4789.5
LID	56	11	5.0	16	0.68	24.2	na	-	-
MePa	59	5	11.8	17	6	3.1	na	-	-
ProPa	128	62	2.1	57	72	1.3	na	-	-
ButPa	138	80	1.7	80	178	2.2	na	-	-
TCS	142	5	28.3	97	9	11.3	na	-	-
AMD	142	295	2.1	88	9	10.1	223.0	2.5	25.4

na: not available, ICF: IndusChemFate, exp. data: experimental data, AMOX: amoxicillin, THEO: theophylline, CAF: caffeine, APAP: acetaminophen, VPA: valproic acid, CyA: cyclosporin A, LID: lidocaine, MePa: methylparaben, ProPa: propylparaben, ButPa: butylparaben, TCS: triclosan, AMD: amiodarone. ^a The ratio represents the 'model simulation': 'observed data' or *vice versa*, depending on what is >1.



SUPPLEMENTARY FIGURE 1 PBK-predicted organ tissue:blood partition coefficients in the human.

SM4 Blood time-course simulation: Additional toxicokinetic studies



SUPPLEMENTARY FIGURE 2 Blood time-course PBK simulations and human observed data. *In vivo* data represent the mean values and the bars (amoxicillin) indicate the standard deviation. Theophylline, 125 mg, single oral dose, eight healthy volunteers (Rovei et al. 1982) caffeine, 270 mg, single oral dose, one healthy volunteer (Lelo et al. 1986); acetaminophen, 1400 mg, single oral dose, six healthy volunteers (Lau and Critchley 1994); lidocaine, intravenous administration of 1 mg/kg, 10 healthy volunteers (Orlando et al. 2004); amoxicillin, 500 mg, single oral dose, nine healthy volunteers (Arancibia et al. 1980); valproic acid, 250 mg, single oral dose, nine healthy volunteers (Chun et al. 1980; Conner et al. 2018).

SM5 *In vivo*-Reported and PBK-model-predicted C_{max}, T_{max}, and AUC values in blood

Substance	Dose(mg)	Experimental measurements		
		C _{max} (mg/L)	T _{max} (hr)	AUC (mg*hr/L) (t: in hrs)
AMOX	500	8.2 (SE:0.9)	1.3 (SE: 0.1)	19.4 (SE:1.3)
AMOX	500	na	na	27.4 (SD:3.1)
LID	207 ^c	13.1 (by eye)	na	na
LID	1 ^d	na	na	na
CAF	100	1.4	1.5	na
CAF	270	4.4	1.6	na
THEO	125	4.1 (range: 3-6.7)	1.6 (range: 1-2)	52 (range: 31-94)(0-inf.)
THEO	250	5.9	3.0	na
APAP	1000	20 (SD: 8.4)	0.35 (SD: 0.17)	45 (SD: 11)
APAP	1400 ^a		na	
APAP	325 (N=8)	3.4 (SD: 0.8)	1.1 (SD:0.6)	14.6 (SD: 3.6)
TCS	4 (N=10)	0.218 (0.17-0.267) ^e	1.5 (1-2)	na
TCS	3.8	0.243	4 (range 2-6)	2.8
VPA	250 (N=9)	27.2 (SD: 4.2)	na	386.4 (SD: 91)
VPA	500 (N=14)	M: 35.6 (SE:5.2) F: 55.3 (SE: 9.4)	2.0	M: 496.6 (SE:55.2, t:0-48) F: 809.4 (SE: 148.4, t:0-48)
AMD	(SD: N=6)	6.9 (SD: 4.2, range: 3-14.2)	4.9 (SD: 1.2, range: 3-6.2)	4.5
CyA	875 ^a (N=15)	range: 0.15-2.56	range: 2-6	range: 2.2-42.6
CyA	280 ^a (infusion, N=8)	2.6	2.5	na
MePA	100 ^b	26.6-38.7 (M-F)	1- 0.5 (M-F)	82.1-143.6 (M-F)
ProPa	100 ^b	11.4-42.3 (M-F)	0.5	58.3-118.1 (M-F)
ButPa	100 ^b	15.2-21 (M-F)	0.5	73.6-99.3 (M-F)

N= Number of participants, SD: standard deviation, SE: standard error, NR: not reported, M: males, F: females, na: not available, AMOX: amoxicillin, THEO: theophylline, CAF: caffeine, APAP: acetaminophen, VPA: valproic acid, CyA: cyclosporin A, LID: lidocaine, MePa: methylparaben, ProPa: propylparaben, ButPa: butylparaben, TCS: trisclorane, AMD: amiodarone

PBK-predictions						Reference
IndusChemFate			TNO Model			
Cmax (mg/L)	Tmax (hr)	AUC (mg*hr/L) (t: in hrs)	Cmax (mg/L)	Tmax (hr)	AUC (mg*hr/L) (t: in hrs)	
5.4	1.2	20.3 (t:0-6)	2.7	2.1	13.3	Adam et al. (1982)
5.4	1.2	22.3 (t:0-12)	2.7	2.1	13 (t:0-12)	Arancibia et al. (1980)
1.2	0.1	0.51 (t:0-3)	13.8	0.05	1.82(t:0-3)	Grillo et al. (2001)
4.6	0.1	1.87(t:0-12)	1.4	0.05	0.68 (t:0-12)	Orlando et al. (2004)
1.7	0.6	16 (t: 0-24)	1.3	1.0	7.7 (t: 0-24)	Zandvliet et al. (2005)
4.5	0.6	43.6 (t: 0-24)	3.6	1.0	20.9 (t:0-24)	Lelo et al. (1986)
2.3	0.6	21.6 (t:0-48)	2.9	1.2	17 (0-48)	Rovei et al. (1982)
4.6	0.7	50.9 (t:0-32)	3.9	1.3	23.8 (t:0-32)	Dadashzadeh and Tajerzaden (2001)
		42.8 (t:0-24)			50.2 (t:0-24)	Prescott (1980)
18.6	0.3	133.2 (t:0-24)	14.0	0.9	68 (t:0-24)	Lau and Critchley (1994)
4.3	0.3	30.7 (t:0-24)	3.2	0.9	16 (t:0-24)	Volak et al. (2013)
0.0066	0.5	0.015 (t:0-24)	0.014	0.500	0.064 (t:0-24)	Sandborgh-Englund et al. (2006)
0.006	0.5	0.017 (t:0-72)	0.012	0.5	0.05 (t:0-72)	Bagley and Lin (2000)
3.4	0.3	33 (t:0-40)	4.9	1.4	24.7 (t:0-40)	Conner et al. (2018)
6.9	0.3	67.6 (t:0-48)	10.3	1.4	51.9 (t:0-48)	Ibarra et al. (2013)
1.6	2.2	19.6 (t:0-24)	2.6	2.0	18.3 (t:0-24)	Kannan et al. (1982)
0.7	2.3	9.2	11.3	1.5	34.9	Bertault-Pères et al. (1985)
1.0	1.0	3.7	13.0	2.5	35.9	Kawai et al. (1998)
79.0	0.6	308.1	na	na	2547.0	Aubert et al. (2012)
73.3	0.6	170.0	na	na	2095.0	Aubert et al. (2012)
69.7	0.6	143.7	na	na	1962.4	Aubert et al. (2012)

References-Supplementary Material

- Adam D, de Visser I, Koeppel P. 1982. Pharmacokinetics of amoxicillin and clavulanic acid administered alone and in combination. *Antimicrob Agents Chemother.* 22(3):353-357.
- Algharably EAH, Kreutz R, Gundert-Remy U. 2019. Importance of *in vitro* conditions for modeling the *in vivo* dose in humans by *in vitro-in vivo* extrapolation (ivive). *Archives of toxicology.* 93(3):615-621.
- Alsenz J, Haenel E. 2003. Development of a 7-day, 96-well caco-2 permeability assay with high-throughput direct uv compound analysis. *Pharm Res.* 20(12):1961-1969.
- Arancibia A, Guttman J, González G, González C. 1980. Absorption and disposition kinetics of amoxicillin in normal human subjects. *Antimicrob Agents Chemother.* 17(2):199-202.
- Ashrap P, Zheng G, Wan Y, Li T, Hu W, Li W, Zhang H, Zhang Z, Hu J. 2017. Discovery of a widespread metabolic pathway within and among phenolic xenobiotics. *Proc Natl Acad Sci U S A.* 114(23):6062-6067.
- Aubert N, Ameller T, Legrand JJ. 2012. Systemic exposure to parabens: Pharmacokinetics, tissue distribution, excretion balance and plasma metabolites of [14c]-methyl-, propyl- and butylparaben in rats after oral, topical or subcutaneous administration. *Food and chemical toxicology : an international journal published for the British Industrial Biological Research Association.* 50(3-4):445-454.
- Bagley DM, Lin YJ. 2000. Clinical evidence for the lack of triclosan accumulation from daily use in dentifrices. *Am J Dent.* 13(3):148-152.
- Bertault-Pérès P, Maranchi D, Carcassonne Y, Cano JP, Barbet J. 1985. Clinical pharmacokinetics of ciclosporin a in bone marrow transplantation patients. *Cancer Chemother Pharmacol.* 15(1):76-81.
- Chiu YY, Higaki K, Neudeck BL, Barnett JL, Welage LS, Amidon GL. 2003. Human jejunal permeability of cyclosporin a: Influence of surfactants on p-glycoprotein efflux in caco-2 cells. *Pharm Res.* 20(5):749-756.
- Chun AH, Hoffman DJ, Friedmann N, Carrigan PJ. 1980. Bioavailability of valproic acid under fasting/nonfasting regimens. *J Clin Pharmacol.* 20(1):30-36.
- Conner TM, Nikolian VC, Georgoff PE, Pai MP, Alam HB, Sun D, Reed RC, Zhang T. 2018. Physiologically based pharmacokinetic modeling of disposition and drug-drug interactions for valproic acid and divalproex. *European journal of pharmaceutical sciences : official journal of the European Federation for Pharmaceutical Sciences.* 111:465-481.
- Dadashzadeh S, Tajerzaden H. 2001. Dose dependent pharmacokinetics of theophylline: Michaelis-menten parameters for its major metabolic pathways. *European journal of drug metabolism and pharmacokinetics.* 26(1-2):77-83.
- Fortaner S, Mendoza-De Gyves E, Cole T, Lostia AM. 2021. Determination of *in vitro* metabolic hepatic clearance of valproic acid (vpa) and five analogues by uplc-ms-qtof, applicable in alternatives to animal testing. *J Chromatogr B Analyt Technol Biomed Life Sci.* 1181:122893.
- Grillo JA, Venitz J, Ornato JP. 2001. Prediction of lidocaine tissue concentrations following different dose regimes during cardiac arrest using a physiologically based pharmacokinetic model. *Resuscitation.* 50(3):331-340.
- Ibarra M, Vázquez M, Fagiolino P, Derendorf H. 2013. Sex related differences on valproic acid pharmacokinetics after oral single dose. *J Pharmacokinet Pharmacodyn.* 40(4):479-486.
- Kannan R, Nademanee K, Hendrickson JA, Rostami HJ, Singh BN. 1982. Amiodarone kinetics after oral doses. *Clinical pharmacology and therapeutics.* 31(4):438-444.
- Kawai R, Mathew D, Tanaka C, Rowland M. 1998. Physiologically based pharmacokinetics of cyclosporine a: Extension to tissue distribution kinetics in rats and scale-up to human. *The Journal of pharmacology and experimental therapeutics.* 287(2):457-468.
- Lakeram M, Lockley DJ, Pendlington R, Forbes B. 2008. Optimisation of the caco-2 permeability assay using experimental design methodology. *Pharm Res.* 25(7):1544-1551.
- Lau GS, Critchley JA. 1994. The estimation of paracetamol and its major metabolites in both plasma and urine by a single high-performance liquid chromatography assay. *J Pharm Biomed Anal.* 12(12):1563-1572.
- Lelo A, Birkett DJ, Robson RA, Miners JO. 1986. Comparative pharmacokinetics of caffeine and its primary demethylated metabolites paraxanthine, theobromine and theophylline in man. *British journal of clinical pharmacology.* 22(2):177-182.
- Louisse J, Alewijn M, Peijnenburg A, Cnubben NHP, Heringa MB, Coecke S, Punt A. 2020. Towards harmonization of test methods for *in vitro* hepatic clearance studies. *Toxicol In vitro.* 63:104722.

- Matsuzaki T, Scotcher D, Darwich AS, Galetin A, Rostami-Hodjegan A. 2019. Towards further verification of physiologically-based kidney models: Predictability of the effects of urine-flow and urine-ph on renal clearance. *The Journal of pharmacology and experimental therapeutics*. 368(2):157-168.
- Oriando R, Piccoli P, De Martin S, Padrini R, Floreani M, Palatini P. 2004. Cytochrome p450 1a2 is a major determinant of lidocaine metabolism *in vivo*: Effects of liver function. *Clinical pharmacology and therapeutics*. 75(1):80-88.
- Paixão P, Gouveia LF, Morais JA. 2012. Prediction of the human oral bioavailability by using *in vitro* and *in silico* drug related parameters in a physiologically based absorption model. *Int J Pharm*. 429(1-2):84-98.
- Peyret T, Poulin P, Krishnan K. 2010. A unified algorithm for predicting partition coefficients for pbpk modeling of drugs and environmental chemicals. *Toxicol Appl Pharmacol*. 249(3):197-207.
- Pichard L, Domergue J, Fourtanier G, Koch P, Schran HF, Maurel P. 1996. Metabolism of the new immunosuppressor cyclosporin g by human liver cytochromes p450. *Biochem Pharmacol*. 51(5):591-598.
- Poulin P, Krishnan K. 1995a. An algorithm for predicting tissue: Blood partition coefficients of organic chemicals from n-octanol: Water partition coefficient data. *J Toxicol Environ Health*. 46(1):117-129.
- Poulin P, Krishnan K. 1995b. A biologically-based algorithm for predicting human tissue: Blood partition coefficients of organic chemicals. *Hum Exp Toxicol*. 14(3):273-280.
- Poulin P, Theil FP. 2002. Prediction of pharmacokinetics prior to *in vivo* studies. 1. Mechanism-based prediction of volume of distribution. *J Pharm Sci*. 91(1):129-156.
- Prescott LF. 1980. Kinetics and metabolism of paracetamol and phenacetin. *British journal of clinical pharmacology*. 10 Suppl 2:291s-298s.
- Rodgers T, Rowland M. 2007. Mechanistic approaches to volume of distribution predictions: Understanding the processes. *Pharm Res*. 24(5):918-933.
- Rovei V, Chanoine F, Strolin Benedetti M. 1982. Pharmacokinetics of theophylline: A dose-range study. *British journal of clinical pharmacology*. 14(6):769-778.
- Sandborgh-Englund G, Adolfsson-Erici M, Odham G, Ekstrand J. 2006. Pharmacokinetics of triclosan following oral ingestion in humans. *Journal of Toxicology and Environmental Health, Part A*. 69(20):1861-1873.
- Sevin E, Dehouck L, Fabulas-da Costa A, Cecchelli R, Dehouck MP, Lundquist S, Culot M. 2013. Accelerated caco-2 cell permeability model for drug discovery. *J Pharmacol Toxicol Methods*. 68(3):334-339.
- Sohlenius-Sternbeck AK, Jones C, Ferguson D, Middleton BJ, Projean D, Floby E, Bylund J, Afzelius L. 2012. Practical use of the regression offset approach for the prediction of *in vivo* intrinsic clearance from hepatocytes. *Xenobiotica*. 42(9):841-853.
- Stec J, Fomovska A, Afanador GA, Muench SP, Zhou Y, Lai BS, El Bissati K, Hickman MR, Lee PJ, Leed SE et al. 2013. Modification of triclosan scaffold in search of improved inhibitors for enoyl-acyl carrier protein (acp) reductase in *Toxoplasma gondii*. *ChemMedChem*. 8(7):1138-1160.
- Taylor RR, Hoffman KL, Schniedewind B, Clavijo C, Galinkin JL, Christians U. 2013. Comparison of the quantification of acetaminophen in plasma, cerebrospinal fluid and dried blood spots using high-performance liquid chromatography-tandem mass spectrometry. *J Pharm Biomed Anal*. 83:1-9.
- Thelen K, Coboeken K, Willmann S, Burghaus R, Dressman JB, Lippert J. 2011. Evolution of a detailed physiological model to simulate the gastrointestinal transit and absorption process in humans, part 1: Oral solutions. *J Pharm Sci*. 100(12):5324-5345.
- Volak LP, Hanley MJ, Masse G, Hazarika S, Harmatz JS, Badmaev V, Majeed M, Greenblatt DJ, Court MH. 2013. Effect of a herbal extract containing curcumin and piperine on midazolam, flurbiprofen and paracetamol (acetaminophen) pharmacokinetics in healthy volunteers. *British journal of clinical pharmacology*. 75(2):450-462.
- Wilson JP. 1967. Surface area of the small intestine in man. *Gut*. 8(6):618-621.
- Yee S. 1997. *In vitro* permeability across caco-2 cells (colonic) can predict *in vivo* (small intestinal) absorption in man--fact or myth. *Pharm Res*. 14(6):763-766.
- Zandvliet AS, Huitema AD, de Jonge ME, den Hoed R, Sparidans RW, Hendriks VM, van den Brink W, van Ree JM, Beijnen JH. 2005. Population pharmacokinetics of caffeine and its metabolites theobromine, paraxanthine and theophylline after inhalation in combination with diacetylmorphine. *Basic Clin Pharmacol Toxicol*. 96(1):71-79.

Section II



Chapter 3

***In vitro* to *in vivo* extrapolation of effective dosimetry in developmental toxicity testing: Application of a generic PBK modelling approach**

Toxicology and Applied Pharmacology, 2017. Oct 1;332:109-120

DOI: [10.1016/j.taap.2017.07.021](https://doi.org/10.1016/j.taap.2017.07.021)

Styliani Fragki¹

Aldert H. Piersma^{1,2}

Emiel Rorije³

Marco J. Zeilmaker⁴

¹ Centre for Health Protection, National Institute for Public Health and the Environment, Bilthoven, the Netherlands

² Institute for Risk Assessment Sciences, Utrecht University, Utrecht, the Netherlands

³ Centre for Safety of Substances and Products, National Institute for Public Health and the Environment (RIVM), Bilthoven, the Netherlands

⁴ Centre for Nutrition, Prevention and Health Services, National Institute for Public Health and the Environment (RIVM), Bilthoven, the Netherlands

Abstract

Incorporation of kinetics to quantitative *in vitro* to *in vivo* extrapolations (QIVIVE) is a key step for the realization of a non-animal testing paradigm, in the sphere of regulatory toxicology. The use of Physiologically-Based Kinetic (PBK) modelling for determining systemic doses of chemicals at the target site is accepted to be an indispensable element for such purposes. Nonetheless, PBK models are usually designed for a single or a group of compounds and are considered demanding, with respect to experimental data needed for model parameterization. Alternatively, we evaluate here the use of a more generic approach, ie. the so-called IndusChemFate model, which is based on incorporated QSAR model parametrization. The model was used to simulate the *in vivo* kinetics of three diverse classes of developmental toxicants: triazoles, glycol ethers' alkoxyacetic acid metabolites and phthalate primary metabolites. The model required specific input per each class of compounds. These compounds were previously tested in three alternative assays: the whole-embryo culture (WEC), the zebrafish embryo test (ZET), and the mouse embryonic stem cell test (EST). Thereafter, the PBK-simulated blood levels at toxic *in vivo* doses were compared to the respective *in vitro* effective concentrations. Comparisons pertaining to relative potency and potency ranking with integration of kinetics were similar to previously obtained comparisons. Additionally, all three *in vitro* systems produced quite comparable results, and hence, a combination of alternative tests is still preferable for predicting the endpoint of developmental toxicity *in vivo*. This approach is put forward as biologically more plausible since plasma concentrations, rather than external administered doses, constitute the most direct *in vivo* dose metric.

Introduction

The transition from animal experiments to alternative mechanism-based *in vitro* assays or assays with lower organisms, as the main information source for chemical risk assessment, meets with significant challenges. To begin with, the toxicity endpoints examined *in vitro* diverge from those assessed *in vivo*, and hence, their relevance for the prediction of adversity at intact organism level needs extrapolation of the underlying toxicodynamics and toxicokinetics (Blaauboer *et al.*, 2008, 2012; Gül den and Seibert, 2005). This problem can partially be overcome by using a combination of *in vitro* and other alternative tests, which can measure several different endpoints and various mechanisms of toxicity, rather than one single assay (Gül den and Seibert, 2005; Kroese *et al.*, 2015; Schenk *et al.*, 2010; Piersma, 2006).

Another critical issue is the quantitative *in vitro* to *in vivo* extrapolation (QIVIVE) of effective concentrations (Blaauboer, 2010; Gül den and Seibert, 2005) corresponding with the points of departure for the risk assessment. *In vitro* and *in vivo* exposure situations differ fundamentally, making such extrapolations complex. In the *in vitro* assays, the compound of interest is directly added to the assay medium, thereby allowing an apparently simple exposure situation when compared to the *in vivo* situation. However, even *in vitro* the exposure situation is not that obvious, as free (active) versus bound (inactive) compound fraction needs to be considered, as well as possible time-dependent decomposition and/or evaporation of the test substance from the culture medium (Kramer *et al.*, 2012; Groothuis *et al.*, 2015). Similarly, *in vivo*, binding of a substance into plasma or serum proteins will make it unavailable for diffusion/transport across cell membranes (Alder *et al.*, 2011; Banker and Clark, 2008). In addition, in an intact organism the route from external exposure to the target organ is confounded with absorption, distribution, metabolism and excretion (ADME) characteristics, determining actual target organ exposure levels both in terms of concentration and in terms of time-dependency. Such processes are lacking in *in vitro* systems.

Clearly, linking the toxic dose metric measured *in vitro* and the *in vivo* relevant effective dose, requires the integration of kinetics of both systems (Alder *et al.*, 2011; NRC, 2007; Blaauboer *et al.*, 2010). Here the use of Physiologically Based Kinetic (PBK) modelling is deemed to be a key element (Alder *et al.*, 2011; Bessems *et al.* 2014; Bouvier d' Yvoire *et al.*, 2007; Hartung *et al.*, 2011; NRC, 2007; Punt *et al.*, 2011; Yoon *et al.*, 2015). PBK models can estimate the systemic effective doses of substances at a specific target site and *vice versa*, whereas with reverse dosimetry, they can be used for the prediction of external effective doses *in vivo* starting from the *in vitro* toxic concentrations, i.e. the presumed target doses (Alder *et al.*, 2011; Blaauboer *et al.*, 2008). Several PBK-reverse dosimetry approaches have been hitherto performed for different toxicity endpoints, as for example: neurotoxicity (Forsby and Blaauboer 2007), nephrotoxicity (Abdulah *et al.*, 2016) and hepatotoxicity (Klein *et al.*, 2016). Furthermore reverse-dosimetry PBK modelling has been applied on high-throughput chemicals on the basis of *in vitro* assays on metabolism and protein binding and QSAR physical-chemical properties (Wambaugh *et al.*, 2015; Wetmore *et al.*, 2012; Wetmore *et al.*, 2013). Here we will focus on the *in vitro/in vivo* extrapolation of the endpoint of developmental toxicity.

We previously correlated directly *in vitro* benchmark concentrations, occurring specifically from three alternative developmental toxicity models, with *in vivo* benchmark doses from existing animal experiments, for a series of embryotoxic compounds (de Jong *et al.*, 2009, 2011; Hermesen *et al.*, 2011; Piersma *et al.*, 2008). The assays employed were the rodent post-implantation Whole- Embryo Culture method (WEC), the zebrafish embryo test (ZET), and the mouse embryonic stem cell test (EST). Amongst these the EST is the only test not requiring the sacrifice of animals, by utilizing a permanent murine cell line. The test uses the capacity of embryonic stem cells to differentiate *in vitro* to contracting cardiac myoblasts. Inhibition of this differentiation process, in the absence of cytotoxicity, is taken as predicting embryotoxicity (Scholz *et al.*, 1999; Seiler and Spielmann, 2011). In contrast to EST, the WEC and ZET involve the development of whole embryos, either after explantation from a pregnant rat or using zebra fish eggs, respectively. In the WEC experimental model, the effects of substances given during a narrow exposure window (early organogenesis, gestation day (GD) 10-12) are examined in culture, after isolation of the embryos from pregnant animals (Chapin *et al.*, 2008; Piersma *et al.*, 2004). On the other hand, the ZET assesses chemical toxicity during up to 120 hours of embryogenesis including hatching of the larva (Brannen *et al.*, 2010; Hill *et al.*, 2005). The advantage of both tests is that they mirror general morphogenesis, at least within a given developmental time window, due to their use of the whole embryo, rather than a plain cell-line (Chapin *et al.*, 2008).

In that research, it was demonstrated that for a more meaningful extrapolation of such alternative methods *in vivo*, integration of kinetics is necessary. Inevitably, this presupposes that the alternative systems sufficiently represent the *in vivo* situation. Regarding the EST assay some examples have been published, where *in vitro* concentration-response data were translated into *in vivo* dose-response data with the use of PBK modelling (glycol ethers and retinoic acid: Lousse *et al.*, 2010, 2015; phenols: Strikwold *et al.*, 2013, 2016; glycol ethers: Verwei *et al.*, 2006). Those studies aimed at deriving a predicted human *in vivo* point of departure to be used for risk assessment, and illustrate the potential of combining *in vitro* results and PBK modelling in deriving human toxicity standards. The PBK model parameters were derived either from combined *in vivo/in vitro* data (Verwei *et al.*, 2006, Lousse *et al.*, 2010), or solely from *in vitro* and *in silico* data (Strikwold *et al.*, 2013, 2016).

Notwithstanding the fact that these studies proved the concept of reverse PBK dosimetry in deriving human toxicity standards, they all needed chemical specific PBK models, whereas the ever increasing number of chemicals would favour a more generic PBK modelling approach (Basketter *et al.*, 2012; Bessems *et al.*, 2014). Proving the suitability of a single PBK model concept, which only requires a minimum input of information, for different groups of chemicals, would facilitate the PBK application for extrapolation purposes, thereby facilitating an animal-free toxicity testing paradigm. Furthermore, the *in vitro* - *in vivo* extrapolation rests on the assumption that the *in vitro* concentrations have equal potency in inducing toxicity in the developing embryo. Finally, the applied reverse dosimetry was limited to the EST assay.

The objectives of the current study were therefore (1) to assess the feasibility of a generic PBK model in order to predict *in vivo* kinetics, (2) to correlate PBK predicted *in vivo* dosimetry, i.e. venous blood plasma concentrations corresponding to toxic *in vivo* effect levels, with the respective *in vitro* effect levels and (3) to extend the foregoing analysis beyond the EST assay, by including other relevant alternative developmental toxicity assays.

The PBK model IndusChemFate (Jongeneelen and Ten Berge 2011) was used, a cross-chemical predictive model, readily accessible, and in a form of an MS EXCEL Spreadsheet. The features of IndusChemFate are in line with what has been previously suggested to form the basis for the build-up of generic PBK-platforms: relatively simple, open access, with inclusion of a physiological data base, multiple exposure routes (oral, inhalatory, dermal) (Basketter *et al.*, 2012; Leist *et al.*, 2014) and species applicability (human, rat, mouse).

Next to the EST, the WEC and the ZET assays were chosen as alternative embryotoxicity assays for comparison. Finally, three different classes of developmentally toxic chemicals were chosen as model compounds, i.e. six 1,2,4-triazole compounds, four glycol ether alkoxyacetic acid metabolites, and two monophthalates. These compounds represent three different classes in terms of challenges for PBK modelling, the complexity of the modelling moving from toxicity induced by the parent compound (triazoles), by hepatic formation of a primary metabolite (glycol ethers) or by metabolite formation in the gastrointestinal tract (phthalates), thereby allowing us to evaluate the extent to which the IndusChemFate model can generically be employed.

Materials and Methods

In vivo toxicity data

1,2,4-Triazoles derivatives

1,2,4-Triazoles derivatives, referred to herein as triazoles, are fungicides some of which are known to induce developmental effects in laboratory animals (EFSA, 2009). The parent compound is known to be more potent than the metabolite free triazole (EFSA, 2009; FAO/WHO, 2008). Six members of the group were used: hexaconazole (HEX), flusilazole (FLU), cyproconazole (CYP), triadimefon (TDI), myclobutanil (MYC), triticonazole (TTC). *In vivo* developmental toxicity studies were used as selected previously by de Jong *et al.* (2011). Study information was collected as presented in that article. In all studies the animal model was the rat, exposed orally (mostly by gavage) during gestation days 6 to 15 or 7 to 16. Other routes of administration and other species were not considered. Benchmark doses at a 10% effect size (BMD10) for skeletal variations¹² were determined by de Jong *et al.* (2011), as this was the most sensitive endpoint for most of the substances (with the exception of flusilazole and myclobutanil). The order followed in Table 1 is based on the BMD10 values (most potent to least potent).

12 Skeletal variation (supernumerary ribs, extra ossification centers in ribs, unossified sternbrae) was chosen as a sensitive developmental endpoint, previously by de Jong *et al.*, 2011. The BMR was defined as a 10% additional incidence of skeletal variations (de Jong *et al.*, 2011).

Glycol ethers

Likewise, existing *in vivo* data were collected for the glycol ethers. *In vivo* BMD10 values for critical embryo toxic endpoints (malformations, fetal viability, skeletal variations) were taken for the glycol ethers ethylene glycol methyl ether (EGME) and ethylene glycol ethyl ether (EGEE) from Hermsen *et al.* (2011), and for ethylene glycol butyl ether (EGBE) from Lousse *et al.* (2010). The corresponding developmental toxicity studies were found either in the published literature or in international evaluations of each compound by US EPA or the EU Risk Assessment Committee (RAC). A standard developmental toxicity test with the parent substance ethylene glycol phenyl ether (EGPE) was identified in the available REACH dossier for this substance (study performed by BASF found at ECHA's website). In this study the tested parent substance EGPE, did not exert any fetotoxic effect. In all four toxicity studies the animal species was the rat, exposed only via the oral route during specific days of the gestation period.

Phthalates

The *in vivo* information for two representatives of the phthalates, was taken from two studies (Table 2), as selected previously (Janer *et al.*, 2008a). The two compounds were di(2-ethylhexyl) phthalate (DEHP) and di(n-butyl) phthalate (DBP), known to be developmentally toxic (Ema *et al.*, 2002; ECB, 2008). As with the two previous sets of chemicals, priority was given to rat studies. The animals were treated orally by gavage during gestation days 7 to 15. BMD50 for malformations and resorptions/implantation loss and BMD05 for fetal body weights were determined (Janer *et al.*, 2008a). For all endpoints the compounds had similar potencies, but the BMD05 for fetal body weight was used here, as the lowest BMD.

TABLE 1 *Developmental toxicity of the triazoles in rats*

Substance	Rat strain	Route	Exposure Period	Dose (mg/kg bw/day)	dLEL (mg/kg bw/day)*	BMD10 skeletal variations (mg/kg bw/day) *
HEX	Wistar	oral gavage	GD 7-16	0, 2.5, 25, 250	2.5	2.5
FLU	CRL:CD (SD)	oral in diet	GD 7-16	0, 0.4, 2, 10, 50, 250	0.4 ^a	2.9
CYP	Wistar	oral gavage	GD 6-15	0, 6, 12, 24, 48	12	15.6
TDI	CRL:CD (SD)	oral gavage	GD 6-15	0, 10, 25, 50, 100	50	26.9
MYC	SD	oral gavage	GD 6-15	0, 31.3, 93.8, 312.6, 468.9	312.6 ^b	314.8
TTC	CRL:CD (SD)	oral gavage	GD 6-15	0, 40, 200, 1000	1000	1182.3 ^c

* dLEL and BMD10 values taken from de Jong *et al.*, 2011 (presented in the paper in $\mu\text{mol/kg}$, transformed here into mg/kg bw/day). The dLEL represents the Low Effect Level for the most sensitive endpoint, i.e. skeletal variations, except for the case of flusilazole and myclobutanyl (see below)

^a This is the dLEL for flusilazole on urogenital malformations, while for skeletal development the dLEL was 10 mg/kg bw/day.

^b dLEL for skeletal variations was not the most sensitive for myclobutanyl; decreased viability index was recorded at 93.8 mg/kg bw/day

^c BMD10 value is above the highest dose tested

Physiologically Based Kinetic model

In order to simulate organ exposure, the PBK model IndusChemFate, developed by Jongeneelen and Ten Berge (Jongeneelen and Berge 2011), was applied to all the selected substances. This model comprises, next to the blood, twelve body compartments¹³, and it can be applied for different routes of exposure (dermal, inhalation or oral), for different species (man, rat, mice) and for different exposure durations (single peak *versus* repeated chronic exposure). In this study, we applied the model for the rat and for single and repeated, daily oral exposure. In order to mimic the fetal exposure, the chemical's average and average-peak concentration in the maternal blood were used as a proxy, in accordance with the developmental toxicity exposure windows. The model thus assumes that the maternal blood is an effective measure for fetal exposure to either of the investigated chemicals.

As input the model requires physiological/anatomical parameters (organ volumes, blood flows, cardiac output and alveolar ventilation), biochemical parameters (hepatic Michaelis-Menten kinetics, *i.e.*, maximal metabolic rate (V_{max}), affinity constant for the parent compound and metabolites (K_M) and physicochemical parameters (octanol-water partition coefficient, vapour pressure, molecular weight, water solubility and density). In the model the latter parameters are used for calculating blood concentration: organ partition coefficients and renal clearance. In IndusChemFate chemical metabolism is implemented in a sequential way, *i.e.*, the parent compound is only metabolized into its primary metabolite followed by metabolism of the primary metabolite into a secondary metabolite, etc. In the case of triazoles this results in the following principal metabolic pathway: biologically parent compound > less active metabolite. In the case of glycol ethers and phthalates the following pathway was modelled: parent compound → toxicologically active acidic metabolite.

Physiological/anatomical parameters for the rat were as described in the IndusChemFate user manual (version 2.00). Physicochemical parameters (organ : blood partition coefficients; renal clearance) were obtained from QSAR models (see Table 3). Three model software packages (KOWWIN, MPBPWIN and WSKOW) automatically give the experimental value used to derive the predictive model, whenever a substance is present in the PhysProp database which is bundled with the EpiSuite software containing the model software packages (Agency) 2016). If an experimental value was available this was preferred over the estimated value. For this particular set of substances the differences between the experimental and estimated values were negligible. All models give a direct estimate of the needed PBK parameter, except for the estimate for the biochemical parameters, *i.e.* hepatic V_{max} and K_M , which is due to lack of general (freely available) QSAR estimation models for these parameters.

¹³ Twelve body compartments: lung, heart, brain, skin, adipose tissue, muscles, bone, bone marrow, stomach and intestines, liver and kidney

TABLE 2 Developmental toxicity of the glycol ethers and two phthalates in rats.

Substance	Rat strain	Route	Exposure Period	Dose (mg/kg bw/day)
EGME (MAA)	SD	oral, in diet	GD 7-18	0, 16, 31, 73, 140, 198, 290, 620
EGEE (EAA)	Wistar	oral gavage	GD 1-21	0, 11.5, 23, 46.5, 93, 186, 372
EGBE (BAA)	F344	oral gavage	GD 9-11	0, 30, 100, 200
EGPE (PAA)	Wistar	oral gavage	GD 6-19	0, 100, 300, 1000

Substance	Rat strain	Route	Exposure\ period	Dose (mg/kg bw/day)
DEHP (MEHP)	Wistar	oral gavage	GD 7-15	0, 40, 200, 1000
DBP (MBP)	Wistar	oral gavage	GD 7-15	0, 500, 630, 750, 1000

* BMD10 values were taken from the respective publications (see below) in $\mu\text{mol/kg bw/day}$ and calculated back to mg/kg bw/day based on the molecular weight of the parent compound

^a Hermsen *et al.*, 2011, ^b Louise *et al.*, 2010, ^c This is the original reference; however, the information presented was taken from the report of the EU RAC Committee on EGEE (2011)

^d This is the original reference; however, data were collected from US EPA evaluation (US EPA, 2009) on EGBE

^e ECHA disseminated dossier on EGPE

The biochemical parameters were obtained as follows. In the case of the triazoles the parent compound itself is known to be developmentally toxic (EFSA, 2009) and much more potent than the metabolite (EFSA, 2009; FAO/WHO, 2008). Hence, the kinetics of the parent fungicides are of major importance. For the modelling of the concentration of parent triazole compounds in maternal blood, the parent triazoles metabolic parameters, i.e. V_{max} and K_M values, are needed. For the triazoles used in this study no PBK models or *in vitro* metabolic data from which V_{max} or K_m may be obtained have yet been developed. However, for these compounds whole body half-lives ranging from 22 to 53 hours are available (for details see supplementary material). Though the whole body half-life *per se* does not provide a PBK metabolism parameter, it allows for the setting of the ratio of the hepatic V_{max}/K_M values as a first-order metabolic rate constant in concordance with the whole body half-life.

For the glycol ethers not the parent compound, but a primary metabolite is responsible for the induced developmental toxicity (Brown *et al.*, 1984, Cheever *et al.*, 1984; Foster *et al.*, 1984; Giavini *et al.*, 1993), i.e. methoxyacetic acid (MAA), ethoxyacetic acid (EAA), butoxyacetic acid (BAA) and phenoxyacetic acid (PAA). Therefore, the kinetics of both the respective parent substance and its alkoxy acetic metabolite have to be modelled. Here existing glycol ether PBK models provided the necessary metabolism parameter information: Hays *et al.* (2000) on EGME metabolism to MAA and urinary excretion of MAA (observed plasma half-life: 20 hr), Gargas *et al.* (2000) on the metabolism of EGEE to EAA and urinary excretion of EAA (observed plasma half-life: 8 hr), Corley *et al.* (1994) on the metabolism of EGBE to BAA and urinary excretion of BAA (observed plasma half-life 1.5 hr) and Troutman *et al.* (2015) on the metabolism of EGPE to PAA, the metabolism of PAA and the urinary excretion of PAA (observed plasma half-life: 0.7 hr). These studies were also used for PBK model verification.

Critical endpoint	dLOAEL (mg/kg bw/day)	BMD10 (mg/kg bw/day)*	Reference
Fetal malformations: cardiovascular	31	38 ^a	Nelson <i>et al.</i> , 1989
Skeletal variations & retardation	46.5	83 ^a	Stenger <i>et al.</i> , 1971 ^c
Fetal viability (resorptions)	200	185 ^b	Sleet <i>et al.</i> , 1989 ^d
No effects on the fetus	NOAEL: 1000	-	ECHA disseminated REACH dossier ^e

Critical endpoint	dLOAEL (mg/kg bw/day)	BMD05 (mg/kg bw/day)	Reference
Growth	1000	507.7	Hellwig <i>et al.</i> , 1997
Growth	500 (lowest dose tested)	528.8	Ema <i>et al.</i> , 1993

For the phthalates DEHP and DBP, the embryo toxic derivatives are their monoesters, mono(2-ethylhexyl)phthalate (MEHP) and mono(n-butyl) phthalate (MBP), respectively, rather than the parent di-ester (Janer *et al.*, 2008). The metabolites are formed in the GI tract by hydrolysis of the di-phthalates (Keys *et al.*, 1999, 2000). Existing PBK models for DEHP (Keys *et al.*, 1999) and DBP (Keys *et al.*, 2000) indicate that this conversion occurs relative fast and that the formed metabolites are absorbed much faster than their respective parents. For this reason the exposure to DEHP and DBP was modelled as instantaneous conversion of an orally administered dose of these compounds to their monoalkyl metabolites, followed by absorption of the formed metabolites. As indicated by Keys *et al.*, (1999) the DEHP → MEHP conversion amounted to 6.5 %, i.e. an oral dose of 100 mg DEHP/kg bw/day resulting in the same systemic exposure to MEHP as an oral dose of 6.5 mg mono(2-ethylhexyl)phthalate/kg bw/day. Similarly, Keys *et al.* (2000) indicate 27% conversion of an oral DBP dose to MBP.

TABLE 3 Models used to estimate input parameters required for the generic PBK model.

Phys Chem parameter	QSAR models used for prediction
Log D at pH 5.4 (intestines) and pH 7.4 (blood serum)	KOWWIN v1.68 (US EPA, 2016), with JChem estimated pKa/pKb for dissociating substances, (Szegezdi and Csizmadia 2007)
Density (g/cm ³)	ChemSketch v.11 (ACD/ChemSketch 2011)
Molecular Weight (g/mol)	Calculated from structural formula
Vapour pressure (Pa)	MPBPWIN v1.43 (US EPA, 2016)
Water Solubility (mg/L)	WSKOW v1.42 (US EPA, 2016)

In vitro toxicity data

Triazoles

Existing *in vitro* data for the six triazoles, were collected from earlier work, as published by de Jong *et al.* (2011) and Hermsen *et al.* (2011). The substances were evaluated in three developmental toxicity alternative assays, the WEC, the ZET and the EST. Critical concentration levels representing thresholds of adverse effects in each of the assays were compiled. The results of all three tests were previously analyzed with a Benchmark Dose (BMD) approach, with the use of the PROAST software, and are presented in the aforesaid publications. The following benchmark responses were used as dose metrics for the *in vitro* assays: in the WEC the concentration associated with a 5% decrease in the Total Morphological Score (TMS), i.e. the $BMC_{05_{TMS}}$ (de Jong *et al.*, 2011), in the ZET the 5% decrease on the General Morphology Score (GMS), i.e. the $BMC_{05_{GMS}}$ (Hermsen *et al.*, 2011), and in the EST the concentration corresponding with a 50% decrease in the number of culture wells with beating embryoid bodies, i.e. BMC_{d50} (de Jong *et al.*, 2011).

TABLE 4 Effect of the triazoles on embryonic development in the WEC and the ZET and on the differentiation of ES cells into beating cardiomyocytes (EST), as collected from published literature.

Substance	WEC $BMC_{05_{TMS}}$ (μM) *	ZET $BMC_{05_{GMS}}$ (μM) *	EST BMC_{d50} (μM) *
FLU	19	4.8	5.7
CYP	335.9	27.7	31.8
TDI	178.6	29.2	32.2
HEX	149.9	7	16.6
MYC	138.6	30.2	30.5
TTC	272.1	80.5	35.8

**In vitro* BMC values taken from de Jong *et al.*, 2011.

Glycol ethers

Likewise, *in vitro* data were collected, as previously performed, for the glycol ethers, but in this case not for the parents, but for their embryotoxic alkoxyacetic acid metabolites. The *in vitro* data (Table 5) were taken from the published studies of de Jong *et al.* (2009) and Hermsen *et al.* (2011), for the EST and ZET, respectively. The tests were conducted directly with the toxic metabolites because the systems essentially lack metabolizing capacity (Piersma *et al.*, 2004; Verwei *et al.*, 2006). For the WEC, only data for three of the metabolites (excluding PAA) were available (Giavini *et al.*, 1993).

As for the fungicides, the Benchmark Concentrations (BMCs) were obtained for ZET and EST from the published results, $BMC_{05_{GMS}}$ (Hermsen *et al.*, 2011) and BMC_{d50} (de Jong *et al.*, 2009), respectively. BAA and PAA did not induce any embryotoxic effects in the ZET. For the WEC only LOAECs were available (Giavini *et al.*, 1993), while no data were found for PAA in this assay.

TABLE 5 Effect of the glycol ethers alkoxyacetic acid metabolites on embryonic development in the WEC and the ZET and on the differentiation of ES cells into beating cardiomyocytes (EST). Effects of the monophthalates in the WEC and EST.

Substance	WEC LOAEC (mM) ^a	ZET BMC05GMS (mM) ^b	EST BMCd50 (mM) ^c
MAA	0.1	2.7	2.4
EAA	0.2	3.1	3.4
BAA	0.4	no effect	5.2
PAA	not tested	no effect	6.2
Substance	WEC BMC05 TMS (µM) ^d	no data on ZET	EST ID50 (µM) ^e
MEHP	600		410
MBP	2900		1440

^a Giavini *et al.*, 1993, ^b Hermesen *et al.*, 2011, ^c de Jong *et al.*, 2009; Presented here is the average between the two lab results (given separately in the publication), ^d Janer *et al.*, 2008, ^e Schulpen *et al.*, 2013.

Phthalates

For the two phthalates DEHP and DBP, *in vitro* data were collected for the respective embryotoxic monoesters (MEHP and MBP), for the WEC and EST (Table 5). Unfortunately, benchmark responses were not available for the EST assay, and hence the ID50 concentrations were used, as presented in the relevant paper (Schulpen *et al.*, 2013). No information on the embryotoxic potential of the two mono-phthalates in the ZET assay could be identified in the public domain.

Correlation analysis

In order to determine correlations between the calculated PBK blood concentrations at the respective *in vivo* BMD10s and the corresponding *in vitro* BMC or LOAEC values, the triazole data were plotted against each other and analysed with a power function in excel. This procedure is in concordance with previous work of our group (de Jong *et al.* (2011), Hermesen *et al.* (2011), Piersma *et al.* (2008)).

Results

Verification of the PBK model

Triazoles

In the case of triazoles the available kinetic information was used for the calculation of the whole body half-life, which ranged from 22 hr for triadimefon to 53 hr for cyproconazole. Without exception, physicochemical QSARs incorporated in the PBK model indicated the lipophilic character for all of these compounds. As expected the PBK model showed highest triazole levels in the maternal adipose tissue. Note the relative small difference between the average blood concentration and the peak concentration (see Figure 1 for flusilazole).

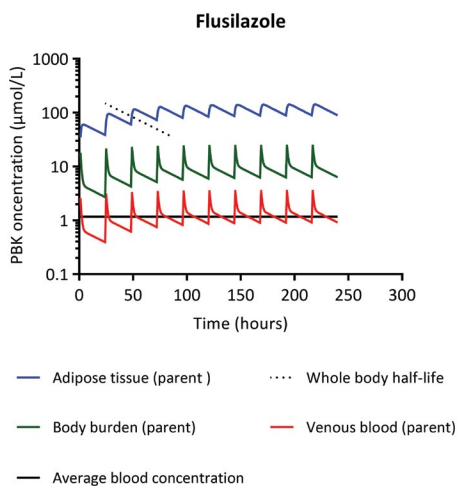


FIGURE 1 Time-course PBK model simulation of flusilazole exposure for the whole body, adipose tissue, venous blood, after oral administration of the substance for 10 consecutive days (external dose used in the simulations is the 2 mg/kg bw/day, chosen from the doses tested in the developmental toxicity study).

In a similar way, respective blood concentrations of the fungicide were calculated, for the dose range applied in the selected *in vivo* developmental toxicity study, i.e. orally 0.4 - 250 mg/kg bw/day during the whole exposure period, i.e. gestation days 7 to 16 (study data shown in Table 1). As the appropriate *in vivo* dose metric for fetal exposure, either the average or the peak-average 10-day maternal blood concentrations could be taken. The predicted blood levels were plotted against the external administered doses (Figure 2). The relationship shown in Figure 2 then was used to calculate the flusilazole average and peak-average concentrations at the BMD10 level of the *in vivo* toxicity experiment (in the case of flusilazole 2.9 mg/kg bw/day). The results indicated that there is no substantial difference between the two blood concentrations (average and average-peak), and potentially they could both represent a suitable *proxy* for fetal exposure. The same procedure was repeated for each of the triazole compounds (data not shown).

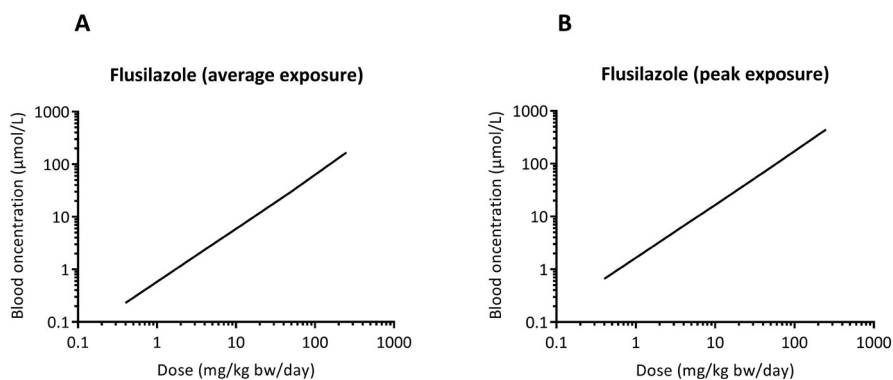


FIGURE 2 Flusilazole average venous blood (A) and peak-average venous blood (B) concentration ($\mu\text{mol/L}$) in relation to the orally administered substance (mg/kg bw/day), for 10 consecutive days, as calculated by PBK-modeling.

Glycol ethers

In the case of glycol ethers existing PBK models provided suitable model verification data, i.e. time-course curves of both the parent compounds and its primary toxic acetic acid metabolite after gavage administration. Initial simulations revealed that the default IndusChemFate, predicting negligible urinary reabsorption of glycol ether metabolites, grossly overpredicted the clearance of such metabolites from the blood (data not shown). This overprediction could be avoided by incorporating substantial urinary reabsorption of glycol ether metabolites from tubular urine, the latter being in concordance with the modelling of the formation of glycol acetic from glycol (Corley *et al.*, 2005). Figure 3 illustrates the PBK simulations for EGME/MAA in venous blood as made with the modified IndusChemFate model, after oral exposure to the parent substance. The produced PBK results were close to the *in vivo* measured concentrations from the experimental study of Hays *et al.* (2000), albeit with slight underprediction (Figure 3).

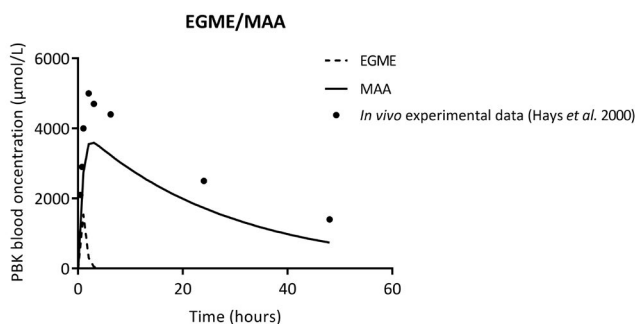


FIGURE 3 Time-course PBK model simulation of the parent substance EGME and its metabolite MAA concentrations in the venous blood, after a single oral administration of EGME (3.3 mmol/kg bw) in the rat. PBK model incorporating reabsorption of MAA from tubular urine.

These results suggest that IndusChemFate can satisfactorily estimate the *in vivo* blood levels of the primary metabolite MAA, after dosing of the parent compound. Similar results were found with the other three glycol ethers and their metabolites (see supplementary material).

As for the triazoles, the PBK model was used to predict both the average and peak-average venous blood concentrations of the glycol ethers' primary metabolites in the rat, after consecutive daily oral exposure to the parent substance, for the whole dose range given in the selected developmental toxicity study (Figure 4).

The average and peak blood levels significantly differed for EAA, BAA and PAA, but not so much for MAA. The differences were more pronounced with the least potent compound BAA and with the non-developmentally toxic PAA (Figure 4).

As with the triazoles, the PBK simulated relationship between the metabolite blood concentrations and the respective oral doses of the parent substances was determined and used to translate the *in vivo* external effect doses of the parent substance, as defined by the benchmark approach (BMD10), into blood concentrations of the corresponding

alkoxyacetic acid metabolite, during the respective exposure period for each substance. As expected the difference between corresponding average and peak levels was remarkable (data not shown).

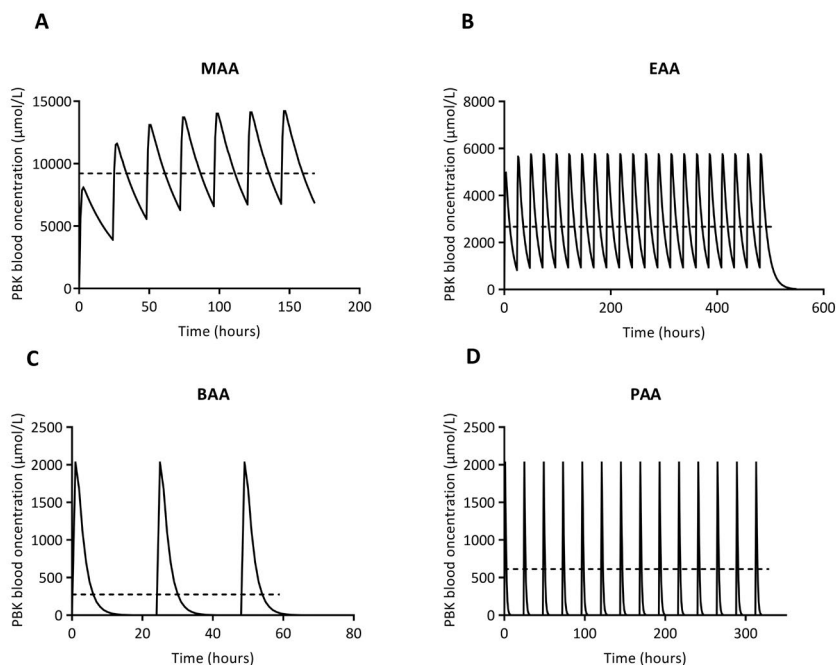


FIGURE 4 (A) Time-course PBK model simulation of MAA in venous blood, after oral administration of eight consecutive daily doses of the parent EGME (dose: 620 mg/kg bw/day). The average venous blood terminal half-life of MAA was 20 hours. (B) Time-course model simulation of EAA in venous blood, after oral administration of 21 consecutive daily doses of the parent EGEE (dose: 372 mg/kg bw/day). The venous blood terminal half-life of EAA was 8 hours. (C) Time-course model simulation of BAA in venous blood, after oral administration of three consecutive daily doses of the parent EGBE (dose: 200 mg/kg bw/day). The venous blood terminal half-life of BAA was 1.5 hours. (D) Time-course model simulation of PAA in venous blood, after oral administration of 14 consecutive daily doses of the parent EGPE (dose: 300 mg/kg bw/day). The venous blood terminal half-life of PAA was 0.7 hours.

Phthalates

As a default the IndusChemFate PBK model describes chemical kinetics as perfusion limited, i.e. kinetics being limited by the blood flowing to the organs. As shown by chemical specific PBK models this concept is unable to describe phthalate kinetics (Keys *et al.*, 1999, 2000). In concordance with the findings of Keys *et al.* indeed it was found that the default IndusChemfate PBK model leads to a gross overestimation of the concentration of mono-phthalate metabolites after gavage exposure to the parent diphtalate (data not shown). However, as also shown by Keys *et al.* the incorporation of enterohepatic circulation leads to a satisfactory description of phthalate kinetics. In the case of phthalates inherent enterohepatic circulation of the IndusChemFate model was taken into account. This lead to a satisfactory description of the time-course of the blood concentrations of toxic monoester phthalates (Figure 5), the PBK simulations are comparable to the verification

data, i.e. *in vivo* measured concentrations from the experimental studies of Keys *et al.*, 1999, 2000). As with the glycol ethers the produced simulations were close to measured data (Keys *et al.*, 1999, 2000).

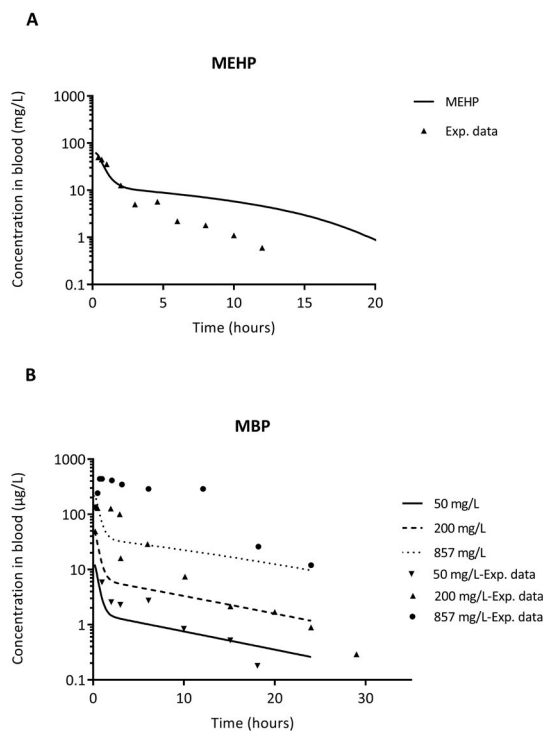


FIGURE 5 (A) Time-course PBK model simulation of MEHP in venous blood, after a single oral administration of the metabolite MEHP (100 mg/kgbw), with the PBK model incorporating enterohepatic circulation of the formed metabolite. The experimental data were taken from Keys *et al.*, (1999, Figure 5). (B) Time-course model simulation of MBP in venous blood, after oral administration of single doses of the parent DBP (doses: 50, 200, 857 mg/kgbw). PBK model incorporating enterohepatic circulation of the formed metabolite. The experimental data were taken from Keys *et al.*, (2000, Figure 4A).

The PBK model was used to predict both the average and peak-average venous blood concentrations of monoesters in the rat, after daily gavage exposure to the di-esters, for the whole dose range given in the selected developmental toxicity study (Figure 6). The two metrics differed between them clearly for both compounds.

As with the triazoles and glycol ethers the PBK simulated relationship between the metabolite blood concentrations and the respective oral doses of the parent substances, the latter being calculated as a % conversion of the parent phthalate. The resulting relationships were used to predict the plasma levels of the metabolite at the corresponding BMD05 on fetal growth (data not shown).

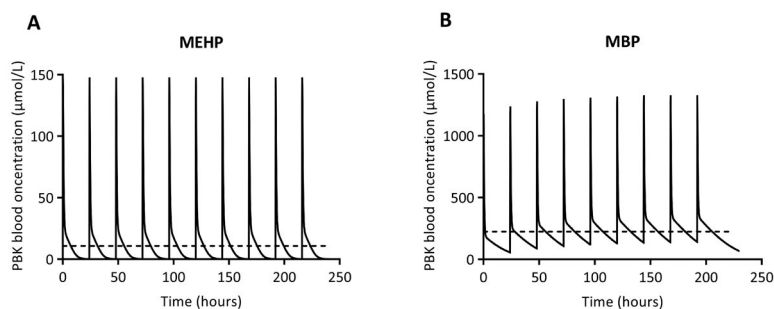


FIGURE 6 (A) Time-course PBK model simulation of the monophthalate MEHP concentrations in the venous blood, after repeated oral administration of the parent (1 g DEHP/kg bw/day \rightarrow 65 mg MEHP/kg bw/day, i.e. 6.5% conversion in the GI tract) in the rat, with activated enterohepatic circulation. (B) Time-course PBK model simulation of the monophthalate DBP concentrations in the venous blood, after repeated oral administration of the parent (1 g DBP/kg bw/d \rightarrow 270 mg MBP/kg bw/day, i.e. 27% conversion in the GI tract) in the rat, with activated enterohepatic circulation.

In vitro-in vivo comparisons

Triazoles

The fetotoxicity potency ranking of the triazoles resulting from the PBK model-predicted blood concentrations (average and peak), at the BMD10 level for skeletal variations, as well as from each alternative developmental toxicity test, is presented in Figure 7. As a dose metric for the *in vitro* assays the corresponding BMC values are used (Table 1). The results show that the triazoles' effective internal concentration (average or average-peak) after oral exposure to each individual substance, produces the same potency ranking as that based on the BMD10 values. Hexaconazole seems to be the most potent compound of all six. The overall ranking is as follows: hexaconazole > flusilazole > cyproconazole > triadimefon > myclobutanil > triticonazole. On the other hand, none of the three alternative assays could rank 100% correctly all six compounds, in agreement with their *in vivo* potency.

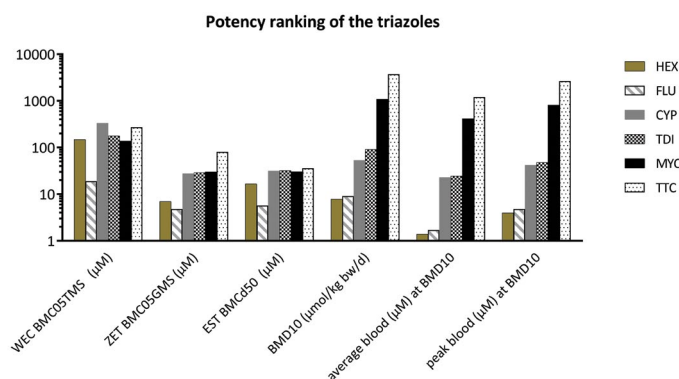


FIGURE 7 Potency ranking of the triazoles as resulting from each developmental toxicity alternative test, *in vivo* experiments and the PBK model-simulated venous blood concentrations. The potency is demonstrated either by the *in vitro* respective BMCs (μM) for the WEC, ZET and EST, the *in vivo* BMD10 skeletal variations, or the PBK simulated average and peak blood concentrations (μM) at the BMD10 level. Note that the higher the graph bar the lower the potency.

For the *in vivo-in vitro* correlations the average blood concentration was chosen as dose metric. Figure 8 illustrates the triazoles predicted average blood concentrations at the *in vivo* BMD10 levels (skeletal variations), in correlation with the BMC values for the triazole compounds, as found in the three alternative developmental toxicity assays. The highest correlation with a coefficient R^2 of 0.85 was produced with the results from the ZET. The EST showed a moderate correlation (R^2 : 0.54), and the WEC a low correlation (R^2 : 0.29).

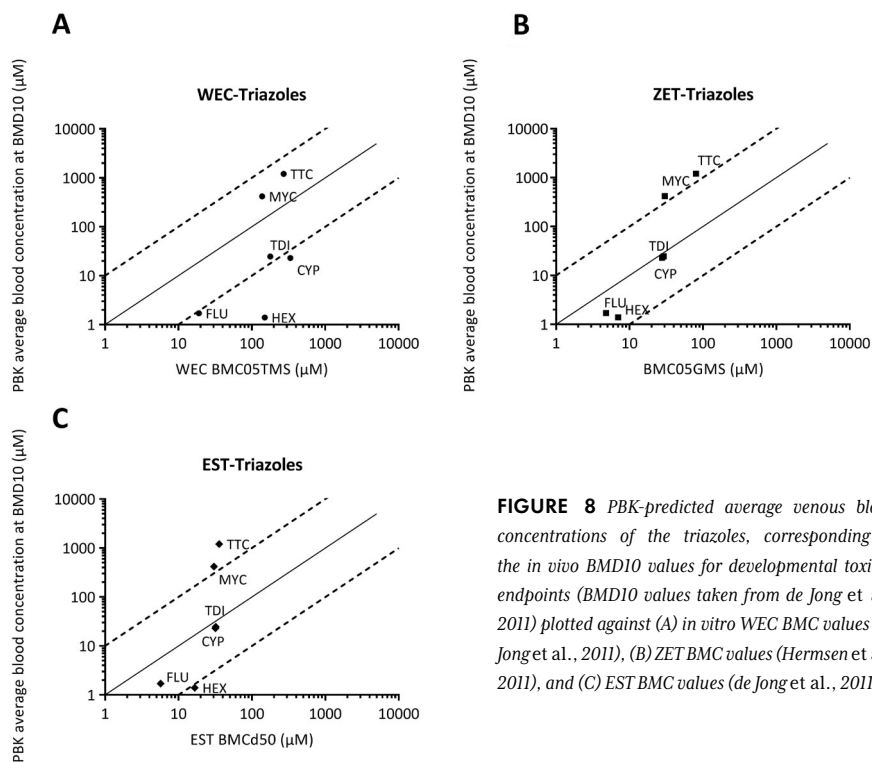


FIGURE 8 PBK-predicted average venous blood concentrations of the triazoles, corresponding to the *in vivo* BMD10 values for developmental toxicity endpoints (BMD10 values taken from de Jong et al., 2011) plotted against (A) *in vitro* WEC BMC values (de Jong et al., 2011), (B) ZET BMC values (Hermesen et al., 2011), and (C) EST BMC values (de Jong et al., 2011).

The line of identity (slope equal to 1) was drawn, in order to depict the absolute differences between effect levels recorded *in vitro* and *in vivo* estimated blood levels (Figure 8); if the data points are precisely on the line of identity the *in vitro* and PBK effect levels are exactly the same. Results within the same order of magnitude are considered to be comparable, since such differences can stem solely from biological variation (Janer *et al.*, 2008a). The compounds TDI and CYP were (almost) on the line of identity for both the ZET and the EST assays. MYC effective concentrations (*in vitro* vs. *in vivo*) differed more than one order of magnitude in these two tests (13.9-fold and 13.7-fold, respectively), with a lower potency *in vivo*. The same was seen for TTC in the ZET (14.9-fold), but a higher difference (33.6-fold) was detected with the EST. Again here, as for MYC, the compound was shown to be more toxic *in vitro* than *in vivo*. In the WEC the main outliers are HEX and CYP, for which the potency is under-predicted (respective differences with blood effect levels: 110-fold, 15-

fold, respectively). The fungicide FLU was borderline in respect to the 10-fold scale (11-fold), which is considered to be a normal variation in *in vivo* toxicity studies (Janer *et al.*, 2008b).

Glycol ethers

In contrast to the result with the triazoles, the embryotoxicity potency ranking of the glycol ethers' primary metabolites, i.e. the alkoxy acetic acids, as resulting from the PBK model-predicted blood concentrations, appeared different for the average and average-peak blood concentrations (Figure 9). The ranking for the internal estimated concentrations corresponding to the peak exposures was in agreement with the order as sorted with the *in vivo* BMD10 values: MAA > EAA > BAA. This outcome suggests that in the case of glycol ethers the developmental effect might be primarily driven by the peak exposures rather than the average exposures of the embryo. The *in vitro* potency ranking of the glycol ether metabolites was the same as the *in vivo* BMD10 ranking, confirming the *in vitro in vivo* extrapolation. BAA and PAA did not induce any embryotoxic effects in the ZET. This is in fact in agreement with the *in vivo* data. BAA is embryotoxic at doses at which maternal toxicity is also observed (Sleet *et al.*, 1989). In the oral developmental toxicity selected for EGPE, the substance, and consequently its metabolite, did not exert any adverse effects on the fetal development. Hence, comparison with these two compounds was not possible.

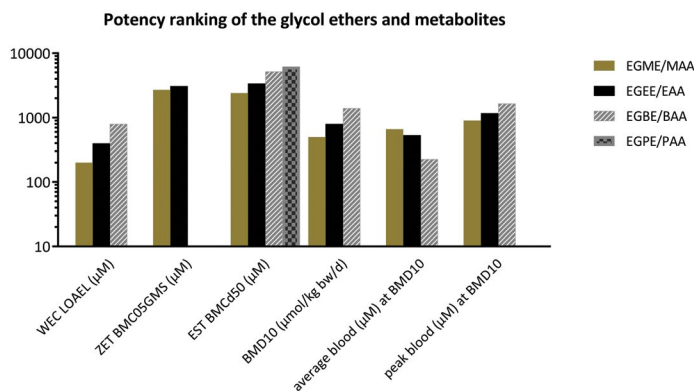


FIGURE 9 Potency ranking of the alkoxy acetic acid metabolites or the respective parents glycol ethers as resulting from each developmental toxicity alternative test, *in vivo* experiments and the PBK model-simulated venous blood concentrations. The potency is demonstrated either by the *in vitro* WEC LOAEL (μM), the *in vitro* respective BMCs (μM) for the ZET and EST, the *in vivo* BMD10 skeletal variations, or the PBK simulated average and peak blood concentrations (μM) at the BMD10 level. Note that the higher the graph bar the lower the potency.

For the *in vivo-in vitro* correlations both the average and average-peak blood concentrations were used. Figure 10 (A and B) illustrates the metabolites' predicted blood concentrations at the *in vivo* BMD10 levels, in correlation with the BMC values for the metabolites, as found in the two alternative developmental toxicity assays. The line of identity in the graphs demonstrates that in the WEC test the effective concentrations are slightly overestimated, as compared to the PBK simulated *in vivo* situation. On the other hand, in the EST the BMC

values are slightly higher in relation to the predicted effect blood concentrations at the BMD levels. This outcome indicates that the alternative assays might be over-sensitive or under-sensitive with respect to predicting the observed *in vivo* toxic effects. Nonetheless, with respect to the calculated peak blood concentrations, equivalent to the *in vivo* BMD10s (critical endpoints), the predicted effect levels by both tests did not differ more than 4.5-fold (2- to 4.5-fold).

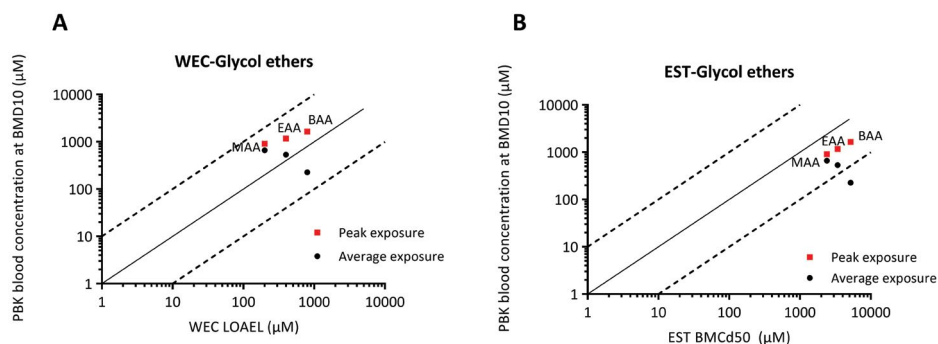


FIGURE 10 PBK-predicted average and peak venous blood concentrations of the glycol ethers alkoxyacetic metabolites (MAA, EAA and BAA), corresponding to the *in vivo* BMD10 values for developmental toxicity endpoints (BMD10 values taken from Hemsen et al., 2011 and Louisse et al., 2010) plotted against (A) *in vitro* WEC LOAEL values (Giavini et al., 1993) and (B) the *in vitro* EST BMCd50 values (de Jong et al., 2009).

Phthalates

In vivo, DEHP and DBP have comparable potency based on the two selected studies, with similar BMD05 values on fetal growth and BMD50s on malformations (Janer *et al.*, 2008). Nevertheless, in the *in vitro* assays WEC and EST, the presumed toxic monophthalate MEHP appears to be more potent than MBP (3.5- to almost 5-fold), which could perhaps be a result of kinetics differences.

Indeed, the estimated blood concentrations of the two metabolites, corresponding to the BMD05 of fetal growth (or the BMD50s on malformations), have larger relative differences than the external BMD05 values. In particular, the peak plasma concentration of MBP was almost 10-fold higher than the respective blood level for the MEHP monoester, despite the similarity in the BMD05 doses. This outcome demonstrates a difference in potency between the two metabolites, in agreement with the observations of the two alternative tests. The PBK calculated peak blood concentrations at the BMD05 and the effect levels measured in the *in vitro* assays differ an order of magnitude or less, i.e. they are within the expected variation observed also in animal experiments *in vivo* (Janer *et al.*, 2008b). However, this is not the case for the average blood concentrations (Figure 11).

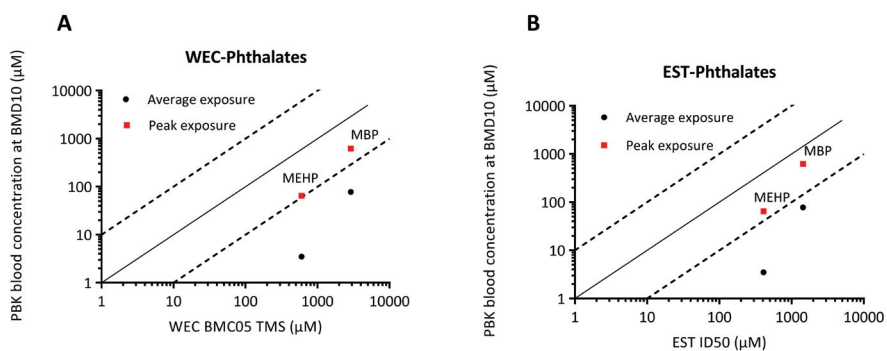


FIGURE 11 PBK-predicted average and peak venous blood concentrations of the monophthalates MEHP and MBP, corresponding to the *in vivo* BMD05 values for developmental toxicity endpoints (BMD05 on fetal growth, taken from Janer et al., 2008) plotted against (A) the *in vitro* WEC BMC05 TMS values (Janer et al., 2008) and (B) the *in vitro* EST ID50 values (Schulpen et al., 2013).

Discussion

A pivotal step towards QIVIVE concerns the correlation of the toxic potency of compounds in *in vitro* systems with that observed *in vivo*. As a first tier this may be obtained by direct comparison of *in vitro* biologically active concentrations with *in vivo* effective doses. This comparison may be improved by comparing biologically active *in vitro* and *in vivo* concentration at the cellular level, i.e. the concentration delivered at the relevant target site. *In vitro* this is relatively easy, initially being the nominal concentrations added to the cells. However, *in vivo* the delivery of an administered dose to the cells is subsequently affected by the ADME processes. In other words, linking *in vitro* to *in vivo* dosimetry, needs the integration of the kinetics of both systems. Though *in vivo* kinetic PBK models have been shown to be an indispensable tool here, they are mostly chemical - (Li *et al.*, 2017; Louisse *et al.*, 2105; Strikwold *et al.*, 2103) or chemical class-(Louisse *et al.*, 2010; Strikwold *et al.*, 2016) specific. The purpose of the present work was, as a proof of principle, to examine whether a PBK model with features which are in line with generic PBK modelling can be used for the extrapolation of *in vitro* observed developmental toxicity to the *in vivo* situation for three different classes of chemicals known to be developmentally toxic in the rat, i.e. the triazoles, the glycol ethers and the phthalates. By employing the model for these diverse classes, we survey the generic nature and applicability domain of the model used.

Feasibility of IndusChemFate a generic PBK model

The results of this study show that PBK modelling is able to extrapolate *in vitro* reproductive toxicity to systemic exposure in the intact organism, thereby refining the extrapolation paradigm previously applied by our group (de Jong *et al.*, 2011; Hermesen *et al.*, 2011). Based on input parameters taken either from previously reported PBK models (metabolism parameters for glycol ethers and phthalates), physicochemical QSARs (all compounds) and from published regulatory literature (whole body half-life of triazoles) our results demonstrate that IndusChemFate can simulate the *in vivo* kinetics in the rat, for widely different chemical compounds. IndusChemFate incorporates several key

features of a generic modelling approach : open access, inclusion of a physiological data base, multiple exposure routes (oral, inhalatory, dermal) (Basketter *et al.*, 2012; Leist *et al.*, 2014) and species (human, rat, mouse). The model avoids the disadvantage common to the development of PBK models which is generally considered quite complex and needs mathematical and programming expertise (Bessemers *et al.*, 2014). Furthermore, it overcomes the problem pertaining to availability of all partitioning model parameters of a substance, by incorporating QSARs, developed to predict such parameters solely from physico-chemical characteristics (Jongeneelen and ten Berge, 2011). However, in addition, the model needs substantial non-QSAR input. Firstly, metabolism parameters should be available. Though such parameters may be obtained from available PBK models or by fitting the model to experimental *in vivo* kinetics preferably they should be obtained from *in vitro* experimental measurements using cellular or subcellular organ fraction. In this context the *in vitro* measurements of these parameters by Green *et al.*, (1996) for glycol ethers still are exemplary. Secondly, essential chemical characteristics such as reabsorption from tubular urine (glycol ether metabolites) and stability in the gastrointestinal tract (phthalate parent compounds) *a priori* should be known in order to lead to successful modelling. In this context the Kow based QSAR for tubular reabsorption clearly was found at variance with the *in vivo* kinetics of glycol ether metabolites.

IndusChemFate: Fine tuning

In IndusChemFate the current model, blood:organ partitioning is based on the distribution of the non-ionised compound, between the blood and the organs. In the case of triazoles, parent glycol ethers and phthalates this is a valid approach for the parent compounds. However for primary glycol ether and phthalate metabolites it may not, because these metabolites contain an acetic acid moiety, which at the pH of the blood or the organs is highly ionised. Though the present study and specific PBK models (Keys, 1999; 2000) indicates that the current PBK model concept gives a satisfactory description of glycol ether and phthalate kinetics without incorporation of a partitioning mechanism, which takes ionisation explicitly into account the extension of the current PBK model concept with pH dependent ionisation partitioning may improve the modelling of ionised compounds. As, in combination with perfusion-diffusion limitation, the non-ionised/ionised partitioning is the most generic chemical PBK distribution mechanism, we currently are extending the IndusChemFate model according to this mechanism.

A potential limitation is the use of maternal blood as a proxy for fetal exposure. Here it should be realised that combining *in vitro* developmental toxicity results with a quantitative measure of placental diffusion (as revealed by the BeWo transport system) was found to increase the predictive power of the *in vitro* reproductive assays with respect to *in vivo* developmental toxicity (Li *et al.*, 2015, 2016, 2017). Clearly, for such compounds *in vitro* toxicity testing should be combined with PBK modelling and the BeWo placental transport system in order to predict *in vivo* reproductive toxicity. As indicated by Li *et al.*, (2017) only in the case of a high placental transfer rate a combination of PBK modelling and an *in vitro*

3

toxicity testing suffices to predict *in vivo* developmental toxicity. In that case, maternal blood is the ideal surrogate for fetal exposure, whereas in the case of chemicals with a low placental transfer rate the PBK model should be extended with a separate fetal sub-compartment. In that case, alterations in chemical kinetics due to physiological changes occurring during pregnancy, or changes in kinetics due to placenta formation have to be taken into account. In this study it was assumed that for all substances the placental barrier is negligible. Nonetheless, as shown for triazoles (Li *et al.*, 2016) it cannot be excluded that the compounds have different transfer rates through the placenta and hence, this can influence the effect levels *in vivo*.

Peak versus average exposure

Developmental toxicity is thought to result from a relatively short exposure period, i.e. a peak, even single, exposure during a well-defined critical time period within organogenesis. The sensitive window of specific morphogenetic processes may amount to less than 2-days. In contrast, toxicity may also be related to more sustained exposure, i.e. a substantial part or even the total duration of pregnancy. Kinetically both exposure situations relate to simulating the maximal (C_{max} approach) or the average (AUC-area under the curve approach) blood concentration. In this study we considered these exposure metrics and the results indicate that, depending on the chemical's kinetic profile, both approaches may lead to different results. For example, triazoles display relatively slow kinetics. As a consequence, after repeated exposure, these chemicals are expected to reach a so-called quasi steady state situation in the body and the blood relatively quickly (see Figure 1). In such a situation additional dosing will lead to relatively low peak concentrations. Hence, the extrapolation of *in vitro* to *in vivo* does not differ much, whether based on a C_{max} or an AUC approach. This contrasts sharply with glycol ethers and phthalates which show much faster kinetics and, consequently, more variable blood kinetics after repeated exposure. As expected, the *in vitro* to *in vivo* extrapolation then may substantially differ when based on the C_{max} or the AUC approach.

In vitro/*in vivo* comparison

Previous work directly correlated *in vivo* reference values of external dose versus *in vitro* effective concentrations, for the triazoles and the glycol ethers (de Jong, *et al.*, 2009, 2011; Hermsen *et al.*, 2011). The current study used a more refined approach, i.e. a comparison of the nominal *in vitro* effective concentration with the PBK simulated concentration in the blood after gavage exposure at the level of *in vivo* reproductive toxicity were used. This comparison showed that for the triazoles, correlations pertaining to relative potency and potency ranking with integration of kinetics, remain comparable with previous correlations (de Jong *et al.*, 2011). For both the ZET and EST assays the fungicides MYC and TTC, were outside the 10-fold scale, which is considered to be a normal variation in *in vivo* toxicity studies (Janer *et al.*, 2008b). Their predicted potencies differed at least one order of magnitude from the PBK estimated plasma concentrations (ZET: 13.9-fold and 14.9-fold, EST: 13.7-fold and 33.6-fold, respectively), while *in vivo* the two compounds appeared less

potent. In the WEC the main outliers are HEX, which exerted a 110-fold lower potency in the *in vitro* assay, compared to its *in vivo* effect level, followed by CYP with a 15-fold difference.

Within the class of glycol ethers, the toxic potency and ranking obtained from all three alternative assays was already in agreement with the ranking based on *in vivo* BMD10 values (embryotoxicity) of the parent substances. The *in vitro* effective concentrations were within the range (one order of magnitude) of estimated blood concentrations, corresponding to external effective doses from animal experiments.

The two chosen phthalates, DEHP and DBP, were shown to have comparable potency in animal experimental studies, with similar BMD05 values on fetal growth and BMD50s on malformations (Janer *et al.*, 2008b). This was not seen in the alternative tests, where MEHP is 3.5- to almost 5-fold more toxic than MBP. Even so, such differences are within the allowable 10-fold scale. The calculated PBK peak blood concentrations showed an analogous pattern to the findings recorded *in vitro*, indicating that integration of kinetics in such extrapolations can quantitatively refine the comparisons. The *in vitro* effective concentrations differed less than an order of magnitude (or in one case an order of magnitude) from the plasma concentrations, corresponding to the *in vivo* BMC05s.

Previously the straightforward assumption was made that equal concentrations at the target site *in vitro* and *in vivo* will induce similar toxic effects (Louisse *et al.*, 2010, 2015; Strikwold *et al.*, 2013, 2016; Li *et al.*, 2017). Nonetheless, the interpretation of reproductive alternative assays as to what effect constitutes adversity versus non-toxic physiological changes and *in vitro* versus *in vivo* toxic potency warrants further elucidation. In the WEC, the ID20 on the total morphological score (TMS) is taken as the standard. This effect size does constitute clear adversity as a 20% reduction of TMS indicates significant retardation of embryo development. For the ZET, the ID20 on the general morphology score (GMS) is defined as the reference value, again based on a significant retardation of development at that effect size. In the EST, the ID50 on cardiomyocyte differentiation has been classically used as the easiest measure to derive on the sigmoid dose-response curves, which this method provides. This standard approach was also applied in the current comparison. The three assays used showed very comparable patterns as to *in vitro* to *in vivo* extrapolation of individual chemicals studied.

In conclusion, the IndusChemFate model was found to be capable of describing the *in vivo* kinetics of the three classes of developmental toxicants employed, though at the expense of several chemical specific adaptations.. However, future modelling will still need fine-tuning, in terms of including for instance a placental-fetal compartment, alternative partitioning mechanisms such as ionization/non-ionization, diffusion-limitation, the fate of chemicals in the GI tract and renal clearance.

Furthermore, we performed comparisons with three different developmental toxicity alternative assays. The current results indicate that for the time being it is not possible to discriminate which of the three assays outweighs the others in predicting *in vivo* toxicity. Hence, a combination of tests is preferable for predicting the endpoint of developmental toxicity.

References

- Abdullah, R., Alhusainy, W., Woutersen, J., Rietjens, I. M. C. M., and Punt, A. Predicting points of departure for risk assessment based on *in vitro* cytotoxicity data and physiologically based kinetic (PBK) modeling: The case of kidney toxicity induced by aristolochic acid I. *Food and Chemical Toxicology*, 2016, 92: 104–116.
- ACD/ChemSketch. 2011. A Free Comprehensive Chemical Drawing Package.
- Alder, S., Basketter, D., Creton, S., Pelkonen, O., van Benthem, J., Zuang, V. *et al.*, Alternative (non-animal) methods for cosmetics testing: current status and future prospects-2010. *Archive of Toxicology*, 2011; 85: 367-485.
- Bailey, J., Oliveri, A. and Levin, E. D. Zebrafish model systems for developmental neurobehavioral toxicology. *Birth Defects Res C Embryo Today*, 2013; 99(1): 14-23.
- Banker, M.J. and Clark, T.C. Plasma / serum protein binding determinations. *Current Drug Metabolism*, 2008; 9: 854-859.
- BASF AG: disseminated dossier by ECHA. Report Phenoxyethanol prenatal developmental toxicity study in Wistar rats oral administration (gavage). Testing laboratory: Schneider S (2006) Report Phenoxyethanol prenatal developmental toxicity study in Wistar rats oral administration (gavage). *Experimental Toxicology and Ecology* BASF Aktiengesellschaft, BPD ID A6.8.1.02. Report No.: 30R0498/01194. Owner company: BASF SE. Report date:2006-12-05.<https://echa.europa.eu/registration-dossier/-/registered-dossier/15160/7/9/3/?documentUUId=0762e89e-9cf7-45db-84e0-7f9c3c0d5e89>
- Basketter, D.A., Clewell, H., Kimber, I., Rossi, A., Blaauboer, B.J., Burrier, R., Daneshian, M., Eskes, C., *et al.*, Roadmap for the development of alternative (non-animal) methods for systemic toxicity testing – t4 report. *ALTEX*, 2012; 29, 3–91.
- Bessemis, J. G., Loizou, G. Krishnan, K., Clewell, H. J., Bernasconi, C. Bois, F. *et al.*, PBTK modelling platforms and parameter estimation tools to enable animal-free risk assessment. Recommendations from a joint EPAA – EURL ECVAM ADME workshop. *Regulatory Toxicology and Pharmacology*, 2014; 68: 119-139.
- Blaauboer, B.J. The contribution of *in vitro* toxicity data in hazard and risk assessment: Current limitations and future perspectives. *Toxicology Letters*, 2008; 180: 81–84.
- Blaauboer, B. J. Biokinetic modeling and *in vitro-in vivo* extrapolations. *Journal of Toxicology and Environmental Health, Part B Critical Reviews*, 2010; 13: 242-252.
- Blaauboer, B. J., Boekelheide, K., Clewell, H. J., Daneshian, M., Dingemans, M. M. L., Goldberg, A. M., Heneweer, M., Jaworska, J., Kramer, N. I., Leist, M., Seibert, H., Testai, E., Vandebriel, R. J., Yager, J. D. , and Zurlo, J. The use of biomarkers of toxicity for integrating *in vitro* hazard estimates into risk assessment for humans. T4 Workshop Report *ALTEX*, 2012; 29, 411–425.
- Bouvier d'Yvoire, M., Prieto, P., Blaauboer, B. J., Bois, F. Y., Boobis, A., Brochot, C., Coecke, S., Freidig, A., Gundert-Remy, U. *et al.*, Physiologically-based kinetic modelling (PBK Modelling): Meeting the 3Rs Agenda. The Report and Recommendations of ECVAM Workshop 63. *ALTA*, 2007; 35: 661-671.
- Brannen, K. C., Panzica-Kelly, J. M., Danberry, T. L. and Augustine-Rauch, K. A. Development of a zebrafish embryo teratogenicity assay and quantitative prediction model. *Birth Defects Research Part B, Developmental and Reproductive Toxicology*, 2010; 89: 66–77.
- Brown, N. A., Holt, D. and Webb, M. The teratogenicity of methoxyacetic acid in the rat. *Toxicology letters*, 1984; 22(1): 93-100.
- Chapin, R., Augustine-Rauch, K., Beyer, B., Daston, G., Finnell, R., Flynn, T., Hunter, S., Mirkes, P., Sue O'Shea, K., Piersma, A., Sandler, D., Vanparys, P., and van Maele-Fabry, G. State of the Art in Developmental Toxicity Screening Methods and a Way Forward: A Meeting Report Addressing Embryonic Stem Cells, Whole Embryo Culture, and Zebrafish. *Birth Defects Research*, 2008 (Part B) 83: 446–456.
- Cheever, K. L., Plotnick, H. B., Richards, D. E., and Weigel, W. W. Metabolism and excretion of 2-ethoxyethanol in the adult male rat. *Environmental Health Perspectives*, 1984; 57: 241–248.
- Corley, R. A., Bormett, G. A., and Ghanayem, B. I. Physiologically based pharmacokinetics of 2-butoxyethanol and its major metabolite, 2-butoxyacetic acid, in rats and humans. *Toxicology and Applied Pharmacology*, 1994; 129: 61-79.
- Corley, R.A., Bartels, M.J., Carney, E.W., Weitz, K.K., Soelberg, R.A. and Thrall, K.D. Development of a physiologically based pharmacokinetic model for ethylene glycol and its metabolite, glycolic acid, in rats and humans. *Toxicological Sciences*, 2005; 85: 476-490.

- de Jong, E., Louisse, J., Verwei, M., Blaauboer, B.J., van de Sandt, J.J., Woutersen, R.A., Rietjens, I.M., and Piersma, A.H. Relative developmental toxicity of glycol ether alkoxy acid metabolites in the embryonic stem cell test as compared with the *in vivo* potency of their parent compounds. *Toxicological Sciences*, 2009; 110: 117-124.
- de Jong, E., Barenys, M., Hermesen, S. A. B., Verhoef, A., Ossendorp, B. C., Bessems, J. G. M., and Piersma, A. Comparison of the mouse embryonic stem cell test, the rat whole embryo culture and the zebrafish embryotoxicity test as alternative methods for developmental toxicity testing of six 1,2,4-triazoles. *Toxicology and Applied Pharmacology*, 2011; 253: 103-11.
- Forsby, A., and Blaauboer, B. Integration of *in vitro* neurotoxicity data with biokinetic modelling for the estimation of *in vivo* neurotoxicity. *Human & Experimental Toxicology*, 2007; 26: 333-338.
- FAO/WHO. Pesticide residues in food 2008. Report of the Joint Meeting of the FAO Panel Experts on Pesticide Residues in Food and the Environment and the WHO Core Assessment Group on pesticide residues, Rome, Italy, 9-18 September 2008.
- EFSA (European Food Safety Authority). Scientific Opinion on risk assessment for a selected group of pesticides from the triazole group to test possible methodologies to assess cumulative effects from exposure through food from these pesticides on human health. *EFSA Journal*, 2009; 7: 1167.
- Ema, M., Amano, H., Itami, T., and Kawasaki, H. Teratogenic evaluation of di-n-butyl phthalate in rats. *Toxicology Letters*, 1993; 69, 197-203.
- Ema, M. Antiandrogenic effects of dibutyl phthalate and its metabolite, monobutyl phthalate, in rats. *Congenital Anomalies*, 2002; 42: 297-308.
- ECB (European Chemical Bureau). European Union Risk Assessment Report for Bis(2-ethylhexyl) phthalate (Consolidated Final Report) 2008.
- EU RAC (Risk Assessment Committee). 2011. Annex I Background document to the Opinion proposing harmonized classification and labelling at Community level of 2-Ethoxyethanol ECHA/RAC/CLH-O-0000001587-67-01/AL.
- Flick, B. and S. Klug. Whole embryo culture: an important tool in developmental toxicology today. *Current pharmaceutical design*, 2006; 12: 1467-1488.
- Foster, P. M., Creasy, D. M., Foster, J. R., and Gray, T. J. Testicular toxicity produced by ethylene glycol monomethyl and monoethyl ethers in the rat. *Environmental Health Perspectives*, 1984; 57: 207-217.
- Gargas, M. L., Tyler, T. R., Sweeney, L. M., Corley, R. A., Weitz, K. K., Mast, T. J., Paustenbach, D. J., and Hays, S. M. A toxicokinetic study of inhaled ethylene glycol ether acetate and validation of a physiologically based pharmacokinetics model for rat and human. *Toxicology and Applied Pharmacology*, 2000; 165: 63-73.
- Genschow, E., Spielmann, H., Scholz, G., Pohl, I., Seiler, A., Clemann, N., Bremer, S., and Becker, K. Validation of the embryonic stem cell test in the international ECVAM validation study on three *in vitro* embryotoxicity tests. *Alternatives to Laboratory Animals*, 2004; 32: 209-244.
- Giavini, E., Broccia, M. L., Menegola, E., and Prati, M. Comparative *in vitro* study of the embryotoxic effects of three glycol ethers and their metabolites, the alkoxyacids. *Toxicology in vitro*, 1993; 7(6): 777-784.
- Green, C. E., Gordon, P. M., Cohen, P. M., Nolen, H. W., Peters, J. H., and Tyson, C. A. *In vitro* metabolism of glycol ethers by human and rat hepatocytes. *Occupational Hygiene*, 1996; 2: 67-75.
- Groothuis, F., A., Heringa, M., B., Nicol, B., Hermens, J. L. M., Blaauboer, B., J., and Kramer, N. Dose metric considerations in *in vitro* assays to improve quantitative *in vitro-in vivo* dose extrapolations. *Toxicology*, 2015; 332: 30-40.
- Gülden, M., and Seibert, H. *In vitro-in vivo* extrapolation of toxic potencies for hazard and risk assessment—problems and new developments. *ALTEX*, 2005; 22(special issue 2):218-225.
- Hartung, T., Blaauboer, B. J., Bosgra, S., Carney, E., Coenen, J., Conolly, R. B., Corsini, E., Green, S., Faustman, E. M., Gaspari, A., Hayashi, M., Hayes, A. W., Hengstler, J. G., Knudsen, L. E., Knudsen, T. B., McKim, J. M., Pfaller, W., and Roggen, E. L. An Expert Consortium Review of the EC-commissioned Report “Alternative (Non-Animal) Methods for Cosmetics Testing: Current Status and Future Prospects – 2010”. Report T4 Workshop Report ALTEX, 2011; 28: 183-209.
- Hays, S. H., Elswick, B. A., Blumenthal, G. M., Welsch, F., Conolly, R. B., and Gargas, M. L. Development of a physiologically based pharmacokinetic model of 2-methoxyethanol and 2-methoxyacetic acid disposition in pregnant rats. *Toxicology and Applied Pharmacology*, 2000; 163: 67-74.
- Hellwig, J., Freudenberger, H., and Jäckh, R. Differential prenatal toxicity of branched phthalate esters in rats. *Food and Chemical Toxicology*, 1997; 35: 501-512.

- Hermesen, S. A. B., van den Brandhof, E. J., van der Ven, L. T. M. and Piersma, A. H. Relative embryotoxicity of two classes of chemicals in a modified zebrafish embryotoxicity test and comparison with their *in vivo* potencies. *Toxicology in vitro*, 2011; 25(3): 745-753.
- Hermesen, S. A., Pronk, T. E., van den Brandof, E.J., van der Ven, L.T. and Piersma, A. H. Concentration-Response Analysis of Differential Gene Expression in the Zebrafish Embryotoxicity Test Following Flusilazole Exposure. *Toxicological Sciences*, 2012; 127(1): 303-312.
- Hill, A. J., Teraoka, H., Heideman, W., and Peterson, R. E. Zebrafish as a model vertebrate for investigating chemical toxicity. *Toxicological Sciences*, 2005; 86: 6-19.
- Janer, G., Verhoef, A., Gilsing, H. D. and Piersma, A.H. Use of the rat postimplantation embryo culture to assess the embryotoxic potency within a chemical category and to identify toxic metabolites. *Toxicology in vitro*, 2008a; 22: 1797-1805
- Janer, G., Slob, W., Hakkert, B. C., Vermeire, T., and Piersma, A. H. A retrospective analysis of developmental toxicity studies in rat and rabbit: What is the added value of the rabbit as an additional test species? *Regulatory Toxicology and Pharmacology*, 2008b; 50: 206-217.
- Jongeneelen, F. J., and Ten Berge, W. F. A generic, cross-chemical predictive PBTK-model with multiple entry routes running as application in MS-EXCEL; Design of the model and comparisons of predictions with experimental results. *Annals Occupational Hygiene*, 2011; 55: 841-864.
- Keys, D. A., Wallace, D. G., Kepler, T. B., Kepler, T. B., and Conolly, R. B. Quantitative evaluation of alternative mechanisms of blood and testes disposition of di(2-ethylhexyl)phthalate and mono(2-ethylhexyl)phthalate in rats. *Toxicological Sciences*, 1999; 49: 172-185.
- Keys, D. A., Wallace, D. G., Kepler, T. B., and Conolly, R. B. Quantitative evaluation of alternative mechanisms of blood disposition of di(*n*-butyl) phthalate and mono(*n*-butyl) phthalate in rats. *Toxicological Sciences*, 2000; 53: 173-184.
- Klein, S., Maggioni, S., Bucher, J., Mueller, D., Niklas, J., Shevchenko, V., Mauch, K., Heinzle, E., and Noor, F. *In silico* modeling for the prediction of dose and pathway-related adverse effects in humans from *in vitro* repeated-dose studies. *Toxicological Sciences*, 2016; 149: 55-66.
- Kramer, N. I., Krismartina, M., Rico-Rico, A., Blaauboer, B. J., Hermens, J/ L. M. Quantifying Processes Determining the Free Concentration of Phenanthrene in Basal Cytotoxicity Assays. *Chemical Research in Toxicology*, 2012; 25 (2): 436-445.
- Kroese, E., Bosgra, S., Buist, H. E., Lewin, G., van der Linden, S. C., Man, H., Piersma, A. H., Rorije, E., Schulpen, S. H. W., Schwarz, M., Uibel, F., van Vust-Lussenburg, B. M. A., Wolterbeek, A. P. M., and van der Burg, B. Evaluation of an alternative *in vitro* test battery for detecting reproductive toxicants in a grouping context. *Reproductive Toxicology*, 2015; 55:11-19.
- Leist, M., Hasiwa, N., Rovida, C., Daneshian, M., Basketter, D., Kimber, I., Clewell, H., Gocht, T., Goldberg, A., Busquet, F., Rossi, A. M., Schwarz, M., Stephens, M., Taalman, R., Knudsen, T. B., McKim, J., Harris, G., Pamies, D. and Hartung, T. Consensus Report on the Future of Animal-Free Systemic Toxicity Testing. *ALTEX*, 2014; 31: 341-356.
- Li, H., Rietjens, I. M. C. M., Louisse, J., Blok, M., Wang, X., Snijders, L., and van Ravenzwaay, B. Use of the ES-D3 cell differentiation assay, combined with the BeWo transport model, to predict relative *in vivo* developmental toxicity of antifungal compounds. *Toxicology In vitro*, 2015; 29: 320-328.
- Li, H., Flick, B., Rietjens, I. M. C. M., Louisse, J., Schneider, S., and van Ravenzwaay, B. Extended evaluation on the ES-D3 cell differentiation assay combined with the BeWo transport model, to predict relative developmental toxicity of triazole compounds. *Archives of Toxicology*, 2016; 90 (5): 1225-37.
- Li, H., Zhang, M., Vervoort, J., Rietjens, I. M. C. M., van Ravenzwaay, B., and Louisse, J. Use of physiologically based kinetic modeling-facilitated reverse dosimetry of *in vitro* toxicity data for prediction of *in vivo* developmental toxicity of tebuconazole in rats. *Toxicology Letters*, 2017; 266: 85-93.
- Louisse, J., de Jong, E., van de Sandt, J. J. M., Blaauboer, B. J., Woutersen, R. A., Piersma A. H., Rietjens, I. M. C. M., and Verwei, M. The use of *in vitro* toxicity data and physiologically based kinetic modeling to predict dose-response curves for *in vivo* developmental toxicity of glycol ethers in rat and man. *Toxicological Sciences*, 2010; 118: 470-484.
- Louisse, J., Bosgra, S., Blaauboer, B. J., Rietjens, I. M. C. M., and Verwei, M. Prediction of *in vivo* developmental toxicity of all-transretinoic acid based on *in vitro* toxicity data and *in silico* physiologically based kinetic modeling. *Archives of Toxicology*, 2015; 89:1135-1148.

- National Research Council. Toxicity Testing in the Twenty-first Century: A Vision and a Strategy. 2007. National Academies Press, Washington, D.C.
- Nelson, B. K., Vorhees, C. V., Scott, W. J. Jr., and Hastings, L. Effects of 2-Methoxyethanol on Fetal Development, Postnatal Behavior, and Embryonic Intracellular pH of Rats. *Neurotoxicology and Teratology*, 1989; 11: 273-284.
- Punt, A., Schifflers, M. J. W. A., Horbach, G. J., van de Sandt, J. J. M., Groothuis, G. M. M., Rietjens, I. M. C. M., and Blaauboer, B. J. Evaluation of research activities and research needs to increase the impact and applicability of alternative testing strategies in risk assessment practice. *Regulatory Toxicology and Pharmacology*, 2011; 61: 105-114.
- Piersma, A. H., Genschow, E., Verhoef A., Spanjersberg, M. Q. I., Brown, N. A. Brady, M., Burns, A., Clemann, N., Seiler, A. and Spielmann, H. Validation of the Postimplantation Rat Whole-embryo Culture Test in the International ECVAM Validation study on three *in vitro* embryotoxicity tests. *ATLA*, 2004; 32: 275-307.
- Piersma, A. H. Alternative methods for developmental toxicity testing. *Basic & Clinical Pharmacology & Toxicology*, 2006; 98:4 27-31.
- Piersma, A. H., Janer, G., Wolterink, G., Bessems, J. G. M., Hakkert, B. C., and Slob, W. Quantitative Extrapolation of *In vitro* Whole Embryo Culture Embryotoxicity Data to Developmental Toxicity *In vivo* Using the Benchmark Dose Approach. *Toxicological Sciences*, 2008; 101(1): 91-100.
- Piersma, A. H., Bosgra, S., van Duursen, M. B. M., Hermsen, S. A. B., Jonker, L. R. A., Kroese, E. D., van der Linden, S.C., Man, H., Roelofs, M. J., Schulpen, S. H., Schwarz, M. Uibel, F., van Vugt-Lussenburg, B. M. Westerhout, J. Wolterbeek, A. P and van der Burg, B. Evaluation of an alternative *in vitro* test battery for detecting reproductive toxicants. *Reproductive Toxicology*, 2013; 38: 53-64.
- Robinson, J. F., Verhoef, A., Pennings, J. L., Pronk, T. E., and Piersma, A. H. A Comparison of Gene Expression Responses in Rat Whole Embryo Culture and *In vivo*: Time-Dependent Retinoic Acid-Induced Teratogenic Response. *Toxicological Sciences*, 2012; 126(1): 242-254.
- Schenk, B., Weimer, M., Bremer, S., van der Burg, B., Cortvrindt, R., Freyberger, A., Lazzari, G., Pellizzer, C., Piersma, A., Schäfer, W. R., Seiler, A., Witters, H., and Schwarz, M. The ReProTect Feasibility Study, a novel comprehensive *in vitro* approach to detect reproductive toxicants. *Reproductive Toxicology*, 2010; 30: 200-18.
- Schulpen, S. H. W., Robinson, J. F., Pennings, J. L. A., van Dartel, D. A. M. and Piersma, A. H. Dose response analysis of monophthalates in the murine embryonic stem cell test assessed by cardiomyocyte differentiation and gene expression. *Reproductive Toxicology*, 2013; 35: 81-88.
- Scholz, G., Genschow, E., Pohl, I., Bremer, S., Paparella, M., Raabe, H., Southee, J., and Spielmann, H. Prevalidation of the Embryonic Stem Cell Test (EST) - A new *in vitro* embryotoxicity test. *Toxicology in vitro*, 1999; 13: 675-681.
- Seiler, A. E. M., and Spielmann, H. The validated embryonic stem cell test to predict embryotoxicity *in vitro*. *Nature protocols*, 2011; 6 (7): 961- 978.
- Sleet, R. B, Price, C. J.,; Marr, M. C. *et al.*, 1989. Teratologic evaluation of ethylene glycol monobutyl ether administered to Fischer 344 rats on either gestational days 9-11 or days 11-13 [final report]. Public Health Service, U.S. Department of Health and Human Services; NTP-CTER-86-103. Available from the National Institute of Environmental Health Sciences, Research Triangle Park, NC.
- Stenger EG, Aeppli L, Müller D, Peheim E, and Thomann P. Zur Toxikologie des Äthylenglykol-Monoäthyläthers. *Arzneimittel-Forschung (Drug Research)*, 1971; 6: 880-885.
- Strikwold, M., Spenkelink, B., Woutersen, R. A., Rietjens, I. M. C. M., and Punt, A. Combining *in vitro* embryotoxicity data with physiologically based kinetic (PBK) modelling to define *in vivo* dose-response curves for developmental toxicity of phenol in rat and human. *Archives of Toxicology*, 2013; 87: 1709-1723.
- Strikwold, M., Spenkelink, B., de Haan, L. H. J., Woutersen, R. A., Punt, A. and Rietjens, I. M. C. M. Integrating *in vitro* data and physiologically based kinetic (PBK) modelling to assess the *in vivo* potential developmental toxicity of a series of phenols. *Archives of Toxicology*, 2016; 19(1): 1-15.
- Szegezdi, J., and Csizmadia, F. A method for calculating the pKa values of small and large molecules. American Chemical Society Spring meeting, 2007.
- Tollefsen, K. E., Scholz, S., Cronin, M. T., Edwards, S. W., de Knecht, J., Crofton, K., Garcia-Reyero, N., Hartung, T., Worth, A., and Patlewicz, G. Applying Adverse Outcome Pathways (AOPs) to support Integrated Approaches to Testing and Assessment (IATA). *Regulatory Toxicology and Pharmacology*, 2014; 70(3): 629-640.

- Troutman, J.A., Rick, D.L., Stuard, S.B., Fisher, J., Bartels, M.J. Development of a physiologically-based pharmacokinetic model of 2-phenoxyethanol and its metabolite phenoxyacetic acid in rats and humans to address toxicokinetic uncertainty in risk assessment. *Regulatory Toxicology and Pharmacology*, 2015; 73: 530-543.
- US EPA. Toxicological review of ethylene glycol monobutyl ether (EGBE). EPA/635/R-08/006D. In Support of Summary Information on the Integrated Risk Information System (IRIS). November 2009.
- US EPA, 2016. Physprop database: <http://www.srcinc.com/what-we-do/environmental/scientific-databases.html>
- Verwei, M., van Burgsteden, J. A., Krul, C. A. M., van de Sandt, J. J. M., and Freidig, A. P. Prediction of *in vivo* embryotoxic effect levels with a combination of *in vitro* studies and PBPK modelling. *Toxicology Letters*, 2006; 165: 79-87.
- Wambaugh, J. F., Wetmore, B. A., Pearce, R., Strobe, C., Goldsmith, R., Sluka, J. P., Sedykh, A., Tropsha, A., Bosgra, S., Shah, I., Judson, R., Thomas, R. S., and Setzer, R. W. Toxicokinetic triage for environmental chemicals. *Toxicological Sciences*, 2015; 147, 55-67.
- Wetmore, B. A., Wambaugh, J. F., Ferguson, S. S., Sochaski, M. A., Rotroff, D. M., Freeman, K., Clewell, H. J., III, Dix, D. J., Andersen, M. E., Houck, K. A., Allen, B., Judson, R. S., Singh, R., Kavlock, R. J., Richard, A. M., and Thomas, R. S. Integration of dosimetry, exposure, and high-throughput screening data in chemical toxicity assessment. *Toxicological Sciences*, 2012; 125, 157-174.
- Wetmore, B. A., Wambaugh, J. F., Ferguson, S. S., Li, L., Clewell, H. J., Judson, R. S., Freeman, K., Bao, W., Sochaski, M. A., Chu, T.-M., Black, M. B., Healy, E., Allen, B., Andersen, M. E., Wolfinger, R. D., and Thomas, R. S. Relative impact of incorporating pharmacokinetics on predicting *in vivo* hazard and mode of action from high-throughput *in vitro* toxicity assays. *Toxicological Sciences*, 2013; 132,327-346.
- Yoon, M., Kedderis, G. L., Zhixia Yan, G., Clewell, H. J. Use of *in vitro* data in developing a physiologically based pharmacokinetic model: Carbaryl as a case study. *Toxicology*, 2015; 332: 52-66.

Supplementary Material

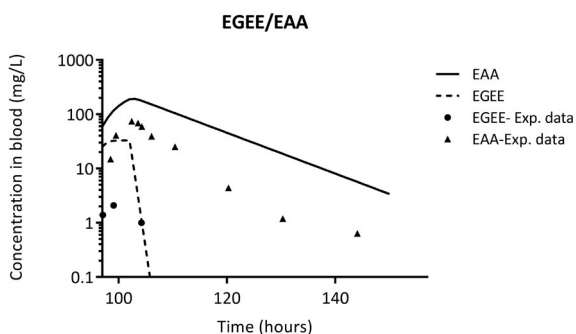
Triazoles

Whole body half-life

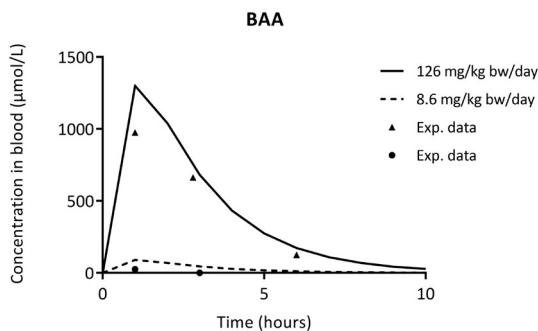
Compound	Whole body half-life (hr)	Source
Fluzilazole	30 (range: 14-57)	FAO/WHO 2007/JMPR 2008
Triadimefon	22	JMPR 2007/IPCS/WHO 2004
Myclobutanil	41 (36-50)	DAR myclobutanil, 2006
Hexaconazole	38 (36-41)	WHO 1990
Cyproconazole	53 (range: 39-62)	DAR cyproconazole, 2006
Triconazole	29 (22-33)	DAR triconazole, 2005

Glycol ethers

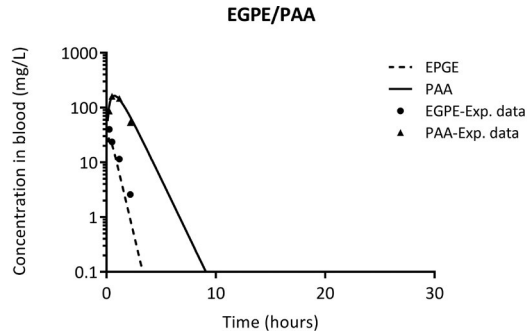
Model verification



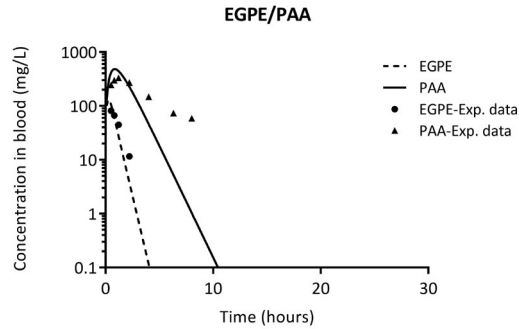
SUPPLEMENTARY FIGURE 1 PBK-model predictions of the parent substance EGEE and its metabolite EAA concentrations in blood, following inhalation of EGEE at 100 ppm (rat, repeated dose). The experimental data are taken from Cargas et al., (2000, Figures 2A & B); rats were exposed during GD 11-15.



SUPPLEMENTARY FIGURE 2 PBK-model predictions of the metabolite EAA concentrations in blood, following oral administration of the parent compound EGEE (two doses: 8.6 and 126 mg/kg bw/day). The experimental data are taken from Corley et al., (1994, Figure 3).



SUPPLEMENTARY FIGURE 3 PBK-model predictions of the parent substance EGPE and its metabolite PAA concentrations in the blood, after oral administration of EGPE (rat, single dose: 152 mg/kg bw). The experimental data are taken from Troutman et al., (2015, Figure 2A).



SUPPLEMENTARY FIGURE 4 PBK-model predictions of the parent substance EGPE and its metabolite PAA concentrations in the blood, after oral administration of EGPE (rat, single dose: 456 mg/kg bw). The experimental data are taken from Troutman et al., (2015, Figure 2B).

References Supplementary Material

- FAO/WHO. Pesticide residues in food. 2009. Toxicological evaluations. Joint meeting of the FAO panel of Experts on Pesticide Residues in Food and the Environment and the WHO Core Assessment Group, Geneva, Switzerland, 18-27 September 2007, ISBN 9789241665230. Flusilazole.
- JMPR. 2008. Pesticide residues in food 2007. Evaluations Part I-Residues. Joint meeting of FAO Plant Production and Protection Paper 192. Flusilazole.
- JMPR. 2007. Pesticide residues in food 2007. Evaluations Part I-Residues. Joint meeting of FAO Plant Production and Protection Paper 191. Triadimefon.
- IPCS/WHO. 2004. Pesticide residues in food-2004. Joint FAO/WHO meeting on Pesticide Residues. Evaluations 2004 Part II-Toxicological. Triadimefon.
- IPCS/WHO. 1990. Pesticide Residues in food. Joint Meeting of the FAO Panel of Experts on Pesticide Residues in Food and the Environment and the WHO Expert Group on Pesticide Residues, Rome, 17-26 September 1990. Toxicological Evaluations. Hexaconazole.
- Draft Assessment Report (DAR). Initial risk assessment provided by the rapporteur Member State Belgium for the existing active substance Myclobutanil of the third stage (part A) of the review programme referred to in Article 8 (2) of Council Directive 91/414/EEC. Volume 3, Annex B, B.6, May 2006.
- Draft Assessment Report (DAR) Initial risk assessment provided by the rapporteur Member State Ireland for the existing active substance Cyproconazole of the third stage (part B) of the review program referred to in Article 8(2) of Council Directive 91/414/EEC. Volume 3, Annex B, B.6, November 2006.
- Draft Assessment Report (DAR) Initial risk assessment provided by the rapporteur Member State Austria for the existing active substance Triticonazole of the second stage of the review program referred to in Article 8 (2) of the Council Derivative 91/414/EEC. Volume 3, Annex B, B.6, February 2005.

Chapter 4

Integrating *in vitro* chemical transplacental passage into a generic PBK model: A QIVIVE approach

Toxicology, 2022, Jan 15;465:153060

DOI: 10.1016/j.tox.2021.153060

Styliani Fragki ^a
Rudolf Hoogenveen ^b
Conny van Oostrom ^a
Paul Schwillens ^a
Aldert H. Piersma ^{a,c}
Marco J. Zeilmaker ^d

^aCentre for Health Protection, National Institute for Public Health and the Environment (RIVM), Bilthoven, the Netherlands

^bCentre for Statistics, Informatics and Modelling, National Institute for Public Health and the Environment (RIVM), Bilthoven, the Netherlands

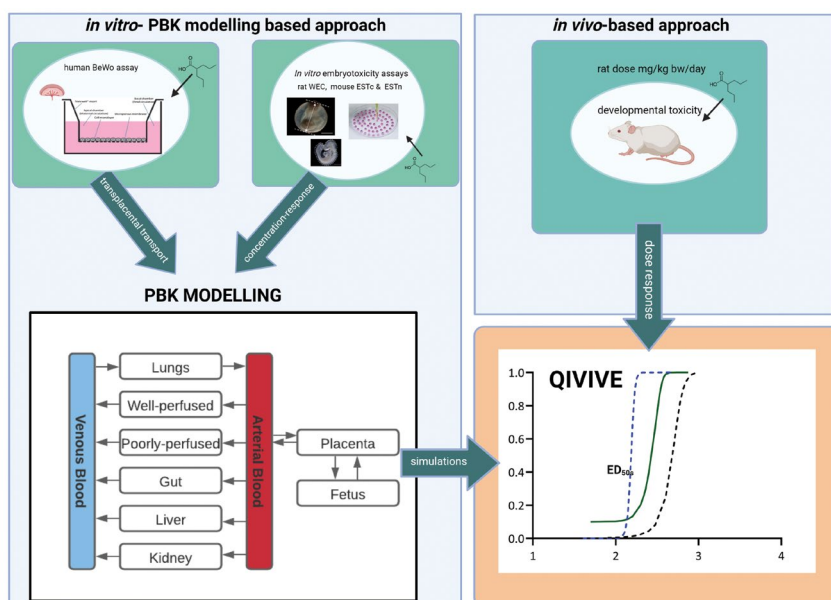
^cInstitute for Risk Assessment Sciences, Utrecht University, P.O. Box 80178, 3508 TD Utrecht, The Netherlands

^dCentre for Nutrition, Prevention and Health Services, National Institute for Public Health and the Environment (RIVM), Bilthoven, the Netherlands

Abstract

With the increasing application of cell culture models as primary tools for predicting chemical safety, the quantitative extrapolation of the effective dose from *in vitro* to *in vivo* (QIVIVE) has become increasingly important. For developmental toxicity this requires scaling the *in vitro* observed concentration effect levels to *in vivo* fetal exposure, by integration of *in vivo* kinetics, including information on the transplacental transfer. This transport of substances across the placental barrier, has been studied here with the use of the *in vitro* BeWo cell assay. Six model compounds with embryotoxic potential have been applied. Subsequently, the BeWo assay results were incorporated in an existing generic Physiologically Based Kinetic (PBK) model, extended for the rat pregnancy as a 'proof of principle'. The BeWo results illustrated different transport profiles of the chemicals across the BeWo monolayer, allocating the substances into two distinct groups: the 'quickly-transported' and the 'slowly-transported'. Exposure PBK-simulations during gestation demonstrated satisfactory kinetic predictions, when compared to experimentally measured maternal blood and fetal concentrations. A PBK modelling reverse dosimetry approach was applied to translate embryotoxicity *in vitro* concentrations-response curves of the chosen chemicals into equivalent *in vivo* dose-response curves. Selected *in vitro* tests were the Whole Embryo Culture (WEC), and the Embryonic Stem Cell test (cardiac:ESTc and neural:ESTn). The *in vitro*-based predictions were compared to rat developmental toxicity data. Overall the *in vitro* to *in vivo* comparisons suggest a promising future for the application of such approaches in the chemical safety assessment of developmental toxicity, at least for screening and prioritization purposes, although the clear need for further optimizations is acknowledged for a wider application such as in risk assessment.

Graphical Abstract



Introduction

During development the predominant physical link between the maternal circulation and the growing fetus is the placenta. As such, this transient organ has a fundamental role in fetal growth with several functions, like the exchange of nutrients and removal of waste products, hormonal secretion and transfer of maternal immunity. Amongst its functions, the placenta serves as an embryonic protection barrier from harmful xenobiotics circulating in the maternal blood (Furukawa et al. 2011; Griffiths and Campbell 2014; Pemathilaka et al. 2019). Even so, many compounds are known to eventually cross the placental passage and influence the development of the fetus; hence, developmental toxicity depends partly on the chemical's ability to transport across the placenta (Furukawa et al. 2011; Griffiths and Campbell 2014).

Transplacental transfer of toxicants can be studied with the use of the BeWo cell assay, an *in vitro* model mimicking *in vivo* transport of a chemical from maternal blood across a cell barrier into the embryo. The BeWo cell line has been derived from a human choriocarcinoma¹⁴ (Pattillo and Gey 1968), and has been confirmed to form a confluent, polarized monolayer. It has been shown to preserve many characteristics of the typical placental trophoblasts, like hormonal secretion and microvillar projections on its apical side (Friedman and Skehan 1979; Liu et al. 1997; Parry and Zhang 2007). BeWo cells consist primarily of undifferentiated cytotrophoblasts (Wice et al. 1990), i.e. the stem cells that *in vivo* form the outermost layer of the placenta villi, which comes into direct contact with the maternal blood (syncytiotrophoblasts) (Furukawa et al. 2011). The cells are grown on transwell inserts, and as such, the formed monolayer divides the well into two distinct sections: the apical maternal compartment and the basolateral embryonic compartment. The apical side is exposed to the respective chemical and its transport to the basolateral side can be measured (Li et al. 2013).

In the field of chemical safety assessment, the evaluation of substances is at the moment evolving towards an animal-free setting and therefore, there is a joint effort on the utilization of *in vitro* approaches for predicting toxicity (Adeleye et al. 2015; Hartung 2018; Knudsen et al. 2015). For the endpoint of developmental toxicity various *in vitro*/alternative assays have been designed, such as the rodent post-implantation WEC (Chapin et al. 2008; Piersma et al. 2004) and the cardiac ESTc (Seiler et al. 2004; Seiler and Spielmann 2011). Both tests have already been scientifically validated by the European Centre for Validation of Alternative Methods (ECVAM) for over two decades, with respect to their capacity to distinguish different classes of embryotoxicants (Brown 2002; Genschow et al. 2002). Although these methods may not represent at the moment complete replacements for current animal tests, they can be used either as part of an *in vitro* testing battery approach or for screening and prioritization, leading as such to a reduction of animal sacrifice (RIVM 2009; Spielmann 2009). Nevertheless, one of their main disadvantages is the fundamentally different exposure conditions when compared to whole organisms, including of course the

14 Choriocarcinoma is a gestational tumor of the placental trophoblast (Friedman 1967).

4

absence of the placental barrier. As such, to overcome this limitation, the BeWo cell assay could potentially be applied for predicting the transport of substances across the placenta. Previously, researchers combined the embryotoxic potential of substances in the ESTc (Dimopoulou et al. 2018; Li et al. 2016; Li et al. 2015; Li et al. 2017a) and WEC (Dimopoulou et al. 2018) with results from the BeWo monolayer, thereby improving the prediction of a chemical's potency to induce *in vivo* developmental toxicity. More specifically, in the BeWo assay chemical characteristics to cross the placenta were quantified by means of the so-called apparent permeability coefficients (Papp). Thereby, Papps were used as correction factors for the *in vitro* derived effect levels, in order to compensate for the absence of placental barrier. The studies illustrated improvement of the correlation between *in vitro* and *in vivo* potency ranking of these compounds, suggesting the potential of the BeWo model application for chemical safety assessment purposes.

In general, linking the environmental chemical exposure that can produce a target tissue concentration in a whole organism to an equivalent *in vitro* toxic concentration, is a prerequisite for the application of these assays for the prediction of developmental toxicity (Blaauboer 2010; Gülden and Seibert 2006; Hartung 2018; Yoon et al. 2015). Due to the different exposure conditions, the integration of *in vivo* kinetics is essential, and thus, they shall be used as a tool for understanding the *in vitro* toxicity results and extrapolating them to human exposure (Basketter et al. 2012; Tsaïoun et al. 2016). As such, for example for developmental toxicity this would require scaling the *in vitro* observed concentration effect levels to *in vivo* actual fetal exposure. In general, implementation of kinetics in QIVIVE can be facilitated by the use of Physiologically Based Kinetic (PBK) models (Adler et al. 2011; Bessems et al. 2014; Bouvier d'Yvoire et al. 2007; Hartung et al. 2011; Punt et al. 2011). Earlier, we employed a generic PBK model (IndusChemFate) in order to compare PBK-predicted blood concentrations which correspond to toxic *in vivo* effect levels from animal studies, with the respective *in vitro* effect levels (Fragki et al. 2017). In this approach, it was hypothesized that maternal blood concentrations could serve as a surrogate for fetal exposure, thus, assuming a negligible effect of the placenta as a barrier for substances reaching the growing fetus. However, xenobiotics are known to have different transplacental transfer rates that depend on their physicochemical properties (Pacifi and Nottoli 1995), and hence, information on the transplacental passage is indispensable for extrapolating *in vitro* observed toxicity to the *in vivo* situation. Furthermore, the applied PBK model was not suited for simulating fetal exposure. Finally, changes in chemical kinetics because of physiological alterations occurring in the maternal body during gestation were not yet considered.

The aim of the present study was to extend the previous QIVIVE generic PBK modelling approach by incorporating physiological alterations occurring in the maternal body during gestation, placental transfer based on the BeWo cell assay and fetal growth. The term generic signifies here a predictive tool that is relatively simple and user-friendly, and can be applied for a range of chemicals, among them data-poor chemicals. The original model

(IndusChemFate) (Jongeneelen and Berge 2011) contains a pre-defined compartmental structure with species-specific information, whereas substance-specific parameters have to be inserted. Several essential parameters, such as organ:blood partition coefficients, are calculated by the model with incorporated QSARs. The previously used IndusChemFate model was extended specifically for the rat pregnancy as a 'proof of principle' approach, considering that it is the most data-rich specie with respect to developmental toxicity. This included its adaptation to account for maternal body changes during pregnancy, as well as the addition of a specific fetoplacental sub-compartment. Subsequently, we: 1) explored the capacity of the BeWo-informed PBK model to predict fetal and maternal dosimetry during pregnancy, 2) applied an *in vitro*-based PBK modelling reverse dosimetry approach in order to predict effective dose levels from *in vitro* developmental toxicity data and 3) compared effective *in vivo* dosimetry with actual *in vivo* toxicity data. To this end, six known embryotoxicants were selected as "proof of principle".

Materials and methods

Test compounds and the BeWo b30 culture

Six known developmental toxicants were selected as model compounds: flusilazole (FLU; CAS 85509-19-9), miconazole (MIC, CAS 22916-47-8), butoxyacetic acid (BAA, CAS 2516-93-0), monobutyl phthalate (MBuP; CAS 131-70-4), valproic acid (VPA; CAS 99-66-1), and 2-ethylhexanoic acid (EHA; CAS 149-57-5). In the case of FLU, VPA and EHA, the parent compound and not its metabolites is known to be the most potent with respect to developmental toxicity (EFSA 2009; FAO/WHO ; Klug et al. 1990). BAA and MBUP are the embryotoxic metabolites of ethylene glycol butyl ether (EGBE) and di(n-butyl) phthalate (DBP), respectively (Giavini et al. 1993; Janer et al. 2008b). BAA is a product of hepatic metabolism, whereas MBuP is formed after hydrolysis very rapidly in the gastrointestinal tract (Keys 2000). No such information was found for MIC. Since it belongs to the azoles' family we assumed this is the same as for other azoles (Giavini and Menegola 2010). Antipyrine (ANTI; CAS 60-80-0) and amoxicillin (AMOX; CAS 26787-78-0) were included as controls of high and low permeability of the BeWo layers, respectively. Test compounds were purchased from Sigma-Aldrich (Zwijndrecht, The Netherlands).

The BeWo b30 cell line was purchased from AddexBio (Cat. #C0030002, Lot. # 7985832; San Diego, USA). It was confirmed to be bacteria, yeast and mycoplasma negative (certificate of analysis from AddexBio). BeWo b30 cells were subcultured 2 times per week in culture medium consisting of DMEM (11960-044) supplemented with 10% (v/v) heat inactivated FBS (Greiner Bio-One) , 1% (v/v) Penicillin/Streptomycin solution (15140-122) and 1% (v/v) L-Glutamine (25030-024) under a humidified atmosphere of 5% CO₂ at 37 °C. For the transport experiments the cells were harvested by exposure to a 0.05% trypsin EDTA solution and transferred to transwell polycarbonate membranes (6.5 mm diameter, 3.0 µm pore size; Cat. # 3415, Corning Costar, USA). Cells were seeded at a density of

$\times 10^5$ cells/cm² in 0.2 mL culture medium (apical compartment), while the basolateral compartment contained 1 mL culture medium, and cultured under standard conditions (37 °C and 5% CO₂). The medium in both compartments was changed 6 - 7 x per week until day 21 of post-seeding, when the transport experiments were performed. All ingredients were obtained from Gibco (Waltham, MA, USA).

Transepithelial electrical resistance of the BeWo layer

Before the start of the transfer experiments, transepithelial electrical resistance (TEER) values were measured using a Millicell ERS-2 voltohmmeter. Millipore TEER values were corrected for wells without the presence of cells, and transformed in $\Omega \times \text{cm}^2$, by multiplying the measured values in Ω by the insert area (0.33 cm²). Only wells showing a TEER value $\geq 150 \Omega \times \text{cm}^2$ were used.

BeWo transport experiments

Transport data has been collected for the aforementioned eight substances (experiments in triplicate per concentration). Fresh stock solutions of the selected compounds were made for each respective concentration (20 mM FLU, 20 mM MIC, 400 mM MBuP, 4 M BAA, 400 mM EHA, 200 mM AMOX and 200 mM ANTI in DMSO, 400 mM VPA in medium). ANTI and AMOX were included as controls of high and low permeability of the BeWo layers, respectively. Subsequent dilutions (10 x or 5 x) in DMSO or medium were made to get the stock solutions for the respective concentrations. All stocks were diluted 400 x in medium to obtain the resulting exposure medium. The resulting exposure concentrations were 50 μM for FLU and MIC, 1000 μM for VPA, EHA and MBuP, 10000 μM for BAA, 50 μM for ANTI and 500 μM for AMOX, with a maximum concentration of 0.25% DMSO in any case. The concentrations selected were non-cytotoxic based on in house information.

At the start of the experiments, 200 μL of the exposure medium was added apically and 1 mL medium was added to the basolateral compartment (in triplicate). Cells were incubated in a humidified atmosphere with 5% CO₂ at 37°C. 100 μL of exposure medium was used as a control (time point 0 hrs). After 2, 4, 6, 8, 24 and 48 hours of incubation, samples of 100 μL were collected from the basolateral compartment for measurement and replaced by an equal volume of medium. To estimate the amount at the basolateral side for the second, the third etc. time point, a correction was made in order to compensate for the removal of the chemical at the earlier time points in accordance with previous literature (Li et al. 2013). At the end of the transport experiments, an additional sample of 100 μL was collected from the apical compartment, for calculating the recovered amount of every tested compound. Collected samples were stored at -20 °C for further analysis by UHPLC-MS analysis. At the end of the transport experiments, the transwells were washed once with medium and equilibrated for 60 min in the incubator, with 0.2 mL medium in the apical, and 1.0 mL medium in the basolateral compartment.

TEER values were determined again to verify the cell barrier integrity. Hereafter, 0.2 mL of MTT working solution was added to the apical compartment. After incubation of 60 min at 37 °C, MTT working solution was replaced by 200 µL DMSO. After 30 s of shaking, 100 µL of samples from the apical compartment were collected in a 96-well plate. The absorbance was measured at wavelengths 570 and 690 nm using an SpectraMax M2 spectrophotometer.

Ultra-high performance liquid chromatography (UHPLC) analysis

Collected samples were analysed using the Sciex Qtrap 6500 mass spectrometer – Shimadzu Nexera ultra-high performance liquid chromatography (UHPLC-MS), in order to quantify the amount of the tested compounds transferred from the apical to the basolateral compartment. Samples with 5-50 µL injection volume were separated, dependent on the analyte, on 2 analytical columns (Waters ACQUITY UPLC HSS C18 1.8 µm, 150 × 2.1 mm Part , No.186003534 or Thermo Scientific HYPERCARB 3.0 µm 50 x 2.1 mm , Part35003-052130) with a pre-column (Waters ACQUITY Part no. 186003981). The UHPLC was performed in the gradient mode. For analyzing the LC-MS data, the operating software Sciex MultiQuant 3.0.3 was used.

Data analysis of the BeWo transport experiments

The time-dependent amounts of each chemical, as measured in the apical and basolateral compartment of the BeWo layer, were described with the use of a two-compartmental model. The first compartment represents the apical side, and the second compartment the basolateral side. The differential equations that describe the change of the amounts over time are presented in the Supplementary Material (1)

Rat pregnancy PBK model structure

A generic PBK model for rat pregnancy has been developed in order to simulate exposure to the selected chemicals throughout gestation (Figure 1). This model is in essence an extension of the existing IndusChemFate model, which can perform kinetic predictions for several species, including the adult rat, but not for pregnancy. IndusChemFate comprises, next to the blood, twelve body compartments, and it can be applied for different routes of exposure (dermal, inhalation or oral), and for different exposure durations (single peak versus repeated chronic exposure). IndusChemFate has been described previously (Jongeneelen and Berge 2011), and therefore, only its extension to simulate rat pregnancy is presented here. The original model runs as an application in MS-EXCEL, but for the current work it was transformed into the R-language (R Core Team 2020). The principal change in the model structure was the addition of separate compartments for the placenta and fetus, as well as, the maternal uterus and mammary tissue. Considering the many alterations occurring within the maternal body and fetus during the gestational period, several tissue volumes and hence, their respective blood flows, were described as growing over time. These include the following: maternal adipose tissue, uterus, and mammary tissue, as

well as the placenta and fetus. The remaining maternal tissues were not considered to change during pregnancy. The body weight of the animal and the total cardiac output were adjusted accordingly. Corresponding time-dependent equations and further description on the model structure can be found in the Supplementary Material. The pregnancy model is based on the earlier published model of O'Flaherty (1994). The mean number of fetuses per litter was set at 12 (O'Flaherty 1994). Uterus: blood and mammary tissue: blood partition coefficients were based on the partition coefficients of rapidly- and slowly-perfused tissues (liver and fat), respectively. The placenta: blood partition coefficient was assumed to be similar to that of a rapidly perfused tissue (liver).

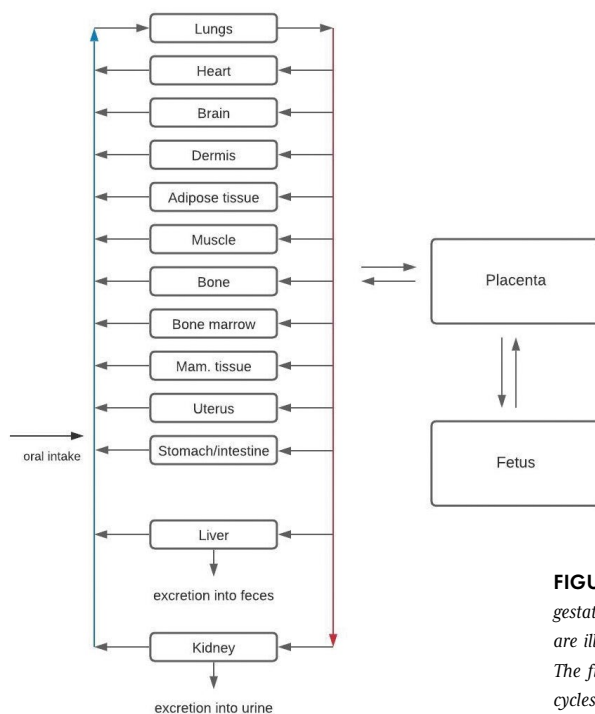


FIGURE 1 Schematic diagram of the generic PBK gestation model for the rat. Arterial and venous blood are illustrated by the red and blue lines, respectively. The figure is for the parent compound, whereas the cycles for the metabolites have a similar PBK structure.

Integration of the BeWo assay data into the PBK model

For simplification and in the context of a generic model, the fetus was considered as one single compartment. Mass of a chemical (i) flowing with arterial blood into the placenta equilibrates instantaneously with placental tissue according to a flow-limited process characterized by arterial blood into the placenta compartment at a certain flow rate ($q_p(t)$; L/hr). The partitioning between the placenta compartment and venous placental blood is characterized by the placental tissue:placental blood partition coefficient ($P_{p,i}$). Furthermore during gestation (GD_x , where x is the gestation day, 0-23) placental tissue equilibrates instantaneously with the fetal compartment characterized by a flow rate. This flow rate is equivalent to clearance (hence, symbolized as $CL_{GDx,i}(t)$ L/hr thereon). The fetal tissue:placental tissue partition coefficients are ($P_{e,i}$). The mathematical equations that

describe the chemical's mass balance throughout gestation are given in the Supplementary Material (3.1).

For ANTI an experimentally determined *in vivo* GD20 clearance has been reported for the rat (Varma and Ramakrishnan 1985). $CL_{GD20, ANTI}$ was therefore used as the starting point for the scaling of antipyrine clearance across pregnancy. Physiological scaling was applied, i.e. antipyrine clearance was assumed to be proportional to the maternal blood flow to the placenta. As mentioned in the Supplementary Material two parameters were estimated by the *in vitro* measured data, 'pc' and 'flow'. The parameter 'flow' is equivalent to 'clearance' of the chemical from one compartment to the other. Using the *in vivo* clearance of ANTI together with the modelled *in vitro* BeWo estimated clearances for each chemical would enable a biologically sound extrapolation of the *in vitro* estimated value into an *in vivo* predicted clearance (see Supplementary Material for the mathematical equations, sections 3.2 & 3.3).

Bile, enterohepatic circulation and fecal excretion

In the original IndusChemFate model the enterohepatic circulation is activated by setting the enterohepatic circulation rate at >0 (ECR, hr^{-1} , default value: 0). The ECR reflects the mass flow in the liver being discharged to the GI via the bile ($\sim ECR * AM_l(t)$, with $AM_l(t)$ the amount in the liver) relative to the mass flow via the venous blood flowing out of the liver ($\sim Q_l * C_l(t)/P_l$, with Q_l being the hepatic blood flow, C_l the liver concentration and P_l the liver: blood partition coefficient). For example, $ECR = 0.5$ thus corresponds with $ECR * AM_l(t) = 0.5 * Q_l * C_l(t)/P_l$. Similarly $ECR = 1$ corresponds with $ECR * AM_l(t) = Q_l * C_l(t)/P_l$. Furthermore it is assumed that all mass discharged via the bile is re-absorbed with a rate constant equal to $0.3 hr^{-1}$, i.e. ten times lower than the (default) absorption rate constant of $3 hr^{-1}$. Note that this way of modeling does not enable fecal excretion as route of excretion. To enable the feces as a route of excretion we have therefore modified the model by allowing a fraction $1-\alpha$ of biliary discharged mass to be excreted into the feces and, hence, a fraction α to be reabsorbed with a rate constant of $0.3 hr^{-1}$.

PBK modelling for the developmental toxicants

As input the model requires chemical-specific physicochemical and biochemical parameters for each substance. In the model complete (100%) absorption is considered default for all compounds, while the absorption rate into the intestinal tissue can be manually adapted. The physicochemical characteristics are used for the calculation of tissue:blood partition coefficients and renal clearance (Jongeneelen and Berge 2011). Such information was obtained from QSARs or measured values when available (Table 1, Supplementary Material). Biochemical parameters (V_{max}/K_M) were also selected from the literature (Table 1, Supplementary Material).

PBK model verification and calibration

A literature search was performed in order to identify the *in vivo* toxicokinetic data during pregnancy for the model verification, (see more details in the Supplementary Material).

PBK model predictions for the maternal blood and embryo (mainly C_{max} and T_{max}, but also AUC when possible) were compared to experimental data when available. When necessary model parameters were optimized for better model fitting.

PBK model predictions for developmental toxicity at BMD₁₀

Developmental toxicity studies relevant for the six substances were also collected from the open literature (Table 1). The animal model was the rat, exposed orally, while other routes of administration and other species were not considered. Exposure periods of standard design, including the critical window for developmental toxicity such as gestation days (GD) 6 to 15, or 7 to 16, were preferred; when not possible other exposure scenarios were included. Studies performed under GLP and based on recognized guidelines were also given priority. In the case of BAA and MBuP, the embryotoxic derivatives of EGBE and DBP, *in vivo* developmental toxicity was based on studies with the parent substances. Studies with at least one control group and three dose groups were chosen in order to allow analysis using the Benchmark Dose (BMD) approach. Benchmark doses for the most sensitive quantal (not continuous) endpoint at a 10% effect size (BMD₁₀), were determined (when possible) with the PROAST software 69.1 (Slob 2002). Eight dose-response models were fitted to the data as instructed for quantal data (EFSA 2017). The performance of each model fit was evaluated and the model with the smallest Akaike's Information Criterion (AIC) was chosen here as superior. Adverse effects for the BMD modelling were favoured when seen at the absence of maternal toxicity. The pregnancy BeWo PBK model was run for each substance at an external dose that equals the BMD₁₀ in order to predict the time-course dosimetry for the maternal blood, placenta and fetus.

TABLE 1 *Developmental toxicity of the selected chemicals in rats.*

Compound	Rat strain	Route	Exposure period
FLU	Sprague Dawley	oral gavage	GD 6-20
VPA	Sprague Dawley	oral gavage	GD 8-17
EHA	Wistar	oral drinking water	GD 6-19
MIC	not available	oral gavage	GD 7-16
EGBE (BAA)	Fischer 344	oral gavage	GD 9-11
DBuP (MBuP)	Wistar	oral gavage	GD 7-15

^a Information taken as reported in JMPR (2008). Data sufficiently provided for PROAST modelling; b information (including BMD₁₀) taken as reported in Dimopoulou et al. (2017). No data provided on the confidence intervals of the BMD₁₀; c calculated by PROAST software unless indicated otherwise.

BeWo PBK model-based reverse dosimetry for *in vitro* developmental toxicity assays

In vitro/alternative developmental toxicity assays performed with the chemicals of interest were collected from the open literature. The assays chosen were the WEC, ESTc, and the mouse neural Embryonic Stem Cell Test (ESTn) (only for VPA and EHA). WEC data for each substance were taken from: FLU and MIC (Dimopoulou et al. 2017), VPA (Klug et al. 1990), BAA (Giavini et al. 1993), MBuP (Saillenfait et al. 2001); ESTc data: FLU (de Jong et al. 2011), MIC (Dimopoulou et al. 2018), VPA (unpublished data-manuscript in preparation), BAA

(de Jong et al. 2009), MBuP (Schulpen et al. 2013); ESTn data for VPA are taken from (de Leeuw et al. 2019). Not all assays were available for all six substances.

The PBK model incorporating the BeWo assay estimates, was applied in a reverse-dosimetry approach so as to convert the *in vitro* toxicity concentration-response curves to *in vivo* dose-response curves. The *in vivo* dose metric selected for relating exposure to toxicity was the maximal concentration in the fetal tissue (C_{max}), since developmental effects are typically attributed to peak concentrations. Therefore, all nominally applied concentrations from the alternative assays were considered equal to the fetal C_{max} concentration and transformed to the corresponding external exposure using the pregnancy PBK model. The calculated external doses were analysed with PROAST (Slob 2002) in order to obtain the predicted *in vivo* dose-response curves. For a quantitative comparison with the experimentally observed *in vivo* data the ED₅₀ 90% confidence interval was calculated, which is denoted by its lower (BMDL₅₀) and upper (BMDU₅₀) limits. The ED₅₀ is defined as the dose that corresponds with an estimated risk of 50% and it was chosen here as it is considered the most stable point of the dose-response curve for quantal data (Slob 1999). Model averaging was applied in order to obtain a single model averaged ED₅₀ 90% confidence interval (EFSA 2017) The following benchmark responses were used: in the WEC the concentration associated with a 50% decrease in the Total Morphological Score (TMS) or 50% increase in the number of abnormal embryos, in the ESTc the concentration corresponding with a 50% decrease in the number of culture wells with beating embryoid bodies, and in the ESTn 50% increase in embryoid bodies defined as less than 75% intact surrounding corona of neurites relative to controls. In all cases these were analysed as quantal data, except for the WEC tests with

Doses mg/kg bw/d	Critical endpoint	BMD ₁₀ mg/kg bw/d (90% CI) ^c	Reference
0, 0.5, 2, 10 or 50	skeletal abnormalities	12 (8.8-16.4)	Munley (2000) ^a
0, 200, 500, 600, or 800	malformations	195 (100-473)	Binkerd et al. (1988)
0, 100,300, or 600	skeletal malformations	190 (68.5-350)	Pennanen et al. (1992)
not available	skeletal abnormalities	107 ^b	Ito (1976)
0, 30, 100, or 200	resorptions	199 (171-264)	Sleet (1989)
0, 500, 630, 750, 1000	resorptions	454 (282-633)	Ema et al. (1993)

TMS responses which were analysed as continuous. Accordingly, for the experimentally observed *in vivo* developmental toxicity data the model averaged ED₅₀ 90% confidence interval was obtained with PROAST, for the same critical endpoint as selected above for the BMD₁₀ derivation (see Table 1, Materials and methods, sub-section PBK modelling for the developmental toxicants). The resulting lower bound of the underlying ED₅₀ (BMDL₅₀) derived from the *in vivo* data was compared to the respective BMDL₅₀ from the *in vitro*-based BeWo PBK modelling reverse dosimetry approach.

Results

In vitro placental transport study

Transport data in the BeWo model have been collected for the six developmental toxicants and the two controls, ANTI and AMOX. Figure 3 illustrates the increasing amount of each chemical entering in the basolateral compartment during the 48 hours of the experiment. The mass balances showed that more than 80% of the initial amount was conserved in each transport experiment, with the exception of MIC (mass balance: ~70%). In all cases, an initial linear increase of each substance was recorded in the basolateral compartment. The results clearly show that transport profiles of the chemicals across the BeWo monolayer can be rather different. In fact, the model compounds can be divided into two distinct categories: the ‘quickly-transported’ (FLU, VPA, EHA) and the ‘slowly-transported’ (MIC, MBuP, BAA). For the first class, the initial linear increase in the basolateral compartment is evolving into a steady state. This steady-state is reached within the first 24 hours, with more than 75% of chemical crossing over to the basolateral compartment. On the other hand, for the second class the transplacental passage shows a linear profile throughout the whole experimental duration, whereas an equilibrium is not yet achieved during the exposure period, implying as such that transport would continue further if the experiment was extended. As such, these data suggest that an equilibrium would be reached after the 48 hours. The slope of the curves is smaller compared to the slopes of the initial linear part in the first class, suggesting transport at considerable slower pace. As expected, ANTI (positive control) showed a high transwell passage, while AMOX (negative control) hardly crossed the cell barrier, remaining mainly at the apical side.

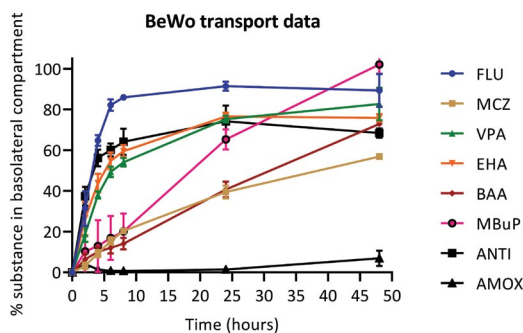


FIGURE 2 The amount of chemical detected in the basolateral compartment of the BeWo monolayer over time, expressed as percentage of the initial amount added at the apical compartment at the beginning of the experiment ($t=0$ hrs).

Data analysis of the BeWo transport experiments

The data analysis of the BeWo results was described with a two-compartmental model (Figure 4). The data describe the results of 3 parallel experiments. Estimated parameters from the BeWo assay results were the ‘flow’ and ‘partition coefficient’ (Table 1). For the substances in the ‘slowly-transported’ group, the data only partially comply with the applied modelling strategy. As such, enforcing such data on this model results in unrealistic

or else non-identifiable calculated partition coefficient values for MBuP, BAA and MIC. Therefore, for the PBK model simulations of these three chemicals thereon, respective 'partition coefficient' values, representing the fetal tissue:placental tissue partition coefficients, were set at 'one' were applied. This choice was based on the comparable water:lipid content in the placenta and fetus, consisting primarily of water (>75%), in both cases (Toro-Ramos et al. 2015).

TABLE 2 'Flow' and 'partition coefficient' parameters for each compound as estimated from the *in vitro* data analysis.

Compound	flow ($\mu\text{L/hr}$)	Partition coefficient
FLU	54.46	1.95
EHA	29.32	0.96
VPA	22.68	1.2
MBuP	7.97	non-identifiable
BAA	5.02	non-identifiable
MIC	4.96	non-identifiable
ANTI	46	0.61
AMOX	0.26	non-identifiable

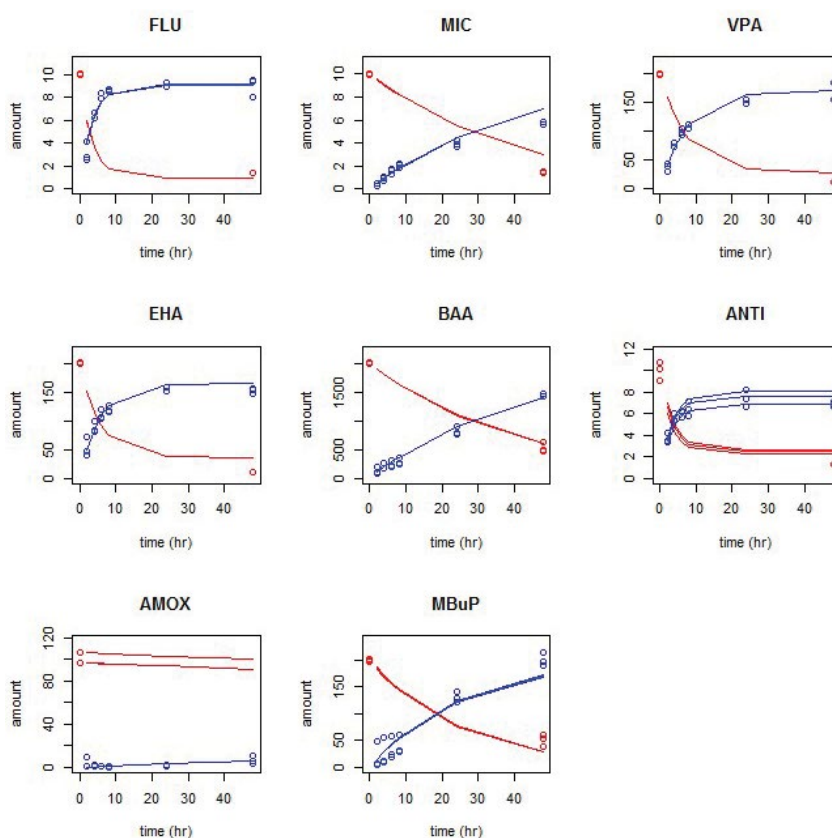


FIGURE 3 Amount of each chemical in the basolateral (blue line) and apical (red line) compartments of the BeWo transwell insert throughout the experiment, as fitted through the data. Dots represent the measured values of three replicate experiments and lines represent the model-based fitted values.

Verification of the rat pregnancy PBK model

The rat pregnancy BeWo PBK model was used to simulate the *in vivo* kinetics in the pregnant rat of the selected embryotoxic compounds. For comparisons chemical toxicokinetic information throughout gestation were collected from the open literature. As such information is scarce, data was only found for three out of the six applied substances: VPA, EHA and MBuP. In our previous work, we could simulate the *in vivo* kinetics of FLU and BAA with the original PBK model IndusChemFate, for the adult non-pregnant rat (Fragki et al. 2017). This was considered sufficient for the purpose of this work and in the absence of specific pregnancy kinetic data, the same biochemical input parameters (V_{max}/K_M) were introduced into the model. Nevertheless, it is acknowledged that such input parameters for a pregnant animal are not necessarily the same as for the non-pregnant. Verification for MIC PBK-predictions was not possible to perform; instead FLU toxicokinetic input parameters were applied for the model simulations.

Existing kinetic rat studies with VPA, EHA and MBuP during segments of pregnancy were used for the pregnancy model verification. Default generic model scenarios were initially applied with respect to absorption rate, enterohepatic cycling (none) and excretion (only renal, no fecal), which were thereafter, adapted for acquiring a better model fit to the experimental data. Initial PBK simulations for VPA revealed a faster clearance of the chemical from the maternal blood and fetus when compared to the measured values (Figure 4). This overestimation of clearance was avoided by altering the enterohepatic circulation rate, which is in accordance with VPA kinetics (Dickinson et al. 1979; Kobayashi et al. 1991; Ogiso et al. 1986). Figure 4B depicts the model predictions of VPA in blood and fetus in comparison to *in vivo* measured concentrations from experimental studies (Binkerd et al. 1988; Scott et al. 1994). The blood peak concentration C_{max} was around 3.4- to 3.9-fold underpredicted by the PBK model for one of the studies (Binkerd et al. 1988), whereas very well predicted (1.1-fold) for the other study (Scott et al. 1994). This could be the result of the different exposure period during pregnancy applied in the two studies, i.e. GD 8 and 12, respectively, or simply the expected variation between two different experiments. The model adequately captured the time of the peak concentration (T_{max} , around 2-fold difference), as well as the fetal C_{max} (1.8-fold lower compared to experimental data) (Scott et al. 1994).

Accordingly, a similar procedure was followed for its analogue EHA, with the activation of enterohepatic circulation for the modelling, albeit including here also a small fraction of fecal excretion (Figure 5); this are again as dictated by *in vivo* kinetics of the substance in the rat (English 1998). Model predictions illustrated a somewhat faster absorption and hence, the absorption rate was adapted accordingly from the 'default' scenario, by fitting the model calculated concentration values to the experimental values. Unfortunately, C_{max} and T_{max} cannot be easily discerned from the available experimental data and were not reported in the respective paper.

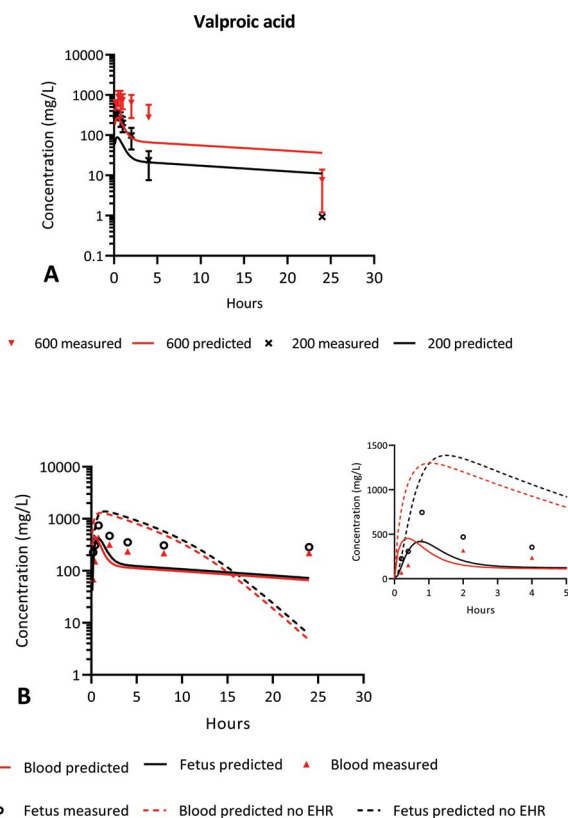


FIGURE 4 A. Concentrations of valproic acid (VPA) in blood after exposure at 200 and 600 mg/kg bw on GD8. Experimental data are taken from Binkerd et al. (1988), and they represent the mean and standard deviation (n=4). B. Concentrations of VPA in blood and fetus after exposure at 940 mg/kg bw on GD12. Experimental data are taken from Scott et al. (1994). The graph illustrates the effect of enterohepatic cycling (ECR) on the model prediction.

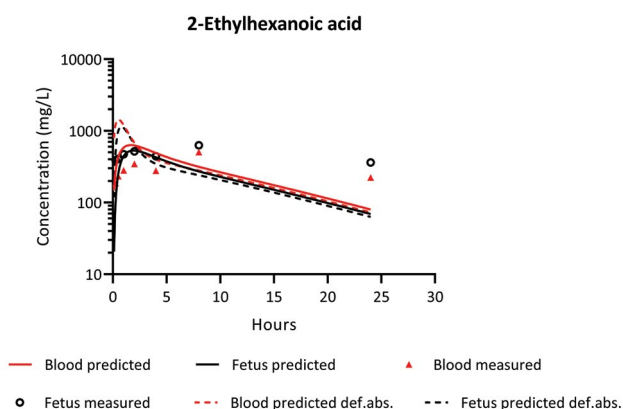


FIGURE 5 Concentrations of 2-ethylhexanoic acid (EHA) in blood and fetus after exposure at 1800 mg/kg bw on GD12. The graph illustrates the effect of absorption rate (def. abs. = default absorption rate) on the model prediction. Experimental data are taken from (Scott et al. 1994).

For both VPA and EHA, PBK-predicted embryonic concentrations were in close proximity to the predicted maternal blood levels, as also observed *in vivo*. The results show that the generic PBK model predicts the toxicokinetics of the two chemicals during certain periods of pregnancy, with less than 4- and around 2-fold differences in the predicted C_{max} and T_{max} values, respectively, for the maternal blood and embryo, when compared to the respective *in vivo* measurements.

For the toxic monoester phthalate MBuP, biochemical model input parameters (V_{max}/K_M) were introduced as previously defined by Fragki et al. (2017), together with the activation of the enterohepatic cycling observed for the phthalates (Keys et al. 1999; 2000). As discussed earlier, the compound is considered the main embryotoxic derivative of its parent DBuP (Clewel et al. 2009), formed by hydrolysis in the gastrointestinal tract (Keys 1999, 2000). This conversion occurs very quickly and the formed MBuP is absorbed much better when compared to the parent chemical, leading as such to a major exposure to MBuP (Keys 2000). The produced PBK-simulations were compared with measured data from pregnant rat toxicokinetic studies at different doses and gestation days (Clewel et al. 2009; Saillenfait et al. 1998) (Figure 6). Although in the *in vivo* studies MBuP was absorbed rapidly after oral administration, and peak maternal blood concentrations were reached within 1 to 2 hours, model predictions show an even faster T_{max} (0.3 hours) (Figure 6, Table 4). For the embryo these differences were smaller (1.3- to 2.3-fold). Adaptation of the absorption rate did not result in a better PBK model prediction (data not shown). Nevertheless, estimated C_{max} values were reasonably predicted by the model when compared to *in vivo* observations: 1.9- to 2.8-fold for the fetus, and 1.4- to 1.7-fold for the maternal blood, whereas AUC (0-8 hrs) differed 1.5- and 3.9-fold, respectively. Application of a very high dose (1500 mg/kg bw) (see Supplementary Material) did not seem to affect differently the predictions.

TABEL 4 *In vivo*-Reported and PBK model-predicted C_{max}, T_{max}, and AUC values in blood and fetus at specific timepoints during pregnancy.

Substance	Dose (mg/kg bw)	Exposure	Experimental measurements					
			Blood			Fetus		
			C _{max} (mg/L)	T _{max} (hr)	AUC (mg*hr/L) (t:hr)	C _{max} (mg/L)	T _{max} (hr)	AUC (mg*hr/L) (t:hr)
VPA	940	GD 12	431	0.8	na	745	0.8	nd
VPA	200	GD 8	341 ± 18	0.5	1019 ± 769 (0-24)	na	na	na
VPA	600	GD 8	911 ± 379	0.8 ± 0.8	6250 ± 3895 (0-24)	na	na	na
EHA	1800	GD 12	na	na	na	na	na	na
MBuP	400	GD 14	351	1.4	1467 (0-8)	84	1.4	289 (t= 0-8)
MBuP	400	GD 19	320	2	na	133	2	na

na: not available; nd: not determined; VPA: valproic acid, EHA: 2-ethylhexanoic acid, MBuP: monobutyl phthalate; hr: hours

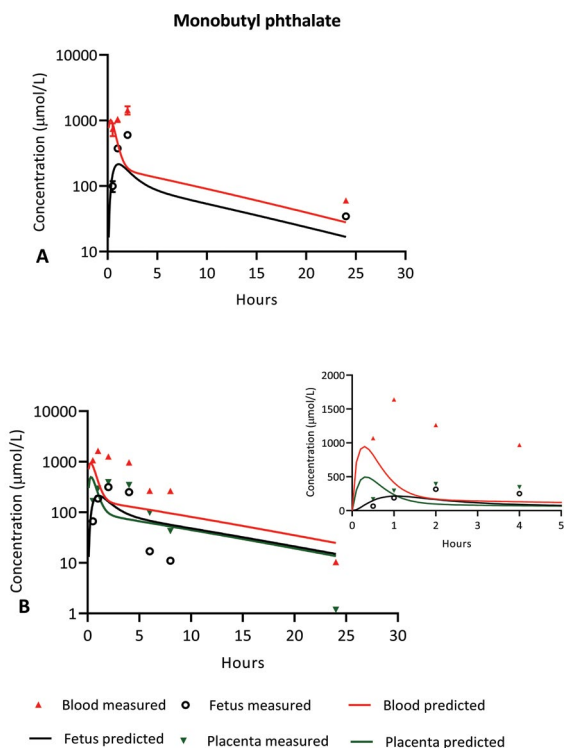


FIGURE 6 Concentrations of MBuP in blood, growing fetus and placenta after exposure to the parent DBuP. A. Dose 500 mg/kg bw (equivalent to 400 mg/kg bw MBuP), GD19, experimental data (mean ± SEM, n=4) taken from Clewell et al. (2008). B. Dose 500 mg/kg bw (equivalent to 400 mg/kg bw MBuP), GD14 experimental data (mean, n=3) taken from Saillenfait et al. (1995).

PBK-predictions						Reference
Blood			Fetus			
Cmax (mg/L)	Tmax (hr)	AUC (mg*hr/L) (t:hr)	Cmax (mg/L)	Tmax (hr)	AUC (mg*hr/L) (t:hr)	
454	0.4	nd	419	0.8	nd	Scott et al. (1994)
89	0.4	469 (0-24)	na	na	na	Binkerd et al. (1988)
271	0.4	1485 (0-24)	na	na	na	Binkerd et al. (1988)
632	1.7	nd	531	1.9	nd	Scott et al. (1994)
210	0.3	372 (0-8)	162	0.6	187 (0-8)	Saillenfait et al. (1998)
227	0.3	nd	48	1.1	nd	Clewell et al. (2009)

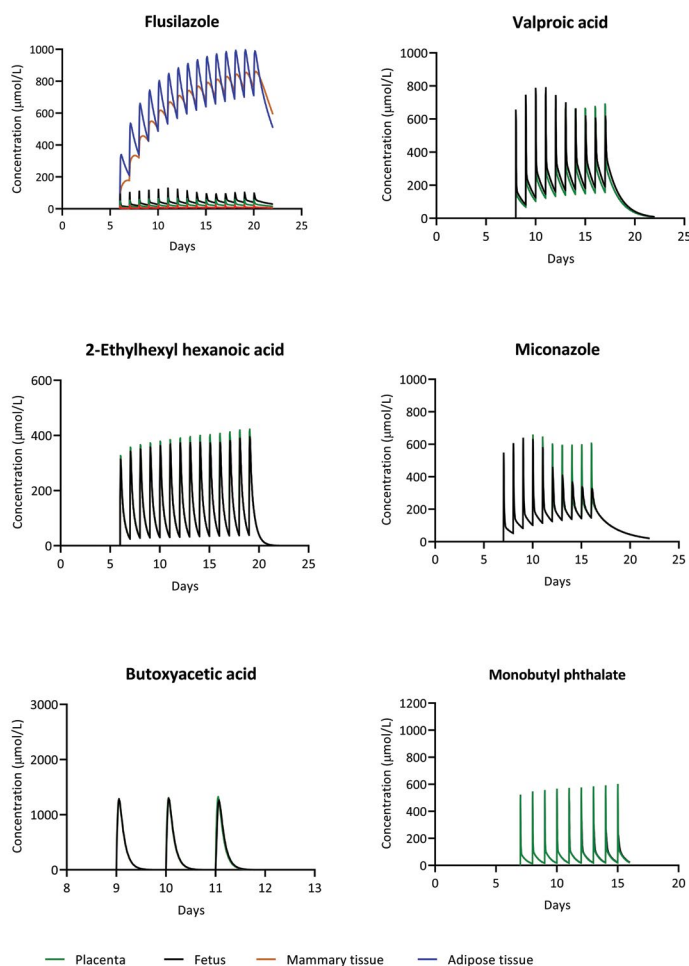


FIGURE 7 Time-course PBK model simulation of chemicals after oral administration during gestation in the rat. Model runs are performed at the BMD_{10} for the selected critical endpoint and the predicted concentrations represent the placenta and growing fetus. For the lipophilic triazoles the adipose and mammary tissue are included.

PBK model predictions at BMD_{10} for the critical endpoints

The pregnancy PBK model was run for each of the substances for the rat at an external dose that equals the BMD_{10} for the selected critical endpoint from the developmental toxicity study (see Table 2- Supplementary Material). The time-course maternal blood, placenta and fetus concentrations are depicted in Figures 7 and 8. The shape of the placental, and consequently, fetal curves show the different dynamics of the placental compartment compared to the other organs, in terms of changes of volume and blood flow. In other words, the ratio of the volume change to the blood flow change alters over time for the placenta, whereas it is a constant for the other organs. In the case of the azoles, the model estimates illustrate the lipophilic character of the compounds with high concentrations in the two fat maternal compartments, adipose and mammary tissue (see for example

flusilazole). For both substances, the PBK model predicts higher concentrations in the growing embryo (Figure 7) compared to the maternal blood (Figure 8). For VPA and EHA simulated concentrations in the two compartments are comparable, whereas for BAA, and MBuP concentrations in the maternal blood are higher compared to the embryonic levels. For VPA, EHA, and MBuP this is in line with the experimental data from animal studies (Binkerd et al. 1988; Saillenfait et al. 1998; Scott et al. 1994), throughout the whole exposure period.

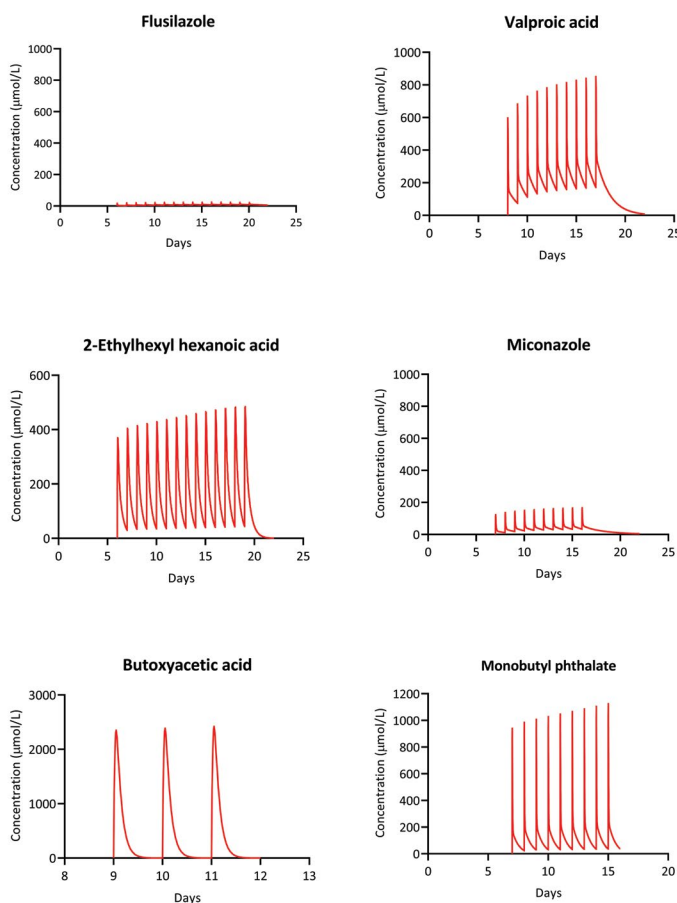


FIGURE 8 Time-course PBK model simulation of chemicals after oral administration during gestation in the rat. Model runs are performed at the BMD_{10} for the selected critical endpoint and the predicted concentrations represent the maternal blood.

Quantitative *in vitro* to *in vivo* extrapolations with the pregnancy PBK model

The predicted *in vitro*-based BeWo PBK dose response curves for embryotoxicity of FLU, VPA, EGBE (embryotoxic metabolite: BAA) and DBuP (embryotoxic metabolite: MBuP) are illustrated in Figure 9. The simulations were performed by equating the nominal *in vitro* concentrations, used in the embryotoxicity assays (ESTc, WEC, or ESTn), to the maximal concentration in the fetal tissue. Thereafter, these concentrations were translated into

respective *in vivo* oral doses with the use of the BeWo PBK model, after which the calculated *in vivo* doses were analysed with the BMD PROAST software.

In the case of BAA and MBuP, the embryotoxic derivatives of EGBE and DBuP, the BeWo PBK model translated the *in vitro* metabolite' doses into equivalent parent external doses. The calculated *in vivo* dose-response curves for the four compounds were compared with the dose-response curve of experimentally observed toxicity. Unfortunately, the information available for EHA and MIC did not allow for the derivation of dose-response curves. Nevertheless, comparisons of the ED₅₀ 90% confidence intervals were still possible for EHA, whereas for MIC the BMD₁₀ value was used (see below Table 4). Overall, the results indicate that the predicted WEC and ESTc *in vitro*-PBK dose-responses calculated by reverse dosimetry give a fairly good prediction of the *in vivo* data for VPA, EGBE and DBuP, but not for FLU.

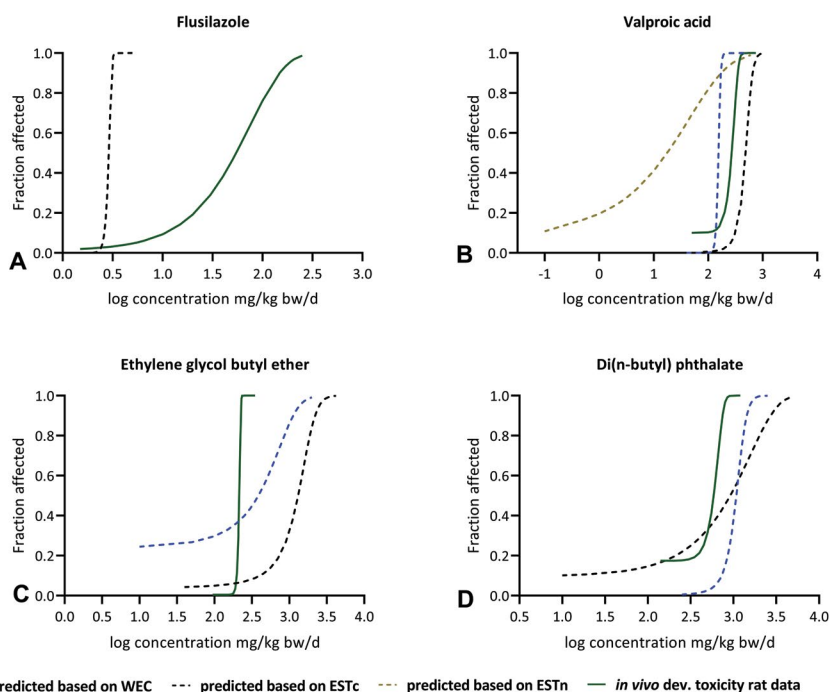


FIGURE 9 Predicted (dashed lines) and *in vivo* (solid green lines) dose-response curves for the developmental toxicity of A. flusilazole (FLU), B. valproic acid (VPA), C. ethylene glycol butyl ether (EGBE), and D. di (n-butyl) phthalate (DBuP). Predicted curves were obtained from *in vitro* concentration-response data with BeWo PBK modelling reverse dosimetry. The Cmax was chosen as dose metric for relating exposure to embryotoxicity. *In vivo* rat developmental toxicity data were collected from the open literature and the critical endpoints for the four substances are the following: skeletal abnormalities (FLU), malformations (VPA), resorptions (EGBE), resorptions (DBuP).

For a quantitative evaluation the 90% confidence interval's lower bound of the underlying ED₅₀ (BMDL₅₀) of each compound, predicted with the *in vitro*-based PBK modelling approach, was compared to the respective lower bound derived from the *in vivo* developmental toxicity studies. The ED₅₀ 90% confidence intervals were derived with PROAST by model averaging (Table 4). ED_{50s} were selected as the metric for comparison since the analysed

data for the dose-response modelling with PROAST were primarily quantal. However, it is not meant here that the ED_{50} s shall necessarily be used as starting points in risk assessment. In general, $BMDL_{50}$ s within the same order of magnitude (10-fold) were considered to be comparable, as such differences are within the range of (inter-species) biological variation (Janer 2008). The reverse dosimetry $BMDL_{50}$ s were within 10-fold (2.3-, 1.4-, 9.8-, 1.5-, 2-fold, for FLU, VPA, MIC, EGBE, and DBuP, respectively) with the WEC as embryotoxicity assay. With the ESTc $BMDL_{50}$ s differed by 1.5-, 5.7- and 1.5-fold for VPA, EGBE and DBuP, respectively, whereas more than 20-fold for the two azoles. This suggests that the ESTc might not be a good predictor of the azole's toxicity *in vivo*. Note here that the comparisons for MIC are based on BMD_{10} (instead of ED_{50}) given the lack of the relevant information. $BMDL_{50}$ predictions based on the ESTn assay for VPA and EHA did not seem to fit the respective *in vivo* $BMDL_{50}$ (>10-fold different).

TABLE 3 Model averaged ED_{50} 90% confidence intervals ($BMDL_{50}$ - $BMDU_{50}$) determined by a BMD analysis from the *in vitro*-based BeWo PBK modelling reverse dosimetry predictions and the *in vivo* developmental toxicity data. BMD analysis performed with PROAST software.

Compound	<i>In vitro</i> -PBK reverse dosimetry			<i>In vivo</i> data
	Model averaging ED_{50} 90% confidence intervals			
	WEC ^a	ESTc ^b	ESTn ^c	Rat dev. toxicity
FLU	21.6-23.2	2.86-3.07	na	49-62.4
VPA	147-162	381-496	15.1-23.1	205-374
EHA	na	na	81-133	932-13500
MIC ^d	10.89 (7.5-16.1)	2.03 (1.77-2.32)	na	107.00
EGBE	145-2530	1220-1430	na	213-996
DBuP	988-1180	737-1060	na	493-651

^a WEC data for each substance taken from: FLU and MIC (Dimopoulou et al. 2017), based on continuous data, VPA (Klug et al. 1990), BAA (Giavini et al. 1993), MBuP (Saillenfait et al. 2001); ^b ESTc data taken from: FLU (de Jong et al. 2011), MIC (Dimopoulou et al. 2018), VPA (unpublished data-manuscript in preparation), BAA (de Jong et al. 2009), MBUP (Schulpen et al. 2013); ^c ESTn data for VPA and EHA are taken from (de Leeuw et al. 2019); ^d For MIC only the BMD_{10} (Dimopoulou et al. 2017) was available without further information to allow for a proper BMD analysis and derivation of confidence intervals. Therefore, the respective BMD_{10} values were estimated for the *in vitro*-based BeWo PBK reverse dosimetry curves of the WEC and ESTc. The model fitting BMD_{50} based on the lowest AIC is presented here.

Discussion

In this study we developed a first-tier methodology that integrates placental passage of chemicals, as derived from the *in vitro* BeWo assay, into a generic PBK model modified for rat pregnancy. In concordance with the generic nature of the PBK model several simplifications of pregnancy were assumed. Within all simplifications made the rat pregnancy BeWo PBK model was found to give a reasonable description of the toxicokinetics of VPA, EHA and MBuP at the level of the rat maternal blood-placental-fetal interface. Based on these findings the BeWo PBK model was used as a proof-of-principle in a QIVIVE reverse dosimetry approach in which the dose-response as observed in three *in vitro* embryotoxicity tests was extrapolated to the *in vivo* situation. In this extrapolation the fetal

C_{max} was taken as the internal dose metric for the induction of developmental toxicity. A comparison of extrapolated dose-response curves with *in vivo* data illustrates a fairly good prediction for the WEC, followed by the EST_c for three out of the five compounds, with differences of the selected dose metric standing within the same order of magnitude (<10-fold).

Transplacental transport with the BeWo assay and mathematical analysis

Transport of chemicals across the placenta was determined with the BeWo cell line, which was previously shown to be a useful *in vitro* model for this purpose (Li et al. 2013; Poulsen et al. 2009; Prouillac and Lecoecur 2010). Earlier, BeWo assay data combined with embryotoxicity information from the EST_c and WEC have improved the prediction of a chemical's potency to induce *in vivo* developmental toxicity (Li et al. 2015, 2016, 2017, Dimopoulou 2018). Commonly, transport rates of substances until so far were expressed with the Papp values, quantifying as such only the initial transplacental transport rate, up to a maximum of 120 minutes (Li 2015, 2016, 2017, Dimopoulou 2018). This approach assumes that the velocity of the transport does not change over the course of the experiment. In our study we explore further the kinetics of chemicals across the BeWo system by prolonging the experimental duration to 48 hours (instead of 2 hours). The observations regarding the transport from the apical to the basolateral chamber reveal in fact a biphasic profile, at least for FLU, VPA, and EHA ('quickly-transported' group), characterized by a fast initial stage, and a subsequent slow stage with an established equilibrium between the two compartments. Within the paradigm of kinetic theory such a dynamic equilibrium is presumably achieved by back-and-forth transport, i.e. not only from the donor to the receiver chamber, but also *vice versa*. Reverse transport experiments with the BeWo cell line have in fact confirmed this bidirectional transport (Heaton et al. 2008; Huang et al. 2016; Magnarin et al. 2008; Utoguchi and Audus 2000), and hence, this was prescribed in the current modelling approach. For the other three substances ('slowly-transported') different kinetics are displayed, with the transplacental passage remaining linear and much slower till the end of the experiment. An equilibrium between the two compartments is not reached and the results showed that this steady state may be reached long after 48 hours. Additional timepoints (after 48 hours) should be included in future BeWo experiments, in order to achieve a steady-state concentration also for these 'slowly-transported' compounds.

Why such a clear division regarding transport profiles exists amongst the studied xenobiotics is not clear from these data. *In vivo*, the main mechanism for passage of chemicals across the placental syncytiotrophoblast is passive diffusion (Magnarin et al. 2008; Syme et al. 2004). In general, this applies to substances with a small molecular weight (<500 Da), moderate lipid solubility, low polarity and low protein binding properties. The transport of highly ionized substances is in principle not favored by the lipid membrane bilayer of the placental cells (Mathiesen et al. 2014; Syme et al. 2004). Nevertheless, active transport of substances mediated by several carrier proteins located on the apical and basal side

of the syncytiotrophoblast has also been described for a wide spectrum of chemicals (Ganapathy et al. 2000; Joshi et al. 2016). Accordingly, *in vitro*, substances cross the BeWo monolayer, being similar to the placental trophoblast, mainly via passive diffusion, but carrier-mediated transport possibly also occurs (Dallmann et al. 2019; Magnarin et al. 2008; Utoguchi et al. 1999). Consequently, mechanism of transport (passive or active), and the physicochemical characteristics will define the transport of compounds across the model cell layer.

The data obtained for passage of chemicals across the BeWo barrier were analyzed with compartmental modelling. A two-compartment model was employed with the first compartment corresponding to the apical side and the second compartment to the basolateral side of the cell layer. The BeWo data-based resulting parameters 'partition coefficient' and 'flow' characterize the transport rate in the place of the static Papp value. It shall be noted here that no discrimination between the nature of the transfer mechanism, passive diffusion or active transport, is performed given that this is implicitly factored into the two transfer parameters. No intracellular compartment was included since such experimental measurements were not performed. The mass balances showed that more than 80% of the initial amount was conserved in each transport experiment, with the exception of MIC with a mass balance of ~ 70%. This suggests that a major part of the material was transferred from one side to the other, and *vice versa*. It shall also be noted that other aspects that may influence the *in vitro* distribution of test compounds, such as non-specific binding, for example to the well's plastic, or evaporation (Kramer et al. 2012), intracellular accumulation and/or metabolism (Dimopoulou et al. 2018; Li et al. 2013) could also be accountable for the observed mass loss. Specific corrections for these aspects were not considered in the present mathematical analysis of the BeWo system (since the mass loss is not large); it cannot, however, be excluded that the calculated transport rate from the apical to the basolateral chamber is in some cases slightly underestimated.

Integration into a generic PBK model

For its integration into the PBK model the BeWo assay was modelled as the first chamber (apical side) representing the placenta and the second the fetus (basolateral side). Previous research with the BeWo assay indicated that the *rate* of transplacental transport is a determinant for developmental toxicity. To mimic *in vivo* transport from the placenta to the embryo a one cellular *in vitro* transport system was incorporated into the PBK model. In contrast to transport measured in a static *in vitro* system, which postulates a constant initial transfer rate, *in vivo* placenta to embryo transport rate is dynamic, i.e. depending on placental, embryonic and placenta-embryo interface growth. Consequently, *in vivo* a constant transfer rate is not expected. For that reason *in vivo* the best measure for induced embryonic toxicity is the time integral of the transport rate, i.e. the amount transported or the embryonic concentration, the latter requiring information on embryonic growth. Using the concentration provides the most generic risk assessment approach based on BeWo measurements, for it assumes induced toxicity to scale directly to an homogeneous

distribution over the embryo. Although this is essentially a rather crude approach, we are here interested in the events at the placenta-embryo surface and therefore, refining the embryonic compartment in sub-compartments is considered beyond the scope of this manuscript.

The PBK-simulated fetal concentrations are defined by the following elements: i) the concentration in the placenta, determined by the physicochemical properties of the substances leading to the QSAR placental tissue:maternal blood partition coefficients, ii) the transplacental clearance, determined from the BeWo parameter 'flow' and iii) the fetus:placenta partition coefficient, given (when feasible) by the BeWo-estimated 'partition coefficient'. The BeWo-derived 'flow' was extrapolated to *in vivo* transplacental clearance rates for each substance ($CL_{BeWo,r}$), by physiological scaling to the placental blood flow (as it changes throughout gestation). Prior to this, the *in vitro* 'flow' was expressed as relative flow to the positive control compound ANTI, for which *in vivo* clearance data in the rat are available (Varma 1985). Our method is in line with and further refines a previous attempt to translate BeWo-derived Papps into *in vivo* transplacental clearance, where allometric instead of physiological scaling was applied (Strikwold et al. 2017).

The fetus:placenta partition coefficients were used *per se* as determined from the *in vitro* model, for the 'quickly-transported' group of chemicals. For the 'slowly-transported' group, with unidentifiable partition coefficients, values of one were applied, suggesting that the chemical concentrations for the two compartments are equal at steady-state. Although this is an arbitrary choice, kinetic animal data during rat pregnancy for MBuP (Saillenfait et al. 1998) suggest that it is defensible, at least for this substance. Such studies could not be found for BAA and MIC. Future BeWo experiments, as suggested above, are expected to clarify this further.

Feasibility of the generic PBK model

Generic PBK models, by definition, may have lower accuracy compared to models designed specifically for a single (or small group) of chemicals, and usually in a data-rich environment, where they can be properly evaluated and calibrated so as to fit the experimental data. Nevertheless, generic models have a much larger applicability domain, they can be run with a relatively small amount of substance-specific input parameters, in contrast to heavy parameterization normally required for specific models (Bessemers et al. 2014; Jamei 2016a), allowing as such their wider application in a data poor environment. Within the context of generic PBK modelling, the model presented here shall be considered to provide reasonable estimations of the *in vivo* pregnancy toxicokinetics for VPA, EHA, MBuP, as shown by some experimental verification data (Binkerd et al. 1988; Clewell et al. 2009; Saillenfait et al. 1998; Scott et al. 1994). This is valid at least with respect to an important dose metric often linked with fetal toxicity, the C_{max} . We have shown here that the PBK model can predict the maternal blood and fetal C_{max} of the three chemicals with a less than 5-fold difference when compared to measured experimental data. In chemical risk assessment, which is currently based on animal data, it is customary to

employ a 10-fold safety factor so as to accommodate for species differences (Herrman and Younes 1999). Within this 10-fold a 4-fold factor accounts for the toxicokinetic differences (Renwick 1993). This supports further the notion that the model can reasonably predict the pregnancy toxicokinetics at least for these three chemicals.

Quantitative *in vitro* - *in vivo* extrapolations

The last part of this study was to describe (when possible) the dose-effect relationships for developmental toxicity, based on the BeWo PBKmodelling reverse dosimetry of *in vitro* toxicity assays. The BeWo PBK model was used to translate the *in vitro* nominally applied concentrations, which were considered equal to levels in the fetus, into equivalent oral doses. For the *in vitro* data, the nominal concentrations were used, as applied at the site of action, and *in vitro* biokinetics were not considered here. The selected *in vitro* tests were the WEC, ESTc and ESTn. The resulting oral doses were analysed with PROAST for the derivation of the respective dose-response curves. A direct comparison of the curves' BMDL₅₀s was also performed. The aim of these comparisons was to quantitatively assess the performance of the BeWo PBK modelling reverse dosimetry approach

In our earlier QIVIVE approach, we compared the nominal *in vitro* effective concentrations with PBK simulated concentrations in the blood after exposure at the level of developmental toxicity, assuming that maternal blood levels represent a good surrogate for fetal exposure (Fragki et al. 2017). The current study puts forward a more refined method, by simulating fetal concentrations with this adapted model, containing a fetal compartment, and capturing important parts of the kinetics during rat gestation. Instead of effective concentrations normally used for risk assessment purposes, such as BMD₁₀, the complete concentration-response curves and the BMDL₅₀ (lowest limit of the model averaged 90% confidence interval of the underlying ED₅₀) are compared. ED₅₀ was chosen for the comparisons since it is recommended for the case of quantal data (Slob 1999).

For the comparisons the question raised was which magnitude in differences between *in vitro*-based and *in vivo*-based BMDL₅₀s may be considered acceptable. An earlier retrospective analysis of developmental toxicity studies has demonstrated that developmental effect limits (NOAELs) for the same substance, species (either rat or rabbit) and exposure route may vary considerably, in fact up to 10-fold (Janer et al. 2008a). Consequently, even a one order of magnitude difference may be within the intervals of biological variation. In addition, earlier PBK modelling reverse dosimetry efforts to translate *in vitro* toxicity into equivalent *in vivo* dose levels, performed with models specifically designed for the substance (or small group of substances) of interest (Louisse et al. 2017; Louisse et al. 2015; Louisse et al. 2010; Strikwold et al. 2017) have illustrated differences within 10-fold. In the present work, comparison of the simulated dose-response curves and respective BMDL₅₀s with *in vivo* data shows BMDL₅₀s standing within the same order of magnitude, for the WEC, followed by the ESTc for three out of the five compounds, suggesting as such a fairly good prediction for this first feasibility study. Nevertheless, the approach has to be further elaborated with more embryotoxicants.

For the current QIVIVE exercise, the assumption was made that the C_{max} is the most appropriate dose metric because embryotoxicity is commonly attributed to peak concentrations, since it can be induced by as little as a single exposure at a critical time window of gestation (Daston et al. 2010). However, it cannot be excluded that in some cases toxicity to the embryo may be better captured with time-dependent parameters, such as the AUC or a time-weighted average concentration. (Groothuis et al. 2015; Lousse et al. 2017). Consequently, a clear approach has to be put forward in the future on the criteria for selection of the most appropriate dose metric for such *in vitro* to *in vivo* extrapolations.

Limitations

The BeWo system was previously evaluated to be a useful *in vitro* model to predict the transport of chemicals across the placenta, by comparisons to the human *ex vivo* placental perfusion model (Li et al. 2013). To our knowledge, data for the validation of the BeWo transport for these specific compounds are currently not available, and consequently, it is not possible to conclude here whether the determined transport rates are well-predicted. In order to validate the BeWo results for the chemicals applied here one has to perform an experiment, for example with the *ex vivo* placental perfusion model (Bassily et al. 1995). However, this method is labor intensive, and depends on the availability of fresh placental tissue, constituting it as such less appealing for safety assessment of large number of substances (Li et al. 2013). Nonetheless, it is acknowledged that investigating the applicability domain of the assay, but also the time of pregnancy it represents would be useful for its wider application.

For the toxicokinetic predictions, activation of the enterohepatic cycling was necessary for VPA, EHA and MBuP. Also, gastrointestinal hydrolysis of the parent phthalate DBuP to MBuP and specific absorption rate parametrization for EHA had to be taken into consideration. This presupposes that some *in vivo* data shall be available beforehand in order to properly calibrate certain model parameters and leading as such to successful predicted results. This is of course an issue considering the lack of information on toxicokinetics during gestation. It shall also be noted here that saturation of metabolic enzymes is not included in the generic structure of the model, and consequently simulations at very high dose levels, where toxicity may influence the toxicokinetics, may not be adequately captured. As such, without appropriate information to evaluate the model performance, its application for different chemicals may be problematic. For FLU and BAA substance-specific model parameterization was done based on former successful kinetic simulations with the original PBK model IndusChemFate for the non-pregnant rat (Fragki et al. 2017). Obviously, whether or not the simulated fetal concentrations are in close proximity with what occurs in reality cannot be discerned here, since, to our knowledge, such data are not available to investigate this further. Considering that toxicokinetic data on rat pregnancy are not commonly available, in particular for environmental chemicals, verification of the model predictions based on non-pregnancy kinetics seems the only option. Human data from cord-blood samples collected at term of pregnancy and/or biomonitoring information from

pregnant women (Bocca et al. 2019; Bocca et al. 2020; Cardenas et al. 2017; Freire et al. 2018) would also be a good alternative, provided that the PBK model is extended for the human.

Furthermore, the PBK model and also the reverse dosimetry approach applied here for the back calculation of external doses from *in vitro* concentrations uses a deterministic model, where all input parameters are fixed and hence, it does not accommodate for any uncertainty for these parameters. Nevertheless, it is acknowledged that parameter value uncertainty shall be taken into consideration when using such models for QIVIVE, although this was considered beyond the scope of the present paper.

The current methodology shall be seen as a 'proof or principle' exercise for QIVIVE purposes for developmental toxicity screening and prioritization. However, it shall be highlighted that species differences related to the source of data may constitute a limitation of the approach. For example, the BeWo cell line is derived from human choriocarcinoma, whereas developmental toxicity data and PBK model adaptations are for the rat animal. The rat model was selected here since it is the most informative with respect to data availability on developmental toxicity. Furthermore, the alternative embryotoxicity assays are based on the rat (WEC), but also on the mouse (ESTc and ESTn) species. It cannot be excluded that these species differences could affect the results for both the transplacental transport and embryotoxicity. Currently, a major effort is put on the development of alternative assays with human embryonic stem cells, which may prove to be a more suitable model for detecting embryotoxicants (Aikawa 2020; Chong et al. 2014; Luz and Tokar 2018). In the future, cell systems of human origin in combination with a PBK model adapted for human pregnancy coupled with human biomonitoring data could possibly be more informative for human risk assessment purposes.

In conclusion, the developed generic PBK model coupled with the BeWo transplacental information for the different embryotoxicants seems a promising tool for simulating pregnancy kinetics in the rat. Further exploration of chemical kinetics in the BeWo assay with advanced experimental designs are expected to improve the PBK model simulations. In addition, the QIVIVE proof-of-principle results suggest a good potential of the applied reverse dosimetry approach to predict *in vivo* developmental toxicity, so as to reduce animal testing. Nevertheless, this is still a work-in-progress and further refinements and improvements are required, in order for such approaches to be applied in chemical risk assessment.

Acknowledgement

The authors acknowledge Anne Kienhuis, National Institute for Public Health and the Environment (RIVM), Bilthoven, The Netherlands, for the critical reading of the paper and valuable comments.

Funding

This work was supported by the Dutch Ministry of Public Health, Welfare and Sports.

References

- Adeleye Y, Andersen M, Clewell R, Davies M, Dent M, Edwards S, Fowler P, Malcomber S, Nicol B, Scott A et al. 2015. Implementing Toxicity Testing in the 21st Century (TT21C): Making safety decisions using toxicity pathways, and progress in a prototype risk assessment. *Toxicology*. 332:102-111. eng.
- Adler S, Basketter D, Creton S, Pelkonen O, van Benthem J, Zuang V, Andersen KE, Angers-Loustau A, Aptula A, Bal-Price A et al. 2011. Alternative (non-animal) methods for cosmetics testing: current status and future prospects-2010. *Archives of toxicology*. 85(5):367-485. eng.
- Aikawa N. 2020. A novel screening test to predict the developmental toxicity of drugs using human induced pluripotent stem cells. *The Journal of Toxicological Sciences*. 45(4):187-199.
- Basketter DA, Clewell H, Kimber I, Rossi A, Blaauboer B, Burrier R, Daneshian M, Eskes C, Goldberg A, Hasiwa N et al. 2012. A roadmap for the development of alternative (non-animal) methods for systemic toxicity testing. *Altex*. 29(1):3-91. eng.
- Bassily M, Ghabrial H, Smallwood RA, Morgan DJ. 1995. Determinants of placental drug transfer: studies in the isolated perfused human placenta. *J Pharm Sci*. 84(9):1054-1060. eng.
- Bessems JG, Loizou G, Krishnan K, Clewell HJ, 3rd, Bernasconi C, Bois F, Coecke S, Collnot EM, Diembeck W, Farcail LR et al. 2014. PBTK modelling platforms and parameter estimation tools to enable animal-free risk assessment: recommendations from a joint EPAA--EURL ECVAM ADME workshop. *Regul Toxicol Pharmacol*. 68(1):119-139. eng.
- Binkerd PE, Rowland JM, Nau H, Hendrickx AG. 1988. Evaluation of valproic acid (VPA) developmental toxicity and pharmacokinetics in Sprague-Dawley rats. *Fundam Appl Toxicol*. 11(3):485-493. eng.
- Blaauboer BJ. 2010. Biokinetic modeling and *in vitro-in vivo* extrapolations. *J Toxicol Environ Health B Crit Rev*. 13(2-4):242-252. eng.
- Bocca B, Ruggieri F, Pino A, Rovira J, Calamandrei G, Martinez M, Domingo JL, Alimonti A, Schuhmacher M. 2019. Human biomonitoring to evaluate exposure to toxic and essential trace elements during pregnancy. Part A: concentrations in maternal blood, urine and cord blood. *Environ Res*. 177:108599. eng.
- Bocca B, Ruggieri F, Pino A, Rovira J, Calamandrei G, Mirabella F, Martínez M, Domingo JL, Alimonti A, Schuhmacher M. 2020. Human biomonitoring to evaluate exposure to toxic and essential trace elements during pregnancy. Part B: Predictors of exposure. *Environ Res*. 182:109108. eng.
- Bouvier d'Yvoire M, Prieto P, Blaauboer BJ, Bois FY, Boobis A, Brochot C, Coecke S, Freidig A, Gundert-Remy U, Hartung T et al. 2007. Physiologically-based Kinetic Modelling (PBK Modelling): meeting the 3Rs agenda. The report and recommendations of ECVAM Workshop 63. *Altern Lab Anim*. 35(6):661-671.
- Brown NA. 2002. Selection of test chemicals for the ECVAM international validation study on *in vitro* embryotoxicity tests. European Centre for the Validation of Alternative Methods. *Altern Lab Anim*. 30(2):177-198. eng.
- Cardenas A, Rifas-Shiman SL, Godderis L, Duca RC, Navas-Acien A, Litonjua AA, DeMeo DL, Brennan KJ, Amarasiwardena CJ, Hivert MF et al. 2017. Prenatal Exposure to Mercury: Associations with Global DNA Methylation and Hydroxymethylation in Cord Blood and in Childhood. *Environ Health Perspect*. 125(8):087022. eng.
- Chapin R, Augustine-Rauch K, Beyer B, Daston G, Finnell R, Flynn T, Hunter S, Mirkes P, O'Shea KS, Piersma A et al. 2008. State of the art in developmental toxicity screening methods and a way forward: a meeting report addressing embryonic stem cells, whole embryo culture, and zebrafish. *Birth Defects Res B Dev Reprod Toxicol*. 83(4):446-456. eng.
- Chong JJ, Yang X, Don CW, Minami E, Liu YW, Weyers JJ, Mahoney WM, Van Biber B, Cook SM, Palpant NJ et al. 2014. Human embryonic-stem-cell-derived cardiomyocytes regenerate non-human primate hearts. *Nature*. 510(7504):273-277. eng.
- Clewell RA, Kremer JJ, Williams CC, Campbell JL, Sochaski MA, Andersen ME, Borghoff SJ. 2009. Kinetics of selected di-n-butyl phthalate metabolites and fetal testosterone following repeated and single administration in pregnant rats. *Toxicology*. 255(1-2):80-90. eng.
- Dallmann A, Liu XI, Burckart GJ, van den Anker J. 2019. Drug Transporters Expressed in the Human Placenta and Models for Studying Maternal-Fetal Drug Transfer. *J Clin Pharmacol*. 59 Suppl 1(Suppl 1):S70-s81. eng.
- Daston GP, Chapin RE, Scialli AR, Piersma AH, Carney EW, Rogers JM, Friedman JM. 2010. A different approach to validating screening assays for developmental toxicity. *Birth Defects Res B Dev Reprod Toxicol*. 89(6):526-530. eng.

- de Jong E, Barenys M, Hermsen SA, Verhoef A, Ossendorp BC, Bessems JG, Piersma AH. 2011. Comparison of the mouse Embryonic Stem cell Test, the rat Whole Embryo Culture and the Zebrafish Embryotoxicity Test as alternative methods for developmental toxicity testing of six 1,2,4-triazoles. *Toxicol Appl Pharmacol.* 253(2):103-111. eng.
- de Jong E, Louisse J, Verwei M, Blaauboer BJ, van de Sandt JJM, Woutersen RA, Rietjens IMCM, Piersma AH. 2009. Relative Developmental Toxicity of Glycol Ether Alkoxy Acid Metabolites in the Embryonic Stem Cell Test as compared with the *In vivo* Potency of their Parent Compounds. *Toxicological Sciences.* 110(1):117-124.
- de Leeuw VC, Hessel EVS, Piersma AH. 2019. Look-alikes may not act alike: Gene expression regulation and cell-type-specific responses of three valproic acid analogues in the neural embryonic stem cell test (ESTn). *Toxicol Lett.* 303:28-37. eng.
- Dickinson RG, Harland RC, Ilias AM, Rodgers RM, Kaufman SN, Lynn RK, Gerber N. 1979. Disposition of valproic acid in the rat: dose-dependent metabolism, distribution, enterohepatic recirculation and choleric effect. *J Pharmacol Exp Ther.* 211(3):583-595. eng.
- Dimopoulou M, Verhoef A, Gomes CA, van Dongen CW, Rietjens I, Piersma AH, van Ravenzwaay B. 2018. A comparison of the embryonic stem cell test and whole embryo culture assay combined with the BeWo placental passage model for predicting the embryotoxicity of azoles. *Toxicol Lett.* 286:10-21. eng.
- Dimopoulou M, Verhoef A, Pennings JLA, van Ravenzwaay B, Rietjens I, Piersma AH. 2017. Embryotoxic and pharmacologic potency ranking of six azoles in the rat whole embryo culture by morphological and transcriptomic analysis. *Toxicol Appl Pharmacol.* 322:15-26. eng.
- EFSA. 2009. (European Food Safety Authority). Scientific Opinion on risk assessment for a selected group of pesticides from the triazole group to test possible methodologies to assess cumulative effects from exposure through food from these pesticides on human health. *EFSA Journal.* 2009; 7, 1167.
- EFSA. 2017. Update: Guidance on the use of the benchmark dose approach in risk assessment. *EFSA Journal* 2017;15(1):4658.
- Ema M, Amano H, Itami T, Kawasaki H. 1993. Teratogenic evaluation of di-n-butyl phthalate in rats. *Toxicol Lett.* 69(2):197-203. eng.
- FAO/WHO. Pesticide residues in food 2008. Report of the Joint Meeting of the FAO Panel Experts on Pesticide residues in food and the environment and the WHO Core Assessment Group on pesticide residues, Rome, Italy, 9-18 September 2008. .
- Fragki S, Piersma AH, Rorije E, Zeilmaker MJ. 2017. *In vitro* to *in vivo* extrapolation of effective dosimetry in developmental toxicity testing: Application of a generic PBK modelling approach. *Toxicol Appl Pharmacol.* 332:109-120. eng.
- Freire C, Amaya E, Gil F, Fernández MF, Murcia M, Llop S, Andiaarena A, Aurrekoetxea J, Bustamante M, Guxens M et al. 2018. Prenatal co-exposure to neurotoxic metals and neurodevelopment in preschool children: The Environment and Childhood (INMA) Project. *Sci Total Environ.* 621:340-351. eng.
- Friedman SJ, Skehan P. 1979. Morphological differentiation of human choriocarcinoma cells induced by methotrexate. *Cancer Res.* 39(6 Pt 1):1960-1967. eng.
- Furukawa S, Hayashi S, Usuda K, Abe M, Hagio S, Ogawa I. 2011. Toxicological pathology in the rat placenta. *J Toxicol Pathol.* 24(2):95-111. eng.
- Ganapathy V, Prasad PD, Ganapathy ME, Leibach FH. 2000. Placental transporters relevant to drug distribution across the maternal-fetal interface. *J Pharmacol Exp Ther.* 294(2):413-420. eng.
- Genschow E, Spielmann H, Scholz G, Seiler A, Brown N, Piersma A, Brady M, Cleemann N, Huuskonen H, Paillard F et al. 2002. The ECVAM international validation study on *in vitro* embryotoxicity tests: results of the definitive phase and evaluation of prediction models. *European Centre for the Validation of Alternative Methods. Altern Lab Anim.* 30(2):151-176. eng.
- Giavini E, Broccia ML, Menegola E, Prati M. 1993. Comparative *in vitro* study of the embryotoxic effects of three glycol ethers and their metabolites, the alkoxyacids. *Toxicol In vitro.* 7(6):777-784. eng.
- Giavini E, Menegola E. 2010. Are azole fungicides a teratogenic risk for human conceptus? *Toxicol Lett.* 198(2):106-111. eng.
- Griffiths SK, Campbell JP. 2014. Placental structure, function and drug transfer. *Continuing Education in Anaesthesia Critical Care & Pain.* 15(2):84-89.
- Groothuis FA, Heringa MB, Nicol B, Hermens JL, Blaauboer BJ, Kramer NI. 2015. Dose metric considerations in *in vitro* assays to improve quantitative *in vitro-in vivo* dose extrapolations. *Toxicology.* 332:30-40. eng.

- Gülden M, Seibert H. 2006. *In vitro-in vivo* extrapolation of toxic potencies for hazard and risk assessment - problems and new developments. ALTEX : Alternativen zu Tierexperimenten. 23 Suppl:218-225.
- Hartung T. 2018. Perspectives on *In vitro* to *In vivo* Extrapolations. Appl *In vitro* Toxicol. 4(4):305-316. eng.
- Hartung T, Blaauboer BJ, Bosgra S, Carney E, Coenen J, Conolly RB, Corsini E, Green S, Faustman EM, Gaspari A et al. 2011. An expert consortium review of the EC-commissioned report "alternative (Non-Animal) methods for cosmetics testing: current status and future prospects - 2010". *Altex*. 28(3):183-209. eng.
- Heaton SJ, Eady JJ, Parker ML, Gotts KL, Dainty JR, Fairweather-Tait SJ, McArdle HJ, Srail KS, Elliott RM. 2008. The use of BeWo cells as an *in vitro* model for placental iron transport. *Am J Physiol Cell Physiol*. 295(5):C1445-C1453. eng.
- Herrman JL, Younes M. 1999. Background to the ADI/TDI/PTWI. *Regul Toxicol Pharmacol*. 30(2 Pt 2):S109-113. eng.
- Huang X, Lüthi M, Ontsouka EC, Kallol S, Baumann MU, Surbek DV, Albrecht C. 2016. Establishment of a confluent monolayer model with human primary trophoblast cells: novel insights into placental glucose transport. *Mol Hum Reprod*. 22(6):442-456. eng.
- Ito C, Shibutanil, Y., Inoue, K., Nakano, K., Ohnishi, H.,.. 1976. Toxicological studies of miconazole (II) teratological studies of miconazole in rats. *IYAKUJIN KENKYU* 7, 367-376.
- Jamei M. 2016. Recent Advances in Development and Application of Physiologically-Based Pharmacokinetic (PBPK) Models: a Transition from Academic Curiosity to Regulatory Acceptance. *Curr Pharmacol Rep*. 2(3):161-169. eng.
- Janer G, Slob W, Hakker BC, Vermeire T, Piersma AH. 2008a. A retrospective analysis of developmental toxicity studies in rat and rabbit: what is the added value of the rabbit as an additional test species? *Regul Toxicol Pharmacol*. 50(2):206-217. eng.
- Janer G, Verhoeft A, Gilsing HD, Piersma AH. 2008b. Use of the rat postimplantation embryo culture to assess the embryotoxic potency within a chemical category and to identify toxic metabolites. *Toxicol In vitro*. 22(7):1797-1805. eng.
- JMPR. 2008. Joint FAO/WHO Meeting on Pesticide Residues. Pesticide residues in food 2007. Evaluations Part I-Residues. Joint meeting of FAO Plant Production and Protection Paper 192. Flusilazole.
- Jongeneelen FJ, Berge WF. 2011. A generic, cross-chemical predictive PBTK model with multiple entry routes running as application in MS Excel; design of the model and comparison of predictions with experimental results. *Ann Occup Hyg*. 55(8):841-864. eng.
- Joshi AA, Vaidya SS, St-Pierre MV, Mikheev AM, Desino KE, Nyandeghe AN, Audus KL, Unadkat JD, Gerk PM. 2016. Placental ABC Transporters: Biological Impact and Pharmaceutical Significance. *Pharm Res*. 33(12):2847-2878. eng.
- Keys DA, Wallace DG, Kepler TB, Conolly RB. 1999. Quantitative evaluation of alternative mechanisms of blood and testes disposition of di(2-ethylhexyl) phthalate and mono(2-ethylhexyl) phthalate in rats. *Toxicol Sci*. 49(2):172-185. eng.
- Keys DA, Wallace DG, Kepler TB, Conolly RB. 2000. Quantitative evaluation of alternative mechanisms of blood disposition of di(n-butyl) phthalate and mono(n-butyl) phthalate in rats. *Toxicol Sci*. 53(2):173-184. eng.
- Klug S, Lewandowski C, Zappel F, Merker HJ, Nau H, Neubert D. 1990. Effects of valproic acid, some of its metabolites and analogues on prenatal development of rats *in vitro* and comparison with effects *in vivo*. *Arch Toxicol*. 64(7):545-553. eng.
- Knudsen TB, Keller DA, Sander M, Carney EW, Doerrner NG, Eaton DL, Fitzpatrick SC, Hastings KL, Mendrick DL, Tice RR et al. 2015. FutureTox II: *in vitro* data and *in silico* models for predictive toxicology. *Toxicol Sci*. 143(2):256-267. eng.
- Kobayashi S, Takai K, Iga T, Hanano M. 1991. Pharmacokinetic analysis of the disposition of valproate in pregnant rats. *Drug Metab Dispos*. 19(5):972-976. eng.
- Kramer NI, Krismartina M, Rico-Rico A, Blaauboer BJ, Hermens JL. 2012. Quantifying processes determining the free concentration of phenanthrene in Basal cytotoxicity assays. *Chem Res Toxicol*. 25(2):436-445. eng.
- Li H, Flick B, Rietjens IM, Louise J, Schneider S, van Ravenzwaay B. 2016. Extended evaluation on the ES-D3 cell differentiation assay combined with the BeWo transport model, to predict relative developmental toxicity of triazole compounds. *Arch Toxicol*. 90(5):1225-1237. eng.

- Li H, Rietjens IM, Louisse J, Blok M, Wang X, Sniijders L, van Ravenzwaay B. 2015. Use of the ES-D3 cell differentiation assay, combined with the BeWo transport model, to predict relative *in vivo* developmental toxicity of antifungal compounds. *Toxicol In vitro*. 29(2):320-328. eng.
- Li H, van Ravenzwaay B, Rietjens IM, Louisse J. 2013. Assessment of an *in vitro* transport model using BeWo b30 cells to predict placental transfer of compounds. *Arch Toxicol*. 87(9):1661-1669. eng.
- Li H, Zhang M, Vervoort J, Rietjens IM, van Ravenzwaay B, Louisse J. 2017. Use of physiologically based kinetic modeling-facilitated reverse dosimetry of *in vitro* toxicity data for prediction of *in vivo* developmental toxicity of tebuconazole in rats. *Toxicol Lett*. 266:85-93. eng.
- Liu F, Soares MJ, Audus KL. 1997. Permeability properties of monolayers of the human trophoblast cell line BeWo. *Am J Physiol*. 273(5):C1596-1604. eng.
- Louisse J, Beekmann K, Rietjens IM. 2017. Use of Physiologically Based Kinetic Modeling-Based Reverse Dosimetry to Predict *in vivo* Toxicity from *in vitro* Data. *Chem Res Toxicol*. 30(1):114-125. eng.
- Louisse J, Bosgra S, Blaauboer BJ, Rietjens IM, Verwei M. 2015. Prediction of *in vivo* developmental toxicity of all-trans-retinoic acid based on *in vitro* toxicity data and *in silico* physiologically based kinetic modeling. *Arch Toxicol*. 89(7):1135-1148. eng.
- Louisse J, de Jong E, van de Sandt JJ, Blaauboer BJ, Woutersen RA, Piersma AH, Rietjens IM, Verwei M. 2010. The use of *in vitro* toxicity data and physiologically based kinetic modeling to predict dose-response curves for *in vivo* developmental toxicity of glycol ethers in rat and man. *Toxicol Sci*. 118(2):470-484. eng.
- Luz AL, Tokar EJ. 2018. Pluripotent Stem Cells in Developmental Toxicity Testing: A Review of Methodological Advances. *Toxicol Sci*. 165(1):31-39. eng.
- Magnarin M, Rosati A, De Iudicibus S, Bartoli F, Decorti G. 2008. Role of ABC Transporters in the BeWo Trophoblast Cell Line. *Toxicol Mech Methods*. 18(9):763-769. eng.
- Mathiesen L, Mørck TA, Zuri G, Andersen MH, Pehrson C, Frederiksen M, Mose T, Rytting E, Poulsen MS, Nielsen JK et al. 2014. Modelling of human transplacental transport as performed in Copenhagen, Denmark. *Basic Clin Pharmacol Toxicol*. 115(1):93-100. eng.
- Munley. 2000. S.M. (2000) Flusilazole technical: developmental toxicity study in rats. Unpublished report No. Dupont-2287 from Haskell Laboratory for Toxicology and Industrial Medicine, DE, USA. Submitted to WHO by E.I. du Pont de Nemours & Co., Inc., DE, USA.
- O'Flaherty EJ. 1994. Physiologically based pharmacokinetic models in developmental toxicology. *Risk Anal*. 14(4):605-611. eng.
- Ogiso T, Ito Y, Iwaki M, Yamahata T. 1986. Disposition and pharmacokinetics of valproic acid in rats. *Chem Pharm Bull (Tokyo)*. 34(7):2950-2956. eng.
- Pacifici GM, Nottoli R. 1995. Placental transfer of drugs administered to the mother. *Clin Pharmacokinet*. 28(3):235-269. eng.
- Parry S, Zhang J. 2007. Multidrug resistance proteins affect drug transmission across the placenta. *Am J Obstet Gynecol*. 196(5):476.e471-476. eng.
- Pattillo RA, Cey GO. 1968. The establishment of a cell line of human hormone-synthesizing trophoblastic cells *in vitro*. *Cancer Res*. 28(7):1231-1236. eng.
- Pemathilaka RL, Reynolds DE, Hashemi NN. 2019. Drug transport across the human placenta: review of placenta-on-a-chip and previous approaches. *Interface Focus*. 9(5):20190031. eng.
- Pennanen S, Tuovinen K, Huuskonen H, Komulainen H. 1992. The developmental toxicity of 2-ethylhexanoic acid in Wistar rats. *Fundam Appl Toxicol*. 19(4):505-511. eng.
- Piersma AH, Genschow E, Verhoef A, Spanjersberg MQ, Brown NA, Brady M, Burns A, Clemann N, Seiler A, Spielmann H. 2004. Validation of the postimplantation rat whole-embryo culture test in the international ECVAM validation study on three *in vitro* embryotoxicity tests. *Altern Lab Anim*. 32(3):275-307. eng.
- Poulsen MS, Rytting E, Mose T, Knudsen LE. 2009. Modeling placental transport: correlation of *in vitro* BeWo cell permeability and ex vivo human placental perfusion. *Toxicol In vitro*. 23(7):1380-1386. eng.
- Prouillac C, Lecoecur S. 2010. The role of the placenta in fetal exposure to xenobiotics: importance of membrane transporters and human models for transfer studies. *Drug Metab Dispos*. 38(10):1623-1635. eng.
- Punt A, Schifflers MJ, Jean Horbach C, van de Sandt JJ, Groothuis GM, Rietjens IM, Blaauboer BJ. 2011. Evaluation of research activities and research needs to increase the impact and applicability of alternative testing strategies in risk assessment practice. *Regulatory toxicology and pharmacology : RTP*. 61(1):105-114. eng.

- mR Core Team. 2020. R: A language and environment for statistical computing. R Foundation for Statistical Computing, Vienna, Austria URL <https://www.R-project.org/>. (version 4.0.2).
- Renwick AG. 1993. Data-derived safety factors for the evaluation of food additives and environmental contaminants. *Food Addit Contam.* 10(3):275-305. eng.
- RIVM. 2009. M. Luijten, A. de Vries, A. Opperhuizen, A.H. Piersma. Alternative methods in reproductive toxicity testing: state of the art. RIVM report 340720002/2007: RIVM.
- Saillenfait AM, Langonné I, Leheup B. 2001. Effects of mono-n-butyl phthalate on the development of rat embryos: *in vivo* and *in vitro* observations. *Pharmacol Toxicol.* 89(2):104-112. eng.
- Saillenfait AM, Payan JP, Fabry JP, Beydon D, Langonne I, Gallissot F, Sabate JP. 1998. Assessment of the developmental toxicity, metabolism, and placental transfer of Di-n-butyl phthalate administered to pregnant rats. *Toxicol Sci.* 45(2):212-224. eng.
- Schulpen SH, Robinson JF, Pennings JL, van Dartel DA, Piersma AH. 2013. Dose response analysis of monophthalates in the murine embryonic stem cell test assessed by cardiomyocyte differentiation and gene expression. *Reprod Toxicol.* 35:81-88. eng.
- Scott WJ, Jr., Collins MD, Nau H. 1994. Pharmacokinetic determinants of embryotoxicity in rats associated with organic acids. *Environ Health Perspect.* 102 Suppl 11(Suppl 11):97-101. eng.
- Seiler A, Visan A, Buesen R, Genschow E, Spielmann H. 2004. Improvement of an *in vitro* stem cell assay for developmental toxicity: the use of molecular endpoints in the embryonic stem cell test. *Reprod Toxicol.* 18(2):231-240. eng.
- Seiler AE, Spielmann H. 2011. The validated embryonic stem cell test to predict embryotoxicity *in vitro*. *Nat Protoc.* 6(7):961-978. eng.
- Sleet. 1989. Teratologic evaluation of ethylene glycol monobutyl ether administered to Fischer 344 rats on either gestational days 9-11 or days 11-13 [final report]. Public Health Service, U.S. Department of Health and Human Services; NTP-CTER-86-103. Available from the National Institute of Environmental Health Sciences, Research Triangle Park, NC.
- Slob W. 1999. Thresholds in Toxicology and Risk Assessment. *International Journal of Toxicology.* 18(4):259-268.
- Slob W. 2002. Dose-Response Modeling of Continuous Endpoints. *Toxicological Sciences.* 66(2):298-312.
- Spielmann H. 2009. The way forward in reproductive/developmental toxicity testing. *Altern Lab Anim.* 37(6):641-656. eng.
- Strikwold M, Spenkelink B, de Haan LHJ, Woutersen RA, Punt A, Rietjens I. 2017. Integrating *in vitro* data and physiologically based kinetic (PBK) modelling to assess the *in vivo* potential developmental toxicity of a series of phenols. *Arch Toxicol.* 91(5):2119-2133. eng.
- Syme MR, Paxton JW, Keelan JA. 2004. Drug transfer and metabolism by the human placenta. *Clin Pharmacokinet.* 43(8):487-514. eng.
- Toro-Ramos T, Paley C, Pi-Sunyer FX, Gallagher D. 2015. Body composition during fetal development and infancy through the age of 5 years. *Eur J Clin Nutr.* 69(12):1279-1289. eng.
- Tsaion K, Blaauboer BJ, Hartung T. 2016. Evidence-based absorption, distribution, metabolism, excretion (ADME) and its interplay with alternative toxicity methods. *Altex.* 33(4):343-358. eng.
- Uotoguchi N, Audus KL. 2000. Carrier-mediated transport of valproic acid in BeWo cells, a human trophoblast cell line. *Int J Pharm.* 195(1-2):115-124. eng.
- Uotoguchi N, Magnusson M, Audus KL. 1999. Carrier-mediated transport of monocarboxylic acids in BeWo cell monolayers as a model of the human trophoblast. *J Pharm Sci.* 88(12):1288-1292. eng.
- Varma DR, Ramakrishnan R. 1985. A rat model for the study of transplacental pharmacokinetics and its assessment with antipyrine and aminoisobutyric acid. *J Pharmacol Methods.* 14(1):61-74. eng.
- Wice B, Menton D, Geuze H, Schwartz AL. 1990. Modulators of cyclic AMP metabolism induce syncytiotrophoblast formation *in vitro*. *Exp Cell Res.* 186(2):306-316. eng.
- Yoon M, Blaauboer BJ, Clewell HJ. 2015. Quantitative *in vitro* to *in vivo* extrapolation (QIVIVE): An essential element for *in vitro*-based risk assessment. *Toxicology.* 332:1-3. eng.

Supplementary Material

Equations of the BeWo transport experiments

$$A1'(t) = \left(\frac{A2(t)}{V2 \times pc} - \frac{A1(t)}{V1} \right) \times \text{flow}$$

$$A2'(t) = -A1'(t)$$

where, A_1, A_2 : amounts in apical (1) and basolateral (2) chamber, respectively (μmol); $A_1(0)$: initial amount added to the apical chamber; $A_2(0)$: 0; t : time V_1, V_2 : volumes of compartments (μL); pc : partition coefficient; flow : flow between the two chambers. The model parameters 'pc: partition coefficient' and 'flow' ($\mu\text{L/hr}$) were estimated from the *in vitro* measured data by the method least of squares, The criterium function to be minimized was the sum of squared differences between data and calculated amounts over all time points and for all 3 parallel experiments. The freely available R-software was used for performing the calculations (<https://www.r-project.org/>).

PBK equations

Fat Volume (L)

$$V_{F,P} = V_P \times [1.0 + (0.0165 \times GD)] \quad (1)$$

where:

$V_{F,P}$: Volume of fat tissue during pregnancy

V_F : Volume of fat tissue adult non-pregnant rat

GD: Gestation Days

Mammary Tissue Volume (L)

$$V_{M,P} = V_M \times [1.0 + (0.27 \times GD)] \quad (2)$$

where:

$V_{M,P}$: Volume of mammary tissue during pregnancy

V_M : Volume of mammary tissue adult rat (= 0.01 x BW)

BW: Body Weight adult non-pregnant rat

GD: Gestation Days

Uterus Volume (L)

$$V_{U,P} = V_U \times 1.0, \text{ if } GD < 3 \quad (3)$$

$$V_{U,P} = V_U \times 1.0 + [0.77 + (GD - 3)^{1.6}], \text{ if } GD \geq 3 \quad (4)$$

where:

$V_{U,P}$: Volume of uterus during pregnancy

V_U : Volume of uterus adult rat (= 0.002 x BW)

BW: Body Weight adult non-pregnant rat

GD: Gestation Days

Body Weight (kg)

$$BW_p = BW + (V_{F,P} - V_F) + (V_{M,P} - V_M) + (V_{U,P} - V_U) + V_{Plac} + V_{Fet} \quad (5)$$

with:

BW_p : body weight during pregnancy

BW : body weight adult non-pregnant rat

V_{Fet} : volume of fetus

Cardiac Output & Blood Flows (L/h)

The increase of the total cardiac output during pregnancy, i.e. $Q_p - Q_C$, is distributed over the adipose tissue, the mammary tissue, the uterus and the placenta, or:

$$Q_p - Q_C = (Q_{F,P} - Q_F) + (Q_{M,P} - Q_M) + (Q_{U,P} - Q_U) + Q_{Plac} \quad (6)$$

With:

Q_p : Cardiac output pregnancy

Q_C : Cardiac output adult non-pregnant rat

$Q_{F,P}$: Blood flow to fat tissue during pregnancy

Q_F : Blood flow to fat tissue adult non-pregnant rat

$Q_{M,P}$: Blood flow to mammary tissue during pregnancy

Q_M : Blood flow to mammary tissue adult non-pregnant rat

$Q_{U,P}$: Blood flow to uterus during pregnancy

Q_U : Blood flow to uterus during adult non-pregnant rat

Q_{plac} : Blood flow to placenta

Conserving the fraction of the cardiac output flowing to the organs, i.e. as age-independent fractions of the cardiac output, scaling the blood flow to the fat, the mammary tissue and the uterus during pregnancy to organ volume then results in :

$$Q_{F,P} = Q_F \times \left(\frac{V_{F,P}}{V_F} \right) \quad (7)$$

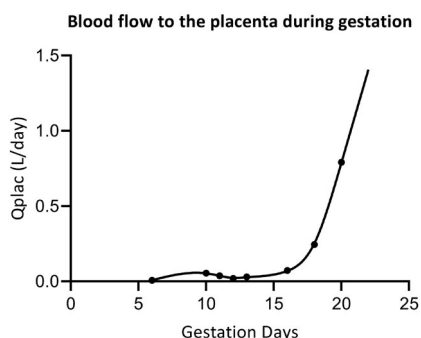
$$Q_{M,P} = Q_M \times \left(\frac{V_{M,P}}{V_M} \right) \quad (8)$$

$$Q_{U,P} = Q_U \times \left(\frac{V_{U,P}}{V_U} \right) \quad (9)$$

Except for placenta: $Q_{placenta}(GD) = f(GD)$ (10) (see below)

Blood flow to the placenta (L/hr)

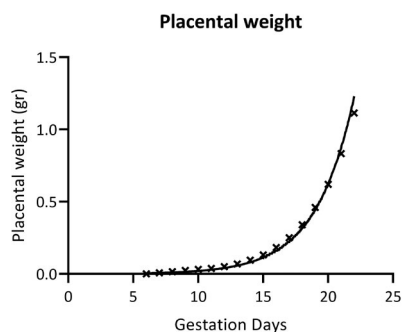
The data used describing the placenta blood flow during gestation and the resulting curve are presented in Figure 1. No simple mathematical function can reproduce the data and hence, a spline function is used (R-function smooth.spline).



SUPPLEMENTARY FIGURE 1 Blood flow to the placenta as a function of time (gestation days) in the rat as predicted by the PBK model (here expressed in L/day). The placenta blood flow in the graph is for a single embryo. The predicted curve is a spline-based curve based on experimental measurements (dots) (Buelke-Sam 1982b, as reported in O’Flaherty 1992). The transient increase around gestation day 10 represents the period of a prominent yolk sac placenta.

Placental weight (kg or else L)

During rat pregnancy the fetus is nourished by two independent placental systems: the yolk-sac system (mainly operating from GD6 to GD12) and the chorioallantoic system (being operational from GD12 onwards). The growth of the yolk sac placenta is modeled as a linear increase (GD6-D10), followed by a gradual decline. A small amount of the yolk sac placenta remains till the end of pregnancy. The growth of the chorioallantoic placenta is modeled as an exponential function of GDs (GD10-23) (O’Flaherty 1992). O’Flaherty et al. (1992) provide reference values for the sum of those two placental systems during GD6-GD23 (see graph).



SUPPLEMENTARY FIGURE 2 Placental weight changes(per single fetus) throughout the gestation period as predicted by the PBK model. Experimental data are taken from (O’Flaherty 1994).

As such the developed equation for the total placental weight is:

$$V_{plac}(t) = \frac{1e^{-6} \times e^{\alpha_1 + \alpha_2 t}}{1000000} \tag{11}(kg)$$

where: $\alpha_1 = 2.133$, $\alpha_2 = 0.0141$

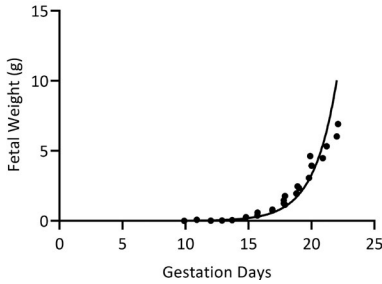
Fetal Growth (kg or L)

The graph below describes the growth weight of an individual fetus during gestation for the rat. Before GD10 the weight of the fetus is almost negligible. Data for fetal growth were obtained from O’Flaherty et al. (1992; Figure 3, as compiled from 4 early studies (1954–1982)).

$$V_{fetus}(t) = \frac{e^{b_1 + b_2 t}}{1000} \tag{12}(kg)$$

where: $b_1 = -7.432$ and $b_2 = 0.023$

Fetal Growth during Gestation



SUPPLEMENTARY FIGURE 3 Rat fetal weight growth during gestation for a single fetus. Experimental data are from O'Flaherty (1994).

Integration of the BeWo assay data into the PBK model-Mathematical equations

The fetoplacental unit

During gestation (GD0-23) the equations that describe mass balance for the change of the amount of a chemical in the placenta (13) and fetus (14) are the following:

$$\frac{d}{dt} A_p(t) = q_p(t) * \left[C_a(t) - \frac{A_p(t)}{V_p(t) * P_{p,i}} \right] + CL_{GDx,i}(t) * \left[\frac{A_e(t)}{V_e(t) * P_{e,i}} - C_p(t) \right] \quad (13)$$

$$\frac{d}{dt} A_e(t) = -CL_{GDx,i}(t) * \left[\frac{A_e(t)}{V_e(t) * P_{e,i}} - C_p(t) \right] \quad (14)$$

where:

$q_p(t)$ Maternal blood flow into the placenta (L/hr) (refers to the total sum of fetuses, assumed here N=12)

$C_a(t)$ Concentration in (arterial) blood flowing into the placenta (amount/L)

$A_p(t)$ Amount in the placental tissue

$V_p(t)$ Placental volume (L)

$P_{p,i}$ Placental tissue:blood partition coefficient

$CL_{GDx,i}(t)$ Clearance on different gestation days (refers to the total sum of fetuses (N=12) and it illustrates the placental exchange with umbilical cord blood)

$A_e(t)$ Amount in the fetus

$V_e(t)$ Volume of fetus (L)

Placental clearance: Antipyrine the index compound

In vivo antipyrine clearances were obtained at any time points across GD0-23:

$$CL_{GDx,ANTI}(t) = \frac{q_p(t)}{q_{p,GD20}} * CL_{GD20,ANTI} \quad (15)$$

where:

$CL_{GDx,ANTI}$ (*t*) *In vivo* clearance of ANTI (L/hr) by the embryo (from placenta tissue) throughout gestation

$q_p(t)$ Blood flow into the placenta (L/hr)

$q_{p,GD20}$ Blood flow into the placenta (L/hr) at GD20

$CL_{GD20,ANTI}$ *In vivo* clearance of ANTI at GD20 (reference value 0.172 L/hr, Varma et al., 1985).

Placental clearance: Incorporation of the BeWo assay results

Consequently, the respective *in vivo* $CL_{GDx,i}(t)$ for each substance will be:

$$CL_{GDx,i}(t) = \frac{CL_{BeWo,i}}{CL_{BeWo,ANTI}} * CL_{GDx,ANTI}(t) \quad (16)$$

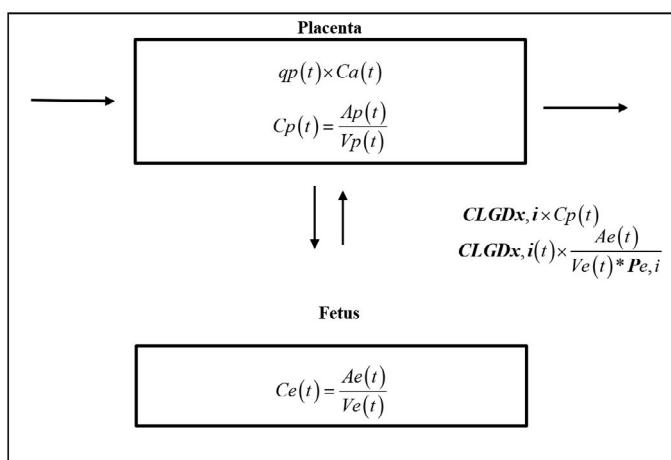
Consequently, from equations (15) and (16):

$$CL_{GDx,i}(t) = \left[\frac{CL_{BeWo,i}}{CL_{BeWo,ANTI}} * \frac{CL_{GD20,ANTI}}{q_{p,GD20}} \right] * q_p(t) \quad (17)$$

where:

- $CL_{GDx,i}(t)$ *In vivo* clearance of compound *i* (L/hr) on different gestation days *x* (refers to the total sum of fetuses (N=12) and it illustrates the placental exchange with umbilical cord blood)
- $CL_{BeWo,i}$ Estimated parameter ‘flow’ from the *in vitro* BeWo assay for substance *i*; equivalent to ‘clearance’ of the chemical from one compartment to the other
- $CL_{BeWo,ANTI}$ Estimated parameter ‘flow’ from the *in vitro* BeWo assay for ANTI
- $CL_{GDx,ANTI}(t)$ *In vivo* clearance of ANTI (L/hr) by the embryo (from placenta tissue) throughout gestation
- $q_{p,GD20}$ Blood flow into the placenta (L/hr) at GD20
- $CL_{GD20,ANTI}$ *In vivo* clearance of ANTI at GD20 (Varma and Ramakrishnan 1985)
- $q_p(t)$ Blood flow into the placenta (L/hr)

The *in vitro* measured parameter ‘pc’ was used as a proxy for the unknown *in vivo* $P_{e,i}$, representing the embryo:placental tissue partition coefficient.



SUPPLEMENTARY FIGURE 4 The fetoplacental unit as incorporated into the generic rat pregnancy PBK model. The rectangular shapes represent compartments and the arrows are showing the direction of transfer of the compounds. The model allows for the use of measured BeWo assay data as input parameters for PBK predictions. The transport between placenta and fetus is proportional to the $q_p(t)$.

PBK model input parameters

SUPPLEMENTARY TABLE 1 Model input parameters for the generic PBK model.

Substance	Parameter	Value	Reference/QSAR model
FLU	Absorption rate	default	
	Density (mg/cm ³ or grams/litre)	1170	ChemSketch v.11 (ACD/ChemSketch 2011)
	Molecular weight	315.4	Calculated from structural formula
	Vapour Pressure (Pa)	3.19E-05	MPBPWIN v1.43 (EpiSuite)
	Log(Kow) at skin pH 5.5	3.7	ChemAxon Marvin Sketch 21.4.0
	Log(Kow) at blood pH 7.4	3.7	ChemAxon Marvin Sketch 21.4.0
	Water solubility (mg/litre)	54	WSKOW v1.42 (EpiSuite)
	Vmax Liver (parent[total] micmol/kg tissue/hr)	6438	Fragki et al. (2017), based on whole body half-life
	Km Liver (parent[total] micmol/litre)	3750	
	Resorption tubuli (?/estimated fraction)	default	
	Enterohepatic removal (relative to liver venous blood)	default	
	Faeces fraction (relative to removal)	default	
	VPA	Absorption rate	default
Density (mg/cm ³ or grams/litre)		950	ChemSketch v.11 (ACD/ChemSketch 2011)
Molecular weight		144.214	Calculated from structural formula
Vapour Pressure (Pa)		11.3	MPBPWIN v1.43 (EpiSuite)
Log(Kow) at skin pH 5.5		2.23	ChemAxon Marvin Sketch 21.4.0
Log(Kow) at blood pH 7.4		0.49	ChemAxon Marvin Sketch 21.4.0
Water solubility (mg/litre)		2000	WSKOW v1.42 (EpiSuite)
Vmax Liver (parent[total] micmol/kg tissue/hr)		13438.36	Kobayashi et al. (1991)
Km Liver (parent[total] micmol/litre)		1941.56	
Resorption tubuli (?/estimated fraction)		default	
Enterohepatic removal (relative to liver venous blood)		0.5	Fitting to experimental data
Faeces fraction (relative to removal)		default	
EHA		Absorption rate	0.5
	Density (mg/cm ³ or grams/litre)	926	ChemSketch v.11 (ACD/ChemSketch 2011)
	Molecular weight	144.212	Calculated from structural formula
	Vapour Pressure (Pa)	4	MPBPWIN v1.43 (EpiSuite)
	Log(Kow) at skin pH 5.5	2.12	ChemAxon Marvin Sketch 21.4.0
	Log(Kow) at blood pH 7.4	0.38	
	Water solubility (mg/litre)	2000	WSKOW v1.42 (EpiSuite)
	Vmax Liver (parent[total] micmol/kg tissue/hr)	20250	Hamdoune et al. (1995)
	Km Liver (parent[total] micmol/litre)	2200	
	Resorption tubuli (?/estimated fraction)	default	
	Enterohepatic removal (relative to liver venous blood)	0.2	Fitting to experimental data
	Faeces fraction (relative to removal)	0.1	Fitting to experimental data
	MCZ	Absorption rate	default
Density (mg/cm ³ or grams/litre)		1400	ChemSketch v.11 (ACD/ChemSketch 2011)
Molecular weight		416.14	Calculated from structural formula
Vapour Pressure (Pa)		2.35E-08	MPBPWIN v1.43 (EpiSuite)
Log(Kow) at skin pH 5.5		5.23	ChemAxon Marvin Sketch 21.4.0
Log(Kow) at blood pH 7.4		6.2	
Water solubility (mg/litre)		0.024	WSKOW v1.42 (EpiSuite)
Vmax Liver (parent[total] micmol/kg tissue/hr)		6438	as for FLU
Km Liver (parent[total] micmol/litre)		3750	

Substance	Parameter	Value	Reference/QSAR model
	Resorption tubuli (?/estimated fraction)	default	
	Enterohepatic removal (relative to liver venous blood)	default	
	Faeces fraction (relative to removal)	default	
EGBE	Absorption rate	default	
	Density (mg/cm ³ or grams/litre)	900	ChemSketch v.11 (ACD/ChemSketch 2011)
	Molecular weight	118.18	Calculated from structural formula
	Vapour Pressure (Pa)	1.17E+02	MPBPWIN v1.43 (EpiSuite)
	Log(Kow) at skin pH 5.5	0.83	ChemAxon Marvin Sketch 21.4.0
	Log(Kow) at blood pH 7.4	0.83	
	Water solubility (mg/litre)	1.00E+06	WSKOW v1.42 (EpiSuite)
	Vmax Liver (parent[total] micromol/kg tissue/hr)	94848	Corley et al. (2005)
	Km Liver (parent[total] micromol/litre)	900	
	Resorption tubuli (?/estimated fraction)	default	
	Enterohepatic removal (relative to liver venous blood)	default	
	Faeces fraction (relative to removal)	default	
BAA	Absorption rate	default	
	Density (mg/cm ³ or grams/litre)	1030	ChemSketch v.11 (ACD/ChemSketch 2011)
	Molecular weight	132.16	Calculated from structural formula
	Vapour Pressure (Pa)	8.98E+00	MPBPWIN v1.43 (EpiSuite)
	Log(Kow) at skin pH 5.5	-0.44	ChemAxon Marvin Sketch 21.4.0
	Log(Kow) at blood pH 7.4	-2.31	
	Water solubility (mg/litre)	46920	WSKOW v1.42 (EpiSuite)
	Vmax Liver (parent[total] micromol/kg tissue/hr)	0	
	Km Liver (parent[total] micromol/litre)	0	
	Resorption tubuli (?/estimated fraction)	0.6	Fitting to experimental data, as in Fragki et al. (2017)
	Enterohepatic removal (relative to liver venous blood)	default	
	Faeces fraction (relative to removal)	default	
MBuP	Absorption rate	default	
	Density (mg/cm ³ or grams/litre)	1170	ChemSketch v.11 (ACD/ChemSketch 2011)
	Molecular weight	222.24	Calculated from structural formula
	Vapour Pressure (Pa)	5.15E-03	MPBPWIN v1.43 (EpiSuite)
	Log(Kow) at skin pH 5.5	0.44	ChemAxon Marvin Sketch 21.4.0
	Log(Kow) at blood pH 7.4	-1.46	
	Water solubility (mg/litre)	1.26E+02	WSKOW v1.42 (EpiSuite)
	Vmax Liver (parent[total] micromol/kg tissue/hr)	1993	Keys et al. (2000)
	Km Liver (parent[total] micromol/litre)	81.9	
	Resorption tubuli (?/estimated fraction)	default	
	Enterohepatic removal (relative to liver venous blood)	0.5	Fitting to experimental data
	Faeces fraction (relative to removal)	default	

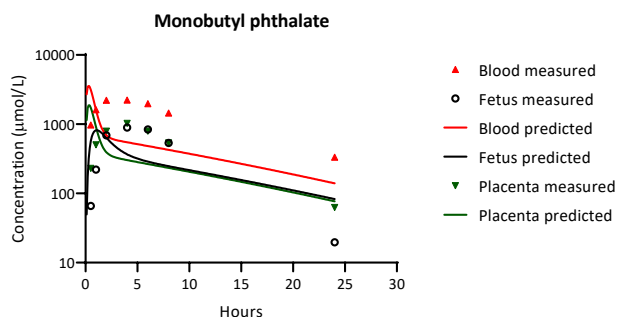
In vivo toxicokinetic and toxicity data

A literature search was performed in PubMed for each of the six substances for retrieving information on toxicokinetics and developmental toxicity in the rat model. The following searches were included in 'All fields':

<substance> AND <rat> AND <pregnancy>; <substance> AND <rat> AND <gestation>; <substance> AND <rat> AND <toxicokinetics>; <substance> AND <rat> AND <transplacental transport> AND <pregnancy>; <substance> AND <rat> AND <developmental toxicity>

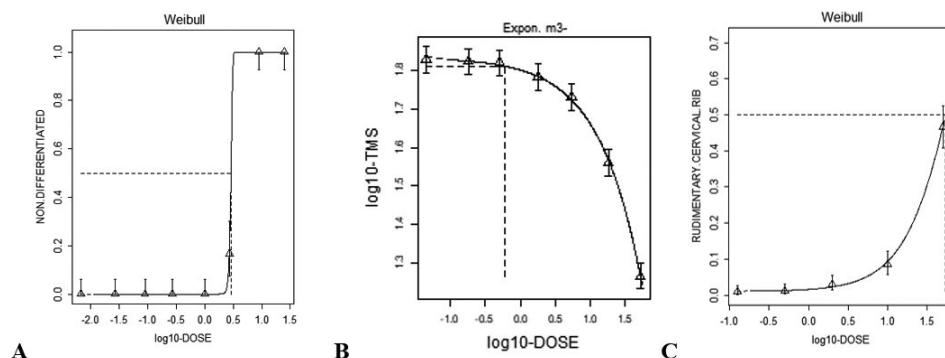
For the pesticide FLU information was collected as presented in the JMPR safety evaluation (JMPR 2008). For EGBE (BAA) and DBP (MBP) international evaluation reports by US EPA and the EU Risk Assessment Committee (RAC) were also consulted (RAC 2012; 2018; US EPA 2009).

MBuP pregnancy toxicokinetics

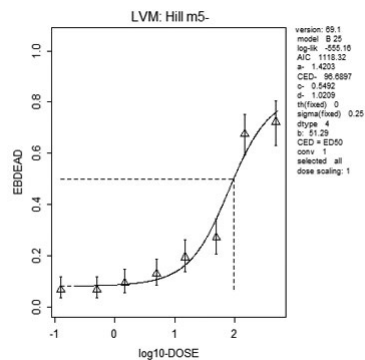
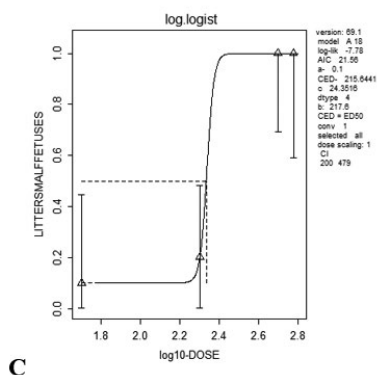
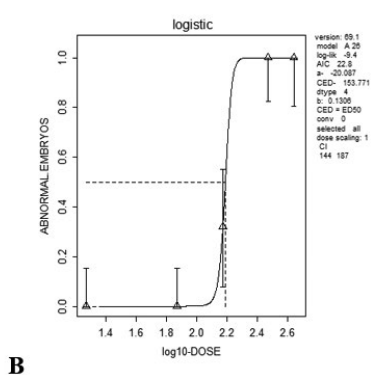
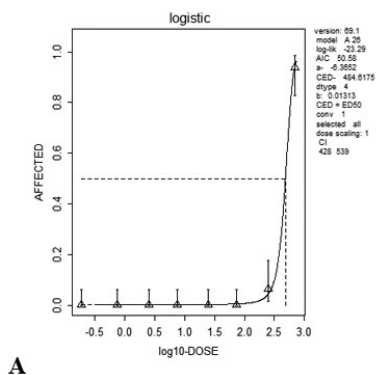


SUPPLEMENTARY FIGURE 5 Concentrations of MBuP in blood, growing fetus and placenta after exposure to the parent DBuP. Dose 1500 mg/kg bw (equivalent to 1400 mg/kg bw MBuP), GD14, experimental data (mean, n=3) taken from Saillenfait *et al.* (1995).

BMD analysis with PROAST



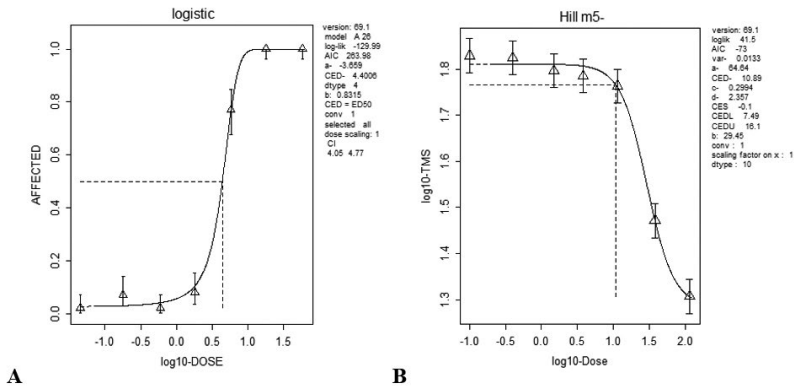
SUPPLEMENTARY FIGURE 6 Dose-response analysis performed with PROAST for flusilazole based on the A. ESTc-based PBK modelling reverse dosimetry, B. WEC-based PBK modelling reverse dosimetry and C. experimental determined *in vivo* developmental toxicity rat data. The model with lowest AIC is presented here. References on the original data sets are provided within the manuscript in the section of Materials & Methods.



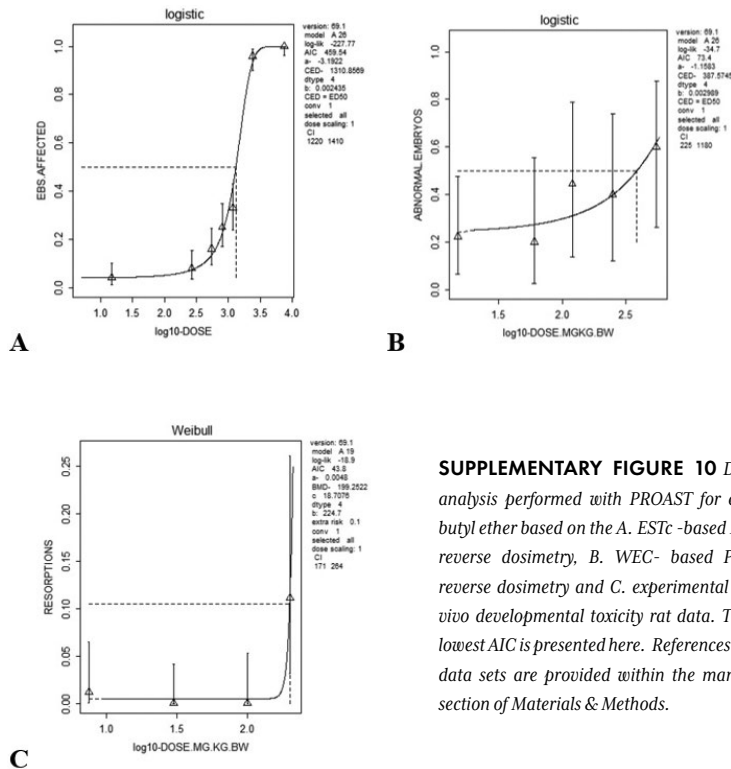
SUPPLEMENTARY FIGURE 7 Dose- response analysis performed with PROAST for valproic acid based on the A. ESTc -based PBK modelling reverse dosimetry, B. WEC- based PBK modelling reverse dosimetry and C. experimental determined in vivo developmental toxicity rat data. The model with lowest AIC is presented here. References on the original data sets are provided within the manuscript in the section of Materials & Methods.

SUPPLEMENTARY FIGURE 8 Dose- response analysis performed with PROAST for 2-ethyl hexanoic acid based on the A. ESTn -based PBK modelling reverse dosimetry. The model with lowest AIC is presented here. References on the original data set is provided within the manuscript in the section of Materials & Methods.

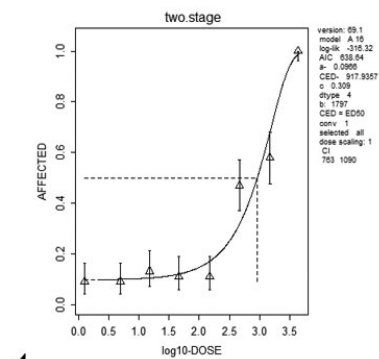




SUPPLEMENTARY FIGURE 9 Dose- response analysis performed with PROAST for miconazole based on the A. ESTc- based PBK modelling reverse dosimetry, and B. WEC- based PBK modelling reverse dosimetry. The model with lowest AIC is presented here. References on the original data sets are provided within the manuscript in the section of Materials & Methods.

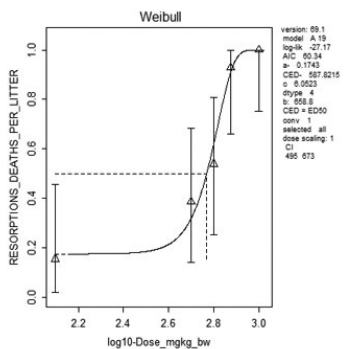
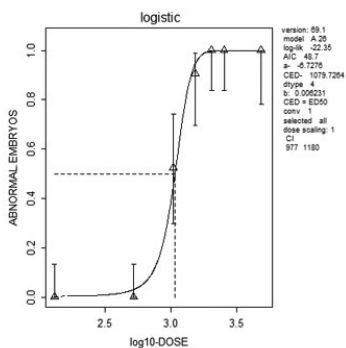


SUPPLEMENTARY FIGURE 10 Dose- response analysis performed with PROAST for ethylene glycol butyl ether based on the A. ESTc- based PBK modelling reverse dosimetry, B. WEC- based PBK modelling reverse dosimetry and C. experimental determined *in vivo* developmental toxicity rat data. The model with lowest AIC is presented here. References on the original data sets are provided within the manuscript in the section of Materials & Methods.



A

B



C

SUPPLEMENTARY FIGURE 11 Dose- response analysis performed with PROAST for dibutyl phthalate based on the A. ESTc -based PBK modelling reverse dosimetry, B. WEC- based PBK modelling reverse dosimetry and C. experimental determined *in vivo* developmental toxicity rat data. The model with lowest AIC is presented here. References to the original data sets are provided within the manuscript in the section of Materials & Methods.

References-Supplementary Material

- Corley RA, Bartels MJ, Carney EW, Weitz KK, Soelberg JJ, Gies RA, Thrall KD. 2005. Development of a physiologically based pharmacokinetic model for ethylene glycol and its metabolite, glycolic Acid, in rats and humans. *Toxicol Sci.* 85(1):476-490. eng.
- Fragki S, Piersma AH, Rorije E, Zeilmaker MJ. 2017. *In vitro* to *in vivo* extrapolation of effective dosimetry in developmental toxicity testing: Application of a generic PBK modelling approach. *Toxicol Appl Pharmacol.* 332:109-120. eng.
- Hamdoune M, Duclos S, Mounie J, Santona L, Lhuguenot JC, Magdalou J, Goudonnet H. 1995. *In vitro* glucuronidation of peroxisomal proliferators: 2-ethylhexanoic acid enantiomers and their structural analogs. *Toxicol Appl Pharmacol.* 131(2):235-243. eng.
- JMPR. 2008. Joint FAO/WHO Meeting on Pesticide Residues. Pesticide residues in food 2007. Evaluations Part I-Residues. Joint meeting of FAO Plant Production and Protection Paper 192. Flusilazole.
- Keys DA, Wallace DG, Kepler TB, Conolly RB. 2000. Quantitative evaluation of alternative mechanisms of blood disposition of di(n-butyl) phthalate and mono(n-butyl) phthalate in rats. *Toxicol Sci.* 53(2):173-184. eng.
- Kobayashi S, Takai K, Iga T, Hanano M. 1991. Pharmacokinetic analysis of the disposition of valproate in pregnant rats. *Drug Metab Dispos.* 19(5):972-976. eng.
- O'Flaherty EJ. 1994. Physiologically based pharmacokinetic models in developmental toxicology. *Risk Anal.* 14(4):605-611. eng.
- RAC. 2012. Committee for Risk Assessment (RAC). Committee for Socio-economic Analysis (SEAC). Background document to the Opinion on the Annex XV dossier proposing restrictions on four phthalates. ECHA/RAC/RES-O-0000001412-86-07/S1. ECHA/SEAC/RES-O-0000001412-86-10/S2. 5 December 2012.
- RAC. 2018. Committee for Risk Assessment, RAC. Annex 1 Background document to the Opinion proposing harmonised classification and labelling at EU level of 2-butoxyethanol; ethylene glycol monobutyl ether. CLH-O-0000001412-86-226/F. Adopted 14 September 2018.
- US EPA. 2009. US EPA, November 2009. Toxicological review of ethylene glycol monobutyl ether (EGBE). EPA/635/R-08/006D. In Support of Summary Information on the Integrated Risk Information System (IRIS).
- Varma DR, Ramakrishnan R. 1985. A rat model for the study of transplacental pharmacokinetics and its assessment with antipyrine and aminoisobutyric acid. *J Pharmacol Methods.* 14(1):61-74. eng.

Section III



Chapter 5

Systemic PFOS and PFOA exposure and disturbed lipid homeostasis in humans: what do we know and what not?

Critical Reviews in Toxicology, 2021. Feb;51 (2):141-164

DOI: 10.1080/10408444.2021.1888073

Styliani Fragki^a

Hubert Dirven^b

Tony Fletcher^c

Bettina Grasl-Kraupp^d

Kristine Bjerve Gützkw^b

Ron Hoogenboom^e

Sander Kersten^f

Birgitte Lindeman^b

Jochem Lousse^e

Ad Peijnenburg^e

Aldert Piersma^{a,g}

Hans M. G. Princen^h

Maria Uhlⁱ

Joost Westerhoutⁱ

Marco Zeilmaker^k

Mirjam Luijten^a

^a Centre for Health Protection, National Institute for Public Health and the Environment (RIVM), Bilthoven, the Netherlands

^b Department of Environmental Health, Norwegian Institute of Public Health, P.O.Box 222, Skøyen, 0213 Oslo, NO

^c Centre for Radiation, Chemical and Environmental Hazards, Public Health England (PHE), Chilton, United Kingdom.

^d M.D., Institut für Krebsforschung, University of Vienna, Borschkegasse 8a, A-1090 Vienna, Austria

^e Wageningen Food Safety Research (WFSR), Wageningen, The Netherlands

^f Nutrition, Metabolism and Genomics Group, Division of Human Nutrition, Wageningen University, The Netherlands

^g Institute for Risk Assessment Sciences, Utrecht University, P.O. Box 80178, 3508 TD Utrecht, The Netherlands

^h Metabolic Health Research, The Netherlands Organization of Applied Scientific Research (TNO), Gaubius Laboratory, Leiden, The Netherlands

ⁱ Environment Agency Austria (EAA), Vienna, Austria

^j Risk Analysis for Products In Development, The Netherlands Organization of Applied Scientific Research (TNO), Utrecht, The Netherlands

^k Centre for Nutrition, Prevention and Health Services, National Institute for Public Health and the Environment (RIVM), Bilthoven, the Netherlands

Abstract

Associations between per- and polyfluoroalkyl substances (PFASs) and increased blood lipids have been repeatedly observed in humans, but a causal relation has been debated. Rodent studies show reverse effects, i.e. decreased blood cholesterol and triglycerides, occurring however at PFAS serum levels at least 100-fold higher than those in humans. This paper aims to present the main issues regarding the modulation of lipid homeostasis by the two most common PFASs, PFOS and PFOA, with emphasis on the underlying mechanisms relevant for humans. Overall, the apparent contrast between human and animal data may be an artefact of dose, with different molecular pathways coming into play upon exposure to PFASs at very low *versus* high levels. Altogether, the interpretation of existing rodent data on PFOS/PFOA-induced lipid perturbations with respect to the human situation is complex. From a mechanistic perspective, research on human liver cells shows that PFOS/PFOA activate the PPAR α pathway, whereas studies on the involvement of other nuclear receptors, like PXR, are less conclusive. Other data indicate that suppression of the nuclear receptor HNF4 α signalling pathway, as well as perturbations of bile acid metabolism and transport might be important cellular events that require further investigation. Future studies with human-relevant test systems would help to obtain more insight into the mechanistic pathways pertinent for humans. These studies shall be designed with a careful consideration of appropriate dosing and toxicokinetics, so as to enable biologically plausible quantitative extrapolations. Such research will increase the understanding of possible perturbed lipid homeostasis related to PFOS/ PFOA exposure and the potential implications for human health.

Introduction

Per- and polyfluoroalkyl substances (PFASs) are man-made substances with unique physicochemical properties, such as oil and water repellence, high temperature and chemical resistance, and emulsifying/surfactant properties. Because of these properties, PFASs have been in use since the 1950s for a wide range of industrial and consumer applications, including food contact materials, water-repellent fabrics, waxes, fire-fighting foams, shampoos and cosmetics, as well as insecticides. Several long-chain PFASs, including the well-known PFOA perfluorooctanoic acid (PFOA) and perfluorooctane sulfonic acid (PFOS), are extremely persistent in the environment and tend to bioaccumulate (OECD 2015). Measurable blood concentrations of PFOA and PFOS, and to a lesser degree other PFASs, have been found in populations worldwide (ATSDR 2018; Ballesteros et al. 2017; EFSA CONTAM Panel 2018a; 2020a; US EPA 2016a; 2016b). Moreover, this class of substances has been associated with various adverse health effects in humans, including serum lipid perturbations, immunotoxicity, and developmental toxicity (ATSDR 2018; EFSA CONTAM Panel 2018a; 2020a; US EPA 2016a; 2016b).

Despite agreements to phase out the production of certain PFASs by industry, part of the European population is still exposed to levels of PFASs¹⁵ exceeding the tolerable weekly intake (TWI) recently proposed by the EFSA CONTAM Panel, based on effects in humans (EFSA CONTAM Panel 2020a). Furthermore, alternative PFASs are increasingly being used without sufficient knowledge on their potential hazards and sources of emissions. Thus, PFASs are a public health concern deserving attention from health authorities and policy makers.

One of the human health concerns associated with PFAS exposure is potential perturbation of triglyceride (TG) and cholesterol homeostasis. PFASs, have been repeatedly found to be positively associated with increased blood cholesterol concentrations, and in some cases TGs, in numerous human epidemiological studies. Increased serum cholesterol (total cholesterol of > 5.2 mmol/L, i.e. >200 mg/dL) (FERENCE et al. 2017; Leritz et al. 2016; Piepoli et al. 2016), and in particular its low density lipoprotein (LDL) fraction, is a well-established risk factor for cardiovascular disease (CVD), including ischemic heart disease and ischemic stroke (Borén et al. 2020; FERENCE et al. 2017; Piepoli et al. 2016). The use of cholesterol-lowering drugs such as statins has been shown to decrease the risk of CVD (FERENCE et al. 2017; Piepoli et al. 2016). Moderate hypertriglyceridemia (>10 mmol/L) is also considered a CVD risk factor, albeit with a smaller correlation when compared to the correlation between hypercholesterolemia and CVD (Nordestgaard and Varbo 2014; Piepoli et al. 2016; Sandesara et al. 2019). Consequently, even a small increase in serum lipids caused by PFASs can be considered a potential human health hazard.

In contrast to the evidence from human data, rodent studies with PFASs, commonly performed with high doses, have demonstrated decreased serum cholesterol and TG levels,

15 EFSA CONTAM Panel has considered four PFASs members for the calculation of a TWI: PFOS, PFOA, PFHxS (perfluorohexanesulfonic acid) and PFNA (perfluorononanoic acid) (EFSA CONTAM Panel 2020).

accompanied by increased intrahepatic lipid (mainly TG) concentrations (Curran et al. 2008; DeWitt et al. 2009; Loveless et al. 2006; NTP 2019a; 2019b; Seacat et al. 2003). Next to this, liver toxicity is one of the most frequently reported effects manifested as hypertrophy, steatosis, and in some cases, even necrosis (NTP 2019a; 2019b; RIVM 2018). The divergent results regarding blood lipids between rodents and humans raise debate about the human relevance of rodent data on lipid perturbation, but also about the causality of the human findings on PFAS-associated elevated serum lipids (EFSA CONTAM Panel 2018c).

Despite the fact that perturbed lipid homeostasis associated with PFAS exposure has received substantial attention, clear understanding of the mechanisms involved in both animals and humans, is still lacking. This is partly due to distinct species differences, pertaining to the combination of toxicokinetics and toxicodynamics, which have obscured the evaluation of causal pathways and their interpretation in the context of human health. Additionally, many studies focused on peroxisome proliferator-activated receptor α (PPAR α)-mediated mechanisms, and less attention has been given to other possible mechanisms explaining the observed effects, such as interactions with other transcription factors.

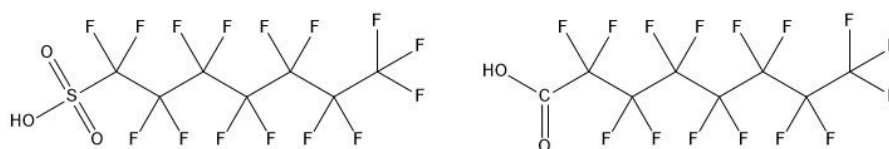


FIGURE 1 Chemical structure of PFOS (left) and PFOA (right).

The goal of the present paper is to present the state of the art knowledge on the disturbance of cholesterol and TG homeostasis by PFASs, and to bring forward the most important issues pertaining to this topic. Possible explanations for the findings and discrepancies observed between different lines of evidence are identified, with an emphasis on the underlying mechanisms, especially those that could be relevant for humans. Elucidating the mechanism through which PFASs might induce lipid perturbations would assist in explaining the epidemiological findings, as well as establishing the human relevance of experimental data. For this purpose, this review presents i) a summary of the main findings on PFAS-mediated lipid dysregulation, as recorded in epidemiological and animal studies, ii) an overview of the most important related mechanistic knowledge, as derived from mechanistic rodent studies and *in vitro* human-relevant test systems, and iii) the importance of PFAS species-specific toxicokinetics. The aim of the work is neither to perform a systematic review nor to evaluate the quality and reliability of all available data, since this has been previously performed (e.g. EFSA CONTAM Panel 2018a; 2020a), and hence, information used is mainly derived from studies that are highlighted in existing reviews and reports published by various agencies (EFSA CONTAM Panel 2018a; 2020a; Pizzurro et al. 2019; RIVM 2018), complemented with some recent scientific publications. The focus is on the two main congeners of the PFAS group, PFOS (Figure 1, left) and PFOA (Figure 1, right). Furthermore, this paper provides some recommendations on how to

address the identified issues and fill the knowledge gaps, and lays down important factors that require careful consideration when designing new studies. Altogether, this paper aims to contribute to a better understanding of PFAS-mediated lipid perturbations and the issues involved in their interpretation for human health risk assessment.

PFOS and PFOA: lipid homeostasis perturbations

Effects observed in human studies

Both, PFOS and PFOA (further referred to as 'PFOS/PFOA' and/or PFASs), have been repeatedly found to be positively associated with increased blood cholesterol concentrations in multiple human epidemiological studies (EFSA CONTAM Panel, 2018). A few examples, which are representative for these findings, are shown in Table 1. The epidemiological evidence mainly comprises cross-sectional associations between serum PFOS/PFOA and increased levels of cholesterol in blood, with a few examples of longitudinal studies (EFSA CONTAM Panel 2018a). Most studies have used general population samples with the "normal" range of PFOS/PFOA concentrations for that country at that time (e.g. Eriksen et al. 2013; Geiger et al. 2014; Nelson et al. 2010; Starling et al. 2014) and some have used specific populations with occupational exposure (e.g. Olsen et al. 2003a; Sakr et al. 2007a; Sakr et al. 2007b) or contaminated community drinking water supplies (e.g. Canova et al. 2020; Frisbee et al. 2010; Li et al. 2020; Steenland et al. 2009). Exposure to the chemicals was in general for several decades. In the majority of these studies, the general pattern observed was a significant increase in the total serum cholesterol or low density lipoprotein cholesterol (LDL-C) associated with increased blood levels of PFOS and/or PFOA, while the results reported for high density lipoprotein cholesterol (HDL-C) were inconsistent. For the general population studies, the magnitude of the increase in total serum cholesterol, based on highest *versus* lowest quantiles, was around 5% (Eriksen et al. 2013: PFOS +4.9%, PFOA +5.6%; Li et al. 2020: PFOA, PFOS +7-9%; Nelson et al. 2010: PFOS +6.8%; Steenland et al. 2009: PFOS +6.4%, PFOA +5.5%), which may correspond to a clinically relevant increase in the risk of CVD (FERENCE et al. 2017; Piepoli et al. 2016).

The largest study is on 46 000 adults from the C8 cohort in the mid-Ohio valley, in which residents were exposed for many decades to various PFOA levels through contaminated drinking water and via food, and show a wide range of serum concentrations (Steenland et al. 2009). This study showed median blood PFOS and PFOA levels of 20 and 27 ng/mL, respectively. Notably, for PFOA very high blood levels (up to ~18 000 ng/mL) were observed in part of the population. Much of the increase is observed at low PFOS/PFOA serum levels and seems to level off at higher levels (above about 50 ng/mL), as also shown by the modelling of the data (EFSA CONTAM Panel 2018a). Another large population with PFAS exposure from contaminated drinking water, predominantly PFOA, is in the Veneto region of Italy (Canova et al. 2020). A cross sectional analysis of PFASs and lipids was carried out in nearly 16 000 people, between 20-39 years. The median PFOA serum concentration

was 35.8 ng/ml, and the pattern broadly consistent with the C8 study, i.e. increasing cholesterol with PFOA concentration and a steeper slope at lower concentrations. Another recent study on a community, living in a PFAS-polluted area and exhibiting raised serum of levels of mainly PFOS (and other PFASs) and to a lesser degree PFOA, also reported positive associations with serum cholesterol (Li et al. 2020). In addition to the cross-sectional analyses associating concurrent serum measurements of PFASs and lipids, the authors included an ecological component showing higher cholesterol in the exposed community compared to subjects sampled in a nearby, non-exposed community.

In contrast to the community studies, the reported magnitude of the effect on cholesterol is lower in workers at much higher serum concentrations, e.g. a +2-3% increase in cholesterol per increase in serum PFOA levels of 1 000 ng/mL (Sakr et al. 2007b) with exposure for several years and higher serum concentrations of PFOS/PFOA (mean or median levels \geq 1 000 ng/mL, PFOA: 7- 92 300 ng/mL, PFOS: 20- 6 240 ng/mL) (e.g. Olsen et al. 2003a; Olsen et al. 2007; Sakr et al. 2007a; Sakr et al. 2007b). Olsen and Zobel (2007) re-analysed the data from 2003 (Olsen et al. 2003a) and after some exclusions, e.g. people using cholesterol lowering drugs, no longer observed an association between total cholesterol and LDL-C. Positive associations between increased serum levels of TGs and PFOS and/or PFOA were also recorded in both workers and the general population, but in relatively few studies (e.g. Olsen et al. 2003a; Olsen and Zobel 2007; Steenland et al. 2009).

TABLE 1 Representative human studies reporting associations between serum levels of PFOS and/or PFOA and serum levels of lipids.¹⁶

Substance	Study information, No of subjects	Findings in serum	Serum levels (ng/mL)	Reference
<i>Cross-sectional studies general population</i>				
PFOS/PFOA	Denmark DCH, 753 individuals	PFOS vs TC \uparrow	Mean PFOS 36,	Eriksen et al. (2013)
		PFOA vs TC \uparrow	Mean PFOA 7.1	
PFOS/PFOA	NHANES, USA, 860 adults	PFOS vs TC \uparrow		Nelson et al. (2010)
		PFOS vs non-HDL-C \uparrow		
		PFOS vs LDL-C \uparrow	Median PFOS 20,	
		PFOA vs TC \uparrow	3.8	
PFOS/PFOA	C8 cohort, 46 000 adults	PFOA vs non-HDL \uparrow		Steenland et al. (2009)
		PFOA vs LDL-C \uparrow		
		PFOS vs TC \uparrow		
		PFOS vs LDL-C \uparrow	Median PFOS 20	
PFOS/PFOA	C8 cohort, 46 000 adults	PFOS vs TGs \uparrow		Steenland et al. (2009)
		PFOA vs TC \uparrow		
		PFOA vs LDL-C \uparrow	Median PFOA 27	
PFOS/PFOA	C8 cohort, 46 000 adults	PFOA vs TGs \uparrow		

¹⁶ Only significant positive or inverse (negative) associations are mentioned in the Table. However, some studies showed also negative findings (no associations).

Substance	Study information, No of subjects	Findings in serum	Serum levels (ng/mL)	Reference
PFOS/PFOA	C8 cohort, 12 500, children, 1–18 y	PFOS vs TC ↑	Mean PFOS 23	Frisbee et al. (2010)
		PFOS vs LDL-C ↑		
		PFOS vs HDL-C ↑		
		PFOA vs TC ↑	Mean PFOA 69	
		PFOA vs LDL-C ↑		
PFOS/PFOA	Sweden, 1945, adults ¹⁷	PFOS vs TC ↑	Median PFOS 157	Li et al. (2020)
		PFOS vs LDL-C ↑		
		PFOA vs TC ↑	Median PFOA 8.6	
		PFOA vs LDL-C ↑		
Cross-sectional studies occupational settings				
PFOS/PFOA	USA (3M), and Belgium, 518 individuals	PFOS vs TC ↑	High, mean PFOS and PFOA about 1 000	Olsen, Burris, et al. (2003)
		PFOS vs TGs ↑		
PFOA	USA (3M) and Belgium, 506 individuals (re-evaluation of 2003 data)	PFOA vs HDL-C ↓	High, median PFOS of 720 (range 20 to 6 240), median PFOA of 2 210 (range 10 to 92 000)	Olsen and Zobel (2007)
		PFOA vs TGs ↑		
PFOA	USA (DuPont), 1 025 individuals	PFOA vs TC ↑	High, median PFOA 114–494 across 4 categories (range 8 to 9550)	Sakr et al. (2007a)
		PFOA vs LDL-C ↑		
		PFOA vs VLDL-C ↑		
Longitudinal studies general population				
PFOS/PFOA	C8 cohort, 560 individuals	PFOS vs TC ↑	Geometric Mean PFOS: from 10 to 8	Fitz-Simon et al. (2013)
		PFOS vs LDL-C ↑		
PFOA	C8 cohort, 32 000 individuals, general population and workers	PFOA vs TC ↑	Geometric Mean PFOA: from 75 to 31	Winqvist and Steenland (2014)
			Median PFOA general population 24 and workers 113. Modelled cumulative PFOA: 20th percentile 215 ng/mL*yr and 80th percentile 1 820 ng/mL*yr	
Longitudinal studies occupational settings				
PFOS/PFOA	USA (3M), and Belgium, 174 individuals	PFOA vs TC ↑	High, mean PFOS and PFOA about 1 000	Olsen, Burris, et al. (2003)
		PFOA vs TGs ↑		
PFOA	USA (DuPont), 454 individuals	PFOA vs TC ↑	High, mean PFOA about 1 000	Sakr et al. (2007b)
Therapeutic studies				
PFOA	49 cancer patients, phase 1 dose-escalation trial, no control group, 50–1200 mg, weekly for 6 weeks	PFOA vs TC ↓	150 000 – 230 000	Convertino et al. (2018)
		PFOA vs LDL-C ↓		

DCH: Diet Cancer and Health; C8: study performed in the 'C8' area where drinking water was contaminated by PFOA from a DuPont plant; '↑' sign illustrates a statistically significant positive association; '↓' sign illustrates inverse a statistically significant association, TC: Total cholesterol, TGs: triglycerides, LDL-C: Low-Density lipoprotein, HDL-C: High-Density lipoprotein.

17 Municipality where one out of two waterworks had been heavily contaminated from aqueous fire-fighting foams, and from a nearby control area.

Although the associations between serum levels of total cholesterol, LDL-C and TGs and serum levels of PFOS/PFOA have been recorded repeatedly, the causality of these exposure-effect relationships is still an issue requiring further scientific inquiry (EFSA CONTAM Panel 2020a). In addition, the available evidence for an association between PFOS/PFOA exposure and an associated adverse outcome, i.e. CVD, is missing (EFSA CONTAM Panel 2020a).

An important limitation of most of the studies, is that they were cross-sectional in design, and so the direction of causality is unknown and may be vulnerable to confounding affecting serum concentrations of both PFOS/PFOA and cholesterol. An example of potential confounding is related to the enterohepatic cycling of PFOS/PFOA and bile acids. PFOS/PFOA have been shown to be excreted to the bile and it was estimated that thereafter, most of the PFOS/PFOA must undergo extensive enterohepatic re-absorption from the gastrointestinal tract to explain the long half-lives in humans (Fujii et al. 2015; Harada et al. 2007) (see section Species differences in toxicokinetic properties of PFOS and PFOA). In line with this, absorption of PFOS/PFOA was shown to be mediated by the transporters that also participate in absorption of bile acids (Zhao et al. 2015b). Given that differences in the absorption of bile acids due to genetic factors, such as interindividual variations, food composition or medicines can result in altered levels of serum cholesterol, it is plausible that confounding related to excretion and re-absorption in the enterohepatic cycling process may play a role in the cross-sectional associations observed for PFOS/PFOA and total serum cholesterol (EFSA CONTAM Panel 2020a).

A few studies had a longitudinal design (see example in Table 1), and as such were subject to a smaller risk of confounding. For example, in a longitudinal study within the C8 cohort, the incidence of the diagnosis of increased serum cholesterol levels was related to the modelled serum PFOA in the population. The exposure model was based on the water concentrations and intake, not individual measurements, and thus was not vulnerable to the confounding described above. A modest, but significant, increase of serum cholesterol levels in relation to modelled PFOA intake was found (Winquist and Steenland 2014). The same study assessed CVD in relation to PFOA and did not find an association. A subgroup of subjects in the C8 study participated in a longitudinal follow-up study with repeated blood testing about 4 years after the first survey (Fitz-Simon et al. 2013), showing a general decline of serum PFOS/PFOA levels by an average of about 60% reflecting the half-life of approximately 3 years. The mean total cholesterol level did not fall, but was slightly increased, which may be explained by increasing age or change in life-style. When stratifying the group according to the extent of decrease in serum PFOS or PFOA levels, it was shown that those with the highest decrease in PFOS/PFOA showed a relative decrease in serum cholesterol levels, compared to the group with the lowest decrease in PFOS/PFOA. These results also suggest that the effect of PFOS/PFOA on cholesterol levels is reversible. The similarity in the direction of results across different study designs (cross sectional, ecologic and longitudinal) supports a causal role for the PFOA in increasing cholesterol. On the other hand, one would expect an exposure-related increase in cardiovascular risk, but there is little evidence for this.

A recently published human study (Convertino et al. 2018) does not seem to support the findings regarding increased cholesterol, as observed in a large number of epidemiological studies. This was a clinical phase I dose-escalation study with 49 cancer patients, who were administered for 6 weeks very high doses of PFOA, resulting in serum levels of 150 000 – 230 000 ng/mL (Table 1). The authors reported a subsequent dose-dependent reduction in total cholesterol and LDL-C levels in blood. However, this study is probably of little relevance for the general and worker population, since it was conducted in a small population of late-stage cancer patients, whose metabolic activity may differ considerably from healthy individuals. In addition, high doses of PFOA were applied for a limited time period.

In parallel to cholesterol changes, an increased incidence of mildly elevated serum levels of the liver enzyme alanine transferase (ALT) associated with PFOA exposure was recorded (Darrow et al. 2013; Gallo et al. 2012a; Gleason et al. 2015; Jain and Ducatman 2019; Lin et al. 2010; Nian et al. 2019; Salihovic et al. 2018). Some studies reported similar findings for PFOS (Gallo et al. 2012a; Lin et al. 2010; Salihovic et al. 2018). Nevertheless, the magnitude of the associations between serum ALT and PFOA (and PFOS) levels was small (~ 3%). In addition, the observed changes in ALT were not accompanied by observable adverse health effects, such as liver damage and metabolic disorders (EFSA CONTAM Panel 2018a; 2020a).

Effects observed in animal toxicity studies

The interpretation of perturbations in lipid homeostasis observed in human studies becomes more challenging when considering the apparent lack of similar effects in rodent models. In fact, rodent data in general demonstrate opposite findings, *i.e.* a hypolipidemic effect characterized by decreased levels of serum cholesterol (~20-40%) and TGs (~30-80%) after exposure to PFOS/PFOA. Some representative studies are presented in Table 2. It should be noted that the purpose of this manuscript is not to perform a comprehensive review; thus, Table 2 lists only examples of typical studies. In rodents, decreases in serum cholesterol and TGs have been observed after repeated exposure (starting already at exposure durations of 2-4 weeks) and at doses between 0.3 to 10 mg/kg bw/d, which resulted in serum levels of 50 000 - 500 000 ng/mL (Bijland et al. 2011; Curran et al. 2008; DeWitt et al. 2009; Loveless et al. 2006; Minata et al. 2010; NTP 2019a; 2019b; see some information in Table 2; Yan et al. 2015b). These PFAS serum levels are much higher than those levels associated with increased serum lipids in humans (observed at mean serum concentrations as low as 20-30 ng/mL; Table 1). For PFOS, decreases in serum cholesterol were also reported after longer exposure durations (13-14 weeks) (Butenhoff et al. 2012a; Seacat et al. 2003), whereas for PFOA these endpoints were not examined in longer-term studies (Butenhoff et al. 2012b; Perkins et al. 2004). Very few investigations in animals used PFOS/PFOA doses that were low enough to have given serum concentrations like those seen in humans. At these low exposure levels, serum lipids were not affected by PFOS/PFOA treatment in rodents (Pouwer et al. 2019; Seacat et al. 2003; Yan et al. 2015b). Nevertheless, only one of these studies illustrates a dose-response (Pouwer et al. 2019), discussed further in sub-section Species differences in lipoprotein homeostasis in relation to PFAS lipid-related effects, whereas only a single dose level was applied in the other two.

Most investigations on the effects of PFOS/PFOA have been performed in rats and mice, with a few exceptions, in which monkeys have been used (examples in Table 2). PFOS lowered the serum cholesterol in cynomolgus monkeys after repeated exposure, when administered at doses comparable to those in the high dose rodent studies (serum: 15 000 – 70 000 ng/mL) (Chang et al. 2017; Seacat et al. 2002). A 6-month oral PFOA administration in monkeys (serum: 70 000 - 160 000 ng/mL) produced a mild increase in circulating TGs, whereas blood cholesterol appeared unaffected (Butenhoff et al. 2002).

In parallel to the hypolipidemic effects in the blood, other lipid disturbances observed include enhanced intrahepatic accumulation of lipids, mainly TGs, in rodents for both PFOS (Bijland et al. 2011; Wan et al. 2012; Wang et al. 2014), and PFOA (Das et al. 2017; Hui et al. 2017; Nakagawa et al. 2012; Schlezinger et al. 2020; Tan et al. 2013; Wang et al. 2013; Wu et al. 2018) (see Table 2 for examples). The liver appears to be a major target organ for both compounds in rats and mice, as indicated by increased liver weight, hypertrophy of centrilobular hepatocytes, induction of peroxisomal and mitochondrial β -oxidation, and in some cases necrosis. Liver damage in rodents is also indicated by increased serum transaminases (Curran et al. 2008; Elcombe et al. 2012; NTP 2019a; 2019b; Son et al. 2008; Yu et al. 2009). Similarly, in primates the liver appears to be a target organ for PFOS/PFOA, with effects manifested as increased liver weights with hepatocellular hypertrophy and vacuolation (Butenhoff et al. 2002; Chang et al. 2017; Seacat et al. 2002). It has been speculated that the observed liver damage, like steatosis and necrosis, can be attributed to the alterations in the hepatic lipid metabolism (EFSA CONTAM Panel 2020a).

TABLE 2 Example studies in animals reporting on lipid perturbations induced by PFOS/PFOA. Only induced effects are reported in the table.

Substance	Experimental design	Lipid perturbation-related findings	LO(A)EL (mg/kg bw/d)	Serum levels at LO(A)EL (μ g/mL)	Liver levels at LO(A)EL (μ g/g)	Reference
Studies in rats						
PFOS	Sprague Dawley rats (m,f), 4 weeks, in feed	↓ serum TC (m)	3.21	20.93 ± 2.36	856.90 ± 353.83	Curran et al. (2008)
	0, 0.14, 1.33, 3.21, 6.34 (m)	↓ serum TGs (m)	3.21	20.93 ± 2.36	856.90 ± 353.83	
	0, 0.15, 1.43, 3.73, 7.58 (f) mg/kg bw/d	↓ serum TC (f)	3.73	31.93 ± 3.6	597 ± 158	
		↓ serum TGs (f)	3.73	31.93 ± 3.6	597 ± 158	
PFOS	Sprague Dawley rats (m,f), 4 weeks, gavage	↓ serum TC (m)	0.312	23.73 ± 1.11	87.17 ± 3.03	NTP (2019a)
	0, 0.312, 0.625, 1.25, 2.5, 5 mg/kg bw/d	↓ serum TGs (m)	5	318.2 ± 8.86	867.1 ± 26.8	
		↓ serum TC (f)	5	413.55 ± 8.07	NR	
		↓ serum TGs (f)	2.5	237.5 ± 5.218	NR	
PFOS	Sprague Dawley rats (m,f), 14 weeks, feed	↓ serum TC (m)	1.5	148 ± 14	568 ± 107	Seacat et al. (2003)
PFOA	Sprague Dawley rats (m), 2 weeks, gavage	↓ serum TC	0.3	20 ± 3.2	NR	Loveless et al. (2006)
	0, 0.3, 1, 3, 10, 30 mg/kg bw/d	↓ serum TGs	0.3	20 ± 3.2		
		↓ non-HDL-C	0.3	65 ± 11		
		↓ HDL-C	3	137 ± 18		

Substance	Experimental design	Lipid perturbation-related findings	LO(A)EL (mg/kg bw/d)	Serum levels at LO(A)EL (µg/mL)	Liver levels at LO(A)EL (µg/g)	Reference	
PFOA	Sprague Dawley rats (m,f), 4 weeks, gavage 0, 0.625, 1.25, 2.5, 5, 10 (m) mg/kg bw/d 0, 6.25, 12.5, 25, 50, 100 (f) mg/kg bw/d	↓ serum TC (m)	0.625	50.69 ± 2.2	54.61 ± 2.23	NTP (2019b)	
		↓ serum TGs (m)	0.625	50.69 ± 2.2	54.61 ± 2.23		
		↑ serum TC (f)	50	9.32 ± 1.82	NR		
		↑ serum TGs (f)	50	9.32 ± 1.82	NR		
Studies in Mice							
PFOS	CD-1 mice (m), 3,7,14,21 days, gavage 0, 1, 5, 10 mg/kg bw	↓ serum TC	5	NR	NR	Wan et al. (2012)	
		↓ serum VLCL-C	5				
		↓ serum LDL-C	5				
		↑ liver lipids	5				
PFOA	SV129 mice (m), 7 days, gavage 0, 10 mg/kg bw	↑ liver lipids	10	NR	NR	Das et al. (2017)	
PFOA	C57BL/6N mice (m), 3 weeks, standard chow or Western type diet 0, 5 mg/kg bw/d	↑ liver lipids	5	NR	NR	Tan et al. (2013)	
PFOA	Crl:CD [®] -1(ICR)BR mice (m), 2 weeks, gavage 0, 0.3, 1, 3, 10, 30 mg/kg bw/d	↓ serum TC	3	69 ± 10	NR	Loveless et al. (2006)	
		↓ HDL-C	3	69 ± 10			
PFOA	29S4/SvlmJ mice (m), 4 weeks, gavage 0, 5.4, 10.8, 21.5 mg/kg bw/d	↓ serum TC	10.8	46.9 ± 3.2	198.8 ± 15.4	Minata et al. (2010)	
PFOA	C57BL/6 & BALB/c mice 6 weeks, in feed, Western type diet (m,f) 0, 0.5 mg/kg bw/d	↑ serum TC (f, C56BL/6)	0.5	8.6	NR	Rebholz et al. (2016)	
		↑ serum TC (m, C56BL/6)		26.9			
		↑ serum TC (m, BALB/c)		28.2			
		↓ liver TC (m,f BALB/c)					
PFOA	BALB/c mice (m), 4 weeks, gavage 0, 0.08, 0.31, 1.25, 5, 20 mg/kg bw/d	↓ liver TC	0.31	NR		(Yan, Wang, et al. 2015)	
Studies in genetically modified mice							
PFOS	APOE*3-Leiden CETP mice (m) 4-6 weeks, in feed, Western type diet 0, 3 mg/kg bw/d	↓ serum TC	3	86-125 (mean range from 3 experiments)		NR	Bijland et al. (2011)
		↓ serum TGs	3	86-125			
		↓ serum non-HDL-C	3	86-125			
		↓ serum HDL-C	3	86-125			
		↑ liver lipids	3	86-125			
PFOA	APOE*3-CETP mice (m) 4-6 weeks, in feed, Western type diet 0, 0.001, 0.03, 3.2 mg/kg bw/d	↓ hepatic CYP7A1 gene expression	3	86-125		NR	Pouwer et al. (2019)
		↓ serum TGs	3.2	90-150			
		↓ serum TC	3.2	90-150			
		↓ non-HDL	3.2	90-150			
		↑ HDL-C	3.2	90-150			
PFOS	WT and PPAR α null mice (m), 7 days 0, 3, 10 mg/kg bw/d	↑ expression of genes related to liver cholesterol biosynthesis	10	NR	NR	Rosen et al. (2010)	
PFOA	hPPAR α mice, 6 weeks, gavage 0, 1, 5 mg/kg bw/d	↓ serum TGs	1	NR	NR	Nakagawa et al. (2012)	
		↑ liver TGs	1				

Substance	Experimental design	Lipid perturbation-related findings	LO(A)EL (mg/kg bw/d)	Serum levels at LO(A)EL (µg/mL)	Liver levels at LO(A)EL (µg/g)	Reference
PFOA	hPPARα mice (m,f), 6 weeks, drinking water, Western type diet 0, 0.7 mg/kg bw/d	↑ liver lipids	0.7	48	NR	Schleizinger et al. (2020)
Studies in Monkeys						
PFOS	Cynomolgous monkeys (m,f) 26 weeks (182 days), gavage 0, 0.03, 0.15, 0.75 mg/kg bw/d	↓ serum TC (m)	0.03	15.8 ± 1.4	17.3 ± 4.7	Seacat et al. (2002)
		↓ serum TGs (m)	0.15	82.6 ± 25.2	58.8 ± 19.5	
		↓ serum HDL-C	0.03	15.8 ± 1.4	17.3 ± 4.7	
		↑ liver lipids (m)	0.75	173 ± 37	395 ± 24	
		↓ serum TC (f)	0.75	171 ± 22	273 ± 14	
		↓ serum HDL-C	0.75	171 ± 22	273 ± 14	
PFOS	Cynomolgous monkeys (m,f) 1 year, gavage applied only on certain and few days during the experimental period 11-17.2 mg/kg bw, given to achieve respective serum levels	↓ serum TC (m)		74		Chang et al. (2017)
		↓ serum HDL-C	NR	74	NR	
		↓ serum TC (f)		76		
		↓ serum HDL-C		76		

m: males, f: females, bw: body weight, NR: not reported, TC: total cholesterol, HDL-C: high-density lipoprotein cholesterol, TGs: triglycerides, hPPARα: human Peroxisome Proliferator-Activated Receptor, WT: wild-type, '↑' sign illustrates a statistically significant increase; '↓' sign illustrates a statistically significant decrease.

Interpretation of human versus rodent data

Several population studies have repeatedly found correlations between increased blood levels of PFOS/PFOA and elevated blood total cholesterol and LDL-C, (and to a lesser extent TGs). Nevertheless, these findings have not been linked to a corresponding adverse health effect and are inconsistent with toxicological animal studies, where high doses of PFOS/PFOA were found to lower serum cholesterol and TGs, and increase liver lipids. These apparent divergent findings thus present the health risk assessors a conundrum. As noted above, some representative studies on these findings are described in Tables 1 and 2. For a complete picture of the epidemiological and animal data the reader is referred to the EFSA CONTAM Panel Opinions (2018a; 2020a).

Considering the large differences in exposure levels between humans and laboratory animals and in order to facilitate the discussion, serum levels of PFOS/PFOA together with externally administered doses are mentioned here, when available. Furthermore, it should be highlighted that not only PFOS/PFOA serum concentrations are of importance in such evaluations, but also the related hepatic concentrations (also reported when available). A relatively higher retention of PFOS/PFOA in the liver in one species compared to another could also play a role in the different outcomes.

Next to the exposure levels, exposure duration may also be divergent, i.e. several decades for humans *versus* several (2-14) weeks for animals¹⁸. Consequently, one could argue that

18 One decade in human life would correspond to approximately 12 weeks for the rat considering its two-year life span.

in humans, PFOS/PFOA chronic exposure leads to a different lipid response and balance, whereas this is not the case for rats exposed for shorter periods. It cannot be excluded that such differences may also contribute to the differential responses between the two species. It shall be noted here that irrespective of the shorter exposure duration, data indicate that a serum steady-state concentration is also reached in the rat for both compounds (Gomis et al. 2018).

Apart from the exposure levels and exposure duration, other reasons are known or suspected to be implicated in the observed differences, including differences in mechanisms underlying the observed effects and in PFAS species-specific toxicokinetics. An understanding of the causal pathway that may lead from chemical exposure to potential adverse outcomes could assist in a better understanding of the epidemiological data. An overview of such mechanisms, which may explain the PFOS/PFOA-mediated lipid disturbances, is presented below. Information discussed stems from mechanistic rodent studies (including genetically modified mice) and *in vitro* test systems performed with human relevant material, such as human hepatocytes. Next to this, PFOS/PFOA species-specific toxicokinetics issues are presented.

Mechanistic pathways involved in PFAS-induced lipid perturbations

Species differences in lipoprotein homeostasis

General information on lipoprotein circulation

The liver is the primary organ tightly controlling lipid homeostasis, in humans, as well as in other primates and rodents, to ensure a balance between influx, generation, and efflux of lipids. Main functions of the liver with respect to lipid homeostasis include the fatty acid β -oxidation for energy supply, cholesterol biosynthesis and lipogenesis. Circulation of the lipids through the body occurs via specific carrier molecules, i.e. the lipoproteins, also synthesized in the liver (Dietschy et al. 1993; Kwiterovich 2000) (Figure 2). Lipoproteins contain a hydrophobic core comprising cholesteryl-esters and TGs, and an amphipathic part, which consists of apolipoproteins and phospholipids (Imes and Austin 2013).

After a meal, the intestine releases chylomicrons, which are mainly composed of TGs and to a lesser extent cholesteryl-esters. Most of the TGs are cleared in the adipose tissue and muscle through the action of lipoprotein lipase. The leftover TGs and the cholesteryl-esters are taken up by the liver as part of chylomicron remnants (Figure 2). The liver uses the cholesterol to synthesize bile acids, which together with cholesterol are secreted into the bile. During fasting, the liver serves as a sink for circulating adipose tissue-derived free fatty acids, which are either fully oxidized or converted into ketone bodies. In addition, incoming fatty acids are esterified into TGs and stored within lipid droplets or secreted as very low-density lipoproteins (VLDL) for delivery of primarily TGs to the peripheral tissues (Zhang et al. 2014). In the blood, VLDL are further metabolized through the removal of

the TG portion into LDL, the latter being the main carrier of cholesterol to many tissues including the liver, and taken up via the LDL-receptor (LDLR). On the other hand, the HDL particles participate in the reverse cholesterol transport pathway, i.e. acquiring excess cholesterol effluxed from peripheral tissues and returning it to the liver. The main apolipoprotein in VLDL and LDL particles is apolipoprotein B (apoB) and in HDL apolipoprotein A-I (apoA-I) (Feingold 2000; Imes and Austin 2013; Marques et al. 2018). Disturbances in these metabolic pathways can promote fatty-liver disease and lead to alterations in plasma lipid levels (Adiels et al. 2008).

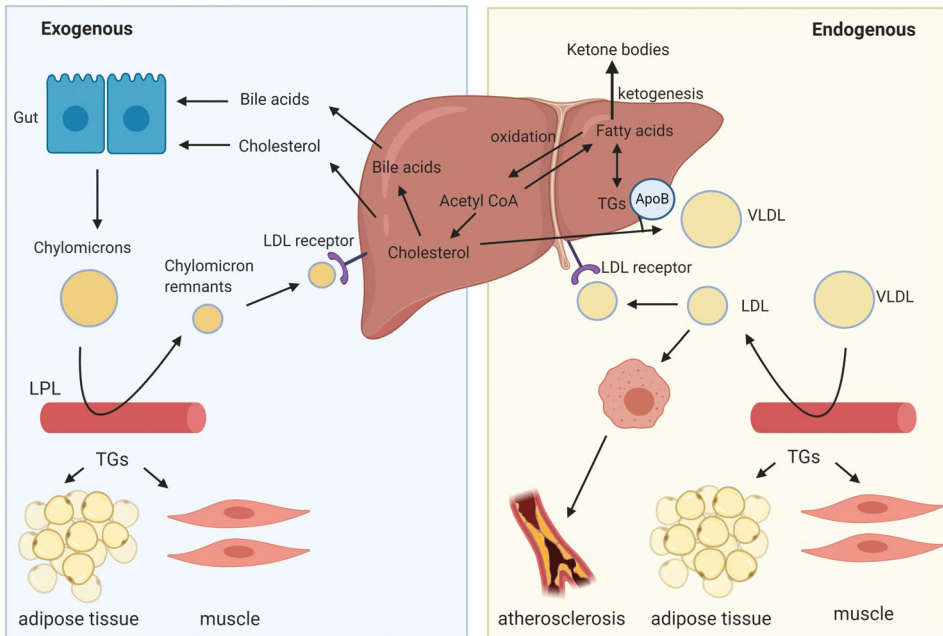


FIGURE 2 Overview of the lipid circulation throughout the human body with their carrier molecules, the lipoproteins. LPL: lipoprotein lipase, LDL: low-density lipoprotein, VLDL: very low-density lipoprotein, TGs: triglycerides, ApoB: apolipoprotein B. (Created with BioRender.com).

The above described processes comprise some general characteristics of lipid homeostasis that overall are well-conserved across species (Bergen and Mersmann 2005; Dietschy et al. 1993). Nevertheless, several aspects of lipid homeostasis are known to be specific for humans or rodents. These include differences pertaining to lipoprotein metabolism (Dietschy and Turley 2002; Princen et al. 2016), which ultimately results in different proportions of the circulating lipoproteins amongst species (Bergen and Mersmann 2005; Kaabia et al. 2018; Lee-Rueckert et al. 2016). Hence, in mice and rats, serum cholesterol is for the major part confined to HDL, while the levels of cholesterol carried by VLDL and LDL are low. In contrast, in humans and non-human primates, the majority of cholesterol is contained in the apoB-containing lipoproteins LDL and to a lesser extent VLDL, thereby resulting in a higher proportion of LDL relative to HDL in the blood (Krause and Princen

1998; Princen et al. 2016). This occurs due to a faster LDL clearance pathway in rodents compared to humans (Dietschy and Turley 2002; Dietschy et al. 1993), and the complete absence of cholesteryl ester transfer protein (CETP) in rats and mice. CETP is a central element in lipoprotein metabolism and is responsible for the transfer of cholesteryl-esters from HDL to apoB-containing lipoproteins in exchange for TGs (Chapman et al. 2010; Morton and Izem 2014; Princen et al. 2016). Consequently, the choice of the animal model should be carefully considered.

Species differences in lipoprotein homeostasis in relation to PFAS lipid-related effects

A few studies attempted to clarify the relevance of such species-specific differences for the observed PFOS/PFOA lipid-disturbing effects (Bijland et al. 2011; Pouwer et al. 2019). For this, the genetically engineered mouse model APOE*3-Leiden.CETP (Westerterp et al. 2006) was used, which mimics human lipoprotein metabolism and the response to clinically used hypolipidemic drugs, such as statins, fibrates, niacin and the novel PCSK9-inhibitors (Ason et al. 2014; Kühnast et al. 2015; Pouwer et al. 2020; Zadelaar et al. 2007). At the two highest doses tested, both PFOS (86 000- 125 000 ng/mL, 4-6 weeks) and PFOA (90 000- 150 000 ng/mL, 4-6 weeks) induced hypolipidemia in the blood, which was characterized by decreased levels of TGs (50-70%) and total cholesterol (30-60%) (mainly the non-HDL fraction)(Bijland et al. 2011; Pouwer et al. 2019). These findings are in line with other studies with PFOS/PFOA conducted in wild-type mice and rats, with similar dose levels and exposure durations. However, in the wild-type animals the decrease in cholesterol is presumed to be mainly due to the HDL fraction. Unfortunately, most of the animal studies did not discriminate between the lipoproteins and mainly measured total cholesterol. Concurrently, PFOS exposure enhanced intrahepatic TG and cholesterol concentrations in APOE*3-Leiden.CETP mice (Bijland et al. 2011), while such lipid changes were not seen with PFOA at a similar dose (Pouwer et al. 2019). Mechanistic studies revealed that the decreased serum lipid levels occurred through PFOS/PFOA-enhanced (lipoprotein lipase-mediated) VLDL-TG clearance and PFOS/PFOA-decreased hepatic VLDL-TG and apoB production. The observations were further supported by gene expression alterations and pathway analysis confirming the changes in lipoprotein metabolism measured (Bijland et al. 2011; Pouwer et al. 2019). It should be noted that these effects were only seen at doses and respective serum levels that are several orders of magnitude higher than those relevant in humans (Table 2), whereas they were absent at lower, human-relevant environmental or occupational serum levels (50- 2 000 ng/mL); only PFOA was tested at these low doses (Pouwer et al. 2019).

These findings from the studies using the APOE*3-Leiden.CETP model indicate that the known differences in lipoprotein metabolism between humans and rodents, as discussed above, cannot sufficiently explain the observed discrepancy in PFOS/PFOA-induced lipid perturbations. Although the APOE*3-Leiden.CETP mouse has a humanized lipoprotein metabolism, it does not integrate other species differences that possibly play a fundamental role in the respective lipid perturbations (see next sections). On the other hand, the findings

observed could be interpreted otherwise, and one could hypothesize that substantial differences in serum PFOA concentrations (at least two or three orders of magnitude) are indeed the main determinant of the interspecies differences reported (the slight reduction in cholesterol reported for cancer patients with very high serum PFOA (Convertino et al. 2018) is consistent with this finding. Perhaps at such high serum levels different pathways come into play, both in humans and animals. Accordingly, exposure to PFOA at low doses may not have a significant effect on serum lipid homeostasis, as illustrated by the findings from the APOE*3-Leiden.CETP mouse. The resulting uncertainty regarding the causality of the epidemiological observations and PFOS/PFOA exposure could be reduced by further elucidation of the mechanism(s) involved.

Additionally, when evaluating the different effects of PFOS/PFOA on blood lipids between humans and rodents, it is important to realize that rodent chow contains much less fat and almost no cholesterol when compared to the high-fat Western type diet of humans. For this reason, some studies were performed with rodents fed with a more human-relevant diet (Bijland et al. 2011; Pouwer et al. 2019; Rebholz et al. 2016; Wang et al. 2014), in order to delineate whether dietary factors are responsible for the absence of the increased blood lipid effect of PFASs in rodents fed conventionally.

Wang et al. (2014) treated BALB/c mice with PFOS combined with a normal or high fat diet (Table 2). Indeed, in the control animals, fed with the high-fat diet alone, a significant increase in blood cholesterol (HDL and LDL), together with an increase in hepatic fat content, was reported (Wang et al. 2014). Nevertheless, unlike the controls, the PFOS-treated mice exhibited reduced levels of serum lipids and lipoproteins, independent of the dietary regimen. Administration of a Western-type diet together with PFOS or PFOA was also employed with the aforementioned studies on the APOE*3-Leiden.CETP mice (Bijland et al. 2011; Pouwer et al. 2019). Similarly, blood cholesterol and TGs were decreased in PFOS or PFOA-treated animals. These results suggest that the dietary fat does not interfere with the PFOS/PFOA-induced lipid perturbations observed in rodents. On the other hand, one single study demonstrated different results, where C57BL/6 mice showed increased blood cholesterol (35% in males, 70% in females), when receiving PFOA together with a cholesterol/lipid-rich diet, in comparison to the animals treated only with the lipid rich diet (Rebholz et al. 2016). A less pronounced increase in blood cholesterol (20%) was seen in male BALB/c mice, whereas blood cholesterol remained unaffected in the PFOA-treated BALB/c female mice when compared to control animals being on the high fat diet alone. The increased cholesterol was contained in the (large) HDL fraction, as expected for the rodents. Unfortunately, only one dose level was applied, while a control group fed on standard chow was not included. Overall, no conclusive differences were identified that can fully justify the contrasting lipid disturbances in rodents *versus* humans upon PFAS exposure; still, it cannot be excluded that diet might play a role, but effects need to be further clarified.

The role of PPAR α in PFOS/PFOA-induced lipid perturbations

General information on the PPAR α

The regulation of hepatic lipid and cholesterol metabolism occurs largely at the level of gene transcription by nutrient-sensitive transcription factors, encompassing several nuclear receptors. One of the main nuclear receptors involved in the regulation of hepatic lipid metabolism is PPAR α , which is primarily activated by fatty acids and various fatty acid derivatives (Göttlicher et al. 1992). The activation of PPAR α in rodent and human hepatocytes induces the expression of numerous genes involved in various pathways of lipid metabolism, such as fatty acid storage, β -oxidation, and transport (Kersten 2014; Kersten and Stienstra 2017). For example, PPAR α serves as direct molecular target of fibrate drugs, which are used in the treatment of dyslipidemia and lower blood lipid levels by inducing lipoprotein lipase-mediated VLDL-TG clearance (Chapman et al. 2010; Fabbrini et al. 2010; Kim and Kim 2020; Schoonjans et al. 1996).

Lipid homeostasis and activation of PPAR α by PFOS/PFOA in rodents

PFOS/PFOA structurally resemble fatty acids and are well-established ligands of PPAR α in the rat and mouse liver (Elcombe et al. 2012; Perkins et al. 2004; Rosen et al. 2017; Rosen et al. 2010; Wolf et al. 2014; Wolf et al. 2012; Wolf et al. 2008). Consequently, activation of the PPAR α signalling pathway upon exposure to PFOS or PFOA is believed to be, at least partly, responsible for the observed perturbations of lipid homeostasis in animals (DWQI 2017; 2018; EFSA CONTAM Panel 2018a). In fact, gene expression studies conducted on liver samples from PFOS/PFOA-exposed rodents revealed that a substantial proportion of the up- or down-regulated genes (e.g. *Cyp4a1*, *Acox1*) are under the control of the PPAR α receptor (Pouwer et al. 2019; Ren et al. 2009; Rosen et al. 2008a; Rosen et al. 2017; Rosen et al. 2010). In terms of the PPAR α activation potency, PFOA was shown to be more potent when compared to PFOS, both in reporter gene assays and in gene expression studies with rat hepatocytes. (Bjork and Wallace 2009; Takacs and Abbott 2007; Wolf et al. 2012; Wolf et al. 2008). Also, in the recent NTP studies in male rats (2019a,b), PFOA appeared to be a more potent inducer of *Acox1* and *Cyp4a1* gene expression in livers than PFOS, despite a lower accumulation in liver.

As prototypical PPAR α agonists, PFOS/PFOA induce the mitochondrial and peroxisomal β -oxidation of fatty acids for their degradation to acyl-CoA-moieties in the rodent liver (Bijland et al. 2011; Pouwer et al. 2019; Rosen et al. 2010; Wan et al. 2012; Wang et al. 2014). Furthermore, they induce the fatty acid transport across the mitochondrial membrane (Bijland et al. 2011; Pouwer et al. 2019; Rosen et al. 2010; Wang et al. 2014). In parallel, they decrease the hepatic VLDL-TG and apoB production, disturbing as such the hepatic secretion of TGs (and indirectly cholesterol) into the blood. Furthermore, they promote lipoprotein lipase-mediated lipolysis of TG-rich plasma lipoproteins (Bijland et al. 2011; Pouwer et al. 2019). These processes appear to contribute to the lowered blood TG levels but also to the enhanced hepatic TG concentrations in PFOS/PFOA-treated rodents.

PPAR α is also known to play a role in cholesterol homeostasis, including inhibition of cholesterol and bile acid synthesis in mice and man) (Li and Chiang 2009; Post et al. 2001), regulation of HDL metabolism and promotion of reverse cholesterol transport (Li and Glass 2004; Li and Chiang 2009; Ory 2004). Nevertheless, the role of PPAR α in the PFAS-induced changes on blood and liver cholesterol in rodents is still elusive. This is further discussed in section Mechanisms linked to disturbance of cholesterol homeostasis.

Although the general view remains that the PPAR α plays a pivotal role in PFOS/PFOA-induced lipid disturbances in rats and mice (ATSDR 2018; EFSA CONTAM Panel 2018a), some evidence suggests its role is of less importance. Actually, the effects observed upon PFOS/PFOA exposure are not *per se* consistent with effects of other well-studied PPAR α activators, such as fibrates and Wyeth (WY)-14643. For example, typical PPAR α activators commonly do not cause liver steatosis in rodents at comparable doses and exposure durations (Larter et al. 2012; Pawlak et al. 2015), contrary to what is seen after exposure to PFOS/PFOA.

Some information from PPAR α -null mice studies further support the notion for the involvement of PPAR α -independent pathways in the PFOS/PFOA-exerted lipid disturbances. However, it is important to emphasize that knocking out the receptor itself in mice affects lipid metabolism, leading to steatosis in the liver of control PPAR α -null mice (Corton et al. 2014a; Das et al. 2017; Howroyd et al. 2004), which might interfere with the interpretation of the results obtained for PFOS/PFOA treated PPAR α -null mice. Still, it has been shown that PPAR α -null mice exhibit hepatic lipid accumulation and/or alterations in genes linked to lipid metabolism upon exposure to PFOA (Das et al. 2017; Minata et al. 2010; Nakagawa et al. 2012; Rosen et al. 2008a; Rosen et al. 2008b) or PFOS (Rosen et al. 2010), which counterargues that these effects should be attributed to PPAR α activation. Nakagawa et al. (2012), for example, demonstrated that the liver steatosis in the PFOA-exposed PPAR α -null mice is more prominent when compared to the WT mice (1 and 5 mg/kg b/d, 6 weeks). In that study, control PPAR α -null mice showed only a slight and not statistically significant increase in hepatic TG accumulation, contrary to what is commonly seen with such knock-out animals (Corton et al. 2014b; Das et al. 2017; Howroyd et al. 2004). Overall, data on PFOA-exposed PPAR α -null mice seem to corroborate the contribution of other PPAR α -independent signalling pathways in the lipid disturbances induced by PFOS/PFOA in rodents.

Are PPAR α -mediated effects in rodents relevant for human health?

The importance of the PPAR α receptor in human liver has been questioned in the past, due to the perceived low expression of PPAR α in humans and minimal responsiveness of human liver cell lines to PPAR α activation (Auboeuf et al. 1997; Palmer et al. 1998; Tugwood et al. 1996). Accordingly, the potential human relevance of the PFOS/PFOA-induced lipid perturbations seen in rodents, and, at least partially, driven by activation of the PPAR α pathway, has been subject to debate (DWQI 2017; 2018; EFSA CONTAM Panel 2018a). However, later research indicates that the quantitative expression of PPAR α is similar

in human and mouse liver (Kersten and Stienstra 2017) and that in human hepatocytes and liver slices, PPAR α is able to effectively induce the expression of genes involved in numerous lipid metabolic pathways. Still, remains to a lesser extent compared to mouse or rat hepatocytes and mouse liver slices (Corton et al. 2014a; Heusinkveld et al. 2018; Janssen et al. 2015; Liss and Finck 2017; Okyere et al. 2014). Indeed, studies using chimeric mice, harbouring murine as well as human hepatocytes in the liver, underscore the more modest PPAR α -mediated gene trans-activation in human hepatocytes compared to their murine counterparts (de la Rosa Rodriguez et al. 2018). Apart from these quantitative interspecies differences, qualitative differences have also been illustrated recently, after comparisons of PPAR α signalling transcriptional networks in primary human hepatocytes and rats (McMullen et al. 2020). Such differences could in principle result in differential effect-responses in humans and rats when exposed to PPAR α -ligands.

With respect to the activation of the human PPAR α (hPPAR α) by PFOS/PFOA, studies with hPPAR α expressing mice suggest a lower response to PFOA, when compared to their wild type (WT) counterpart. This is seen by lower increase in transcripts and protein levels of PPAR α target genes (Nakagawa et al. 2012; Nakamura et al. 2009). Still, in combination with these gene expression changes, PFOA-treated hPPAR α mice showed increased lipid accumulation in liver (Nakagawa et al. 2012; Schlezinger et al. 2020). Actually, despite the reduced responsiveness of hPPAR α to PFOA, hPPAR α mice appeared to be substantially more susceptible to liver steatosis than the WT mice, as shown by larger increases in hepatic TG levels (Nakagawa et al. 2012). This further supports that the PFOA-induced liver steatosis, specifically the increase in TG levels, might be driven by PPAR α -independent pathways. With respect to cholesterol, blood levels remained unaffected by the treatment in hPPAR α mice, contrary to the WT mice that showed the typical decrease, when exposed to PFOA. Similar studies with PFOS have not been identified in the literature.

The activation of the hPPAR α by PFOA, but also PFOS, was likewise seen with *in vitro* assays performed in human liver cells, such as human primary hepatocytes, or human liver cell lines (HepG2 and HepaRG) (Beggs et al. 2016; Behr et al. 2020b; Bjork et al. 2011; Louise et al. 2020c). These studies support the activation of PPAR α signalling, at concentrations commonly ranging from 10 μ M to 100 μ M (PFOA: ~4 000 to 40 000 ng/mL, PFOS: ~5 000 to 50 000 ng/mL). These concentrations are high when compared directly to the serum levels recorded even at the highly exposed populations or at workers in occupational settings. However, in one study, gene expression network analysis showed a simulation of the PPAR α signalling already at a concentration of 1 μ M for PFOA (Buhrke et al. 2015). As seen *in vivo* for PFOA, *in vitro* studies comparing responses upon PFOS/PFOA exposure between rodent and human primary hepatocytes support the view that induction of PPAR α transcriptional responses are more pronounced in rodent than in human hepatocytes (Bjork et al. 2011; Bjork and Wallace 2009).

As already stressed for rodents, some *in vitro* studies have demonstrated differences with respect to the hPPAR α activation potency between PFOS and PFOA. Again, PFOA seems a

more potent activator of the hPPAR α than PFOS in reporter gene assays (Takacs and Abbott 2007; Wolf et al. 2012; Wolf et al. 2008), but also in gene expression studies with human hepatocytes (Bjork et al. 2011; Buhrke et al. 2015; Louise et al. 2020c). These differences can be also related to the differences in cellular uptake. For example, cellular uptake of the PFASs in HepG2 cells was shown to be low for PFOA (0.24%), but 10-fold lower for PFOS (0.04%) (at a concentration of 10 μ M, 10% serum), with absolute cellular concentrations of 39 and 4 nmol/mg protein for PFOA and PFOS, respectively (Rosenmai et al. 2018). In that study, PFOA induced PPAR α -mediated reporter gene expression at relatively high concentrations (30 and 100 μ M) whereas PFOS did not induce PPAR α -mediated reporter gene expression, possibly reflecting the differences in cellular uptake, but perhaps also in PPAR α affinity. However, preliminary data on human HepaRG cells (own unpublished data) indicate the reverse, i.e. PFOS accumulating more in the cells than PFOA. To our knowledge, data on cellular uptake of PFASs are currently very limited. It should be emphasized here that overall the lack of information on this aspect is an important limitation of these *in vitro* data. Such measurements would in principle assist in more appropriate comparisons on actual exposure levels, since the nominal concentrations applied in the *in vitro* systems might not be a good proxy for serum levels. As such it is difficult to assess at this state whether the effective concentrations *in vitro* are relevant for human exposure.

Conclusions

The role of PPAR α activation by PFOA in the observed lipid perturbations in rodents, but also its relevance for human health, has been extensively studied, including examinations in hPPAR α and PPAR α -null mice, and in rodent and human hepatocytes. For PFOS less data are available. Overall, PFOA and to a lesser extent PFOS activate PPAR α , both its murine and human version, and the observed lipid alterations may depend to a certain extent on the PPAR α -signalling pathway. Effects on PPAR α -null mice indicate, however, the involvement of other pathways. With respect to the human situation, the large differences in exposure scenarios when compared to rodents, combined with the reduced hPPAR α responsiveness to PFOS/PFOA, warrant the need for careful consideration when comparing rodent and human findings. It cannot be excluded that in humans higher exposure is required for the manifestation of the effects on lipid metabolism, but it should be stressed that certain PFASs accumulate to a higher extent in humans than in rats and mice (see section Species differences in toxicokinetic properties of PFOS and PFOA). As such, due to the life-long exposure of humans to such substances, along with high exposure rates, a certain critical body burden necessary to affect lipid homeostasis by this pathway might be achieved.

Other nuclear receptors potentially involved in PFOS/PFOA-mediated lipid disturbances

PPAR, CAR and other signalling pathways

As discussed above, it is suggested that PPAR α -independent signalling pathways are also involved in the lipid disturbances induced by PFOS/PFOA. In particular the transactivation of other nuclear receptors by PFOS/PFOA, such as PPAR γ , constitutive androstane receptor (CAR), pregnane X receptor (PXR), liver X receptor (LXR) and farnesoid X receptor (FXR), have been studied in rats and mice. It has been suggested that the nuclear receptors PPAR γ (Rosen et al. 2008b), CAR (Abe et al. 2017; Ren et al. 2009; Rosen et al. 2008b; Schlezinger et al. 2020) and PXR (Bjork et al. 2011; Pouwer et al. 2019; Ren et al. 2009), are also activated by PFOS/PFOA in the murine liver. These receptors are in general associated with cholesterol and TG homeostasis (Ory 2004; Yan et al. 2015a; Yin et al. 2011), implying that they might also play a role in the effects induced by PFOS/PFOA. Considering that gene expression is rarely dependent on a sole transcription factor, and that cross-talk between various transcription factors is known to occur, PFOS/PFOA effects in rodents are probably a result of multiple inter-linked pathways.

In vitro studies with human relevant material reported somewhat contradicting results, which could also be the outcome of variable experimental designs, i.e. different concentrations, exposure durations, cell systems etc. In human primary hepatocytes (Bjork et al. 2011), in HepaRG (Abe et al. 2017) and in HepG2 cells (Zhang et al. 2017), multiple nuclear receptors (CAR, PXR, LXR) were activated by PFOS and PFOA, as illustrated by increased expression in some selected marker genes. Yet, other gene expression studies in human hepatocytes and/or reporter gene assays have shown that PFOS/PFOA may activate to a very limited (if any) extent all these receptors, including PPAR γ and FXR (Behr et al. 2020b; Buhrke et al. 2015; Louisse et al. 2020c; Vanden Heuvel et al. 2006). Louisse et al. (2020c) compared the effects of PFOS/PFOA on gene expression in HepaRG cells with the effects of a known LXR-agonist and a FXR-agonist (data from Wigger et al. 2019), suggesting that PFOS/PFOA do not activate these receptors.

Disruption of HNF4 α signalling pathway by PFOS/PFOA

Amongst the other nuclear receptors, of particular interest is the hepatocyte nuclear factor HNF4 α , that seems to be affected by PFOS/PFOA (Beggs et al. 2016; Pouwer et al. 2019; Yan et al. 2015b). HNF4 α is considered a master regulator of liver-specific gene expression and essential for liver development and liver function, including lipid homeostasis (Hayhurst et al. 2001; Yeh et al. 2019; Yin et al. 2011). Dysregulation of HNF4 α function has been associated with a large number of human diseases, including non-alcoholic fatty liver disease (Yeh et al. 2019). There is cross-talk between HNF4 α and other nuclear receptors like PPAR α , for which both antagonism and synergism have been reported (Chamouton and Latruffe 2012; Lu 2016). There is also evidence for inhibitory cross-talk between PXR and HNF4 α as well as CAR and HNF4 α in hepatic lipid metabolism. While HNF4 α is a transcriptional activator of

CYP7A1, the rate-limiting enzyme in bile acid biosynthesis, PPAR α and PXR inhibit *CYP7A1* expression, probably by competing with HNF4 α for a common transcriptional coactivator (Li and Chiang 2005; Miao et al. 2006). Similarly, CAR downregulates HNF4 α target genes (Miao et al. 2006). Repression of *CYP7A1* results in decreased transformation of cholesterol into bile acids (see sub-section Intrahepatic disturbances in the enterohepatic cycle and bile acid formation), leading to lipid accumulation in the liver and increased LDL-C levels in humans (Lasker et al. 2017).

In studies with mice, PFOS and PFOA exerted reduction in the HNF4 α protein expression (10 and 3 mg/kg bw/d, respectively), after a short, *i.e.* 7-day exposure, while HNF4 α mRNA levels were not affected (Beggs et al. 2016). Upon a longer exposure to PFOA (1.25 and 5 mg/kg bw/d, 28 days), HNF4 α mRNA levels were slightly decreased; still, this reduction of the transcription factor was not reflected in representative target genes (Yan et al. 2015b). In the humanized APOE*3.Leiden.CETP mouse, the expression of HNF4 α mRNA was mildly increased after treatment with a similar dose, *i.e.* 3.2 mg/kg bw/d (serum levels ~ 90 000 ng/mL at 4 weeks), whereas *in silico* prediction of transcription factor activity based on the expression changes of known target genes was decreased (Pouwer et al. 2019).

Data from *in vitro* assays with human cells exposed to PFOS/PFOA also point towards a downregulation of the HNF4 α pathway. A proteomic study with human HepG2 cells (Scharmach et al. 2012) showed inhibition of HNF4 α signalling upon exposure to 25 μ M of PFOA (10 000 ng/mL). Such effects were also seen in primary human hepatocytes after a 96-h treatment with PFOS or PFOA (Beggs et al. 2016), with protein levels of HNF4 α (but not mRNA levels) decreasing at the highest concentration tested (10 μ M; ~4 000 ng/mL). PFOA-induced inhibition of HNF4 α in primary human hepatocytes was also observed in another study, albeit at higher concentrations (25 and 100 μ M; 10 000 – 42 000 ng/mL) (Buhrke et al. 2015). In human HepaRG cells, Behr et al. (2020a) reported a downregulation of HNF4 α gene expression at concentrations of 50 μ M and above after a 24- or 48-hour exposure. In another HepaRG study, HNF4A was not significantly downregulated by 100 μ M PFOS/PFOA, but expression of *CYP7A1* was decreased (Louisse et al. 2020c).

Conclusions

In conclusion, there is evidence indicating the involvement of other nuclear receptors important in lipid homeostasis, such as PXR, in the PFOS/PFOA-induced lipid dysregulation in rodents. With respect to human liver cells, such data are limited and hence, their relevance for the potential induced lipid perturbations by PFOS/PFOA in humans, is not clear. Regarding the HNF4 α pathway there are some indications that it might be involved in potential effects of PFOS/PFOA on cholesterol and lipid homeostasis. However, this evidence is not so strong and more investigations are required to potentially support this mechanism. In addition, it remains unclear whether in reality PFOS/PFOA exposures result in serum levels at which suppression of the HNF4 α pathway is likely to occur. More *in vitro* studies on primary human hepatocytes and liver cell lines would help elucidate this further.

Mechanisms linked to disturbance of cholesterol homeostasis

Cholesterol biosynthetic pathway and hepatic uptake

Regarding PFOS/PFOA-induced changes in cholesterol observed in humans, it is of interest to also consider a possible direct effect on the intrahepatic cholesterol biosynthetic pathway, and/or perturbation on its import to/export from the liver. In the liver, regulation of cholesterol levels is achieved through a negative feedback mechanism, in which hepatic cholesterol accumulation suppresses its *de novo* synthesis, and concurrently, the liver's uptake of cholesterol from the blood (Brown and Goldstein 1997; DeBose-Boyd 2008; Feingold 2000). The expression of genes that are involved in *de novo* cholesterol synthesis, but also uptake, is under control of the hepatic transcription factor sterol regulatory element-binding proteins (SREBP) (Horton et al. 2002; Jeon and Osborne 2012; Shao and Espenshade 2012). Amongst these genes are the *HMGCR* (3-hydroxy-3-methyl-glutaryl (HMG)-coenzyme A reductase), encoding the rate-limiting enzyme of the cholesterol biosynthetic pathway (converts HMG-CoA to mevalonate; Figure 3), as well as the gene encoding the LDL receptor (LDLR). The LDLR is the main receptor involved in cholesterol uptake from the blood to the liver via endocytosis, and its activity regulates the plasma levels of cholesterol (Brown and Goldstein 1997). SREBP stimulates in parallel the hepatic cholesterol synthesis and clearance from the blood and thus, the balance between these two processes determines ultimately the levels of cholesterol in the liver and serum circulation (Brown and Goldstein 1997; Horton et al. 2002). Cholesterol export from the liver into the circulation occurs via the VLDL particles, which are metabolized into LDL-C in the blood.

Exposure to high PFOS/PFOA doses has been demonstrated to decrease the hepatic VLDL-TG and apoB production in the liver of the APOE*3-Leiden.CETP mouse concomitantly with enhanced lipoprotein lipase-mediated VLDL clearance (Bijland et al. 2011; Pouwer et al. 2019), resulting in decreased cholesterol and TG levels in serum. In these studies with the APOE*3-Leiden.CETP mouse, hepatic accumulation of cholesterol and TGs was only seen upon PFOS exposure and not with PFOA (see sub-section Species differences in lipoprotein homeostasis in relation to PFAS lipid-related effects).

There are some reports on the effect of PFOS/PFOA on intrahepatic cholesterol synthesis, as well as on hepatic cholesterol uptake from the bloodstream. In murine liver, PFOA and PFOS were shown to enhance SREBP activity, as indicated by an increased expression on both the transcriptional and protein level. In parallel, a significant upregulation of relevant target genes, such as *HMGCR* and *LDLR*, was detected (Rosen et al. 2010: 10 mg/kg bw/d, 7 days; Yan et al. 2015b: 1.25-20 mg/kg bw/d, 4 weeks). However, histopathological examinations did not reveal hepatic lipid accumulation in the case of PFOS (Rosen et al. 2010), while total hepatic cholesterol levels were reduced after PFOA exposure (Yan et al. 2015b). In contrast to the two aforementioned studies, others reported reduced expression of certain SREBP target genes, accompanied by elevated intrahepatic cholesterol levels. In rats, both PFOS/PFOA lowered hepatic cholesterol synthesis, as reflected by a reduced activity of liver HMGCR enzyme (Haughom and Spydevold 1992) or mRNA levels (Guruge et al. 2006: 5 mg/kg bw/d,

3 weeks). Similarly, the expression of *HMGCR* and *LDLR* was decreased by PFOA in both WT and hPPAR α mice (Schlezingner et al. 2020: 0.7 mg/kg b/d, 6 weeks). Despite the lowered expression of the biosynthetic genes, exposures to PFOS or PFOA led to a pronounced hepatic cholesterol accumulation. These data imply that increased intrahepatic cholesterol, as seen in rodents after exposure to PFOS/PFOA, might not be directly related to *de novo* cholesterol biosynthesis. Instead, the effects could be the consequence of other impaired pathways, such as the secretion as VLDL particles and/or cholesterol metabolism into bile acids.

In vitro results with human cells pertaining to affected genes involved in cholesterol synthesis and PFOS/PFOA seem to be somewhat inconsistent. Using a human fetal liver cell line (L-02), Peng et al. (2013) combined a gene expression and metabolomics analysis, and reported an effect of PFOA on cholesterol biosynthesis. Measurement of cholesterol suggested a concentration-dependent increase in intracellular levels (significant at the high concentration: 120 μ M, 72 h). In addition, several cholesterol biosynthesis genes were upregulated at the same concentration. Opposing to these findings, Behr et al. (2020a) reported a downregulation of such genes (e.g. *HMGCR*, *SQLE*, and *LDLR*) and the transcription factor SREBP in HepaRG cells after 24 or 48 h, at concentrations ≥ 10 and 25 μ M for PFOA and PFOS, respectively. Intracellular cholesterol levels were not affected. Similar results were obtained for PFOA and PFOS in a recent transcriptomics study with HepaRG cells (Louisse et al. 2020c; 100 μ M, 24 h), showing a downregulation of gene sets related to cholesterol biosynthesis and SREBP signalling. In primary human hepatocytes, PFOA induced a concurrent upregulation (e.g. *MVK*: mevalonate kinase, *PMVK*: phosphomevalonate kinase) and downregulation (e.g. *SQLE*, *FDFTI*: farnesyl-diphosphate farnesyltransferase 1) of few cholesterol biosynthesis genes, whereas most remained unaffected (Buhrke et al. 2015; 100 μ M, 24 h).

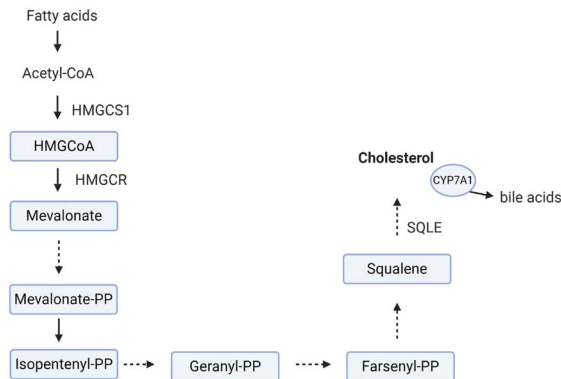


FIGURE 3 The principal steps of the hepatic cholesterol biosynthetic pathway (figure created with BioRender.com). HMGCS1: HMG-CoA synthase 1, HMGCR: HMG-CoA reductase. HMGCS1 catalyzes the condensation of acetyl-CoA with acetoacetyl-CoA to HMG-CoA. In a following step HMG-CoA is converted by HMGCR to mevalonate. Subsequently, several enzymatic reactions are required for the synthesis of cholesterol. SQLE: Squalene epoxidase. SQLE catalyzes the first oxygenation step in sterol biosynthesis. CYP7A1: cholesterol 7- α hydroxylase. CYP7A1 catalyzes the transformation of excess cholesterol into bile acids. (Created with BioRender.com).

Intrahepatic disturbances in the enterohepatic cycle and bile acid formation

Another possible explanation for the PFOS/PFOA-induced changes in blood and liver cholesterol is perturbation of bile acid synthesis from cholesterol. Excess cholesterol in the liver is stored, exported or converted into bile acids; the predominant pathway in human liver is the classic bile acid synthesis pathway, which is initiated by the rate-limiting enzyme cholesterol 7- α hydroxylase (CYP7A1) (Chiang 2017; Princen et al. 1997). The enzyme's gene expression and the bile acid synthesis rate are inhibited by bile acids, which return to the liver through the enterohepatic circulation (Chiang 1998; Li and Chiang 2009; Thompson 1996). Hence, an elevated hepatic re-uptake of bile acids induces a negative feedback loop via the farnesoid X receptor (FXR) to lower the *de novo* synthesis of bile acids from cholesterol, by CYP7A1 inhibition. Alterations in serum bile acid levels suggest either a direct disruption of the bile acid flow or/and a disturbance of the intrahepatic bile acid synthesis from cholesterol (Thompson 1996).

In rats, PFOS/PFOA have been shown to increase the levels of serum bile acids (PFOS at 2.5 and PFOA at 5 mg/kg bw/d) after a 28-day exposure (NTP 2019a; 2019b). In APOE*3-Leiden. CETP mice, PFOS, inhibited bile acid excretion in the feces (Bijland et al. 2011: 3 mg/kg bw/d, 4-6 weeks). In addition, downregulation of hepatic CYP7A1 gene expression upon exposure to PFOS (Bijland et al. 2011; Wang et al. 2014: 5 mg/kg bw/d, 2 weeks) or PFOA (Pouwer et al. 2019; Schlezinger et al. 2020) was seen. These findings show impairment of the bile flow and synthesis, through which PFOS/PFOA may affect cholesterol homeostasis. It should be noted that next to the FXR the main transcription factors regulating CYP7A1 include HNF4 α and PPAR α (Chen et al. 2001; Kir et al. 2012), which have already been suggested as molecular target of PFOS and PFOA (see section Mechanistic pathways involved in PFAS-induced lipid perturbations).

Reduction of CYP7A1 expression has been also demonstrated *in vitro*, in human hepatocytes (Beggs et al. 2016: 10 μ M, 96 h) and in HepaRG cells (Behr et al. 2020a: 10 μ M, 48 h; Louise et al. 2020c: 100 μ M, 24 h).

Interference of PFOS/PFOA with the enterohepatic cycling may also play a role. PFOS/PFOA have been shown to be excreted in the bile (Fujii et al. 2015; Harada et al. 2007), and thereafter, are believed to be substantially re-absorbed from the gastrointestinal tract (see section Species differences in toxicokinetic properties of PFOS and PFOA). Both substances have been reported to share the same transporters (e.g. NTCP: Na⁺/taurocholate co-transporting polypeptide, ASBT: apical sodium-dependent bile salt transporter, OATPs: organic anion transporting polypeptides) as bile acids for excretion via bile into the intestine and re-absorption in the ileum (Zhao et al. 2015b; Zhao et al. 2017a). Therefore, PFOS/PFOA may alter the absorption of bile acids through competition for the same transporter, interfering as such with the negative feedback control of the conversion of cholesterol to bile acids and perturbing cholesterol levels. For example, losses of bile acids are compensated by enhanced bile acid synthesis from cholesterol, the mechanism behind the cholesterol lowering effect of the drug cholestyramine. This resin binds bile

acids in the gastrointestinal lumen to prevent reabsorption and indirectly lowers serum cholesterol levels via enhanced conversion of cholesterol to bile acids, which in turn leads to activation of SREBP-mediated LDLR expression. Interestingly, in rats application of cholestyramine also strongly increased the excretion of PFOA via feces (Genuis et al. 2010; Genuis et al. 2013).

With respect to the enterohepatic circulation in humans, differences in the absorption of bile acids due to genetic factors, food composition or medicines can lead into altered levels of serum cholesterol. For example, dietary fiber intake was recently reported to be associated with lower PFAS serum concentrations in humans (Dzierlenga et al. 2020b). Consequently, it is plausible that confounding related to excretion and re-absorption in the enterohepatic cycling process may play a role in the associations for PFOS/PFOA and total serum cholesterol reported repeatedly in the cross-sectional epidemiological studies. Nevertheless, confounding due to this biological mechanism is till now only a postulation with no available supporting evidence (see section PFOS and PFOA: lipid homeostasis perturbations; *effects observed in human studies*) (EFSA CONTAM Panel 2020a).

Conclusions

Collectively, there are indications that PFOS/PFOA influence different aspects of cholesterol metabolism, including biosynthesis, import/export from the liver and conversion into bile acids. Despite this, the molecular events leading to the alterations in serum cholesterol that may be caused by PFOS/PFOA exposure in animals and humans remain unclear. More insight into the mechanisms involved is needed in order to understand the molecular events that are potentially triggered by PFOS/PFOA and how these may ultimately lead to cholesterol alterations in blood and/or liver. Additionally, it should be noted once more that for the interpretation of such findings the exposure levels should be taken into consideration, which are different between animals and humans. For interpretation of data from *in vitro* assays difference in the free fraction between the *in vitro* assay and the *in vivo* situation has to be considered. Currently, this is hindered by lack of data on the free fraction of PFOS/PFOA in the medium of different *in vitro* studies and/or the related cellular concentrations in *in vitro* systems.

Species differences in toxicokinetic properties of PFOS and PFOA

Apart from the toxicodynamic differences analysed above, toxicokinetic differences have been reported for the PFASs, with most data on PFOS and PFOA. In general, both chemicals are well absorbed from the intestinal tract and are excreted unmetabolized (ATSDR 2018; EFSA CONTAM Panel 2018a; US EPA 2016a; 2016b). Once absorbed, PFOS/PFOA bind extensively to serum albumin (>90%), as shown in several species (Beesoon and Martin 2015; Ehresman et al. 2007; Han et al. 2012), while also binding to the liver fatty acid binding protein (L-FABP) has also been reported for the rat and human (Luebker et al. 2002a; Woodcroft et al. 2010).

With regard to organ distribution it is often mentioned that PFOS/PFOA accumulate in the liver and kidney (EFSA CONTAM Panel 2018a). However, as shown recently, PFOA does not deposit preferentially in the liver (NTP 2019b), based on the average liver: plasma partition coefficient (PC) in male rats after a 28-day exposure¹⁹ (range across doses: 0.87-1.17). This is somewhat lower than what has been previously shown in other studies in the male rat with a single PFOA exposure (showing PCs of for example 2.2 and 0.8 at a low and high dose (Kudo et al. 2007) and 2.3 (Kim et al. 2016). The NTP finding is important considering the repeated exposure, which is not commonly applied in toxicokinetic studies. For PFOS current evidence indicates a higher retention in the liver (Curran et al. 2008; NTP 2019a; Seacat et al. 2003). In this case, the liver: plasma PCs obtained for example from a 14-week exposure (Seacat et al. 2003) are in the range of 6.3 to 12.2 across doses, but lower after shorter (NTP 2019a: 4 weeks, range across doses: 2.74-3.76) and single (Kim et al. 2016; mean: 2.6) exposures. With regard to the kidney, neither of the two substances show accumulation in the rat, with kidney: plasma PCs of ~0.4 to 1 for PFOA (Dzierlenga et al. 2020a; Kim et al. 2016; Kudo et al. 2007) and ~0.3 to 1 for PFOS (Huang et al. 2019; Kim et al. 2016).

Human data are unfortunately very limited in number (Ericson et al. 2007; Olsen et al. 2003b; Perez et al. 2013). In order to facilitate a preliminary comparison with the rat data, human organ:plasma PCs were calculated (Table 3, N=20) based on the available information. It should be mentioned though that for these calculations data of PFOS/PFOA levels in the tissues and blood plasma do not stem from the same study (see Table 3, furthermore note the high variability of organ measurements), i.e. they come from different persons; they are, however, from the same region. The results suggest a substantial higher distribution to the liver for both PFOA and PFOS in a substantial part of the human population, probably reflecting the long human exposure period. Calculated kidney:plasma PCs, in humans *versus* rats, are comparable for PFOA, whereas PFOS seems to accumulate more in some human kidneys compared to the rat kidney (Dzierlenga et al. 2020a; Huang et al. 2019; Kim et al. 2016; Kudo et al. 2007). For the time being, and in the absence of more information, these data imply that at comparable blood concentrations a substantial part of the human population may have higher intrahepatic levels of PFOS/PFOA and higher intrarenal PFOS levels when compared to rodents.

Species differences also exist regarding the elimination and excretion mechanisms. An overview of the blood terminal half-lives is presented in Table 4, designating much longer half-lives in humans as compared to rodents and monkeys. PFOS shows accumulating properties in all species, with an elimination half-life in the range of a month for the rat and mouse (20-40 days), and with a remarkable half-life of ~ 5 years recorded in humans. In the case of PFOS, limited differences are observed between males and females of the same species. PFOA also shows high accumulation potential in many species, except for the rat (0.15 to 2 days). In addition, in the rat a remarkable gender difference has been observed for PFOA, which is briefly discussed below.

¹⁹ Liver levels were not analyzed in female rats.

In most species, urinary clearance seems to be the primary elimination pathway (EFSA CONTAM Panel 2018a). For PFOA, clear differences have been reported between male and female rats pertaining to the renal elimination and they have been linked specifically to the active protein-mediated transport that governs tubular secretion and re-absorption (from the pre-urine back to the kidney and blood circulation) (Han et al. 2012). Sex-hormone mediated expression of organic anion transporting polypeptide (Oatp)1a1, located on the apical tubular membrane, was demonstrated to play a role in the observed renal re-absorption of PFOA in the male rat (Yang et al. 2009). However, more transporters, including organic anion transporters (OATs) may be involved (Kudo et al. 2002). This information provides an explanation on the observed faster renal excretion of PFOA in female as opposed to male rats.

TABLE 3 PFOS/PFOA organ concentrations in humans and calculated human organ: plasma partition coefficients (based on mean/median organ concentrations).

	Organ concentrations (ng/mL) (mean \pm SD ^a , median ^b ; range ^c)		Calculated human organ : plasma partition coefficients (median, range ^c)	
	PFOA	PFOS	PFOA	PFOS
Blood ¹	1.80 \pm 0.66 ^a 1.65 ^b	7.64 \pm 3.54 ^c 7.60 ^b		
Plasma ²	3.2 \pm 1.2 ^a	13.6 \pm 6.3 ^a	1	1
Liver ³	4.0 ^b 3-98.9 ^c	41.9 ^b 3-405 ^c	1.3 0.9 - 30.9	3.1 0.2 - 29.8
Brain ³	< LOD (=2.45)	1.9 ^b 3-22.5 ^c	Not available	0.1 0.2-1.6
Lung ³	12.1 ^b 6-87.9 ^c	28.4 ^b 3-61.8 ^c	3.8 1.9 - 27.5	2.1 0.1-2.0
Kidney ³	1.5 ^b 3-11.9 ^c	55 ^b 3-369 ^c	0.5 0.9-3.7	4.0 0.2 - 27.1

¹Ericson et al. (2007), N=48, age: 55.5 \pm 5.5 years; ²Fàbrega et al. (2014), applying a 0.56 blood \rightarrow plasma conversion while ignoring erythrocyte binding; ³Perez et al. (2013), N=20 age: 28- 83 years.

TABLE 4 Information of terminal half-lives for PFOS and PFOA in various species (taken from RIVM (2018) and complemented with more recent data).

Substance	Species/Terminal half- life			
	Rat	Mouse	Pig	Monkey
PFOS	27.8 days (m) 24.8 days (f) (Kim et al. 2016)	42.8 days (m) 37.8 days (f) (Chang et al. 2012)	634 days (Numata et al. 2014)	132 days (m) 110 days (f) (Chang et al. 2012)
PFOA	1.6-1.8 days (m) 0.15-0.19 days (f) (Kim et al. 2016)	21.7 days (m) 15.6 days (f) (Lou et al., 2009)	236 days (Numata et al. 2014)	21 days (m) 30 days (f) (Butenhoff et al. 2004)

m: males, f: females

Elimination of PFOS/PFOA in humans is thought to be primarily via urinary excretion. However, there is a clear lack of studies on fecal excretion (EFSA CONTAM Panel 2018a). PFOS and PFOA are shown to be highly excreted in the bile; still, most of the quantity excreted into the gut is believed to undergo extensive enterohepatic re-absorption (>97%) (Harada et al. 2007) (Fuji et al 2015). Renal re-absorption via kidney transporters has been demonstrated for PFOS and PFOA (Han et al. 2012; Nakagawa et al. 2009). Such re-absorption processes, both renal and intestinal, are believed to contribute substantially to the observed long elimination half-lives of both PFOS and PFOA in humans.

Overall, from a kinetic perspective there are species- (and gender)-dependent differences, primarily regarding the terminal half-life, intra-hepatic and -renal concentrations and excretion patterns for PFOS/PFOA. These differences further complicate the extrapolation of rodent data to the human situation. Kinetic differences have to be carefully considered prior to such extrapolations, by scaling of rodent data to humans and *vice versa*. For risk assessment purposes it is important to consider body burdens or serum levels rather than the exposure levels. Toxicokinetic modelling, based on available data from animal and human studies, may provide a better basis for such extrapolations. *In vitro* kinetic studies may also provide insight into the various input parameters for such models. It is emphasized here that with regard to the *in vitro* toxicity assays toxicokinetics are also very important to consider, prior to extrapolations of effective doses to humans. A direct comparison of the nominally applied concentration of PFOS/PFOA *in vitro* with the respective human PFOS/PFOA blood levels is not necessarily a good approach. Given that *in vitro* and *in vivo* exposure situations differ fundamentally, extrapolations from these cell systems to humans are complex and shall not be performed without integration of the kinetic aspects.

Species/Terminal half- life
Humans
Occupational workers: 5.4 years (Olsen and Zobel 2007) Community (contaminated drinking water): 3.4 years (Li et al. 2020)
Occupational workers: 3.8 years (Olsen and Zobel 2007) Adults (contaminated drinking water): 2.3 years (Bartell et al. 2010), 3.3 years (Brede et al. 2010) Community (contaminated drinking water): 2.7 years (Li et al. 2020)

Conclusions and recommendations

Many epidemiological studies have shown associations between increased blood levels of PFOS/PFOA and increased blood total cholesterol, and in some cases TGs. Exposure to the substances have occurred for several decades. Nonetheless, many of these studies are cross-sectional and consequently, the extent to which the relationships between PFOS/PFOA exposure and these altered levels of blood lipids are causal remains uncertain. Also, there are no associations with related adverse outcomes, like CVD. Even so, given the very small changes in the involved risk factors, such effects could be possibly detected only in very large studies. The recorded associations could also be the result of confounding related to excretion and re-absorption in the enterohepatic cycling process of PFOS/PFOA and bile acids, which can affect serum cholesterol levels. However, until now this remains only a postulation that requires experimental evidence.

Intriguingly, studies with shorter durations and high exposures of PFOS/PFOA in rodents and in some cases monkeys, have demonstrated opposite effects, i.e. decreased serum cholesterol and TGs. Such effects occur at much higher (at least >100-fold) serum levels and are commonly accompanied by enhanced intrahepatic lipid (mainly TG) concentrations. This complicates the interpretation of the human findings. In order to support (or not) a causal inference and to elucidate whether such findings are a real health concern for humans, a clear mechanistic understanding relevant for humans is essential.

Mechanistic evidence discussed in this manuscript stems from studies performed primarily with rodents and with human liver-derived cells. In rodents, most of the studies focus on the role of PPAR α , and its activation by PFOS/PFOA appears to play, at least partially, a role in PFOS/PFOA-induced lipid perturbations, but it is not the sole mechanism. With respect to humans, studies in hPPAR α mice demonstrate a reduced responsiveness of the human PPAR α to PFOA when compared to rodents. The same is recorded for both PFOS/PFOA in human liver cells. This, together with the large differences in exposure levels and durations between animals and humans, indicates that comparisons between rodent and human findings shall be done with caution. Also, other pathways that do not directly involve PPAR α seem to play a role in the PFOS/PFOA-induced lipid disturbances, as shown in rodents and rodent-derived hepatocytes. These relate to the activation of other nuclear receptors important for lipid homeostasis, such PXR and CAR. Nonetheless, studies with PFOS/PFOA on human hepatocytes indicate contradicting results, rendering the relevance of these receptors for humans uncertain. A possible role of these receptors remains to be clarified.

In addition, available data suggest that the effect of PFOS/PFOA on cholesterol and lipid homeostasis may also be mediated via suppression of the HNF4 α pathway. Furthermore, there are indications that PFOS/PFOA may affect the cholesterol levels, by interfering with its metabolism and specifically its transformation into bile acids (including interference with CYP7A1), as well as the transport of the latter. Such observations are indeed valuable for better understanding of the mode of action, but they require further elucidation. In

summary, the underlying mechanism of PFOS/PFOA-induced lipid disturbances seems to be rather complex and hitherto, not fully delineated.

Similarly, there is no simple mechanistic explanation for the differences in findings between animals and humans. The discrepancy in effects between rodents and humans may be related to profound interspecies differences in physiology regarding lipid homeostasis, and/or PFAS-species differences in toxicokinetics, as well as basic nutrition. These differences and potential interpretations are discussed throughout the manuscript (summarized in Figure 4).

The explanation for the observed differences in health effects in rodents *versus* humans may also lie with the large differences in exposure levels and durations between animals and humans. Cholesterol and TG changes in humans are recorded after chronic exposure and at serum concentrations of PFOS/PFOA at least two to three orders of magnitude lower, when compared to the respective serum concentrations in rodents. This is mainly due to the higher doses commonly used for the performance of the animal studies, while animal studies using low doses, resulting in serum PFOS/PFOA levels that are comparable to the human situation, are scarce. One single 4-week study using more relevant exposure levels in APOE*3-Leiden.CETP mice showed recently that environmental (approximately 50 ng/ml) or occupational (approximately 1500 ng/ml) levels of PFOA exposure, representative for exposed community populations and fluorochemical production workers respectively, did not increase plasma cholesterol and TG levels, whereas exposure to high PFOA levels (90 000-150 000 ng/ml) did decrease TGs, total cholesterol and non-HDL-C levels and increased HDL-C level (Pouwer et al. 2019). This is in accordance with the slight reduction in cholesterol reported for cancer patients exposed for 6 weeks to very high PFOA levels (Convertino et al. 2018), although the interpretation of these data is difficult due to some methodological issues (see section PFOS and PFOA: *lipid homeostasis perturbations; effects observed in human studies*). Perhaps at such high serum levels and such exposure durations, both in humans and animals, different pathways come into play, than at the much lower concentrations and longer exposure durations observed in background populations and even in areas with increased exposure. Therefore, there are indeed few indications that the discrepancy in findings between humans and rodents might be the result of the large differences in exposure conditions. Nevertheless, it must be highlighted that PFOS/PFOA accumulate much more in humans than in rodents, as illustrated by the terminal half-lives measured in occupational workers and a highly exposed population (Table 4). In addition, human data (although limited) suggest that at comparable blood concentrations humans may have higher intrahepatic levels of PFOS/PFOA and higher intrarenal PFOS levels when compared to rodents. The life-long exposure of humans to PFOS/PFOA could possibly lead to continuously elevated body burdens, sufficient to cause effects on lipid homeostasis. Overall, it appears that the interpretation of the existing rodent data on PFOS/PFOA-induced lipid perturbations, with respect to the human situation, is complex.

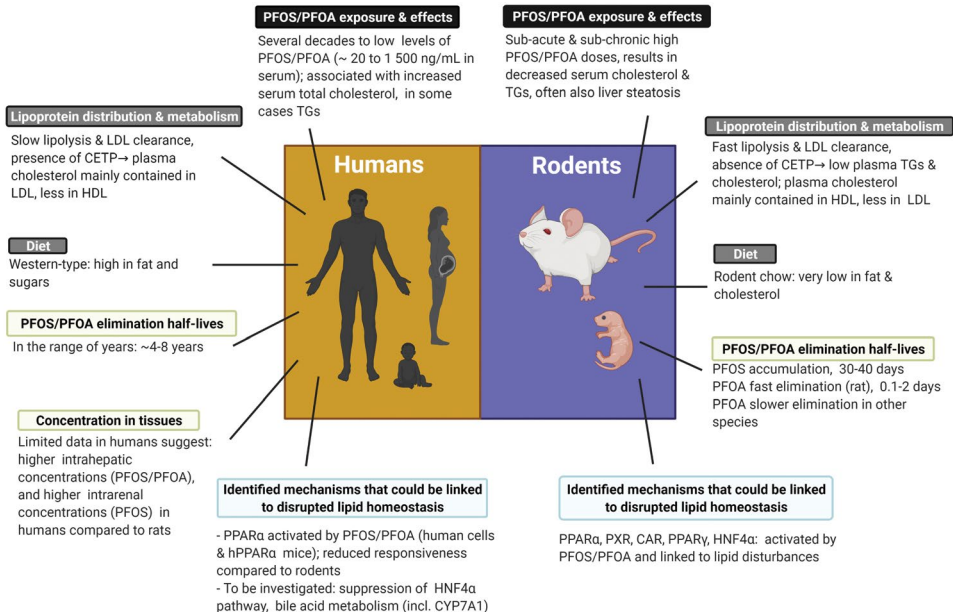


FIGURE 4 Summarized human- and rodent- specific differences related to PFOS/PFOA exposure, as well as species-specific differences with respect to lipoprotein metabolism and nutrition. CETP: cholesteryl ester transfer protein, LDL: low-density lipoprotein, HDL: high-density lipoprotein, TGs: triglycerides, PPARα: peroxisome proliferator-activated receptor α, hPPARα: human PPARα, HNF4α: hepatocyte nuclear factor 4 α, CYP7A1: cholesterol 7-α hydroxylase (rate-limiting enzyme in bile acid synthesis), PXR: pregnane X receptor, CAR: constitutive androstane receptor, PPARγ: peroxisome proliferator-activated receptor γ (Created with BioRender.com).

In the case of the *in vitro* experiments with human hepatocytes, only single short exposures are generally used, attempting to mimic effects occurring *in vivo* after repeated chronic exposures. In addition, only nominal concentrations applied into the cell cultures are reported, whereas actual intracellular concentrations are rarely reported. These nominal concentrations in the culture medium are commonly much higher, when compared directly to serum PFOS/PFOA levels associated with increased cholesterol and TGs in humans. However, it is unclear whether these PFOS/PFOA *in vitro* concentrations constitute an appropriate surrogate for serum levels, especially considering the very high protein binding of these compounds. Quantitative *in vitro* to *in vivo* extrapolations (QIVIVE) would assist in translating effect levels observed in the *in vitro* test systems into the equivalent human PFOS/PFOA serum levels. This shall be done with the integration of kinetics, while preferably the cellular uptake of the chemicals shall be determined experimentally.

An important new asset to delineate the species differences and the inherent differences in signalling pathways between rodents and humans is to make use of mice with a humanized chimeric liver (Tateno et al. 2004). In these mice > 80% of the mouse hepatocytes are replaced by human hepatocytes. The chimeric mice exhibit a “humanized” circulating lipoprotein cholesterol profile with an LDL-C/HDL-C ratio similar to that observed in humans, as well as bile acid regulation more characteristic of humans (Ellis et al. 2013). Importantly, with respect to the substantial species differences in PPARα expression and

affinity of PFOS/PFOA for the receptor expression levels of human PPAR α are as in humans and their interaction with other relevant transcription factors have a human context. The same applies to other relevant biological processes. These mice have been used to elucidate the discrepancy in circulating cholesterol induced by obeticholic acid, an FXR-agonist and clinical candidate for treatment of NASH, between rodent models and humans, where obeticholic acid increased LDL-C in humans and consistently reduced total cholesterol levels in rodents (Papazyan et al. 2018). Studies with these mice, and importantly with different escalating exposure levels relevant to humans, may help elucidate the mechanism of action of PFOS/PFOA relevant for humans.

Together with studies on chimeric mice, further *in vitro* investigations with human hepatocytes may help clarify the pathway underlying the potential PFOS/PFOA-induced lipid perturbations. Specifically, more information is needed on the involvement of the HNF4 α signalling pathway, as well as interference of PFOS/PFOA with cholesterol transformation into bile acids. Still, given the specific limitations of such *in vitro* models, the extrapolation of the effects to humans shall be done carefully by taking into consideration the dosing and integrating the kinetic aspects. The latter can be achieved with the use of physiologically-based kinetic modelling, together with measurements of the actual intracellular concentrations of the compounds. If such studies are finetuned to the human situation and interpreted in the context of the intact human, they can generate valuable information that will contribute to a better understanding of PFAS-mediated lipid perturbations and the issues involved in their interpretation for human health risk assessment.

Acknowledgements

This work is conducted within the HBM4EU project. HBM4EU represents a joint effort of 28 countries, the European Environment Agency and the European Commission, co-funded by Horizon 2020. The main aim of the initiative is to coordinate and advance human biomonitoring in Europe. HBM4EU provides evidence of the actual exposure of citizens to chemicals and the possible health effects to support policy making. The project involves collaboration between several Commission services, EU agencies, national representatives, stakeholders and scientists, demonstrating how research funding can build bridges between the research and policy worlds. The authors acknowledge Shalenie den Braver-Sewradj and Wieneke Bil, National Institute for Public Health and the Environment (RIVM), Bilthoven, The Netherlands, for their critical reading of the paper and valuable comments. The authors cordially thank the reviewers the Editor selected, whose identity was anonymous, for their thoughtful insight and comments towards the improvement of the manuscript.

Funding

This work was supported by the European Union's Horizon 2020 research and innovation programme under Grant agreement No 733032 HBM4EU (www.HBM4EU.eu). Additional funding sources are the TNO research program "Biomedical Health".

Disclosures of interest

Hans M.G. Princen does not have competing interests other than employment in contract facilities at TNO Metabolic Health Research which received previously funds from 3M Company for contract services. The authors report no conflicts of interest. This work was supported by the European Union's Horizon 2020 research and innovation programme under Grant agreement No 733032 HBM4EU (www.HBM4EU.eu). Additional funding sources are the TNO research program "Biomedical Health". The employment affiliations of the authors are shown on the cover page. None of the authors have been involved in legal or regulatory matters related to the contents of the article.

References

- Abe T, Takahashi M, Kano M, Amaike Y, Ishii C, Maeda K, Kudoh Y, Morishita T, Hosaka T, Sasaki T et al. 2017. Activation of nuclear receptor CAR by an environmental pollutant perfluorooctanoic acid. *Arch Toxicol*. 91(6):2365-2374. eng.
- Adiels M, Olofsson SO, Taskinen MR, Borén J. 2008. Overproduction of very low-density lipoproteins is the hallmark of the dyslipidemia in the metabolic syndrome. *Arterioscler Thromb Vasc Biol*. 28(7):1225-1236. eng.
- Ason B, van der Hoorn JWA, Chan J, Lee E, Pieterman EJ, Nguyen KK, Di M, Shetterly S, Tang J, Yeh W-C et al. 2014. PCSK9 inhibition fails to alter hepatic LDLR, circulating cholesterol, and atherosclerosis in the absence of ApoE. *Journal of lipid research*. 55(11):2370-2379. eng.
- mATSDR. 2018. Toxicological Profile for Perfluoroalkyls. Draft for Public Comment June 2018. <https://www.atsdr.cdc.gov/toxprofiles/tp200.pdf>, 2018-11-10.
- Auboeuf D, Rieusset J, Fajas L, Vallier P, Frereng V, Riou JP, Staels B, Auwerx J, Laville M, Vidal H. 1997. Tissue distribution and quantification of the expression of mRNAs of peroxisome proliferator-activated receptors and liver X receptor-alpha in humans: no alteration in adipose tissue of obese and NIDDM patients. *Diabetes*. 46(8):1319-1327. eng.
- Ballesteros V, Costa O, Iniguez C, Fletcher T, Ballester F, Lopez-Espinosa MJ. 2017. Exposure to perfluoroalkyl substances and thyroid function in pregnant women and children: A systematic review of epidemiologic studies. *Environment international*. 99:15-28. eng.
- Bartell SM, Calafat AM, Lyu C, Kato K, Ryan PB, Steenland K. 2010. Rate of decline in serum PFOA concentrations after granular activated carbon filtration at two public water systems in Ohio and West Virginia. *Environmental health perspectives*. 118(2):222-228. eng.
- Beeson S, Martin JW. 2015. Isomer-Specific Binding Affinity of Perfluorooctanesulfonate (PFOS) and Perfluorooctanoate (PFOA) to Serum Proteins. *Environmental science & technology*. 49(9):5722-5731. eng.
- Beggs KM, McGreal SR, McCarthy A, Gunewardena S, Lampe JN, Lau C, Apte U. 2016. The role of hepatocyte nuclear factor 4-alpha in perfluorooctanoic acid- and perfluorooctanesulfonic acid-induced hepatocellular dysfunction. *Toxicol Appl Pharmacol*. 304:18-29. eng.
- Behr AC, Kwiatkowski A, Ståhlman M, Schmidt FF, Luckert C, Braeuning A, Buhrke T. 2020a. Impairment of bile acid metabolism by perfluorooctanoic acid (PFOA) and perfluorooctanesulfonic acid (PFOS) in human HepaRG hepatoma cells. *Arch Toxicol*. 94(5):1673-1686. eng.
- Behr AC, Plinsch C, Braeuning A, Buhrke T. 2020b. Activation of human nuclear receptors by perfluoroalkylated substances (PFAS). *Toxicol In vitro*. 62:104700. eng.
- Bergen WG, Mersmann HJ. 2005. Comparative Aspects of Lipid Metabolism: Impact on Contemporary Research and Use of Animal Models. *The Journal of Nutrition*. 135(11):2499-2502.
- Bijland S, Rensen PC, Pieterman EJ, Maas AC, van der Hoorn JW, van Erk MJ, Havekes LM, Willems van Dijk K, Chang SC, Ehresman DJ et al. 2011. Perfluoroalkyl sulfonates cause alkyl chain length-dependent hepatic steatosis and hypolipidemia mainly by impairing lipoprotein production in APOE*3-Leiden CETP mice. *Toxicological sciences : an official journal of the Society of Toxicology*. 123(1):290-303. eng.
- Bjork JA, Butenhoff JL, Wallace KB. 2011. Multiplicity of nuclear receptor activation by PFOA and PFOS in primary human and rodent hepatocytes. *Toxicology*. 288(1-3):8-17. eng.
- Bjork JA, Wallace KB. 2009. Structure-activity relationships and human relevance for perfluoroalkyl acid-induced transcriptional activation of peroxisome proliferation in liver cell cultures. *Toxicological sciences : an official journal of the Society of Toxicology*. 111(1):89-99. eng.
- Borén J, Chapman MJ, Krauss RM, Packard CJ, Bentzon JF, Binder CJ, Daemen MJ, Demer LL, Hegele RA, Nicholls SJ et al. 2020. Low-density lipoproteins cause atherosclerotic cardiovascular disease: pathophysiological, genetic, and therapeutic insights: a consensus statement from the European Atherosclerosis Society Consensus Panel. *European Heart Journal*. 41(24):2313-2330.
- Brede E, Wilhelm M, Goen T, Muller J, Rauchfuss K, Kraft M, Holzer J. 2010. Two-year follow-up biomonitoring pilot study of residents' and controls' PFC plasma levels after PFOA reduction in public water system in Arnsberg, Germany. *International journal of hygiene and environmental health*. 213(3):217-223. eng.
- Brown MS, Goldstein JL. 1997. The SREBP pathway: regulation of cholesterol metabolism by proteolysis of a membrane-bound transcription factor. *Cell*. 89(3):331-340. eng.

- Buhrke T, Krüger E, Pevny S, Rößler M, Bitter K, Lampen A. 2015. Perfluorooctanoic acid (PFOA) affects distinct molecular signalling pathways in human primary hepatocytes. *Toxicology*. 333:53-62. eng.
- Butenhoff J, Costa G, Elcombe C, Farrar D, Hansen K, Iwai H, Jung R, Kennedy G, Jr., Lieder P, Olsen G et al. 2002. Toxicity of ammonium perfluorooctanoate in male cynomolgus monkeys after oral dosing for 6 months. *Toxicological sciences : an official journal of the Society of Toxicology*. 69(1):244-257. eng.
- Butenhoff JL, Chang SC, Olsen GW, Thomford PJ. 2012a. Chronic dietary toxicity and carcinogenicity study with potassium perfluorooctanesulfonate in Sprague Dawley rats. *Toxicology*. 293(1-3):1-15. eng.
- Butenhoff JL, Kennedy GL, Jr., Chang SC, Olsen GW. 2012b. Chronic dietary toxicity and carcinogenicity study with ammonium perfluorooctanoate in Sprague-Dawley rats. *Toxicology*. 298(1-3):1-13. eng.
- Butenhoff JL, Kennedy GL, Jr., Hinderliter PM, Lieder PH, Jung R, Hansen KJ, Gorman GS, Noker PE, Thomford PJ. 2004. Pharmacokinetics of perfluorooctanoate in cynomolgus monkeys. *Toxicological sciences : an official journal of the Society of Toxicology*. 82(2):394-406. eng.
- Canova C, Barbieri G, Zare Jeddi M, Gion M, Fabricio A, Daprà F, Russo F, Fletcher T, Pitter G. 2020. Associations between perfluoroalkyl substances and lipid profile in a highly exposed young adult population in the Veneto Region. *Environment international*. 145:106117.
- Chamouton J, Latruffe N. 2012. PPAR α /HNF4 α interplay on diversified responsive elements. Relevance in the regulation of liver peroxisomal fatty acid catabolism. *Curr Drug Metab*. 13(10):1436-1453. eng.
- Chang S, Allen BC, Andres KL, Ehresman DJ, Falvo R, Provencher A, Olsen GW, Butenhoff JL. 2017. Evaluation of Serum Lipid, Thyroid, and Hepatic Clinical Chemistries in Association With Serum Perfluorooctanesulfonate (PFOS) in Cynomolgus Monkeys After Oral Dosing With Potassium PFOS. *Toxicological sciences : an official journal of the Society of Toxicology*. 156(2):387-401. eng.
- Chang SC, Noker PE, Gorman GS, Gibson SJ, Hart JA, Ehresman DJ, Butenhoff JL. 2012. Comparative pharmacokinetics of perfluorooctanesulfonate (PFOS) in rats, mice, and monkeys. *Reproductive toxicology (Elmsford, NY)*. 33(4):428-440. eng.
- Chapman MJ, Le Goff W, Guerin M, Kontush A. 2010. Cholesteryl ester transfer protein: at the heart of the action of lipid-modulating therapy with statins, fibrates, niacin, and cholesteryl ester transfer protein inhibitors. *Eur Heart J*. 31(2):149-164. eng.
- Chen W, Owsley E, Yang Y, Stroup D, Chiang JY. 2001. Nuclear receptor-mediated repression of human cholesterol 7 α -hydroxylase gene transcription by bile acids. *J Lipid Res*. 42(9):1402-1412. eng.
- Chiang JY. 1998. Regulation of bile acid synthesis. *Front Biosci*. 3:d176-193. eng.
- Chiang JY. 2017. Recent advances in understanding bile acid homeostasis. *Fl000Res*. 6:2029-2029. eng.
- Convertino M, Church TR, Olsen GW, Liu Y, Doyle E, Elcombe CR, Barnett AL, Samuel LM, MacPherson IR, Evans TRJ. 2018. Stochastic Pharmacokinetic-Pharmacodynamic Modeling for Assessing the Systemic Health Risk of Perfluorooctanoate (PFOA). *Toxicological sciences : an official journal of the Society of Toxicology*. 163(1):293-306. eng.
- Corton JC, Cunningham ML, Hummer BT, Lau C, Meek B, Peters JM, Popp JA, Rhomberg L, Seed J, Klaunig JE. 2014a. Mode of action framework analysis for receptor-mediated toxicity: The peroxisome proliferator-activated receptor alpha (PPAR α) as a case study. *Crit Rev Toxicol*. 44(1):1-49. eng.
- Corton JC, Cunningham ML, Hummer BT, Lau C, Meek B, Peters JM, Popp JA, Rhomberg L, Seed J, Klaunig JE. 2014b. Mode of action framework analysis for receptor-mediated toxicity: The peroxisome proliferator-activated receptor alpha (PPAR α) as a case study. *Crit Rev Toxicol*. 44(1):1-49. eng.
- Curran I, Hierlihy SL, Liston V, Pantazopoulos P, Nunnikhoven A, Tittlemier S, Barker M, Trick K, Bondy G. 2008. Altered Fatty Acid Homeostasis and Related Toxicologic Sequelae in Rats Exposed to Dietary Potassium Perfluorooctanesulfonate (PFOS). *Journal of Toxicology and Environmental Health, Part A*. 71(23):1526-1541.
- Darrow LA, Stein CR, Steenland K. 2013. Serum Perfluorooctanoic Acid and Perfluorooctane Sulfonate Concentrations in Relation to Birth Outcomes in the Mid-Ohio Valley, 2005–2010. *Environmental health perspectives*. 121(10):1207-1213.
- Das KP, Wood CR, Lin MT, Starkov AA, Lau C, Wallace KB, Corton JC, Abbott BD. 2017. Perfluoroalkyl acids-induced liver steatosis: Effects on genes controlling lipid homeostasis. *Toxicology*. 378:37-52. eng.
- de la Rosa Rodriguez MA, Sugahara G, Hooiveld G, Ishida Y, Tateno C, Kersten S. 2018. The whole transcriptome effects of the PPAR α agonist fenofibrate on livers of hepatocyte humanized mice. *BMC Genomics*. 19(1):443. eng.

- DeBose-Boyd RA. 2008. Feedback regulation of cholesterol synthesis: sterol-accelerated ubiquitination and degradation of HMG CoA reductase. *Cell Res.* 18(6):609-621. eng.
- DeWitt JC, Shnyra A, Badr MZ, Loveless SE, Hoban D, Frame SR, Cunard R, Anderson SE, Meade BJ, Peden-Adams MM et al. 2009. Immunotoxicity of perfluorooctanoic acid and perfluorooctane sulfonate and the role of peroxisome proliferator-activated receptor alpha. *Crit Rev Toxicol.* 39(1):76-94. eng.
- Dietschy JM, Turley SD. 2002. Control of cholesterol turnover in the mouse. *J Biol Chem.* 277(6):3801-3804. eng.
- Dietschy JM, Turley SD, Spady DK. 1993. Role of liver in the maintenance of cholesterol and low density lipoprotein homeostasis in different animal species, including humans. *J Lipid Res.* 34(10):1637-1659. eng.
- DWQI. 2017. New Jersey Drinking Water Quality Institute Health Effects Subcommittee. Health-based maximum contaminant level support document: perfluorooctanoic acid (PFOA). February 15, 2017.
- DWQI. 2018. New Jersey Drinking Water Quality Institute Health Effects Subcommittee. Health-based maximum contaminant level support document: perfluorooctane sulfonate (PFOS). June 5, 2018.
- Dzierlenga AL, Robinson VG, Waidyanatha S, DeVito MJ, Eifrid MA, Gibbs ST, Granville CA, Blystone CR. 2020a. Toxicokinetics of perfluorohexanoic acid (PFHxA), perfluorooctanoic acid (PFOA) and perfluorodecanoic acid (PFDA) in male and female Hsd:Sprague dawley SD rats following intravenous or gavage administration. *Xenobiotica.* 50(6):722-732. eng.
- Dzierlenga MW, Keast DR, Longnecker MP. 2020b. The concentration of several perfluoroalkyl acids in serum appears to be reduced by dietary fiber. medRxiv.2020.2007.2015.20154922.
- EFSA CONTAM Panel. 2018a. (EFSA Panel on Contaminants in the Food Chain), Knutsen HK, Alexander J, Barregard L, Bignami M, Bruschweiler B, Ceccatelli S, Cottrill B, Dinovi M, Edler L, Grasl-Kraupp B, Hogstrand C, Hoogenboom LR, Nebbia CS, Oswald IP, Petersen A, Rose M, Roudot A-C, Vleminckx C, Vollmer G, Wallace H, Bodin L, Cravedi J-P, Halldorsson TI, Haug LS, Johansson N, van Loveren H, Gergelova P, Mackay K, Levorato S, van Manen M and Schwerdtle T, 2018. Scientific Opinion on the risk to human health related to the presence of perfluorooctane sulfonic acid and perfluorooctanoic acid in food. *EFSA Journal* 2018;16(12):5194, 284 pp. <https://doi.org/10.2903/j.efsa.2018.5194> [Scientific Opinion]. Minutes of the expert meeting on perfluorooctane sulfonic acid and perfluorooctanoic acid in food assessment. 2018b.
- EFSA CONTAM Panel. 2020. (EFSA Panel on Contaminants in the Food Chain), Schrenk D, Bignami M, Bodin L, Chipman JK, del Mazo J, Grasl-Kraupp B, Hogstrand C, Hoogenboom LR, Leblanc J-C, Nebbia CS, Nielsen E, Ntzani E, Petersen A, Sand S, Vleminckx C, Wallace H, Barregard L, Ceccatelli S, Cravedi J-P, Halldorsson TI, Haug LS, Johansson N, Knutsen HK, Rose M, Roudot A-C, Van Loveren H, Vollmer G, Mackay K, Riolo F and Schwerdtle T, 2020. Scientific Opinion on the risk to human health related to the presence of perfluoroalkyl substances in food. *EFSA Journal* 2020;18(9):6223, 391 pp. <https://doi.org/10.2903/j.efsa.2020.6223>
- Ehresman DJ, Froehlich JW, Olsen GW, Chang SC, Butenhoff JL. 2007. Comparison of human whole blood, plasma, and serum matrices for the determination of perfluorooctanesulfonate (PFOS), perfluorooctanoate (PFOA), and other fluorochemicals. *Environmental research.* 103(2):176-184. eng.
- Elcombe CR, Elcombe BM, Foster JR, Chang SC, Ehresman DJ, Butenhoff JL. 2012. Hepatocellular hypertrophy and cell proliferation in Sprague-Dawley rats from dietary exposure to potassium perfluorooctanesulfonate results from increased expression of xenosensor nuclear receptors PPARalpha and CAR/PXR. *Toxicology.* 293(1-3):16-29. eng.
- Ellis EC, Naugler WE, Parini P, Mörk LM, Jorns C, Zemack H, Sandblom AL, Björkhem I, Ericzon BG, Wilson EM et al. 2013. Mice with chimeric livers are an improved model for human lipoprotein metabolism. *PLoS One.* 8(11):e78550. eng.
- Ericson I, Gómez M, Nadal M, van Bavel B, Lindström G, Domingo JL. 2007. Perfluorinated chemicals in blood of residents in Catalonia (Spain) in relation to age and gender: a pilot study. *Environment international.* 33(5):616-623. eng.
- Eriksen KT, Raaschou-Nielsen O, McLaughlin JK, Lipworth L, Tjønneland A, Overvad K, Sørensen M. 2013. Association between plasma PFOA and PFOS levels and total cholesterol in a middle-aged Danish population. *PloS one.* 8(2):e56969-e56969. eng.
- Fabbri E, Mohammed BS, Korenblat KM, Magkos F, McCreia J, Patterson BW, Klein S. 2010. Effect of fenofibrate and niacin on intrahepatic triglyceride content, very low-density lipoprotein kinetics, and insulin action in obese subjects with nonalcoholic fatty liver disease. *J Clin Endocrinol Metab.* 95(6):2727-2735. eng.

- Fàbrega F, Kumar V, Schuhmacher M, Domingo JL, Nadal M. 2014. PBPK modeling for PFOS and PFOA: validation with human experimental data. *Toxicology letters*. 230(2):244-251. eng.
- Feingold. 2000. KR. Grunfeld C, Introduction to Lipids and Lipoproteins. [Updated 2018 Feb 2]. In: Feingold KR, Anawalt B, Boyce A, et al., editors. *Endotext* [Internet]. South Dartmouth (MA): MDText.com, Inc.; 2000-. Available from: <https://www.ncbi.nlm.nih.gov/books/NBK305896/>.
- Ference BA, Ginsberg HN, Graham I, Ray KK, Packard CJ, Bruckert E, Hegele RA, Krauss RM, Raal FJ, Schunkert H et al. 2017. Low-density lipoproteins cause atherosclerotic cardiovascular disease. 1. Evidence from genetic, epidemiologic, and clinical studies. A consensus statement from the European Atherosclerosis Society Consensus Panel. *European heart journal*. 38(32):2459-2472. eng.
- Fitz-Simon N, Fletcher T, Luster MI, Steenland K, Calafat AM, Kato K, Armstrong B. 2013. Reductions in serum lipids with a 4-year decline in serum perfluorooctanoic acid and perfluorooctanesulfonic acid. *Epidemiology (Cambridge, Mass)*. 24(4):569-576. eng.
- Frisbee SJ, Shankar A, Knox SS, Steenland K, Savitz DA, Fletcher T, Ducatman AM. 2010. Perfluorooctanoic acid, perfluorooctanesulfonate, and serum lipids in children and adolescents: results from the C8 Health Project. *Arch Pediatr Adolesc Med*. 164(9):860-869. eng.
- Fujii Y, Niisoe T, Harada KH, Uemoto S, Ogura Y, Takenaka K, Koizumi A. 2015. Toxicokinetics of perfluoroalkyl carboxylic acids with different carbon chain lengths in mice and humans. *Journal of Occupational Health*. 57(1):1-12.
- Gallo V, Leonardi G, Genser B, Lopez-Espinosa M-J, Frisbee SJ, Karlsson L, Ducatman AM, Fletcher T. 2012. Serum Perfluorooctanoate (PFOA) and Perfluorooctane Sulfonate (PFOS) Concentrations and Liver Function Biomarkers in a Population with Elevated PFOA Exposure. *Environmental health perspectives*. 120(5):655-660.
- Geiger SD, Xiao J, Ducatman A, Frisbee S, Innes K, Shankar A. 2014. The association between PFOA, PFOS and serum lipid levels in adolescents. *Chemosphere*. 98:78-83. eng.
- Genius SJ, Birkholz D, Ralitsch M, Thibault N. 2010. Human detoxification of perfluorinated compounds. *Public Health*. 124(7):367-375. eng.
- Genius SJ, Curtis L, Birkholz D. 2013. Gastrointestinal Elimination of Perfluorinated Compounds Using Cholestyramine and *Chlorella pyrenoidosa*. *ISRN Toxicology*. 2013:657849.
- Gleason JA, Post GB, Faglino JA. 2015. Associations of perfluorinated chemical serum concentrations and biomarkers of liver function and uric acid in the US population (NHANES), 2007-2010. *Environmental research*. 136:8-14. eng.
- Gomis MI, Vestergren R, Borg D, Cousins IT. 2018. Comparing the toxic potency *in vivo* of long-chain perfluoroalkyl acids and fluorinated alternatives. *Environment international*. 113:1-9. eng.
- Göttlicher M, Widmark E, Li Q, Gustafsson JA. 1992. Fatty acids activate a chimera of the clofibrilic acid-activated receptor and the glucocorticoid receptor. *Proc Natl Acad Sci U S A*. 89(10):4653-4657. eng.
- Guruge KS, Yeung LW, Yamanaka N, Miyazaki S, Lam PK, Giesy JP, Jones PD, Yamashita N. 2006. Gene expression profiles in rat liver treated with perfluorooctanoic acid (PFOA). *Toxicological sciences : an official journal of the Society of Toxicology*. 89(1):93-107. eng.
- Han X, Nabb DL, Russell MH, Kennedy GL, Rickard RW. 2012. Renal elimination of perfluorocarboxylates (PFCAs). *Chemical research in toxicology*. 25(1):35-46. eng.
- Harada KH, Hashida S, Kaneko T, Takenaka K, Minata M, Inoue K, Saito N, Koizumi A. 2007. Biliary excretion and cerebrospinal fluid partition of perfluorooctanoate and perfluorooctane sulfonate in humans. *Environmental toxicology and pharmacology*. 24(2):134-139. eng.
- Haughom B, Spydevold O. 1992. The mechanism underlying the hypolipemic effect of perfluorooctanoic acid (PFOA), perfluorooctane sulphonic acid (PFOSA) and clofibrilic acid. *Biochim Biophys Acta*. 1128(1):65-72. eng.
- Hayhurst GP, Lee YH, Lambert G, Ward JM, Gonzalez FJ. 2001. Hepatocyte nuclear factor 4alpha (nuclear receptor 2A1) is essential for maintenance of hepatic gene expression and lipid homeostasis. *Mol Cell Biol*. 21(4):1393-1403. eng.
- Heusinkveld HJ, Wackers PFK, Schoonen WC, van der Ven L, Pennings JLA, Luijten M. 2018. Application of the comparison approach to open TG-GATES: A useful toxicogenomics tool for detecting modes of action in chemical risk assessment. *Food and chemical toxicology : an international journal published for the British Industrial Biological Research Association*. 121:115-123. eng.

- Horton JD, Goldstein JL, Brown MS. 2002. SREBPs: activators of the complete program of cholesterol and fatty acid synthesis in the liver. *J Clin Invest.* 109(9):1125-1131. eng.
- Howroyd P, Swanson C, Dunn C, Cattley RC, Corton JC. 2004. Decreased longevity and enhancement of age-dependent lesions in mice lacking the nuclear receptor peroxisome proliferator-activated receptor alpha (PPARalpha). *Toxicol Pathol.* 32(5):591-599. eng.
- Huang MC, Dzierlenga AL, Robinson VG, Waidyanatha S, DeVito MJ, Eifrid MA, Granville CA, Gibbs ST, Blystone CR. 2019. Toxicokinetics of perfluorobutane sulfonate (PFBS), perfluorohexane-1-sulphonic acid (PFHxS), and perfluorooctane sulfonic acid (PFOS) in male and female Hsd:Sprague Dawley SD rats after intravenous and gavage administration. *Toxicology reports.* 6:645-655. eng.
- Hui Z, Li R, Chen L. 2017. The impact of exposure to environmental contaminant on hepatocellular lipid metabolism. *Gene.* 622:67-71. eng.
- Imes CC, Austin MA. 2013. Low-density lipoprotein cholesterol, apolipoprotein B, and risk of coronary heart disease: from familial hyperlipidemia to genomics. *Biol Res Nurs.* 15(3):292-308. eng.
- Jain RB, Ducatman A. 2019. Selective Associations of Recent Low Concentrations of Perfluoroalkyl Substances With Liver Function Biomarkers: NHANES 2011 to 2014 Data on US Adults Aged ≥ 20 Years. *J Occup Environ Med.* 61(4):293-302. eng.
- Janssen AW, Betzel B, Stoopen G, Berends FJ, Janssen IM, Peijnenburg AA, Kersten S. 2015. The impact of PPAR α activation on whole genome gene expression in human precision cut liver slices. *BMC Genomics.* 16:760. eng.
- Jeon TI, Osborne TF. 2012. SREBPs: metabolic integrators in physiology and metabolism. *Trends Endocrinol Metab.* 23(2):65-72. eng.
- Kaabia Z, Poirier J, Moughaizel M, Aguesse A, Billon-Crossouard S, Fall F, Durand M, Dagher E, Krempf M, Croyal M. 2018. Plasma lipidomic analysis reveals strong similarities between lipid fingerprints in human, hamster and mouse compared to other animal species. *Scientific Reports.* 8(1):15893.
- Kersten S. 2014. Integrated physiology and systems biology of PPAR α . *Mol Metab.* 3(4):354-371. eng.
- Kersten S, Stienstra R. 2017. The role and regulation of the peroxisome proliferator activated receptor alpha in human liver. *Biochimie.* 136:75-84. eng.
- Kim NH, Kim SG. 2020. Fibrates Revisited: Potential Role in Cardiovascular Risk Reduction. *Diabetes Metab J.* 44(2):213-221. eng.
- Kim SJ, Heo SH, Lee DS, Hwang IG, Lee YB, Cho HY. 2016. Gender differences in pharmacokinetics and tissue distribution of 3 perfluoroalkyl and polyfluoroalkyl substances in rats. *Food and chemical toxicology : an international journal published for the British Industrial Biological Research Association.* 97:243-255. eng.
- Kir S, Zhang Y, Gerard RD, Klierer SA, Mangelsdorf DJ. 2012. Nuclear receptors HNF4 α and LRH-1 cooperate in regulating Cyp7a1 *in vivo*. *J Biol Chem.* 287(49):41334-41341. eng.
- Krause BR, Princen HM. 1998. Lack of predictability of classical animal models for hypolipidemic activity: a good time for mice? *Atherosclerosis.* 140(1):15-24. eng.
- Kudo N, Katakura M, Sato Y, Kawashima Y. 2002. Sex hormone-regulated renal transport of perfluorooctanoic acid. *Chem Biol Interact.* 139(3):301-316. eng.
- Kudo N, Sakai A, Mitsumoto A, Hibino Y, Tsuda T, Kawashima Y. 2007. Tissue distribution and hepatic subcellular distribution of perfluorooctanoic acid at low dose are different from those at high dose in rats. *Biological & pharmaceutical bulletin.* 30(8):1535-1540. eng.
- Kühnast S, Fiocco M, van der Hoorn JW, Princen HM, Jukema JW. 2015. Innovative pharmaceutical interventions in cardiovascular disease: Focusing on the contribution of non-HDL-C/LDL-C-lowering versus HDL-C-raising: A systematic review and meta-analysis of relevant preclinical studies and clinical trials. *Eur J Pharmacol.* 763(Pt A):48-63. eng.
- Kwiterovich PO, Jr. 2000. The metabolic pathways of high-density lipoprotein, low-density lipoprotein, and triglycerides: a current review. *Am J Cardiol.* 86(12a):51-101. eng.
- Larter CZ, Yeh MM, Van Rooyen DM, Brooling J, Ghatora K, Farrell GC. 2012. Peroxisome proliferator-activated receptor- α agonist, Wy 14,643, improves metabolic indices, steatosis and ballooning in diabetic mice with non-alcoholic steatohepatitis. *J Gastroenterol Hepatol.* 27(2):341-350. eng.
- Lee-Rueckert M, Escola-Gil JC, Kovanan PT. 2016. HDL functionality in reverse cholesterol transport – Challenges in translating data emerging from mouse models to human disease. *Biochimica et Biophysica Acta (BBA) - Molecular and Cell Biology of Lipids.* 1861(7):566-583.

- Leritz EC, McGlinchey RE, Salat DH, Milberg WP. 2016. Elevated levels of serum cholesterol are associated with better performance on tasks of episodic memory. *Metab Brain Dis.* 31(2):465-473. eng.
- Li AC, Glass CK. 2004. PPAR- and LXR-dependent pathways controlling lipid metabolism and the development of atherosclerosis. *J Lipid Res.* 45(12):2161-2173. eng.
- Li T, Chiang JY. 2005. Mechanism of rifampicin and pregnane X receptor inhibition of human cholesterol 7 alpha-hydroxylase gene transcription. *Am J Physiol Gastrointest Liver Physiol.* 288(1):G74-84. eng.
- Li T, Chiang JY. 2009. Regulation of bile acid and cholesterol metabolism by PPARs. *PPAR Res.* 2009:501739. eng.
- Li Y, Barregard L, Xu Y, Scott K, Pineda D, Lindh CH, Jakobsson K, Fletcher T. 2020. Associations between perfluoroalkyl substances and serum lipids in a Swedish adult population with contaminated drinking water. *Environ Health.* 19(1):33. eng.
- Lin CY, Lin LY, Chiang CK, Wang WJ, Su YN, Hung KY, Chen PC. 2010. Investigation of the associations between low-dose serum perfluorinated chemicals and liver enzymes in US adults. *Am J Gastroenterol.* 105(6):1354-1363. eng.
- Liss KH, Finck BN. 2017. PPARs and nonalcoholic fatty liver disease. *Biochimie.* 136:65-74. eng.
- Louisse J, Rijkers D, Stoopen G, Janssen A, Staats M, Hoogenboom R, Kersten S, Peijnenburg A. 2020. Perfluorooctanoic acid (PFOA), perfluorooctane sulfonic acid (PFOS), and perfluorononanoic acid (PFNA) increase triglyceride levels and decrease cholesterologenic gene expression in human HepaRG liver cells. *Arch Toxicol.* eng.
- Loveless SE, Finlay C, Everds NE, Frame SR, Gillies PJ, O'Connor JC, Powley CR, Kennedy GL. 2006. Comparative responses of rats and mice exposed to linear/branched, linear, or branched ammonium perfluorooctanoate (APFO). *Toxicology.* 220(2-3):203-217. eng.
- Lu H. 2016. Crosstalk of HNF4 α with extracellular and intracellular signaling pathways in the regulation of hepatic metabolism of drugs and lipids. *Acta Pharm Sin B.* 6(5):393-408. eng.
- Luebker DJ, Hansen KJ, Bass NM, Butenhoff JL, Seacat AM. 2002. Interactions of fluorochemicals with rat liver fatty acid-binding protein. *Toxicology.* 176(3):175-185. eng.
- Marques LR, Diniz TA, Antunes BM, Rossi FE, Caperuto EC, Lira FS, Gonçalves DC. 2018. Reverse Cholesterol Transport: Molecular Mechanisms and the Non-medical Approach to Enhance HDL Cholesterol. *Front Physiol.* 9:526. eng.
- McMullen PD, Bhattacharya S, Woods CG, Pendse SN, McBride MT, Soldatow VY, Deisenroth C, LeCluyse EL, Clewell RA, Andersen ME. 2020. Identifying qualitative differences in PPAR α signaling networks in human and rat hepatocytes and their significance for next generation chemical risk assessment methods. *Toxicol In vitro.* 64:104463. eng.
- Miao J, Fang S, Bae Y, Kemper JK. 2006. Functional inhibitory cross-talk between constitutive androstane receptor and hepatic nuclear factor-4 in hepatic lipid/glucose metabolism is mediated by competition for binding to the DRI motif and to the common coactivators, GRIP-1 and PGC-1 α . *J Biol Chem.* 281(21):14537-14546. eng.
- Minata M, Harada KH, Kärrman A, Hitomi T, Hirotsawa M, Murata M, Gonzalez FJ, Koizumi A. 2010. Role of peroxisome proliferator-activated receptor- α in hepatobiliary injury induced by ammonium perfluorooctanoate in mouse liver. *Ind Health.* 48(1):96-107. eng.
- Morton RE, Izem L. 2014. Cholesteryl ester transfer proteins from different species do not have equivalent activities. *Journal of lipid research.* 55(2):258-265. eng.
- Nakagawa H, Terada T, Harada KH, Hitomi T, Inoue K, Inui K, Koizumi A. 2009. Human organic anion transporter hOAT4 is a transporter of perfluorooctanoic acid. *Basic & clinical pharmacology & toxicology.* 105(2):136-138. eng.
- Nakagawa T, Ramdhan DH, Tanaka N, Naito H, Tamada H, Ito Y, Li Y, Hayashi Y, Yamagishi N, Yanagiba Y et al. 2012. Modulation of ammonium perfluorooctanoate-induced hepatic damage by genetically different PPAR α in mice. *Arch Toxicol.* 86(1):63-74. eng.
- Nakamura T, Ito Y, Yanagiba Y, Ramdhan DH, Kono Y, Naito H, Hayashi Y, Li Y, Aoyama T, Gonzalez FJ et al. 2009. Microgram-order ammonium perfluorooctanoate may activate mouse peroxisome proliferator-activated receptor α , but not human PPAR α . *Toxicology.* 265(1-2):27-33. eng.

- Nelson JW, Hatch EE, Webster TF. 2010. Exposure to Polyfluoroalkyl Chemicals and Cholesterol, Body Weight, and Insulin Resistance in the General U.S. Population. *Environmental health perspectives*. 118(2):197-202.
- Nian M, Li QQ, Bloom M, Qian ZM, Syberg KM, Vaughn MG, Wang SQ, Wei Q, Zeeshan M, Gurram N et al. 2019. Liver function biomarkers disorder is associated with exposure to perfluoroalkyl acids in adults: Isomers of C8 Health Project in China. *Environmental research*. 172:81-88. eng.
- Nordestgaard BG, Varbo A. 2014. Triglycerides and cardiovascular disease. *Lancet*. 384(9943):626-635. eng.
- NTP. 2019a. NTP technical report on the toxicity studies of perfluoroalkyl sulfonates (perfluorobutane sulfonic acid, perfluorohexane sulfonate potassium salt, and perfluorooctane sulfonic acid) administered by gavage to Sprague Dawley (Hsd:Sprague Dawley SD) rats. Research Triangle Park, NC: National Toxicology Program. Toxicity Report 96.
- NTP. 2019b. NTP technical report on the toxicity studies of perfluoroalkyl carboxylates (perfluorohexanoic acid, perfluorooctanoic acid, perfluorononanoic acid, and perfluorodecanoic acid) administered by gavage to Sprague Dawley (Hsd:Sprague Dawley SD) rats. Research Triangle Park, NC: National Toxicology Program. Toxicity Report 97.
- Numata J, Kowalczyk J, Adolphs J, Ehlers S, Schafft H, Fuerst P, Muller-Graf C, Lahrssen-Wiederholt M, Greiner M. 2014. Toxicokinetics of seven perfluoroalkyl sulfonic and carboxylic acids in pigs fed a contaminated diet. *Journal of agricultural and food chemistry*. 62(28):6861-6870. eng.
- OECD. 2015. RISK REDUCTION APPROACHES FOR PFASS – A CROSSCOUNTRY ANALYSIS.
- Okyere J, Oppon E, Dzidzienyo D, Sharma L, Ball G. 2014. Cross-species gene expression analysis of species specific differences in the preclinical assessment of pharmaceutical compounds. *PloS one*. 9(5):e96853-e96853. eng.
- Olsen GW, Burriss JM, Burllew MM, Mandel JH. 2003a. Epidemiologic assessment of worker serum perfluorooctanesulfonate (PFOS) and perfluorooctanoate (PFOA) concentrations and medical surveillance examinations. *J Occup Environ Med*. 45(3):260-270. eng.
- Olsen GW, Burriss JM, Ehresman DJ, Froehlich JW, Seacat AM, Butenhoff JL, Zobel LR. 2007a. Half-life of serum elimination of perfluorooctanesulfonate, perfluorohexanesulfonate, and perfluorooctanoate in retired fluorochemical production workers. *Environmental health perspectives*. 115(9):1298-1305. eng.
- Olsen GW, Hansen KJ, Stevenson LA, Burriss JM, Mandel JH. 2003b. Human donor liver and serum concentrations of perfluorooctanesulfonate and other perfluorochemicals. *Environmental science & technology*. 37(5):888-891. eng.
- Olsen GW, Zobel LR. 2007b. Assessment of lipid, hepatic, and thyroid parameters with serum perfluorooctanoate (PFOA) concentrations in fluorochemical production workers. *International archives of occupational and environmental health*. 81(2):231-246. eng.
- Ory DS. 2004. Nuclear receptor signaling in the control of cholesterol homeostasis: have the orphans found a home? *Circ Res*. 95(7):660-670. eng.
- Palmer CN, Hsu MH, Griffin KJ, Raucy JL, Johnson EF. 1998. Peroxisome proliferator activated receptor- α expression in human liver. *Mol Pharmacol*. 53(1):14-22. eng.
- Papazyan R, Liu X, Liu J, Dong B, Plummer EM, Lewis RD, 2nd, Roth JD, Young MA. 2018. FXR activation by obeticholic acid or nonsteroidal agonists induces a human-like lipoprotein cholesterol change in mice with humanized chimeric liver. *J Lipid Res*. 59(6):982-993. eng.
- Pawlak M, Lefebvre P, Staels B. 2015. Molecular mechanism of PPAR α action and its impact on lipid metabolism, inflammation and fibrosis in non-alcoholic fatty liver disease. *J Hepatol*. 62(3):720-733. eng.
- Peng S, Yan L, Zhang J, Wang Z, Tian M, Shen H. 2013. An integrated metabolomics and transcriptomics approach to understanding metabolic pathway disturbance induced by perfluorooctanoic acid. *J Pharm Biomed Anal*. 86:56-64. eng.
- Perez F, Nadal M, Navarro-Ortega A, Fabrega F, Domingo JL, Barcelo D, Farre M. 2013. Accumulation of perfluoroalkyl substances in human tissues. *Environment international*. 59:354-362. eng.
- Perkins RG, Butenhoff JL, Kennedy GL, Jr., Palazzolo MJ. 2004. 13-week dietary toxicity study of ammonium perfluorooctanoate (APFO) in male rats. *Drug Chem Toxicol*. 27(4):361-378. eng.

- Piepoli MF, Hoes AW, Agewall S, Albus C, Brotons C, Catapano AL, Cooney M-T, Corrà U, Cosyns B, Deaton C et al. 2016. 2016 European Guidelines on cardiovascular disease prevention in clinical practice: The Sixth Joint Task Force of the European Society of Cardiology and Other Societies on Cardiovascular Disease Prevention in Clinical Practice (constituted by representatives of 10 societies and by invited experts) Developed with the special contribution of the European Association for Cardiovascular Prevention & Rehabilitation (EACPR). *European Heart Journal*. 37(29):2315-2381.
- Pizzurro DM, Seeley M, Kerper LE, Beck BD. 2019. Interspecies differences in perfluoroalkyl substances (PFAS) toxicokinetics and application to health-based criteria. *Regulatory toxicology and pharmacology : RTP*. 106:239-250. eng.
- Post SM, Duez H, Gervois PP, Staels B, Kuipers F, Princen HM. 2001. Fibrates suppress bile acid synthesis via peroxisome proliferator-activated receptor- α -mediated downregulation of cholesterol 7 α -hydroxylase and sterol 27-hydroxylase expression. *Arterioscler Thromb Vasc Biol*. 21(11):1840-1845. eng.
- Pouwer MG, Pieterman EJ, Chang SC, Olsen GW, Caspers MPM, Verschuren L, Jukema JW, Princen HMG. 2019. Dose Effects of Ammonium Perfluorooctanoate on Lipoprotein Metabolism in APOE*3-Leiden.CETP Mice. *Toxicological sciences : an official journal of the Society of Toxicology*. 168(2):519-534. eng.
- Pouwer MG, Pieterman EJ, Worms N, Keijzer N, Jukema JW, Gromada J, Gusarova V, Princen HMG. 2020. Alirocumab, evinacumab, and atorvastatin triple therapy regresses plaque lesions and improves lesion composition in mice. *J Lipid Res*. 61(3):365-375. eng.
- Princen H, Post S, Twisk J. 1997. Regulation of Bile Acid Biosynthesis. *Current Pharmaceutical Design*. 3:59-84.
- Princen HMG, Pouwer MG, Pieterman EJ. 2016. Comment on "Hypercholesterolemia with consumption of PFOA-laced Western diets is dependent on strain and sex of mice" by Rebholz S.L. et al. *Toxicol. Rep*. 2016 (3) 46-54. *Toxicology reports*. 3:306-309. eng.
- Rebholz SL, Jones T, Herrick RL, Xie C, Calafat AM, Pinney SM, Woollett LA. 2016. Hypercholesterolemia with consumption of PFOA-laced Western diets is dependent on strain and sex of mice. *Toxicology reports*. 3:46-54. eng.
- Ren H, Vallanat B, Nelson DM, Yeung LWY, Guruge KS, Lam PKS, Lehman-McKeeman LD, Corton JC. 2009. Evidence for the involvement of xenobiotic-responsive nuclear receptors in transcriptional effects upon perfluoroalkyl acid exposure in diverse species. *Reproductive toxicology (Elmsford, NY)*. 27(3-4):266-277. eng.
- RIVM. 2018. Mixture exposure to PFAS: A Relative Potency Factor approach. National Institute for Public Health and the Environment, The Netherlands. RIVM Report 2018-0070. M.J. Zeilmaker et al.
- Rosen MB, Abbott BD, Wolf DC, Corton JC, Wood CR, Schmid JE, Das KP, Zehr RD, Blair ET, Lau C. 2008a. Gene profiling in the livers of wild-type and PPAR α -null mice exposed to perfluorooctanoic acid. *Toxicol Pathol*. 36(4):592-607. eng.
- Rosen MB, Das KP, Rooney J, Abbott B, Lau C, Corton JC. 2017. PPAR α -independent transcriptional targets of perfluoroalkyl acids revealed by transcript profiling. *Toxicology*. 387:95-107. eng.
- Rosen MB, Lee JS, Ren H, Vallanat B, Liu J, Waalkes MP, Abbott BD, Lau C, Corton JC. 2008b. Toxicogenomic dissection of the perfluorooctanoic acid transcript profile in mouse liver: evidence for the involvement of nuclear receptors PPAR α and CAR. *Toxicological sciences : an official journal of the Society of Toxicology*. 103(1):46-56. eng.
- Rosen MB, Schmid JR, Corton JC, Zehr RD, Das KP, Abbott BD, Lau C. 2010. Gene Expression Profiling in Wild-Type and PPAR α -Null Mice Exposed to Perfluorooctane Sulfonate Reveals PPAR α -Independent Effects. *PPAR Res*. 2010:794739. eng.
- Rosenmai AK, Ahrens L, le Godec T, Lundqvist J, Oskarsson A. 2018. Relationship between peroxisome proliferator-activated receptor α activity and cellular concentration of 14 perfluoroalkyl substances in HepG2 cells. *J Appl Toxicol*. 38(2):219-226. eng.
- Sakr CJ, Kreckmann KH, Green JW, Gillies PJ, Reynolds JL, Leonard RC. 2007a. Cross-sectional study of lipids and liver enzymes related to a serum biomarker of exposure (ammonium perfluorooctanoate or APFO) as part of a general health survey in a cohort of occupationally exposed workers. *J Occup Environ Med*. 49(10):1086-1096. eng.
- Sakr CJ, Leonard RC, Kreckmann KH, Slade MD, Cullen MR. 2007b. Longitudinal study of serum lipids and liver enzymes in workers with occupational exposure to ammonium perfluorooctanoate. *J Occup Environ Med*. 49(8):872-879. eng.

- Salihovic S, Stubleski J, Kärrman A, Larsson A, Fall T, Lind L, Lind PM. 2018. Changes in markers of liver function in relation to changes in perfluoroalkyl substances - A longitudinal study. *Environment international*. 117:196-203. eng.
- Sandesara PB, Virani SS, Fazio S, Shapiro MD. 2019. The Forgotten Lipids: Triglycerides, Remnant Cholesterol, and Atherosclerotic Cardiovascular Disease Risk. *Endocr Rev*. 40(2):537-557. eng.
- Scharmach E, Buhrke T, Lichtenstein D, Lampen A. 2012. Perfluorooctanoic acid affects the activity of the hepatocyte nuclear factor 4 alpha (HNF4alpha). *Toxicology letters*. 212(2):106-112. eng.
- Schlezingner J, Puckett H, Oliver J, Nielsen G, Heiger-Bernays W, Webster T. 2020. Perfluorooctanoic acid activates multiple nuclear receptor pathways and skews expression of genes regulating cholesterol homeostasis in liver of humanized PPAR α mice fed an American diet. *bioRxiv*.2020.2001.2030.926642.
- Schoonjans K, Staels B, Auwerx J. 1996. Role of the peroxisome proliferator-activated receptor (PPAR) in mediating the effects of fibrates and fatty acids on gene expression. *J Lipid Res*. 37(5):907-925. eng.
- Seacat AM, Thomford PJ, Hansen KJ, Clemen LA, Eldridge SR, Elcombe CR, Butenhoff JL. 2003. Sub-chronic dietary toxicity of potassium perfluorooctanesulfonate in rats. *Toxicology*. 183(1-3):117-131. eng.
- Seacat AM, Thomford PJ, Hansen KJ, Olsen GW, Case MT, Butenhoff JL. 2002. Subchronic toxicity studies on perfluorooctanesulfonate potassium salt in cynomolgus monkeys. *Toxicological sciences : an official journal of the Society of Toxicology*. 68(1):249-264. eng.
- Shao W, Espenshade PJ. 2012. Expanding roles for SREBP in metabolism. *Cell Metab*. 16(4):414-419. eng.
- Son HY, Kim SH, Shin HI, Bae HI, Yang JH. 2008. Perfluorooctanoic acid-induced hepatic toxicity following 21-day oral exposure in mice. *Arch Toxicol*. 82(4):239-246. eng.
- Starling AP, Engel SM, Whitworth KW, Richardson DB, Stuebe AM, Daniels JL, Haug LS, Eggesbø M, Becher G, Sabaredzovic A et al. 2014. Perfluoroalkyl substances and lipid concentrations in plasma during pregnancy among women in the Norwegian Mother and Child Cohort Study. *Environment international*. 62:104-112. eng.
- Steenland K, Tinker S, Frisbee S, Ducatman A, Vaccarino V. 2009. Association of perfluorooctanoic acid and perfluorooctane sulfonate with serum lipids among adults living near a chemical plant. *Am J Epidemiol*. 170(10):1268-1278. eng.
- Takacs ML, Abbott BD. 2007. Activation of mouse and human peroxisome proliferator-activated receptors (alpha, beta/delta, gamma) by perfluorooctanoic acid and perfluorooctane sulfonate. *Toxicological sciences : an official journal of the Society of Toxicology*. 95(1):108-117. eng.
- Tan X, Xie G, Sun X, Li Q, Zhong W, Qiao P, Sun X, Jia W, Zhou Z. 2013. High fat diet feeding exaggerates perfluorooctanoic acid-induced liver injury in mice via modulating multiple metabolic pathways. *PLoS One*. 8(4):e61409. eng.
- Tateno C, Yoshizane Y, Saito N, Kataoka M, Utoh R, Yamasaki C, Tachibana A, Soeno Y, Asahina K, Hino H et al. 2004. Near completely humanized liver in mice shows human-type metabolic responses to drugs. *Am J Pathol*. 165(3):901-912. eng.
- Thompson MB. 1996. Bile acids in the assessment of hepatocellular function. *Toxicol Pathol*. 24(1):62-71. eng.
- Tugwood JD, Aldridge TC, Lambe KG, Macdonald N, Woodyatt NJ. 1996. Peroxisome proliferator-activated receptors: structures and function. *Ann N Y Acad Sci*. 804:252-265. eng.
- mUS EPA. 2016a. Drinking Water Health Advisory for Perfluorooctanoic Acid (PFOA). In: US EPA Office of Water (4304T) Health and Ecological Criteria Division Washington D, EPA Document Number: 822-R-16-005, May 2016, editor.
- mUS EPA. 2016b. Drinking Water Health Advisory for Perfluorooctane Sulfonate (PFOS). In: US EPA Office of Water (4304T) Health and Ecological Criteria Division Washington D, EPA Document Number: 822-R-16-004, May 2016, editor.
- Vanden Heuvel JP, Thompson JT, Frame SR, Gillies PJ. 2006. Differential activation of nuclear receptors by perfluorinated fatty acid analogs and natural fatty acids: a comparison of human, mouse, and rat peroxisome proliferator-activated receptor-alpha, -beta, and -gamma, liver X receptor-beta, and retinoid X receptor-alpha. *Toxicological sciences : an official journal of the Society of Toxicology*. 92(2):476-489. eng.
- Wan HT, Zhao YG, Wei X, Hui KY, Giesy JP, Wong CK. 2012. PFOS-induced hepatic steatosis, the mechanistic actions on β -oxidation and lipid transport. *Biochim Biophys Acta*. 1820(7):1092-1101. eng.

- Wang L, Wang Y, Liang Y, Li J, Liu Y, Zhang J, Zhang A, Fu J, Jiang G. 2013. Specific accumulation of lipid droplets in hepatocyte nuclei of PFOA-exposed BALB/c mice. *Sci Rep.* 3:2174. eng.
- Wang L, Wang Y, Liang Y, Li J, Liu Y, Zhang J, Zhang A, Fu J, Jiang G. 2014. PFOS induced lipid metabolism disturbances in BALB/c mice through inhibition of low density lipoproteins excretion. *Sci Rep.* 4:4582. eng.
- Westerterp M, van der Hoogt CC, de Haan W, Offerman EH, Dallinga-Thie GM, Jukema JW, Havekes LM, Rensen PC. 2006. Cholesteryl ester transfer protein decreases high-density lipoprotein and severely aggravates atherosclerosis in APOE*3-Leiden mice. *Arterioscler Thromb Vasc Biol.* 26(11):2552-2559. eng.
- Wigger L, Casals-Casas C, Baruchet M, Trang KB, Pradervand S, Naldi A, Desvergne B. 2019. System analysis of cross-talk between nuclear receptors reveals an opposite regulation of the cell cycle by LXR and FXR in human HepaRG liver cells. *PLoS One.* 14(8):e0220894. eng.
- Winqvist A, Steenland K. 2014. Modeled PFOA exposure and coronary artery disease, hypertension, and high cholesterol in community and worker cohorts. *Environmental health perspectives.* 122(12):1299-1305. eng.
- Wolf CJ, Rider CV, Lau C, Abbott BD. 2014. Evaluating the additivity of perfluoroalkyl acids in binary combinations on peroxisome proliferator-activated receptor- α activation. *Toxicology.* 316:43-54. eng.
- Wolf CJ, Schmid JE, Lau C, Abbott BD. 2012. Activation of mouse and human peroxisome proliferator-activated receptor- α (PPAR α) by perfluoroalkyl acids (PFAAs): further investigation of C4-C12 compounds. *Reproductive toxicology (Elmsford, NY).* 33(4):546-551. eng.
- Wolf CJ, Takacs ML, Schmid JE, Lau C, Abbott BD. 2008. Activation of mouse and human peroxisome proliferator-activated receptor α by perfluoroalkyl acids of different functional groups and chain lengths. *Toxicological sciences : an official journal of the Society of Toxicology.* 106(1):162-171. eng.
- Woodcroft MW, Ellis DA, Rafferty SP, Burns DC, March RE, Stock NL, Trumpour KS, Yee J, Munro K. 2010. Experimental characterization of the mechanism of perfluorocarboxylic acids' liver protein bioaccumulation: the key role of the neutral species. *Environmental toxicology and chemistry.* 29(8):1669-1677. eng.
- Wu X, Xie G, Xu X, Wu W, Yang B. 2018. Adverse bioeffect of perfluorooctanoic acid on liver metabolic function in mice. *Environ Sci Pollut Res Int.* 25(5):4787-4793. eng.
- Yan J, Chen B, Lu J, Xie W. 2015a. Deciphering the roles of the constitutive androstane receptor in energy metabolism. *Acta Pharmacologica Sinica.* 36(1):62-70.
- Yan S, Wang J, Dai J. 2015b. Activation of sterol regulatory element-binding proteins in mice exposed to perfluorooctanoic acid for 28 days. *Arch Toxicol.* 89(9):1569-1578. eng.
- Yang CH, Glover KP, Han X. 2009. Organic anion transporting polypeptide (Oatp) 1a1-mediated perfluorooctanoate transport and evidence for a renal reabsorption mechanism of Oatp1a1 in renal elimination of perfluorocarboxylates in rats. *Toxicology letters.* 190(2):163-171. eng.
- Yeh MM, Bosch DE, Daoud SS. 2019. Role of hepatocyte nuclear factor 4- α in gastrointestinal and liver diseases. *World J Gastroenterol.* 25(30):4074-4091. eng.
- Yin L, Ma H, Ge X, Edwards PA, Zhang Y. 2011. Hepatic hepatocyte nuclear factor 4 α is essential for maintaining triglyceride and cholesterol homeostasis. *Arterioscler Thromb Vasc Biol.* 31(2):328-336. eng.
- Yu WG, Liu W, Jin YH. 2009. Effects of perfluorooctane sulfonate on rat thyroid hormone biosynthesis and metabolism. *Environmental toxicology and chemistry.* 28(5):990-996. eng.
- Zadelaar S, Kleemann R, Verschuren L, de Vries-Van der Weij J, van der Hoorn J, Princen HM, Kooistra T. 2007. Mouse models for atherosclerosis and pharmaceutical modifiers. *Arterioscler Thromb Vasc Biol.* 27(8):1706-1721. eng.
- Zhang H, Temel RE, Martel C. 2014. Cholesterol and lipoprotein metabolism: Early Career Committee contribution. *Arterioscler Thromb Vasc Biol.* 34(9):1791-1794. eng.
- Zhang YM, Dong XY, Fan LJ, Zhang ZL, Wang Q, Jiang N, Yang XS. 2017. Poly- and perfluorinated compounds activate human pregnane X receptor. *Toxicology.* 380:23-29. eng.

- Zhao W, Zitzow JD, Ehresman DJ, Chang SC, Butenhoff JL, Forster J, Hagenbuch B. 2015. Na⁺/Taurocholate Cotransporting Polypeptide and Apical Sodium-Dependent Bile Acid Transporter Are Involved in the Disposition of Perfluoroalkyl Sulfonates in Humans and Rats. *Toxicological sciences : an official journal of the Society of Toxicology*. 146(2):363-373. eng.
- Zhao W, Zitzow JD, Weaver Y, Ehresman DJ, Chang S-C, Butenhoff JL, Hagenbuch B. 2017. Organic Anion Transporting Polypeptides Contribute to the Disposition of Perfluoroalkyl Acids in Humans and Rats. *Toxicological sciences : an official journal of the Society of Toxicology*. 156(1):84-95. eng.

Chapter 6

Determination of *in vitro* hepatotoxic potencies of a series of perfluoroalkyl substances (PFASs) based on gene expression changes in HepaRG liver cells

Accepted, in press Archives of Toxicology

Jochem Louisse¹
Styliani Fragki²
Deborah Rijkers¹
Aafke Janssen¹
Martijn Staats¹
Bas Bokkers³
Marco Zeilmaker⁴
Aldert Piersma^{2,5}
Mirjam Luijten²
Ron Hoogenboom¹
Ad Peijnenburg¹

¹ Wageningen Food Safety Research (WFSR), Wageningen, The Netherlands

² Centre for Health Protection, National Institute for Public Health and the Environment (RIVM), Bilthoven, The Netherlands

³ Centre for Safety of Substances and Products, National Institute for Public Health and the Environment (RIVM), Bilthoven, The Netherlands

⁴ Centre for Nutrition, Prevention and Health Services, National Institute for Public Health and the Environment (RIVM), Bilthoven, The Netherlands

⁵ Institute for Risk Assessment Sciences, Utrecht University, Utrecht, The Netherlands

Abstract

Per- and polyfluoroalkyl substances (PFASs) are omnipresent and have been shown to induce a wide range of adverse health effects, including hepatotoxicity, developmental toxicity and immunotoxicity. The aim of the present work was to assess whether human HepaRG liver cells can be used to obtain insight into differences in hepatotoxic potencies of a series of PFASs. Therefore, the effects of 18 PFASs on cellular triglyceride accumulation (AdipoRed assay) and gene expression (DNA microarray for PFOS and RT-qPCR for all 18 PFASs) were studied in HepaRG cells. BMDExpress analysis of the PFOS microarray data indicated that various cellular processes were affected at the gene expression level. From these data, ten genes were selected to assess the concentration-effect relationship of all 18 PFASs using qRT-PCR analysis. The AdipoRed data and the qRT-PCR data were used for the derivation of *in vitro* relative potencies using PROAST analysis. *In vitro* relative potency factors (RPFs) could be obtained for 8 PFASs (including index chemical PFOA) based on the AdipoRed data, whereas for the selected genes *in vitro* RPFs could be obtained for 11-18 PFASs (including index chemical PFOA). For the readout *OAT5* expression, *in vitro* RPFs were obtained for all PFASs. *In vitro* RPFs were found to correlate in general well with each other (Spearman correlation) except for the PPAR target genes *ANGPTL4* and *PDK4*. Comparison of *in vitro* RPFs with RPFs obtained from *in vivo* studies in rats indicate that best correlations (Spearman correlation) were obtained for *in vitro* RPFs based on *OAT5* and *CXCL10* expression changes and external *in vivo* RPFs. HFPO-TA was found to be the most potent PFAS tested, being around 10-fold more potent than PFOA. Altogether, it may be concluded that the HepaRG model may provide relevant data to provide insight into which PFASs are relevant regarding their hepatotoxic effects and that it can be applied as a screening tool to prioritize other PFASs for further hazard and risk assessment.

Introduction

Per- and polyfluoroalkyl substances (PFASs) are very persistent chemicals and omnipresent in the environment (Wang et al., 2017). PFASs are defined as “fluorinated substances that contain at least one fully fluorinated methyl or methylene carbon atom (without any H/Cl/Br/I atom attached to it)” (OECD, 2021). They are widely used in various industrial and consumer applications, such as firefighting foams, electronics, textiles, food contact materials, and cosmetics. The production and use of the most studied PFASs, perfluorooctanoic acid (PFOA) and perfluorooctane sulfonic acid (PFOS), have been restricted given the concerns of adverse effects to human health and the environment (EU, 2019; EU, 2020; UNEP, 2009).

In experimental animals, PFASs have been shown to induce a wide range of adverse effects, including hepatotoxicity, developmental toxicity, immunotoxicity, and a decrease in thyroid hormone levels (ATSDR, 2021; EFSA CONTAM Panel, 2018, 2020). The most consistent endpoint is increased liver weight, characterized by a combined hyperplasia and hypertrophy, which has been observed for many PFASs with clear differences in potencies. Disturbances in lipid metabolism, including hepatocellular steatosis and other hepatotoxic effects, have also been reported (EFSA CONTAM Panel, 2020). Also in humans, rather low serum levels of PFOS and PFOA have been associated with disturbed lipid homeostasis, in which the liver may play a role. However, the causality of this relationship has been debated (see for a recent review Fragki et al. (2021)). Furthermore, epidemiological evidence has correlated serum levels of both PFOS and PFOA to a small elevation in serum levels of the hepatic enzyme ALT (alanine transferase), a biomarker for liver damage (Gallo et al., 2012). However, whether that limited increase in ALT reflects serious liver damage is questionable.

Bil et al. (2021; 2022a) used data on hepatotoxicity in individual studies with male rats to derive external relative potency factors (RPFs) for 16 PFASs (using PFOA as index chemical). External RPFs of 7 other PFASs were estimated based on read across. In addition, Bil et al. (2022b) reported eight internal RPFs, which are based on the same toxicological information as the external RPFs reported by Bil et al. (2021; 2022a), but estimated by translating external doses to internal blood concentrations using kinetic models. For assessment of risks upon combined exposure to PFASs, such RPFs may be of use to take potency differences in PFASs into account. In that regard, external RPFs may be of use when considering external exposure and internal RPFs when considering internal exposure.

The number of existing PFASs is estimated to be around a few thousands, and for many of these toxicity data are lacking. Performing *in vivo* animal studies to obtain toxicity data for all these PFASs is not considered feasible, given the high costs and demand of resources, and also not desirable, because of ethical issues and the uncertainty related to possible species differences between laboratory animals and humans. Instead, application of novel approach methodologies (NAMs), such as *in vitro* toxicity assays, may be used, in the first

place to prioritize those PFASs for which a more extensive hazard and risk assessment would be considered most relevant, and within a next generation risk assessment paradigm, to provide *in vitro* effect concentrations that can be translated to *in vivo* oral equivalent dose levels (Punt et al., 2021), providing data that may be used for the risk assessment.

Recently, we demonstrated that treatment of human HepaRG liver cells with PFOA, PFOS, and PFNA resulted in an increase in triglyceride levels (Louisse et al., 2020), which is considered to be a potential relevant readout for PFAS-induced liver toxicity (Fragki et al., 2021). Furthermore, microarray analysis indicated that these three PFASs, at a concentration of 100 μM , downregulated genes involved in cholesterol biosynthesis. The data also pointed to, amongst others, changes in cellular processes, such as PERK/ATF4 signalling, tRNA aminoacylation and expression of amino acid transporters by PFOA, PFOS and PFNA. It is of interest to assess whether such *in vitro* effects may be of use for obtaining insight into potency differences of different PFASs. Therefore, the present study aimed to assess the concentration-dependent effects of 18 PFASs (Figure 1) on triglyceride levels (applying the AdipoRed assay) and expression of genes (as measured with RT-qPCR) in HepaRG cells. This study includes 11 perfluoroalkyl carboxylic acids (PFCAs), 5-perfluoroalkyl sulfonic acids (PFSA) and 2 perfluoroalkyl ether carboxylic acids (PFECAs, including GenX (HFPO-DA)). To identify genes for RT-qPCR analysis, concentration-dependent PFOS transcriptomic data were analysed with BMDExpress software, providing insight into PFOS-induced effects on gene expression and their concentration-dependency in HepaRG cells. Based on these data, genes were selected to assess the concentration-dependent changes in expression upon exposure to the 18 PFASs (Figure 1). Concentration-response data on the increase in triglyceride levels and effects on gene expression of the selected genes were analysed with PROAST software to obtain insight into *in vitro* potency differences for the 18 PFASs. The obtained *in vitro* RPFs were compared with reported external and internal RPFs obtained from animal studies to provide insights into differences and similarities in the outcomes of using *in vitro* human cell-based and *in vivo* animal-based approaches.

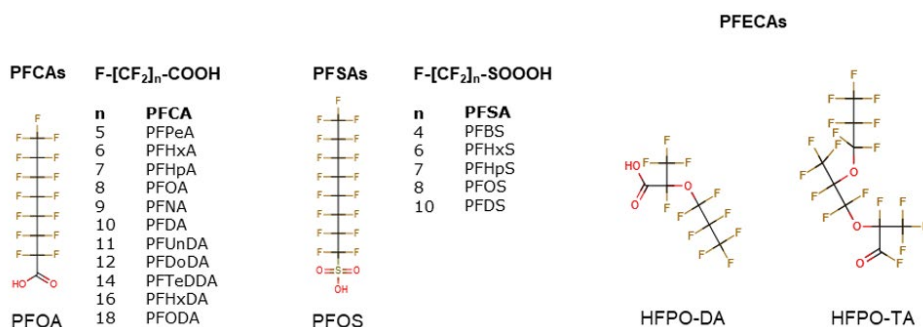


FIGURE 1 Chemical structures of the PFASs tested in the present study. Full names of abbreviations are provided in the Materials and methods section under 'Chemicals'.

Materials and methods

Chemicals

The following PFASs were tested in the present study: perfluoropentanoic acid (PFPeA; C5), perfluorohexanoic acid (PFHxA; C6), perfluoroheptanoic acid (PFHpA; C7), perfluorooctanoic acid (PFOA; C8), perfluorononanoic acid (PFNA; C9), perfluorodecanoic acid (PFDA; C10), perfluoroundecanoic acid (PFUnDA; C11), perfluorododecanoic acid (PFDoDA; C12), perfluorotetradecanoic acid (PFTeDA; C14), perfluorohexadecanoic acid (PFHxDA; C16), perfluorooctadecanoic acid (PFODA; C18), perfluorobutane sulfonate (PFBS; C4), perfluorohexane sulfonate (PFHxS; C6), perfluoroheptane sulfonate (PFHpS; C7), perfluorooctane sulfonate (PFOS; C8), perfluorodecane sulfonate (PFDS; C10), hexafluoropropylene oxide dimer acid (HFPO-DA, also known as GenX; C6) and hexafluoropropylene oxide trimer acid (HFPO-TA; C9) (Figure 1). All stocks were prepared in 100% dimethyl sulfoxide (DMSO HybriMax, Sigma-Aldrich), which were stored at -20 °C. More information about suppliers, purity, catalog numbers, CAS numbers and maximum concentrations tested in the present study is presented in Supplementary Table 1. The highest concentration tested was determined by the degree of solubility of each PFAS.

HepaRG cell culture

The human hepatic cell line HepaRG was obtained from Biopredic International (Rennes, France) and cultured in growth medium consisting of William's Medium E + GlutaMAX™ (ThermoFisher Scientific, Landsmeer, The Netherlands) supplemented with 10% fetal bovine serum (FBS; Corning (35-079-CV), United States of America), 1% PS (100 U/mL penicillin, 100 µg/mL streptomycin; Capricorn Scientific, Ebsdorfergrund, Germany), 50 µM hydrocortisone hemisuccinate (sodium salt) (Sigma-Aldrich), and 5 µg/mL human insulin (PAN™ Biotech). Seeding, trypsinization (using 0.05% Trypsin-EDTA (ThermoFisher Scientific)) and maintenance of the cells was performed according to the HepaRG instruction manual from Biopredic International. For cell viability and triglyceride accumulation studies, cells were seeded in black-coated 96-well plates (Greiner Bio-One, Frickenhausen, Germany; 9000 cells per well in 100 µL). For gene expression studies, cells were seeded in 24-well plates (Corning, Corning, NY; 55000 cells per well in 500 µL). After two weeks on growth medium, cells were cultured for two days in growth medium supplemented with 0.85% DMSO to induce differentiation. Subsequently, cells were cultured for 12 days in growth medium supplemented with 1.7% DMSO (differentiation medium) for final differentiation. At this stage, cells were ready to be used for toxicity studies. Cells that were not immediately used were kept on differentiation medium for a maximum of three additional weeks. Cell cultures were maintained in an incubator (humidified atmosphere with 5% CO₂ at 37°C) and the medium was refreshed every 2-3 days during culturing. Prior to toxicity studies, differentiated cells were incubated for 24 h in assay medium (growth medium containing 2% FBS) supplemented with 0.5% DMSO.

Cell exposure

Test chemicals were diluted from 200-fold concentrated stock solutions in assay medium, providing a final DMSO concentration of 0.5%. In each experiment a solvent control (0.5% DMSO) was included. PFASs were tested in concentrations up to 400 μM (if solubility allowed). After exposure, effects of the PFASs on cell viability and gene expression were assessed. Highest tested concentrations that could be tested for each PFAS are presented in Supplementary Table 1.

Stability studies HFPO-DA and HFPO-TA

To assess whether HFPO-DA and HFPO-TA are stable under the culture conditions applied in this study, we incubated 50 μM HFPO-DA or HFPO-TA in culture medium (0.5% DMSO) for 24 h in an incubator (humidified atmosphere with 5% CO_2 at 37°C) and took samples at $t = 0$ h, 6 h and 24 h for quantification using LC-MS analysis. We also assessed the stability of stock solutions in DMSO kept at -20 °C. To 50 μL culture medium, 850 μL methanol (Actual Chemicals, Oss, The Netherlands) containing internal standard (13C3-GenX (Wellington Laboratories, Canada)) was added. These dilutions were vortexed well before centrifugation at maximum speed for 10 minutes at 4 °C. Samples were further another 1200 times diluted with methanol and internal standard and HFPO-DA and HFPO-TA concentrations were determined using LC-MS/MS analysis. LC-MS/MS analysis was based on a Sciex UHPLC system containing: 2 pumps (ExionLC AD); column oven (ExionLC AC); controller (ExionLC); degasser (ExionLC); and sample tray holder (ExionLC AD) (Sciex, Framingham, MA, USA). An Luna Omega PS C18 analytical column (100Å , 100 × 2.1 mm i.d., 1.6 μm , Phenomenex, Torrance, CA, USA), was used to separate the PFASs at a column temperature of 40°C. Additionally, a Gemini C18 analytical column (110Å , 50 × 3 mm i.d., 3 μm , Phenomenex, Torrance, CA, USA) was used as an isolator column, placed between the pump and the injector valve to isolate and delay interferences out of the LC system. The mobile phase consisted of 20 mM ammonium acetate (Merck Millipore, Darmstadt, Germany) in water Ultra LC/MS grade (Actu-All Chemicals, Oss, The Netherlands) (mobile phase A) and Acetonitrile ULC/MS grade (Biosolve, Dieuze, France) (mobile phase B). The injection volume used was 20 μL . The chromatographic gradient was operated at a flow rate of 0.8 mL min^{-1} starting from 15% mobile phase B in the first 1.0 min, a linear increase to 98% B in 6 min with a final hold of 0.5 min. The gradient was returned to 15% B within 0.1 min for 0.7 min to equilibrate before the next injection, resulting in a total run of 8.3 min. Detection was carried out by MS/MS using a Sciex QTRAP 7500 system (Sciex, Framingham, MA, USA) in negative electrospray ionization (ESI-) mode, with the following conditions: ion spray voltage (IS) of -1500 V; curtain gas (CUR) of 45 psi; source temperature (TEM) of 400°C; gas 1 (GS1) of 40 psi; gas 2 (GS2) of 80 psi; and collision gas (CAD) 9. The PFASs were fragmented using collision induced dissociation (CID) using argon as target gas. The analyses were performed in multiple reaction monitoring (MRM) mode, using two mass transitions per component selected based on the abundance of the signal and the selectivity of the transition. In Supplementary Table 2 information on the MRM transitions, entrance potential (EP), collision energy (CE) and cell

exit potential (CXP) are presented. Data were acquired using SciexOS and processed using MultiQuant™ software (Sciex, Framingham, MA, USA).

Cell viability studies

The effects of the 18 PFASs on the viability of HepaRG cells cultured in 96-well plates, was determined using the WST-1 assay. This assay determines the conversion of the tetrazolium salt WST-1 (4-[3-(4-iodophenyl)-2-(4-nitrophenyl)-2H-5-tetrazolio]-1,3-benzene disulfonate) to formazan by metabolically active cells. For PFOA, PFNA, PFHxS and PFOS, the effects on cell viability were studied upon a 24-h and a 72-h exposure, given that both exposure times were studied for optimization of the exposure time for assessing effects of these PFASs on triglyceride accumulation. All other PFASs were only tested upon a 24-h exposure. After exposure, the medium was removed and the cells were washed with Dulbecco's Phosphate Buffered Saline (DPBS; ThermoFisher Scientific). Next, WST-1 solution (Sigma-Aldrich) was added to the cell culture medium (1:10 dilution) and 100 μ L was added to each well. After 1 h incubation in an incubator (humidified atmosphere with 5% CO₂ at 37°C), the plate was shaken at 1000 rpm for 1 min, and absorbance at 450 nm was measured (background absorbance at 630 nm was subtracted) using a Synergy HT Microplate Reader (BioTek, Winooski, VT). Three independent studies, with in each study three technical replicates per condition, were performed. Cell viability upon PFAS treatments was expressed as percentage of the cell viability of the solvent control.

Triglyceride accumulation studies

The effect of the 18 PFASs on triglyceride levels was determined using the AdipoRed assay essentially according to the instructions of the supplier (Lonza, Basel, Switzerland). We used the approach as applied in the study of Luckert et al. (2018), in which HepaRG cells were exposed to the steatotic compound cyproconazole. In that study, 72 hours was shown to be the optimal time point to assess the effects of cyproconazole on triglyceride accumulation as determined with the AdipoRed assay. We first assessed whether this time point was also the optimal time point for assessing effects of PFASs on triglyceride accumulation, by studying the effects of a 24-h or a 72-h exposure to PFOA, PFNA, PFHxS and PFOS in the AdipoRed assay, also including cyproconazole as positive control. After exposure for 24 or 72 h, the medium was removed and the cells were washed with 200 μ L DPBS and subsequently incubated for 10 min at room temperature with 200 μ L AdipoRed-DPBS solution. The latter solution was prepared by adding 25 μ L AdipoRed to 1 mL DPBS. Subsequently, fluorescence was measured using a 485/20 nm excitation and 590/35 emission filter set on the Synergy HT Microplate Reader. The results from that study indicate that a 24-h exposure was considered better than a 72-h exposure to study effects of PFASs (see Results section). Therefore, all other PFASs were tested upon a 24-h exposure. For each PFAS, three independent biological replicates, with three technical replicates per condition were obtained. Data were used for dose-response analysis using PROAST software (see below).

Whole genome gene expression: microarray hybridisations and BMDEExpress analysis

To obtain insight into the PFOS concentration-dependent induced gene expression changes, differentiated cells were exposed for 24 h to 6.25, 12.5, 25, 50, 100, 200 or 400 μ M PFOS. An exposure duration of 24 h was selected based on our previous study (Louisse et al., 2020). After exposure, total RNA was isolated and purified using the RNeasy Minikit (Qiagen). RNA quality and integrity was assessed using the RNA 6000 Nano chips on the Agilent 2100 Bioanalyzer (Agilent Technologies, Amsterdam, The Netherlands). Purified RNA (100 ng) was labeled with the Ambion WT expression kit (Invitrogen) and hybridized to Affymetrix Human Gene 2.1 ST arrays (Affymetrix, Santa Clara, CA). Hybridization, washing, and scanning were carried out on an Affymetrix GeneTitan platform according to the instruction by the manufacturer. Obtained data (CEL-files) were further processed using Bioconductor in R, performing quality control and normalization. For array normalization, the Robust Multiarray Average method (Bolstad et al., 2003; Irizarry et al., 2003) was applied. Probe sets were defined according to Dai et al. (2005). In this method probes are assigned to Entrez IDs as a unique gene identifier. CEL file normalization was performed with the Robust Multichip Average method using the Bioconductor oligo package (version 3.8) and the human Entrez-Gene custom CDF annotation from Brain Array version 23.0.0 containing 965365 probes and 29635 probesets (http://brainarray.mbni.med.umich.edu/Brainarray/Database/CustomCDF/CDF_download.asp).

BMDEExpress is a software tool for BMD analysis of transcriptomic data (Yang et al., 2007; Philips et al., 2018). BMDEExpress2 (Version 2.20.0180) was applied following the workflow (loading expression data, filtering, BMD analysis, and Pathway analysis (functional analysis)) as described on <https://github.com/auerbachs/BMDEExpress-2/wiki>. Expression data were organized in a tab-delimited plain text file and are provided as Supplementary Material. Each column in the data matrix corresponds to an individual expression experiment. The first row contains information in the sample label, the second row on the PFOS concentration and all further rows the data for one probe ID. Regarding loading of the expression data, 'Generic' was selected for the platform, and 'BASE2' for the Log Transformation. Regarding the filtering, ANOVA was used, using a P-value Cutoff of 0.05, applying the Benjaminin & Hochberg correction for multiple testing, filtering out control genes, and without applying a Fold Change Filter (i.e. Fold Change Value of 1.0 was selected). Regarding BMD analysis, the continuous models Exp2, Exp3, Exp4, Exp5, Linear, Poly2, Poly3, Hill and Power were selected. A BMR factor of 1.021 was selected. At 1.021 times the standard deviation of the control group the gene expression is thought to change by 5% compared to background as also applied by Chang et al. (2020). Applying such a low response as BMR allows inclusion of genes that may show limited changes in expression. Application of a higher BMR may provide more robust BMC estimations, but may exclude genes (and as a possible consequence related gene sets) that show limited gene expression changes that could be relevant from a biological perspective. Regarding the functional analysis, we performed a defined category analysis using gene sets from

the Reactome Pathway Database (<https://reactome.org/>; Wu and Haw, 2017), applying the following data source options: 'Remove Promiscuous Probes', 'Remove BMD > Highest Dose from Category Descriptive Statistics', 'Remove BMD with p-Value < Cutoff: 0.1', 'Remove genes with BMD/BMDL >: 20', 'Remove genes with BMDU/BMDL >: 40', 'Remove Genes With Max Fold Change <: 1.2', and 'Identify conflicting probe sets: 0.5'. The applied probe file and category file used for the analysis are provided in the Supplementary Materials. For further analysis we applied the following filters: Fisher's Exact Two Tail ≤ 0.1 , 'genes that passed all filters' of a gene set were set at 5, and the percentage of genes regulated of the gene was set at $\geq 20\%$. For the gene sets remaining upon application of these filters, information was collected and organized in an Excel file, which is available as Supplementary Material.

RT-qPCR

For selected genes, concentration-dependent expression levels were determined in PFAS-exposed HepaRG cells. To that end, cells were exposed to increasing concentrations of the 18 PFASs for 24 h and total RNA was extracted from the cells using the RNeasy Mini Kit (Qiagen, Venlo, The Netherlands). Subsequently, 500 ng RNA was used to synthesize cDNA using the iScript cDNA synthesis kit (Bio-Rad Laboratories, Veenendaal, The Netherlands). Changes in gene expression were determined by RT-qPCR on a CFX384 real-time PCR detection system (Bio-Rad Laboratories) by using SensiMix (Bioline; GC Biotech, Alphen aan den Rijn, The Netherlands). The PCR conditions consisted of an initial denaturation at 95°C for 10 min, followed by 40 cycles of denaturation at 95°C for 10 s and annealing extension at 60°C for 15 s. Relative gene expression was quantified with the standard curve method, using a standard curve generated from a serial dilution of pooled sample cDNA, and subsequently normalized to RPL27 gene expression. Primer sequences were taken from the Harvard PrimerBank and ordered from Eurogentec (Liège, Belgium). Sequences of the used primers are listed in Table 1. The concentration-response data were subjected to dose-response analysis using PROAST software as described below.

TABLE 1 Primer sequences used for RT-qPCR

Name	Primer Sequence	
	Forward	Reverse
<i>ANGPTL4</i>	CACAGCCTGCAGACAACTC	GGAGGCCAACTGGCTTTGC
<i>ATF4</i>	CCCTTCACCTTCTTACAACCTC	TGCCCAGCTCTAAACTAAAGGA
<i>CXCL10</i>	GAACGTIACGCTGTACCTGCA	TTGATGGCCTTCGATTCTGGA
<i>HMGR</i>	TGATTGACCTTTCCAGAGCAAG	CTAAAATTGCCATTCCACGAGC
<i>LSS</i>	GCACTGGACGGGTGATTATGG	TCTCTTCTCTGTATCCGGCTG
<i>OAT5</i>	TGGTGTITGCTCCAGCTTG	GCCTTATCCACTCAGTAATGGCC
<i>PK4</i>	TGGAGCATTCTCGCGCTAC	ACAGGCAATTCTGTGCGCAA
<i>RPL27</i>	ATCGCAAGAGATCAAAGATAA	TCTGAAGACATCCTTATTGACC
<i>SLC7A11</i>	GGTCCATTACCAGCTTTTGTACG	AATGTAGCGTCCAAATGCCAG
<i>THRSP</i>	CAGGTGCTAACCAAGCGTTAC	CAGAAGGCTGGGGATCATCA
<i>YARS1</i>	TGGTCACACAGCACGATTCC	CGGGGTATAAGAGGCCACTC

Dose-response analysis of AdipoRed and RT-qPCR data with PROAST

AdipoRed data and RT-qPCR data were used for concentration-response modelling with dose-response analysis software PROAST version 70.2 and 70.7tmp (National Institute for Public Health and the Environment 2018) in R (version 4.2.0). Data were available from three independent experiments. First, it was determined whether differences between the independent experiments (for individual PFASs) exist. For this, PROAST version 70.2 was used. This analysis was performed using the data of *OAT5* gene expression. It appeared that the background (parameter a) differed for some PFASs between different experiments, based on which it was decided to not use summary data for the further dose-response analysis to determine RPFs, but to run the PROAST analyses (in version 70.7tmp) with the following covariates: substance (parameter b and var) and substance-experiment (parameter a). Data of all PFASs were analysed simultaneously to ensure the parallel curves required to derive RPFs (Bosgra et al., 2009; Bil et al., 2021; 2022a; 2022b; van der Ven et al., 2022; van den Brand et al., 2022). Tab-delimited text files containing data on concentration, effect and experiment number were made and analysed as continuous data. Non-normalized gene expression and AdipoRed data were used for dose-response analysis since possible differences in background are accounted for by the covariate on background parameter a. Then, the exponential model, with parameters a, b, c, and d describing the response at dose 0 (background value), the potency of the PFAS, maximum fold change in response compared with background response (upper or lower plateau), and steepness of the curve (on a log-dose scale), respectively, was fitted with and without fixing parameter c to a large value to determine if a maximum fold change could be established. The model (with or without fixed parameter c) with the lowest Akaike information criterion (AIC) was chosen to determine the RPFs and the corresponding 90% confidence intervals (Bil et al., 2022a,b; van den Brand et al., 2022). PFOA was used as the index chemical. For some PFASs it was not possible to determine an RPF and for some compounds determination of the lower bound RPF (RPFL) was not possible, because the data did not show a clear trend.

Comparisons of obtained *in vitro* RPFs and reported *in vivo* RPFs

We compared the RPFs obtained from the different *in vitro* readouts (AdipoRed and selected genes) to assess whether different conclusions would be drawn based on the readout selection. Subsequently we compared the *in vitro* RPFs with RPFs reported in the literature obtained from *in vivo* rat studies, for which RPFs are available for external (Bil et al., 2021; 2022a) and internal exposure (Bil et al., 2022b).

Results

Stability studies HFPO-DA and HFPO-TA

HFPO-DA and HFPO-TA were added to cell culture medium (0.5% DMSO) at a concentration of 50 μ M and incubated in an incubator (humidified atmosphere with 5% CO₂ at 37°C).

Samples were taken at $t = 0$ h, 6 h and 24 h, and were measured using LC-MS analysis. Results indicate that under these conditions HFPO-DA and HFPO-TA are stable (Supplementary Figure 1), indicating that these culture conditions are adequate to determine the effects of these PFASs on the HepaRG cells.

Cell viability studies

The effect of a 24-h (all PFASs) and 72-h (PFOA, PFNA, PFHxS and PFOS) exposure of HepaRG cells to the PFASs on cell viability was determined using the WST-1 assay. Concentrations up to 400 μM were used, except for PFDoDA/ PFTeDA (up to 100 μM) and PFHxDA/PFODA (up to 25 μM), due to limited solubility of these PFASs (Supplementary Table 1). The results of the 72-h exposure studies indicate that PFOA is clearly cytotoxic at 400 μM , PFNA at 200 and 400 μM and that no effects were found for PFHxS and PFOS (Supplementary Figure 2). The results of the 24-h exposure studies indicate that four of the 18 tested PFASs decrease cell viability in a concentration-dependent manner, being PFNA, PFDA, PFHpS and HPFO-TA (Supplementary Figure 3), with HFPO-TA being the most potent PFAS, followed by PFDA and PFNA. The other PFASs did not show cytotoxicity in the WST-1 assay for the concentration range tested (Supplementary Figure 3). Maximum concentrations for the further studies were selected as the highest concentrations causing less than 25% decrease in cell-based WST-1 conversion, amounting to 50 μM HPFO-TA, 100 μM PFNA, 100 μM PFDA and 200 μM PFHpS.

Triglyceride accumulation studies

We first assessed whether a 24-h or a 72-h exposure was considered optimal to assess effects of PFASs on triglyceride accumulation, as measured with the AdipoRed assay, by determining the effects for PFOA, PFNA, PFHxS and PFOS, also including cyproconazole, for which earlier studies indicated that most effects were found upon a 72-h exposure (Luckert et al., 2018). The results show that for the four PFASs, in contrast to cyproconazole, more effects were observed upon exposure for 24 h compared to a 72-h exposure (Supplementary Figure 4). Therefore, for all other PFASs, the effect of a 24-h exposure to the PFASs on triglyceride accumulation in HepaRG cells was determined. In general, changes in AdipoRed signal were limited, at maximum amounting to a 1.4-fold increase at 50 μM HPFO-TA compared to the solvent control (Supplementary Figure 5), comparing to a measured maximum 1.6-fold increase for the positive control cyproconazole (Supplementary Figure 4). Dose-response analysis using parallel curve fitting was applied on the AdipoRed data to determine *in vitro* RPF values, which could be obtained for PFNA, PFDoDA, PFHxDA, PFHxS, PFOS and PFDS (Figure 2). PFNA, PFDoDA, PFHxDA and HFPO-TA were more potent than PFOA, but it must be noted that confidence intervals of PFHxDA's RPF are large (Figure 2). PFOS showed a similar potency as PFOA, and PFHxS and PFDS were slightly less potent than PFOA (Figure 2).

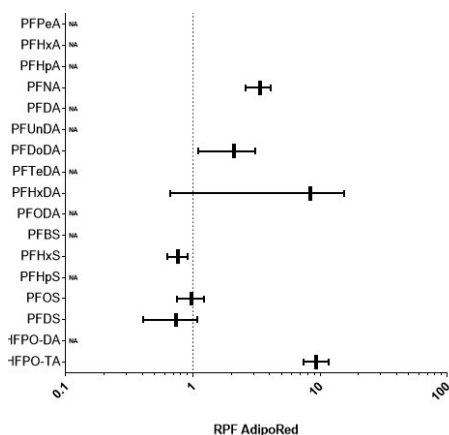


FIGURE 2 *In vitro* RPFs based on PROAST dose-response analysis of AdipoRed data obtained from HepaRG cells exposed to various PFASs. RPFs are presented as vertical lines, with the 5% lower bound and 95% upper bound of the confidence interval as whiskers. PFOA was used as index chemical, i.e., has an RPF of 1 (dotted line). NA: not applicable, RPF could not be determined.

Transcriptomics studies PFOS-exposed HepaRG cells and BMDExpress analysis

HepaRG cells were exposed for 24 h to 0 (solvent control), 6.25, 12.5, 25, 50, 100, 200 or 400 μ M PFOS and subjected to DNA microarray analysis. Data were analysed using BMDExpress as described in the Materials and Methods section. With the applied criteria for the identification of regulated gene sets (Fisher's Exact Two Tail ≤ 0.1 , number of genes that passed all filters of a gene set ≤ 5 , and the percentage of genes of the gene set regulated ≥ 20 , see Materials and Methods section), 18 Reactome gene sets were upregulated ($\geq 60\%$ of the regulated genes upregulated) and 90 downregulated ($\geq 60\%$ of regulated genes downregulated). Figure 3 shows for each of the 108 regulated gene sets the percentage of genes that is affected by PFOS plotted against the median BMC value of the regulated genes. One can conclude that, in general, high micromolar concentrations of PFOS are required to cause effects and that differences in effect concentrations between gene sets are considered minor, based on the comparison of median BMC values. Gene sets related to cellular processes that were previously identified to be affected by PFOA, PFNA and PFOS (Louisse et al., 2020) are indicated in Figure 3. For the selection of genes to assess differences in potencies between different PFASs, genes related to these gene sets may be of particular interest, as these have been shown before to be regulated by at least three PFASs in HepaRG cells (Louisse et al., 2020). The expression data for the regulated genes for these selected gene sets are presented in Figure 4. It must be noted that another 11 Reactome gene sets were identified to be regulated using the applied selection criteria (Fisher's Exact Two Tail ≤ 0.1 , number of genes that passed all filters of a gene set ≤ 5 , and the percentage of genes regulated of the gene set ≥ 20 , see Materials and Methods section) that were not clearly up- or downregulated, i.e. 40-60% of the regulated genes were upregulated and the other 40-60% of the regulated genes were downregulated. More detailed information on the results of the BMDExpress analysis for all these 119 regulated gene sets (90 downregulated, 18 upregulated, 11 not clearly up- or downregulated) are provided in the Supplementary Materials.

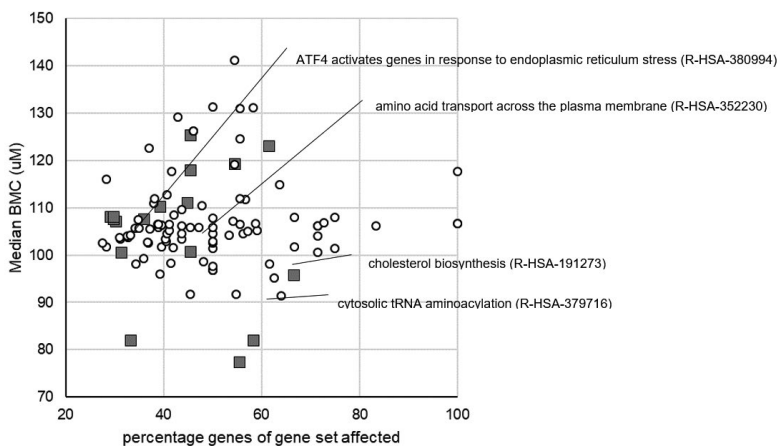
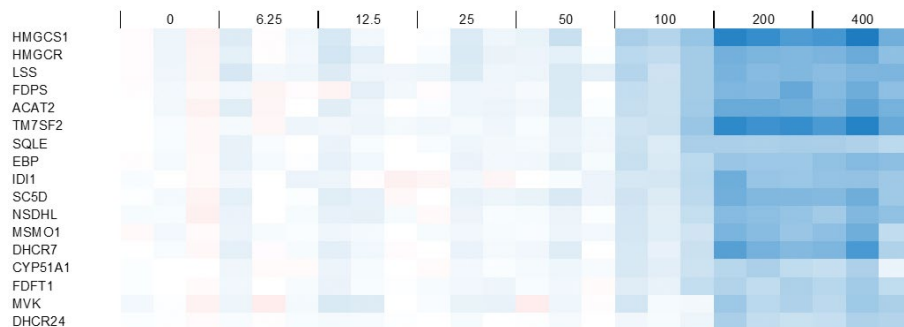
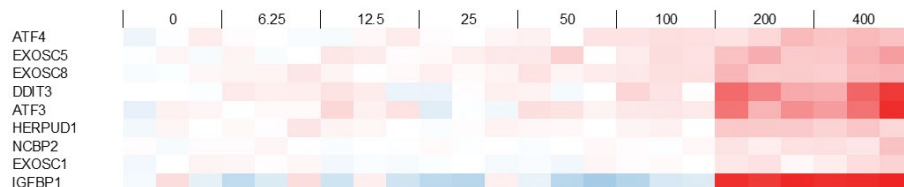


FIGURE 3 Overview of upregulated (grey squares) and downregulated (white circles) Reactome gene sets based on microarray data of PFOS-exposed HepaRG cells as analysed with BMDEExpress. Each gene set is positioned based on the percentage of affected genes of the gene set and the median BMC value of the gene set. Gene sets related to cellular processes that were previously found to be affected by PFOA, PFOS and PFNA in HepaRG cells (Louisse et al., 2020) are indicated. More information on the regulated genes of these gene sets is presented in Figure 4. More information on all affected gene sets is presented in the Supplementary Materials.

A: cholesterol biosynthesis (R-HSA-191273)



B: ATF4 activates genes in response to endoplasmic reticulum stress (R-HSA-380994)



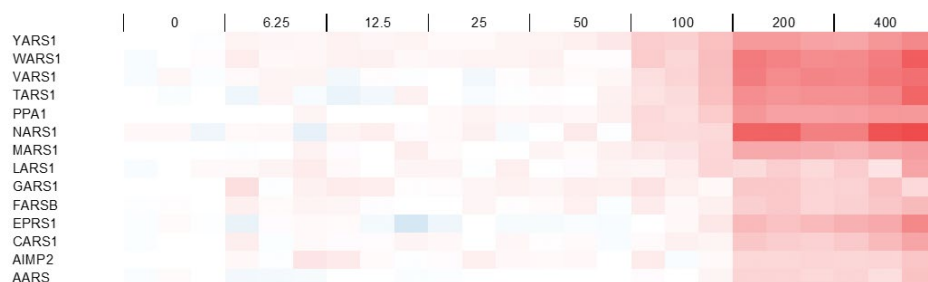
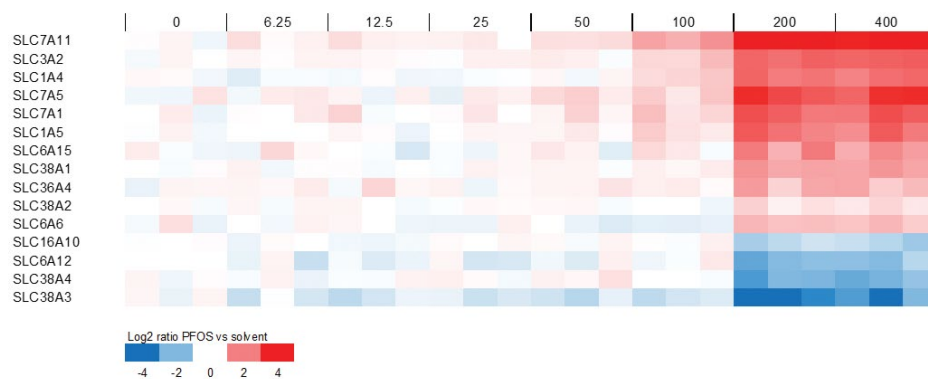
C: cytosolic tRNA aminoacylation (R-HSA-379716)**D: amino acid transport across the plasma membrane (R-HSA-352230)**

FIGURE 4 Concentration-dependent modulation of genes belonging to a selection of Reactome gene sets that are regulated in HepaRG cells upon PFOS exposure. Regulated gene sets presented here are A) 'cholesterol biosynthesis' (R-HSA-191273), B) 'ATF4 activates genes in response to endoplasmic reticulum stress' (R-HSA-380994), C) 'cytosolic tRNA aminoacylation' (R-HSA-379716), and D) 'amino acid transport across the plasma membrane' (R-HSA-352230). For each PFOS exposure (concentration given in μM above the plots), data from three independent samples (independent studies) are shown. Expression is normalized against average expression of the solvent control (0), showing the Log_2 ratio of expression upon PFOS treatment versus expression in the control.

As a next step, the concentration-response data were analysed to identify genes that were relatively sensitive to PFOS treatment. Besides those selected from gene sets as indicated in Figures 3 and 4, such genes may be good candidates to assess relative potency differences between PFASs, as also PFASs with a relatively low potency may induce a response. For this, genes were selected for which a BMC value was obtained and that showed at 100 μM at least a 2-fold change compared to the solvent control. Microarray expression data of these genes are presented in Figure 5. It is of interest to note that some of these are part of the selected gene sets presented in Figure 4, whereas many are not.

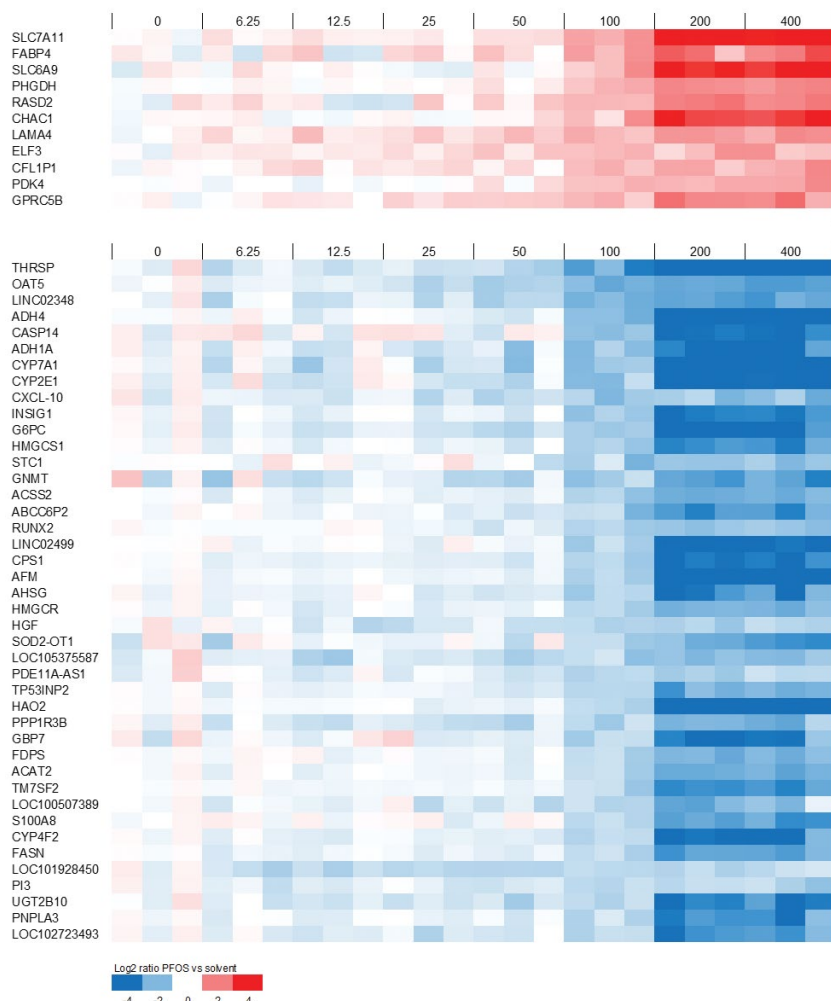


FIGURE 5 Concentration-dependent modulation of selected sensitive genes in HepaRG cells upon PFOS exposure. Data for genes are presented for which a BMC was obtained and that showed an average fold-change at 100 μM of at least 2 compared to the solvent control.

In addition, the microarray data for PPAR α response genes were examined, given that PPAR α is a cellular target often mentioned in relation with PFAS-induced (liver) toxicity. Figure 6 shows the microarray data for PFOS-exposed cells for genes that were previously shown to be regulated by both the PPAR α agonist GW7646 (Wigger et al., 2019) and by PFOS (Louisse et al., 2020) in HepaRG cells. It is of interest to note that some of these genes showed a non-typical concentration-response (*PLIN1*, *SLC27A2*, *CPT2*), i.e., showing a concentration-dependent increase in expression up to and including 100 μM , and a decrease at 200 and 400 μM (Figure 6).

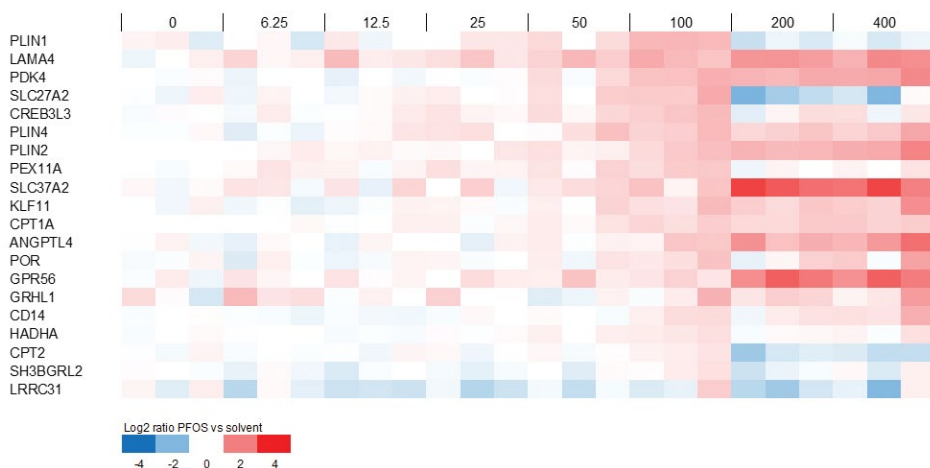


FIGURE 6 Concentration-dependent modulation of PPAR α -regulated genes by PFOS in HepaRG cells. Data for genes are presented that were previously shown to be induced by the PPAR α agonist GW7646 (Wigger et al., 2019) and by PFOS (Louisse et al., 2020) in HepaRG cells.

Selection of genes for RT-qPCR analysis to assess potency differences of 18 PFASs

Subsequently, the concentration-response microarray data presented in Figures 4 to 6 were analysed in more detail to select genes suitable for analysing the concentration-dependent effects of 18 PFASs (Figure 1) and to provide insights into potency differences. To that end, genes were selected that showed clear concentration-response curves for PFOS and covering diverse biological processes, as well as genes with relatively low BMC values. The ten genes selected include five genes that were upregulated and five that were downregulated upon PFOS treatment (see concentration-response data for microarray data in Supplementary Figure 6), and are shortly described below.

ATF4: Activating transcription factor 4 (ATF4) is a transcription factor activated upon endoplasmic reticulum stress and/or amino acid starvation (Harding et al., 2000), upregulating genes that play a role in cell recovery, adaptation to stress conditions, and restoration of cell homeostasis (Rozpedek et al., 2016). Member of the upregulated gene set ‘ATF4 activates genes in response to endoplasmic reticulum stress’ (Figure 4B).

SLC7A11: The *SLC7A11* gene codes for an amino acid transporter importing cysteine and exporting glutamate. It is one of the amino acid transporters that is upregulated by ATF4 upon amino acid starvation (Adams 2007; Shan et al., 2016; Krokowski et al., 2013; Han et al., 2013). Member of the upregulated gene set ‘Amino acid transport across the plasma membrane’ (Figure 4D). Highly upregulated even at relatively low PFOS concentrations (Figure 5).

YARS1: Tyrosyl-tRNA synthetase (YARS) is an aminoacyl-tRNA synthetase (ARS) catalyzing the aminoacylation of transfer RNA (tRNA) by its cognate amino acid tyrosine. It is one of the ARS genes that is upregulated by ATF4 upon amino acid starvation (Adams 2007; Shan et al., 2016; Krokowski et al., 2013; Han et al., 2013). Member of the upregulated gene set ‘Cytosolic tRNA aminoacylation’ (Figure 4C).

PDK4: pyruvate dehydrogenase (PDH) kinase 4 (PDK4) (Kwon and Harris, 2004) diminishes PDH activity, thereby reducing the conversion of pyruvate to acetyl-CoA. PDK4 expression has been reported to be upregulated upon fasting and/or a switching from glucose to fatty acids as an energy source (Zhang et al., 2014; Pettersen et al., 2019). PDK4 expression has been reported to be regulated by retinoic acid receptors (Kwon and Harris, 2004) and by PPAR α (e.g. Wigger et al., 2019). Thus, considered to be a PPAR α response gene (Figure 6). Highly upregulated even at relatively low PFOS concentrations (Figure 5).

ANGPTL4: angiopoietin-like protein 4 (ANGPTL4) is a member of the angiopoietin-related family, and has been reported to play a crucial role in regulating angiogenesis and glucolipid metabolism (Hato et al., 2008). Regulation of *ANGPTL4* gene expression has been reported to be mediated via PPARs and HIF-1 α (La Paglia et al., 2017). Thus, considered to be a PPAR α response gene (Figure 6).

LSS: The protein encoded by the *LSS* gene catalyzes the conversion of (S)-2,3 oxidosqualene to lanosterol in the cholesterol biosynthesis pathway (Wada et al., 2020). Member of the downregulated gene set 'Cholesterol biosynthesis' (Figure 4A).

HMGCR: The gene codes for HMG-CoA reductase, the rate-limiting enzyme in the cholesterol biosynthetic pathway, which catalyzes the conversion of HMG-CoA to mevalonic acid (Luskey and Stevens, 1985). Member of the downregulated gene set 'Cholesterol biosynthesis' (Figure 4A). Highly downregulated even at relatively low PFOS concentrations (Figure 5).

OAT5: Organic anion transporter 5 (OAT5) is an anion exchanger. Expression in the liver has been reported to be regulated via hepatocyte nuclear factor-1 α (HNF-1 α) (Klein et al., 2010). Highly downregulated even at relatively low PFOS concentrations (Figure 5).

THRSP: Thyroid hormone responsive (THRSP) is primarily a nuclear protein that plays a role in the regulation of lipid metabolism. Expression has been reported to be downregulated upon fasting (Kuemmerle and Kinlaw, 2011). Highly downregulated even at relatively low PFOS concentrations (Figure 5).

CXCL10: C-X-C motif chemokine ligand 10 (CXCL10) is a chemokine capable of stimulation of monocytes, natural killer cell and T-cell migration, regulation of T-cell and bone marrow progenitor maturation, modulation of adhesion molecule expression, and inhibition of angiogenesis (Neville et al., 1997). Highly downregulated even at relatively low PFOS concentrations (Figure 5).

Effects of 18 PFASs on expression of selected genes

In order to determine the relative potencies of the 18 PFASs, HepaRG cells were exposed for 24 h to increasing concentrations of the 18 PFASs shown in Figure 1. After exposure, RNA was collected and used for RT-qPCR analysis of the ten selected genes. Supplementary Figure 7 shows concentration-response data of these genes for PFOS, PFOA and HPFO-TA, the latter being the PFAS that was found to be most potent in the present study based on cell viability

and triglyceride accumulation as well as for gene expression modulation. Concentration-response data for the 18 PFASs for all genes are presented in the Supplementary Materials. These data were then used to perform PROAST dose-response analysis using parallel curve fitting to obtain *in vitro* RPFs related to PFAS-induced gene expression changes. For the selected genes, only for *OAT5* RPFs could be obtained for all tested PFASs (18 including PFOA). For *CXCL10* and *THRSP*, RPFs were obtained for 14 PFASs, for *LSS*, *HMGCR* and *ANGPTL4* for 13 PFASs, for *ATF4* and *PDK4* for 12 PFASs, and for *SLC7A11* and *YARS1* for 11 PFASs. Figure 7 presents the RPFs based on gene expression data for *PDK4*, *HMGCR*, *OAT5* and *THRSP*. RPFs for all genes are presented in Supplementary Figure 8.

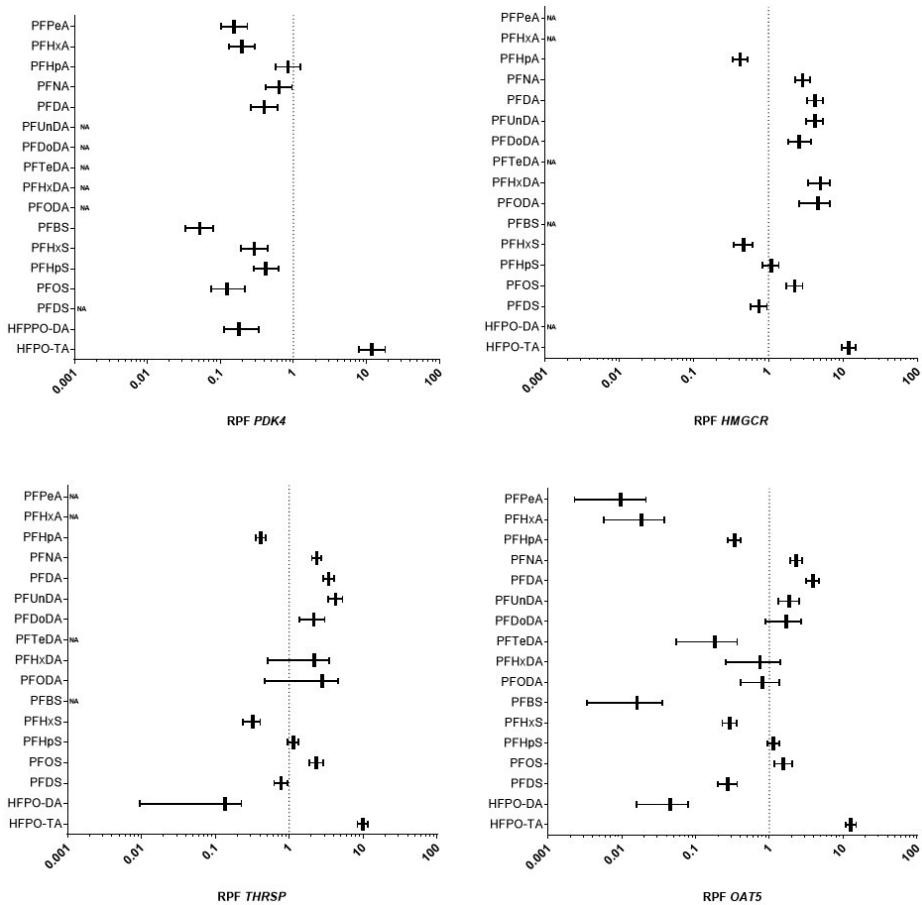


FIGURE 7 *In vitro* RPFs based on PROAST dose-response analysis of gene expression and AdipoRed data obtained from HepaRG cells exposed to various PFASs. RPFs are presented as vertical lines, with the 5% lower bound and 95% upper bound of the confidence interval as whiskers. PFOA was used as index chemical, i.e., has an RPF of 1 (dotted line). NA: not applicable, RPF could not be determined.

Gene-specific differences in RPF values were observed, although some general patterns could be identified. In general, RPFs obtained for the PPAR response genes *PDK4* and *ANGPTL4* were similar, but differed for many PFASs from RPFs obtained from the other

genes (Supplementary Figures 8 and 9). For *PK4* and *ANGPTL4*, all studied PFASs, except HFPO-TA, were less potent than PFOA. For the majority of the other genes (*ATF4*, *SLC7A11*, *YARS1*, *LSS*, *HMGCR*, *OAT5*, and *THRSP*), PFNA, PFDA, PFUnDA, PFDoDA, PFHpS, PFOS and HFPO-TA were consistently more potent than PFOA, and PFHpA, PFHxS and PFDS less potent than PFOA.

For PFNA, PFHxS, PFOS, and HFPO-TA *in vitro* RPFs were obtained for all readouts (AdipoRed data and gene expression data), whereas for other PFASs this was not the case (Supplementary Figure 9). Of these 4 PFASs, RPFs related to all *in vitro* readouts were smaller than 1 for PFHxS. RPF patterns of PFPeA, PFHxA, PFHpA, PFBS, PFDS and HFPO-DA were similar as for PFHxS, i.e., having in general RPFs lower than 1 (Supplementary Figure 9). HFPO-TA was the only PFAS tested for which all *in vitro* RPFs were found to be larger than 1. For PFNA, RPFs related to expression of PPAR response genes (*PK4* and *ANGPTL4*) were smaller than 1, whereas these were larger than 1 for the other readouts. For PFOS, potencies for the two PPAR response genes and *CXCL10* were lower than that of PFOA, whereas for other genes these were similar or slightly higher. PFHpS showed a similar RPF pattern as that of PFOS, as well as PFDoDA, although for the latter PFAS no RPFs could be determined for the PPAR response genes (Supplementary Figure 8). For the longer-chain PFASs PFTeDA, PFHxDA and PFODA, RPFs were only obtained for 2, 4 and 5 readouts, respectively (Supplementary Figure 6).

Comparison *in vitro* RPFs with internal *in vivo* RPFs

We then performed a Spearman correlation analysis using GraphPad Prism 9 to assess whether potency rankings obtained with different readouts are correlated and to assess whether certain *in vitro*-based potency rankings correlated with *in vivo* potency rankings based on reported external *in vivo* RPFs (Bil et al., 2021; 2022a) or internal *in vivo* RPFs (Bil et al., 2022b). The results of the correlation analysis point to a reasonable correlation between most of the *in vitro* RPFs, except for *ANGPTL4* and *PK4*, both PPAR target genes (Supplementary Figure 10). A reasonable correlation was found between the *in vitro* RPFs based on *CXCL* or *OAT5* expression and external *in vivo* RPFs (Supplementary Figure 10). Regarding internal RPFs, the best correlation was found for *HMGCR* expression, but it must be noted that this was only based on data for 4 PFASs. Figure 8 presents the external and internal *in vivo* RPFs in comparison with the *in vitro* RPFs for *OAT5* and *CXCL10* expression, and *OAT5* and *HMGCR* expression, respectively. Although *in vitro* RPFs based on changes in *OAT5* expression correlated well with external *in vivo* RPFs (Supplementary Figure 10), PFHxDA and PFODA are major outliers, showing *in vitro* RPFs > 1 and *in vivo* external RPFs < 0.1 (Figure 8A). The slightly better correlation between *in vitro* RPFs based on *CXCL10* expression and external *in vivo* RPFs (Supplementary Figure 10), may relate to the fact that for PFHxDA and PFODA, no *in vitro* RPFs could be obtained (Supplementary Figures 8 and 9), being therefore excluded from the correlation analysis. *In vitro* RPFs correlated to a lesser extent to internal RPFs than to external RPFs (Supplementary Figure 10), showing the best correlation for RPFs based on *HMGCR* expression (Figure 8B). As indicated above, this was

only based on data for 4 PFASs. When comparing *in vitro* RPFs based on *OAT5* with internal *in vivo* RPFs, it becomes clear that PFHxA and HFPO-DA are the main outliers, showing *in vitro* RPFs < 0.1 and *in vivo* RPFs > 1 (Figure 8B). All *in vitro* and *in vivo* RPFs used for these analyses are presented in an Excel-file that can be found in the Supplementary Materials.

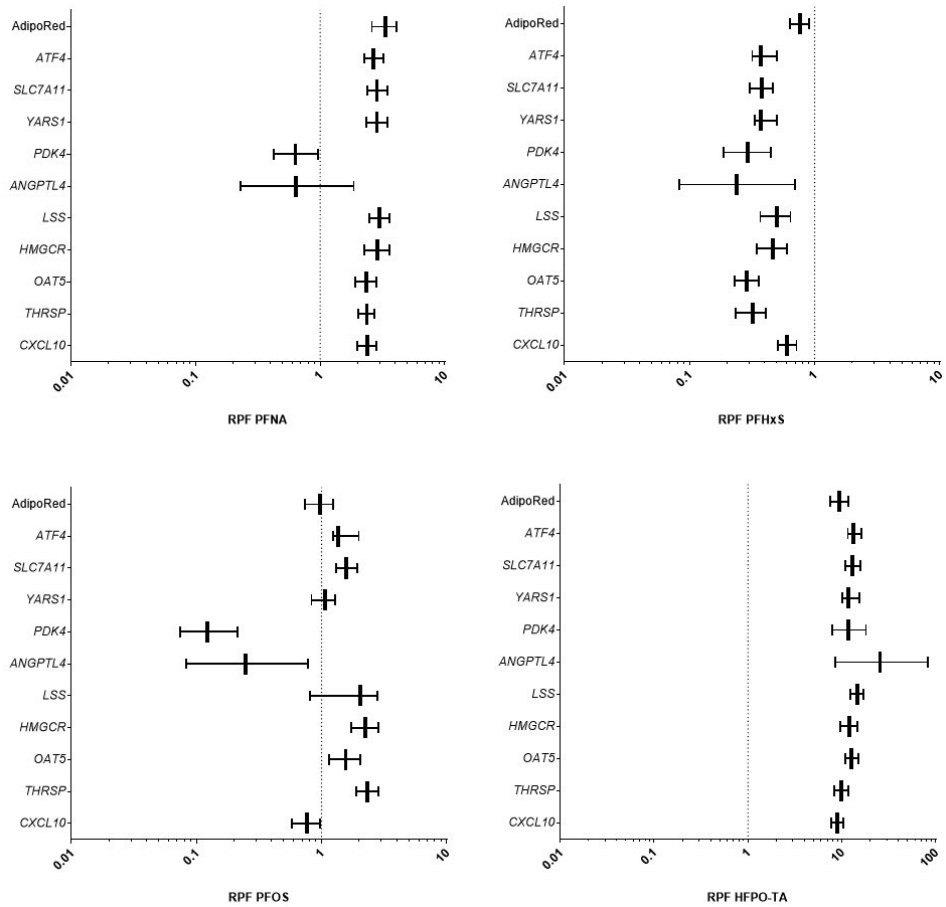


FIGURE 8 Comparison of A) *in vitro* RPFs based on *OAT5* or *CXCL10* gene expression data with reported external RPFs for PFAS-induced liver toxicity in rats and B) *in vitro* RPFs based on *OAT5* or *HMGCR* gene expression data with reported internal RPFs for PFAS-induced liver toxicity in rats.

Discussion

The present study evaluated the *in vitro* toxicity of 18 PFASs in human HepaRG liver cells, by studying the effects on cellular triglyceride accumulation and gene expression changes, and assessed whether these *in vitro* data can be used to obtain insight into potency differences regarding hepatotoxicity of PFASs. *In vitro* RPFs could be obtained for 8 PFASs (including index chemical PFOA) based on the triglyceride accumulation data, whereas for the selected genes *in vitro* RPFs could be obtained for 11-18 PFASs (including index

chemical PFOA). Only for PFNA, PFHxS, PFOS, and HFPO-TA *in vitro* RPFs were obtained for all readouts. For the readout *OAT5* expression, *in vitro* RPFs were obtained for all PFASs. *In vitro* RPFs were found to correlate in general well with each other (Spearman correlation) except for the PPAR target genes *ANGPTL4* and *PDK4*. Comparison of *in vitro* RPFs with reported *in vivo* RPFs in rats indicate that best correlations (Spearman correlation) were obtained for *in vitro* RPFs based on *OAT5* and *CXCL10* expression changes and external *in vivo* RPFs. HFPO-TA was found to be the most potent PFAS tested, being around 10-fold more potent than PFOA.

To assess effects of PFASs on triglyceride accumulation, we applied the AdipoRed assay. Interestingly, we found for the PFASs a more pronounced effects (and better concentration-dependent effects) upon a 24-h exposure than upon a 72-h exposure, in contrast to cyproconazole, for which a 72-h exposure was found to show most effects, and which was used as a model steatotic compound in an *in vitro* study on adverse outcome pathway (AOP)-driven analysis of liver steatosis (Luckert et al., 2018). This may relate to different modes of action underlying chemical-induced steatotic effects, as indicated by the available AOPs on this endpoint (Vinken, 2013; 2015; Mellor et al., 2016). It is of interest to note that upon a 72-h exposure, the AdipoRed signal returned in various exposure conditions for PFHxS and PFOS to the same levels as in the solvent control (Supplementary Figure 4). The toxicological meaning of that finding is not clear, but it may point to a possible cellular response to increased cellular triglyceride levels at earlier time points. Various studies have shown PFAS-induced increased hepatic triglyceride levels in experimental animals. PFOA, PFNA, PFHxS and PFOS have been shown to increase hepatic triglycerides in male mice (Bijland et al., 2011; Das et al., 2017; Huck et al., 2018; Hui et al., 2017; Wan et al., 2012). As indicated in recent Opinions of the EFSA CONTAM Panel, thorough knowledge of the mode of action underlying the development of hepatocellular steatosis in PFAS-treated rodents is missing (EFSA CONTAM Panel 2018; 2020).

Although we identified some genes that can be considered relevant readouts to screen PFASs for possible liver toxicity, one would like to mechanistically relate the gene expression change(s) to adverse effects to the liver. Ideally such gene expression changes would be a key event (KE) of an AOP related to liver toxicity. The AOP-wiki was consulted to assess whether *in vitro* effects measured in the present study are part of (putative) AOPs related to liver toxicity (<https://aopwiki.org/>; latest access: 28-12-2022). Of the *in vitro* readouts of the present study, triglyceride accumulation was found in the AOP-wiki as proposed key event related to liver steatosis. In light of the possible endoplasmic reticulum stress induced by the PFASs tested (indicated by activation of ATF4 signalling), it is of interest to note that the updated AOP on liver steatosis (from Mellor et al. (2016) based on earlier work of Vinken (2013; 2015) includes an induction of endoplasmic reticulum stress as a key event following increase of triglyceride accumulation. The selected genes are not present as key events in the AOPs present in the AOP-wiki, but it may still be possible that changes in expression of the genes can be related to certain KEs of relevance for liver toxicity, which would require

a more extensive assessment. In the Supplementary Materials, some more information on the possible link of gene expression changes of the selected genes assessed in the present study in relation to (liver) toxicity is provided.

When comparing RPFs obtained for the different readouts, it was shown that for most readouts good correlations were found. Correlations were rather poor, though, for the PPAR response genes *PDK4* or *ANGPTL4* and the other readouts. It must be noted that for the 8 genes for which the RPFs correlate well, still considerable differences in RPFs are found. It is difficult to select one gene that would provide the best data on relative potencies, and it can be expected that the study set-up, including the choice of exposure time (24 h in the present study) will affect the RPFs obtained. The data should therefore rather be used to obtain a general indication of whether a certain PFAS is expected to be a relatively potent hepatotoxicant or whether it will be of less concern related to its hepatotoxic effects. As we obtained RPFs for all PFASs based on changes in *OAT5* expression, the comparison of *OAT5*-based RPFs with available external and internal RPFs reported in the literature is of specific interest (Figure 8). From that comparison, *in vitro* RPFs were in general good in line with RPFs based on *in vivo* studies, with most striking exceptions for PFHxDA and PFODA for external RPFs and PFHxA and HFPO-DA for internal RPFs. The discrepancy for PFHxDA and PFODA regarding external RPFs (high *in vitro* RPFs vs low external *in vivo* RPFs) may relate to a relatively low systemic uptake of these large molecules upon oral exposure. Relative differences in systemic exposure is accounted for by using internal RPFs, for which kinetic models were applied to estimate internal exposure (Bil et al., 2022b). Internal RPFs are, however, not available for PFHxDA and PFODA. The discrepancy for PFHxA and HFPO-DA regarding internal RPFs (low *in vitro* RPFs vs high internal *in vivo* RPFs) is more difficult to explain. It is of interest to further investigate these *in vitro*-*in vivo* differences in future studies. They may, amongst others, relate to possible species differences in PFAS-induced effects on the liver (Fragki et al., 2021). Of course, also differences in exposure duration or other differences between the *in vitro* and *in vivo* situation may play a role. Studies that assess possible species differences in human and rat liver cells *in vitro* may shed more light on this. It shall be noted here that the evaluation of the predictive capability of *in vitro* assays should not necessarily be based on a comparison to animal *in vivo* data (van der Zalm et al., 2022). Ideally, one would like to compare the *in vitro* HepaRG data with effect data in humans. Epidemiological evidence has correlated PFOS and PFOA exposure to a small elevation in serum levels of the hepatic enzyme ALT (alanine transferase), a biomarker for liver damage (Gallo et al., 2012). As indicated before, whether that limited increase in ALT is causal and reflects serious liver damage is questionable. Also, data on other PFASs are scarce or lacking, making these *in vitro* human vs *in vivo* human comparisons cumbersome. It would be interesting to compare the present *in vitro* potency ranking from human HepaRG cells with similar data obtained from rodent hepatic cells, which may provide possible insights into species-dependent differences in toxicodynamics. To obtain *in vivo* relative potencies based on *in vitro* toxicity data, information on toxicokinetics should be included in the assessment. In that regard, we have been working on the quantitative *in*

vitro to *in vivo* extrapolation (QIVIVE) of the toxicity data of PFOA, PFNA, PFHxS and PFOS, translating cell-associated PFAS levels to oral equivalent doses using physiologically based kinetic (PBK) modelling, providing information that will be of use in the assessment of relative potencies of PFASs in humans (Fragki et al., 2023).

Although the main aim of this study was to select *in vitro* readouts related to liver toxicity that can be used to determine *in vitro* potency differences for PFASs, the obtained concentration-response microarray data may be of use to increase our insights into mechanisms related to the liver toxicity of PFASs in humans. The BMDExpress analysis indicated 18 gene sets to be upregulated and 90 gene sets to be downregulated. Many of the regulated gene sets are related to cholesterol biosynthesis and lipid metabolism as also indicated by Rowan-Carroll et al. (2021), who assessed the concentration- and time-dependent effects of PFOA, PFBS, PFOS and PFDS on gene expression in human primary hepatocyte spheroids. In a later study, this work was extended to include more PFASs and to estimate relative potencies (Reardon et al., 2021), testing carboxylates (PCFAs), sulfonates (PFSAs) and fluorotelomers and sulfonamides. In general, PCFAs and PFSAs caused gene expression changes with increased potency with increasing carbon chain-length (Reardon et al., 2021), being in line with findings for some of the genes in the present study. In general, effective concentrations in the present study are for most genes in the high micromolar range, which are not expected to be reached *in vivo* in relevant exposure scenarios. Rowan-Carroll et al. (2021) and Reardon et al. (2021) found effects at low micromolar concentrations, which may relate to the difference in test system used (2D culture HepaRG cells in present study vs. 3D primary hepatocyte model) as well as difference in exposure duration (24 h vs. up to 14 days in the study of Rowan-Carroll et al. (2021) and up to 10 days in the study of Reardon et al. (2021). We recently showed that HepaRG cells cultured in an organ-on-a-chip device can be cultured for at least 8 weeks, allowing chronic exposure studies (Duivenvoorde et al., 2021). Such long-term studies may provide more insights into effects at more relevant human effect concentrations, but given the low throughput, such models are less suitable for screening a large number of PFASs.

Of the PFASs tested in the present study, HFPO-TA was shown to be the most potent. Sheng et al. (2018) assessed the effects of HPFO-TA in mice and concluded it to be a potent hepatotoxicant, causing hepatomegaly, necrosis, and increase in serum ALT, as well as a dose-dependent decrease in total cholesterol and triglycerides in the liver, and they concluded it to be more potent than PFOA, which was tested in an earlier study from the same group (Yan et al., 2014). In 2017, Pan and coworkers were the first to report on the environmental occurrence (Xiaoqing River in China), bioaccumulation (in carp) and presence in human serum of HFPO-TA, concluding that the emerging usage of HFPO-TA in the fluoropolymer manufacturing industry raises concerns about its toxicity and potential health risks to aquatic organisms and humans (Pan et al., 2017). In a more recent study, HFPO-TA was measured in the serum of residents living near a fluorochemical plant in Shandong, China, showing median serum concentrations of ~2 ng/mL (low pM range),

almost 100 times lower than the median PFOA serum concentrations of these individuals (Yao et al., 2020). Based on our *in vitro* studies, which seems to be in line with the limited *in vivo* evidence (Sheng et al., 2018), HFPO-TA is a rather toxic PFAS, suggesting that its production and/or application should be discouraged and that human exposure should be prevented.

Altogether, the present study shows an approach to select *in vitro* gene expression readouts in HepaRG cells that can be used to obtain information on relative potencies of PFASs related to liver toxicity *in vitro*. It may be concluded that the HepaRG model may provide relevant data to provide insight into which PFASs are relevant regarding their hepatotoxic effects and that it can be applied as a screening tool to prioritize other PFASs for further hazard and risk assessment.

Acknowledgements

This work was funded by the Dutch Ministry of Agriculture, Nature and Food Quality (project KB-37-002-009/010) and by the European Unions' Horizon 2020 Research and Innovation Programme under grant agreement No 733032 HBM4EU. The authors would like to thank Bas van Dijk and Liz Leenders for their help with the LC-MS analyses.

Conflict of interest statement

The authors declare that they have no conflict of interest.

References

- Adams CM (2007). Role of the transcription factor ATF4 in the anabolic actions of insulin and the anti-anabolic actions of glucocorticoids. *J Biol Chem.* 282(23): 16744-16753.
- ATSDR (2021). Toxicological Profile for Perfluoroalkyls. Version May 2021. <https://www.atsdr.cdc.gov/toxprofiles/tp200.pdf>.
- Bijland S, Rensen PC, Pieterman EJ, Maas AC, van der Hoorn JW, van Erk MJ, Havekes LM, Willems van Dijk K, Chang SC, Ehresman DJ, Butenhoff JL, Princen HM (2011). Perfluoroalkyl sulfonates cause alkyl chain length-dependent hepatic steatosis and hypolipidemia mainly by impairing lipoprotein production in APOE*3-Leiden CETP mice. *Toxicological Sciences*, 123: 290-303.
- Bil W, Zeilmaker M, Fragki S, Lijzen J, Verbruggen E, Bokkers B (2021). Risk Assessment of Per- and Polyfluoroalkyl Substance Mixtures: A Relative Potency Factor Approach. *Environ Toxicol Chem.* 40(3): 859-870.
- Bil W, Zeilmaker M, Fragki S, Lijzen J, Verbruggen E, Bokkers B (2022a). Response to Letter to the Editor on Bil et al. 2021 "Risk Assessment of Per- and Polyfluoroalkyl Substance Mixtures: A Relative Potency Factor Approach". *Environ Toxicol Chem.* 41(1): 13-18.
- Bil W, Zeilmaker MJ, Bokkers BGH (2022b). Internal Relative Potency Factors for the Risk Assessment of Mixtures of Per- and Polyfluoroalkyl Substances (PFAS) in Human Biomonitoring. *Environ Health Perspect.* 130(7):77005.
- Bolstad BM, Irizarry RA, Astrand M, Speed TP (2003). A comparison of normalization methods for high density oligonucleotide array data based on variance and bias. *Bioinformatics.* 19: 185-193.
- Bosgra S, van der Voet H, Boon PE, Slob W (2009). An integrated probabilistic framework for cumulative risk assessment of common mechanism chemicals in food: an example with organophosphorus pesticides. *Regul Toxicol Pharmacol.* 54(2): 124-133.
- Chang Y, Huynh CTT, Bastin KM, Rivera BN, Siddens LK, Tilton SC (2020). Classifying polycyclic aromatic hydrocarbons by carcinogenic potency using in vivo biosignatures. *Toxicol In Vitro.* 69: 104991.
- Dai M, Wang P, Boyd AD, Kostov G, Athey B, Jones EG, Bunnay WE, Myers RM, Speed TP, Akil H, Watson SJ, Meng F (2005). Evolving gene/transcript definitions significantly alter the interpretation of GeneChip data. *Nucleic Acids Res.* 33: e175.
- Das KP, Wood CR, Lin MT, Starkov AA, Lau C, Wallace KB, Corton JC, Abbott BD (2017). Perfluoroalkyl acids-induced liver steatosis: Effects on genes controlling lipid homeostasis. *Toxicology.* 378: 37-52.
- Duivenvoorde LPM, Louise J, Pinckaers NET, Nguyen T, van der Zande M (2021). Comparison of gene expression and biotransformation activity of HepaRG cells under static and dynamic culture conditions. *Sci Rep.* 11(1): 10327.
- EFSA CONTAM Panel (2018). Scientific Opinion. Risk to human health related to the presence of perfluorooctane sulfonic acid and perfluorooctanoic acid in food. *EFSA Journal* 16 (12):5194.
- EFSA CONTAM Panel (2020). Scientific Opinion. Risk to human health related to the presence of perfluoroalkyl substances in food. *EFSA Journal* 18 (9):6223.
- EU (2019). Regulation (EU) 2019/1021 of the European Parliament and of the Council of 20 June 2019 on persistent organic pollutants (recast). *Off J EU* 25.6.2019 L 169/45.
- EU (2020). Commission Delegated Regulation (EU) 2020/784 of 8 April 2020 amending Annex I to Regulation (EU) 2019/1021 of the European Parliament and of the Council as regards the listing of perfluorooctanoic acid (PFOA), its salts and PFOA-related compounds. *Off J EU* 15.6.2020 L 188 I/1.
- Fragki S, Dirven H, Fletcher T, Grasl-Kraupp B, Bjerve Gützkow K, Hoogenboom R, Kersten S, Lindeman B, Louise J, Peijnenburg A, Piersma AH, Princen HMG, Uhl M, Westerhout J, Zeilmaker MJ, Luijten M (2021). Systemic PFOS and PFOA exposure and disturbed lipid homeostasis in humans: what do we know and what not? *Crit Rev Toxicol.* 51(2): 141-164.
- Fragki S, Louise J, Bokkers B, Luijten M, Peijnenburg A, Rijkers D, Piersma A, Zeilmaker M (2023). New Approach Methodologies: A Quantitative *In Vitro* to *In Vivo* Extrapolation case study with PFASs. *Food Chem Toxicol.* 172: 113559.
- Gallo V, Leonardi G, Genser B, Lopez-Espinosa MJ, Frisbee SJ, Karlsson L, Ducatman AM, Fletcher T (2012). Serum perfluorooctanoate (PFOA) and perfluorooctane sulfonate (PFOS) concentrations and liver function biomarkers in a population with elevated PFOA exposure. *Environ Health Perspect.* 120(5): 655-660.

- Han J, Back SH, Hur J, Lin YH, Gildersleeve R, Shan J, Yuan CL, Krokowski D, Wang S, Hatzoglou M, Kilberg MS, Sartor MA, Kaufman RJ (2013). ER-stress-induced transcriptional regulation increases protein synthesis leading to cell death. *Nat Cell Biol.* 15: 481-490.
- Harding HP, Novoa I, Zhang Y, Zeng H, Wek R, Schapira M, Ron D (2000). Regulated translation initiation controls stress-induced gene expression in mammalian cells. *Mol Cell.* 6(5): 1099-1108.
- Hato T, Tabata M, Oike Y (2008). The role of angiopoietin-like proteins in angiogenesis and metabolism. *Trends Cardiovasc Med.* 18(1): 6-14.
- Huck I, Beggs K, Apte U (2018). Paradoxical protective effect of perfluorooctanesulfonic acid against high-fat diet-induced hepatic steatosis in mice. *International Journal of Toxicology.* 37: 383-392.
- Hui Z, Li R, Chen L (2017). The impact of exposure to environmental contaminant on hepatocellular lipid metabolism. *Gene* 622: 67-71.
- Irizarry RA, Bolstad BM, Collin F, Cope LM, Hobbs B, Speed TP (2003). Summaries of Affymetrix GeneChip probe level data. *Nucleic Acids Res.* 31: e15.
- Klein K, Jüngst C, Mwinyi J, Stieger B, Krempler F, Patsch W, Eloranta JJ, Kullak-Ublick GA (2010). The human organic anion transporter genes OAT5 and OAT7 are transactivated by hepatocyte nuclear factor-1 α (HNF-1 α). *Mol Pharmacol.* 78(6): 1079-1087.
- Krokowski D, Han J, Saikia M, Majumder M, Yuan CL, Guan BJ, Bevilacqua E, Bussolati O, Bröer S, Arvan P, Tchórzewski M, Snider MD, Puchowicz M, Croniger CM, Kimball SR, Pan T, Koromilas AE, Kaufman RJ, Hatzoglou M (2013). A self-defeating anabolic program leads to β -cell apoptosis in endoplasmic reticulum stress-induced diabetes via regulation of amino acid flux. *J Biol Chem.* 288: 17202-17213.
- Kuemmerle NB, Kinlaw WB (2011). THRSP (thyroid hormone responsive). *Atlas Genet Cytogenet Oncol Haematol.* 15(6): 480-482.
- Kwon HS, Harris RA (2004). Mechanisms responsible for regulation of pyruvate dehydrogenase kinase 4 gene expression. *Adv Enzyme Regul.* 44: 109-121.
- La Paglia L, Listi A, Caruso S, Amodeo V, Passiglia F, Bazan V, Fanale D (2017). Potential Role of ANGPTL4 in the Cross Talk between Metabolism and Cancer through PPAR Signaling Pathway. *PPAR Res.* 2017: 8187235.
- Louisse J, Rijkers D, Stoop G, Janssen A, Staats M, Hoogenboom R, Kersten S, Peijnenburg A (2020). Perfluorooctanoic acid (PFOA), perfluorooctane sulfonic acid (PFOS), and perfluorononanoic acid (PFNA) increase triglyceride levels and decrease cholesterogenic gene expression in human HepaRG liver cells. *Arch Toxicol.* 94(9): 3137-3155.
- Luckert C, Braeuning A, de Sousa G, Durinck S, Katsanou ES, Konstantinidou P, Machera K, Milani ES, Peijnenburg AACM, Rahmani R, Rajkovic A, Rijkers D, Spyropoulou A, Stamou M, Stoop G, Sturla S, Wollscheid B, Zucchini-Pascal N, Lampen A (2018). Adverse Outcome Pathway-Driven Analysis of Liver Steatosis *in Vitro*: A Case Study with Cyproconazole. *Chem Res Toxicol.* 31(8): 784-798.
- Luskey KL, Stevens B (1985). Human 3-hydroxy-3-methylglutaryl coenzyme A reductase. Conserved domains responsible for catalytic activity and sterol-regulated degradation. *J Biol Chem.* 260(18): 10271-10277.
- Mellor CL, Steinmetz FP, Cronin MT (2016). The identification of nuclear receptors associated with hepatic steatosis to develop and extend adverse outcome pathways. *Crit Rev Toxicol.* 46(2): 138-52.
- National Institute for Public Health and the Environment (2018). PROAST. Bilthoven, The Netherlands. [02-11-2018]. Available from: <https://www.rivm.nl/proast>
- Neville LF, Mathiak G, Bagasra O (1997). The immunobiology of interferon-gamma inducible protein 10 kD (IP-10): a novel, pleiotropic member of the C-X-C chemokine superfamily. *Cytokine Growth Factor Rev.* 8(3): 207-219.
- NTP (National Toxicology Program), 2019a. NTP technical report on the toxicity studies of perfluoroalkyl carboxylates (perfluorohexanoic acid, perfluorooctanoic acid, perfluorononanoic acid, and perfluorodecanoic acid) administered by gavage to sprague dawley (Hsd:Sprague Dawley SD) rats. NTP TOX 97. Research Triangle Park, North Carolina, USA. Available online: <http://ntp.niehs.nih.gov>
- NTP (National Toxicology Program), 2019b. NTP technical report on the toxicity studies of perfluoroalkyl sulfonates (perfluorobutane sulfonic acid, perfluorohexane sulfonate potassium salt, and perfluorooctane sulfonic acid) administered by gavage to sprague dawley (Hsd:Sprague Dawley SD) rats. NTP TOX 96. Research Triangle Park, North Carolina, USA. Available online: <http://ntp.niehs.nih.gov>
- OECD (2021). Reconciling Terminology of the Universe of Per- and Polyfluoroalkyl Substances: Recommendations and Practical Guidance. Series on Risk Management No.61. ENV/CBC/MONO(2021)25.

- Pan Y, Zhang H, Cui Q, Sheng N, Yeung LWY, Guo Y, Sun Y, Dai J (2017). First Report on the Occurrence and Bioaccumulation of Hexafluoropropylene Oxide Trimer Acid: An Emerging Concern. *Environ Sci Technol.* 51(17): 9553-9560.
- Petersen IK, Tusubira D, Ashrafi H, Dyrstad SE, Hansen L, Liu XZ, Nilsson LIH, Lovsletten NG, Berge K, Wergedahl H, Bjørndal B, Fluge Ø, Bruland O, Rustan AC, Halberg N, Røslund GV, Berge RK, Tronstad KJ (2019). Upregulated PDK4 expression is a sensitive marker of increased fatty acid oxidation. *Mitochondrion.* 49: 97-110.
- Phillips JR, Svoboda DL, Tandon A, Patel S, Sedykh A, Mav D, Kuo B, Yauk CL, Yang L, Thomas RS, Gift JS, Davis JA, Olszyk L, Merrick BA, Paules RS, Parham F, Saddler T, Shah RR, Auerbach SS (2019). BMDExpress 2: enhanced transcriptomic dose-response analysis workflow. *Bioinformatics.* 35(10): 1780-1782.
- Punt A, Pinckaers N, Peijnenburg A, Lousse J. Development of a Web-Based Toolbox to Support Quantitative In-Vitro-to-In-Vivo Extrapolations (QVIVE) within Nonanimal Testing Strategies. *Chem Res Toxicol.* 34(2): 460-472.
- Reardon AJF, Rowan-Carroll A, Ferguson SS, Leingartner K, Gagne R, Kuo B, Williams A, Lorusso L, Bourdon-Lacombe JA, Carrier R, Moffat I, Yauk CL, Atlas E (2021). Potency Ranking of Per- and Polyfluoroalkyl Substances Using High-Throughput Transcriptomic Analysis of Human Liver Spheroids. *Toxicol Sci.* 184(1):154-169.
- Rowan-Carroll A, Reardon A, Leingartner K, Gagné R, Williams A, Meier MJ, Kuo B, Bourdon-Lacombe J, Moffat I, Carrier R, Nong A, Lorusso L, Ferguson SS, Atlas E, Yauk C (2021). High-Throughput Transcriptomic Analysis of Human Primary Hepatocyte Spheroids Exposed to Per- and Polyfluoroalkyl Substances as a Platform for Relative Potency Characterization. *Toxicol Sci.* 181(2): 199-214.
- Rozpedek W, Pytel D, Mucha B, Leszczynska H, Diehl JA, Majsterek I (2016). The Role of the PERK/eIF2 α /ATF4/CHOP Signaling Pathway in Tumor Progression During Endoplasmic Reticulum Stress. *Curr Mol Med.* 16: 533-544.
- Shan J, Zhang F, Sharkey J, Tang TA, Örd T, Kilberg MS (2016). The C/ebp-Atf response element (CARE) location reveals two distinct Atf4-dependent, elongation-mediated mechanisms for transcriptional induction of aminoacyl-tRNA synthetase genes in response to amino acid limitation. *Nucleic Acids Res.* 44: 9719-9732.
- Sheng N, Pan Y, Guo Y, Sun Y, Dai J (2018). Hepatotoxic Effects of Hexafluoropropylene Oxide Trimer Acid (HFPO-TA), A Novel Perfluorooctanoic Acid (PFOA) Alternative, on Mice. *Environ Sci Technol.* 52(14): 8005-8015.
- UNEP (2009). Recommendations of the Persistent Organic Pollutants Review Committee of the Stockholm Convention to amend Annexes A, B or C of the Convention. *UNEP/POPS/COP.4/17.*
- van den Brand AD, Bokkers BGH, Te Biesebeek JD, Mengelers MJB (2022). Combined Exposure to Multiple Mycotoxins: An Example of Using a Tiered Approach in a Mixture Risk Assessment. *Toxins (Basel).* 14(5): 303.
- van der Ven LTM, van Ommeren P, Zwart EP, Gremmer ER, Hodemaekers HM, Heusinkveld HJ, van Klaveren JD, Rorije E (2022). Dose Addition in the Induction of Craniofacial Malformations in Zebrafish Embryos Exposed to a Complex Mixture of Food-Relevant Chemicals with Dissimilar Modes of Action. *Environ Health Perspect.* 130(4): 47003.
- van der Zalm AJ, Barroso J, Browne P, Casey W, Gordon J, Henry TR, Kleinstreuer NC, Lowit AB, Perron M, Clippinger AJ (2022). A framework for establishing scientific confidence in new approach methodologies. *Arch Toxicol.* Online ahead of print.
- Vinken M (2013). The adverse outcome pathway concept: a pragmatic tool in toxicology. *Toxicology* 312: 158-165.
- Vinken M (2015). Adverse outcome pathways and drug-induced liver injury. *Chem Res Toxicol* 28: 1391-1397.
- Wada Y, Kikuchi A, Kaga A, Shimizu N, Ito J, Onuma R, Fujishima F, Totsune E, Sato R, Niihori T, Shirota M, Funayama R, Sato K, Nakazawa T, Nakayama K, Aoki Y, Aiba S, Nakagawa K, Kure S (2020). Metabolic and pathologic profiles of human LSS deficiency recapitulated in mice. *PLoS Genet.* 16(2): e1008628.
- Wang Z, DeWitt JC, Higgins CP, Cousins IT (2017). A Never-Ending Story of Per- and Polyfluoroalkyl Substances (PFASs)? *Environ Sci Technol.* 51: 2508-2518.
- Wigger L, Casals-Casas C, Baruchet M, Trang KB, Pradervand A, Naldi A, Desvergne B (2019). System analysis of cross-talk between nuclear receptors reveals an opposite regulation of the cell cycle by LXR and FXR in human HepaRG liver cells. *PLoS One.* 14: e0220894.
- Wu G, Haw R (2017). Functional Interaction Network Construction and Analysis for Disease Discovery. *Methods Mol Biol.* 1558: 235-253.

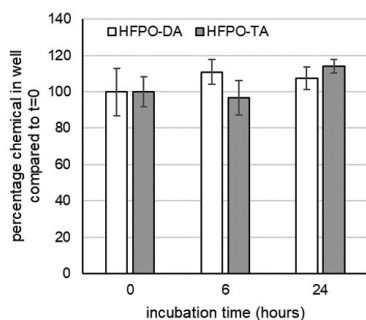
- Yan S, Wang J, Zhang W, Dai J (2014). Circulating microRNA profiles altered in mice after 28 d exposure to perfluorooctanoic acid. *Toxicol Lett.* 224(1): 24-31.
- Yang L, Allen BC, Thomas RS (2007). BMDExpress: a software tool for the benchmark dose analyses of genomic data. *BMC Genomics.* 8: 387.
- Yao J, Pan Y, Sheng N, Su Z, Guo Y, Wang J, Dai J (2020). Novel Perfluoroalkyl Ether Carboxylic Acids (PFECAs) and Sulfonic Acids (PFESAs): Occurrence and Association with Serum Biochemical Parameters in Residents Living Near a Fluorochemical Plant in China. *Environ Sci Technol.* 54(21): 13389-13398.
- Zhang S, Hulver MW, McMillan RP, Cline MA, Gilbert ER (2014). The pivotal role of pyruvate dehydrogenase kinases in metabolic flexibility. *Nutr Metab (Lond).* 11(1): 10.
- Zhang C, McElroy AC, Liberatore HK, Alexander NLM, Knappe DRU (2022). Stability of Per- and Polyfluoroalkyl Substances in Solvents Relevant to Environmental and Toxicological Analysis. *Environ Sci Technol.* 56(10): 6103-6112.

Supplementary Material

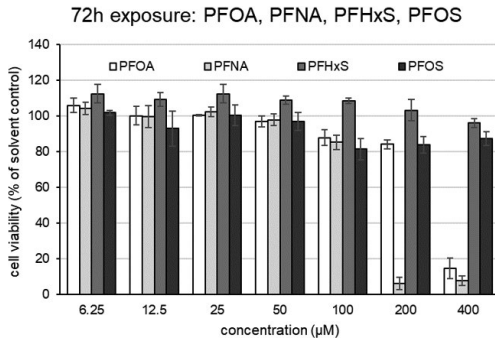
SUPPLEMENTARY TABLE 1 Suppliers, purity, catalog numbers, CAS numbers and maximum concentrations of PFASs tested in the present study.

PFAS	Full name	Supplier	Purity	Catalog number	CAS number	Highest tested concentration (µM)
PFPeA	perfluoropentanoic acid	Sigma-Aldrich	97%	396575-5ML	2706-90-3	400
PFHxA	perfluorohexanoic acid	Synquest laboratories	97%	2121-3-39	307-24-4	400
PFHpA	perfluoroheptanoic acid	Sigma-Aldrich	99%	342041-5G	375-85-9	400
PFOA	perfluorooctanoic acid	Sigma-Aldrich	95%	171468-5G	335-67-1	400
PFNA	perfluorononanoic acid	Sigma-Aldrich	99%	91977-50MG	375-95-1	400
PFDA	perfluorodecanoic acid	Sigma-Aldrich	98%	177741-5G	335-76-2	400
PFUnDA	perfluoroundecanoic acid	Sigma-Aldrich	95%	446777-5G	2058-94-8	400
PFDoDA	perfluorododecanoic acid	Sigma-Aldrich	95%	406449-1G	307-55-1	100
PFTeDA	perfluorotetradecanoic acid	Sigma-Aldrich	96%	446785-5G	376-06-7	100
PFHxDA	perfluorohexadecanoic acid	abcr GmbH	95%	AB 108458	67905-19-5	25
PFODA	perfluorooctadecanoic acid	abcr GmbH	95%	AB 108482	16517-11-6	25
PFBS	perfluorobutane sulfonate	Sigma-Aldrich	97%	562629-5G	375-73-5	400
PFHxS	perfluorohexane sulfonate	Synquest laboratories	95%	6164-3-2T	355-46-4	400
PFHpS	perfluoroheptane sulfonate	Synquest laboratories	99%	6164-3-2S	375-92-8	400
PFOS	perfluorooctane sulfonate	Synquest laboratories	97%	6164-3-08	1763-23-1	400
PFDS	perfluorodecane sulfonate	Toronto Research Chemicals	*	P286540	335-77-3	200
HFPO-DA (GenX)	hexafluoropropylene oxide dimer acid	Synquest laboratories	97%	2121-3-13	13252-13-6	400
HFPO-TA	hexafluoropropylene oxide trimer acid	abcr GmbH	97%	164194-5G	13252-14-7	400

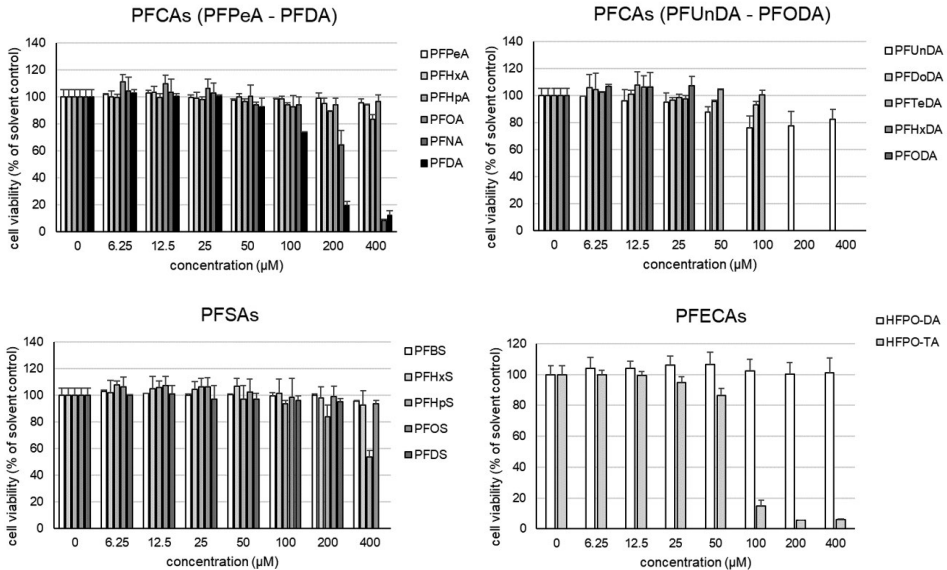
* Information on purity not provided by supplier.



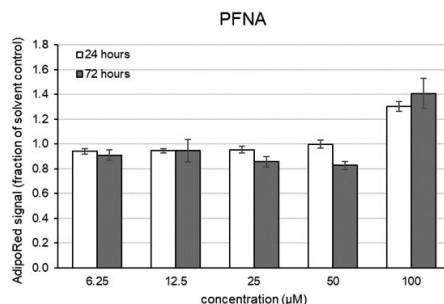
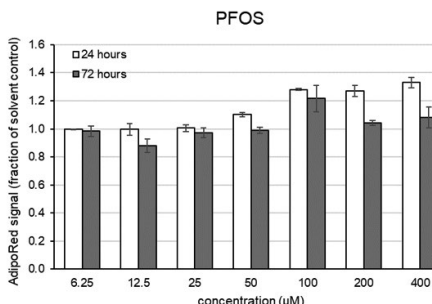
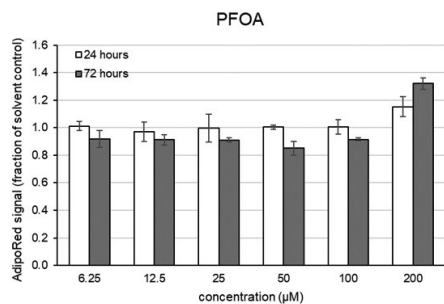
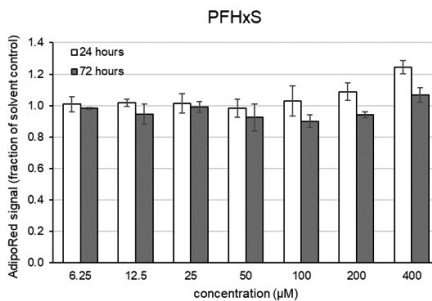
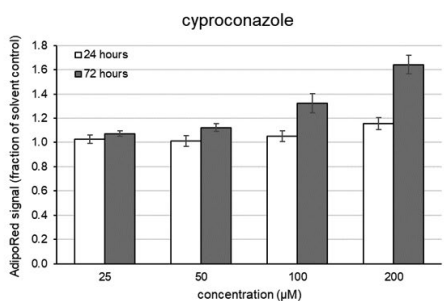
SUPPLEMENTARY FIGURE 1 HFPO-DA and HFPO-TA levels in culture medium upon 0, 6 or 24 hour incubation.



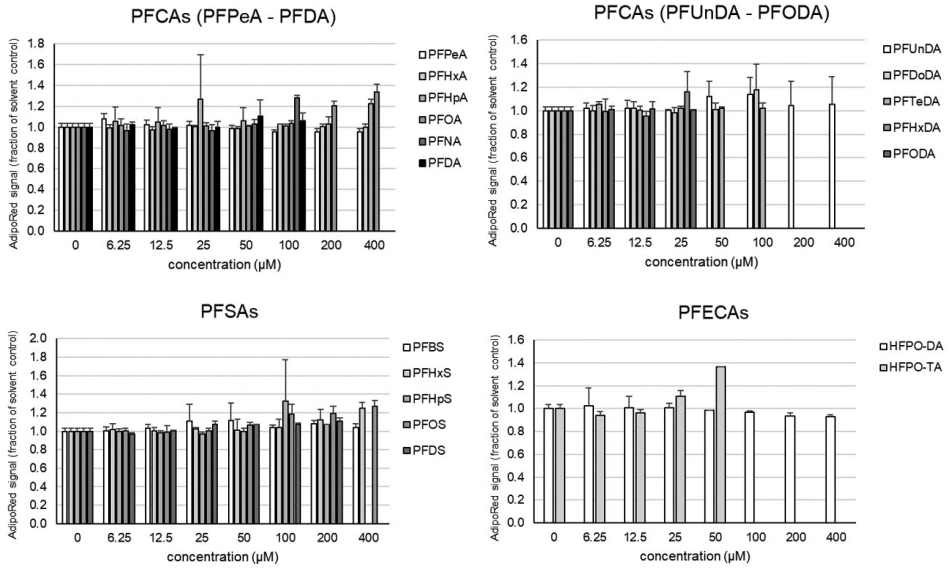
SUPPLEMENTARY FIGURE 2 Effect of 72-h exposure to PFOA, PFNA, PFHxS or PFOS on viability of HepaRG cells as determined with the WST-1 assay and expressed as percentage of the solvent control (0.5% DMSO). Data are presented as mean \pm SD of three independent experiments (using per independent experiment the mean of three technical replicates).



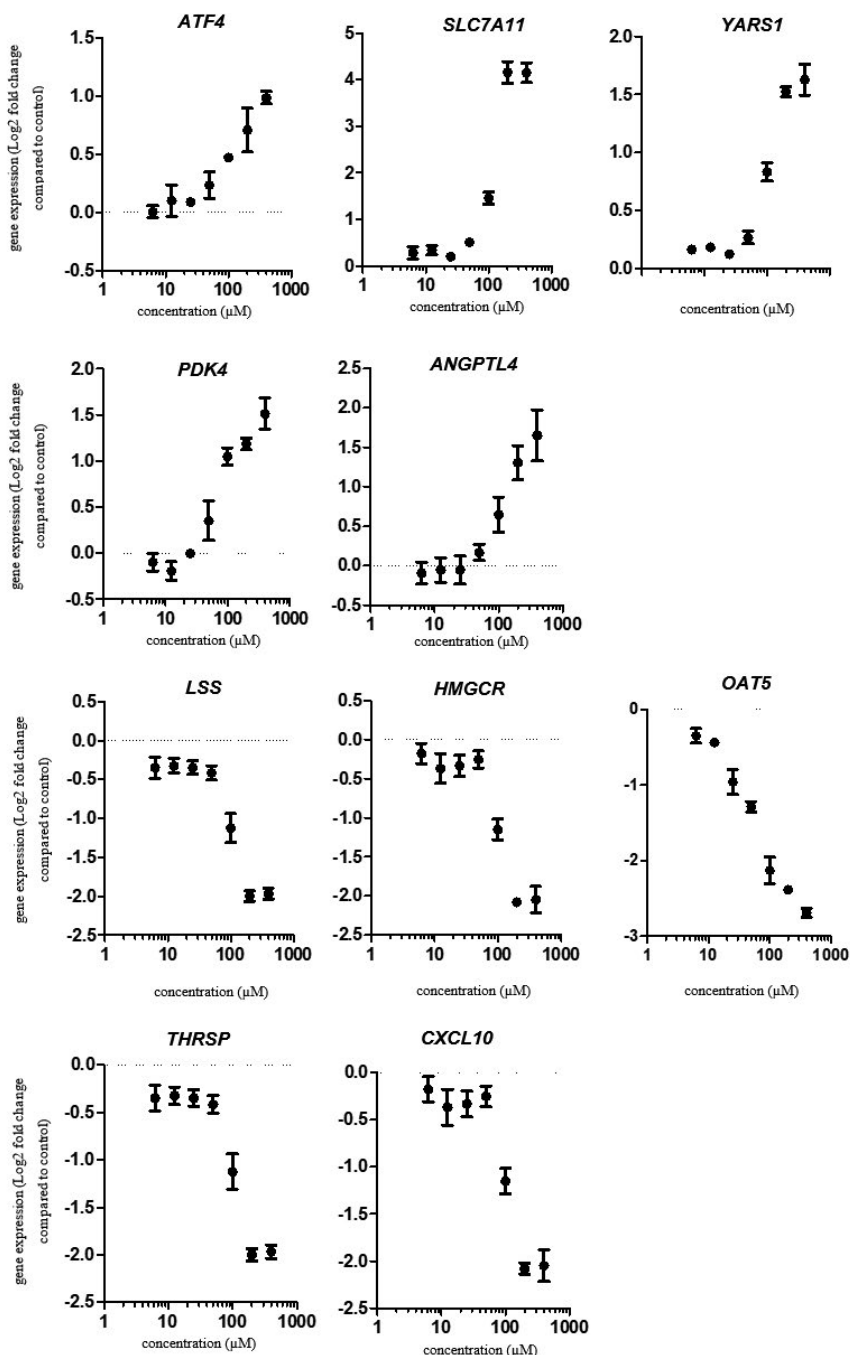
SUPPLEMENTARY FIGURE 3 Effect of 24-h exposure to PFASs on viability of HepaRG cells as determined with the WST-1 assay and expressed as percentage of the solvent control (0.5% DMSO). Data are presented as mean \pm SD of three independent experiments (using per independent experiment the mean of three technical replicates).



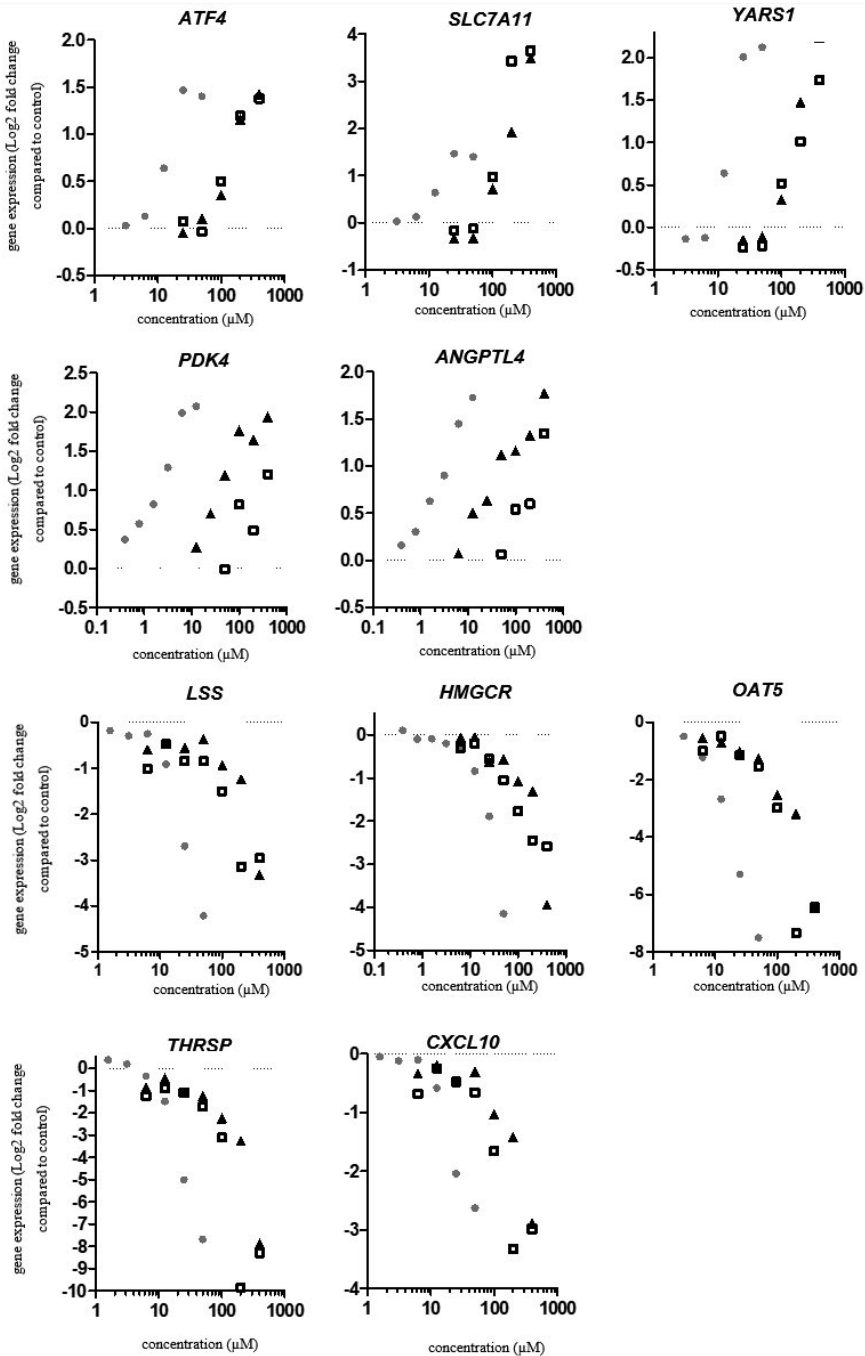
SUPPLEMENTARY FIGURE 4 Effect of 24-h or 72-h exposure to cyproconazole, PFOA, PFNA, PFHxS or PFOS on triglyceride levels in HepaRG cells as determined with the AdipoRed assay and expressed as percentage of the solvent control (0.5% DMSO). Data are presented as mean \pm SD of three independent experiments (using per independent experiment the mean of three technical replicates).



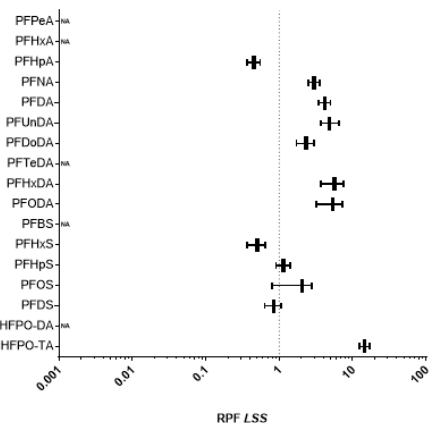
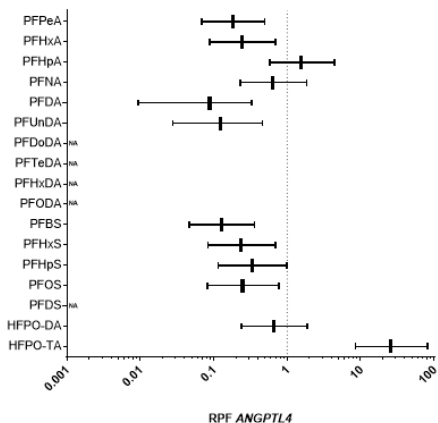
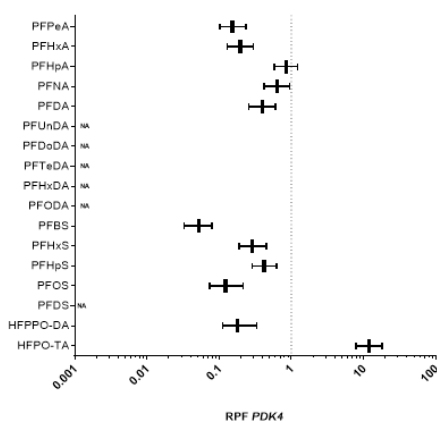
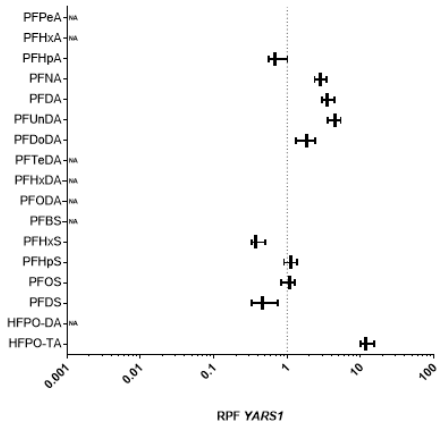
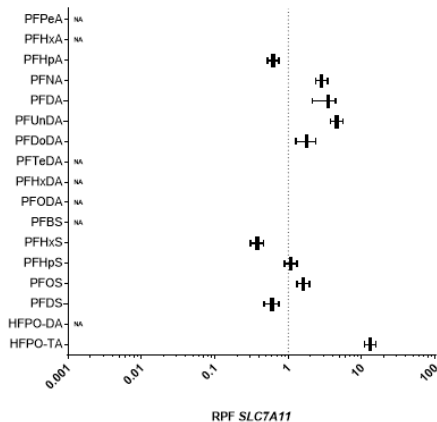
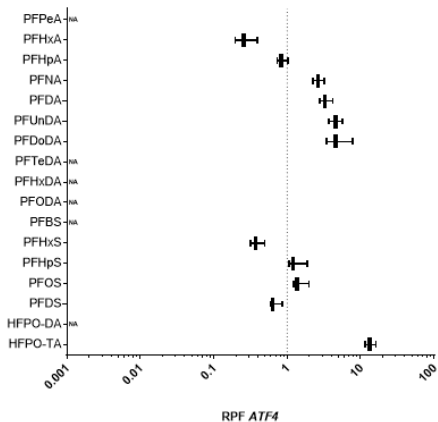
SUPPLEMENTARY FIGURE 5 Effect of 24-h exposure to PFASs on triglyceride levels in HepaRG cells as determined with the AdipoRed assay and expressed as percentage of the solvent control (0.5% DMSO). Data are presented as mean \pm SD of three independent experiments (using per independent experiment the mean of three technical replicates).

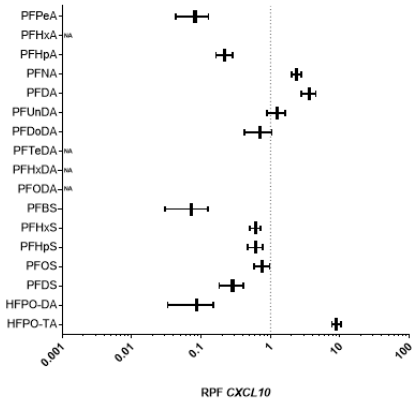
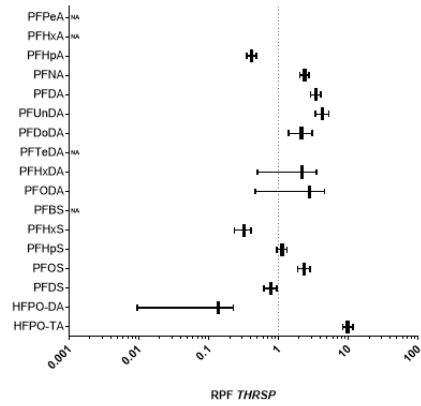
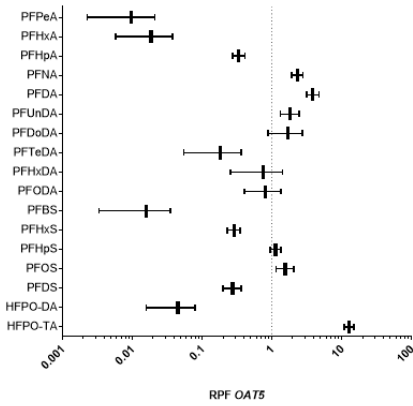
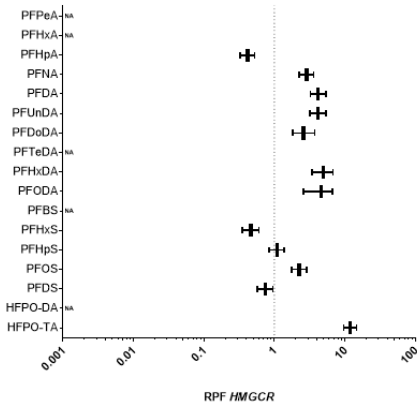


SUPPLEMENTARY FIGURE 6 Concentration-response microarray data of PFOS for selected genes to determine *in vitro* potency differences of PFASs. Average values and standard deviations of data from three independent studies are presented.



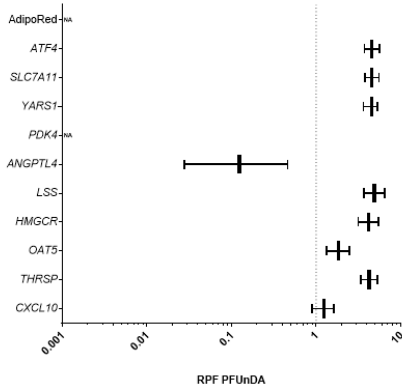
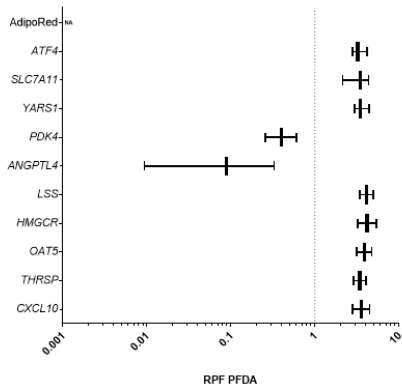
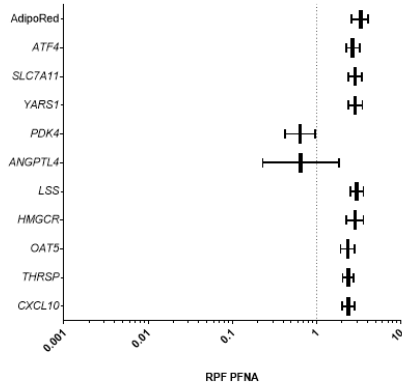
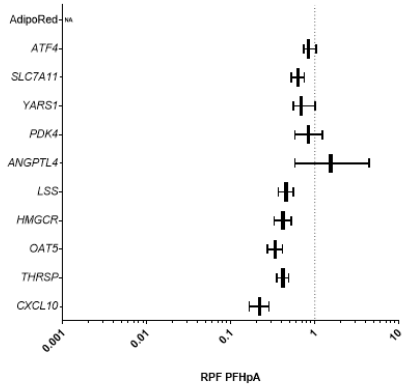
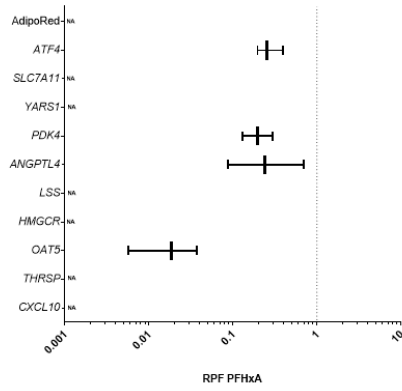
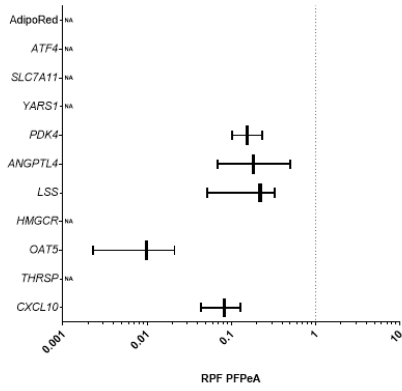
SUPPLEMENTARY FIGURE 7 Concentration-response data of PFOA- (black triangles), PFOS- (white squares) and HFPO-TA- (grey circles) induced effects on the expression of selected genes based on RT-qPCR analysis. Average values of data from three independent studies are presented.

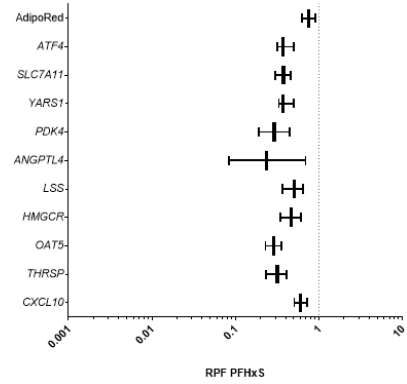
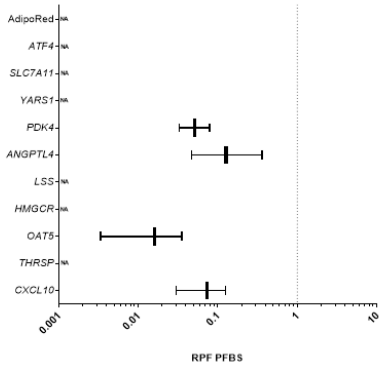
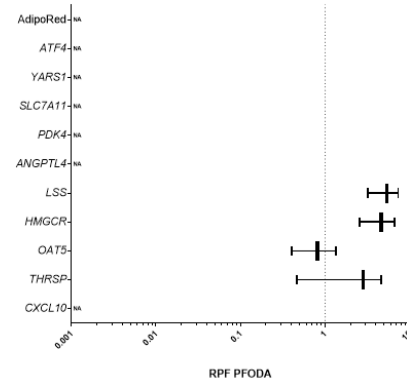
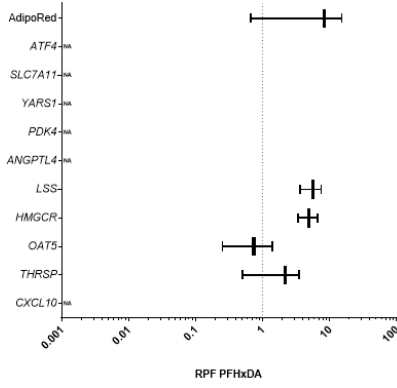
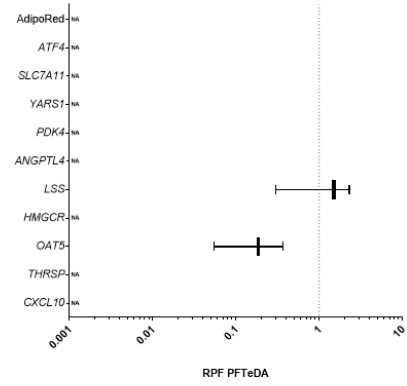
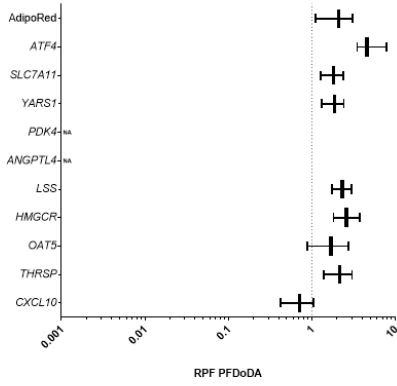


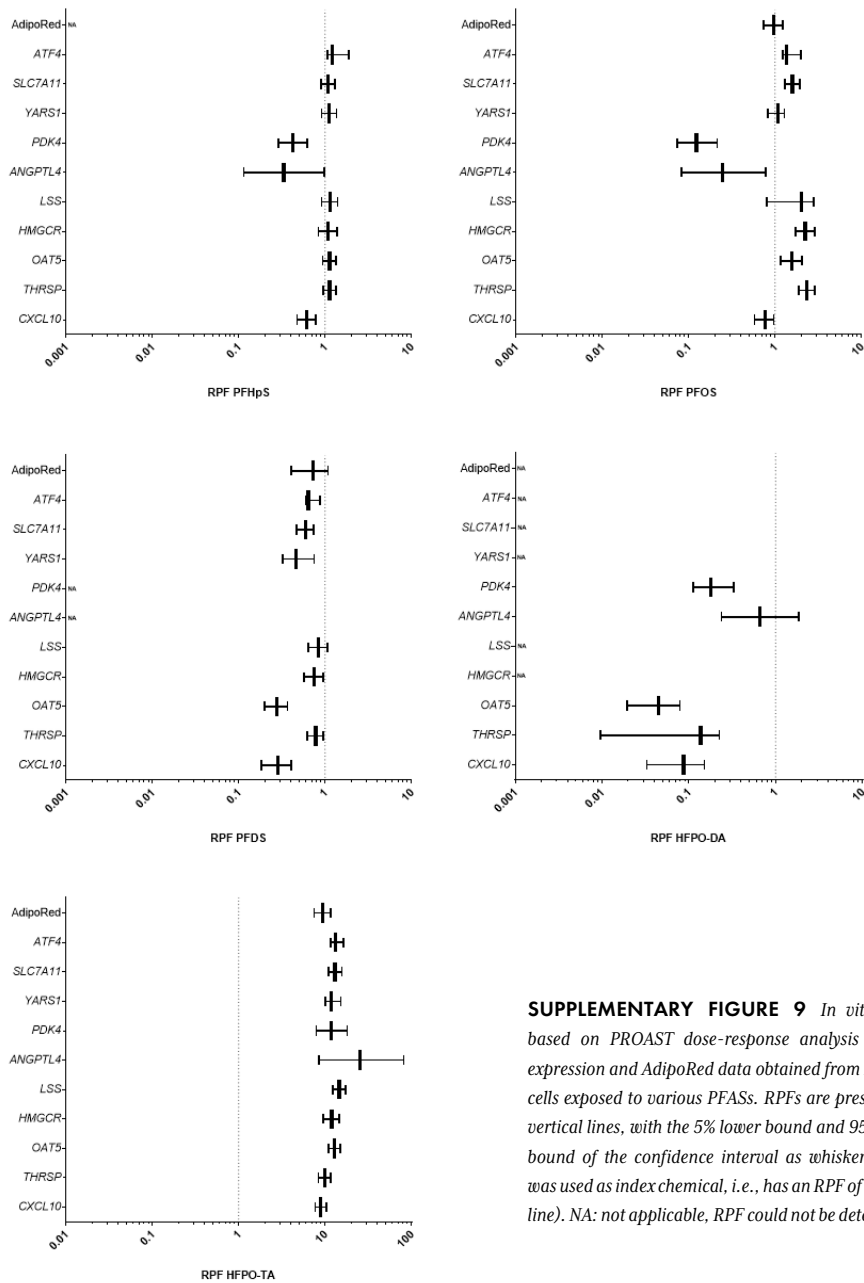


SUPPLEMENTARY FIGURE 8 *In vitro* RPFs based on PROAST dose-response analysis of *ATF4*, *SLC7A11*, *YARS1*, *PDK4*, *ANGPTL4*, *LSS*, *HMGCR*, *OAT5*, *THRSP* and *CXCL10* gene expression data obtained from HepaRG cells exposed to various PFASs. RPFs are presented as vertical lines, with the 5% lower bound and 95% upper bound of the confidence interval as whiskers. PFOA was used as index chemical, i.e., has an RPF of 1 (dotted line). NA: not applicable, RPF could not be determined.

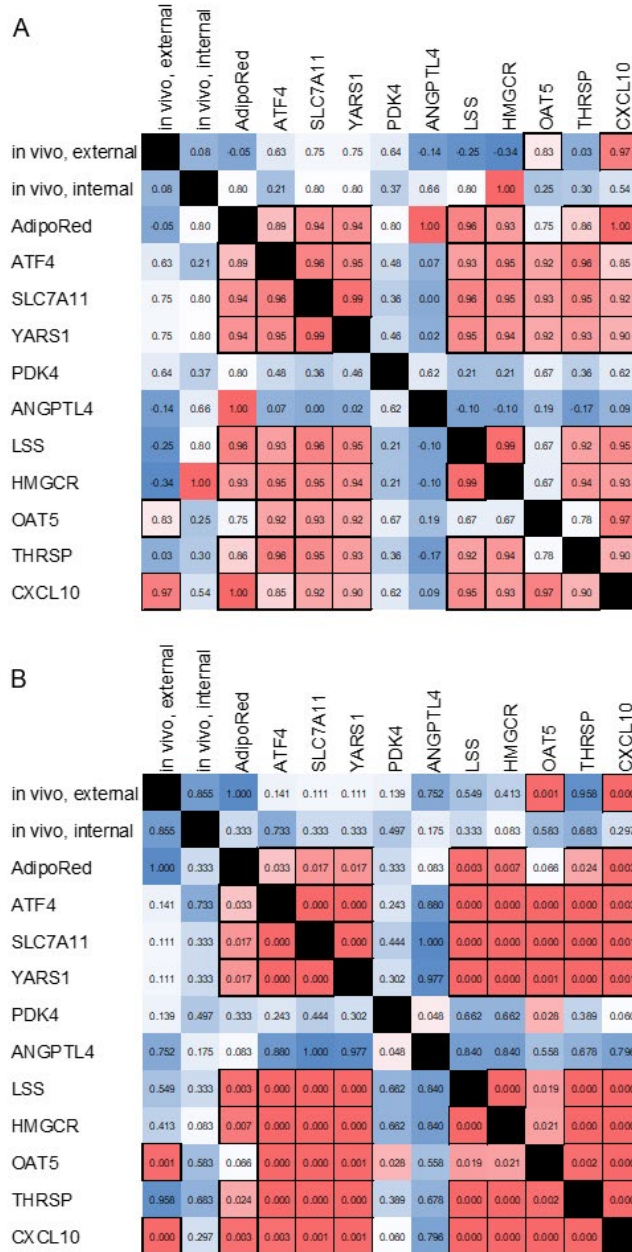
Exploration of NAMs for the perfluoroalkyl substances







SUPPLEMENTARY FIGURE 9 *In vitro* RPFs based on PROAST dose-response analysis of gene expression and AdipoRed data obtained from HepaRG cells exposed to various PFASs. RPFs are presented as vertical lines, with the 5% lower bound and 95% upper bound of the confidence interval as whiskers. PFOA was used as index chemical, i.e., has an RPF of 1 (dotted line). NA: not applicable, RPF could not be determined.



SUPPLEMENTARY FIGURE 10 Results of Spearman correlation analysis performed using Graphpad Prism 9, presenting obtained *r*-values (A) and *p*-values (B). Correlation with both an *r*-value > 0.8 and a *p*-value < 0.05 are accentuated by a black border.

Information on selected genes and possible relation to liver toxicity

OAT5

Limited information on the function and regulation of expression of OAT5 is available. Klein et al. (2010) showed that OAT5 expression in the liver is regulated via HNF-1 α . A downregulation of OAT5 may therefore relate to a downregulation and/or diminished action of HNF-1 α . Interestingly, HNF-1 α was shown to be an essential regulator of bile acid and plasma cholesterol metabolism in mice (Shih et al., 2001). An important role of HNF-4 α deregulation in PFAS-induced disturbance of lipid homeostasis has been suggested (recently reviewed by Fragki et al., 2021). Diminished HNF-1 α activity may be linked to diminished HNF-4 α activity, as HNF-4 α has been shown to act as an HNF-1 α coactivator (Eeckhoutte et al., 2014). This may indicate that PFAS-induced OAT5 downregulation is possibly (also) accomplished through PFAS-induced diminished HNF-4 α activity, but more focused studies would be required to conclude on this, which was out of the scope of the present study. It is of interest to mention that HNF-4 α is a transcriptional activator of the rate-limiting enzyme CYP7A1 in the bile acid biosynthesis (Miao et al. 2006). Although not selected here as a basis for the RPF derivation, CYP7A1 was downregulated by PFOS in the present study (Figure 5). Reduction of CYP7A1 expression has been observed before in HepaRG cells (Behr et al., 2020, Louisse et al., 2020), but also in human hepatocytes (Beggs et al. 2016) after exposure to PFASs. Currently, an AOP is under development on 'HNF4alpha suppression leading to hepatic steatosis' (access AOP-wiki 18-07-2022).

ATF4, SLC7A11, YARS1

Upon endoplasmic reticulum stress and/or amino acid starvation (Harding et al., 2000), genes that play a role in cell recovery, adaptation to stress conditions, and restoration of cell homeostasis are upregulated by the transcription factor ATF4 (Rozpedek et al., 2016). SLC7A11 and YARS1 have been described to be regulated by ATF4 (Adams, 2007; Shan et al., 2016; Krokowski et al., 2013; Han et al., 2013). Various of the PFASs tested in the present study caused an increase in the expression of ATF4, SLC7A11 and/or YARS1. The SLC7A11 gene codes for an amino acid transporter, and the YARS1 gene codes for the aminoacyl-tRNA synthetase (ARS) that catalyzes the aminoacylation of tRNA with tyrosine. Although these processes may not directly play a role in liver toxicity, they may point to (PFAS-induced) endoplasmic reticulum stress and/or amino acid starvation that can be related to adverse effects to the liver. PFOA-induced endoplasmic reticulum stress in the liver has been reported *in vivo* in mice, and related liver toxicity was attenuated by the endoplasmic reticulum stress inhibitor 4-phenylbutyrate (Yan et al., 2015). Also other studies point to a possible role of endoplasmic reticulum stress in liver disease (Malhi and Kaufman, 2011; Maiers and Malhi, 2019).

PDK4 and ANGPTL4

PDK4 and *ANGPTL4* are PPAR α -response genes, where it must be noted that *PDK4* expression is also regulated by retinoic acid receptors (Kwon and Harris, 2004). The present study shows that the PFCAs and PFSAs up to C10/C11 are activators of *PDK4* and *ANGPTL4* expression, whereas the longer chain PFASs (PFDoDA, PFTeDA, PFHxDA, PFODA and PFDS) are not. PPAR α activity of the shorter chain PFASs has been reported before by Behr et al. (2020), whereas they did not test the effects of the longer chain PFAS that were not active in our study. Interestingly, the long-chain PFASs have been reported to be rather potent *in vivo* with regard to liver toxicity, which may suggest that liver toxicity is not necessarily related to PPAR α activation. Although PPAR α activation has been suggested to play a role in certain adverse effects to the liver, it is not typically related to the relative liver weight increase which was the endpoint used for RPF derivation based on *in vivo* studies (Bil et al., 2021; 2022a; 2022b; Hall et al., 2012).

HMGCR and LSS

HMGCR and *LSS* are cholesterologenic genes that were already found to be downregulated by PFOA, PFOS and PFNA in our previous study (Louisse et al., 2020). Various human (epidemiological) studies have reported a relationship between PFOA/PFOS (internal) exposure and increased cholesterol levels, but the causality is debated, and an established mode of action supporting such a relationship is lacking (Fragki et al., 2021). The downregulation of these genes found in HepaRG cells may at first seem better in line with the reported PFOA-induced decrease in cholesterol as observed in late-stage cancer patients in a phase I dose-escalation trial exposed to high doses of PFOA for six weeks (Convertino et al., 2018) as well as the PFAS-induced decrease in cholesterol in several animal studies (see review in Fragki et al. (2021)). On the other hand, suppressed *de novo* biosynthesis of cholesterol may point to an increase in intrahepatic cholesterol (Brown and Goldstein, 1997; Feingold et al. 2000; DeBose-Boyd, 2008). It is of importance to note that processes involved in regulation of cholesterol homeostasis *in vivo* are complex, and extrapolation of findings from a single cell model *in vitro* to consequences for in the *in vivo* situation is not straightforward.

CXCL10

CXCL10 may play a role in liver disease, but this is reported to be related to interaction with the immune system, playing a role in inflammation reactions upon liver damage (Chen et al., 2013). The impact of a decrease in *CXCL10* gene expression in liver cells upon PFAS exposure as observed in the present study on liver function is not known. It is, however, tempting to speculate about a possible role of a decrease in *CXCL10* on the immune system, as an immunotoxic effect (decreased response to vaccination) has been selected as the critical endpoint for derivation of the health based guidance value of combined exposure to PFOA, PFNA, PFHxS and PFOS by EFSA (EFSA CONTAM Panel, 2020). *CXCL10* is a chemokine playing a role in the stimulation and migration of immune cells and the

regulation of T-cell and bone marrow progenitor maturation (Neville et al., 1997). PFOA and PFOS were shown before to decrease *CXCL10* gene expression in primary human liver cells (Beggs et al., 2016) and to decrease *CXCL10* excretion by human bronchial epithelial cells (HBEC3-KT cell line) (Sørli et al., 2020). *CXCL10* has been shown to work as an adjuvant, i.e., triggering an immune response to injected antigens in a mouse model (Kratzwohl and Anderson, 2006). It is therefore tempting to speculate on a possible role of PFAS-induced *CXCL10* suppression in the decreased vaccine response in humans (Grandjean et al., 2012; Abraham et al., 2020) and the decreased T-cell-dependent antibody response (TDAR) in experimental animals (Peden Adams et al., 2008; DeWitt et al., 2008; DeWitt et al., 2009; Dong et al., 2009), given that the mode of action underlying the immunotoxicity of PFASs has not been unraveled yet. *CXCL10* has been shown to be directly involved in the generation of a parasite specific CD8⁺ T cell-mediated immune response in mice, evidenced by a significant reduction of CD8⁺ T cells in mice depleted of *CXCL10* (Majumder et al., 2012). A PFAS-induced decrease in *CXCL10* has not been reported *in vivo*, so any role in the immunotoxicity of PFASs is to be further investigated.

THRSP

THRSP has been reported to be involved in the regulation of lipid metabolism. It is induced by thyroid hormone, progestin, glucose and estradiol (Kuemmerle and Kinlaw, 2011; Ren et al., 2017). Expression has been reported to be downregulated upon fasting. A role of THRSP in PFAS-induced hepatotoxicity has not been described. *Thrsp* was up-regulated in livers of two mouse models (db/db mice and high-fat-diet-fed mice) for studying nonalcoholic fatty liver disease pathogenesis (Wu et al., 2013). This study also showed that hepatic overexpression of *Thrsp* increased triglyceride accumulation with enhanced lipogenesis in livers of C57Bl/6 mice, and that hepatic *Thrsp* gene silencing attenuated the fatty liver phenotype in db/db mice. THRSP expression has been reported to be regulated via various transcription factors, such as TH, PXR and CAR. Our previous study, compared the expression changes induced by PFOA, PFNA and PFOS in HepaRG cells with data published by Wigger et al. (2019) on the LXR agonist GW3965. Whereas the PFASs decreased *THRSP* expression, the LXR agonist GW3965 increased *THRSP* expression. Also various other genes induced by GW3965 were downregulated by the PFASs, suggesting a PFAS-induced downregulation of LXR-regulated genes. LXR activation has been described as the molecular initiating event in an AOP for liver steatosis (Vinken, 2015). A role of inhibition of LXR-mediated gene expression in chemical-induced liver toxicity has not been described.

References-Supplementary Material

- Abraham K, Mielke H, Fromme H, Völkel W, Menzel J, Peiser M, Zepp F, Willich SN, Weikert C (2020). Internal exposure to perfluoroalkyl substances (PFASs) and biological markers in 101 healthy 1-year-old children: associations between levels of perfluorooctanoic acid (PFOA) and vaccine response. *Arch Toxicol.* 94(6): 2131-2147.
- Adams CM (2007). Role of the transcription factor ATF4 in the anabolic actions of insulin and the anti-anabolic actions of glucocorticoids. *J Biol Chem.* 282(23): 16744-16753.
- Beggs KM, McGreal SR, McCarthy A, Gunewardena S, Lampe JN, Lau C, Apte U (2016). The role of hepatocyte nuclear factor 4- α in perfluorooctanoic acid- and perfluorooctanesulfonic acid-induced hepatocellular dysfunction. *Toxicol Appl Pharmacol.* 304: 18-29.
- Behr AC, Plinsch C, Braeuning A, Buhrke T (2020). Activation of human nuclear receptors by perfluoroalkylated substances (PFAS). *Toxicol In Vitro.* 62: 104700.
- Bil W, Zeilmaker M, Fragki S, Lijzen J, Verbruggen E, Bokkers B (2021). Risk Assessment of Per- and Polyfluoroalkyl Substance Mixtures: A Relative Potency Factor Approach. *Environ Toxicol Chem.* 40(3): 859-870.
- Bil W, Zeilmaker M, Fragki S, Lijzen J, Verbruggen E, Bokkers B (2022). Response to Letter to the Editor on Bil et al. 2021 "Risk Assessment of Per- and Polyfluoroalkyl Substance Mixtures: A Relative Potency Factor Approach". *Environ Toxicol Chem.* 41(1): 13-18.
- Bil W, Zeilmaker MJ, Bokkers BGH (2022b). Internal Relative Potency Factors for the Risk Assessment of Mixtures of Per- and Polyfluoroalkyl Substances (PFAS) in Human Biomonitoring. *Environ Health Perspect.* 130(7):77005.
- Brown MS, Goldstein JL (1997). The SREBP pathway: regulation of cholesterol metabolism by proteolysis of a membrane-bound transcription factor. *Cell.* 89(3): 331-340.
- Chen LJ, Lv J, Wen XY, Niu JQ (2013). CXCL10: a key actor in liver disease? *Hepatol Int.* 7(3): 798-804.
- Convertino M, Church TR, Olsen GW, Liu Y, Doyle E, Elcombe CR, Barnett AL, Samuel LM, MacPherson IR, Evans TRJ (2018). Stochastic Pharmacokinetic-Pharmacodynamic Modeling for Assessing the Systemic Health Risk of Perfluorooctanoate (PFOA). *Toxicol Sci.* 163(1): 293-306.
- DeBose-Boyd RA (2008). Feedback regulation of cholesterol synthesis: sterol-accelerated ubiquitination and degradation of HMG CoA reductase. *Cell Res.* 18(6): 609-621.
- Dewitt JC, Copeland CB, Strynar MJ, Luebke RW (2008). Perfluorooctanoic acid-induced immunomodulation in adult C57BL/6J or C57BL/6N female mice. *Environ Health Perspect.* 116(5): 644-650.
- DeWitt JC, Copeland CB, Luebke RW (2009). Suppression of humoral immunity by perfluorooctanoic acid is independent of elevated serum corticosterone concentration in mice. *Toxicol Sci.* 109(1): 106-112.
- Dong GH, Zhang YH, Zheng L, Liu W, Jin YH, He QC (2009). Chronic effects of perfluorooctanesulfonate exposure on immunotoxicity in adult male C57BL/6 mice. *Archives of Toxicology.* 83, 805-815.
- Eeckhoutte J, Formstecher P, Laine B (2004). Hepatocyte Nuclear Factor 4 α enhances the Hepatocyte Nuclear Factor 1 α -mediated activation of transcription. *Nucleic Acids Research* 32(8): 2586-2593.
- EFSA CONTAM Panel (2020). Scientific Opinion. Risk to human health related to the presence of perfluoroalkyl substances in food. *EFSA Journal* 18 (9):6223.
- Feingold KR. 2000. Introduction to lipids and lipoproteins. In: Feingold KR, Anawalt B, Boyce A, Chrousos G, de Herder WW, Dungan K, Grossman A, Hershman JM, Hofland J, Kaltsas G, editors. *Endotext* [Internet]. South Dartmouth (MA): MDText.com. [Updated 2018 Feb 2]. Available from: <https://www.ncbi.nlm.nih.gov/books/NBK305896/>.
- Fragki S, Dirven H, Fletcher T, Grasl-Kraupp B, Bjerve Gützkow K, Hoogenboom R, Kersten S, Lindeman B, Lousse J, Peijnenburg A, Piersma AH, Princen HMG, Uhl M, Westerhout J, Zeilmaker MJ, Luijten M (2021). Systemic PFOS and PFOA exposure and disturbed lipid homeostasis in humans: what do we know and what not? *Crit Rev Toxicol.* 51(2): 141-164.
- Grandjean P, Andersen EW, Budtz-Jørgensen E, Nielsen F, Mølbak K, Weihe P, Heilmann C (2012). Serum vaccine antibody concentrations in children exposed to perfluorinated compounds. *JAMA.* 307(4): 391-397.
- Hall AP, Elcombe CR, Foster JR, Harada T, Kaufmann W, Knippel A, Küttler K, Malarkey DE, Maronpot RR, Nishikawa A, Nolte T, Schulte A, Strauss V, York MJ (2012). Liver hypertrophy: a review of adaptive (adverse and non-adverse) changes - conclusions from the 3rd International ESTP Expert Workshop. *Toxicol Pathol.* 40(7): 971-994.
- Han J, Back SH, Hur J, Lin YH, Gildersleeve R, Shan J, Yuan CL, Krokowski D, Wang S, Hatzoglou M, Kilberg MS, Sartor MA, Kaufman RJ (2013). ER-stress-induced transcriptional regulation increases protein synthesis leading to cell death. *Nat Cell Biol.* 15: 481-490.
- Harding HP, Novoa I, Zhang Y, Zeng H, Wek R, Schapira M, Ron D (2000). Regulated translation initiation controls stress-induced gene expression in mammalian cells. *Mol Cell.* 6(5): 1099-1108.

- Klein K, Jüngst C, Mwinyi J, Stieger B, Krempler F, Patsch W, Eloranta JJ, Kullak-Ublick GA (2010). The human organic anion transporter genes OAT5 and OAT7 are transactivated by hepatocyte nuclear factor-1 α (HNF-1 α). *Mol Pharmacol*. 78(6): 1079-1087.
- Krathwohl MD, Anderson JL (2006). Chemokine CXCL10 (IP-10) is sufficient to trigger an immune response to injected antigens in a mouse model. *Vaccine*. 24(15): 2987-2993.
- Krokowski D, Han J, Saikia M, Majumder M, Yuan CL, Guan BJ, Bevilacqua E, Bussolati O, Bröer S, Arvan P, Tchórzewski M, Snider MD, Puchowicz M, Croniger CM, Kimball SR, Pan T, Koromilas AE, Kaufman RJ, Hatzoglou M (2013). A self-defeating anabolic program leads to β -cell apoptosis in endoplasmic reticulum stress-induced diabetes via regulation of amino acid flux. *J Biol Chem*. 288: 17202-17213.
- Kuemmerle NB, Kinlaw WB (2011). THRSP (thyroid hormone responsive). *Atlas Genet Cytogenet Oncol Haematol*. 15(6): 480-482.
- Kwon HS, Harris RA (2004). Mechanisms responsible for regulation of pyruvate dehydrogenase kinase 4 gene expression. *Adv Enzyme Regul*. 44: 109-121.
- Louise J, Rijkers D, Stoopen G, Janssen A, Staats M, Hoogenboom R, Kersten S, Peijnenburg A (2020). Perfluorooctanoic acid (PFOA), perfluorooctane sulfonic acid (PFOS), and perfluorononanoic acid (PFNA) increase triglyceride levels and decrease cholesterologenic gene expression in human HepaRG liver cells. *Arch Toxicol*. 94(9): 3137-3155.
- Maiers JL, Malhi H (2019). Endoplasmic Reticulum Stress in Metabolic Liver Diseases and Hepatic Fibrosis. *Semin Liver Dis*. 39(2): 235-248.
- Majumder S, Bhattacharjee S, Paul Chowdhury B, Majumdar S (2012). CXCL10 is critical for the generation of protective CD8 T cell response induced by antigen pulsed CpG-ODN activated dendritic cells. *PLoS One*. 7(11): e48727.
- Malhi H, Kaufman RJ (2011). Endoplasmic reticulum stress in liver disease. *J Hepatol*. 54(4): 795-809.
- Miao J, Fang S, Bae Y, Kemper JK (2006). Functional inhibitory cross-talk between constitutive androstane receptor and hepatic nuclear factor-4 in hepatic lipid/glucose metabolism is mediated by competition for binding to the DRI motif and to the common coactivators, GRIP-1 and PGC-1 α . *J Biol Chem*. 281(21): 14537-14546.
- Neville LF, Mathiak G, Bagasra O (1997). The immunobiology of interferon-gamma inducible protein 10 kD (IP-10): a novel, pleiotropic member of the C-X-C chemokine superfamily. *Cytokine Growth Factor Rev*. 8(3): 207-219.
- Peden-Adams MM, Keller JM, Eudaly JG, Berger J, Gilkeson GS, Keil DE (2008). Suppression of humoral immunity in mice following exposure to perfluorooctane sulfonate. *Toxicol Sci*. 104: 144-154.
- Ren J, Xu N, Zheng H, Tian W, Li H, Li Z, Wang Y, Tian Y, Kang X, Liu X (2017). Expression of Thyroid Hormone Responsive SPOT 14 Gene Is Regulated by Estrogen in Chicken (*Gallus gallus*). *Sci Rep*. 7(1): 10243.
- Rozpedek W, Pytel D, Mucha B, Leszczynska H, Diehl JA, Majsterek I (2016). The Role of the PERK/eIF2 α /ATF4/CHOP Signaling Pathway in Tumor Progression During Endoplasmic Reticulum Stress. *Curr Mol Med*. 16: 533-544.
- Shan J, Zhang F, Sharkey J, Tang TA, Örd T, Kilberg MS (2016). The C/ebp-Atf response element (CARE) location reveals two distinct Atf4-dependent, elongation-mediated mechanisms for transcriptional induction of aminoacyl-tRNA synthetase genes in response to amino acid limitation. *Nucleic Acids Res*. 44: 9719-9732.
- Shih DQ, Bussen M, Sehayek E, Ananthanarayanan M, Shneider BL, Suchy FJ, Shefer S, Bollileni JS, Gonzalez FJ, Breslow JL, Stoffel M (2001). Hepatocyte nuclear factor-1 α is an essential regulator of bile acid and plasma cholesterol metabolism. *Nat Genet*. 27(4): 375-382.
- Sørli JB, Låg M, Ekeren L, Perez-Gil J, Haug LS, Da Silva E, Matrod MN, Gützkow KB, Lindeman B (2020). Per- and polyfluoroalkyl substances (PFASs) modify lung surfactant function and pro-inflammatory responses in human bronchial epithelial cells. *Toxicol In Vitro*. 62: 104656.
- Vinken M (2015). Adverse Outcome Pathways and Drug-Induced Liver Injury Testing. *Chem Res Toxicol*. 28(7): 1391-1397.
- Wigger L, Casals-Casas C, Baruchet M, Trang KB, Pradervand A, Naldi A, Desvergne B (2019). System analysis of cross-talk between nuclear receptors reveals an opposite regulation of the cell cycle by LXR and FXR in human HepaRG liver cells. *PLoS One*. 14: e0220894.
- Wu J, Wang C, Li S, Li S, Wang W, Li J, Chi Y, Yang H, Kong X, Zhou Y, Dong C, Wang F, Xu G, Yang J, Gustafsson JÅ, Guan Y (2013). Thyroid hormone-responsive SPOT 14 homolog promotes hepatic lipogenesis, and its expression is regulated by liver X receptor α through a sterol regulatory element-binding protein 1c-dependent mechanism in mice. *Hepatology*. 58(2): 617-628.
- Yan S, Zhang H, Wang J, Zheng F, Dai J (2015). Perfluorooctanoic acid exposure induces endoplasmic reticulum stress in the liver and its effects are ameliorated by 4-phenylbutyrate. *Free Radic Biol Med*. 87: 300-311.

Chapter 7

New Approach Methodologies: A quantitative *in vitro* to *in vivo* extrapolation case study with PFASs

Food and Chemical Toxicology, 2023 Feb; 172: 113559

DOI: 10.1016/j.fct.2022.113559

Styliani Fragki¹

Jochem Louisse³

Bas Bokkers⁴

Mirjam Luijten¹

Ad Peijnenburg³

Deborah Rijkers³

Aldert Piersma^{1,5}

Marco Zeilmaker²

¹ Centre for Health Protection, National Institute for Public Health and the Environment (RIVM), Bilthoven, The Netherlands

² Centre for Nutrition, Prevention and Health Services, National Institute for Public Health and the Environment (RIVM), Bilthoven, the Netherlands

³ Wageningen Food Safety Research (WFSR), Wageningen, The Netherlands

⁴ Centre for Safety of Substances and Products, National Institute for Public Health and the Environment (RIVM), Bilthoven, the Netherlands

⁵ Institute for Risk Assessment Sciences, Utrecht University, P.O. Box 80178, 3508 TD Utrecht, The Netherlands

Abstract

Per- and polyfluoroalkyl substances (PFASs) have been associated with increased blood lipids in humans. Perfluorooctanoic acid (PFOA) has been also linked with elevated alanine transferase (ALT) serum levels in humans, and in rodents the liver is a main target organ for many PFASs. With the focus on New Approach Methodologies, the chronic oral equivalent effect doses were calculated for PFOA, PFNA (perfluorononanoic acid), PFHxS (perfluorohexanesulfonic acid) and PFOS (perfluorooctane sulfonic acid) based on *in vitro* effects measured in the HepaRG cell line. Selected *in vitro* readouts were considered biomarkers for lipid disturbances and hepatotoxicity. Concentration-response data obtained from HepaRG cells on triglyceride (TG) accumulation and expression changes of 12 selected genes (some involved in cholesterol homeostasis) were converted into corresponding human dose-response data, using physiologically based kinetic (PBK) model-facilitated reverse dosimetry. Next to this, the biokinetics of the chemicals were studied in the cell system. The current European dietary PFASs exposure overlaps with the calculated oral equivalent effect doses, indicating that the latter may lead to interference with hepatic gene expression and lipid metabolism. These findings illustrate an *in vitro-in silico* methodology, which can be applied for more PFASs, to select those that should be prioritized for further hazard characterization.

Introduction

Perfluoroalkyl and polyfluoroalkyl substances (PFASs) are a large group of synthetic chemicals, comprising more than 4700 members (OECD 2018), with a broad range of industrial and consumer applications. They all contain carbon-fluorine bonds, which impart to these substances unique physicochemical properties, rendering them non-degradable in the environment and therefore, known as the ‘forever chemicals’. As such, PFASs contaminate soil, and groundwater, but also enter in the food chain via food and drinking water. Certain PFASs are known to persist for years in man (Bartell et al. 2010; Olsen et al. 2007; Zhang et al. 2013b) and have been associated with numerous adverse human health effects, including serum lipid perturbations, which are considered risk factors for cardiovascular disease (CVD), immunotoxicity, and developmental toxicity (ATSDR 2018; EFSA CONTAM Panel 2018b; 2020b). The use of two main family congeners, perfluorooctane sulfonic acid (PFOS) and perfluorooctanoic acid (PFOA), as well as of their precursors, has been restricted within the EU (Regulation (EU) 2019/1021, 2020/784), but also globally (UNEP/POPS/COP.4/17 2009). Currently, the national authorities of five EU Member States are working on the restriction of all PFASs in the EU (<https://www.rivm.nl/en/pfas/pfas-news>), whereas an EU ban of 200 group members will begin in February 2023 (<https://pfascentral.org/news/press-release-the-eu-bans-200-pfas-substances-on-swedish-initiative>). At the moment, human exposure data indicate that part of the European population is exposed to levels higher than the Tolerable Weekly Intake (TWI) established by European Food Safety Authority (EFSA) for the sum of four PFASs: PFOA, PFNA (perfluorononanoic acid), PFHxS (perfluorohexanesulfonic acid), and PFOS (EFSA, 2020). This was further confirmed by recent human biomonitoring data obtained within the European HBM4EU project²⁰.

In several epidemiological studies, increased serum levels of PFASs (PFOS, PFOA and PFNA) have been repeatedly associated with lipid disturbances, mainly seen as elevated blood cholesterol (total and Low Density Lipoprotein-Cholesterol: LDL-C) and (in some cases) triglycerides (TG) (Eriksen et al. 2013; Olsen et al. 2003a; Steenland et al. 2009). Still, these findings could not be linked to a corresponding adverse health outcome (like CVD) and contradict the evidence from animal toxicity studies, where much higher PFASs doses frequently decreased serum cholesterol and TGs, and increased intrahepatic lipid levels (steatosis) (recently reviewed by Fragki et al. 2021). Administration of very high PFOA doses to end-term cancer patients for 6-weeks was found to slightly reduce blood total cholesterol (Convertino et al. 2018), supporting that the divergent outcomes between humans and animals may be related to different PFASs exposure conditions (chronic low dose *vs.* short-term high dose). It has been postulated that, next to the PFAS exposure levels, interspecies differences in lipid homeostasis, as well as toxicokinetics, may play a role in the observed species differences of PFAS-induced effects (Fragki et al. 2021). In parallel with the lipid perturbations, human studies have also associated PFAS exposure with a small elevation in

20 HBM4EU data can be found here: EU HBM Dashboard – HBM4EU – science and policy for a healthy future.

serum levels of the hepatic enzyme ALT (alanine transferase), a liver damage biomarker (Gallo et al. 2012b). These results are in line with the observations from animal studies, where liver toxicity is one of the most commonly recorded effects, exhibited as increased liver weight (hypertrophy and hyperplasia), steatosis, or even necrosis (Bil et al. 2021; NTP 2019a; 2019b). Nevertheless, this information is only available for a small number of the PFASs.

Given the large number of existing PFASs and the lack of *in vivo* toxicity data for the majority of the congeners, application of novel approach methodologies (NAMs), combined with information on (estimated) exposure, may assist in their toxicological screening and prioritization for further hazard assessment. NAMs are emerging tools in chemical risk assessment, which include *in vitro* approaches and *in silico* approaches or combinations thereof (Ball et al. 2022; Carmichael et al. 2022b; Dent et al. 2021b; Punt et al. 2020). For the case of PFASs, *in vitro* toxicity readouts to build such NAMs may be obtained from studies with human hepatocytes or liver cell lines, considering their potential for causing hepatotoxicity and the liver playing a fundamental role in the regulation of cholesterol and lipid homeostasis. Exposure of human HepaRG liver cells (Behr et al. 2020a; Lousse et al. 2020b) (also Lousse et al. 2023, in press), and human primary hepatocyte spheroids (Reardon et al. 2021; Rowan-Carroll et al. 2021), to various PFASs was shown to induce a downregulation of several genes related to the cholesterol biosynthesis pathway, cholesterol uptake from the liver and SREBP²¹ signaling. Additionally, PFOS and PFOA were shown to strongly decrease bile acid synthesis, the main catabolic product of cholesterol (Behr et al. 2020a) and induce a concentration-dependent increase in TG accumulation in HepaRG cells (Lousse et al. 2020b) (Lousse et al. 2023, in press).

Application of NAMs for human health risk assessment should also include a quantitative interpretation of the *in vitro* toxicity data in the context of the intact human. *In vitro* concentrations have to be extrapolated into the equivalent PFASs serum levels, and corresponding external exposure, i.e. the oral equivalent doses. This extrapolation, known as QIVIVE (quantitative *in vitro* to *in vivo* extrapolations), needs the integration of human toxicokinetics and, preferably, the biokinetics of the *in vitro* system. In this manuscript, a PFAS QIVIVE approach is presented and applied to *in vitro* concentration-response data of PFAS-induced TG accumulation and changes in expression of selected genes in the HepaRG cell line. Genes were selected on the basis of concentration-response data from whole-genome gene expression studies with PFOS-exposed HepaRG cells (see Lousse et al. 2023, in press) and represented various biological processes and cellular pathways, including those related to cholesterol homeostasis. As a case study, data on four members of the PFASs family were used: PFOA, PFNA, PFHxS and PFOS. Chemical toxicokinetics were implemented in the QIVIVE following a reverse dosimetry approach facilitated by physiologically-based kinetic (PBK) modelling. For PFOA and PFOS the existing human

21 SREBP: sterol regulatory element-binding protein; cellular cholesterol biosynthesis is regulated by intracellular cholesterol levels, which is mediated by SREBPs 1 and 2 DeBose-Boyd RA. 2008. Feedback regulation of cholesterol synthesis: Sterol-accelerated ubiquitination and degradation of hmg coa reductase. Cell Res. 18(6):609-621, DeBose-Boyd RA, Ye J. 2018. Srebps in lipid metabolism, insulin signaling, and beyond. Trends Biochem Sci. 43(5):358-368.

PBK models of Loccisano et al. (2011) were applied. The models were extended in order to describe the toxicokinetics of PFNA and PFHxS, based on information on their reported elimination half-lives (Olsen et al. 2007; Zhang et al. 2013b). A specific exposure scenario was considered to be of interest: a long (50-year) exposure in accordance with EFSA's assessment (EFSA CONTAM Panel 2018b; 2020b). For PFOA specifically a shorter 6-week exposure was applied in accordance with the Convertino clinical study (Convertino et al. 2018). Although in most reverse dosimetry approaches with PBK modelling, nominally applied *in vitro* concentrations are seen as the proxy for blood or target tissue concentrations (Fragki et al. 2022; Fragki et al. 2017; Li et al. 2017a; Louisse et al. 2017; Louisse et al. 2015), we put forward here the use of experimentally measured PFAS cell-associated concentrations. As such, the biokinetics of PFASs in the HepaRG cells were assessed in the present study by determining time- and concentration-dependent cell-associated concentrations of the chemicals. These data provided relevant *in vitro* dosimetry information for the QIVIVE. The QIVIVE resulted in the calculation of the chronic daily human intake, or else oral equivalent effect dose, corresponding with a (predefined) *in vitro* effect level. The calculated oral equivalent effect doses were compared to current chronic dietary human exposure estimates (EFSA CONTAM Panel 2020b). The results indicate that the current European dietary PFASs exposure overlaps with the calculated oral equivalent effect doses, suggesting that it may interfere with hepatic gene expression and lipid metabolism.

Materials and Methods

Test chemicals

Perfluorooctanoic acid (PFOA, 95% purity) and perfluorononanoic acid (PFNA, 99% purity) were obtained from Sigma-Aldrich (Zwijndrecht, The Netherlands). Perfluorohexane sulfonate (PFHxS, 95% purity) and perfluorooctane sulfonate (PFOS, 97% purity) were obtained from Synquest laboratories (Alachua FL, USA). All stocks were prepared in 100% dimethyl sulfoxide (DMSO HybriMax, Sigma-Aldrich).

HepaRG cell culture

The cell line human hepatic HepaRG was obtained from Biopredic International (Rennes, France) and it was cultured in growth medium consisting of William's Medium E + GlutaMAX™ (ThermoFisher Scientific, Landsmeer, The Netherlands) supplemented with 10% fetal bovine serum (FBS; Corning (35-079-CV), United States of America), 1% PS (100 U/mL penicillin, 100 µg/mL streptomycin; Capricorn Scientific, Ebsdorfergrund, Germany), 50 µM hydrocortisone hemisuccinate (sodium salt) (Sigma-Aldrich), and 5 µg/mL human insulin (PAN™ Biotech). Seeding, trypsinization (using 0.05% Trypsin-EDTA (ThermoFisher Scientific)) and maintenance of the cells was performed according to the HepaRG instruction manual from Biopredic International. HepaRG cells were

seeded in 24-well plates (Corning, Corning, NY; 55000 cells per well in 500 μL). The cells remained two weeks on growth medium, and thereafter, they were cultured for two days in growth medium supplemented with 0.85% DMSO so as to induce differentiation. Subsequently, cells were cultured for 12 days in growth medium supplemented with 1.7% DMSO (differentiation medium) for final differentiation. At this final stage, the cells were considered ready to be used for biokinetic studies. Cells that were not immediately used were kept on differentiation medium for a maximum of three additional weeks. Cell cultures were maintained in an incubator (humidified atmosphere with 5% CO_2 at 37°C) and the medium was refreshed every 2–3 days during culturing. Prior to biokinetic studies, differentiated HepaRG cells were incubated for 24 h in assay medium (growth medium containing 2% FBS) supplemented with 0.5% DMSO, being the same as the conditions used in our previous *in vitro* studies (Louisse et al. 2023, in press).

***In vitro* biokinetic studies**

In vitro biokinetic studies were designed based on the study of Rosenmai et al. (2018), who assessed the cellular accumulation of PFASs in HepG2 cells. Test chemicals were diluted from 200-fold concentrated stock solutions in assay medium, providing exposure medium with a final DMSO concentration of 0.5%. PFOA and PFOS biokinetics were first assessed upon a nominal exposure to 6.25 μM for 5, 15, 60 minutes or 6 or 24 hours. Biokinetics of all PFASs were assessed upon a 24-hour exposure to 6.25, 12.5, 25, 50 and 100 μM . Cells were exposed to 550 μL exposure medium and at $t=0$, a 50 μL medium sample was taken from the well to allow for mass-balance analysis. At the desired time point, all remaining medium (500 μL) was removed. Medium samples were stored in Eppendorf vials at -80 °C and thawed when needed for LC-MS analysis. Cells were washed 5 times with Dulbecco's Phosphate Buffered Saline (DPBS; ThermoFisher Scientific). Subsequently, 250 μL lysis buffer (Thermo Scientific, Waltham, MA) was added to lyse the cells. Cell lysates were stored in Eppendorf vials at -80 °C and thawed when needed for LC-MS analysis and for quantification of the protein concentration.

Sample preparation and LC-MS analysis

Methanol (850 μL) (Actual Chemicals, Oss, The Netherlands) containing internal standards ($^{13}\text{C}_4$ -PFOA, $^{13}\text{C}_5$ -PFNA, $^{18}\text{O}_2$ -PFHxS and $^{13}\text{C}_4$ -PFOS (Wellington Laboratories, Canada) was added to 50 μL cell lysate or medium sample. These dilutions were vortexed well before centrifugation at maximum speed for 10 minutes at 4 °C. PFAS concentrations in the supernatant were determined using LC-MS/MS analysis. If needed, samples were further diluted using methanol with internal standards. LC-MS/MS analysis was based on a Shimadzu UHPLC system containing: 2 pumps (LC 20AD xr); column oven (Shimadzu CTO-20AC); pump switch (Shimadzu FCV-11AL); degasser (Shimadzu DGU-20A3); and sample tray holder (Shimadzu SIL-20 AC XR model) (Shimadzu Corporation, Kyoto, Japan). An Acquity BEH-C18 analytical column (50 \times 2.1 mm i.d., 1.7 μm , Waters, Milford, MA, USA) was used to separate the PFAS at a column temperature of 35°C. Additionally, a symmetry C18 analytical column (50 \times 2.1 mm i.d., 5 μm , Waters, Milford, MA, USA) was

used as a guard column, placed between the pump and the injector valve to isolate and delay interferences out of the LC system. The mobile phase consisted of 2 mM ammonium acetate (Merck Millipore, Darmstadt, Germany) in Milli-Q water (prepared using a Milli-Q system with a resistivity of at least $18.2 \text{ M } \Omega \text{ cm}^{-1}$ (Merck Millipore)) (mobile phase A) and Acetonitrile ULC/MS grade (Actu-All Chemicals, Oss, The Netherlands) (mobile phase B). The injection volume used was 20 μL . The chromatographic gradient was operated at a flow rate of 0.3 mL min^{-1} starting from 25% mobile phase B in the first 0.1 min, a linear increase to 100% B in 6 min with a final hold of 2.5 min. The gradient was returned to 25% B within 0.1 min for 3.9 min to equilibrate before the next injection, resulting in a total run of 12.5 min.

Detection was carried out by MS/MS using a Sciex QTRAP 5500 system (Sciex, Framingham, MA, USA) in negative electrospray ionization (ESI-) mode, with the following conditions: ion spray voltage (IS) of -4500 V ; curtain gas (CUR) of 30 L h^{-1} ; source temperature (TEM) of $350 \text{ }^\circ\text{C}$; gas 1 (GS1) of 55 L h^{-1} ; gas 2 (GS2) of 60 L h^{-1} ; and collision gas (CAD) high. The PFAS were fragmented using collision induced dissociation (CID) using argon as target gas. The analyses were performed in multiple reaction monitoring (MRM) mode, using two mass transitions per component selected based on the abundance of the signal and the selectivity of the transition. In Supplementary Table I information on the MRM transitions, declustering potential (DP), entrance potential (EP), collision energy (CE) and cell exit potential (CXP) are presented. Data were acquired using Analyst software and processed using MultiQuantTM software (Sciex, Framingham, MA, USA).

Determination protein concentration

Cellular PFAS content was normalized to cellular protein. To that end, 25 μL from each cell lysate was used to determine the protein concentration (technical duplicate) using the Pierce BCA Protein Assay Kit (Thermo Scientific, Waltham, MA). First, samples were diluted two times with lysis buffer directly in a 96-wells plate (PS, F-bottom, clear; Greiner Bio-One, Alphen aan den Rijn, The Netherlands) and in each plate a BSA standard curve (0.05 – 2 mg/mL in lysis buffer) was included allowing protein quantification of the samples. The manufacturer's protocol was followed for the subsequent steps and absorbance was measured using a microplate reader (SynergyTM HT BioTek, Winooski, VT) at 562 nm.

Selection of the *in vitro* readouts for QIVIVE

In our other study (Louisse et al. 2023, in press), the effect of the four PFASs on TG levels in HepaRG cells was determined using the AdipoRed assay. *In vitro* concentration-response data on TG, were used as a basis for the QIVIVE. Accordingly, *in vitro* gene expression concentration-response data, as collected the same study (Louisse et al. 2023, in press), were used as a basis for the QIVIVE. In this study, the effects of PFASs on the gene expression of 10 selected genes (as measured by RT-qPCR) were used for the derivation of *in vitro* relative potency factors (RPFs). These ten genes (*ATF4*, *SLC7A11*, *PDK4*, *YARS1*, *ANGPTL4*, *LSS*, *HMGCGR*, *OAT5*, *THRSP*, and *CXCL10*) were selected based on concentration-response curves

from microarray studies with PFOS-exposed HepaRG cells, being members of modulated genes sets and covering various biological processes (see Louisse et al., 2023, in press). Some information on these genes is presented below:

ATF4: encodes for the activating transcription factor 4, activated upon endoplasmic reticulum stress and amino acid starvation (Harding et al. 2003), upregulating genes important for cell recovery, adapting to stress conditions, and cell homeostasis (Rozpedek et al. 2016). Within the upregulated gene set 'ATF4 activates genes in response to endoplasmic reticulum stress' (see Louisse et al. 2023, in press).

SLC7A11: encodes for an amino acid transporter and upregulated by ATF4 upon amino acid starvation (Martin and Gardner 2015). Within the upregulated gene set 'Amino acid transport across the plasma membrane' (see Louisse et al. 2023, in press).

YARS1: encodes for tyrosyl-tRNA synthetase, upregulated by ATF4 upon amino acid starvation (Han et al. 2013; Krokowski et al. 2013). Within the upregulated gene set 'Cytosolic tRNA aminoacylation' (see Louisse et al. 2023, in press).

PDK4: encodes for pyruvate dehydrogenase kinase 4; it has been reported to be regulated by PPAR α (Wigger et al. 2019). Considered to be part of the PPAR α response genes (see Louisse et al. 2023, in press).

ANGPTL4: encodes for angiopoietin-like protein 4 (ANGPTL4), important in regulating angiogenesis and glucolipid metabolism (Hato et al. 2008). The regulation of its expression has been reported to be mediated via PPARs and HIF-1 α (La Paglia et al. 2017). Considered to be part of the PPAR α response genes (see Louisse et al. 2023, in press).

HMGCR: encodes for the rate-limiting enzyme of the cholesterol biosynthetic pathway hydroxy-3-methylglutaryl coenzyme A reductase (converts HMG-CoA to mevalonate) in the liver (Brown and Goldstein 1997; Trapani et al. 2012). Member of the downregulated gene set 'Cholesterol biosynthesis' (see Louisse et al. 2023, in press).

LSS: encodes for lanosterol synthase which catalyzes the conversion of (S)-2,3-oxidosqualene to lanosterol in the cholesterol biosynthesis pathway (Wada et al. 2020). Member of the downregulated gene set 'Cholesterol biosynthesis' (see Louisse et al. 2023, in press).

OAT5: encodes for the organic anion transporter 5, which is an anion exchanger. The hepatic expression of the transport in the liver has been reported to be regulated via hepatocyte nuclear factor-1 α (HNF-1 α) (Klein et al., 2010).

THRSP: encodes for the thyroid hormone responsive protein that plays a role in the regulation of lipid metabolism. Expression has been reported to be downregulated upon fasting (Kuemmerle and Kinlaw 2011).

CXCL10: encodes a chemokine of the CXC subfamily, which is involved in monocyte, natural killer cell and T-cell migration, regulation of T-cell and bone marrow progenitor maturation, modulation of adhesion molecule expression, and inhibition of angiogenesis (Neville et al. 1997).

It was previously suggested that PFOA and PFOS may affect different aspects of cholesterol homeostasis, including its intrahepatic *de novo* biosynthesis, import/export from the liver, as well as its catabolism to bile acids (Fragki et al. 2021). As such, a set of key genes of these three processes were selected, including two genes that were studied in our previous study (Louisse et al. 2023, in press):

HMGCR and *LSS*: see information above

CYP7A1: regulates the pathway of cholesterol conversion into bile acid, by encoding the rate-limiting enzyme cholesterol 7- α -hydroxylase (Tavares-Sanchez et al. 2015).

CYP8B1: encodes for the protein sterol 12- α -hydroxylase, a key regulatory enzyme in the bile acid formation from cholesterol (Tavares-Sanchez et al. 2015).

LDLR: encodes for the low density lipoprotein receptor, main receptor involved in the uptake of cholesterol from the blood to the liver, regulating as such serum cholesterol levels (Brown and Goldstein 1997; Trapani et al. 2012).

SREBF2: gene encoding the sterol regulatory element binding protein 2 (isoform 2); transcription factor that stimulates in parallel the *de novo* hepatic cholesterol synthesis and its clearance from the blood. *HMGCR*, *LDLR*, as well as many other genes of the cholesterol biosynthesis pathway are under the control of SREBF (Horton et al. 2002; Shao and Espenshade 2012). Member of the downregulated gene set 'Regulation of cholesterol biosynthesis by SREBP (SREBF)' (Louise et al. 2023, in press).

For the two genes *HMGCR* and *LSS* of the cholesterol biosynthetic pathway, RT-qPCR gene expression concentration-response data were used as generated earlier (Louisse et al. 2023, in press). An RT-qPCR analysis of the concentration-dependent effects of all four PFASs (PFOA, PFNA, PFHxS, PFOS) on the other four genes was performed in the present study.

RT-qPCR for the four cholesterol-related genes: CYP7A1, CYP8B1, LDLR, and SREBF2

For the four selected genes linked to cholesterol homeostasis, concentration-dependent expression levels were determined in PFAS-exposed HepaRG cells. cDNA samples from our earlier study (Louisse et al. 2023, in press) were used. Changes in the expression of genes were determined by RT-qPCR on a CFX384 real-time PCR detection system (Bio-Rad Laboratories) by the application of SensiMix (Bioline; GC Biotech, Alphen aan den Rijn, The Netherlands). The PCR conditions consisted of an initial denaturation at 95°C for 10 min, followed by 40 cycles of denaturation at 95°C for 10 s and annealing extension at 60°C for 15 s. Relative gene expression was quantified with the standard curve method, using a standard curve generated from a serial dilution of pooled sample cDNA, and subsequently normalized to the housekeeping gene RPL27. Primer sequences were taken from the Harvard PrimerBank and ordered from Eurogentec (Liège, Belgium) and are presented in Table 1. Statistical differences were assessed by performing a one-way ANOVA followed by Dunnett's multiple comparison test on the normalized data (fold-change compared

to the solvent control) using Graphpad Prism 9.3.1, considering a p value < 0.05 as being statistically significant. The concentration–response data were used for the QIVIVE and consequent benchmark dose (BMD) analysis as described below.

TABLE 1 Primer sequences used for RT-qPCR.

Primer Sequence		
Name	Forward	Reverse
CYP7A1	TGATGATCTGGAGAAGCCAAGA	AGAAAGTCGCTGGAATGGTGTIT
CYP8B1	CTTGTTCCGGCTACACGAAGGA	GCAGGGAGTAGACAAACCTTG
SREBP2	GGCTGTTTGGACTGGATGAT	CACAAAGACGCTCAGGACAA
LDLR	GACGTGGCGTGAACATCTG	CTGGCAGGCAATGCTTTGG
RPL27	ATCGCCAAGAGATCAAAGATAA	TCTGAAGACATCCTTATTGACG

PBK model-based reverse dosimetry approach

General outline

The PBK model-based reverse dosimetry approach consists of the extrapolation of short term (24 hours) *in vitro* concentrations to the corresponding chronic human dietary exposure. This approach starts with the definition of the *in vitro* Point of Departure (PoD). In this manuscript two PoD options were considered: the PFASs nominally added *in vitro* concentrations (scenarios 1 and 2) or the cell-associated concentrations (scenario 3; considered as intracellular concentrations). As PFOA, PFNA, PFHxS and PFOS have long elimination half-lives (in the range of years) and (dietary) human exposure lasts chronically, an AUC approach was applied. As such, the aforementioned *in vitro* PoDs were converted into 24 hour Area Under the Curve values (AUC_{24hr}) (see below for more information). Thereafter, PBK modelling was applied for the calculation of the corresponding chronic human dietary exposure which (over time) would lead to the same AUC value in the target organ of interest, in this case the human liver. As an exposure scenario the 50 years (i.e. AUC_{50yr}) were used, since it was considered to represent the lifetime exposure to PFASs, in accordance with EFSA (EFSA CONTAM Panel 2020b). In other words, the approach contains the underlying assumption that AUC_{24hr} *in vitro* and AUC_{50yr} *in vivo* are equipotent in inducing gene expression changes and/or TG accumulation. In this way for each of the *in vitro* tested concentrations a corresponding chronic human exposure was obtained. Finally, the latter were analysed with BMD modelling to obtain the exposure levels corresponding with a benchmark response (BMR) of 20% for lipid accumulation and 50% for gene expression (oral equivalent effect dose). The selected BMRs were here a practical choice since it is currently not clear whether such changes (%) are associated with an adverse outcome. The 20% BMR for lipid accumulation was chosen as a level just above the normal variation in the control data and therefore, can be considered a minimally measurable effect size. The 50% BMR for gene expression was chosen given the large variation in gene expression responses per concentration tested.

Finally, the calculated oral equivalent effect doses were compared to the mean current European dietary exposure.

Selection of the *in vitro* Point of Departure: three possible scenarios

Since liver cells (HepaRG) are used *in vitro* either one of the following three extrapolation scenarios was applied:

Scenario 1: The nominal PFAS concentration in the medium added to the HepaRG cells equals to the PFAS concentration in the liver.

Scenario 2: The nominal PFAS concentration in the medium added to the HepaRG cells equals the PFAS concentration in blood flowing to the liver tissue. As such, the PFAS concentration in the liver equals the nominal PFAS concentration in the medium multiplied by the liver:blood partition coefficient.

Scenario 3: The cell-associated concentration measured in HepaRG cells equals to the PFAS liver concentration. To ensure the same concentration metric of both concentrations, the cell-associated concentration expressed in mol/g protein was converted into a liver concentration (in mol/kg liver) (see Supplementary Table 2)

For the details on the calculations see Supplementary Material (Table 2).

Application of the PBK models (QIVIVE)

For both PFOA and PFOS the existing human PBK models of Loccisano et al. (2011) were used, with the modified Berkeley Madonna (BM) code of EFSA (EFSA CONTAM Panel 2018b). To our knowledge, no PBK models are available for PFNA and PFHxS. Therefore, the PFOA and PFOS PBK models were re-scaled with respect to the PBK transporter maximum capacity for renal tubular reabsorption in order to reach the reported human elimination half-lives of PFNA and PFHxS.

Mean elimination half-lives of 3.2 and 8.2 years were applied for PFNA and PFHxS, (Olsen et al. 2007; Zhang et al. 2013b). Prior to the renal reabsorption, tissue: blood partition coefficients were adapted for the liver and kidney for both chemicals (see for data Supplementary Table 3). By applying the PBK model reverse dosimetry approach the *in vitro* concentration-response TG accumulation and gene expression data were translated into their corresponding oral human equivalent *in vivo* dose-response data for all three scenarios mentioned above. As mentioned above, due to the long elimination half-lives (in the range of years) and chronic human exposure, an AUC approach was applied. The concentration-response data from the HepaRG cells were translated to AUC-response data (AUC_{24hr}) by multiplying the target concentration (separately for the three scenarios) with the assay duration (24 hours) (Daston et al. 2010). As such, the liver AUC to be reached with the PBK modelling (irrespective of the exposure scenario applied) equals to:

Scenario 1: the nominal *in vitro* concentration * 24 hrs.

Scenario 2: the nominal *in vitro* concentration * the liver: blood partition coefficient* 24 hrs.

Scenario 3: the cell-associated concentration * 24 hrs.

Derivation of human oral equivalent doses

As mentioned above the *in vitro* concentration-response gene expression data as well as the TG accumulation data were translated via PBK modelling into their corresponding oral human equivalent *in vivo* dose-response data. The original *in vitro* data for TG accumulation and gene expression (of the 10 genes) are presented in Louisse et al. (2023, in press). BMD modelling was applied on the estimated human oral equivalent dose-response data resulting from the reverse-dosimetry approach, using the PROAST software (version 70.6) (Slob 2002). The data were analysed as continuous and benchmark doses (BMD) were determined for a benchmark response (BMR) of 20% for TG accumulation and 50% for gene expression. The applied benchmark responses were here a pragmatic choice, but it is currently not clear whether such changes (%) are associated with an adverse outcome.

Dose-response modelling was applied using the exponential model:

$$y = a * c^{1 - \exp(-(x/b)^d)}$$

with parameters a, b and d describing the response at dose 0 (background value), the potency of the chemical, maximum fold change in response compared with background response (upper or lower plateau), and steepness of the curve (on a log-dose scale), respectively. The models were fitted to the data of all PFASs simultaneously by using covariate analysis (EFSA 2017) to ensure parallel curves (on a log dose scale). The model was fitted with and without estimating parameter c, and the fit with the lowest Akaike information criterion (AIC) was selected. Some datasets do not provide information on the maximum fold change in response, and do not allow the estimation of parameter c. As such the BMD_{20} and BMD_{50} and their underlying 90% confidence interval (lower bound: BMDL, upper bound: BMDU) were estimated for TG accumulation and for each of the selected genes, respectively, and represent the oral equivalent effect doses based on these *in vitro* data.

Comparison with reference values for dietary exposure

The resulting oral equivalent effect dose confidence intervals (CI) were compared with the chronic dietary intake as recently evaluated by EFSA for the four chemicals (EFSA CONTAM Panel 2020b). In its evaluation EFSA (see EFSA report Table 10) provides the following summary statistics of the mean and 95th percentile lower bound (LB) and upper bound (UB) chronic dietary exposure for PFOA, PFNA, PFHxS and PFOS for adults across European countries. For the comparisons with the calculated oral equivalent effect doses the mean median LB and UB exposures were used here (Table 2).

TABLE 2 Dietary exposure of adults to the four PFASs as presented by EFSA (EFSA CONTAM Panel 2020b).

PFAS	Range of mean dietary exposure in adults (LB-UB)(ng/kg bw per day)					
	Mean LB dietary exposure			Mean UB dietary exposure		
	Minimum	Median	Maximum	Minimum	Median	Maximum
PFOA	0.13	0.18	0.28	3.60	4.18	5.71
PFNA	0.02	0.04	0.07	3.08	3.68	5.25
PFHxS	0.06	0.08	0.11	2.86	3.45	5.06
PFOS	0.29	0.58	0.93	3.82	4.47	5.94

PFAS	Range of P95 percentile dietary exposure in adults (LB-UB)(ng/kg bw per day)					
	95 th percentile LB dietary exposure			95 th percentile UB dietary exposure		
	Minimum	Median	Maximum	Minimum	Median	Maximum
PFOA	0.32	0.40	0.59	7.76	8.37	15.92
PFNA	0.06	0.10	0.18	5.80	7.46	15.42
PFHxS	0.15	0.18	0.24	5.36	7.13	15.22
PFOS	0.84	1.71	4.79	7.53	9.31	16.31

Comparison with clinical trial with administration of high PFOA doses

An additional QIVIVE was performed only for PFOA in order to compare *in vitro* based equivalent effect dose for changes in gene expression of cholesterol-related genes with doses shown to decrease serum cholesterol in cancer patients (Convertino et al. 2018). In accordance with the Convertino clinical study, a different exposure scenario was used here, i.e. administration of PFOA for 6 weeks (one exposure per week). The same procedure as described above was applied, but in this case only for *scenario 3*, since it was considered to be the most relevant dose metric.

Results

In vitro biokinetic assays

The time-dependent cellular uptake was determined for 6.25 μM PFOS and 6.25 μM PFOA, and the concentration-dependent uptake was determined upon 24 hours exposure for all PFASs tested in this study. In these biokinetic studies, protein concentrations of cell lysates were determined and cellular PFAS content was normalized to total measured cellular protein (expressed as amount PFAS per mg protein). Total protein content appeared stable across the different treatments for all PFASs, except for the highest concentration level for PFNA (100 μM ; Supplementary Figure 1 & 2). In the experiment on time-dependency, HepaRG cells were exposed to a single concentration (6.25 μM) of PFOA or PFOS for 5, 15, 60 minutes or 6 or 24 hours, to identify the time-point at which steady-state cellular concentrations are reached. Maximum cellular concentrations were achieved already at around 1 hour of exposure, which remains to be stable up to the final time point assessed (24 hours), suggesting that a steady-state concentration is reached rather quickly (Figure

1A). As expected based on PFAS-physicochemical properties, these data clearly illustrate the stability of the chemicals in the *in vitro* system over time. Based on these results a 24-hour exposure was considered relevant for the continuation of the experiments, as the *in vitro* effects studies used for QIVIVE were also performed upon a 24-hour exposure.

HepaRG cells were exposed for 24 hours to increasing concentrations (0, 6.25, 12.5, 25, 50, and 100 μM) of the four PFASs: PFOA, PFNA, PFHxS, PFOS and their cellular levels were determined. The results demonstrate that at equal nominal concentrations, different cellular exposure occurs depending on the PFAS, suggesting the importance of determining the cellular levels of such compounds (Figure 1B). Overall, the highest cellular concentrations over the concentration-range were reached by PFOS, followed by PFNA that also achieved an equally high cellular level when applied at the maximum nominal concentration (100 μM). Nevertheless, given the observed low protein content (Supplementary Figure 1) this concentration level was excluded from the QIVIVE analysis, as this may indicate a possible cytotoxic effect at this condition, even though this concentration was not considered to be cytotoxic based on data obtained from the WST-1 assay in our previous study (Louisse et al. 2023, in press).

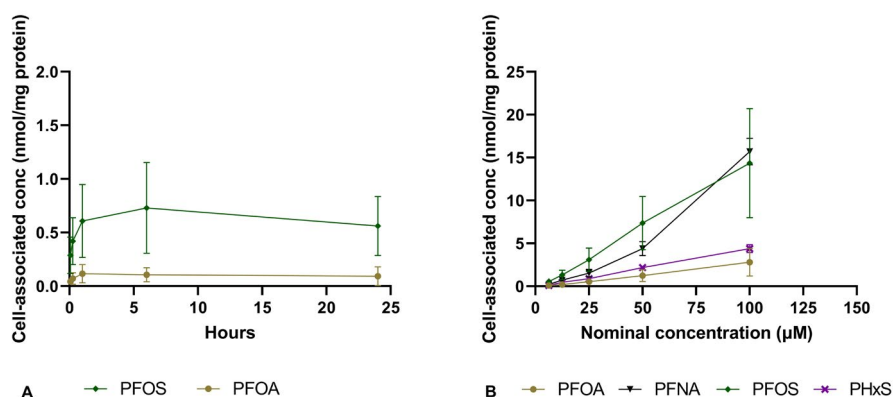
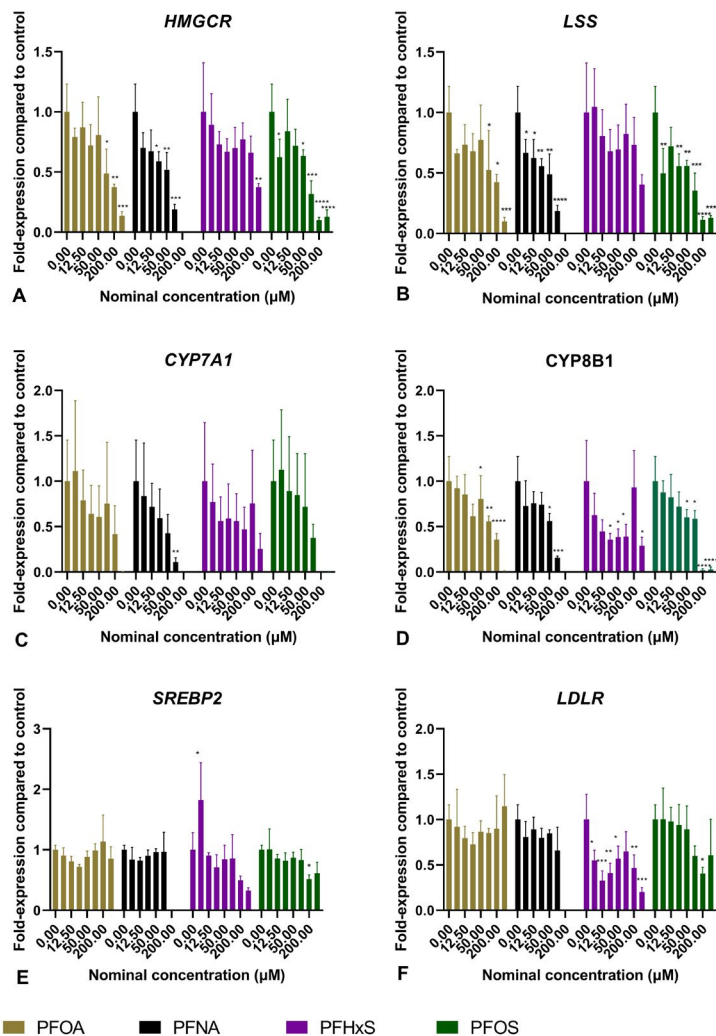


FIGURE 1 Biokinetic assays in the HepaRG cells. A. Time-dependent cell-associated concentrations upon exposure to 6.25 μM of PFOA or PFOS. B. Cell-associated concentrations upon 24-hour exposure to different concentrations (6.25, 12.5, 25, 50, and 100 μM) of PFOA, PFNA, PFHxS or PFOS. Data presented as mean and SD (data from three individual experiments with three replicates each).

The PFASs fraction taken up by the liver cells was estimated as the measured cell-associated mass divided by the initial total mass applied nominally to the culture medium (Table 3). In general, PFOS showed the highest uptake amongst the four chemicals, followed by PFNA. PFOA and PFHxS had lower uptake compared to the other two PFASs and their uptake was almost equivalent.

TABLE 3 Cellular uptake (%) of the four PFASs upon increasing concentrations after a 24-hour exposure. Mean values of three individual experiments (three replicates each) are presented per substance and for each concentration.

HepaRG uptake (%) of PFASs					
Nominal concentration (μM)	6.25	12.5	25	50	100
PFOA	0.55	0.84	1.23	1.34	1.55
PFNA	1.12	2.34	2.65	3.46	5.00
PFHxS	0.40	1.23	1.33	1.49	1.64
PFOS	3.87	4.52	5.91	11.22	10.94

**FIGURE 2** Concentration-dependent effects induced by PFASs on the expression of genes related to cholesterol homeostasis: HMGCR (rate-limiting enzyme cholesterol biosynthesis), LSS (cholesterol biosynthesis pathway), CYP7A1 (rate-limiting enzyme bile acid synthesis from cholesterol), CYP8B1 (bile acid synthesis from cholesterol), SREBFP2 (transcription factor cholesterol biosynthesis and clearance from the blood), LDLR (main receptor cholesterol uptake from the blood to the liver). Gene expression was normalized to the housekeeping gene RPL27, and subsequently normalized to the solvent control (set at 1). Data represent the mean \pm SD of three independent experiments. Gene expression of the solvent control was set at 1. Statistically significant differences in effects compared to the solvent control are shown with * ($p \leq 0.05$), ** ($p \leq 0.01$), *** ($p \leq 0.001$), **** ($p \leq 0.0001$) (one way ANOVA, Dunnett's multiple comparison test (GraphPad Prism 9.3.1)).

RT-qPCR analysis for the genes related to cholesterol homeostasis

Six genes that have been earlier identified to play a functional role in cholesterol homeostasis (Fragki et al. 2021) and showing clear concentration-response curves for PFOS (PFOS microarray analysis-Louisse et al. 2023, in press) were selected as relevant gene expression readouts that may play a role in cholesterol perturbations *in vivo*: *HMGR*, *LSS*, *CYP7A1*, *CYP8B*, *LDLR*, *SREBF2*. The results of the RT-qPCR analysis of the concentration-dependent effects for all four PFASs (PFOA, PFNA, PFHxS, PFOS) and for all selected cholesterol key genes are shown in Figure 2. Concentration-dependent decreases in the expression of *HMGR*, *LSS*, *CYP7A1* and *CYP8B1* were recorded for the four PFASs, although not statistically significant for *CYP7A1*. Effects on *SREBP2* and *LDLR* were limited and appeared to be chemical-specific; still, there is no consistency with regard to dose response of these findings. For these reasons, these two genes were excluded from the QIVIVE analysis.

Estimation of oral equivalent doses with PBK model based reverse dosimetry

To quantitatively predict *in vivo* effects based on previously measured *in vitro* TG changes (Louisse et al. 2023, in press) and gene expression changes measured in HepaRG cells, three scenarios were explored with different dose metrics representing the concentration at target tissue (see details Supplementary Table 2). In *scenario 1* the nominal concentration applied in the culture medium was considered to equal the PFASs liver concentration. In *scenario 2* the PFASs liver concentration was determined by the liver: blood partition coefficient. Lastly, in *scenario 3* the experimentally measured cell-associated concentrations were used. Figure 3 shows the related concentration-response data for the four PFASs for the liver based on these three scenarios, using the *LSS* gene as an example. Details on the conversion of nominal concentrations to oral equivalent doses using the three scenarios are presented in Supplementary Table 2.

Daily, continuous oral exposure

The *in vitro* concentration-response data for gene expression and TG changes upon PFASs exposure were translated into the corresponding *in vivo* oral equivalent dose response-data. As a starting point for corresponding liver tissue concentration the three scenarios were applied (Figure 3). For each scenario, toxicity was related to the AUC, considering the chronic, low exposure of humans to PFASs as well as their accumulation within the body. The resulting *in vivo* dose response curves were analysed with a BMD analysis and the BMD, as well as the corresponding lower (BMDL) and upper (BMDU) bounds were defined for the two readouts TG accumulation and up- or down-regulation of the selected genes.

The calculated oral equivalent effect doses are shown separately for the three scenarios in Figures 4 and 5, while results of *scenario 3* are presented in more detail in Table 4 (for scenarios 1 and 2 see Supplementary Table 4). The BMD analysis is reported in the Supplementary Material. The bars in the Figures illustrate the confidence intervals (CIs); in Figure 4 these are $BMDU_{50}$ - $BMDL_{50}$, while in Figure 5 this is $BMDU_{20}$ - $BMDL_{20}$. These

are here referred to as oral equivalent effect doses, resulting from the *in vitro* data for a 50% benchmark response on gene expression or a 20% benchmark response on TG level, respectively. For PFNA, PFHxS and PFOS (but not PFOA) *scenario 3* leads to higher oral equivalent effect doses, compared to the other two scenarios.

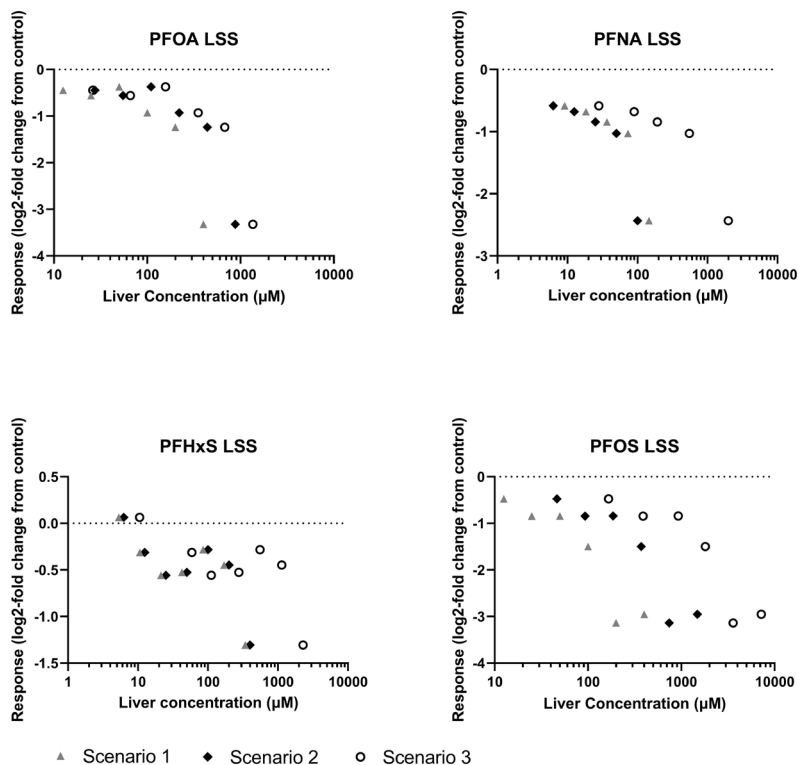


FIGURE 3 Concentration-response data of PFOA, PFNA, PFHxS and PFOS- induced effect on the expression of the LSS gene from the cholesterol biosynthesis pathway, in HepaRG cells. Gene expression was quantified with RT-qPCR. Nominal concentrations were converted to liver concentrations using the three scenarios as described in the text.

In the case of PFOA, values resulting from *scenarios 2* and *3* are comparable. Differences between oral equivalent effect doses based on *scenarios 1* and *2* are marginal, with *scenario 2* resulting in slightly higher values in the case of PFOA, PFOS and PFNA and slightly lower values in the case of PFHxS.

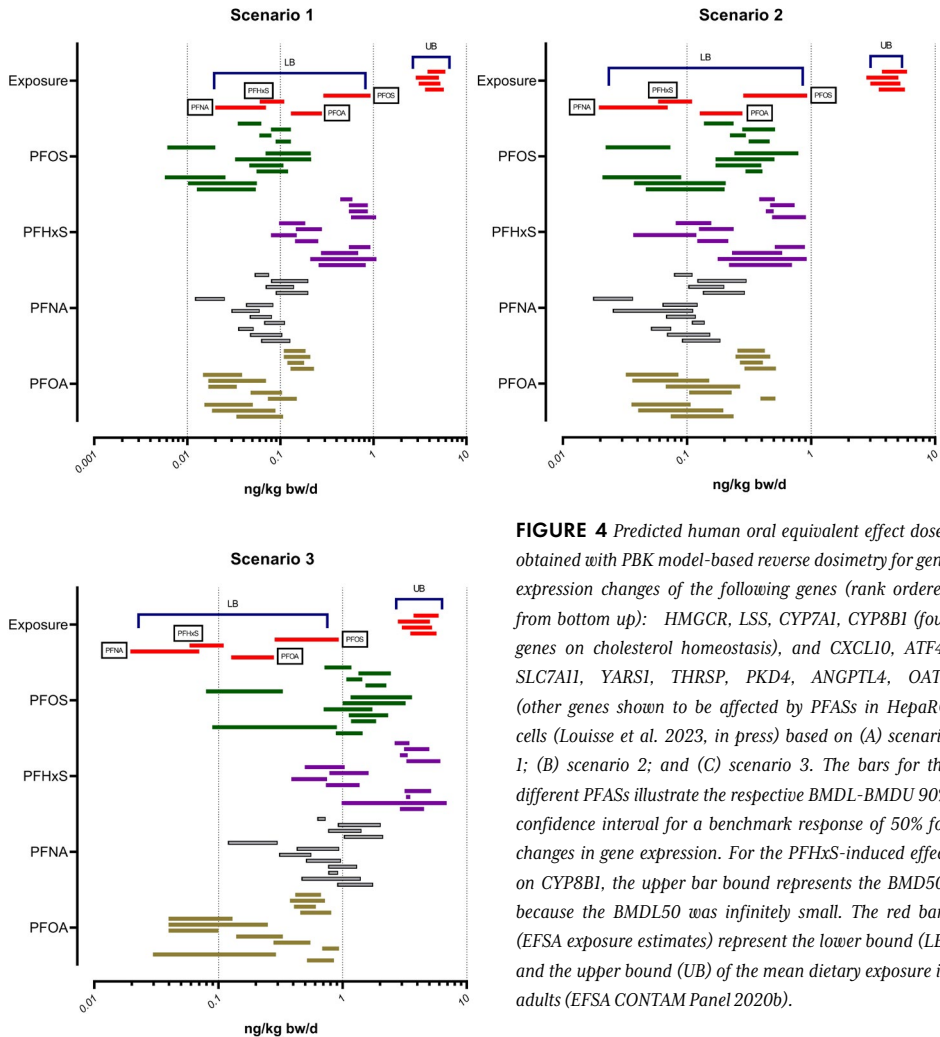


FIGURE 4 Predicted human oral equivalent effect doses obtained with PBK model-based reverse dosimetry for gene expression changes of the following genes (rank ordered from bottom up): *HMGCR*, *LSS*, *CYP7A1*, *CYP8B1* (four genes on cholesterol homeostasis), and *CXCL10*, *ATF4*, *SLC7A11*, *YARS1*, *THRSP*, *PKD4*, *ANGPTL4*, *OAT5* (other genes shown to be affected by PFASs in HepaRG cells (Louisse et al. 2023, in press) based on (A) scenario 1; (B) scenario 2; and (C) scenario 3. The bars for the different PFASs illustrate the respective BMDL-BMDU 90% confidence interval for a benchmark response of 50% for changes in gene expression. For the PFHxS-induced effect on *CYP8B1*, the upper bar bound represents the BMD50, because the BMDL50 was infinitely small. The red bars (EFSA exposure estimates) represent the lower bound (LB) and the upper bound (UB) of the mean dietary exposure in adults (EFSA CONTAM Panel 2020b).

It is important to note that the oral equivalent effect doses derived based on TG accumulation data appear to be in the same range as the oral equivalent effect doses based on gene expression changes, for PFOA, PFHxS and PFOS. However, this is not the case for PFNA, where TG-based values seem overall higher than these based on gene expression

The *in vitro*-PBK model based oral equivalent effect doses were compared to the mean chronic dietary exposure data estimated by EFSA (EFSA CONTAM Panel 2020b). When exposure is based on the lower bound (LB), gene expression changes may be expected with scenarios 1 and 2. In the case of scenario 3 mean LB exposure exceeds the gene expression-based oral equivalent effect doses for PFOA and PFOS, but not for PFNA and PFHxS. With regards to TG accumulation, LB dietary exposure of PFNA and PFHxS is lower than the calculated effect doses, irrespective of the applied scenario. For PFOA and PFOS this is the case only with scenario 3. Comparison with the mean upper bound (UB) exposure values

shows that dietary PFAS levels, may interfere with gene expression and hepatic lipid homeostasis.

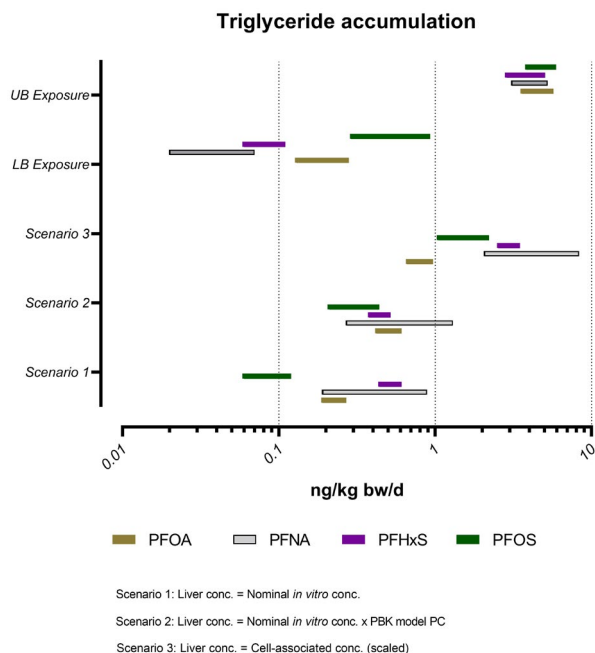


FIGURE 5 Predicted human oral equivalent effect doses obtained with PBK model-based reverse dosimetry for data on TG increase in the HepaRG cells based on (A) scenario 1; (B) scenario 2; and (C) scenario 3. The bars for PFASs illustrate the respective BMDL-BMDU 90% confidence interval for a benchmark response of 20% for triglyceride increase. LB: lower bound and UB: upper bound of the mean dietary exposure in adults (EFSA CONTAM Panel 2020b).

TABLE 4 Predicted human oral equivalent effect doses (ng/kg bw/d) (BMD_{50} s for gene expression, BMD_{20} s for TG accumulation, and underlying CI) with PBK model-based reverse dosimetry for the 12 selected genes, applying scenario 3. Exposure conditions: continuous oral exposure, 50 years.

	PFOA	PFNA	PFHxS	PFOS
HMCCR	0.7 0.52-0.85	1.2 0.91-1.76	3.6 2.92-4.53	1.2 0.89-1.45
LSS	0.1 0.03-0.29	0.8 0.47-1.4	2.4 0.99-6.9	0.3 0.09-0.9
CYP7A1	0.8 0.69-0.94	0.8 0.77-0.92	3.5 3.27-3.51	1.4 1.18-1.52
CYP8B1	0.4 0.28-0.55	1.0 0.77-1.31	5.2 3.18-inf.	1.7 1.13-2.33
CXCL10	0.2 0.14-0.33	0.7 0.51-0.97	1.0 0.74-1.37	1.1 0.71-1.74
PKD4	0.06 0.04-0.1	0.4 0.31-0.56	0.5 0.39-0.75	2.0 1.01-3.22
ANGPTL4	0.09 0.04-0.25	0.7 0.43-0.94	1.1 0.79-1.62	2.2 1.17-3.62

	PFOA	PFNA	PFHxS	PFOS
<i>OAT5</i>	0.08 0.04-0.13	0.2 0.12-0.3	0.7 0.5-1.04	0.2 0.08-0.33
<i>ATF4</i>	0.6 0.46-0.81	1.4 1.03-2.12	4.2 3.29-6.13	1.9 1.54-2.25
<i>SLC7A11</i>	0.5 0.41-0.61	0.9 0.77-1.42	3.4 2.92-3.35	1.3 1.08-1.44
<i>YARS1</i>	0.5 0.38-0.72	1.2 0.92-2.03	3.8 3.15-4.99	1.9 1.35-2.45
<i>THRSP</i>	0.5 0.42-0.67	0.7 0.63-0.73	3.0 2.65-3.45	1.0 0.72-1.18
Triglyceride accumulation	0.8 0.66-0.97	3.2 2.06-8.35	3.0 2.53-3.49	1.5 1.05-2.21

Subacute oral exposure

An additional simulation was performed for PFOA in order to simulate the exposure conditions as applied in the Convertino et al. study (2018) (6 weeks, once per week). In this phase I clinical trial, PFOA was administered to cancer patients (50-1200 mg), once per week, for six consecutive weeks. A decline in total blood cholesterol was reported at plasma PFOA levels starting at 420-565 μM (approximately 175,000-230,000 ng/mL) and corresponding to administered doses of 450 mg and above. The modelled plasma concentrations of PFOA over time and for the different dose groups is shown in Figure 6. Comparisons with the *in vivo* data from Convertino et al. (2018) (see Figure 2 of original paper) demonstrate a good PBK model prediction, supporting the use of the model for this QIVIVE.

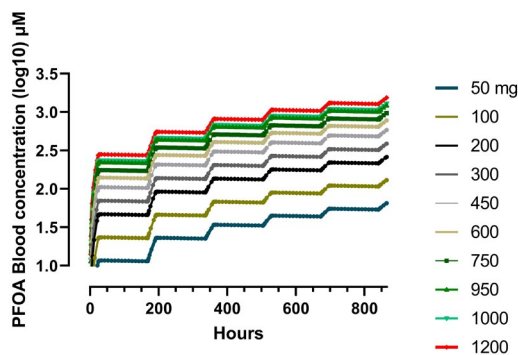


FIGURE 6 PBK model predicted blood concentrations of PFOA over time when administered orally at different doses, once per week, for six consecutive weeks (simulating exposure used in Convertino et al. (2018)).

Similarly as for the earlier simulations for a continuous exposure the *in vitro* concentration-response data of the cholesterol homeostasis genes were translated into *in vivo* oral equivalent dose response-data by PBK model-based reverse dosimetry, but this time based on the Convertino et al. (2018) exposure conditions. As a starting point for the extrapolations the measured PFASs cell-associated concentrations were used (*scenario 3*),

since this was considered to be the most relevant *in vitro* dose metric. Since the Convertino et al. (2018) measured effects on cholesterol levels in the patients, only the four genes directly relevant for cholesterol homeostasis were used. Subsequently, the results were processed with a BMD analysis. Again here, toxicity was related to the AUC, considering the toxicokinetic profile of PFASs and their accumulation within the body. This is considered justified given the PFOA blood level trajectory during the 6-week period, where a Cmax cannot be identified (Figure 6). Table 5 depicts the predicted *in vivo* human oral equivalent doses for PFOA, which appear to be considerably lower (40- to 60-fold) compared to the starting dose (450 mg) at which decreased cholesterol was reported in the clinical trial (Convertino et al. 2018).

TABLE 5 Predicted human oral equivalent effect doses (in mg) (BMD_{50} s and the underlying CI) with the PBK model-based reverse dosimetry for the cholesterol-related genes. Exposure conditions: oral repeated dose, once per week, for six weeks.

Gene	HMGCR	LSS	CYP7A1	CYP8B1
BMD_{50}	7.1	11.0	7.4	7.3
BMDL-BMDU	4.3-9.9	8.8-13.2	5.6-9.5	6.1-8.7

Discussion

The aim of this study was to assess the feasibility of determining human oral equivalent effect doses of PFAS-induced lipid perturbations and hepatotoxicity, for the four PFASs: PFOA, PFNA, PFHxS and PFOS, by a combined *in vitro-in silico* approach. *In vitro* concentration-response data (TG accumulation and gene expression changes of 12 selected genes) measured in HepaRG cells were translated into equivalent human dose-response curves, with PBK model-facilitated reverse dosimetry. An exposure scenario of 50 years was considered in order to represent the lifetime chronic exposure to PFASs. For reverse dosimetry, cellular PFAS levels were determined in the HepaRG cells to link *in vitro* exposure to *in vivo* internal exposure in the liver. A BMD analysis of the obtained dose-response data resulted in oral equivalent effect doses, i.e. the chronic human dietary exposure, which may be indicative of hepatic lipid perturbation and liver toxicity. Finally the oral equivalent effect doses were compared with the human dietary exposure as recently determined by EFSA for the European population. For the case of PFOA, oral equivalent effect doses were also compared to serum levels found to induce blood cholesterol decrease in cancer patients, with an exposure scenario of 6 weeks. Oral equivalent effect doses were found to be in the same range as estimated human exposure levels, in particular when the UB estimates were considered. Effect doses of PFOA on expression of cholesterol-related genes were estimated to be 40- to 60-fold lower than the doses causing effects on cholesterol in cancer patients. This approach used in this study may be used to obtain points of departure (PODs) for screening, hazard identification and prioritization of other PFASs for which data are lacking.

Applied QIVIVE starting point scenarios

For the present QIVIVE three different types of *in vitro* dose metrics were used to relate to the observed responses, as potential surrogates for the PBK liver concentration: the nominal assay concentration (*scenario 1*), the nominal concentration corrected for *in vivo* liver: blood partitioning (*scenario 2*), and the measured cell-associated concentration scaled to the whole liver (*scenario 3*). The results of the three scenarios were compared with each other. *A priori*, it has been suggested that the most appropriate dose metric to relate to an *in vitro* response would be the concentration at the site of action (Escher and Hermens 2004; Groothuis et al. 2015), so here the PFASs concentration within the HepaRG cells or else, the cell-associated concentration (*scenario 3*). The results of the present study demonstrate oral equivalent effect doses based on *scenario 3* to be the least conservative, i.e. resulting in higher effect doses, followed by *scenario 2*, and *scenario 1*, for PFNA, PFHxS and PFOS (but not for PFOA). Differences between scenarios 1 and 2 were marginal, as expected here, since the applied liver: blood PCs do not deviate much from 1 (SM Table 3, range 0.85 – 3.73). However, for other chemicals with larger PCs *scenario 1* and 2 would deviate more from each other. Findings were different for PFOA, where oral equivalent effect doses for *scenarios 2* and 3 were overall comparable, whereas *scenario 1* gave lower values. Assuming that *scenario 3*, as applied here, represents by theoretical considerations the best QIVIVE dose metric (Groothuis et al. 2015), and seeing clearly that it makes a difference for three out of the four chemicals, we favor the use of experimentally measured *in vitro* intracellular concentrations for the PFASs. Nevertheless, due to practical difficulties intracellular concentrations are seldomly measured in *in vitro* toxicity assays (Groothuis et al. 2015). In that case, *scenario 2* may be used as a proxy, applying *in vivo* measured organ: blood partition coefficients or, when unavailable, partition coefficients estimated based on chemical characteristics like LogP and pKa.

HepaRG cell uptake and *in vivo* organ: blood partitioning

In most *in vitro* studies with PFASs, only the concentrations applied to the medium are presented, whereas actual intracellular concentrations are not considered. An important contribution of this study is the reporting of actual PFAS cell-associated concentrations in the *in vitro* system, by measuring the fraction retained in the cells 24 hours after exposure. The data demonstrate differences between the four PFASs with regard to cellular uptake. Cell-associated concentration increased with increasing treatment concentrations, whereas it appears to level off at higher levels, suggesting saturation of binding sites. The levelling off is more profound for the two sulfonates. At the same concentration (50 μM) PFOS cell-associated concentration was shown to be ~ 11% of the applied amount, whereas this was 7-fold lower for PFOA and PFHxS. For PFNA cell-associated concentration was around 3% at the same concentration (PFOS > PFNA > PFOA ~ PFHxS). This result is in line with *in vivo* data on liver: plasma partitioning for PFASs in rats from recent NTP studies (NTP 2019a; 2019b), where PFOS shows the highest distribution/accumulation within the liver, compared to the other three compounds. This is probably due to differential binding

to hepatic proteins, like for example, the human liver fatty acid binding protein (L-FABP), which has as main function the transport and uptake of fatty acids (Thumser and Wilton 1996). All four PFASs are reported to bind to L-FABP (Luebker et al. 2002b; Sheng et al. 2016; Woodcroft et al. 2010; Zhang et al. 2013a); however, with PFOS and PFNA showing the highest affinity (Zhang et al. 2013a). Possibly, simple binding studies with PFASs and such proteins can provide insight into which members of the group are expected to show higher partitioning into tissues *in vivo*. Next to this, organic cation transporters OATP1B1, OATP1B3, and OATP2B1, as well as Na⁺/taurocholate co-transporting polypeptide (NTCP), which are expressed in the liver, are known to transfer PFAS across the cell membrane in the cytosol (Ruggiero et al. 2021; Zhao et al. 2015a; Zhao et al. 2017b). Again here, transporter affinity and transport efficiency differ between PFASs, with PFOS showing the most efficient transport.

It is interesting to note that in another study with human hepatocarcinoma HepG2 cell line, PFOS cellular uptake was significantly lower compared to the other three chemicals (Rosenmai et al. 2018). Next to this, for the four PFASs the percentage uptake was much lower (0.04-0.33%) in the HepG2 cells compared to our study. This difference might stem from the fact that HepaRG cell line possesses unique characteristics in transporter expression (Kotani et al. 2012; Le Vee et al. 2006), whereas HepG2 cells show very low expression of these uptake transporters (Cui et al. 2003; Le Vee et al. 2006). Another explanation could be different used serum concentrations (2 vs 10%) that have probably resulted in less bioavailable PFASs for uptake in the cell medium. The latter seems a reasonable hypothesis, considering the known high binding to the medium serum proteins, of these chemicals (Beesoon and Martin 2015; Ehresman et al. 2007; Han et al. 2012)

Applied QIVIVE dose metric: exposure metric

From an exposure perspective, the toxicity of a chemical can be linked to different internal dose metrics, like the peak concentration (C_{max}), or the AUC. The parameter to use for relating exposure to toxicity depends on the mode of action of the chemical (Groothuis et al. 2015; Louisse et al. 2017), its toxicokinetic properties, but also the exposure conditions (Groothuis et al. 2015). In the current literature, QIVIVE with reverse dosimetry is often based on the C_{max} (Chen et al. 2018b; Fragki et al. 2022; Li et al. 2017a) and less commonly on the AUC (Louisse et al. 2015). Here, the assumption was made that the toxic effect is best related to a time-dependent dose metric, since exposure of humans to PFASs is chronic and their elimination half-lives are rather long (in the range of years). In addition, the effects *per se*, i.e. the PFAS-induced increases in serum cholesterol (and occasionally TG), but also in serum ALT (for PFOA) as reported in epidemiological studies, are a result of continuous exposure, supporting further the choice of a cumulative metric, in this case the AUC.

This approach for extrapolating from a single 24-hour exposure occurring *in vitro* to a life-time *in vivo* exposure is uncertain, but can serve at least as a first tier in human health risk assessment provided the appropriate *in vitro* data are available. For a wider application of QIVIVE in risk assessment, well-defined criteria for selecting the most appropriate dose

metric have to be put forward, in order to extrapolate short-term *in vitro* data to chronic toxicity (Macko et al. 2021).

Applied PBK models

For PFOA and PFOS the existing human PBK models (Loccisano et al. 2011) were used as adapted by EFSA (EFSA CONTAM Panel 2018b). Given the lack of available models for PFNA and PFHxS, the models of PFOA and PFOS, respectively, were used after adaptations. These changes pertain to adaptation in substance specific liver: and kidney: blood partition coefficients, but also to the transporter capacity for renal tubular re-absorption (Tmc). As such the transporter capacity was modified for each substance in order to achieve the correct half-life for PFNA (3.2 years) and PFHxS (8.2 years) (Olsen et al. 2007; Zhang et al. 2013b). However, due to the absence of suitable human biomonitoring data, the PFNA and PFHxS models could not be verified directly on such data, as it has been done for PFOA and PFOS (EFSA CONTAM Panel 2018b; Loccisano et al. 2011). It is of interest to note, though, that the fitted values for renal tubular re-absorption (Tmc) are in line with recently reported *in vitro* Vmax values for OAT4-mediated reabsorption of PFASs, i.e. showing the highest Vmax and Tmc for PFNA, followed by PFHxS, PFOA and PFOS (Louisse et al. 2022). This suggests that, in the absence of *in vivo* kinetic data, *in vitro* kinetic data may be of use to extend the PFOA/PFOS/PFNA/PFHxS PBK model for even more PFASs.

As a general remark, it is highlighted that the PBK models (for all four PFASs) and also the reverse dosimetry approach applied for the translation of *in vitro* concentrations to external doses use a deterministic approach, with all parameters fixed and as such, it does not accommodate for any uncertainty. It is acknowledged that parameter value uncertainty shall be taken into consideration when using such models for QIVIVE, although this was considered beyond the scope of the present paper.

Toxicological relevance of *in vitro* effects and comparison with dietary exposure

In the current approach, the BMRs 20 and 50% were selected, for cellular TG accumulation and gene expression changes, respectively. This was a pragmatic approach, considering that the degree of change associated with adversity for these *in vitro* readouts, in particular with regard to gene expression, is not clearly known at the moment. TG accumulation in HepaRG cells was selected since PFASs are positively associated with blood TG levels in humans (for example Frisbee et al. 2010; Olsen et al. 2003a; Steenland et al. 2009) and are known to cause hepatotoxicity and liver steatosis in animals (Das et al. 2017; NTP 2019a; 2019b; Wan et al. 2012), although it remains unclear whether the latter effect is relevant for humans (Fragki et al. 2021). All four PFASs induced a concentration-dependent increase in TG accumulation in the hepatic cells (Louisse et al. 2023, in press). TG accumulation within the HepaRG cells has been suggested to be a biomarker for liver steatosis and hepatotoxicity (Lichtenstein et al. 2020). Comparison of the TG accumulation-based oral equivalent effect doses with the chronic dietary exposure data known for the adult European population (EFSA CONTAM Panel 2020b), suggests a possible interference with

hepatic lipid homeostasis, for the case of PFOA and PFOS, when the most conservative scenarios 1 and 2 are applied. It shall be noted that this result is very much dependent on the critical effect size selected, here being 20%.

Another read-out was the transcriptional changes for six genes that are known to play a key role in cholesterol homeostasis. These genes were selected to mechanistically relate changes in gene expression to the known changes in serum total cholesterol that have been repeatedly associated with PFASs blood levels (for example Eriksen et al. 2013; Nelson et al. 2010; Steenland et al. 2009). The RT-qPCR results showed a concentration-dependent decrease in four (*HMGCR*, *LSS* from Lousse et al. in preparation; *CYP7A1*, *CYP8B1*) out of the six genes induced by all chemicals. This is in agreement with other *in vitro* studies, where exposure of HepaRG cells (Behr et al. 2020a; Lousse et al. 2020c), but also human primary hepatocyte spheroids (Rowan-Carroll et al. 2021), to various PFASs was shown to induce a downregulation of several genes in the cholesterol biosynthetic pathway. Additionally, PFOS and PFOA were reported to strongly decrease bile acid synthesis, the main catabolic product of cholesterol, in HepaRG cells, both at a protein and transcriptional level (Behr et al. 2020a), like it is shown here with the downregulation of *CYP7A1* and *CYP8B1*. *CYP7A1* catalyzes the rate-limiting step for the classic bile acid synthesis from cholesterol. These results were not corroborated by intracellular changes in cholesterol levels, since these appeared to be hardly affected upon exposure to PFOS, PFOA (Behr et al. 2020a; Lousse et al. 2020c) or PFNA (Lousse et al. 2020c). This outcome suggests the presence of mechanisms balancing cholesterol levels in the HepaRG cells after PFAS-induced perturbations, as expected considering its known tight regulation within the liver (Dietschy et al. 1993; Kwiterovich 2000; Trapani et al. 2012). Consequently, measuring actual cholesterol changes (if any) within the cell system may require a more specific experimental design that would allow for the quantification of small modifications in cholesterol levels (e.g. measuring effects on *de novo* cholesterol synthesis, using labelled precursors). For the genes *SREBP2* and *LDLR* limited effects were observed after exposure to all four PFASs, in contrast to what has been reported earlier in another study (Behr et al. 2020a). It would be interesting to speculate on a potential mechanism occurring in the liver and ultimately leading to increases in serum cholesterol based on these findings. As suggested earlier by Behr and colleagues (2020a) the inhibitory effect of PFASs on *CYP7A1* could serve as the molecular initiating or key event, leading to bile acid metabolism and cholesterol perturbations. We therefore consider perturbation of *CYP7A1* expression as a sensitive biomarker for perturbed cholesterol metabolism.

Next to the cholesterol homeostasis genes, up- or downregulation of eight other genes was included as *in vitro* read-out for the QIVIVE. These genes cover diverse biological processes and they were identified in an earlier study as potential markers for liver toxicity, based on a whole genome microarray analysis performed for PFOS (Lousse et al. 2023, in press).

In the presented calculations, oral equivalent effect doses for gene expression, given the currently selected effect size (50%), are lower than the UB chronic dietary exposure

estimates. When comparing to the LB values, exceedance of the effect levels occurs with *scenarios 1 and 2* for the four PFASs, and with *scenario 3* only for PFOA and PFOS. In other words, the current dietary PFASs exposure may lead to interference with gene expression in the liver, considering the continuous, lifetime exposure to these chemicals. Linking altered expression of genes to actual measures of adversity has of course to be done with caution (Buesen et al. 2017; Sauer et al. 2017). Ideally, these genes would have been described as molecular initiating events or other key events in Adverse Outcome Pathways (AOPs), but this information is currently lacking. However, it is important to note that two of the cholesterol-related genes (*HMGCR* and *CYP7A1*) are encoding for the rate-limiting enzymes in the biosynthesis and catabolism of cholesterol, respectively. In other words, they have been assigned a pivotal biological function in these pathways and any modification of their expression could have major implications for the respective phenotype (Buesen et al. 2017). As such, we speculate that interference with the expression of these genes could ultimately result in perturbed *in vivo* cholesterol homeostasis, and consequently, in perturbed levels of blood cholesterol. Nevertheless, this should be studied in more detail, and not only at the gene expression level, but also by measurements of the activities of corresponding enzymes in the cholesterol pathway and the net effect on the cholesterol levels. Next to this, studies that assess the impact of time of exposure in the *in vitro* systems would be of interest to assess whether the extrapolation from a 24-hr exposure *in vitro* to a chronic exposure *in vivo* can be justified.

Comparison to the data from the human clinical trial

In the present QIVIVE, the exposure scenario as applied in a phase I clinical trial (Convertino et al. 2018) was also simulated for the cholesterol-homeostasis genes, given the observed decreased cholesterol seen in the patients, only for *scenario 3*. However, here the predicted oral equivalent effect doses for PFOA, were considerably lower (between 40- to 60-fold), compared to the starting dose (450 mg) at which decreased cholesterol was reported in the patients of the clinical trial (Convertino et al. 2018). Perhaps these gene expression biomarkers measured in the *in vitro* system are more sensitive as readouts compared to an *in vivo* change in blood cholesterol. In general, gene expression alterations in a biological system upon exposure to xenobiotics may serve as early indicators of eventual toxicity, and as such they may start at lower exposure levels prior to manifestation of the respective toxicity phenotype that may occur at higher doses (Gatzidou et al. 2007; Joseph 2017; Smith et al. 2020). As mentioned earlier, interpretation of changes in gene expression with regards to eventual adverse effects shall be done with caution. On the other hand, this difference could also relate to the fact that the patients exposed to these large dose of PFOA in the clinical trial, were a small population of late-stage cancer patients, perhaps with a compromised metabolic activity. Consequently, it could be that the results of the Convertino et al. (2018) study are not of relevance for the general population. Ideally, the *in vitro*-based equivalent effect doses (for the cholesterol homeostasis genes) would be compared with dose-response data from epidemiological studies that associate exposure to PFASs with

increased serum cholesterol (e.g. Eriksen et al. 2013; Frisbee et al. 2010; Steenland et al. 2009). Unfortunately, data in these publications are insufficiently reported and do not allow for a proper dose-response analysis (Minutes on the Expert Meeting;EFSA CONTAM Panel 2018c) and hence, this comparison was not considered further in our study.

Altogether, the present combined *in vitro* PBK modelling-facilitated QIVIVE illustrates that suitable PFASs *in vitro* concentration-response data can be highly valuable for the screening, prioritization and potentially risk assessment of these chemicals. This shall be done after careful consideration of the *in vitro* dose metric to be used for the extrapolations.

Acknowledgements

This work was funded by the European Unions' Horizon 2020 Research and Innovation Programme under grant agreement No 733032 HBM4EU and by the Dutch Ministry of Agriculture, Nature and Food Quality (project KB-37-002-009/010).

Conflict of interest statement

The authors declare that they have no conflict of interest.

References

- ATSDR. 2018. Toxicological profile for perfluoroalkyls. Draft for public comment june 2018. <https://www.atsdr.cdc.gov/toxprofiles/tp200.pdf>, 2018-11-10.
- Ball N, Bars R, Botham PA, Cuciureanu A, Cronin MTD, Doe JE, Dudzina T, Gant TW, Leist M, van Ravenzwaay B. 2022. A framework for chemical safety assessment incorporating new approach methodologies within reach. *Archives of toxicology*. 96(3):743-766.
- Bartell SM, Calafat AM, Lyu C, Kato K, Ryan PB, Steenland K. 2010. Rate of decline in serum pfoa concentrations after granular activated carbon filtration at two public water systems in ohio and west virginia. *Environ Health Perspect*. 118(2):222-228.
- Beesoon S, Martin JW. 2015. Isomer-specific binding affinity of perfluorooctanesulfonate (pfos) and perfluorooctanoate (pfoa) to serum proteins. *Environmental science & technology*. 49(9):5722-5731.
- Behr AC, Kwiatkowski A, Ståhlman M, Schmidt FF, Luckert C, Braeuning A, Buhrke T. 2020. Impairment of bile acid metabolism by perfluorooctanoic acid (pfoa) and perfluorooctanesulfonic acid (pfos) in human heparg hepatoma cells. *Arch Toxicol*. 94(5):1673-1686.
- Bil W, Zeilmaker M, Fragki S, Lijzen J, Verbruggen E, Bokkers B. 2021. Risk assessment of per- and polyfluoroalkyl substance mixtures: A relative potency factor approach. *Environ Toxicol Chem*. 40(3):859-870.
- Brown MS, Goldstein JL. 1997. The srebp pathway: Regulation of cholesterol metabolism by proteolysis of a membrane-bound transcription factor. *Cell*. 89(3):331-340.
- Buesen R, Chorley BN, da Silva Lima B, Daston G, Deferme L, Ebbels T, Gant TW, Goetz A, Grealley J, Gribaldo L et al. 2017. Applying 'omics technologies in chemicals risk assessment: Report of an ecetoc workshop. *Regul Toxicol Pharmacol*. 91 Suppl 1(Suppl 1):S3-s13.
- Carmichael PL, Baltazar MT, Cable S, Cochrane S, Dent M, Li H, Middleton A, Muller I, Reynolds G, Westmoreland C et al. 2022. Ready for regulatory use: Nams and ngra for chemical safety assurance. *Altex*.
- Chen L, Ning J, Louise J, Wesseling S, Rietjens IMCM. 2018. Use of physiologically based kinetic modelling-facilitated reverse dosimetry to convert *in vitro* cytotoxicity data to predicted *in vivo* liver toxicity of lasiocarpine and riddelliine in rat. *Food and Chemical Toxicology*. 116:216-226.
- Convertino M, Church TR, Olsen GW, Liu Y, Doyle E, Elcombe CR, Barnett AL, Samuel LM, MacPherson IR, Evans TRJ. 2018. Stochastic pharmacokinetic-pharmacodynamic modeling for assessing the systemic health risk of perfluorooctanoate (pfoa). *Toxicol Sci*. 163(1):293-306.
- Cui Y, König J, Nies AT, Pfanschmidt M, Hergt M, Franke WW, Alt W, Moll R, Keppler D. 2003. Detection of the human organic anion transporters slc21a6 (oatp2) and slc21a8 (oatp8) in liver and hepatocellular carcinoma. *Lab Invest*. 83(4):527-538.
- Das KP, Wood CR, Lin MT, Starkov AA, Lau C, Wallace KB, Corton JC, Abbott BD. 2017. Perfluoroalkyl acids-induced liver steatosis: Effects on genes controlling lipid homeostasis. *Toxicology*. 378:37-52.
- Daston GP, Chapin RE, Scialli AR, Piersma AH, Carney EW, Rogers JM, Friedman JM. 2010. A different approach to validating screening assays for developmental toxicity. *Birth Defects Res B Dev Reprod Toxicol*. 89(6):526-530.
- DeBose-Boyd RA. 2008. Feedback regulation of cholesterol synthesis: Sterol-accelerated ubiquitination and degradation of hmg coa reductase. *Cell Res*. 18(6):609-621.
- DeBose-Boyd RA, Ye J. 2018. Srebps in lipid metabolism, insulin signaling, and beyond. *Trends Biochem Sci*. 43(5):358-368.
- Dent MP, Vaillancourt E, Thomas RS, Carmichael PL, Ouedraogo G, Kojima H, Barroso J, Ansell J, Barton-Maclaren TS, Bennekou SH et al. 2021. Paving the way for application of next generation risk assessment to safety decision-making for cosmetic ingredients. *Regul Toxicol Pharmacol*. 125:105026.
- Dietschy JM, Turley SD, Spady DK. 1993. Role of liver in the maintenance of cholesterol and low density lipoprotein homeostasis in different animal species, including humans. *J Lipid Res*. 34(10):1637-1659.
- EFSA. 2017. Update: Guidance on the use of the benchmark dose approach in risk assessment. *Efsa journal* 2017;15(1):4658.
- EFSA CONTAM Panel. 2018a. Knutsen hk, alexander j, barregard l, bignami m, bruschweiler b, ceccatelli s, cottrill b, dinovi m, edler l, grasl-kraupp b, hogstrand c, hoogenboom lr, nebbia cs, oswald ip, petersen a, rose m, roudot a-c, vlemincx c, vollmer g, wallace h, bodin l, cravedi j-p, halldorsson ti, haug ls, johansson n, van loveren h, gergelova p, mackay k, levorato s, van manen m and schwerdtle t, 2018. Scientific opinion on the risk to human health related to the presence of perfluorooctane sulfonic acid and perfluorooctanoic acid in food. *Efsa journal* 2018;16(12):5194, 284 pp. <https://doi.org/10.2903/j.efsa.2018.5194>

- . Minutes of the expert meeting on perfluorooctane sulfonic acid and perfluorooctanoic acid in food assessment. 2018b.
- EFSA CONTAM Panel. 2020. Schrenk d, bignami m, bodin l, chipman jk, del mazo j, grasl-kraupp b, hogstrand c, hoogenboom lr, leblanc j-c, nebbia cs, nielsen e, ntzani e, petersen a, sand s, vlemincx c, wallace h, barregard l, ceccatelli s, cravedi j-p, halldorsson ti, haug ls, johansson n, knutsen hk, rose m, roudot a-c, van loveren h, vollmer g, mackay k, riolo f and schwerdtle t, 2020. Scientific opinion on the risk to human health related to the presence of perfluoroalkyl substances in food. Efsa journal 2020;18(9):6223, 391 pp. <https://doi.org/10.2903/j.efsa.2020.6223>
- Ehresman DJ, Froehlich JW, Olsen GW, Chang SC, Butenhoff JL. 2007. Comparison of human whole blood, plasma, and serum matrices for the determination of perfluorooctanesulfonate (pfos), perfluorooctanoate (pfoa), and other fluorochemicals. Environmental research. 103(2):176-184.
- Eriksen KT, Raaschou-Nielsen O, McLaughlin JK, Lipworth L, Tjønneland A, Overvad K, Sørensen M. 2013. Association between plasma pfoa and pfos levels and total cholesterol in a middle-aged danish population. PloS one. 8(2):e56969-e56969.
- Escher BI, Hermens JL. 2004. Internal exposure: Linking bioavailability to effects. Environ Sci Technol. 38(23):455a-462a.
- Fragki S, Dirven H, Fletcher T, Grasl-Kraupp B, Bjerve Gützkow K, Hoogenboom R, Kersten S, Lindeman B, Louise J, Peijnenburg A et al. 2021. Systemic pfos and pfoa exposure and disturbed lipid homeostasis in humans: What do we know and what not? Crit Rev Toxicol. 51(2):141-164.
- Fragki S, Hoogenveen R, van Oostrom C, Schwillens P, Piersma AH, Zeilmaker MJ. 2022. Integrating *in vitro* chemical transplacental passage into a generic pbk model: A qvive approach. Toxicology. 465:153060.
- Fragki S, Piersma AH, Rorije E, Zeilmaker MJ. 2017. *In vitro* to *in vivo* extrapolation of effective dosimetry in developmental toxicity testing: Application of a generic pbk modelling approach. Toxicol Appl Pharmacol. 332:109-120.
- Frisbee SJ, Shankar A, Knox SS, Steenland K, Savitz DA, Fletcher T, Ducatman AM. 2010. Perfluorooctanoic acid, perfluorooctanesulfonate, and serum lipids in children and adolescents: Results from the c8 health project. Archives of pediatrics & adolescent medicine. 164(9):860-869.
- Gallo V, Leonardi G, Genser B, Lopez-Espinosa MJ, Frisbee SJ, Karlsson L, Ducatman AM, Fletcher T. 2012. Serum perfluorooctanoate (pfoa) and perfluorooctane sulfonate (pfos) concentrations and liver function biomarkers in a population with elevated pfoa exposure. Environ Health Perspect. 120(5):655-660.
- Gatzidou ET, Zira AN, Theocharis SE. 2007. Toxicogenomics: A pivotal piece in the puzzle of toxicological research. J Appl Toxicol. 27(4):302-309.
- Groothuis FA, Heringa MB, Nicol B, Hermens JL, Blaauboer BJ, Kramer NI. 2015. Dose metric considerations in *in vitro* assays to improve quantitative *in vitro-in vivo* dose extrapolations. Toxicology. 332:30-40.
- Han J, Back SH, Hur J, Lin Y-H, Gildersleeve R, Shan J, Yuan CL, Krokowski D, Wang S, Hatzoglou M et al. 2013. Er-stress-induced transcriptional regulation increases protein synthesis leading to cell death. Nature Cell Biology. 15(5):481-490.
- Han X, Nabb DL, Russell MH, Kennedy GL, Rickard RW. 2012. Renal elimination of perfluorocarboxylates (pfcas). Chemical research in toxicology. 25(1):35-46.
- Harding HP, Zhang Y, Zeng H, Novoa I, Lu PD, Calfon M, Sadri N, Yun C, Popko B, Paules R et al. 2003. An integrated stress response regulates amino acid metabolism and resistance to oxidative stress. Mol Cell. 11(3):619-633.
- Hato T, Tabata M, Oike Y. 2008. The role of angiopoietin-like proteins in angiogenesis and metabolism. Trends Cardiovasc Med. 18(1):6-14.
- Horton JD, Goldstein JL, Brown MS. 2002. Srebps: Activators of the complete program of cholesterol and fatty acid synthesis in the liver. J Clin Invest. 109(9):1125-1131.
- Joseph P. 2017. Transcriptomics in toxicology. Food Chem Toxicol. 109(Pt 1):650-662.
- Kotani N, Maeda K, Debori Y, Camus S, Li R, Chesne C, Sugiyama Y. 2012. Expression and transport function of drug uptake transporters in differentiated heparg cells. Mol Pharm. 9(12):3434-3441.
- Krokowski D, Han J, Saikia M, Majumder M, Yuan CL, Guan BJ, Bevilacqua E, Bussolati O, Bröer S, Arvan P et al. 2013. A self-defeating anabolic program leads to β -cell apoptosis in endoplasmic reticulum stress-induced diabetes via regulation of amino acid flux. J Biol Chem. 288(24):17202-17213.

- Kuemmerle NB, Kinlaw WB. 2011. Thrsp (thyroid hormone responsive). *Atlas Genet Cytogenet Oncol Haematol*. 15(6):480-482.
- Kwiterovich PO, Jr. 2000. The metabolic pathways of high-density lipoprotein, low-density lipoprotein, and triglycerides: A current review. *Am J Cardiol*. 86(12a):51-101.
- La Paglia L, Listi A, Caruso S, Amodeo V, Passiglia F, Bazan V, Fanale D. 2017. Potential role of angptl4 in the cross talk between metabolism and cancer through ppar signaling pathway. *PPAR Res*. 2017:8187235.
- Le Vee M, Jigorel E, Glaise D, Gripon P, Guguen-Guillouzo C, Fardel O. 2006. Functional expression of sinusoidal and canalicular hepatic drug transporters in the differentiated human hepatoma heparg cell line. *Eur J Pharm Sci*. 28(1-2):109-117.
- Li H, Zhang M, Vervoort J, Rietjens IM, van Ravenzwaay B, Louise J. 2017. Use of physiologically based kinetic modeling-facilitated reverse dosimetry of *in vitro* toxicity data for prediction of *in vivo* developmental toxicity of tebuconazole in rats. *Toxicology letters*. 266:85-93.
- Lichtenstein D, Luckert C, Alarcán J, de Sousa G, Gioutlakis M, Katsanou ES, Konstantinidou P, Machera K, Milani ES, Peijnenburg A et al. 2020. An adverse outcome pathway-based approach to assess steatotic mixture effects of hepatotoxic pesticides *in vitro*. *Food Chem Toxicol*. 139:111283.
- Loccisano AE, Campbell JL, Jr., Andersen ME, Clewell HJ, 3rd. 2011. Evaluation and prediction of pharmacokinetics of pfoa and pfos in the monkey and human using a pbpk model. *Regulatory toxicology and pharmacology* : RTP. 59(1):157-175.
- Louisse J, Beekmann K, Rietjens IM. 2017. Use of physiologically based kinetic modeling-based reverse dosimetry to predict *in vivo* toxicity from *in vitro* data. *Chem Res Toxicol*. 30(1):114-125.
- Louisse J, Bosgra S, Blaauboer BJ, Rietjens IM, Verwei M. 2015. Prediction of *in vivo* developmental toxicity of all-trans-retinoic acid based on *in vitro* toxicity data and *in silico* physiologically based kinetic modeling. *Archives of toxicology*. 89(7):1135-1148.
- Louisse J, Rijkers D, Stoopen G, Janssen A, Staats M, Hoogenboom R, Kersten S, Peijnenburg A. 2020. Perfluorooctanoic acid (pfoa), perfluorooctane sulfonic acid (pfos), and perfluorononanoic acid (pfna) increase triglyceride levels and decrease cholesterologenic gene expression in human heparg liver cells. *Arch Toxicol*.
- Luebker DJ, Hansen KJ, Bass NM, Butenhoff JL, Seacat AM. 2002. Interactions of fluorochemicals with rat liver fatty acid-binding protein. *Toxicology*. 176(3):175-185.
- Macko P, Palosaari T, Whelan M. 2021. Extrapolating from acute to chronic toxicity *in vitro*. *Toxicology in vitro*. 76:105206.
- Martin L, Gardner LB. 2015. Stress-induced inhibition of nonsense-mediated rna decay regulates intracellular cystine transport and intracellular glutathione through regulation of the cystine/glutamate exchanger slc7a11. *Oncogene*. 34(32):4211-4218.
- Nelson JW, Hatch EE, Webster TF. 2010. Exposure to polyfluoroalkyl chemicals and cholesterol, body weight, and insulin resistance in the general u.s. Population. *Environmental health perspectives*. 118(2):197-202.
- Neville LF, Mathiak G, Bagasra O. 1997. The immunobiology of interferon-gamma inducible protein 10 kd (ip-10): A novel, pleiotropic member of the c-x-c chemokine superfamily. *Cytokine Growth Factor Rev*. 8(3):207-219.
- NTP. 2019a. Ntp technical report on the toxicity studies of perfluoroalkyl sulfonates (perfluorobutane sulfonic acid, perfluorohexane sulfonate potassium salt, and perfluorooctane sulfonic acid) administered by gavage to sprague dawley (hsd:Sprague dawley sd) rats. Research triangle park, nc: National toxicology program. Toxicity report 96.
- NTP. 2019b. Ntp technical report on the toxicity studies of perfluoroalkyl carboxylates (perfluorohexanoic acid, perfluorooctanoic acid, perfluorononanoic acid, and perfluorodecanoic acid) administered by gavage to sprague dawley (hsd:Sprague dawley sd) rats. Research triangle park, nc: National toxicology program. Toxicity report 97.
- OECD. 2018. Toward a new comprehensive global database of per- and polyfluoroalkyl substances (pfass): Summary on updating the oecd 2007 list of per-and polyfluoroalkyl substances (pfass). .
- Olsen GW, Burris JM, Burrell MM, Mandel JH. 2003. Epidemiologic assessment of worker serum perfluorooctanesulfonate (pfos) and perfluorooctanoate (pfoa) concentrations and medical surveillance examinations. *J Occup Environ Med*. 45(3):260-270.

- Olsen GW, Burris JM, Ehresman DJ, Froehlich JW, Seacat AM, Butenhoff JL, Zobel LR. 2007. Half-life of serum elimination of perfluorooctanesulfonate, perfluorohexanesulfonate, and perfluorooctanoate in retired fluorochemical production workers. *Environ Health Perspect.* 115(9):1298-1305.
- Punt A, Bouwmeester H, Blaauboer BJ, Coecke S, Hakkert B, Hendriks DFG, Jennings P, Kramer NI, Neuhoff S, Masereeuw R et al. 2020. New approach methodologies (nam) for human-relevant biokinetics predictions. Meeting the paradigm shift in toxicology towards an animal-free chemical risk assessment. *Altex.* 37(4):607-622.
- Rosenmai AK, Ahrens L, le Godec T, Lundqvist J, Oskarsson A. 2018. Relationship between peroxisome proliferator-activated receptor alpha activity and cellular concentration of 14 perfluoroalkyl substances in hepg2 cells. *J Appl Toxicol.* 38(2):219-226.
- Rowan-Carroll A, Reardon A, Leingartner K, Gagné R, Williams A, Meier MJ, Kuo B, Bourdon-Lacombe J, Moffat I, Carrier R et al. 2021. High-throughput transcriptomic analysis of human primary hepatocyte spheroids exposed to per- and polyfluoroalkyl substances as a platform for relative potency characterization. *Toxicol Sci.* 181(2):199-214.
- Rozpedek W, Pytel D, Mucha B, Leszczynska H, Diehl JA, Majsterek I. 2016. The role of the perk/eif2 α /atf4/chop signaling pathway in tumor progression during endoplasmic reticulum stress. *Curr Mol Med.* 16(6):533-544.
- Ruggiero MJ, Miller H, Idowu JY, Zitzow JD, Chang S-C, Hagenbuch B. 2021. Perfluoroalkyl carboxylic acids interact with the human bile acid transporter ntcp. *Livers.* 1(4):221-229.
- Sauer UG, Deferme L, Gribaldo L, Hacker Müller J, Tralau T, van Ravenzwaay B, Yauk C, Poole A, Tong W, Gant TW. 2017. The challenge of the application of 'omics technologies in chemicals risk assessment: Background and outlook. *Regulatory Toxicology and Pharmacology.* 91:S14-S26.
- Shao W, Espenshade PJ. 2012. Expanding roles for srebp in metabolism. *Cell Metab.* 16(4):414-419.
- Sheng N, Li J, Liu H, Zhang A, Dai J. 2016. Interaction of perfluoroalkyl acids with human liver fatty acid-binding protein. *Arch Toxicol.* 90(1):217-227.
- Slob W. 2002. Dose-response modeling of continuous endpoints. *Toxicological Sciences.* 66(2):298-312.
- Smith BP, Auviel LS, Welge M, Bushell CB, Bhargava R, Elango N, Johnson K, Madak-Erdogan Z. 2020. Identification of early liver toxicity gene biomarkers using comparative supervised machine learning. *Scientific Reports.* 10(1):19128.
- Steenland K, Tinker S, Frisbee S, Ducatman A, Vaccarino V. 2009. Association of perfluorooctanoic acid and perfluorooctane sulfonate with serum lipids among adults living near a chemical plant. *Am J Epidemiol.* 170(10):1268-1278.
- Tavares-Sanchez OL, Rodriguez C, Gortares-Moroyoqui P, Estrada MI. 2015. Hepatocyte nuclear factor-4 α , a multifunctional nuclear receptor associated with cardiovascular disease and cholesterol catabolism. *Int J Environ Health Res.* 25(2):126-139.
- Thumser AE, Wilton DC. 1996. The binding of cholesterol and bile salts to recombinant rat liver fatty acid-binding protein. *Biochem J.* 320 (Pt 3)(Pt 3):729-733.
- Trapani L, Segatto M, Pallottini V. 2012. Regulation and deregulation of cholesterol homeostasis: The liver as a metabolic "power station". *World J Hepatol.* 4(6):184-190.
- UNEP/POPS/COP.4/17 SC. 2009. Recommendations of the persistent organic pollutants review committee of the stockholm convention to amend annexes a, b or c of the convention. Conference of the Parties of the Stockholm, Convention on Persistent Organic Pollutants. Fourth meeting, Geneva, 4-8 May 2009.
- Wada Y, Kikuchi A, Kaga A, Shimizu N, Ito J, Onuma R, Fujishima F, Totsune E, Sato R, Niihori T et al. 2020. Metabolic and pathologic profiles of human lss deficiency recapitulated in mice. *PLoS Genet.* 16(2):e1008628-e1008628.
- Wan HT, Zhao YG, Wei X, Hui KY, Giesy JP, Wong CK. 2012. Pfos-induced hepatic steatosis, the mechanistic actions on β -oxidation and lipid transport. *Biochim Biophys Acta.* 1820(7):1092-1101.
- Wigger L, Casals-Casas C, Baruchet M, Trang KB, Pradervand S, Naldi A, Desvergne B. 2019. System analysis of cross-talk between nuclear receptors reveals an opposite regulation of the cell cycle by lxr and fxr in human hepg2 liver cells. *PLoS One.* 14(8):e0220894.
- Woodcroft MW, Ellis DA, Rafferty SP, Burns DC, March RE, Stock NL, Trumpour KS, Yee J, Munro K. 2010. Experimental characterization of the mechanism of perfluorocarboxylic acids' liver protein bioaccumulation: The key role of the neutral species. *Environ Toxicol Chem.* 29(8):1669-1677.

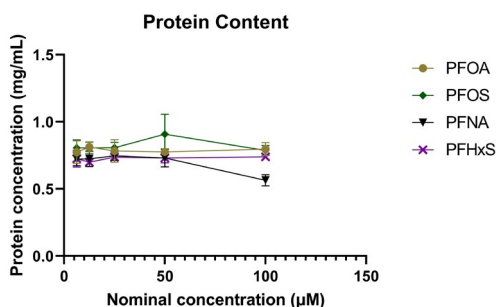
- Zhang L, Ren XM, Guo LH. 2013a. Structure-based investigation on the interaction of perfluorinated compounds with human liver fatty acid binding protein. *Environ Sci Technol.* 47(19):11293-11301.
- Zhang Y, Beesoon S, Zhu L, Martin JW. 2013b. Biomonitoring of perfluoroalkyl acids in human urine and estimates of biological half-life. *Environ Sci Technol.* 47(18):10619-10627.
- Zhao W, Zitzow JD, Ehresman DJ, Chang S-C, Butenhoff JL, Forster J, Hagenbuch B. 2015. Na⁺/taurocholate cotransporting polypeptide and apical sodium-dependent bile acid transporter are involved in the disposition of perfluoroalkyl sulfonates in humans and rats. *Toxicological sciences : an official journal of the Society of Toxicology.* 146(2):363-373.
- Zhao W, Zitzow JD, Weaver Y, Ehresman DJ, Chang SC, Butenhoff JL, Hagenbuch B. 2017. Organic anion transporting polypeptides contribute to the disposition of perfluoroalkyl acids in humans and rats. *Toxicol Sci.* 156(1):84-95.

Supplementary Material

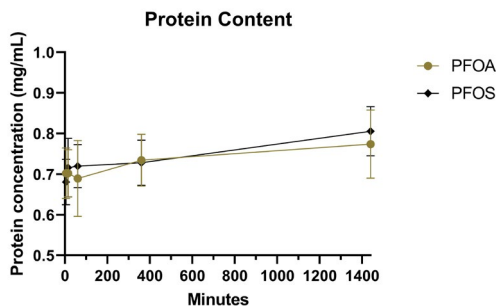
Biokinetic studies in HepaRG cells

SUPPLEMENTARY TABLE 1 MRM transitions of the PFASs tested in the present study.

Name	Q1 Mass Da	Q3 Mass Da	Dwell (msec)	DP	EP	CE	CXP
¹³ C ₄ -PFOA	416.9	371.9	4.0	-40	-15	-24	-19
¹³ C ₅ -PFNA	468.0	423.0	4.0	-75	-10	-16	-27
¹⁸ O ₂ -PFHxS	403.0	84.0	4.0	-30	-10	-40	-8
¹³ C ₄ -PFOS	502.9	99.0	4.0	-80	-5	-34	-7
PFOA	412.9	369.1	4.0	-40	-10	-14	-11
PFOA	412.9	169.0	4.0	-40	-15	-24	-19
PFNA	462.9	419.1	4.0	-75	-10	-16	-27
PFNA	462.9	169.0	4.0	-75	-10	-26	-11
PFHxS	398.9	80.0	4.0	-110	-10	-104	-17
PFHxS	398.9	98.9	4.0	-110	-10	-42	-15
PFOS	498.9	99.0	4.0	-80	-5	-94	-7
PFOS	498.9	80.0	4.0	-80	-5	-100	-11



SUPPLEMENTARY FIGURE 1 Total protein content (mg/mL) upon 24-hours exposure to the four PFASs at concentrations of 6.25, 12.5, 25, 50, and 100 μ M. Data presented as mean and SD (three individual experiments with three replicates each).



SUPPLEMENTARY FIGURE 2 Total protein content (mg/mL) upon various exposure durations (5, 15, 60, 360 minutes, 6 or 24 hours) to PFOS or PFOA at a single concentrations of 6.25 μ M. Data presented as mean and SD (three individual experiments with three replicates each).

SUPPLEMENTARY TABLE 2 Details for the calculations of scenarios 1, 2 and 3.

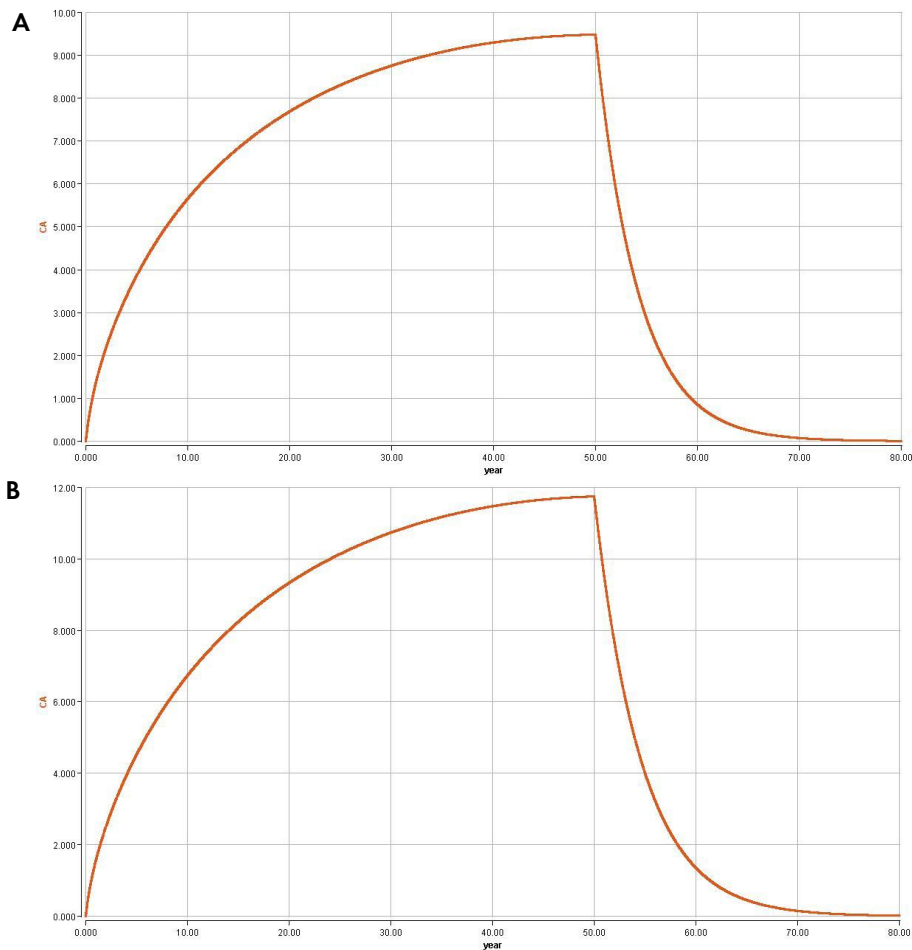
PF/CA	Scenario 1				Scenario 2				Scenario 3				
	in vitro nominal conc (µM)	in vitro nominal conc (µg/L)	AUC µg/L*24hr	Oral equivalent dose (ng/kg bw/d)	predicted liver conc (µM)	predicted liver conc (µg/L)	AUC µg/L*24hr	Oral equivalent dose (ng/kg bw/d)	nmol/mg protein	µmol/kg liver (=µmol/L)	µg/L	AUC µg/L*24hr	Oral equivalent dose (ng/kg bw/d)
PF/CA	0	0	0	0.0000	0	0	0	0.0000	0	0.000	0	0	0
	6.25	6.25	2,588	0.0074	13.75	5,693	136,020	0.0162	0.09226	11.02	4.813	115,502	0.0137
	12.5	12.5	5,175	0.0148	27.5	11,385	273,240	0.0325	0.20381	26.06	10.788	238,919	0.0305
	25	25	10,350	0.0295	55	22,770	546,480	0.0648	0.40762	65.91	27.285	654,837	0.0777
	50	50	20,700	0.0589	110	45,540	1,092,960	0.1296	1.24559	156.82	64.923	1,538,152	0.1850
	100	100	41,400	0.1170	220	91,080	2,185,920	0.2590	2.49119	361.93	145.689	3,496,772	0.4150
200	200	82,800	0.2300	440	182,160	4,371,840	0.5180	5.38000	677.88	280.642	6,735,416	0.8000	
400	400	165,600	0.4780	880	364,320	8,743,680	1.0400	10.76000	1355.76	561.285	19,470,831	1.6000	
PF/CS	0	0	0	0.0000	0	0	0	0.0000	0	0.000	0	0	0
	6.25	6.25	3,125	0.0055	23.25	11,625	279,000	0.0203	0.50046	70.62	35.309	847,415	0.061575
	12.5	12.5	6,250	0.0109	46.5	23,250	558,000	0.0405	1.31866	166.15	83.075	1,993,808	0.1449
	25	25	12,500	0.0218	93	46,500	1,116,000	0.0811	3.09028	390.13	195.066	4,681,578	0.3400
	50	50	25,000	0.0436	186	93,000	2,232,000	0.1622	7.38919	908.32	464.299	11,142,212	0.8100
	100	100	50,000	0.0872	372	186,000	4,464,000	0.3244	14.34799	1807.84	903.921	21,694,112	1.5700
200	200	100,000	0.1745	744	372,000	8,928,000	0.6487	28.54000	3596.04	1,798.000	43,152,480	3.1400	
400	400	200,000	0.3490	1488	744,000	17,856,000	1.2974	57.08000	7192.08	3,596.040	86,304,960	6.2700	
PF/VA	0	0	0	0	0	0	0	0	0.00000	0.000	0.000	0	0
	6.25	6.25	2,900	0.006125	9.125	4,234	101,616	0.014	0.22203	27.98	12.981	311.542	0.04000
	12.5	12.5	5,800	0.019225	18.25	8,468	203,232	0.028	0.71015	89.48	41.518	996.438	0.13755
	25	25	11,600	0.03845	36.5	16,936	406,464	0.056	1.52540	192.20	88.181	2,140,347	0.28550
	50	50	23,200	0.0769	73	33,872	812,928	0.112	4.37700	551.59	255.938	6,142,508	0.84815
	100	100	46,400	0.1538	146	67,744	1,625,856	0.225	15.69467	1977.53	917.573	22,021,764	3.04070
PF/HCS	0	0	0	0	0	0	0	0	0.00000	0.000	0.000	0	0
	6.25	6.25	2,500	0.010575	5.3125	2,125	51,000	0.008985	0.08359	10.53	4.213	101,114	0.018
	12.5	12.5	5,000	0.02115	10.625	4,250	102,000	0.01797	0.46716	58.86	23.545	565,078	0.100
	25	25	10,000	0.0423	21.25	8,500	204,000	0.03594	0.88456	111.45	44.582	1,069,961	0.189
	50	50	20,000	0.0846	42.5	17,000	408,000	0.07188	2.18716	275.58	110.233	2,645,586	0.466
	100	100	40,000	0.1692	85	34,000	816,000	0.14370	4.39058	553.21	221.285	5,310,843	0.936
200	200	80,000	0.3384	170	68,000	1,632,000	0.28752	8.98670	1132.32	452.930	10,870,312	1.9152	
400	400	160,000	0.67652	340	136,000	3,264,000	0.57504	18.14670	2286.48	914.584	21,950,248	3.8675	

For scenario 3, the *in vitro* measured cell-associated concentrations were expressed per mg protein in the culture. To scale this to a whole liver a value of 126 mg total protein/g liver was used as reported in the literature (Vasilogianni et al. 2021). The two highest concentrations (200 and 400 µM) were linearly extrapolated based on the experimental measurements (0-100 µM).

SUPPLEMENTARY TABLE 3 Parameters as used for the four compounds for the PBK model based reverse dosimetry approach.

	PFOA	PFNA	PFHxS	PFOS
liver:blood PC	2.20 ^a	1.46 ^b	0.85 ^b	3.72 ^a
kidney:blood PC	1.05 ^a	0.60 ^b	0.30 ^b	0.80 ^a
maximum resorption rate (Tmc)	6000 ^c	7900 ^d	7000 ^d	3500 ^c

^a taken from Loccisano et al. (2011); ^{b,c} taken from NTP (2019 a,b); ^c corresponding to a half-life of 3 years for PFOA, and 6 years for PFOS (based on the EFSA’s model code); ^d calibrated to result in half-lives of 3.2 years (range: 0.34-20) for PFNA and 8.2 years (95% CI 6.4-10.6) for PFHxS (Olsen et al. 2007; Zhang et al. 2013b).



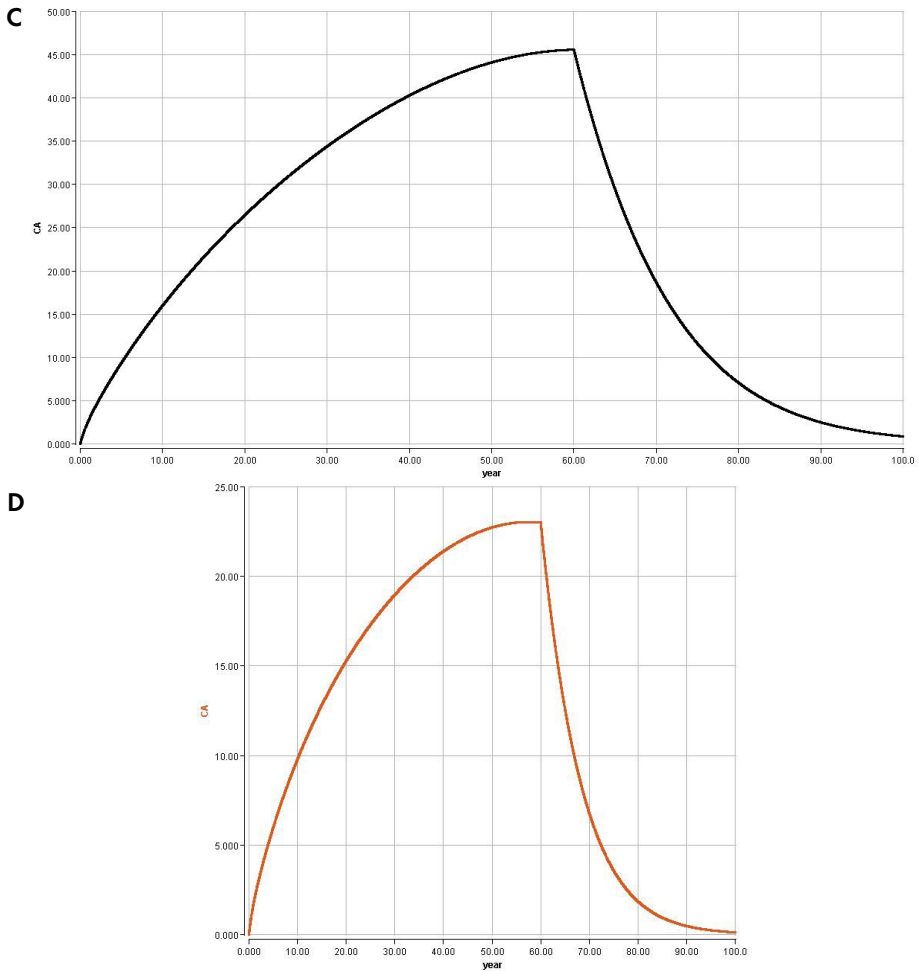


FIGURE 3 Simulation of blood concentrations ($\mu\text{g/L}$) of A. PFOA, B. PFNA, C. PFHxS, and D. PFOS by the PBK models. Chronic daily constant exposure (PFOA: 0.85, PFNA: 0.85, PFHxS: 1.85, PFOS: 1.85 ng/kg bw/day).

PBK Model code

Model Code for PFOA

```

METHOD Stiff
STARTTIME = 0
STOPTIME=438000 ;end of simulation (h), 50 years
DT = 0.01
TOLERANCE = 0.01
DTMAX = 10.0
DTMIN = 0.000001
year= TIME/(24*365)

```

;Physiological parameters (from Brown, et al 1997)

; fractional blood flows

QCC = 12.5 ; Cardiac blood output (L/h/kg^{0.75})

QFC = 0.052 ; Fraction cardiac output going to fat

QLC = 0.069 ; Fraction cardiac output going to liver, through hepatic artery

QKC = 0.175 ; Fraction cardiac output going to kidney

QSkC = 0.058 ; Fraction cardiac output going to skin

QGC = 0.181 ; Fraction of cardiac output going to gut and in the liver via portal artery

; Not used ;QfilC = 0.035 ; Fraction cardiac output to the filtrate compartment (20% of kidney blood flow)

; BW = 70 ; Body weight (kg) for men; 58 kg for women

; weight algorithm based on french survey (French total Diet Study)

BW=3.68+4.47*year-0.093*year²+0.00061*year³

fractional tissue volumes

VLC = 0.026 ; Fraction liver volume

VFC = 0.214 ; Fraction fat volume

VKC = 0.004 ; Fraction kidney volume

VfilC = 0.0004 ; Fraction filtrate compartment volume (10% of kidney volume)

VGC = 0.0171 ; Fraction gut volume

VPlasC = 0.0428 ; Fraction plasma volume (58% of blood)

Htc = 0.44 ; hematocrit

for dermal exposure

SkinTarea = 9.1*(BW*1000)**0.666 ; Total area of skin (cm²)

Skinthickness = 0.1 ; Skin thickness (cm)

; Chemical-specific parameters for PFOA

Tmc = 6000 ; Maximum resorption rate (µg/h/kg^{0.75}), changed from 6 in the original Loccisano 2011 model and expressed in µg, to be consistent with other parameters

Kt = 55.0 ; Resorption affinity (µg/L), changed from 0.055 in the original Loccisano 2011 model and expressed in µg, to be consistent with other parameters

Free = 0.02 ; Free fraction of PFOA in plasma

PL = 2.2 ; Liver/plasma partition coefficient

PF = 0.04 ; Fat/ plasma partition coefficient

PK = 1.05 ; Kidney/ plasma partition coefficient

PSk = 0.1 ; Skin/ plasma partition coefficient

PR = 0.12 ; Rest of the body/ plasma partition coefficient

PG = 0.05 ; Gut/ plasma partition coeff.

kurinec = 0.0003 ; urinary elimination rate constant (/h/kg^{-0.25}); estimated from Harada, et al 2005

kurine = kurinec*BW**(-0.25)

Free fraction of chemical in tissues

FreeL = Free/PL ; liver

FreeF = Free/PF ; fat

FreeK = Free/PK ; kidney

FreeSk = Free/PSk ; skin

FreeR = Free/PR ; rest of tissues

FreeG = Free/PG ; gut

```

; Exposure parameters
tchng =438000 ; Duration of exposure (h); 50 years

; turn dose on/off
DoseOn = IF time<tchng THEN 1.0 else 0.0

; Dermal exposure
Dermconc = 0.0 ; Dermal concentration (µg/mL)
Dermvol = 0.0 ; Dermal exposure volume (mL)
Dermdose = Dermconc*Dermvol*1000 ; (µg)
Skinarea = 5 ; Exposed area on skin (cm^2)

; Oral exposure
Oralconc =0.00085 ; Oral uptake (µg/kg/day)
Oraldose = Oralconc*BW ; (µg/day)

; Drinking water exposure
Drinkconc = 0.0 ; Drinking water concentration (µg/L or ppb)
Drinkrate = 13 ; Drinking water rate (mL/kg/day)
Drinkdose = (Drinkconc*Drinkrate/1000)*BW ; (µg/day)

; Inhalation exposure
Inhalation = 0.0 ; Inhalation dose (ppm)
Tinput = 24.0 ; duration of dose (h), the CONTAM Panel increased the Tinput to 24h (instead
of 0.6) considering continuous exposure from food

; oral dose
Input1 = IF MOD(time,24) <=Tinput THEN Oraldose/Tinput ELSE 0.0

; drinking water
Input2 = IF MOD(time,24) <= Tinput THEN Drinkdose/Tinput ELSE 0.0

; Scaling parameters
QC = QCC*BW**0.75 ; Cardiac output (L/h)
QCP = QC*(1-Htc) ; adjust for plasma flow
QL = QLC*QCP ; Plasma flow to liver (L/h)
QF = QFC*QCP ; Plasma flow to fat (L/h)
QK = QKC*QCP ; Plasma flow to kidney (L/h)
Qfil = 0.2*QK ; Plasma flow to filtrate compartment (L/h); 20% of QK
QG = QGC*QCP ; Plasma flow to gut (L/h)

QSk = IF Dermconc >0.0 THEN QSkC*QCP*(Skinarea/SkinTarea) else 0.0 ;plasma flow to skin
QR = QCP - QL - QF - QK - QG - QSk ; Plasma flow to rest
of the body (L/h)

Qbal = QCP - (QR+QL+QF+QK+QG+QSk) ; balance check--better be 0
VL = VLC*BW ; Liver volume (L)
VF = VFC*BW ; Fat volume (L)
VK = VKC*BW ; Kidney volume (L)
Vfil = VfILC*BW ; Filtrate compartment volume (L)
VG = VGC*BW ; Gut volume (L)
VPlas = VPlasC*BW ; Plasma volume (L)

```



```

; Skin compartment
ASk' = QSk*(CA*Free-CSk*FreeSk) ; Rate of change in skin (µg/h)
init ASk = DermDose
Csk = ASk/VSk ; Concentration in skin compartment (µg/L)
CVSk = Csk/PSk ; Concentration leaving skin compartment (µg/L)

```

```

; Rest of the body
AR' = QR*(CA*Free-CR*FreeR) ; Rate of change in rest of the body (µg/h)
init AR = 0.0
CR = AR/VR ; Concentration in rest of the body (µg/L)
CVR = CR/PR ; Concentration leaving rest of the body (µg/L)

```

```

Display Drinkconc, Dermconc, Oralconc, Inhalation, TInput, Tmc, Kt, Free, PL,PK,PF,PR,PSK,PG,
tchng,input1,input2,drinkrate,BW,QCC,QFC,QLC,QKC,QSkC,QGC,VLC,VFC,VKC,VfilC,VGC,VPlasC,kurinec,
year , APlas, AG, AL, AF, AF, AK, ASK, AR ; for parameters window
Display CA, CG, CL, CF, CR, CK, CAFREE, Qbal , year, FreeL ; for plotting

```

Model Code for PFNA adapted from code on PFOA

```

METHOD Stiff
STARTTIME = 0
STOPTIME=438000 ;end of simulation (h), 50 years
DT = 0.01
TOLERANCE = 0.01
DTMAX = 10.0
DTMIN = 0.000001
year= TIME/(24*365)
;Physiological parameters (from Brown, et al 1997)
; fractional blood flows
QCC = 12.5 ; Cardiac blood output (L/h/kg^0.75)
QFC = 0.052 ; Fraction cardiac output going to fat
QLC = 0.069 ; Fraction cardiac output going to liver, through hepatic artery
QKC = 0.175 ; Fraction cardiac output going to kidney
QSkC = 0.058 ; Fraction cardiac output going to skin
QGC = 0.181 ; Fraction of cardiac output going to gut and in the liver via portal artery

; Not used ;QfilC = 0.035 ; Fraction cardiac output to the filtrate compartment (20% of kidney blood flow)

; BW = 70 ; Body weight (kg) for men; 58 kg for women
; weight algorithm based on french survey (French total Diet Study)
BW=3.68+4.47*year-0.093*year^2+0.00061*year^3

```

fractional tissue volumes

```

VLC = 0.026 ; Fraction liver volume
VFC = 0.214 ; Fraction fat volume
VKC = 0.004 ; Fraction kidney volume
VfilC = 0.0004 ; Fraction filtrate compartment volume (10% of kidney volume)
VGC = 0.0171 ; Fraction gut volume
VPlasC = 0.0428 ; Fraction plasma volume (58% of blood)
Htc = 0.44 ; hematocrit

```

for dermal exposure

```

SkinTarea = 9.1*((BW*1000)**0.666) ; Total area of skin (cm^2)
Skinthickness = 0.1 ; Skin thickness (cm)

```


; Chemical-specific parameters for PFNA

Tmc = 7900 ; Maximum resorption rate ($\mu\text{g}/\text{h}/\text{kg}^{0.75}$), changed from original 6000 (EFSA, 2018) for PFOA, fitted in order to achieve a half-life of 3.2 years

Kt = 55.0 ; Resorption affinity ($\mu\text{g}/\text{L}$)

Free = 0.02 ; Free fraction of PFNA (PFOA) in plasma

PL = 1.46 ; Liver/plasma partition coefficient (NTP study, 2019a)

PF = 0.04 ; Fat/ plasma partition coefficient (based on PFOA)

PK = 0.6 ; Kidney/ plasma partition coefficient (NTP study, 2019a)

PSk = 0.1 ; Skin/ plasma partition coefficient (based on PFOA)

PR = 0.12 ; Rest of the body/ plasma partition coefficient

PG = 0.05 ; Gut/ plasma partition coeff.

kurinec = 0.0003 ; urinary elimination rate constant ($1/\text{h}/\text{kg}^{-0.25}$); estimated from Harada, et al 2005

kurine = kurinec*BW**(-0.25)

Free fraction of chemical in tissues

FreeL = Free/PL ; liver

FreeF = Free/PF ; fat

FreeK = Free/PK ; kidney

FreeSk = Free/PSk ; skin

FreeR = Free/PR ; rest of tissues

FreeG = Free/PG ; gut

; Exposure parameters

tchng = 438000 ; Duration of exposure (h); 50 years

; turn dose on/off

DoseOn = IF time < tchng THEN 1.0 else 0.0

; Dermal exposure

Dermconc = 0.0 ; Dermal concentration ($\mu\text{g}/\text{mL}$)

Dermvol = 0.0 ; Dermal exposure volume (mL)

Dermdose = Dermconc*Dermvol*1000 ; (μg)

Skinarea = 5 ; Exposed area on skin (cm^2)

; Oral exposure

Oralconc = 0.00085 ; Oral uptake ($\mu\text{g}/\text{kg}/\text{day}$)

Oraldose = Oralconc*BW ; ($\mu\text{g}/\text{day}$)

; Drinking water exposure

Drinkconc = 0.0 ; Drinking water concentration ($\mu\text{g}/\text{L}$ or ppb)

Drinkrate = 13 ; Drinking water rate (mL/kg/day)

Drinkdose = (Drinkconc*Drinkrate/1000)*BW ; ($\mu\text{g}/\text{day}$)

; Inhalation exposure

Inhalation = 0.0 ; Inhalation dose (ppm)

Tinput = 24.0 ; duration of dose (h), the CONTAM Panel increased the Tinput to 24h (instead of 0.6) considering continuous exposure from food

; oral dose

Input1 = IF MOD(time,24) <= Tinput THEN Oraldose/Tinput ELSE 0.0


```

CF = AF/VF ; Concentration in fat (µg/L)
CVF = CF/PF ; Concentration leaving fat (µg/L)
; Fat compartment

; Kidney compartment
AK' = QK*(CA*Free-CK*FreeK) + Tm*Cfil/(Kt+Cfil) ; Rate of change in kidneys (µg/h)
init AK = 0.0
CK = AK/VK ; Concentration in kidneys (µg/L)
CVK = CK/PK ; Concentration leaving kidneys (µg/L)

; Filtrate compartment
Afil' = Qfil*(CA*Free-Cfil) - Tm*Cfil/(Kt+Cfil) ; Rate of change in filtrate compartment (µg/h)
init Afil = 0.0
Cfil = Afil/Vfil ; Concentration in filtrate compartment (µg/L)

; Storage compartment for urine
; Adelay' = Qfil*Cfil-kurine*Adelay
; init Adelay = 0.0

; Urine
;Aurine' = kurine*Adelay
Aurine' = Qfil*Cfil - kurine*Aurine
init Aurine = 0.0

; Skin compartment
ASK' = QSk*(CA*Free-CSk*FreeSk) ; Rate of change in skin (µg/h)
init ASk = DermDose
CSk = ASk/VSk ; Concentration in skin compartment (µg/L)
CVSk = CSk/PSk ; Concentration leaving skin compartment (µg/L)

; Rest of the body
AR' = QR*(CA*Free-CR*FreeR) ; Rate of change in rest of the body (µg/h)
init AR = 0.0
CR = AR/VR ; Concentration in rest of the body (µg/L)
CVR = CR/PR ; Concentration leaving rest of the body (µg/L)

Display Drinkconc, Dermconc, Oralconc, Inhalation, TInput, Tmc, Kt, Free, PL,PK,PF,PR,PSK,PG,
tchng,input1,input2,drinkrate,BW,QCC,QFC,QLC,QKC,QSkC,QGC,VLC,VFC,VKC,VfilC,VGC,VPlasC,kurinec,
year , APlas, AG, AL, AF, AF, AK, ASK, AR ; for parameters window
Display CA, CG, CL, CF, CR, CK, CAFREE, Qbal , year, FreeL ; for plotting

```

Model Code for PFHxS adapted from code on PFOS

```

METHOD Stiff
STARTTIME = 0
STOPTIME=438000 ;end of simulation (h): 50 years
DT = 0.01
TOLERANCE = 0.01 ;default tolerance
DTMAX = 10.0
DTMIN = 0.000001
year= TIME/(24*365)

```

; Physiological parameters (from Brown et al., 1997) start



;fractional blood flows

QCC = 12.5 ; Cardiac blood output (L/h/kg^{0.75})

QFC = 0.052 ; Fraction cardiac output going to fat

QLC = 0.069 ; Fraction cardiac output going to liver, through hepatic artery

QKC = 0.175 ; Fraction cardiac output going to kidney

QSkC = 0.058 ; Fraction cardiac output going to skin

QGC = 0.181 ; Fraction of cardiac output going to gut and in the liver via portal artery

; Not used ;QfilC = 0.035 ; Fraction cardiac output to the filtrate compartment (20% of kidney blood flow)

;BW = 70 ; Body weight (kg) for men; 58 kg for women

;weight algorithm based on french survey (French total Diet Study)

BW=3.68+4.47*year-0.093*year²+0.00061*year³

;fractional tissue volumes

VLC = 0.026 ; Fraction liver volume

VFC = 0.214 ; Fraction fat volume

VKC = 0.004 ; Fraction kidney volume

VfilC = 0.0004 ; Fraction filtrate compartment volume (10% of kidney volume)

VGC = 0.0171 ; Fraction gut volume

VPlasC = 0.0428 ; Fraction plasma volume (58% of blood)

Htc = 0.44 ; hematocrit

;for dermal exposure

SkinTarea = 9.1*(BW*1000)**0.666 ; Total area of skin (cm²)

Skinthickness = 0.1 ; Skin thickness (cm)

; Chemical-specific parameters (PFHxS)

Tmc = 7000 ; Maximum resorption rate (µg/h/kg^{0.75}), changed from original 3500 (EFSA, 2018) for PFOS, fitted in order to achieve a half-life of 8.2 years

Kt = 23.0 ; Resorption affinity (µg/L)

Free = 0.025 ; Free fraction of PFHxS in plasma (based on PFOS)

PL = 0.85 ; Liver/plasma partition coefficient (NTP study, 2019b)

PF = 0.14 ; Fat/ plasma partition coefficient (based on PFOS)

PK = 0.30 ; Kidney/ plasma partition coefficient (based on NTP study, 2019, in rats)

PSk = 0.29 ; Skin/ plasma partition coefficient (based on PFOS)

PR = 0.2 ; Rest of the body/ plasma partition coefficient (based on PFOS)

PG = 0.57 ; Gut/ plasma partition coeff. (based on PFOS)

kurinec = 0.001 ; urinary elimination rate constant (/h/kg^{-0.25}); estimated from Harada, et al 2005, (based on PFOS)

kurine = kurinec*BW**(-0.25)

; Free fraction of chemical in tissues

FreeL = Free/PL ;liver

FreeF = Free/PF ;fat

FreeK = Free/PK ;kidney

FreeSk = Free/PSk ;skin

FreeR = Free/PR ;rest of tissues

FreeG = Free/PG ;gut

; Exposure parameters

tchng = 438000 ; Duration of exposure (h); 50 years

; turn dose on/off

DoseOn = IF time < tchng THEN 1.0 else 0.0

; Dermal exposure

Dermconc = 0.0 ; Dermal concentration (µg/mL)

Dermvol = 0.0 ; Dermal exposure volume (mL)

Dermdose = Dermconc * Dermvol * 1000 ; (µg)

Skinarea = 5 ; Exposed area on skin (cm²)

; Oral exposure

Oralconc = 0.00185 ; Oral uptake (µg/kg/day)

Oraldose = Oralconc * BW ; (µg/day)

; Drinking water exposure

Drinkconc = 0.0 ; Drinking water concentration (µg/L or ppb)

Drinkrate = 13 ; Drinking water rate (mL/kg/day)

Drinkdose = (Drinkconc * Drinkrate / 1000) * BW ; (µg/day)

; Inhalation exposure

Inhalation = 0.0 ; Inhalation dose (ppm)

Tinput = 24 ; duration of dose (h) the CONTAM Panel increased the Tinput to 24h (instead of 0.6) considering continuous exposure from food.

; oral dose

Input1 = IF MOD(time, 24) <= Tinput THEN Oraldose / Tinput ELSE 0.0

; drinking water

Input2 = IF MOD(time, 24) <= Tinput THEN Drinkdose / Tinput ELSE 0.0

; Scaling parameters

QC = QCC * BW ** 0.75 ; Cardiac output (L/h)

QCP = QC * (1 - Htc) ; adjust for plasma flow

QL = QLC * QCP ; Plasma flow to liver (L/h)

QF = QFC * QCP ; Plasma flow to fat (L/h)

QK = QKC * QCP ; Plasma flow to kidney (L/h)

Qfil = 0.2 * QK ; Plasma flow to filtrate compartment (L/h); 20% of QK

QG = QGC * QCP ; Plasma flow to gut (L/h)

QSk = IF Dermconc > 0.0 THEN QSkC * QCP * (Skinarea / SkinTarea) else 0.0 ; plasma flow to skin

QR = QCP - QL - QF - QK - QG - QSk ; Plasma flow to rest of the body (L/h)

Qbal = QCP - (QR + QL + QF + QK + QG + QSk) ; balance check -- better be 0

VL = VLC * BW ; Liver volume (L)

VF = VFC * BW ; Fat volume (L)

VK = VKC * BW ; Kidney volume (L)

Vfil = VfilC * BW ; Filtrate compartment volume (L)

VG = VGC * BW ; Gut volume (L)

VPlas = VPlasC * BW ; Plasma volume (L)

VSk = (Skinarea * Skinthickness) / 1000 ; Skin volume (L)

CSk = ASk/VSk ; Concentration in skin compartment ($\mu\text{g/L}$)
 CVSk = CSk/PSk ; Concentration leaving skin compartment ($\mu\text{g/L}$)

; Rest of the body

AR' = QR*(CA*Free-CR*FreeR) ; Rate of change in rest of the body ($\mu\text{g/h}$)

init AR = 0.0

CR = AR/VR ; Concentration in rest of the body ($\mu\text{g/L}$)

CVR = CR/PR ; Concentration leaving rest of the body ($\mu\text{g/L}$)

Display Drinkconc, Dermconc, Oralconc, Inhalation, TInput, Tmc, Kt, Free, PL,PK,PF,PR,PSK,PG,
 tchnng,

input1,input2,drinkrate,BW,QCC,QFC,QLC,QKC,QSkC,QGC,VLC,VFC,VKC,VfIlC,VGC,VPlasC,kurinec, year ,

APlas, AG, AL, AF, AF, AK, ASK, AR ;for parameters window

Display CA, CG, CL, CF, CR, CK, CAFREE, Qbal , year ;for plotting

Model Code for PFOS

METHOD Stiff

STARTTIME = 0

STOPTIME=438000 ;end of simulation (h); 50 years

DT = 0.01

TOLERANCE = 0.01 ;default tolerance

DTMAX = 10.0

DTMIN = 0.000001

year= TIME/(24*365)

; Physiological parameters (from Brown et al., 1997) start

;fractional blood flows

QCC = 12.5 ; Cardiac blood output ($\text{L/h/kg}^{0.75}$)

QFC = 0.052 ; Fraction cardiac output going to fat

QLC = 0.069 ; Fraction cardiac output going to liver, through hepatic artery

QKC = 0.175 ; Fraction cardiac output going to kidney

QSkC = 0.058 ; Fraction cardiac output going to skin

QGC = 0.181 ; Fraction of cardiac output going to gut and in the liver via portal artery

; Not used ;QfilC = 0.035 ; Fraction cardiac output to the filtrate compartment (20% of kidney blood flow)

;BW = 70 ; Body weight (kg) for men; 58 kg for women

;weight algorithm based on french survey (French total Diet Study)

BW=3.68+4.47*year-0.093*year^2+0.00061*year^3

;fractional tissue volumes

VLC = 0.026 ; Fraction liver volume

VFC = 0.214 ; Fraction fat volume

VKC = 0.004 ; Fraction kidney volume

VfIlC = 0.0004 ; Fraction filtrate compartment volume (10% of kidney volume)

VGC = 0.0171 ; Fraction gut volume

VPlasC = 0.0428 ; Fraction plasma volume (58% of blood)

Htc = 0.44 ; hematocrit

;for dermal exposure

SkinTarea = $9.1 * ((BW * 1000) ** 0.666)$; Total area of skin (cm²)
 Skinthickness = 0.1 ; Skin thickness (cm)

; Chemical-specific parameters (PFOS)

Tmc = 3500 ; Maximum resorption rate ($\mu\text{g}/\text{h}/\text{kg}^{0.75}$); changed from 3.5 in the original
 Loccisano 2011 model and expressed in μg , to be consistent with other parameters

Kt = 23.0 ; Resorption affinity ($\mu\text{g}/\text{L}$); changed from 0.023 in the original Loccisano 2011 model and
 expressed in μg , to be consistent with other parameters

Free = 0.025 ; Free fraction of PFOS in plasma

PL = 3.72 ; Liver/plasma partition coefficient

PF = 0.14 ; Fat/ plasma partition coefficient

PK = 0.8 ; Kidney/ plasma partition coefficient

PSk = 0.29 ; Skin/ plasma partition coefficient

PR = 0.2 ; Rest of the body/ plasma partition coefficient

PG = 0.57 ; Gut/ plasma partition coeff.

kurinec = 0.001 ; urinary elimination rate constant ($1/\text{h}/\text{kg}^{-0.25}$); estimated from Harada, et al 2005

kurine = kurinec * BW ** (-0.25)

; Free fraction of chemical in tissues

FreeL = Free/PL ;liver

FreeF = Free/PF ;fat

FreeK = Free/PK ;kidney

FreeSk = Free/PSk ;skin

FreeR = Free/PR ;rest of tissues

FreeG = Free/PG ;gut

; Exposure parameters

tchng = 438000 ;Duration of exposure (h); 50 years

;turn dose on/off

DoseOn = IF time < tchng THEN 1.0 else 0.0

; Dermal exposure

Dermconc = 0.0 ; Dermal concentration ($\mu\text{g}/\text{mL}$)

Dermvol = 0.0 ; Dermal exposure volume (mL)

Dermdose = Dermconc * Dermvol * 1000 ; (μg)

Skinarea = 5 ; Exposed area on skin (cm²)

; Oral exposure

Oralconc = 0.00185 ; Oral uptake ($\mu\text{g}/\text{kg}/\text{day}$)

Oraldose = Oralconc * BW ; ($\mu\text{g}/\text{day}$)

; Drinking water exposure

Drinkconc = 0.0 ; Drinking water concentration ($\mu\text{g}/\text{L}$ or ppb)

Drinkrate = 13 ; Drinking water rate (mL/kg/day)

Drinkdose = (Drinkconc * Drinkrate / 1000) * BW ; ($\mu\text{g}/\text{day}$)

; Inhalation exposure

Inhalation = 0.0 ; Inhalation dose (ppm)

Tinput = 24 ; duration of dose (h) the CONTAM Panel increased the Tinput to 24h (instead of 0.6) considering
 continuous exposure from food.


```

AF' = QF*(CA*Free-CF*FreeF) ; Rate of change in fat (µg/h)
init AF = 0.0
CF = AF/VF ; Concentration in fat (µg/L)
CVF = CF/PF ; Concentration leaving fat (µg/L)

; Kidney compartment
AK' = QK*(CA*Free-CK*FreeK) + Tm*Cfil/(Kt+Cfil) ; Rate of change in kidneys (µg/h)
init AK = 0.0
CK = AK/VK ; Concentration in kidneys (µg/L)
CVK = CK/PK ; Concentration leaving kidneys (µg/L)

; Filtrate compartment
Afil' = Qfil*(CA*Free-Cfil) - Tm*Cfil/(Kt+Cfil) ; Rate of change in filtrate compartment (µg/h)
init Afil = 0.0
Cfil = Afil/Vfil ; Concentration in filtrate compartment (µg/L)

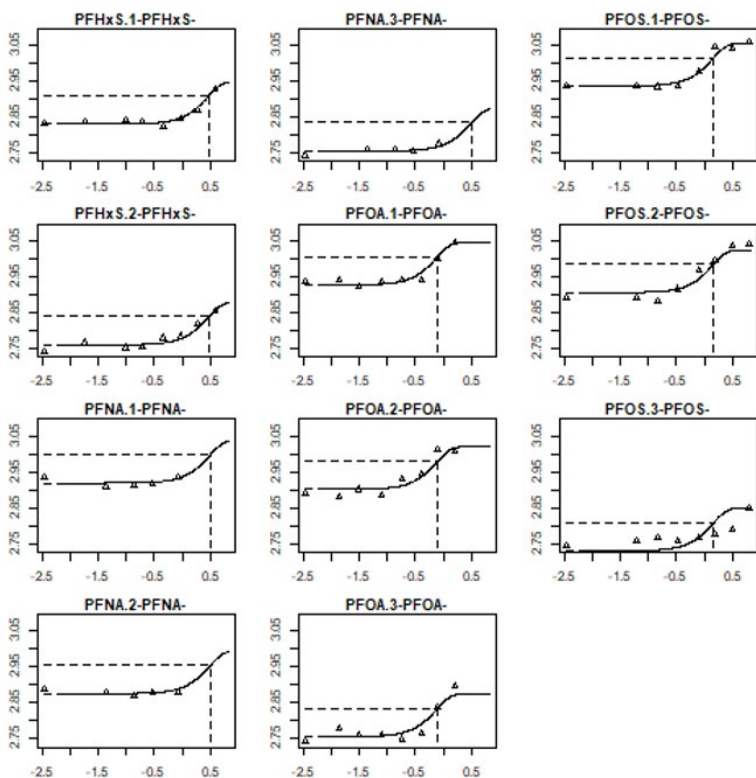
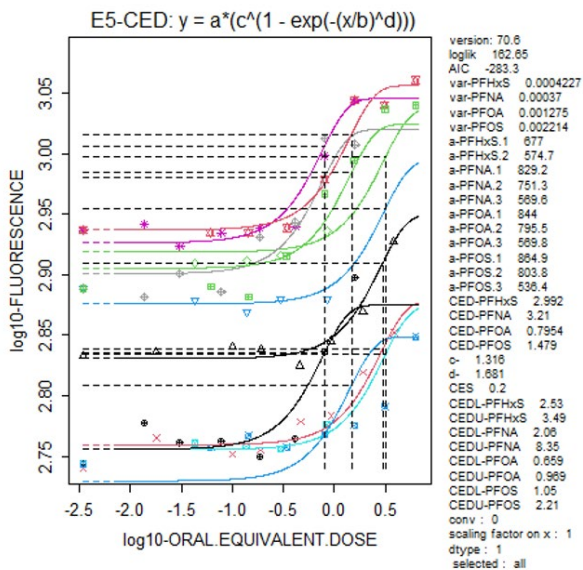
; Storage compartment for urine
;Adelay' = Qfil*Cfil - kurine*Adelay
;init Adelay = 0.0
; Urine
;Aurine' = kurine*Adelay
Aurine' = Qfil*Cfil - kurine*Aurine
init Aurine = 0.0
; Skin compartment
ASk' = QSk*(CA*Free-CSk*FreeSk) ; Rate of change in skin (µg/h)
init ASk = DermDose
CSk = ASk/VSk ; Concentration in skin compartment (µg/L)
CVSk = CSk/PSk ; Concentration leaving skin compartment (µg/L)

; Rest of the body
AR' = QR*(CA*Free-CR*FreeR) ; Rate of change in rest of the body (µg/h)
init AR = 0.0
CR = AR/VR ; Concentration in rest of the body (µg/L)
CVR = CR/PR ; Concentration leaving rest of the body (µg/L)

Display Drinkconc, Dermconc, Oralconc, Inhalation, TInput, Tmc, Kt, Free, PL,PK,PF,PR,PSK,PG,
tchnng.
input1,input2,drinkrate,BW,QCC,QFC,QLC,QKC,QSkC,QGC,VLC,VFC,VKC,VFilC,VGC,VPlasC,kurinec, year ,
APlas, AG, AL, AF, AF, AK, ASK, AR ;for parameters window
Display CA, CG, CL, CF, CR, CK, CAFREE, Qbal , year ;for plotting

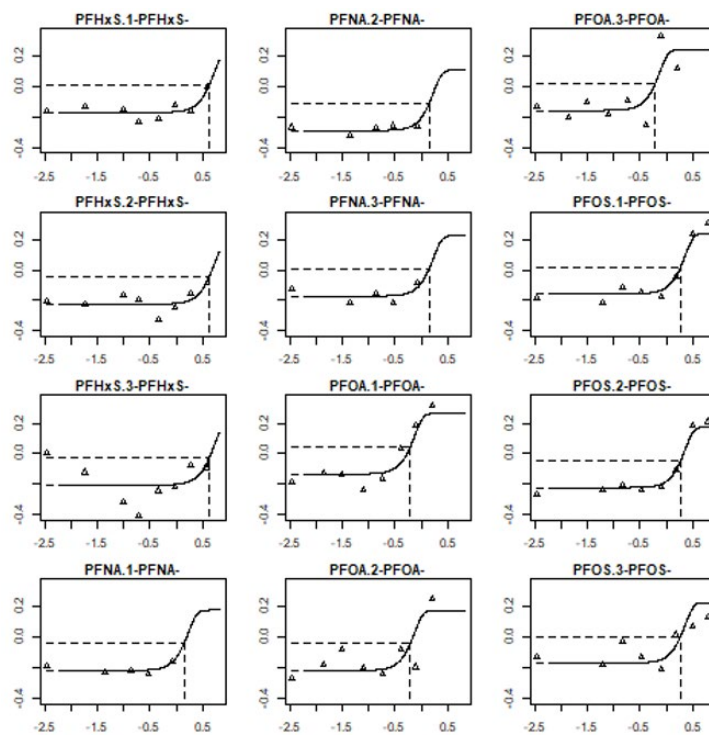
```

Triglycerides- BMD Analysis Scenario 3



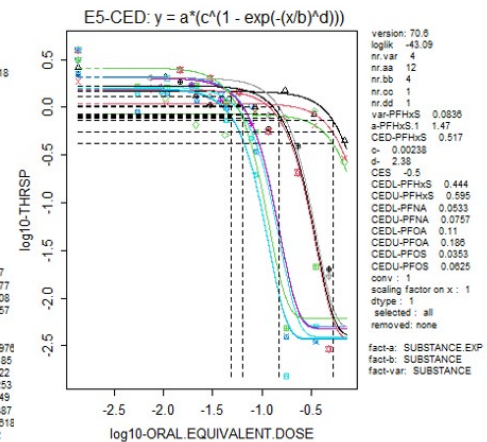
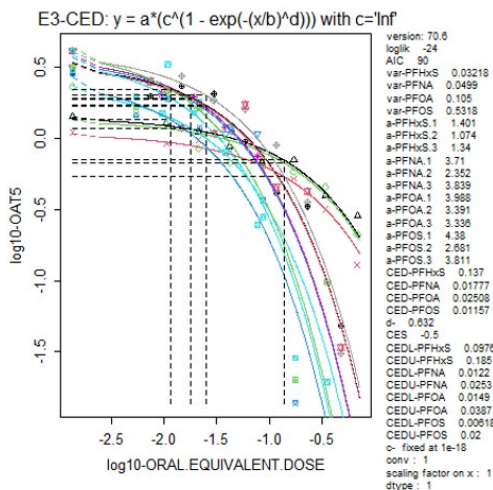
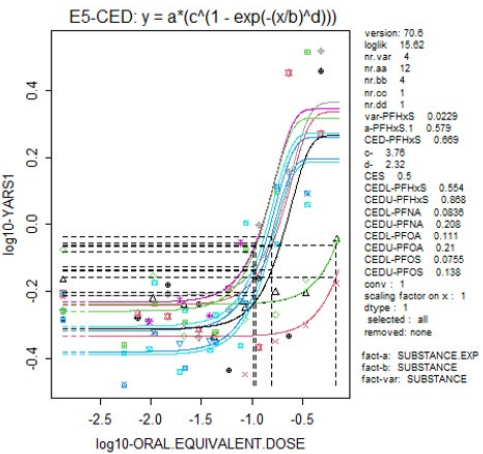
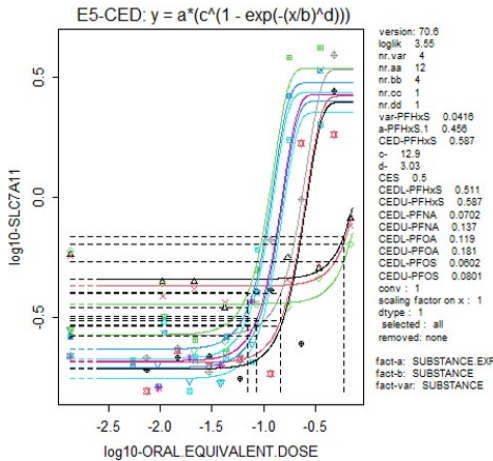
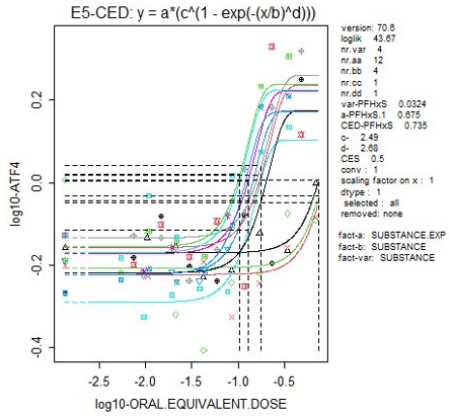
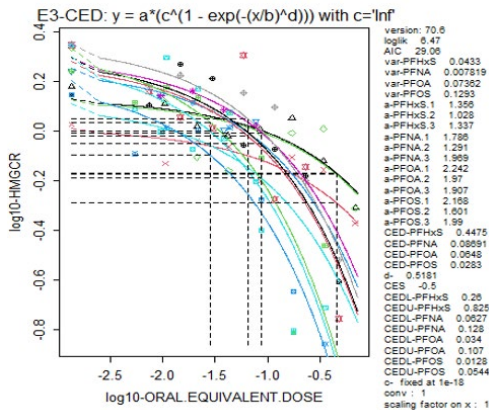
BMD Analysis- gene expression data, example for individual experiment analysis, Scenario 3

ATF4 (individual experiments)

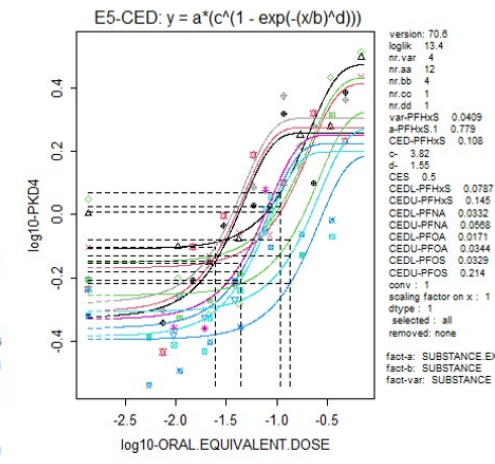
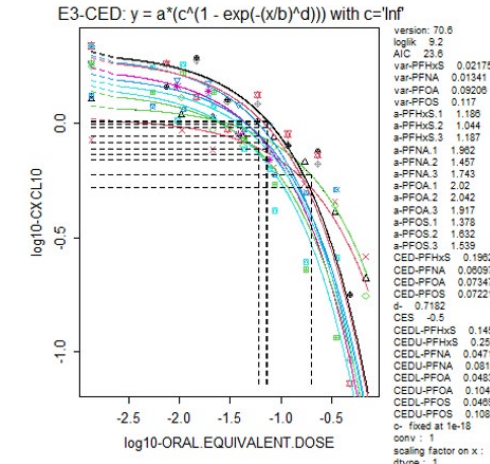
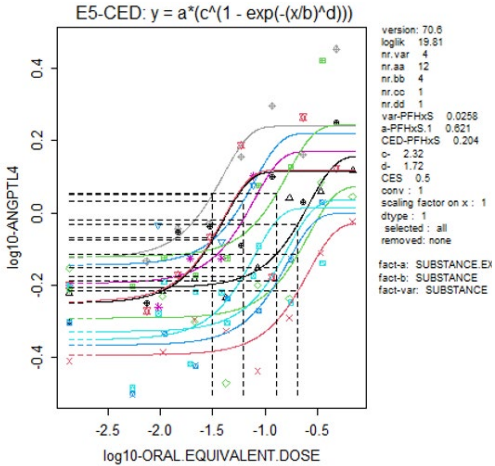
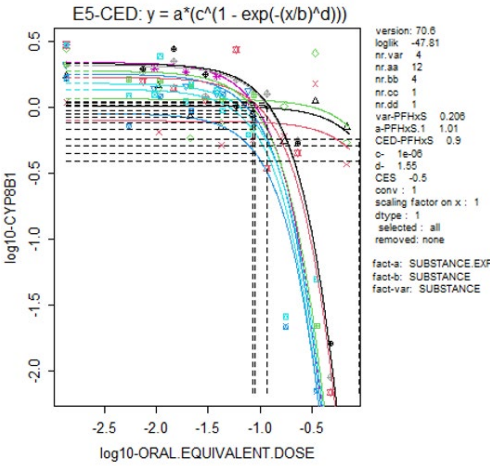
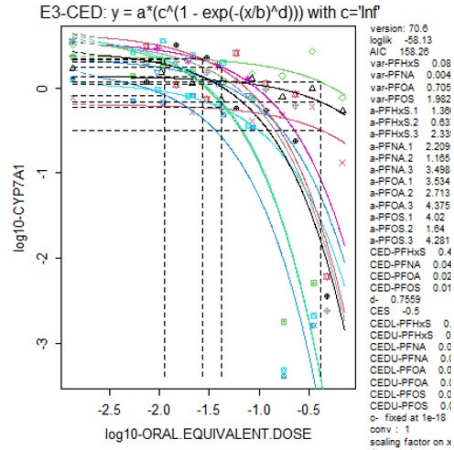
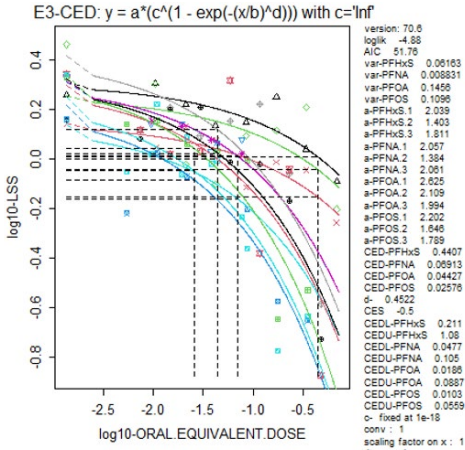


BMD Analysis-gene expression data, all genes

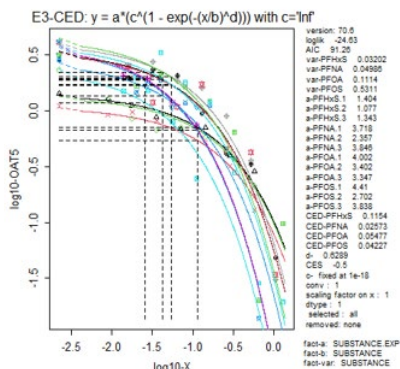
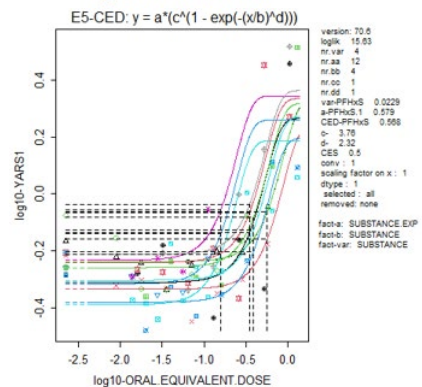
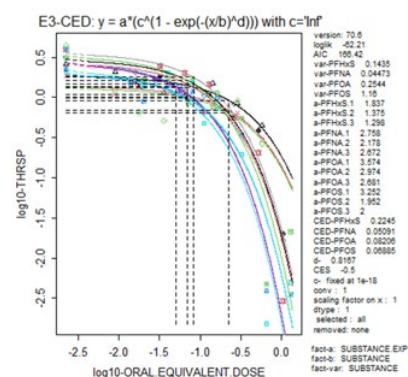
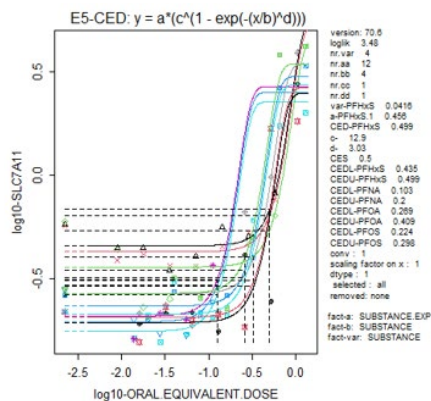
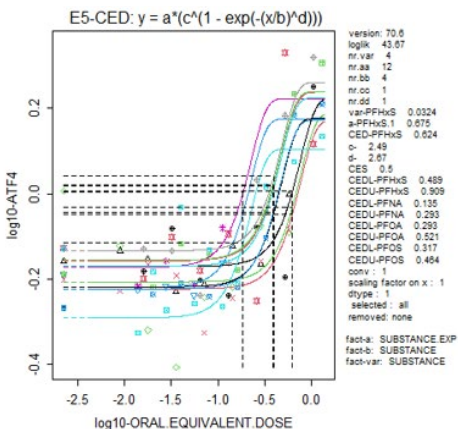
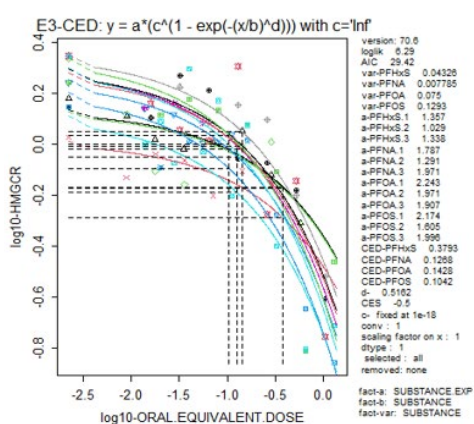
Scenario 1

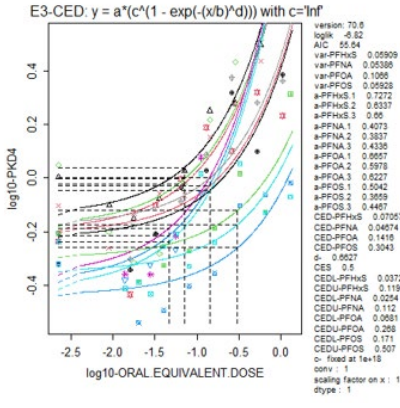
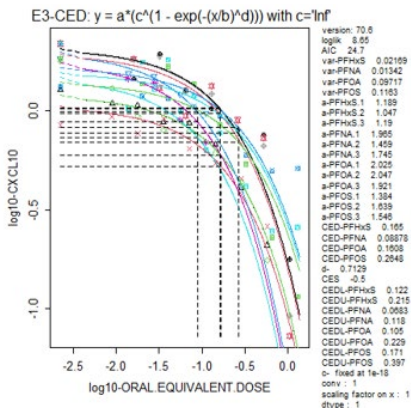
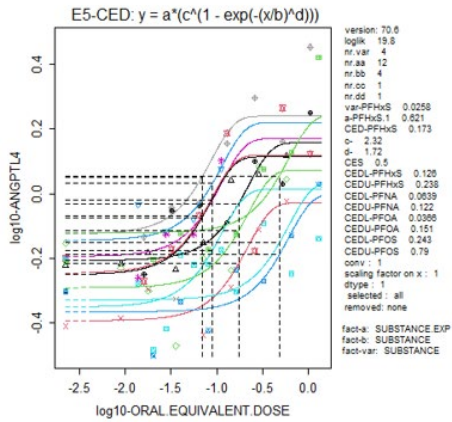
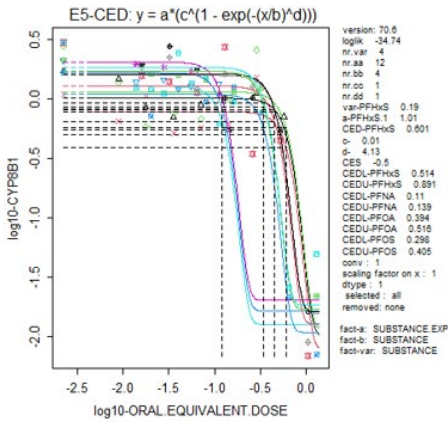
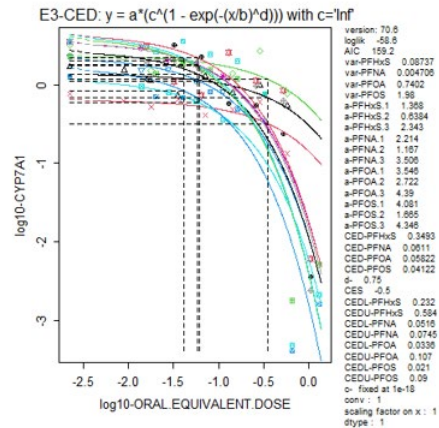
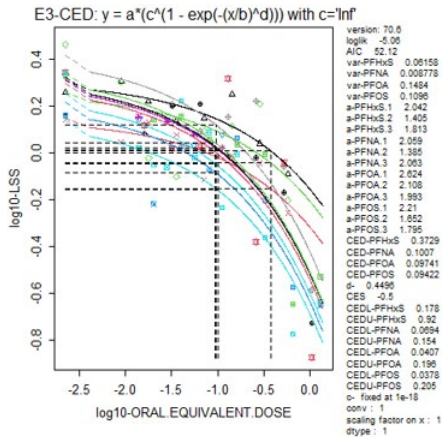


7

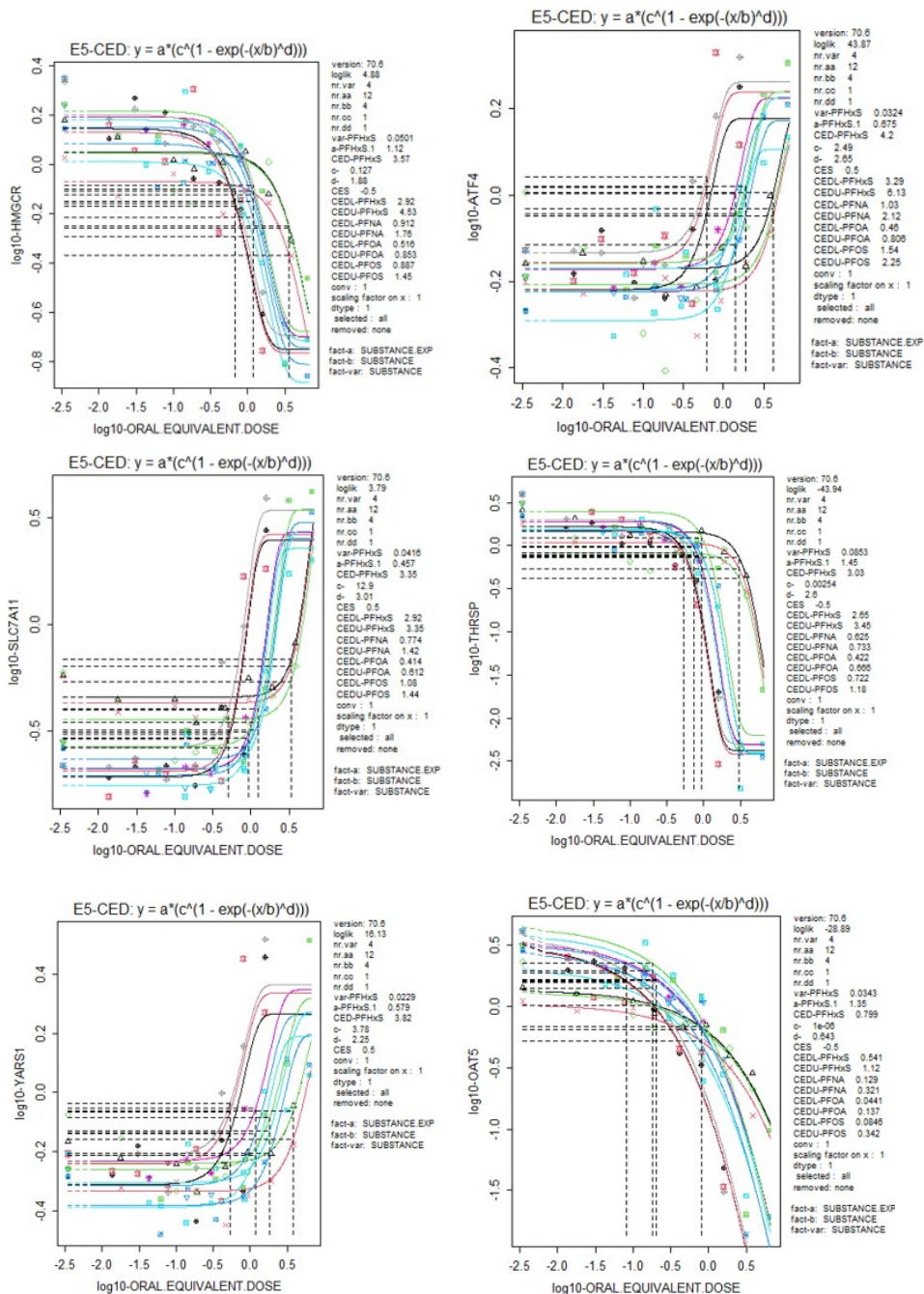


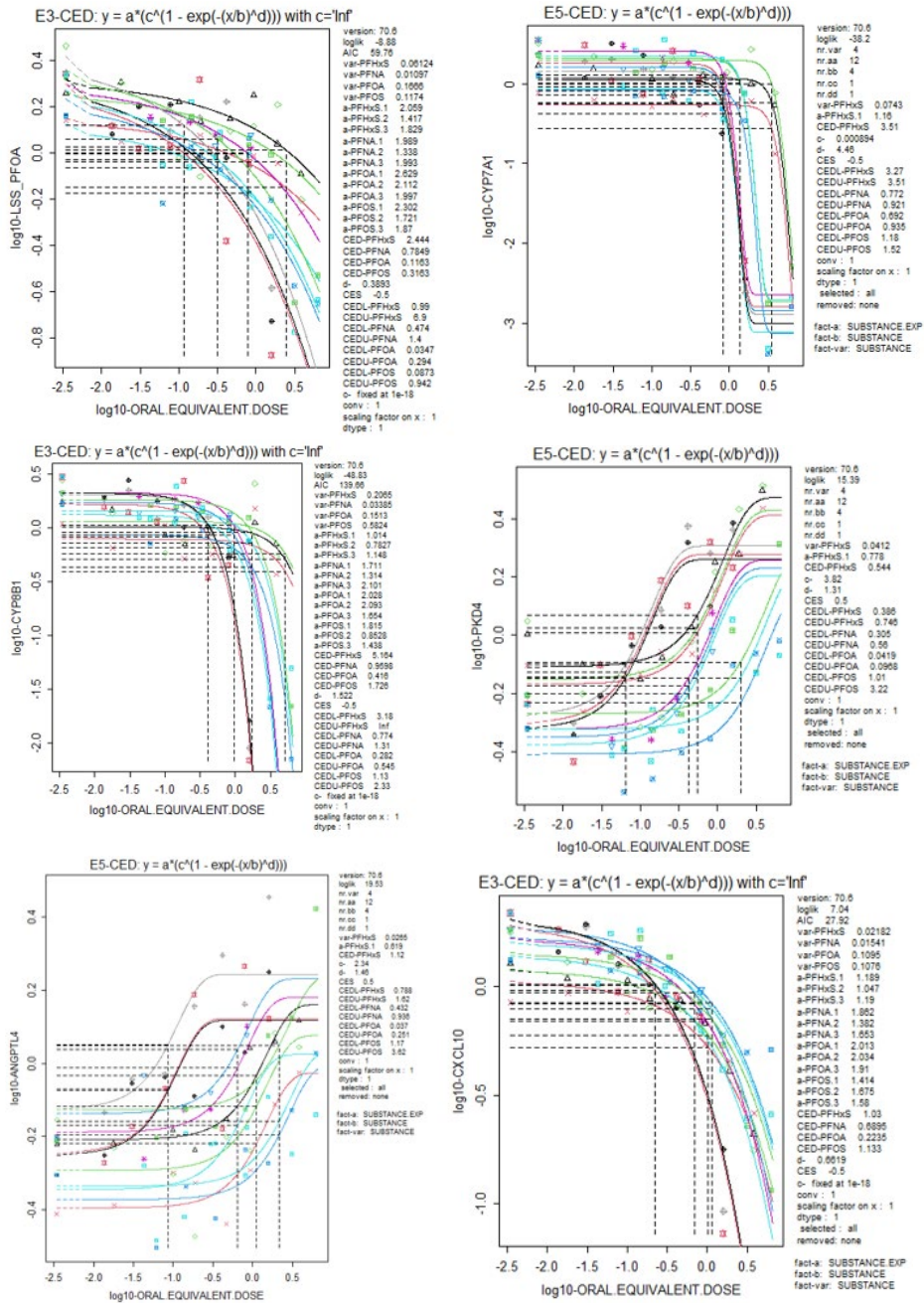
Scenario 2





Scenario 3





SUPPLEMENTARY FIGURE 4 Predicted human oral equivalent dose-response curves for the up- or down-regulation of the 12 genes as induced by PFASs. The 'response' represents the expression of each gene in the HepaRG cells (normalized to housekeeping gene RPL27) exposed to the individual PFASs. A covariate on substance and experiment was applied on the background response (parameter a) to account for possible differences between substances and experiments. A covariate on substance was applied on the potency parameter (b) and the residual variance. Oral equivalent doses are in ng/kg bw/d. The curves were obtained from the *in vitro* concentration-response data based on Scenarios 1, 2 and 3 with PBK model-based reverse dosimetry and a subsequent BMD analysis. The BMD₅₀s and the underlying 95% CIs are presented.

SUPPLEMENTARY TABLE 4 Predicted BMD50s and BMDL-BMDU confidence intervals for the 12 selected genes for the three scenarios.

Genes	Scenario 1			
	PFOA	PFNA	PFHxS	PFOS
HMGCR	0.065 0.034-0.107	0.087 0.0627-0.128	0.448 0.26-0.825	0.028 0.0128-0.0544
LSS	0.044 0.02-0.09	0.069 0.048-0.105	0.441 0.21-1.08	0.026 0.01-0.056
CYP7A1	0.027 0.015-0.051	0.042 0.03550-0.0517	0.413 0.276-0.686	0.011 0.00579-0.0257
CYP8B1	0.113 0.0741-0.150	0.083 0.0673-0.112	0.928 0.5510-Inf	0.088 0.0559-0.121
CXCL10	0.073 0.0483-0.104	0.061 0.0471-0.0811	0.196 0.145-0.255	0.072 0.0469-0.108
PKD4	0.024 0.017-0.034	0.044 0.03-0.06	0.108 0.08-0.15	0.134 0.033-0.214
ANGPTL4	0.031 0.017-0.07	0.062 0.043-0.084	0.204 0.148-0.28	0.13 0.07-0.212
OAT5	0.025 0.0149-0.0387	0.018 0.0122-0.0253	0.137 0.0976-0.185	0.012 0.00618-0.02
ATF4	0.18 0.13-0.23	0.13 0.09-0.2	0.73 0.58-1.07	0.1 0.09-0.13
SLC7A11	0.15 0.12-0.18	0.09 0.07-0.14	0.59 0.51-0.59	0.07 0.06-0.08
YARS1	0.16 0.11-0.21	0.11 0.08-0.2	0.67 0.55-0.87	0.1 0.08-0.13
THRSP	0.147 0.11-0.186	0.063 0.0533-0.0757	0.517 0.444-0.595	0.049 0.0353-0.0625

Genes	Scenario 2			
	PFOA	PFNA	PFHxS	PFOS
HMGCR	0.143 0.0746-0.237	0.127 0.0915-0.186	0.379 0.22-0.701	0.104 0.047-0.201
LSS	0.097 0.041-0.2	0.101 0.069-0.15	0.373 0.18-0.92	0.094 0.038-0.21
CYP7A1	0.058 0.0336-0.1070	0.061 0.0516-0.0745	0.349 0.2320-0.584	0.041 0.021-0.09
CYP8B1	0.256 0.394-0.516	0.122 0.11-0.139	0.78 0.514-0.891	0.338 0.298-0.405
CXCL10	0.161 0.105-0.229	0.089 0.0683-0.118	0.165 0.122-0.215	0.265 0.171-0.397
PKD4	0.1416 0.0681-0.268	0.04674 0.0254-0.112	0.07057 0.0372-0.119	0.3043 0.171-0.507
ANGPTL4	0.06897 0.0366-0.151	0.0898 0.0639-0.122	0.1733 0.126-0.238	0.4803 0.243-0.79
OAT5	0.055 0.0324-0.0852	0.026 0.0176-0.0368	0.115 0.0818-0.1570	0.042 0.0223-0.0736
ATF4	0.3969 0.293-0.521	0.1856 0.135-0.293	0.6244 0.489-0.909	0.3861 0.317-0.464
SLC7A11	0.3284 0.269-0.409	0.1251 0.103-0.2	0.4986 0.435-0.499	0.2612 0.224-0.298
YARS1	0.3492 0.248-0.469	0.1581 0.122-0.302	0.5684 0.471-0.737	0.3864 0.281-0.512
THRSP	0.339 0.257-0.424	0.093 0.0792-0.111	0.445 0.385-0.509	0.188 0.138-0.237

Genes	Scenario 3			
	PFOA	PFNA	PFHxS	PFOS
HMGCR	0.68	1.17	3.57	1.18
	0.52-0.85	0.91-1.76	2.92-4.53	0.89-1.45
LSS	0.12	0.78	2.44	0.32
	0.03-0.29	0.47-1.4	0.99-6.9	0.09-0.9
CYP7A1	0.82	0.83	3.51	1.36
	0.692-0.935	0.772-0.921	3.27-3.51	1.18-1.52
CYP8B1	0.42	0.96	5.16	1.73
	0.28-0.55	0.77-1.31	3.18-inf.	1.13-2.33
CXCL10	0.22	0.69	1.03	1.13
	0.14-0.33	0.51-0.97	0.74-1.37	0.71-1.74
PKD4	0.06	0.42	0.54	1.98
	0.04-0.1	0.31-0.56	0.39-0.75	1.01-3.22
ANGPTL4	0.09	0.65	1.13	2.16
	0.04-0.25	0.43-0.94	0.79-1.62	1.17-3.62
OAT5	0.08	0.19	0.74	0.18
	0.04-0.13	0.12-0.3	0.5-1.04	0.08-0.33
ATF4	0.61	1.4	4.2	1.88
	0.46-0.81	1.03-2.12	3.29-6.13	1.54-2.25
SLC7A11	0.5	0.94	3.35	1.26
	0.41-0.61	0.77-1.42	2.92-3.35	1.08-1.44
YARS1	0.53	1.18	3.82	1.85
	0.38-0.72	0.92-2.03	3.15-4.99	1.35-2.45
THRSP	0.54	0.73	3.03	0.95
	0.42-0.67	0.63-0.73	2.65-3.45	0.72-1.18

PBK Model code for Convertino et al. (2018) simulation**Model Code for PFOA**

METHOD Stiff

STARTTIME = 0

STOPTIME=1008 ;end of simulation (h), 6 weeks

DT = 0.01

TOLERANCE = 0.01

DTMAX = 10.0

DTMIN = 0.000001

year= TIME/(24*365)

;Physiological parameters (from Brown, et al 1997)

; fractional blood flows

QCC = 12.5 ; Cardiac blood output (L/h/kg^{0.75})

QFC = 0.052 ; Fraction cardiac output going to fat

QLC = 0.069 ; Fraction cardiac output going to liver, through hepatic artery

QKC = 0.175 ; Fraction cardiac output going to kidney

QSkC = 0.058 ; Fraction cardiac output going to skin

QGC = 0.181 ; Fraction of cardiac output going to gut and in the liver via portal artery

; Not used ;QfilC = 0.035 ; Fraction cardiac output to the filtrate compartment (20% of kidney blood flow)

; BW = 70 ; Body weight (kg) for men; 58 kg for women

; weight algorithm based on french survey (French total Diet Study)

BW=3.68+4.47*year-0.093*year²+0.00061*year³

fractional tissue volumes

VLC = 0.026 ; Fraction liver volume

VFC = 0.214 ; Fraction fat volume

VKC = 0.004 ; Fraction kidney volume

VfilC = 0.0004 ; Fraction filtrate compartment volume (10% of kidney volume)

VGC = 0.0171 ; Fraction gut volume

VPlasC = 0.0428 ; Fraction plasma volume (58% of blood)

Htc = 0.44 ; hematocrit

for dermal exposure

SkinTarea = 9.1*((BW*1000)**0.666) ; Total area of skin (cm²)

Skinthickness = 0.1 ; Skin thickness (cm)

; Chemical-specific parameters for PFOA

Tmc = 6000 ; Maximum resorption rate ($\mu\text{g}/\text{h}/\text{kg}^{0.75}$), changed from 6 in the original Loccisano 2011 model and expressed in μg , to be consistent with other parametersKt = 55.0 ; Resorption affinity ($\mu\text{g}/\text{L}$), changed from 0.055 in the original Loccisano 2011 model and expressed in μg , to be consistent with other parameters

Free = 0.02 ; Free fraction of PFOA in plasma

PL = 2.2 ; Liver/plasma partition coefficient

PF = 0.04 ; Fat/ plasma partition coefficient

PK = 1.05 ; Kidney/ plasma partition coefficient

PSk = 0.1 ; Skin/ plasma partition coefficient

$PR = 0.12$; Rest of the body/ plasma partition coefficient
 $PG = 0.05$; Gut/ plasma partition coeff.
 $kurinec = 0.0003$; urinary elimination rate constant ($/h/kg^{-0.25}$) ; estimated from Harada, et al
 2005
 $kurine = kurinec * BW^{**}(-0.25)$

Free fraction of chemical in tissues

$FreeL = Free/PL$; liver
 $FreeF = Free/PF$; fat
 $FreeK = Free/PK$; kidney
 $FreeSk = Free/PSk$; skin
 $FreeR = Free/PR$; rest of tissues
 $FreeG = Free/PG$; gut

; Exposure parameters

$tchng = 1008$; Duration of exposure (h); 6 weeks

; turn dose on/off

$DoseOn = IF\ time < tchng\ THEN\ 1.0\ else\ 0.0$

; Dermal exposure

$Dermconc = 0.0$; Dermal concentration ($\mu g/mL$)
 $Dermvol = 0.0$; Dermal exposure volume (mL)
 $Dermdose = Dermconc * Dermvol * 1000$; (μg)
 $Skinarea = 5$; Exposed area on skin (cm^2)

; Oral exposure

$Oralconc = 0.00085$; Oral uptake ($\mu g/kg/day$)
 $Oraldose = Oralconc * BW$; ($\mu g/day$)

; Drinking water exposure

$Drinkconc = 0.0$; Drinking water concentration ($\mu g/L$ or ppb)
 $Drinkrate = 13$; Drinking water rate (mL/kg/day)
 $Drinkdose = (Drinkconc * Drinkrate / 1000) * BW$; ($\mu g/day$)

; Inhalation exposure

$Inhalation = 0.0$; Inhalation dose (ppm)
 $Tinput = 24.0$; duration of dose (h), the CONTAM Panel increased the Tinput to 24h (instead
 of 0.6) considering continuous exposure from food

; oral dose

$Input1 = IF\ MOD(time, 168) <= Tinput\ THEN\ Oraldose / Tinput\ ELSE\ 0.0$; exposure once per week (once
 per 168 h)

; drinking water

$Input2 = IF\ MOD(time, 168) <= Tinput\ THEN\ Drinkdose / Tinput\ ELSE\ 0.0$

; Scaling parameters

$QC = QCC * BW^{**}0.75$; Cardiac output (L/h)
 $QCP = QC * (1 - Htc)$; adjust for plasma flow


```

; Kidney compartment
AK' = QK*(CA*Free-CK*FreeK) + Tm*Cfil/(Kt+Cfil) ; Rate of change in kidneys (µg/h)
init AK = 0.0
CK = AK/VK ; Concentration in kidneys (µg/L)
CVK = CK/PK ; Concentration leaving kidneys (µg/L)

; Filtrate compartment
Afil' = Qfil*(CA*Free-Cfil) - Tm*Cfil/(Kt+Cfil) ; Rate of change in filtrate compartment (µg/h)
init Afil = 0.0
Cfil = Afil/Vfil ; Concentration in filtrate compartment (µg/L)

; Storage compartment for urine
; Adelay' = Qfil*Cfil-kurine*Adelay
; init Adelay = 0.0
; Urine
; Aurine' = kurine*Adelay
Aurine' = Qfil*Cfil - kurine*Aurine
init Aurine = 0.0

; Skin compartment
ASK' = QSk*(CA*Free-CSk*FreeSk) ; Rate of change in skin (µg/h)
init ASk = DermDose
CSk = ASk/VSk ; Concentration in skin compartment (µg/L)
CVSk = CSk/PSk ; Concentration leaving skin compartment (µg/L)

; Rest of the body
AR' = QR*(CA*Free-CR*FreeR) ; Rate of change in rest of the body (µg/h)
init AR = 0.0
CR = AR/VR ; Concentration in rest of the body (µg/L)
CVR = CR/PR ; Concentration leaving rest of the body (µg/L)

Display Drinkconc, Dermconc, Oralconc, Inhalation, TInput, Tmc, Kt, Free, PL,PK,PF,PR,PSK,PG,
tchng,input1,input2,drinkrate,BW,QCC,QFC,QLC,QKC,QSkC,QGC,VLC,VFC,VKC,VFilC,VGC,VPlasC,kurinec,
year , APlas, AG, AL, AF, AF, AK, ASK, AR ; for parameters window
Display CA, CG, CL, CF, CR, CK, CAFREE, Qbal , year, FreeL ; for plotting

```


References-Supplementary Material

- Convertino M, Church TR, Olsen GW, Liu Y, Doyle E, Elcombe CR, Barnett AL, Samuel LM, MacPherson IR, Evans TRJ. 2018. Stochastic pharmacokinetic-pharmacodynamic modeling for assessing the systemic health risk of perfluorooctanoate (pfoa). *Toxicol Sci.* 163(1):293-306.
- Huang MC, Dzierlenga AL, Robinson VG, Waidyanatha S, DeVito MJ, Eifrid MA, Granville CA, Gibbs ST, Blystone CR. 2019. Toxicokinetics of perfluorobutane sulfonate (pfbs), perfluorohexane-1-sulphonic acid (pfhxs), and perfluorooctane sulfonic acid (pfos) in male and female hsd:Sprague dawley sd rats after intravenous and gavage administration. *Toxicology reports.* 6:645-655.
- Loccisano AE, Campbell JL, Jr., Andersen ME, Clewell HJ, 3rd. 2011. Evaluation and prediction of pharmacokinetics of pfoa and pfos in the monkey and human using a pbpk model. *Regulatory toxicology and pharmacology* : RTP. 59(1):157-175.
- NTP. 2019. Toxicity studies of perfluoroalkyl carboxylates administered by gavage to sprague dawley (hsd:Sprague dawley sd) rats. *Toxic Rep Ser.* (97).
- Olsen GW, Burris JM, Ehresman DJ, Froehlich JW, Seacat AM, Butenhoff JL, Zobel LR. 2007. Half-life of serum elimination of perfluorooctanesulfonate, perfluorohexanesulfonate, and perfluorooctanoate in retired fluorochemical production workers. *Environ Health Perspect.* 115(9):1298-1305.
- Vasilogianni AM, Achour B, Scotcher D, Peters SA, Al-Majdoub ZM, Barber J, Rostami-Hodjegan A. 2021. Hepatic scaling factors for *in vitro-in vivo* extrapolation of metabolic drug clearance in patients with colorectal cancer with liver metastasis. *Drug Metab Dispos.* 49(7):563-571.
- Zhang Y, Beesoon S, Zhu L, Martin JW. 2013. Biomonitoring of perfluoroalkyl acids in human urine and estimates of biological half-life. *Environ Sci Technol.* 47(18):10619-10627.

Chapter 8

Summary and General Discussion



In order to protect the environment and people from detrimental effects of chemicals a universal tool has been employed, the so-called risk assessment. Traditionally, risk assessment relied upon data derived from animal studies. However, these tests are subject to several ethical considerations, they are expensive and time consuming. As such, generating safety information for the thousands of commercial chemicals is unrealistic, not only due to the high demand in animal sacrifice, but also due to practical reasons. Additionally, a lot of data suggest that toxicity testing in experimental animals may not always predict toxic effects pertinent to humans. As such, the scientific premise behind animal models being the golden standard for assessing chemical safety appears flawed. The field of toxicology is moving towards the next generation risk assessment that will use the New Approach Methodologies (NAMs). Novel approaches to hazard characterization will be driven by well-designed *in vitro* assays and the development of mechanism-based biomarkers. These assays will help establish the underlying biological mechanisms that can likely result in an *in vivo* adverse outcome, thereby facilitating the shift from apical endpoints at an organism level to mechanistically-anchored endpoints. Relying on these methodologies for predicting toxicity presupposes to quantitatively relate *in vitro* readouts to *in vivo* responses, the so-called Quantitative *In vitro* to *In vivo* Extrapolation(QIVIVE). An effective framework for performing QIVIVE is provided with the application of physiologically based kinetic (PBK) modelling with reverse dosimetry. These models can be used for predicting the *in vivo* external exposure that would produce chemical concentrations in the target tissue equivalent to the concentrations at which effects were observed with *in vitro* assays. Parameterization of the models is facilitated with the use of *in vitro*- and *in silico*-derived substance-specific characteristics. This thesis explores the implementation of PBK models in a number of QIVIVE approaches. Different examples of QIVIVE are described ranging from approaches using generic PBK models to approaches employing substance-specific models.

Summary

This thesis consists of three different parts. In the first part (**Section I**), the performance of two generic PBK models with incorporated QSAR model parameterization was evaluated, in terms of their capacity to predict toxicokinetics of a wide span of chemicals, regarding certain physicochemical and biological properties (**Chapter 2**). In essence, in this Chapter, a previous evaluation of the applicability domain of the generic PBK model IndusChemFate was extended (Fragki et al. 2017). Thereafter, the model was compared to its more complex biological complement (“TNO Model”). The TNO model incorporates more detailed organ:blood partition, liver metabolism and absorption kinetics. Both models run with incorporated organ:blood and renal excretion QSARs and require minimum parameterization. The results revealed that the “simpler” performed best, illustrating that IndusChemFate can be a useful first-tier for simulating toxicokinetics based on QSARs and *in vitro* parameters.

In **Section II**, IndusChemFate was selected for performing QIVIVE for the endpoint of developmental toxicity, with the use of data from alternative embryotoxicity assays. This required the scaling of *in vitro* observed dose-response characteristics to *in vivo* fetal exposure. In **Chapter 3**, three different classes of developmentally toxic chemicals were chosen as model compounds: triazoles, glycol ethers' alkoxyacetic acid metabolites and phthalate primary metabolites. These compounds were previously tested in three alternative assays: the whole- embryo culture (WEC), the zebrafish embryo test (ZET), and the mouse embryonic stem cell test (EST). Here chemical maternal blood concentrations were used as a proxy for fetal exposure and the model required specific input per each class of compounds. The IndusChemFate model was capable of describing the *in vivo* kinetics of the three classes of developmental toxicants employed, though at the expense of several chemical specific adaptations. Furthermore, comparisons were performed of the PBK-simulated blood levels at toxic *in vivo* doses to the respective *in vitro* effective concentrations, with the three different assays. The results indicated that a combination of tests is preferable for predicting the endpoint of developmental toxicity.

In **Chapter 4 (Section II)**, the approach was extended with the adaptation of the PBK model, by incorporating physiological alterations in the maternal body during gestation, placental transfer, and fetal growth. Placental transfer was studied *in vitro* with the BeWo cell assay for six model compounds with embryotoxic potential. The BeWo results illustrated different transport profiles of the chemicals across the BeWo monolayer, allocating the substances into two distinct groups: the 'quickly-transported' and the 'slowly-transported'. These results were incorporated in the IndusChemFate PBK model extended for the rat pregnancy. Exposure PBK-simulations during gestation demonstrated satisfactory kinetic predictions, when compared to experimentally measured maternal blood and fetal concentrations. A PBK modelling reverse dosimetry approach was applied to translate embryotoxicity *in vitro* concentrations-response curves of the chosen chemicals into equivalent *in vivo* dose-response curves. Here, the fetal C_{max} was taken as the internal dose metric for the induction of developmental toxicity. Selected *in vitro* tests were the WEC and the EST (cardiac:EST_c and neural:EST_n). The *in vitro*-based predictions were compared to rat developmental toxicity data. This comparison illustrated a fairly good prediction for the WEC, followed by the EST_c (for three out of the five compounds), with differences of the selected dose metric standing within the same order of magnitude (<10-fold). Overall the *in vitro* to *in vivo* comparisons suggest a promising future for the application of such approaches in the chemical safety assessment of developmental toxicity, at least for screening and prioritization purposes, although the clear need for further optimizations is acknowledged for a wider application such as in risk assessment.

In the last part (**Section III**), a NAMs case study is presented for per- and polyfluoroalkyl substances (PFASs). The number of existing PFASs is estimated to be around a few thousands, and for many of these *in vivo* toxicity data are lacking. For this reason, application of NAMs can be useful for the screening of PFASs and the identification of compounds to be prioritized for a more comprehensive hazard characterization. The endpoint selected here was hepatotoxicity

and perturbations in lipid homeostasis. In **Chapter 5** the main issues related to modulation of lipid homeostasis by the two most common congeners PFOA and PFOS were discussed, with emphasis on the underlying mechanisms relevant for humans. Several population studies have repeatedly found correlations between increased blood levels of PFOS/PFOA and elevated blood total cholesterol and LDL-C, (and to a lesser extent TGs). Nevertheless, these findings have not been linked to a corresponding adverse health effect and are inconsistent with toxicological animal studies, where high doses of PFOS/PFOA were found to lower serum cholesterol and TGs, and increase liver lipids. These apparent divergent findings thus present health risk assessors a conundrum. Overall, this contrast between human and animal data may be an artefact of dose, or a result of interspecies differences in physiology regarding lipid homeostasis, and/or PFAS-species differences in toxicokinetics, as well as basic nutrition. No simple mechanistic explanation could be given. This study highlighted the need for future studies with human-relevant test systems that would assist in getting more insight into the mechanistic pathways pertinent for humans.

In **Chapter 6**, the effects of 18 PFASs on cellular triglyceride accumulation (AdipoRed assay) and gene expression (DNA microarray for PFOS and RT-qPCR for all 18 PFASs) was studied in human HepaRG cells. BMDEExpress analysis of the PFOS microarray data was used as a guide for selecting ten genes to assess the concentration-effect relationship of all 18 PFASs with qRT-PCR analysis. The AdipoRed data and the qRT-PCR data were used for the derivation of *in vitro* relative potencies. *In vitro* relative potency factors (RPFs) could be obtained for 8 PFASs based on the AdipoRed data, whereas for the selected genes *in vitro* RPFs could be obtained for 11-18 PFASs. For the readout *OAT5* expression, *in vitro* RPFs were obtained for all PFASs, suggesting that *OAT5* gene expression, together with some of the other genes, may be a suitable readout to determine relative *in vitro* liver toxicity potencies of PFASs. For 7 of the 10 chosen genes the *in vitro*-based RPFs were in line with data reported for PFAS-induced liver toxicity in rats. When combined with information on the toxicokinetics of the PFASs in humans, these *in vitro* data may be used to estimate potency differences of PFASs in humans *in vivo*.

As a next step in **Chapter 7**, a PFASs QIVIVE case study is presented PFASs: PFOA, PFNA, PFHxS and PFOS. *In vitro* concentration-response data (TG accumulation and gene expression changes of 12 selected genes) obtained in HepaRG cells were converted into dose-response curves, with PBK model-facilitated reverse dosimetry. For this study, cellular PFAS levels were determined in the HepaRG cells to link *in vitro* exposure to *in vivo* internal exposure in the liver. An exposure scenario of 50 years was considered in order to represent the lifetime chronic exposure to PFASs. Finally the predicted oral equivalent effect doses were compared with the human dietary exposure for the European population. Oral equivalent effect doses predicted in this QIVIVE analysis were found to be in the same range as estimated human exposure levels, in particular when the upper bound exposure estimates were considered. This QIVIVE case study, illustrates how *in vitro* assay data can be used for determining points of departure (PODs) for screening, hazard identification and prioritization of other PFASs for which *in vivo* data are lacking.

General discussion

The procedure for QIVIVE with PBK model reverse dosimetry

QIVIVE is the process of converting an *in vitro* concentration (or concentration-response) to an external exposure level (or dose-response relationship). Figure 1 illustrates a basic workflow of a QIVIVE analysis. For the QIVIVE extrapolation an implicit assumption is made: equal concentrations at the target site *in vitro* and *in vivo* will result in equal effects. As a first step, an *in vitro* system that will provide the concentration-response curves of a test chemical for a selected readout is required. A toxicologically meaningful *in vitro* biomarker has to be selected, i.e. a biomarker being a relevant surrogate for an *in vivo* adverse effect. BMD modelling can be applied to the *in vitro* results for the derivation of a benchmark concentration (BMC), i.e. the effect concentration above which the substance is considered to perturb the *in vitro* system. The BMC is the starting point for the PBK model reverse dosimetry, where it is translated into the equivalent human *in vivo* effect dose (BMD). Alternatively, the entire *in vitro* concentration-response curve can be transformed into the corresponding *in vivo* dose response curve. BMD modelling can then be applied to the extrapolated *in vivo* dose response relationship, in order to obtain a benchmark dose level (BMD). Either of the two ways, the predicted effect doses (BMDs) have been commonly referenced as equivalent administered dose (EAD), administered equivalent dose (AED), or for the case of oral exposure oral equivalent dose (Chang et al. 2022). They serve as the point of departure (POD) for the hazard characterization and risk assessment.

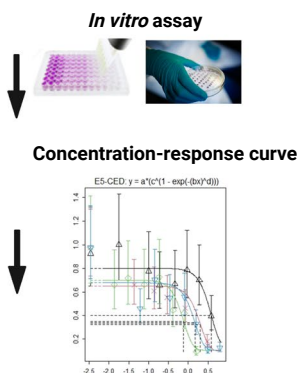
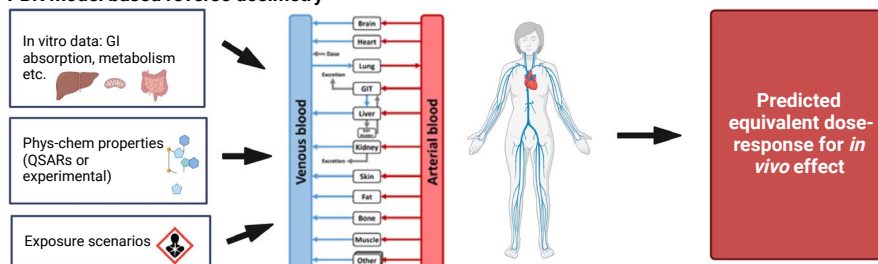


FIGURE 1 Schematic overview of the QIVIVE analysis with PBK model based reverse dosimetry (Created with Biorender.com).

PBK model based reverse dosimetry



***In vitro* test system and biomarkers: what is a meaningful readout?**

Shifting to cell or tissue-based testing, signifies that the traditional apical endpoints commonly measured in the animal studies will be substituted by *in vitro* effect biomarkers. One of the challenges here is to establish a link between the *in vitro* measurements and a hazardous outcome in an intact living organism. Ideally, the *in vitro* measured readout to be used for the QIVIVE will provide quantitative information predictive of adverse outcomes *in vivo* (Blaauboer et al. 2012; Zhang et al. 2018c).

For the work of this thesis on QIVIVE for developmental toxicity, as laid down in Chapters 3 and 4, a number of alternative (some not completely animal-free) tests were selected: the rodent post-implantation Whole- Embryo Culture method (WEC) (Chapin et al. 2008; Piersma et al. 2004), the zebrafish embryo test (ZET) (Brannen et al. 2010; Hill et al. 2005), and the mouse embryonic stem cell test (EST) (Seiler et al. 2004; Seiler and Spielmann 2011). The EST completely eliminates the sacrifice of animals by utilizing a permanent murine cell line (Scholz et al. 1999; Seiler and Spielmann 2011) and the assay's readouts used here were physiological (e.g. beating of cardiomyocytes in the ESTc), rather than mechanism-based. Since these readouts are only surrogates for *in vivo* adverse effects (e.g. decreased fetal weight, skeletal malformations etc.) a lot of research is currently focused on understanding better the underlying mechanisms, and formulating AOPs that can result in embryotoxicity (Piersma et al. 2022). On the other hand, the WEC and ZET involve the development of whole embryos, either after explantation from a pregnant rat or using zebra fish eggs, respectively (Chapin et al. 2008; Piersma 2006). The advantage of both tests is that they mirror general morphogenesis, at least within a given developmental time window, due to their use of the whole embryo, rather than a plain cell-line (Chapin *et al.*, 2008). It shall be noted that, the EST cardiac and WEC have already been scientifically validated by the European Centre for Validation of Alternative Methods (ECVAM) for over two decades, with respect to their capacity to distinguish different classes of embryotoxicants (Brown 2002; Genschow et al. 2002). Although these methods may not represent at the moment complete replacements for current animal tests, they can be used either as part of an *in vitro* testing battery approach or for screening and prioritization (RIVM 2009; Spielmann 2009) and hence, they were selected for our QIVIVE for developmental toxicity.

In the case of the PFAS QIVIVE (Chapter 7), the adverse effects to be captured *in vitro* were hepatotoxicity and perturbations in lipid homeostasis. Here, a more mechanism-based approach was followed. Initially, available information on the underlying mechanisms, through which PFASs might induce lipide perturbations, were reviewed (Chapter 5). This review (Fragki et al. 2021) highlighted the need for new studies with human hepatocytes in order to clarify the mechanism of action of these chemicals. For this purpose, *in vitro* studies were performed using the hepatic stem cell line HepaRG, a human progenitor cell line that can differentiate into two different phenotypes (hepatocytes and biliary cells) (McGill et al. 2011). Hepatocytes play an important role in lipid metabolism and cholesterol homeostasis, indicating the relevance of hepatocytes as model in this study. HepaRG cells

are claimed to share important characteristics and properties with adult hepatocytes, and are considered a valuable surrogate for primary human hepatocytes (McGill et al. 2011; Szabo et al. 2013).

One of the *in vitro* readouts measured in the HepaRG system was triglyceride (TG) accumulation, since it has been suggested to constitute a biomarker for liver steatosis and hepatotoxicity (Lichtenstein et al. 2020). Another readout was the transcriptional changes for six genes that are known to play a key role in cholesterol homeostasis. These genes were chosen in an attempt to mechanistically relate changes in gene expression to the known changes in serum total cholesterol that have been repeatedly associated with PFASs blood levels. Nevertheless, it shall be highlighted that it is currently not clear on how to link altered expression of genes to actual measures of adversity (Buesen et al. 2017; Sauer et al. 2017). Next to the cholesterol homeostasis genes, up- or downregulation of eight other genes was included as *in vitro* readout for the QIVIVE. These genes cover diverse biological processes and were considered potential markers for liver toxicity. Ideally, these genes would have been described as molecular initiating events or other key events in Adverse Outcome Pathways (AOPs), but this information is currently lacking.

To conclude, prior to the application of QIVIVE models a toxicologically meaningful assay and/or readout has to be considered. As such, it has to be given thought whether an observed cellular perturbation will ultimately result in a pathology or if it shall be seen as an adaptive, non-adverse response. The elucidation of AOPs will assist in understanding the relevance of these observations and establishing the relationship between: the *in vitro* readouts at the biochemical or cellular level and the *in vivo* health effects at an organism level.

Consideration of *in vitro* biokinetics

One challenge associated with QIVIVE pertains to the proper definition of an *in vitro* metric to be the starting point for the extrapolations. Traditionally, nominally applied *in vitro* concentrations to which the system is directly exposed are used as the basis for concentration-effect relationships (Fischer et al. 2017; Groothuis et al. 2015). Accordingly, in many of published QIVIVE examples the nominal effect concentration is seen as the proxy for blood or target tissue concentrations (Forsby and Blaauboer 2007; Fragki et al. 2022; Fragki et al. 2017; Henneberger et al. 2021; Louisse et al. 2010; Martin et al. 2015; Proença et al. 2021; Strikwold et al. 2013; Zhao et al. 2019). Nominal concentrations are easily accessible and hence this approach, represents the simplest QIVIVE. Nevertheless, the use of the nominal concentration may not always be appropriate as it ignores any partitioning or loss processes that may affect the effective concentration of a substance (Henneberger et al. 2021; Proença et al. 2021). Given that it is the free (unbound) fraction of a chemical that is expected to induce any toxic effect (Groothuis et al. 2015) correcting the nominal concentration prior to its use for QIVIVE definitely requires some consideration (Henneberger et al. 2021).

There are several factors that may influence the free concentration of a substance in the *in vitro* system, such as binding to the protein or other medium components, binding to the plastic culture vessel or evaporation etc. (Groothuis et al. 2015; Kramer et al. 2012). In the *in vitro* assays, a fundamental factor reducing the bioavailability of a compound is the presence of serum protein (mainly albumin) in the medium (Gülden and Seibert 2003; 2005; Kramer et al. 2012; Smith et al. 2010). For this purpose, corrections for protein binding (*in vitro* vs *in vivo*) have been used in several QIVIVE papers (for example Fabian et al. 2019; Lousse et al. 2015; Wetmore et al. 2013; Wetmore et al. 2012; Zhang et al. 2018b). On the other hand, the overall *in vitro* distribution kinetics are often ignored (Proença et al. 2021).

In Chapters 3 and 4 of this thesis, QIVIVE for developmental toxicity were presented for a number of chemicals. Here, for the sake of simplicity, the nominal concentrations were used, representing the sum of free and bound chemical. In Chapter 3, the assumption was that *in vitro* nominal effect concentrations are equivalent to the maternal blood concentrations. Here, maternal blood was seen as a surrogate for embryonic exposure. In Chapter 4, where the PBK model was specifically fit for pregnancy, nominally applied concentrations from the alternative assays were considered equal to the *in vivo* fetal concentration. In other words, this approach presumes that the nominal *in vitro* concentration equals the total *in vivo* effect concentration, which was a practical choice. Instead, the free concentration may be a better metric for QIVIVE, as it accounts for differences in the bioavailability between the *in vitro* and *in vivo* systems (Fischer et al. 2017; Henneberger et al. 2021; Heringa et al. 2004; Proença et al. 2021). Nevertheless, for practical reasons, QIVIVE based on the nominally applied concentrations may be used, as the simplest, first-tier approach, for example for screening and prioritization purposes. In fact, it has been demonstrated that such QIVIVE models are precautionary and do not underestimate the health risk (Henneberger et al. 2019). For higher tiers, further refinement of the QIVIVE models is necessary by determination of the free (unbound) concentration, in particular for chemicals that show high binding to proteins in the medium and blood plasma. Determination of the free concentration shall ideally be done experimentally, whereas in the absence of experimental data *in silico* distribution models (Armitage et al. 2014; Fischer et al. 2017; Fisher et al. 2019; Kramer et al. 2012; Paini et al. 2017) can be used. Application of such models shall be done with caution, since they may not give good predictions in the case the free concentration changes over time, for example due to saturation of binding to the medium proteins (Henneberger et al. 2021). To enable their wider application in risk assessment, they need to be harmonized and their applicability domain has to be clearly defined, so as to facilitate the selection of the appropriate model by the general scientific public.

Several of these *in silico* models can also predict, next to the free (unbound) concentration, the cell-associated concentration, i.e. the chemical's concentration accumulated in the cells. It has been suggested that the cell-associated concentration (or else assumed intracellular concentration) may provide an even more refined metric for QIVIVE (Escher

and Hermens 2004; Groothuis et al. 2015; Kisitu et al. 2019; Proença et al. 2021). As for the free concentration in the medium, cell-associated concentrations, are seldomly reported in *in vitro* assays due to practical difficulties, and consequently, distribution models can be of assistance here. Nevertheless, as mentioned above they come with quite some uncertainties and their domain of applicability still has to be clarified. In the case of PFASs, in Chapter 7, cell-associated concentrations were experimentally measured in the HepaRG cell system. This was particularly important, considering that these chemicals are transported across cell membranes via specific transporters and not via passive diffusion. Published *in vitro* distribution models do not include, so far, these processes for chemical transport into the cells (Proença et al. 2021). As such, for substances like PFASs, the experimentally measured *in vitro* cell-associated concentrations may be the most meaningful metric for QIVIVE.

In conclusion, careful selection of the *in vitro* metric to be used for each QIVIVE model is fundamental. In order to achieve more accurate estimations of *in vivo* toxic dose levels based on *in vitro*-measured readouts, sufficient guidance shall be provided to scientists and risk assessors on which approach to follow, based on the chemical of interest.

Exposure dose metrics and dependency on time

Another important element to be considered for the QIVIVE analysis pertains to the selection of an appropriate exposure metric (Li et al. 2021). Typical parameters linked to the toxicity of a chemical are the peak concentration (C_{max}), or the AUC. The parameter to use for relating exposure to toxicity depends on the mode of action of the chemical and the endpoint of interest (Groothuis et al. 2015; Louisse et al. 2017; Rietjens et al. 2019), its toxicokinetic properties, but also the exposure conditions (Groothuis et al. 2015).

In the published literature, QIVIVE with reverse dosimetry is often based on the C_{max} (Chen et al. 2018b; Fragki et al. 2022; Li et al. 2017a) and less commonly on the AUC (Louisse et al. 2015). Peak concentrations are often a very important metric (Daston et al. 2010). For instance, the C_{max} is of importance when a peak exposure leads to saturation of detoxification. Another example is the toxicity to the developing fetus, which can be caused by as little as a single exposure at a critical time window of gestation, and consequently, it is more likely dependent on the C_{max}. In Chapter 4, we embraced this assumption and we used the C_{max} for QIVIVE. Nevertheless, it cannot be excluded that in some cases embryotoxicity may also be related to a more sustained exposure, i.e. a substantial part or even the total duration of pregnancy. As such, in some cases it may be better captured with time-dependent parameters, such as the AUC or a time-weighted average concentration (Groothuis et al. 2015; Louisse et al. 2017). In Chapter 3, we applied both the C_{max} and a time-weighted average concentration. Knowledge of the underlying mechanism and the chemical toxicokinetics will assist in picking up the best exposure metric.

Although very relevant for the endpoint of developmental toxicity, the peak concentrations do not account for damage accumulation over time, such as occurring after long-term exposure to accumulating compounds. For example, in the case of PFASs having elimination

half-lives in the range of years, it is questionable whether a peak exposure metric would be meaningful for the PFAS-induced increases in serum cholesterol (and TG), but also in serum ALT (for PFOA), being a result of continuous exposure, throughout lifetime. Also, their elimination half-lives are rather long (in the range of years). Therefore, in the PFAS QIVIVE (Chapter 7), it was hypothesized that the toxic effect is best related to a time-dependent cumulative dose metric, in this case the AUC (Gaylor 2000). It is acknowledged that the applied extrapolation from a single 24-hour exposure occurring *in vitro* to a lifetime *in vivo* exposure contains may be questioned, but it is claimed here that this approach can serve at least as a first tier in human health risk assessment provided the appropriate *in vitro* data are available.

For a wider application of QIVIVE in risk assessment, well-defined criteria for selecting the most appropriate exposure metric have to be agreed upon. Next to this, more attention has to be put on how to interpret and convincingly extrapolate short-term *in vitro* assay findings to chronic toxicity, i.e. by extrapolating the *in vitro* established AUC time dependency across exposure duration. (Macko et al. 2021).

How is the appropriate PBK model selected?

In an animal-free human health risk assessment, it is apparent that PBK models combined with *in vitro* and *in silico* data will be the translation tool for the quantitative interpretation of *in vitro* assay readouts. PBK models may be of a generic nature or chemical-specific, depending on the substance of interest and the information available that would allow for the toxicokinetic modeling. In general, it is advised that a PBK model to be used for regulatory applications shall be as complex as needed on a case-by-case basis, in accordance with the principle of parsimony (OECD 2021b). As such, simpler models may be preferred when sufficient, whereas increasing model complexity for improving predictive performance shall be added only when essential (Cohen Hubal et al. 2019; Najjar et al. 2022). In such a tiered-approach system, for start, minimal generic PBK models may suffice as a first-tier tool to simulate toxicokinetics. For chemicals with non-generic characteristics, where other chemical-specific physiological processes (for example enterohepatic circulation or active-transport uptake mechanisms) play a fundamental role, more elaborate or chemical-specific tailored-made models may be employed (Breen et al. 2021; Najjar et al. 2022). This can only be performed when biologically plausible and if experimental data allow the numeric identification of such processes. Generic PBK model testing may initially be based on the average kinetics, integrating inter-individual variability at a later stage.

Generic PBK models in support for QIVIVE

In the case of generic PBK models, a pre-defined compartmental structure is in place, which contains the essential anatomical and physiological parameters, whereas chemical-specific input has to be provided. Enclosed QSARs predict model parameters based on the molecular structure and physicochemical properties of the compounds (Peyret et al.

2010; Rodgers and Rowland 2007), overcoming the issue of *in vivo* kinetic data paucity for parameterization. Considering the thousands of data-poor chemicals in the environment, the employment of generic PBK models will facilitate QIVIVE for the broader category of environmental chemicals. As their application in chemical risk assessment will become crucial, there is a clear need for their standardization, in order to ensure regulatory acceptance. Some of the major challenges pertaining to their acceptance are discussed below.

Challenge #1: Defining the applicability domain

One primary bottle-neck for the acceptance of generic PBK models relates to the lack of a clearly defined applicability domain. Evaluation of a model's applicability domain requires the comparison of the model's predictions for a number of compounds to *in vivo* toxicokinetic data (Bell et al. 2018). Despite the fact that, a considerable number of platforms have emerged that can perform such simulations (Hack et al. 2020; OECD 2021b), their applicability domain has not yet been comprehensively assessed (Najjar et al. 2022). A number of these models/platforms have been evaluated for their ability to describe *in vivo* kinetics of a diverse set of chemicals in the rat (Kamiya et al. 2021; Kamiya et al. 2019; Kamiya et al. 2020; Punt et al. 2022; Wambaugh et al. 2015). These studies provide important insight into the predictive performance of these models, which will assist in defining their underlying chemical space. However, a more systematic comparison of the various generic PBK model concepts is necessary in order to streamline the further application of such modelling approaches in risk assessment. Next to this, modelling evaluations were done primarily based on animal data, whereas the modelling of human kinetics was only presented in Wambaugh et al. (2015) for a very limited amount of compounds. This stresses the need for additional analyses using human kinetic data as proposed by Breen et al. (2021) and (Sayre et al. 2020), with the available PBK models.

In Chapter 2 of this thesis, the two generic PBK models selected were evaluated on simulating human kinetics over a wide span of chemicals, regarding physicochemical and biological properties. In particular, substances selected for the simulations had a broad span in lipophilicity, blood ionization and blood protein binding, and were in parallel eliminated primarily via the liver. This was done with the purpose of identifying specific properties that could determine the models' predictivity. Although the amount of chemicals applied was limited, this study provides an example on how to evaluate further more substances so as to define better their 'prediction space'. Ideally, physicochemical and biological properties of a chemical will form the basis for determining *a priori* whether a generic PBK model can (or cannot) predict their toxicokinetics.

Challenge #2: Evaluation of model predictions

While a vast amount of animal studies and clinical trials exist for pharmaceuticals, and animal studies exist for certain chemical categories, such as pesticides, the human population is exposed indirectly to many of the commercially produced chemicals, for which limited toxicokinetic data are available (Judson et al. 2009; Najjar et al. 2022; Sayre et al. 2020). As an illustrative example, within the EU REACH Regulation implemented

for industrial chemicals, which resulted in a huge number of newly performed animal studies since 2007, a toxicokinetic assessment is not a formal requirement. This is also the case for several other chemical categories, such as food contact materials, food additives, and food contaminants (Punt et al. 2017). Next to this, controlled human toxicokinetic data for environmental and industrial chemicals are scarce (Judson et al. 2011; Wambaugh et al. 2015). This lack of structured databases for these chemicals makes the systematic evaluation of PBK model performance cumbersome, at least with the traditional way of benchmarking against measured experimental data. Even more so, within the NGRA animal testing will be severely reduced or even eliminated and consequently, comparison of model predictions to *in vivo* data will be restricted. Consequently, it is essential to find other ways to evaluate these models. As mentioned in the previous section robust consideration of chemical domain of applicability of the models is required, so that it can be predetermined whether a chemical would fit a model's purpose. It is key to identify which chemical characteristics have a major influence on the quality of the predictions (Wambaugh et al. 2015).

Next to this, in the absence of *in vivo* kinetic data, the predictive ability of a PBK model for a certain chemical ('target chemical') can also be determined with the use of structural analogues ('source chemicals'), i.e. the read-across approach. In other words, when a model can predict the kinetics of the analogues, it can be applied for simulating the kinetics of the chemical of interest (OECD 2021b; Paini et al. 2021a; Paini et al. 2021c).

Challenge #3: What is a satisfactory prediction for generic models?

A crucial issue that needs to be addressed is the expected accuracy of the generic PBK model predictions (Shebley et al. 2018), an issue currently without consensus. The goodness-of-fit criterion that is commonly applied for PBK models (WHO 2010) dictates that the model simulations should be on average within a factor of 2 from the experimental data. This precision is prescribed for specific PBK models designed for a single or small group of chemicals, usually in a data-rich environment, where they can be properly evaluated and calibrated to fit the *in vivo* kinetics. Employing an evaluation threshold of the same accuracy for generic models, with a much broader applicability domain, is unrealistic (Cohen Hubal et al. 2019; Najjar et al. 2022). At first, biological variability is nowhere near the WHO threshold. For example, several meta-analyses of *in vivo* data have shown that repeating guideline-based mammalian toxicity studies with the same chemical may result in NOAELs/LOAELs differing between 5- to 10-fold (Janer et al. 2007a; Janer et al. 2007b; Janer et al. 2008a; Knudsen et al. 2009; Ly Pham et al. 2020). In another example, a recent analysis of TK data of 389 chemicals performed by US EPA illustrated that replicate *in vivo* measurements are ~ 80% of the time within a factor of two of themselves (Cook et al. 2022). Generic PBK-estimated dose metrics were very frequently seen to be within 10-fold of the empirical data (Abdullah et al. 2016; Breen et al. 2021; Lautz et al. 2020; Pletz et al. 2020; Punt et al. 2021b; Zhang et al. 2018a). In many cases even better predictions were recorded: 70% within 3-fold (Lautz et al. 2020), 50% within 5-fold (Punt et al. 2022), 50%

within 3-fold (Breen et al. 2021). Accordingly, model predictions with IndusChemFate, were within a factor of 5 for 19 out of the 24 compounds tested (Chapters 2 and 3). In fact, these results demonstrate that prediction of generic models are often within accepted variability of data underlying current chemical safety assessment. As such, understanding the quantitative variability of traditional mammalian studies is pivotal before putting an acceptability threshold for these generic models. Overall, it seems that a more flexible threshold or range needs to be considered.

For example, in a recent paper Punt et al. (2022) proposes a quantitative criterion for the C_{max} parameter determined by generic PBK modelling: a 5-fold difference (predicted *vs* observed) is considered *adequate*, whereas a 10-fold difference, although less precise, is still seen as relevant. Following this proposal, it is concluded that IndusChemFate gives adequate predictions; still, additional analyses are needed to confirm this result, as well as to define the specific modifications needed to satisfactorily describe the kinetics of compounds that are not well predicted.

PBK model parameterization with *in vitro* and *in silico* data

For a truly animal-free testing paradigm, physicochemical and toxicokinetic data for the PBK model parametrization should also be derived from *in vitro*/alternative and/or *in silico* methods (Louisse et al. 2020a; Paini et al. 2019). To date, several *in vitro* and *in silico* methods for predictions of the ADME processes have been developed and used for PBK models; still, they remain non-validated in their vast majority. One good example, pertains to the *in vitro* determination of hepatic clearance. Intrinsic clearance can be determined with primary hepatocytes, S9, or microsomes. Despite several methods being available, guidance for performing such studies is lagging behind, hampering as such their systematic characterization and harmonization (Gouliarmou et al. 2018). Intrinsic clearance values for the same chemical, determined in different hepatocyte studies, were recently found to have a very high variation, ranging by more than one order of magnitude for most substances included in that study (Louisse et al. 2020a). Parameterization with high variation would substantially affect the toxicokinetics' predictions of the PBK models. Accordingly, this is important for other PBK input parameters, like the distribution partition coefficients, often calculated *in silico* and for which several methods exist (DeJongh et al. 1997; Peyret et al. 2010; Poulin and Krishnan 1995a; 1996; Rodgers et al. 2005; Rodgers and Rowland 2006; Schmitt 2008a). Obviously, the choice of input parameters that will feed the PBK model will affect its outcome, underpinning the importance for the standardization of the *in vitro* and *in silico* assays, but also for clear guidance on which method to use.

Predicted equivalent effect doses

With the application of QIVIVE analysis equivalent effect doses are estimated, which may be used as PoDs for risk assessment or for screening and prioritization, thereby substituting the classical NOAELs (or BMD10s/ BMD05s). The question that arises is how these NAM-based PoDs can be validated in terms of their credibility and accuracy

(Andersen 2010). This is definitely a key element for building confidence in NAMs and for convincing the regulators and other stakeholders towards the shift to NGRA (Ball et al. 2022). The conservative approach prescribes a 1:1 comparison to traditional methods, i.e. animal studies (Ball et al. 2022; Leist et al. 2012) as shown in many published QIVIVE examples (Chen et al. 2018a; Fragki et al. 2022; Fragki et al. 2017; Li et al. 2017a; Lousse et al. 2015; Lousse et al. 2010; Ning et al. 2019b; Strikwold et al. 2017; Strikwold et al. 2013). Accordingly, in Chapters 3 and 4, we benchmarked our developmental toxicity QIVIVE results against effect doses from *in vivo* animal studies. This may be valid as a first comparison; however, the limitations of such comparisons shall be acknowledged. First, in an animal-free risk assessment framework animal toxicity studies will not be available for such comparisons. Second, the alternative assay readouts are very different than the apical endpoints and consequently, they will not necessarily match the rat NOAELs. Third, the aim of NAMs is to assess safety for humans rather than reproducing the results of experimental animal studies. As such, mechanism-based assays, measuring perturbations in signaling pathways, will be eventually performed in cells/tissues of human origin, and hence, such comparisons are not necessarily meaningful.

Currently, new approaches for establishing confidence in NAMs are under development, which are using underlying toxicity mechanisms and human biology (Parish et al. 2020). It shall be remembered, that the foremost goal to be ensured is that the NAMs-based PoDs provide limits that are protective (Carmichael et al. 2022a). Thus, despite the historical risk assessment approach that is hazard-driven, it has been proposed that NGRA shall be driven by exposure (Berggren et al. 2017; Dent et al. 2018). In an exposure-led approach the exposure assessment will determine the data needed for the hazard assessment and will drive the testing thereon (Dent et al. 2018).

In the QIVIVE for PFASs (Chapter 7), in order to make a first assessment of the predicted equivalent effect doses we compared them to PFAS dietary exposure estimates of the EU population. The result suggested that current exposure may interfere with hepatic lipid homeostasis and gene expression, suggesting the need for better hazard characterization.

Final remarks and conclusions

Animal use in chemical safety assessment continues to be the norm under many regulatory frameworks within the EU, despite the tremendous advances in non-animal safety science over the last 20 years. Nevertheless, a scientific consensus seems to be at the rise dictating that a tiered *in vitro-in silico-in vivo* exposure-led approach shall substitute the current regulatory testing paradigm (Cronin et al. 2021).

Application of NAMs in chemical risk assessment presupposes the interpretation of *in vitro* assay findings for quantitative hazard characterization. PBK models are considered an indispensable component of these quantifications. QIVIVE with the implementation of PBK modelling is essential for the dose-response assessment of *in vitro* data and consequently, their use by risk assessors and toxicologists shall be encouraged and facilitated.

Regulatory acceptance of QIVIVE is unfortunately still limited and in order to promote this a number of critical steps have to be undertaken. Consequently, concrete guidance has to be laid down for their performance, and specific criteria have to be defined for their evaluation and validation. These pertain for example to the selection of appropriate *in vitro* readouts and dose metrics to be used as starting point for the extrapolations, but also to the selection of the PBK modeling approach and to the evaluation of model performance. This dissertation presents case studies of QIVIVE with the implementation of PBK modeling with the aim of exploring their 'know-how' and with the hope of contributing in building confidence in their application for regulatory purposes.

References

- Abdullah R, Alhusainy W, Woutersen J, Rietjens IM, Punt A. 2016. Predicting points of departure for risk assessment based on in vitro cytotoxicity data and physiologically based kinetic (pbk) modeling: The case of kidney toxicity induced by aristolochic acid i. *Food and chemical toxicology : an international journal published for the British Industrial Biological Research Association*. 92:104-116.
- Abe T, Takahashi M, Kano M, Amaike Y, Ishii C, Maeda K, Kudoh Y, Morishita T, Hosaka T, Sasaki T et al. 2017. Activation of nuclear receptor car by an environmental pollutant perfluorooctanoic acid. *Arch Toxicol*. 91(6):2365-2374.
- ACD/ChemSketch. 2011. A free comprehensive chemical drawing package.
- Adam D, de Visser I, Koeppel P. 1982. Pharmacokinetics of amoxicillin and clavulanic acid administered alone and in combination. *Antimicrob Agents Chemother*. 22(3):353-357.
- Adeleye Y, Andersen M, Clewell R, Davies M, Dent M, Edwards S, Fowler P, Malcomber S, Nicol B, Scott A et al. 2015. Implementing toxicity testing in the 21st century (tt21c): Making safety decisions using toxicity pathways, and progress in a prototype risk assessment. *Toxicology*. 332:102-111.
- Adiels M, Olofsson SO, Taskinen MR, Borén J. 2008. Overproduction of very low-density lipoproteins is the hallmark of the dyslipidemia in the metabolic syndrome. *Arterioscler Thromb Vasc Biol*. 28(7):1225-1236.
- Adler S, Basketter D, Creton S, Pelkonen O, van Benthem J, Zuang V, Andersen KE, Angers-Loustau A, Aptula A, Bal-Price A et al. 2011. Alternative (non-animal) methods for cosmetics testing: Current status and future prospects-2010. *Archives of toxicology*. 85(5):367-485.
- Agency) UUSEP. 2016. Estimation programs interface suite™ for microsoft® windows, v 4.11. . Washington, DC, USA.
- Aikawa N. 2020. A novel screening test to predict the developmental toxicity of drugs using human induced pluripotent stem cells. *The Journal of Toxicological Sciences*. 45(4):187-199.
- Albrecht W, Kappenberg F, Brecklinghaus T, Stoeber R, Marchan R, Zhang M, Ebbert K, Kirschner H, Grinberg M, Leist M et al. 2019. Prediction of human drug-induced liver injury (dili) in relation to oral doses and blood concentrations. *Archives of toxicology*. 93(6):1609-1637.
- Alexson SE, Diczfalusy M, Halldin M, Swedmark S. 2002. Involvement of liver carboxylesterases in the in vitro metabolism of lidocaine. *Drug metabolism and disposition: the biological fate of chemicals*. 30(6):643-647.
- Algharably EAH, Kreutz R, Gundert-Remy U. 2019. Importance of in vitro conditions for modeling the in vivo dose in humans by in vitro-in vivo extrapolation (ivive). *Archives of toxicology*. 93(3):615-621.
- Alsenz J, Haenel E. 2003. Development of a 7-day, 96-well caco-2 permeability assay with high-throughput direct uv compound analysis. *Pharm Res*. 20(12):1961-1969.
- Andersen ME. 2010. Calling on science: Making "alternatives" the new gold standard. *ALTEX - Alternatives to animal experimentation*. 27(2):135-143.
- Andersson TB, Kanebratt KP, Kenna JG. 2012. The heparg cell line: A unique in vitro tool for understanding drug metabolism and toxicology in human. *Expert Opin Drug Metab Toxicol*. 8(7):909-920.
- Ankley GT, Bennett RS, Erickson RJ, Hoff DJ, Hornung MW, Johnson RD, Mount DR, Nichols JW, Russom CL, Schmieder PK et al. 2010. Adverse outcome pathways: A conceptual framework to support ecotoxicology research and risk assessment. *Environ Toxicol Chem*. 29(3):730-741.
- Arancibia A, Guttmann J, González G, González C. 1980. Absorption and disposition kinetics of amoxicillin in normal human subjects. *Antimicrob Agents Chemother*. 17(2):199-202.
- Argikar UA, Rimmel RP. 2009. Effect of aging on glucuronidation of valproic acid in human liver microsomes and the role of udp-glucuronosyltransferase ugt1a4, ugt1a8, and ugt1a10. *Drug metabolism and disposition: the biological fate of chemicals*. 37(1):229-236.
- Armitage JM, Wania F, Arnot JA. 2014. Application of mass balance models and the chemical activity concept to facilitate the use of in vitro toxicity data for risk assessment. *Environ Sci Technol*. 48(16):9770-9779.
- Arnaud MJ. 2011. Pharmacokinetics and metabolism of natural methylxanthines in animal and man. *Handb Exp Pharmacol*. (200):33-91.
- Ashrap P, Zheng G, Wan Y, Li T, Hu W, Li W, Zhang H, Zhang Z, Hu J. 2017. Discovery of a widespread metabolic pathway within and among phenolic xenobiotics. *Proc Natl Acad Sci U S A*. 114(23):6062-6067.

- Ason B, van der Hoorn JWA, Chan J, Lee E, Pieterman EJ, Nguyen KK, Di M, Shetterly S, Tang J, Yeh W-C et al. 2014. Pcsk9 inhibition fails to alter hepatic ldlr, circulating cholesterol, and atherosclerosis in the absence of apoe. *Journal of lipid research*. 55(11):2370-2379.
- ATSDR. 2018. Toxicological profile for perfluoroalkyls. Draft for public comment june 2018. <https://www.atsdr.cdc.gov/toxprofiles/tp200.pdf>, 2018-11-10.
- Aubert N, Ameller T, Legrand JJ. 2012. Systemic exposure to parabens: Pharmacokinetics, tissue distribution, excretion balance and plasma metabolites of [14c]-methyl-, propyl- and butylparaben in rats after oral, topical or subcutaneous administration. *Food and chemical toxicology : an international journal published for the British Industrial Biological Research Association*. 50(3-4):445-454.
- Auboeuf D, Rieusset J, Fajas L, Vallier P, Frering V, Riou JP, Staels B, Auwerx J, Laville M, Vidal H. 1997. Tissue distribution and quantification of the expression of mrnas of peroxisome proliferator-activated receptors and liver x receptor-alpha in humans: No alteration in adipose tissue of obese and niddm patients. *Diabetes*. 46(8):1319-1327.
- Bagley DM, Lin YJ. 2000. Clinical evidence for the lack of triclosan accumulation from daily use in dentifrices. *Am J Dent*. 13(3):148-152.
- Bailey J, Thew M, Balls M. 2014. An analysis of the use of animal models in predicting human toxicology and drug safety. *Altern Lab Anim*. 42(3):181-199.
- Bailey J, Thew M, Balls M. 2015. Predicting human drug toxicity and safety via animal tests: Can any one species predict drug toxicity in any other, and do monkeys help? *Altern Lab Anim*. 43(6):393-403.
- Bal-Price A, Meek MEB. 2017. Adverse outcome pathways: Application to enhance mechanistic understanding of neurotoxicity. *Pharmacology & therapeutics*. 179:84-95.
- Ball N, Bars R, Botham PA, Cuciureanu A, Cronin MTD, Doe JE, Dudzina T, Gant TW, Leist M, van Ravenzwaay B. 2022. A framework for chemical safety assessment incorporating new approach methodologies within reach. *Archives of toxicology*. 96(3):743-766.
- Ballesteros V, Costa O, Iniguez C, Fletcher T, Ballester F, Lopez-Espinosa MJ. 2017. Exposure to perfluoroalkyl substances and thyroid function in pregnant women and children: A systematic review of epidemiologic studies. *Environment international*. 99:15-28.
- Bartell SM, Calafat AM, Lyu C, Kato K, Ryan PB, Steenland K. 2010. Rate of decline in serum pfoa concentrations after granular activated carbon filtration at two public water systems in ohio and west virginia. *Environ Health Perspect*. 118(2):222-228.
- Barter ZE, Bayliss MK, Beaune PH, Boobis AR, Carlile DJ, Edwards RJ, Houston JB, Lake BG, Lipscomb JC, Pelkonen OR et al. 2007. Scaling factors for the extrapolation of in vivo metabolic drug clearance from in vitro data: Reaching a consensus on values of human microsomal protein and hepatocellularity per gram of liver. *Curr Drug Metab*. 8(1):33-45.
- Basketter DA, Clewell H, Kimber I, Rossi A, Blaauboer B, Burrier R, Daneshian M, Eskes C, Goldberg A, Hasiwa N et al. 2012. A roadmap for the development of alternative (non-animal) methods for systemic toxicity testing. *Altex*. 29(1):3-91.
- Bassily M, Ghabrial H, Smallwood RA, Morgan DJ. 1995. Determinants of placental drug transfer: Studies in the isolated perfused human placenta. *J Pharm Sci*. 84(9):1054-1060.
- Beesoon S, Martin JW. 2015. Isomer-specific binding affinity of perfluorooctanesulfonate (pfos) and perfluorooctanoate (pfoa) to serum proteins. *Environmental science & technology*. 49(9):5722-5731.
- Beggs KM, McGreal SR, McCarthy A, Gunewardena S, Lampe JN, Lau C, Apte U. 2016. The role of hepatocyte nuclear factor 4-alpha in perfluorooctanoic acid- and perfluorooctanesulfonic acid-induced hepatocellular dysfunction. *Toxicol Appl Pharmacol*. 304:18-29.
- Behr AC, Kwiatkowski A, Ståhlman M, Schmidt FF, Luckert C, Braeuning A, Bührke T. 2020a. Impairment of bile acid metabolism by perfluorooctanoic acid (pfoa) and perfluorooctanesulfonic acid (pfos) in human heparg hepatoma cells. *Arch Toxicol*. 94(5):1673-1686.
- Behr AC, Plinsch C, Braeuning A, Bührke T. 2020b. Activation of human nuclear receptors by perfluoroalkylated substances (pfas). *Toxicol In Vitro*. 62:104700.
- Bell SM, Chang X, Wambaugh JF, Allen DG, Bartels M, Brouwer KLR, Casey WM, Choksi N, Ferguson SS, Fraczekiewicz G et al. 2018. In vitro to in vivo extrapolation for high throughput prioritization and decision making. *Toxicol In Vitro*. 47:213-227.

- Bergen WG, Mersmann HJ. 2005. Comparative aspects of lipid metabolism: Impact on contemporary research and use of animal models. *The Journal of Nutrition*. 135(11):2499-2502.
- Berggren E, White A, Ouedraogo G, Paini A, Richarz AN, Bois FY, Exner T, Leite S, Grunsven LAV, Worth A et al. 2017. Ab initio chemical safety assessment: A workflow based on exposure considerations and non-animal methods. *Comput Toxicol*. 4:31-44.
- Bertault-Pères P, Maraninchi D, Carcassonne Y, Cano JP, Barbet J. 1985. Clinical pharmacokinetics of ciclosporin a in bone marrow transplantation patients. *Cancer Chemother Pharmacol*. 15(1):76-81.
- Bessemers JG, Loizou G, Krishnan K, Clewell HJ, 3rd, Bernasconi C, Bois F, Coecke S, Collnot EM, Diembeck W, Farcial LR et al. 2014. Pbtok modelling platforms and parameter estimation tools to enable animal-free risk assessment: Recommendations from a joint epaa--eurl ecvam adme workshop. *Regulatory toxicology and pharmacology* : RTP. 68(1):119-139.
- Bhattacharya S, Zhang Q, Carmichael PL, Boekelheide K, Andersen ME. 2011. Toxicity testing in the 21 century: Defining new risk assessment approaches based on perturbation of intracellular toxicity pathways. *PLoS One*. 6(6):e20887.
- Bijland S, Rensen PC, Pieterman EJ, Maas AC, van der Hoorn JW, van Erk MJ, Havekes LM, Willems van Dijk K, Chang SC, Ehresman DJ et al. 2011. Perfluoroalkyl sulfonates cause alkyl chain length-dependent hepatic steatosis and hypolipidemia mainly by impairing lipoprotein production in apoe*3-leiden cetp mice. *Toxicological sciences : an official journal of the Society of Toxicology*. 123(1):290-303.
- Bil W, Zeilmaker M, Fragki S, Lijzen J, Verbruggen E, Bokkers B. 2021. Risk assessment of per- and polyfluoroalkyl substance mixtures: A relative potency factor approach. *Environ Toxicol Chem*. 40(3):859-870.
- Binkerd PE, Rowland JM, Nau H, Hendrickx AG. 1988. Evaluation of valproic acid (vpa) developmental toxicity and pharmacokinetics in sprague-dawley rats. *Fundam Appl Toxicol*. 11(3):485-493.
- Bjork JA, Butenhoff JL, Wallace KB. 2011. Multiplicity of nuclear receptor activation by pfoa and pfos in primary human and rodent hepatocytes. *Toxicology*. 288(1-3):8-17.
- Bjork JA, Wallace KB. 2009. Structure-activity relationships and human relevance for perfluoroalkyl acid-induced transcriptional activation of peroxisome proliferation in liver cell cultures. *Toxicological sciences : an official journal of the Society of Toxicology*. 111(1):89-99.
- Blaauboer BJ. 2008. The contribution of in vitro toxicity data in hazard and risk assessment: Current limitations and future perspectives. *Toxicology letters*. 180(2):81-84.
- Blaauboer BJ. 2010. Biokinetic modeling and in vitro-in vivo extrapolations. *J Toxicol Environ Health B Crit Rev*. 13(2-4):242-252.
- Blaauboer BJ, Boekelheide K, Clewell HJ, Daneshian M, Dingemans MM, Goldberg AM, Heneweer M, Jaworska J, Kramer NI, Leist M et al. 2012. The use of biomarkers of toxicity for integrating in vitro hazard estimates into risk assessment for humans. *Altex*. 29(4):411-425.
- Bocca B, Ruggieri F, Pino A, Rovira J, Calamandrei G, Martinez M, Domingo JL, Alimonti A, Schuhmacher M. 2019. Human biomonitoring to evaluate exposure to toxic and essential trace elements during pregnancy. Part a. Concentrations in maternal blood, urine and cord blood. *Environ Res*. 177:108599.
- Bocca B, Ruggieri F, Pino A, Rovira J, Calamandrei G, Mirabella F, Martínez M, Domingo JL, Alimonti A, Schuhmacher M. 2020. Human biomonitoring to evaluate exposure to toxic and essential trace elements during pregnancy. Part b: Predictors of exposure. *Environ Res*. 182:109108.
- Bois FY, Jamei M, Clewell HJ. 2010. Pbpk modelling of inter-individual variability in the pharmacokinetics of environmental chemicals. *Toxicology*. 278(3):256-267.
- Borén J, Chapman MJ, Krauss RM, Packard CJ, Bentzon JF, Binder CJ, Daemen MJ, Demer LL, Hegele RA, Nicholls SJ et al. 2020. Low-density lipoproteins cause atherosclerotic cardiovascular disease: Pathophysiological, genetic, and therapeutic insights: A consensus statement from the european atherosclerosis society consensus panel. *European Heart Journal*. 41(24):2313-2330.
- Bouvier d'Yvoire M, Prieto P, Blaauboer BJ, Bois FY, Boobis A, Brochot C, Coecke S, Freidig A, Gundert-Remy U, Hartung T et al. 2007. Physiologically-based kinetic modelling (pbk modelling): Meeting the 3rs agenda. The report and recommendations of ecvam workshop 63. *Altern Lab Anim*. 35(6):661-671.
- Brannen KC, Panzica-Kelly JM, Danberry TL, Augustine-Rauch KA. 2010. Development of a zebrafish embryo teratogenicity assay and quantitative prediction model. *Birth Defects Res B Dev Reprod Toxicol*. 89(1):66-77.

- Brede E, Wilhelm M, Goen T, Muller J, Rauchfuss K, Kraft M, Holzer J. 2010. Two-year follow-up biomonitoring pilot study of residents' and controls' pfc plasma levels after pfoa reduction in public water system in arnsberg, germany. *International journal of hygiene and environmental health*. 213(3):217-223.
- Breen M, Ring CL, Kreutz A, Goldsmith MR, Wambaugh JF. 2021. High-throughput pbtk models for in vitro to in vivo extrapolation. *Expert Opin Drug Metab Toxicol*. 17(8):903-921.
- Brown MS, Goldstein JL. 1997. The srebp pathway: Regulation of cholesterol metabolism by proteolysis of a membrane-bound transcription factor. *Cell*. 89(3):331-340.
- Brown NA. 2002. Selection of test chemicals for the ecvam international validation study on in vitro embryotoxicity tests. European centre for the validation of alternative methods. *Altern Lab Anim*. 30(2):177-198.
- Buesen R, Chorley BN, da Silva Lima B, Daston G, Deferme L, Ebbels T, Gant TW, Goetz A, Greally J, Gribaldo L et al. 2017. Applying 'omics technologies in chemicals risk assessment: Report of an ecetoc workshop. *Regul Toxicol Pharmacol*. 91 Suppl 1(Suppl 1):S3-s13.
- Buggey J, Kappus M, Lagoo AS, Brady CW. 2015. Amiodarone-induced liver injury and cirrhosis. *ACG Case Rep J*. 2(2):116-118.
- Buhrke T, Krüger E, Pevny S, Rößler M, Bitter K, Lampen A. 2015. Perfluorooctanoic acid (pfoa) affects distinct molecular signalling pathways in human primary hepatocytes. *Toxicology*. 333:53-62.
- Bunchorntavakul C, Reddy KR. 2013. Acetaminophen-related hepatotoxicity. *Clin Liver Dis*. 17(4):587-607, viii.
- Butenhoff J, Costa G, Elcombe C, Farrar D, Hansen K, Iwai H, Jung R, Kennedy G, Jr., Lieder P, Olsen G et al. 2002. Toxicity of ammonium perfluorooctanoate in male cynomolgus monkeys after oral dosing for 6 months. *Toxicological sciences : an official journal of the Society of Toxicology*. 69(1):244-257.
- Butenhoff JL, Chang SC, Olsen GW, Thomford PJ. 2012a. Chronic dietary toxicity and carcinogenicity study with potassium perfluorooctanesulfonate in sprague dawley rats. *Toxicology*. 293(1-3):1-15.
- Butenhoff JL, Kennedy GL, Jr., Chang SC, Olsen GW. 2012b. Chronic dietary toxicity and carcinogenicity study with ammonium perfluorooctanoate in sprague-dawley rats. *Toxicology*. 298(1-3):1-13.
- Butenhoff JL, Kennedy GL, Jr., Hinderliter PM, Lieder PH, Jung R, Hansen KJ, Gorman GS, Noker PE, Thomford PJ. 2004. Pharmacokinetics of perfluorooctanoate in cynomolgus monkeys. *Toxicological sciences : an official journal of the Society of Toxicology*. 82(2):394-406.
- Campbell JL, Yoon M, Clewell HJ. 2015. A case study on quantitative in vitro to in vivo extrapolation for environmental esters: Methyl-, propyl- and butylparaben. *Toxicology*. 332:67-76.
- Canova C, Barbieri G, Zare Jeddi M, Gion M, Fabricio A, Daprà F, Russo F, Fletcher T, Pitter G. 2020. Associations between perfluoroalkyl substances and lipid profile in a highly exposed young adult population in the veneto region. *Environment international*. 145:106117.
- Cardenas A, Rifas-Shiman SL, Godderis L, Duca RC, Navas-Acien A, Litonjua AA, DeMeo DL, Brennan KJ, Amarasiriwardena CJ, Hivert MF et al. 2017. Prenatal exposure to mercury: Associations with global DNA methylation and hydroxymethylation in cord blood and in childhood. *Environ Health Perspect*. 125(8):087022.
- Carmichael PL, Baltazar MT, Cable S, Cochrane S, Dent M, Li H, Middleton A, Muller I, Reynolds G, Westmoreland C et al. 2022a. Ready for regulatory use: Nams and ngra for chemical safety assurance. *Altex*.
- Carmichael PL, Baltazar MT, Cable S, Cochrane S, Dent M, Li H, Middleton A, Muller I, Reynolds G, Westmoreland C et al. 2022b. Ready for regulatory use: Nams and ngra for chemical safety assurance. *Altex*. 39(3):359-366.
- Chamouton J, Latruffe N. 2012. Ppara/hnf4a interplay on diversified responsive elements. Relevance in the regulation of liver peroxisomal fatty acid catabolism. *Curr Drug Metab*. 13(10):1436-1453.
- Chang S, Allen BC, Andres KL, Ehresman DJ, Falvo R, Provencher A, Olsen GW, Butenhoff JL. 2017. Evaluation of serum lipid, thyroid, and hepatic clinical chemistries in association with serum perfluorooctanesulfonate (pfos) in cynomolgus monkeys after oral dosing with potassium pfos. *Toxicological sciences : an official journal of the Society of Toxicology*. 156(2):387-401.
- Chang SC, Noker PE, Gorman GS, Gibson SJ, Hart JA, Ehresman DJ, Butenhoff JL. 2012. Comparative pharmacokinetics of perfluorooctanesulfonate (pfos) in rats, mice, and monkeys. *Reproductive toxicology (Elmsford, NY)*. 33(4):428-440.
- Chang X, Tan YM, Allen DG, Bell S, Brown PC, Browning L, Ceger P, Gearhart J, Hakkinen PJ, Kabadi SV et al. 2022. Ivive: Facilitating the use of in vitro toxicity data in risk assessment and decision making. *Toxics*. 10(5).

- Chapin R, Augustine-Rauch K, Beyer B, Daston G, Finnell R, Flynn T, Hunter S, Mirkes P, O'Shea KS, Piersma A et al. 2008. State of the art in developmental toxicity screening methods and a way forward: A meeting report addressing embryonic stem cells, whole embryo culture, and zebrafish. *Birth Defects Res B Dev Reprod Toxicol.* 83(4):446-456.
- Chapman MJ, Le Goff W, Guerin M, Kontush A. 2010. Cholesteryl ester transfer protein: At the heart of the action of lipid-modulating therapy with statins, fibrates, niacin, and cholesteryl ester transfer protein inhibitors. *Eur Heart J.* 31(2):149-164.
- Chen L, Ning J, Louisse J, Wesseling S, Rietjens I. 2018a. Use of physiologically based kinetic modelling-facilitated reverse dosimetry to convert in vitro cytotoxicity data to predicted in vivo liver toxicity of lasiocarpine and riddelliine in rat. *Food and chemical toxicology : an international journal published for the British Industrial Biological Research Association.* 116(Pt B):216-226.
- Chen L, Ning J, Louisse J, Wesseling S, Rietjens IMCM. 2018b. Use of physiologically based kinetic modelling-facilitated reverse dosimetry to convert in vitro cytotoxicity data to predicted in vivo liver toxicity of lasiocarpine and riddelliine in rat. *Food and Chemical Toxicology.* 116:216-226.
- Chen W, Owsley E, Yang Y, Stroup D, Chiang JY. 2001. Nuclear receptor-mediated repression of human cholesterol 7 α -hydroxylase gene transcription by bile acids. *J Lipid Res.* 42(9):1402-1412.
- Chen Y, Mao J, Hop CE. 2015. Physiologically based pharmacokinetic modeling to predict drug-drug interactions involving inhibitory metabolite: A case study of amiodarone. *Drug metabolism and disposition: the biological fate of chemicals.* 43(2):182-189.
- Chiang JY. 1998. Regulation of bile acid synthesis. *Front Biosci.* 3:d176-193.
- Chiang JY. 2017. Recent advances in understanding bile acid homeostasis. *Fl000Res.* 6:2029-2029.
- Chiu YY, Higaki K, Neudeck BL, Barnett JL, Welage LS, Amidon GL. 2003. Human jejunal permeability of cyclosporin a: Influence of surfactants on p-glycoprotein efflux in caco-2 cells. *Pharm Res.* 20(5):749-756.
- Chong JJ, Yang X, Don CW, Minami E, Liu YW, Weyers JJ, Mahoney WM, Van Biber B, Cook SM, Palpant NJ et al. 2014. Human embryonic-stem-cell-derived cardiomyocytes regenerate non-human primate hearts. *Nature.* 510(7504):273-277.
- Chun AH, Hoffman DJ, Friedmann N, Carrigan PJ. 1980. Bioavailability of valproic acid under fasting/nonfasting regimens. *J Clin Pharmacol.* 20(1):30-36.
- Clewell RA, Clewell HJ, 3rd. 2008. Development and specification of physiologically based pharmacokinetic models for use in risk assessment. *Regulatory toxicology and pharmacology : RTP.* 50(1):129-143.
- Clewell RA, Kremer JJ, Williams CC, Campbell JL, Sochaski MA, Andersen ME, Borghoff SJ. 2009. Kinetics of selected di-n-butyl phthalate metabolites and fetal testosterone following repeated and single administration in pregnant rats. *Toxicology.* 255(1-2):80-90.
- Cohen Hubal EA, Wetmore BA, Wambaugh JF, El-Masri H, Sibus JR, Bahadori T. 2019. Advancing internal exposure and physiologically-based toxicokinetic modeling for 21st-century risk assessments. *Journal of Exposure Science & Environmental Epidemiology.* 29(1):11-20.
- Conner TM, Nikolian VC, Georgoff PE, Pai MP, Alam HB, Sun D, Reed RC, Zhang T. 2018. Physiologically based pharmacokinetic modeling of disposition and drug-drug interactions for valproic acid and divalproex. *European journal of pharmaceutical sciences : official journal of the European Federation for Pharmaceutical Sciences.* 111:465-481.
- Convertino M, Church TR, Olsen GW, Liu Y, Doyle E, Elcombe CR, Barnett AL, Samuel LM, MacPherson IR, Evans TRJ. 2018. Stochastic pharmacokinetic-pharmacodynamic modeling for assessing the systemic health risk of perfluorooctanoate (pfoa). *Toxicol Sci.* 163(1):293-306.
- Cook C, Lucas A, Grace C, Brenda CE, Derik H, Nancy MH. 2022. Epa's concentration versus time database: A resource for extrapolating toxicokinetic trends across chemicals. *The united states environmental protection agency's center for computational toxicology and exposure.* .
- Corley RA, Bartels MJ, Carney EW, Weitz KK, Soelberg JJ, Gies RA, Thrall KD. 2005. Development of a physiologically based pharmacokinetic model for ethylene glycol and its metabolite, glycolic acid, in rats and humans. *Toxicol Sci.* 85(1):476-490.
- Corton JC, Cunningham ML, Hummer BT, Lau C, Meek B, Peters JM, Popp JA, Rhomberg L, Seed J, Klaunig JE. 2014a. Mode of action framework analysis for receptor-mediated toxicity: The peroxisome proliferator-activated receptor alpha (pparalpha) as a case study. *Crit Rev Toxicol.* 44(1):1-49.

- Corton JC, Cunningham ML, Hummer BT, Lau C, Meek B, Peters JM, Popp JA, Rhomberg L, Seed J, Klaunig JE. 2014b. Mode of action framework analysis for receptor-mediated toxicity: The peroxisome proliferator-activated receptor alpha (ppar α) as a case study. *Crit Rev Toxicol*. 44(1):1-49.
- Creton S, Billington R, Davies W, Dent MP, Hawksworth GM, Parry S, Travis KZ. 2009. Application of toxicokinetics to improve chemical risk assessment: Implications for the use of animals. *Regulatory toxicology and pharmacology : RTP*. 55(3):291-299.
- Cronin M, Doe J, Pereira M, Willett C. 2021. Re: A call for action on the development and implementation of new methodologies for safety assessment of chemical-based products in the eu - a short communication. *Regulatory toxicology and pharmacology : RTP*. 122:104911.
- Cui Y, König J, Nies AT, Pfannschmidt M, Hergt M, Franke WW, Alt W, Moll R, Keppler D. 2003. Detection of the human organic anion transporters slc21a6 (oatp2) and slc21a8 (oatp8) in liver and hepatocellular carcinoma. *Lab Invest*. 83(4):527-538.
- Curran I, Hierlihy SL, Liston V, Pantazopoulos P, Nunnikhoven A, Tittlemier S, Barker M, Trick K, Bondy G. 2008. Altered fatty acid homeostasis and related toxicologic sequelae in rats exposed to dietary potassium perfluorooctanesulfonate (pfos). *Journal of Toxicology and Environmental Health, Part A*. 71(23):1526-1541.
- Dadashzadeh S, Tajerzaden H. 2001. Dose dependent pharmacokinetics of theophylline: Michaelis-menten parameters for its major metabolic pathways. *European journal of drug metabolism and pharmacokinetics*. 26(1-2):77-83.
- Dallmann A, Liu XI, Burckart GJ, van den Anker J. 2019. Drug transporters expressed in the human placenta and models for studying maternal-fetal drug transfer. *J Clin Pharmacol*. 59 Suppl 1(Suppl 1):S70-s81.
- Darrow LA, Stein CR, Steenland K. 2013. Serum perfluorooctanoic acid and perfluorooctane sulfonate concentrations in relation to birth outcomes in the mid-ohio valley, 2005–2010. *Environmental health perspectives*. 121(10):1207-1213.
- Das KP, Wood CR, Lin MT, Starkov AA, Lau C, Wallace KB, Corton JC, Abbott BD. 2017. Perfluoroalkyl acids-induced liver steatosis: Effects on genes controlling lipid homeostasis. *Toxicology*. 378:37-52.
- Daston GP, Chapin RE, Scialli AR, Piersma AH, Carney EW, Rogers JM, Friedman JM. 2010. A different approach to validating screening assays for developmental toxicity. *Birth Defects Res B Dev Reprod Toxicol*. 89(6):526-530.
- de Jong E, Barenys M, Hermsen SA, Verhoef A, Ossendorp BC, Bessems JG, Piersma AH. 2011. Comparison of the mouse embryonic stem cell test, the rat whole embryo culture and the zebrafish embryotoxicity test as alternative methods for developmental toxicity testing of six 1,2,4-triazoles. *Toxicol Appl Pharmacol*. 253(2):103-111.
- de Jong E, Louisse J, Verwei M, Blaauboer BJ, van de Sandt JJM, Woutersen RA, Rietjens IMCM, Piersma AH. 2009. Relative developmental toxicity of glycol ether alkoxy acid metabolites in the embryonic stem cell test as compared with the in vivo potency of their parent compounds. *Toxicological Sciences*. 110(1):117-124.
- de la Rosa Rodriguez MA, Sugahara G, Hooiveld G, Ishida Y, Tateno C, Kersten S. 2018. The whole transcriptome effects of the ppar α agonist fenofibrate on livers of hepatocyte humanized mice. *BMC Genomics*. 19(1):443.
- de Leeuw VC, Hessel EVS, Piersma AH. 2019. Look-alikes may not act alike: Gene expression regulation and cell-type-specific responses of three valproic acid analogues in the neural embryonic stem cell test (estn). *Toxicol Lett*. 303:28-37.
- DeBose-Boyd RA. 2008. Feedback regulation of cholesterol synthesis: Sterol-accelerated ubiquitination and degradation of hmg coa reductase. *Cell Res*. 18(6):609-621.
- DeBose-Boyd RA, Ye J. 2018. Srebps in lipid metabolism, insulin signaling, and beyond. *Trends Biochem Sci*. 43(5):358-368.
- DeJongh J, Verhaar HJ, Hermens JL. 1997. A quantitative property-property relationship (qppr) approach to estimate in vitro tissue-blood partition coefficients of organic chemicals in rats and humans. *Archives of toxicology*. 72(1):17-25.
- Deng P, You T, Chen X, Yuan T, Huang H, Zhong D. 2011. Identification of amiodarone metabolites in human bile by ultraperformance liquid chromatography/quadrupole time-of-flight mass spectrometry. *Drug metabolism and disposition: the biological fate of chemicals*. 39(6):1058-1069.
- Dent M, Amaral RT, Da Silva PA, Ansell J, Boisleve F, Hatao M, Hirose A, Kasai Y, Kern P, Kreiling R et al. 2018. Principles underpinning the use of new methodologies in the risk assessment of cosmetic ingredients. *Computational Toxicology*. 7:20-26.

- Dent MP, Vaillancourt E, Thomas RS, Carmichael PL, Ouedraogo G, Kojima H, Barroso J, Ansell J, Barton-Maclaren TS, Bennekou SH et al. 2021a. Paving the way for application of next generation risk assessment to safety decision-making for cosmetic ingredients. *Regulatory Toxicology and Pharmacology*. 125:105026.
- Dent MP, Vaillancourt E, Thomas RS, Carmichael PL, Ouedraogo G, Kojima H, Barroso J, Ansell J, Barton-Maclaren TS, Bennekou SH et al. 2021b. Paving the way for application of next generation risk assessment to safety decision-making for cosmetic ingredients. *Regul Toxicol Pharmacol*. 125:105026.
- DeWitt JC, Shnyra A, Badr MZ, Loveless SE, Hoban D, Frame SR, Cunard R, Anderson SE, Meade BJ, Peden-Adams MM et al. 2009. Immunotoxicity of perfluorooctanoic acid and perfluorooctane sulfonate and the role of peroxisome proliferator-activated receptor alpha. *Crit Rev Toxicol*. 39(1):76-94.
- Dickinson RG, Harland RC, Ilias AM, Rodgers RM, Kaufman SN, Lynn RK, Gerber N. 1979. Disposition of valproic acid in the rat: Dose-dependent metabolism, distribution, enterohepatic recirculation and choleric effect. *J Pharmacol Exp Ther*. 211(3):583-595.
- Dietschy JM, Turley SD. 2002. Control of cholesterol turnover in the mouse. *J Biol Chem*. 277(6):3801-3804.
- Dietschy JM, Turley SD, Spady DK. 1993. Role of liver in the maintenance of cholesterol and low density lipoprotein homeostasis in different animal species, including humans. *J Lipid Res*. 34(10):1637-1659.
- Dimopoulou M, Verhoef A, Gomes CA, van Dongen CW, Rietjens I, Piersma AH, van Ravenzwaay B. 2018. A comparison of the embryonic stem cell test and whole embryo culture assay combined with the bewo placental passage model for predicting the embryotoxicity of azoles. *Toxicol Lett*. 286:10-21.
- Dimopoulou M, Verhoef A, Pennings JLA, van Ravenzwaay B, Rietjens I, Piersma AH. 2017. Embryotoxic and pharmacologic potency ranking of six azoles in the rat whole embryo culture by morphological and transcriptomic analysis. *Toxicol Appl Pharmacol*. 322:15-26.
- DWQI. 2017. New jersey drinking water quality institute health effects subcommittee. Health-based maximum contaminant level support document: Perfluorooctanoic acid (pfoa). February 15, 2017.
- DWQI. 2018. New jersey drinking water quality institute health effects subcommittee. Health-based maximum contaminant level support document: Perfluorooctane sulfonate (pfos). June 5, 2018.
- Dzierlenga AL, Robinson VG, Waidyanatha S, DeVito MJ, Eifrid MA, Gibbs ST, Granville CA, Blystone CR. 2020a. Toxicokinetics of perfluorohexanoic acid (pfhxa), perfluorooctanoic acid (pfoa) and perfluorodecanoic acid (pfda) in male and female hsd:Sprague dawley sd rats following intravenous or gavage administration. *Xenobiotica*. 50(6):722-732.
- Dzierlenga MW, Keast DR, Longnecker MP. 2020b. The concentration of several perfluoroalkyl acids in serum appears to be reduced by dietary fiber. *medRxiv*.2020.2007.2015.20154922.
- ECETOC. 2003. European centre for ecotoxicology and toxicology of chemicals. Derivation of assessment factors for human health risk assessment. Tr086.
- ECHA. 2017. Non-animal approaches—current status of regulatory applicability under the reach, clp and biocidal products regulations. ECHA Helsinki, Finland.
- Edginton AN, Schmitt W, Willmann S. 2006. Development and evaluation of a generic physiologically based pharmacokinetic model for children. *Clinical pharmacokinetics*. 45(10):1013-1034.
- EFSA. 2009. (european food safety authority). Scientific opinion on risk assessment for a selected group of pesticides from the triazole group to test possible methodologies to assess cumulative effects from exposure through food from these pesticides on human health. *Efsa journal*, 2009; 7, 1167.
- EFSA. 2017. Update: Guidance on the use of the benchmark dose approach in risk assessment. *Efsa journal* 2017;15(1):4658.
- EFSA CONTAM Panel. 2018a. (efsa panel on contaminants in the food chain), knutsen hk, alexander j, barregard l, bignami m, bruschweiler b, ceccatelli s, cottrill b, dinovi m, edler l, grasl-kraupp b, hogstrand c, hoogenboom lr, nebbia cs, oswald ip, petersen a, rose m, roudot a-c, vlemminckx c, vollmer g, wallace h, bodin l, cravedi j-p, halldorsson ti, haug ls, johansson n, van loveren h, gergelova p, mackay k, levorato s, van manen m and schwerdtle t. 2018. Scientific opinion on the risk to human health related to the presence of perfluorooctane sulfonic acid and perfluorooctanoic acid in food. *Efsa journal* 2018;16(12):5194, 284 pp. <https://doi.org/10.2903/j.efsa.2018.5194>

- EFSA CONTAM Panel. 2018b. Knutsen hk, alexander j, barregard l, bignami m, bruschweiler b, ceccatelli s, cottrill b, dinovi m, edler l, grasl-kraupp b, hogstrand c, hoogenboom lr, nebbia cs, oswald ip, petersen a, rose m, roudot a-c, vlemminckx c, vollmer g, wallace h, bodin l, cravedi j-p, halldorsson ti, haug ls, johansson n, van loveren h, gergelova p, mackay k, levorato s, van manen m and schwerdtle t, 2018. Scientific opinion on the risk to human health related to the presence of perfluorooctane sulfonic acid and perfluorooctanoic acid in food. *Efsa journal* 2018;16(12):5194, 284 pp. <https://doi.org/10.2903/j.Efsa.2018.5194>
- . Minutes of the expert meeting on perfluorooctane sulfonic acid and perfluorooctanoic acid in food assessment. 2018c.
- EFSA CONTAM Panel. 2020a. (efsa panel on contaminants in the food chain), schrenk d, bignami m, bodin l, chipman jk, del mazo j, grasl-kraupp b, hogstrand c, hoogenboom lr, leblanc j-c, nebbia cs, nielsen e, ntzani e, petersen a, sand s, vlemminckx c, wallace h, barregard l, ceccatelli s, cravedi j-p, halldorsson ti, haug ls, johansson n, knutsen hk, rose m, roudot a-c, van loveren h, vollmer g, mackay k, riolo f and schwerdtle t, 2020. Scientific opinion on the risk to human health related to the presence of perfluoroalkyl substances in food. *Efsa journal* 2020;18(9):6223, 391 pp. <https://doi.org/10.2903/j.Efsa.2020.6223>
- EFSA CONTAM Panel. 2020b. Schrenk d, bignami m, bodin l, chipman jk, del mazo j, grasl-kraupp b, hogstrand c, hoogenboom lr, leblanc j-c, nebbia cs, nielsen e, ntzani e, petersen a, sand s, vlemminckx c, wallace h, barregard l, ceccatelli s, cravedi j-p, halldorsson ti, haug ls, johansson n, knutsen hk, rose m, roudot a-c, van loveren h, vollmer g, mackay k, riolo f and schwerdtle t, 2020. Scientific opinion on the risk to human health related to the presence of perfluoroalkyl substances in food. *Efsa journal* 2020;18(9):6223, 391 pp. <https://doi.org/10.2903/j.Efsa.2020.6223>
- Ehresman DJ, Froehlich JW, Olsen GW, Chang SC, Butenhoff JL. 2007. Comparison of human whole blood, plasma, and serum matrices for the determination of perfluorooctanesulfonate (pfos), perfluorooctanoate (pfoa), and other fluorochemicals. *Environmental research*. 103(2):176-184.
- Elcombe CR, Elcombe BM, Foster JR, Chang SC, Ehresman DJ, Butenhoff JL. 2012. Hepatocellular hypertrophy and cell proliferation in sprague-dawley rats from dietary exposure to potassium perfluorooctanesulfonate results from increased expression of xenosensor nuclear receptors pparalpha and car/pxr. *Toxicology*. 293(1-3):16-29.
- Ellis EC, Naugler WE, Parini P, Mörk LM, Jorns C, Zemack H, Sandblom AL, Björkhem I, Ericzon BG, Wilson EM et al. 2013. Mice with chimeric livers are an improved model for human lipoprotein metabolism. *PLoS One*. 8(11):e78550.
- Ema M, Amano H, Itami T, Kawasaki H. 1993. Teratogenic evaluation of di-n-butyl phthalate in rats. *Toxicol Lett*. 69(2):197-203.
- Ericson I, Gómez M, Nadal M, van Bavel B, Lindström G, Domingo JL. 2007. Perfluorinated chemicals in blood of residents in catalonia (spain) in relation to age and gender: A pilot study. *Environment international*. 33(5):616-623.
- Eriksen KT, Raaschou-Nielsen O, McLaughlin JK, Lipworth L, Tjønneland A, Overvad K, Sørensen M. 2013. Association between plasma pfoa and pfos levels and total cholesterol in a middle-aged danish population. *PloS one*. 8(2):e56969-e56969.
- Escher BI, Hermens JL. 2004. Internal exposure: Linking bioavailability to effects. *Environ Sci Technol*. 38(23):455a-462a.
- Evans MV, Andersen ME. 2000. Sensitivity analysis of a physiological model for 2,3,7,8-tetrachlorodibenzo-p-dioxin (tcdd): Assessing the impact of specific model parameters on sequestration in liver and fat in the rat. *Toxicol Sci*. 54(1):71-80.
- Fabbri E, Mohammed BS, Korenblat KM, Magkos F, McCreary J, Patterson BW, Klein S. 2010. Effect of fenofibrate and niacin on intrahepatic triglyceride content, very low-density lipoprotein kinetics, and insulin action in obese subjects with nonalcoholic fatty liver disease. *J Clin Endocrinol Metab*. 95(6):2727-2735.
- Fabian E, Gomes C, Birk B, Williford T, Hernandez TR, Haase C, Zbrank R, van Ravenzwaay B, Landsiedel R. 2019. In vitro-to-in vivo extrapolation (ivive) by pbtk modeling for animal-free risk assessment approaches of potential endocrine-disrupting compounds. *Archives of toxicology*. 93(2):401-416.
- Fàbrega F, Kumar V, Schuhmacher M, Domingo JL, Nadal M. 2014. Pbpk modeling for pfos and pfoa: Validation with human experimental data. *Toxicology letters*. 230(2):244-251.

- Falk-Filipsson A, Hanberg A, Victorin K, Warholm M, Wallén M. 2007. Assessment factors—applications in health risk assessment of chemicals. *Environmental Research*. 104(1):108-127.
- FAO/WHO. Pesticide residues in food 2008. Report of the joint meeting of the fao panel experts on pesticide residues in food and the environment and the who core assessment group on pesticide residues, rome, italy, 9-18 september 2008. .
- FDA. 2010. Fda report on lidocaine.
- Feingold. 2000. Kr. Grunfeld c, introduction to lipids and lipoproteins. [updated 2018 feb 2]. In: Feingold kr, anawalt b, boyce a, et al., editors. *Endotext* [internet]. South dartmouth (ma): Mdtex.Com, inc.; 2000-. Available from: <https://www.Ncbi.Nlm.Nih.Gov/books/nbk305896/>.
- Fentem J, Malcomber I, Maxwell G, Westmoreland C. 2021. Upholding the eu's commitment to 'animal testing as a last resort' under reach requires a paradigm shift in how we assess chemical safety to close the gap between regulatory testing and modern safety science. *Alternatives to Laboratory Animals*. 49(4):122-132.
- Ference BA, Ginsberg HN, Graham I, Ray KK, Packard CJ, Bruckert E, Hegele RA, Krauss RM, Raal FJ, Schunkert H et al. 2017. Low-density lipoproteins cause atherosclerotic cardiovascular disease. 1. Evidence from genetic, epidemiologic, and clinical studies. A consensus statement from the european atherosclerosis society consensus panel. *European heart journal*. 38(32):2459-2472.
- Ferreira GS, Veening-Griffioen DH, Boon WPC, Moors EHM, Gispens-de Wied CC, Schellekens H, van Meer PJK. 2019. A standardised framework to identify optimal animal models for efficacy assessment in drug development. *PLoS One*. 14(6):e0218014.
- Fischer FC, Henneberger L, König M, Bittermann K, Linden L, Goss KU, Escher BI. 2017. Modeling exposure in the tox21 in vitro bioassays. *Chemical research in toxicology*. 30(5):1197-1208.
- Fisher C, Siméon S, Jamei M, Gardner I, Bois YF. 2019. Vivid: Virtual in vitro distribution model for the mechanistic prediction of intracellular concentrations of chemicals in in vitro toxicity assays. *Toxicol In Vitro*. 58:42-50.
- Fitz-Simon N, Fletcher T, Luster MI, Steenland K, Calafat AM, Kato K, Armstrong B. 2013. Reductions in serum lipids with a 4-year decline in serum perfluorooctanoic acid and perfluorooctanesulfonic acid. *Epidemiology (Cambridge, Mass)*. 24(4):569-576.
- Forsby A, Blaauboer B. 2007. Integration of in vitro neurotoxicity data with biokinetic modelling for the estimation of in vivo neurotoxicity. *Human & experimental toxicology*. 26(4):333-338.
- Fortaner S, Mendoza-De Gyves E, Cole T, Lostia AM. 2021. Determination of in vitro metabolic hepatic clearance of valproic acid (vpa) and five analogues by uplc-ms-qtof, applicable in alternatives to animal testing. *J Chromatogr B Analyt Technol Biomed Life Sci*. 1181:122893.
- Fragki S, Dirven H, Fletcher T, Grasl-Kraupp B, Bjerve Gützkow K, Hoogenboom R, Kersten S, Lindeman B, Louise J, Peijnenburg A et al. 2021. Systemic pfoa and pfoa exposure and disturbed lipid homeostasis in humans: What do we know and what not? *Crit Rev Toxicol*. 51(2):141-164.
- Fragki S, Hoogenveen R, van Oostrom C, Schwillens P, Piersma AH, Zeilmaker MJ. 2022. Integrating in vitro chemical transplacental passage into a generic pbk model: A qivive approach. *Toxicology*. 465:153060.
- Fragki S, Piersma AH, Rorije E, Zeilmaker MJ. 2017. In vitro to in vivo extrapolation of effective dosimetry in developmental toxicity testing: Application of a generic pbk modelling approach. *Toxicol Appl Pharmacol*. 332:109-120.
- Freire C, Amaya E, Gil F, Fernández MF, Murcia M, Llop S, Andiaarena A, Aurrekoetxea J, Bustamante M, Guxens M et al. 2018. Prenatal co-exposure to neurotoxic metals and neurodevelopment in preschool children: The environment and childhood (inma) project. *Sci Total Environ*. 621:340-351.
- Friedman SJ, Skehan P. 1979. Morphological differentiation of human choriocarcinoma cells induced by methotrexate. *Cancer Res*. 39(6 Pt 1):1960-1967.
- Frisbee SJ, Shankar A, Knox SS, Steenland K, Savitz DA, Fletcher T, Ducatman AM. 2010. Perfluorooctanoic acid, perfluorooctanesulfonate, and serum lipids in children and adolescents: Results from the e8 health project. *Arch Pediatr Adolesc Med*. 164(9):860-869.
- Fujii Y, Niisoe T, Harada KH, Uemoto S, Ogura Y, Takenaka K, Koizumi A. 2015. Toxicokinetics of perfluoroalkyl carboxylic acids with different carbon chain lengths in mice and humans. *Journal of Occupational Health*. 57(1):1-12.
- Furukawa S, Hayashi S, Usuda K, Abe M, Hagio S, Ogawa I. 2011. Toxicological pathology in the rat placenta. *J Toxicol Pathol*. 24(2):95-111.

- Gad S. *Animal models in toxicology* (2nd ed.). Crc press. .
- Gallo V, Leonardi G, Genser B, Lopez-Espinosa M-J, Frisbee SJ, Karlsson L, Ducatman AM, Fletcher T. 2012a. Serum perfluorooctanoate (pfoa) and perfluorooctane sulfonate (pfos) concentrations and liver function biomarkers in a population with elevated pfoa exposure. *Environmental health perspectives*. 120(5):655-660.
- Gallo V, Leonardi G, Genser B, Lopez-Espinosa MJ, Frisbee SJ, Karlsson L, Ducatman AM, Fletcher T. 2012b. Serum perfluorooctanoate (pfoa) and perfluorooctane sulfonate (pfos) concentrations and liver function biomarkers in a population with elevated pfoa exposure. *Environ Health Perspect*. 120(5):655-660.
- Ganapathy V, Prasad PD, Ganapathy ME, Leibach FH. 2000. Placental transporters relevant to drug distribution across the maternal-fetal interface. *J Pharmacol Exp Ther*. 294(2):413-420.
- Gatzidou ET, Zira AN, Theocharis SE. 2007. Toxicogenomics: A pivotal piece in the puzzle of toxicological research. *J Appl Toxicol*. 27(4):302-309.
- Gaylor DW. 2000. The use of haber's law in standard setting and risk assessment. *Toxicology*. 149(1):17-19.
- Geiger SD, Xiao J, Ducatman A, Frisbee S, Innes K, Shankar A. 2014. The association between pfoa, pfos and serum lipid levels in adolescents. *Chemosphere*. 98:78-83.
- Genschow E, Spielmann H, Scholz G, Seiler A, Brown N, Piersma A, Brady M, Clemann N, Huuskonen H, Paillard F et al. 2002. The ecvam international validation study on in vitro embryotoxicity tests: Results of the definitive phase and evaluation of prediction models. *European centre for the validation of alternative methods*. *Altern Lab Anim*. 30(2):151-176.
- Genius SJ, Birkholz D, Ralitsch M, Thibault N. 2010. Human detoxification of perfluorinated compounds. *Public Health*. 124(7):367-375.
- Genius SJ, Curtis L, Birkholz D. 2013. Gastrointestinal elimination of perfluorinated compounds using cholestyramine and *Chlorella pyrenoidosa*. *ISRN Toxicology*. 2013:657849.
- Giavini E, Broccia ML, Menegola E, Prati M. 1993. Comparative in vitro study of the embryotoxic effects of three glycol ethers and their metabolites, the alkoxyacids. *Toxicol In Vitro*. 7(6):777-784.
- Giavini E, Menegola E. 2010. Are azole fungicides a teratogenic risk for human conceptus? *Toxicol Lett*. 198(2):106-111.
- Gilbert-Sandoval I, Wesseling S, Rietjens I. 2020. Predicting the acute liver toxicity of aflatoxin b1 in rats and humans by an in vitro-in silico testing strategy. *Mol Nutr Food Res*. 64(13):e2000063.
- Gleason JA, Post GB, Fagliano JA. 2015. Associations of perfluorinated chemical serum concentrations and biomarkers of liver function and uric acid in the us population (nhanes), 2007-2010. *Environmental research*. 136:8-14.
- Gomis MI, Vestergren R, Borg D, Cousins IT. 2018. Comparing the toxic potency in vivo of long-chain perfluoroalkyl acids and fluorinated alternatives. *Environment international*. 113:1-9.
- Göttlicher M, Widmark E, Li Q, Gustafsson JA. 1992. Fatty acids activate a chimera of the clofibrac acid-activated receptor and the glucocorticoid receptor. *Proc Natl Acad Sci U S A*. 89(10):4653-4657.
- Gouliarmou V, Lostia AM, Coecke S, Bernasconi C, Bessems J, Dorne JL, Ferguson S, Testai E, Remy UG, Brian Houston J et al. 2018. Establishing a systematic framework to characterise in vitro methods for human hepatic metabolic clearance. *Toxicol In Vitro*. 53:233-244.
- Griffiths SK, Campbell JP. 2014. Placental structure, function and drug transfer. *Continuing Education in Anaesthesia Critical Care & Pain*. 15(2):84-89.
- Grillo JA, Venitz J, Ornato JP. 2001. Prediction of lidocaine tissue concentrations following different dose regimes during cardiac arrest using a physiologically based pharmacokinetic model. *Resuscitation*. 50(3):331-340.
- Groothuis FA, Heringa MB, Nicol B, Hermens JL, Blaauboer BJ, Kramer NI. 2015. Dose metric considerations in in vitro assays to improve quantitative in vitro-in vivo dose extrapolations. *Toxicology*. 332:30-40.
- Gülden M, Seibert H. 2003. In vitro-in vivo extrapolation: Estimation of human serum concentrations of chemicals equivalent to cytotoxic concentrations in vitro. *Toxicology*. 189(3):211-222.
- Gülden M, Seibert H. 2005. Impact of bioavailability on the correlation between in vitro cytotoxic and in vivo acute fish toxic concentrations of chemicals. *Aquat Toxicol*. 72(4):327-337.
- Gülden M, Seibert H. 2006. In vitro-in vivo extrapolation of toxic potencies for hazard and risk assessment - problems and new developments. *ALTEX : Alternativen zu Tiereperimenten*. 23 Suppl:218-225.

- Guruge KS, Yeung LW, Yamanaka N, Miyazaki S, Lam PK, Giesy JP, Jones PD, Yamashita N. 2006. Gene expression profiles in rat liver treated with perfluorooctanoic acid (pfoa). *Toxicological sciences : an official journal of the Society of Toxicology*. 89(1):93-107.
- Hack CE, Efremenko AY, Pendse SN, Ellison CA, Najjar A, Hewitt N, Schepky A, Clewell HJ. 2020. Chapter 4 - physiologically based pharmacokinetic modeling software. In: Fisher JW, Gearhart JM, Lin Z, editors. *Physiologically based pharmacokinetic (pbpk) modeling*. Academic Press. p. 81-126.
- Hackam DG, Redelmeier DA. 2006. Translation of research evidence from animals to humans. *JAMA*. 296(14):1727-1732.
- Haddad S, Restieri C, Krishnan K. 2001. Characterization of age-related changes in body weight and organ weights from birth to adolescence in humans. *J Toxicol Environ Health A*. 64(6):453-464.
- Hamdoune M, Duclos S, Mounie J, Santona L, Lhuguenot JC, Magdalou J, Goudonnet H. 1995. In vitro glucuronidation of peroxisomal proliferators: 2-ethylhexanoic acid enantiomers and their structural analogs. *Toxicol Appl Pharmacol*. 131(2):235-243.
- Han J, Back SH, Hur J, Lin Y-H, Gildersleeve R, Shan J, Yuan CL, Krokowski D, Wang S, Hatzoglou M et al. 2013. Er-stress-induced transcriptional regulation increases protein synthesis leading to cell death. *Nature Cell Biology*. 15(5):481-490.
- Han X, Nabb DL, Russell MH, Kennedy GL, Rickard RW. 2012. Renal elimination of perfluorocarboxylates (pfcas). *Chemical research in toxicology*. 25(1):35-46.
- Harada KH, Hashida S, Kaneko T, Takenaka K, Minata M, Inoue K, Saito N, Koizumi A. 2007. Biliary excretion and cerebrospinal fluid partition of perfluorooctanoate and perfluorooctane sulfonate in humans. *Environmental toxicology and pharmacology*. 24(2):134-139.
- Harding HP, Zhang Y, Zeng H, Novoa I, Lu PD, Calfon M, Sadri N, Yun C, Popko B, Paules R et al. 2003. An integrated stress response regulates amino acid metabolism and resistance to oxidative stress. *Mol Cell*. 11(3):619-633.
- Hartung T. 2018. Perspectives on in vitro to in vivo extrapolations. *Appl In Vitro Toxicol*. 4(4):305-316.
- Hartung T, Blaauboer BJ, Bosgra S, Carney E, Coenen J, Conolly RB, Corsini E, Green S, Faustman EM, Gaspari A et al. 2011. An expert consortium review of the ec-commissioned report "alternative (non-animal) methods for cosmetics testing: Current status and future prospects - 2010". *Altex*. 28(3):183-209.
- Hato T, Tabata M, Oike Y. 2008. The role of angiopoietin-like proteins in angiogenesis and metabolism. *Trends Cardiovasc Med*. 18(1):6-14.
- Haughom B, Spydevold O. 1992. The mechanism underlying the hypolipemic effect of perfluorooctanoic acid (pfoa), perfluorooctane sulphonic acid (pfosa) and clofibrilic acid. *Biochim Biophys Acta*. 1128(1):65-72.
- Hayhurst GP, Lee YH, Lambert G, Ward JM, Gonzalez FJ. 2001. Hepatocyte nuclear factor 4alpha (nuclear receptor 2a1) is essential for maintenance of hepatic gene expression and lipid homeostasis. *Mol Cell Biol*. 21(4):1393-1403.
- Heaton SJ, Eady JJ, Parker ML, Gotts KL, Dainty JR, Fairweather-Tait SJ, McArdle HJ, Srai KS, Elliott RM. 2008. The use of bewo cells as an in vitro model for placental iron transport. *Am J Physiol Cell Physiol*. 295(5):C1445-C1453.
- Henneberger L, Huchthausen J, Wojtyasiak N, Escher BI. 2021. Quantitative in vitro-to-in vivo extrapolation: Nominal versus freely dissolved concentration. *Chemical research in toxicology*. 34(4):1175-1182.
- Henneberger L, Mühlenbrink M, König M, Schlichting R, Fischer FC, Escher BI. 2019. Quantification of freely dissolved effect concentrations in in vitro cell-based bioassays. *Archives of toxicology*. 93(8):2295-2305.
- Henry CJ. 2003. Distinguished service award: Evolution of toxicology for risk assessment. *International Journal of Toxicology*. 22(1):3-7.
- Heringa MB, Schreurs RH, Busser F, van der Saag PT, van der Burg B, Hermens JL. 2004. Toward more useful in vitro toxicity data with measured free concentrations. *Environ Sci Technol*. 38(23):6263-6270.
- Herrman JL, Younes M. 1999. Background to the adi/tdi/ptwi. *Regul Toxicol Pharmacol*. 30(2 Pt 2):S109-113.
- Heusinkveld HJ, Wackers PFK, Schoonen WG, van der Ven L, Pennings JLA, Luijten M. 2018. Application of the comparison approach to open tg-gates: A useful toxicogenomics tool for detecting modes of action in chemical risk assessment. *Food and chemical toxicology : an international journal published for the British Industrial Biological Research Association*. 121:115-123.
- Hill AJ, Teraoka H, Heideman W, Peterson RE. 2005. Zebrafish as a model vertebrate for investigating chemical toxicity. *Toxicological sciences : an official journal of the Society of Toxicology*. 86(1):6-19.

- Horton JD, Goldstein JL, Brown MS. 2002. Srebps: Activators of the complete program of cholesterol and fatty acid synthesis in the liver. *J Clin Invest.* 109(9):1125-1131.
- Howroyd P, Swanson C, Dunn C, Cattley RC, Corton JC. 2004. Decreased longevity and enhancement of age-dependent lesions in mice lacking the nuclear receptor peroxisome proliferator-activated receptor alpha (pparalpha). *Toxicol Pathol.* 32(5):591-599.
- Huang MC, Dzierlenga AL, Robinson VG, Waidyanatha S, DeVito MJ, Eifrid MA, Granville CA, Gibbs ST, Blystone CR. 2019. Toxicokinetics of perfluorobutane sulfonate (pfbs), perfluorohexane-1-sulphonic acid (pfhxs), and perfluorooctane sulfonic acid (pfos) in male and female hsd:Sprague dawley sd rats after intravenous and gavage administration. *Toxicology reports.* 6:645-655.
- Huang X, Lüthi M, Ontsouka EC, Kallol S, Baumann MU, Surbek DV, Albrecht C. 2016. Establishment of a confluent monolayer model with human primary trophoblast cells: Novel insights into placental glucose transport. *Mol Hum Reprod.* 22(6):442-456.
- Huff J, Jacobson MF, Davis DL. 2008. The limits of two-year bioassay exposure regimens for identifying chemical carcinogens. *Environ Health Perspect.* 116(11):1439-1442.
- Hui Z, Li R, Chen L. 2017. The impact of exposure to environmental contaminant on hepatocellular lipid metabolism. *Gene.* 622:67-71.
- Ibarra M, Vázquez M, Fagiolino P, Derendorf H. 2013. Sex related differences on valproic acid pharmacokinetics after oral single dose. *J Pharmacokin Pharmacodyn.* 40(4):479-486.
- ICRP. 2002. Basic anatomical and physiological data for use in radiological protection: Reference values. A report of age- and gender-related differences in the anatomical and physiological characteristics of reference individuals. *Icrp publication 89. Ann ICRP.* 32(3-4):5-265.
- Imes CC, Austin MA. 2013. Low-density lipoprotein cholesterol, apolipoprotein b, and risk of coronary heart disease: From familial hyperlipidemia to genomics. *Biol Res Nurs.* 15(3):292-308.
- Institute of Medicine's Roundtable on Environmental Health Sciences R, and Medicine 2014. Roundtable on environmental health sciences, research, and medicine; board on population health and public health practice; institute of medicine. Identifying and reducing environmental health risks of chemicals in our society: Workshop summary. Washington (dc): National academies press (us); 2014 oct 2. 2, the challenge: Chemicals in today's society. Available from: <https://www.ncbi.nlm.nih.gov/books/nbk268889/>.
- Ito C, Shibutani Y., Inoue, K., Nakano, K., Ohnishi, H.,.. 1976. Toxicological studies of miconazole (ii) teratological studies of miconazole in rats. *Iyakuhi kenkyu* 7, 367-376.
- Jaeschke H, McGill MR, Williams CD, Ramachandran A. 2011. Current issues with acetaminophen hepatotoxicity - a clinically relevant model to test the efficacy of natural products. *Life Sci.* 88(17-18):737-745.
- Jain RB, Ducatman A. 2019. Selective associations of recent low concentrations of perfluoroalkyl substances with liver function biomarkers: Nhanes 2011 to 2014 data on us adults aged ≥20 years. *J Occup Environ Med.* 61(4):293-302.
- Jamei M. 2016a. Recent advances in development and application of physiologically-based pharmacokinetic (pbpk) models: A transition from academic curiosity to regulatory acceptance. *Curr Pharmacol Rep.* 2(3):161-169.
- Jamei M. 2016b. Recent advances in development and application of physiologically-based pharmacokinetic (pbpk) models: A transition from academic curiosity to regulatory acceptance. *Current pharmacology reports.* 2:161-169.
- Janer G, Hakkert BC, Piersma AH, Vermeire T, Slob W. 2007a. A retrospective analysis of the added value of the rat two-generation reproductive toxicity study versus the rat subchronic toxicity study. *Reprod Toxicol.* 24(1):103-113.
- Janer G, Hakkert BC, Slob W, Vermeire T, Piersma AH. 2007b. A retrospective analysis of the two-generation study: What is the added value of the second generation? *Reprod Toxicol.* 24(1):97-102.
- Janer G, Slob W, Hakkert BC, Vermeire T, Piersma AH. 2008a. A retrospective analysis of developmental toxicity studies in rat and rabbit: What is the added value of the rabbit as an additional test species? *Regulatory toxicology and pharmacology* : RTP. 50(2):206-217.
- Janer G, Verhoef A, Gilsing HD, Piersma AH. 2008b. Use of the rat postimplantation embryo culture to assess the embryotoxic potency within a chemical category and to identify toxic metabolites. *Toxicol In Vitro.* 22(7):1797-1805.

- Janssen AW, Betzel B, Stoopen G, Berends FJ, Janssen IM, Peijnenburg AA, Kersten S. 2015. The impact of ppara activation on whole genome gene expression in human precision cut liver slices. *BMC Genomics*. 16:760.
- Jawien W, Wilimowska J, Klys M, Piekoszewski W. 2017. Population pharmacokinetic modelling of valproic acid and its selected metabolites in acute vpa poisoning. *Pharmacological reports : PR*. 69(2):340-349.
- Jeon TI, Osborne TF. 2012. Srebps: Metabolic integrators in physiology and metabolism. *Trends Endocrinol Metab*. 23(2):65-72.
- JMPR. 2008. Joint fao/who meeting on pesticide residues. Pesticide residues in food 2007. Evaluations part i-residues. Joint meeting of fao plant production and protection paper 192. Flusilazole.
- Johannessen CU, Johannessen SI. 2003. Valproate: Past, present, and future. *CNS Drug Rev*. 9(2):199-216.
- Jones H, Rowland-Yeo K. 2013. Basic concepts in physiologically based pharmacokinetic modeling in drug discovery and development. *CPT Pharmacometrics Syst Pharmacol*. 2(8):e63.
- Jongeneelen FJ, Berge WF. 2011. A generic, cross-chemical predictive pbtk model with multiple entry routes running as application in ms excel; design of the model and comparison of predictions with experimental results. *The Annals of occupational hygiene*. 55(8):841-864.
- Jönsson L, Liu X, Jönsson BA, Ljungberg M, Strand SE. 2002. A dosimetry model for the small intestine incorporating intestinal wall activity and cross-doses. *J Nucl Med*. 43(12):1657-1664.
- Joseph P. 2017. Transcriptomics in toxicology. *Food Chem Toxicol*. 109(Pt 1):650-662.
- Joshi AA, Vaidya SS, St-Pierre MV, Mikheev AM, Desino KE, Nyandege AN, Audus KL, Unadkat JD, Gerk PM. 2016. Placental abc transporters: Biological impact and pharmaceutical significance. *Pharm Res*. 33(12):2847-2878.
- Judson R, Richard A, Dix DJ, Houck K, Martin M, Kavlock R, Dellarco V, Henry T, Holderman T, Sayre P et al. 2009. The toxicity data landscape for environmental chemicals. *Environ Health Perspect*. 117(5):685-695.
- Judson RS, Kavlock RJ, Setzer RW, Hubal EA, Martin MT, Knudsen TB, Houck KA, Thomas RS, Wetmore BA, Dix DJ. 2011. Estimating toxicity-related biological pathway altering doses for high-throughput chemical risk assessment. *Chemical research in toxicology*. 24(4):451-462.
- Kaabia Z, Poirier J, Moughaizel M, Aguesse A, Billon-Crossouard S, Fall F, Durand M, Dagher E, Krempf M, Croyal M. 2018. Plasma lipidomic analysis reveals strong similarities between lipid fingerprints in human, hamster and mouse compared to other animal species. *Scientific Reports*. 8(1):15893.
- Kamiya Y, Handa K, Miura T, Yanagi M, Shigeta K, Hina S, Shimizu M, Kitajima M, Shono F, Funatsu K et al. 2021. In silico prediction of input parameters for simplified physiologically based pharmacokinetic models for estimating plasma, liver, and kidney exposures in rats after oral doses of 246 disparate chemicals. *Chemical research in toxicology*. 34(2):507-513.
- Kamiya Y, Otsuka S, Miura T, Takaku H, Yamada R, Nakazato M, Nakamura H, Mizuno S, Shono F, Funatsu K et al. 2019. Plasma and hepatic concentrations of chemicals after virtual oral administrations extrapolated using rat plasma data and simple physiologically based pharmacokinetic models. *Chemical research in toxicology*. 32(1):211-218.
- Kamiya Y, Otsuka S, Miura T, Yoshizawa M, Nakano A, Iwasaki M, Kobayashi Y, Shimizu M, Kitajima M, Shono F et al. 2020. Physiologically based pharmacokinetic models predicting renal and hepatic concentrations of industrial chemicals after virtual oral doses in rats. *Chemical research in toxicology*. 33(7):1736-1751.
- Kannan R, Nademanee K, Hendrickson JA, Rostami HJ, Singh BN. 1982. Amiodarone kinetics after oral doses. *Clinical pharmacology and therapeutics*. 31(4):438-444.
- Kasteel EEJ, Lautz LS, Culot M, Kramer NI, Zwartsen A. 2021. Application of in vitro data in physiologically-based kinetic models for quantitative in vitro-in vivo extrapolation: A case-study for baclofen. *Toxicol In Vitro*. 76:105223.
- Katinka van der Jagt SM, Jens Tørslov & Jack de Bruijn. 2004. Assessment of additional testing needs under reach. Effects of (q)sars, risk based testing and voluntary industry initiatives. File:///c:/users/fragkis/downloads/eur%2021405%20en.Pdf.
- Kawai R, Mathew D, Tanaka C, Rowland M. 1998. Physiologically based pharmacokinetics of cyclosporine a: Extension to tissue distribution kinetics in rats and scale-up to human. *The Journal of pharmacology and experimental therapeutics*. 287(2):457-468.
- Kersten S. 2014. Integrated physiology and systems biology of ppara. *Mol Metab*. 3(4):354-371.
- Kersten S, Stienstra R. 2017. The role and regulation of the peroxisome proliferator activated receptor alpha in human liver. *Biochimie*. 136:75-84.

- Keys DA, Wallace DG, Kepler TB, Conolly RB. 1999. Quantitative evaluation of alternative mechanisms of blood and testes disposition of di(2-ethylhexyl) phthalate and mono(2-ethylhexyl) phthalate in rats. *Toxicol Sci.* 49(2):172-185.
- Keys DA, Wallace DG, Kepler TB, Conolly RB. 2000. Quantitative evaluation of alternative mechanisms of blood disposition of di(n-butyl) phthalate and mono(n-butyl) phthalate in rats. *Toxicol Sci.* 53(2):173-184.
- Kim NH, Kim SG. 2020. Fibrates revisited: Potential role in cardiovascular risk reduction. *Diabetes Metab J.* 44(2):213-221.
- Kim SJ, Heo SH, Lee DS, Hwang IG, Lee YB, Cho HY. 2016. Gender differences in pharmacokinetics and tissue distribution of 3 perfluoroalkyl and polyfluoroalkyl substances in rats. *Food and chemical toxicology : an international journal published for the British Industrial Biological Research Association.* 97:243-255.
- Kir S, Zhang Y, Gerard RD, Kliever SA, Mangelsdorf DJ. 2012. Nuclear receptors hnf4 α and Irh-1 cooperate in regulating cyp7a1 in vivo. *J Biol Chem.* 287(49):41334-41341.
- Kisitu J, Hougaard Bennekou S, Leist M. 2019. Chemical concentrations in cell culture compartments (c5) - concentration definitions. *Altex.* 36(1):154-160.
- Klintmalm GB, Iwatsuki S, Starzl TE. 1981. Cyclosporin a hepatotoxicity in 66 renal allograft recipients. *Transplantation.* 32(6):488-489.
- Klug S, Lewandowski C, Zappel F, Merker HJ, Nau H, Neubert D. 1990. Effects of valproic acid, some of its metabolites and analogues on prenatal development of rats in vitro and comparison with effects in vivo. *Arch Toxicol.* 64(7):545-553.
- Knight DJ, Deluyker H, Chaudhry Q, Vidal JM, de Boer A. 2021. A call for action on the development and implementation of new methodologies for safety assessment of chemical-based products in the eu - a short communication. *Regulatory toxicology and pharmacology : RTP.* 119:104837.
- Knudsen TB, Keller DA, Sander M, Carney EW, Doerrer NG, Eaton DL, Fitzpatrick SC, Hastings KL, Mendrick DL, Tice RR et al. 2015. Futuretox ii: In vitro data and in silico models for predictive toxicology. *Toxicological sciences : an official journal of the Society of Toxicology.* 143(2):256-267.
- Knudsen TB, Martin MT, Kavlock RJ, Judson RS, Dix DJ, Singh AV. 2009. Profiling the activity of environmental chemicals in prenatal developmental toxicity studies using the u.s. Epa's toxrefdb. *Reprod Toxicol.* 28(2):209-219.
- Kobayashi S, Takai K, Iga T, Hanano M. 1991. Pharmacokinetic analysis of the disposition of valproate in pregnant rats. *Drug metabolism and disposition: the biological fate of chemicals.* 19(5):972-976.
- Kotani N, Maeda K, Debori Y, Camus S, Li R, Chesna C, Sugiyama Y. 2012. Expression and transport function of drug uptake transporters in differentiated heparg cells. *Mol Pharm.* 9(12):3434-3441.
- Kramer N. 2010. Measuring, modeling, and increasing the free concentration of test chemicals in cell assays. Utrecht.
- Kramer NI, Di Consiglio E, Blaauboer BJ, Testai E. 2015. Biokinetics in repeated-dosing in vitro drug toxicity studies. *Toxicol In Vitro.* 30(1 Pt A):217-224.
- Kramer NI, Krismartina M, Rico-Rico A, Blaauboer BJ, Hermens JL. 2012. Quantifying processes determining the free concentration of phenanthrene in basal cytotoxicity assays. *Chemical research in toxicology.* 25(2):436-445.
- Krause BR, Princen HM. 1998. Lack of predictability of classical animal models for hypolipidemic activity: A good time for mice? *Atherosclerosis.* 140(1):15-24.
- Krewski D, Acosta D, Jr., Andersen M, Anderson H, Bailar JC, 3rd, Boekelheide K, Brent R, Charnley G, Cheung VG, Green S, Jr. et al. 2010. Toxicity testing in the 21st century: A vision and a strategy. *J Toxicol Environ Health B Crit Rev.* 13(2-4):51-138.
- Krewski D, Andersen ME, Mantus E, Zeise L. 2009. Toxicity testing in the 21st century: Implications for human health risk assessment. *Risk Anal.* 29(4):474-479.
- Krokowski D, Han J, Saikia M, Majumder M, Yuan CL, Guan BJ, Bevilacqua E, Bussolati O, Bröer S, Arvan P et al. 2013. A self-defeating anabolic program leads to β -cell apoptosis in endoplasmic reticulum stress-induced diabetes via regulation of amino acid flux. *J Biol Chem.* 288(24):17202-17213.
- Kudo N, Katakura M, Sato Y, Kawashima Y. 2002. Sex hormone-regulated renal transport of perfluorooctanoic acid. *Chem Biol Interact.* 139(3):301-316.
- Kudo N, Sakai A, Mitsumoto A, Hibino Y, Tsuda T, Kawashima Y. 2007. Tissue distribution and hepatic subcellular distribution of perfluorooctanoic acid at low dose are different from those at high dose in rats. *Biological & pharmaceutical bulletin.* 30(8):1535-1540.

- Kuemmerle NB, Kinlaw WB. 2011. Thrsp (thyroid hormone responsive). *Atlas Genet Cytogenet Oncol Haematol*. 15(6):480-482.
- Kuepfer L, Niederalt C, Wendl T, Schlender JF, Willmann S, Lippert J, Block M, Eissing T, Teutonico D. 2016. Applied concepts in pbpk modeling: How to build a pbpk/pd model. *CPT Pharmacometrics Syst Pharmacol*. 5(10):516-531.
- Kühnast S, Fiocco M, van der Hoorn JW, Princen HM, Jukema JW. 2015. Innovative pharmaceutical interventions in cardiovascular disease: Focusing on the contribution of non-hdl-c/ldl-c-lowering versus hdl-c-raising: A systematic review and meta-analysis of relevant preclinical studies and clinical trials. *Eur J Pharmacol*. 763(Pt A):48-63.
- Kwiterovich PO, Jr. 2000. The metabolic pathways of high-density lipoprotein, low-density lipoprotein, and triglycerides: A current review. *Am J Cardiol*. 86(12a):51-101.
- La Paglia L, Listi A, Caruso S, Amodeo V, Passiglia F, Bazan V, Fanale D. 2017. Potential role of angptl4 in the cross talk between metabolism and cancer through ppar signaling pathway. *PPAR Res*. 2017:8187235.
- Lakeram M, Lockley DJ, Pendlington R, Forbes B. 2008. Optimisation of the caco-2 permeability assay using experimental design methodology. *Pharm Res*. 25(7):1544-1551.
- Larter CZ, Yeh MM, Van Rooyen DM, Brooling J, Gatora K, Farrell GC. 2012. Peroxisome proliferator-activated receptor- α agonist, wy 14,643, improves metabolic indices, steatosis and ballooning in diabetic mice with non-alcoholic steatohepatitis. *J Gastroenterol Hepatol*. 27(2):341-350.
- Lau GS, Critchley JA. 1994. The estimation of paracetamol and its major metabolites in both plasma and urine by a single high-performance liquid chromatography assay. *J Pharm Biomed Anal*. 12(12):1563-1572.
- Lautz LS, Nebbia C, Hoeks S, Oldenkamp R, Hendriks AJ, Ragas AMJ, Dorne JLCM. 2020. An open source physiologically based kinetic model for the chicken (*Gallus gallus domesticus*): Calibration and validation for the prediction residues in tissues and eggs. *Environment International*. 136:105488.
- Le Vee M, Jigorel E, Glaise D, Gripon P, Guguen-Guillouzo C, Fardel O. 2006. Functional expression of sinusoidal and canalicular hepatic drug transporters in the differentiated human hepatoma hepg2 cell line. *Eur J Pharm Sci*. 28(1-2):109-117.
- Lee-Rueckert M, Escola-Gil JC, Kovanen PT. 2016. Hdl functionality in reverse cholesterol transport – challenges in translating data emerging from mouse models to human disease. *Biochimica et Biophysica Acta (BBA) - Molecular and Cell Biology of Lipids*. 1861(7):566-583.
- Leist M, Hasiwa N, Daneshian M, Hartung T. 2012. Validation and quality control of replacement alternatives – current status and future challenges. *Toxicology Research*. 1(1):8-22.
- Leist M, Hasiwa N, Rovida C, Daneshian M, Basketter D, Kimber I, Clewell H, Gocht T, Goldberg A, Busquet F et al. 2014. Consensus report on the future of animal-free systemic toxicity testing. *Altex*. 31(3):341-356.
- Lelo A, Birkett DJ, Robson RA, Miners JO. 1986. Comparative pharmacokinetics of caffeine and its primary demethylated metabolites paraxanthine, theobromine and theophylline in man. *British journal of clinical pharmacology*. 22(2):177-182.
- Leritz EC, McGlinchey RE, Salat DH, Milberg WP. 2016. Elevated levels of serum cholesterol are associated with better performance on tasks of episodic memory. *Metab Brain Dis*. 31(2):465-473.
- Levitt DG, Heymsfield SB, Pierson RN, Jr., Shapses SA, Kral JG. 2007. Physiological models of body composition and human obesity. *Nutr Metab (Lond)*. 4:19.
- Li AC, Glass CK. 2004. Ppar- and lxr-dependent pathways controlling lipid metabolism and the development of atherosclerosis. *J Lipid Res*. 45(12):2161-2173.
- Li H, Flick B, Rietjens IM, Louise J, Schneider S, van Ravenzwaay B. 2016. Extended evaluation on the es-d3 cell differentiation assay combined with the bewo transport model, to predict relative developmental toxicity of triazole compounds. *Arch Toxicol*. 90(5):1225-1237.
- Li H, Rietjens IM, Louise J, Blok M, Wang X, Sniijders L, van Ravenzwaay B. 2015. Use of the es-d3 cell differentiation assay, combined with the bewo transport model, to predict relative in vivo developmental toxicity of antifungal compounds. *Toxicol In Vitro*. 29(2):320-328.
- Li H, van Ravenzwaay B, Rietjens IM, Louise J. 2013. Assessment of an in vitro transport model using bewo b30 cells to predict placental transfer of compounds. *Arch Toxicol*. 87(9):1661-1669.
- Li H, Yuan H, Middleton A, Li J, Nicol B, Carmichael P, Guo J, Peng S, Zhang Q. 2021. Next generation risk assessment (ngra): Bridging in vitro points-of-departure to human safety assessment using physiologically-based kinetic (pbk) modelling - a case study of doxorubicin with dose metrics considerations. *Toxicol In Vitro*. 74:105171.

- Li H, Zhang M, Vervoort J, Rietjens IM, van Ravenzwaay B, Louisse J. 2017a. Use of physiologically based kinetic modeling-facilitated reverse dosimetry of in vitro toxicity data for prediction of in vivo developmental toxicity of tebuconazole in rats. *Toxicology letters*. 266:85-93.
- Li M, Gehring R, Riviere JE, Lin Z. 2017b. Development and application of a population physiologically based pharmacokinetic model for penicillin g in swine and cattle for food safety assessment. *Food and Chemical Toxicology*. 107:74-87.
- Li T, Chiang JY. 2005. Mechanism of rifampicin and pregnane x receptor inhibition of human cholesterol 7 alpha-hydroxylase gene transcription. *Am J Physiol Gastrointest Liver Physiol*. 288(1):G74-84.
- Li T, Chiang JY. 2009. Regulation of bile acid and cholesterol metabolism by ppars. *PPAR Res*. 2009:501739.
- Li Y, Barregard L, Xu Y, Scott K, Pineda D, Lindh CH, Jakobsson K, Fletcher T. 2020. Associations between perfluoroalkyl substances and serum lipids in a swedish adult population with contaminated drinking water. *Environ Health*. 19(1):33.
- Lichtenstein D, Luckert C, Alarcán J, de Sousa G, Gioutlakis M, Katsanou ES, Konstantinidou P, Machera K, Milani ES, Peijnenburg A et al. 2020. An adverse outcome pathway-based approach to assess steatotic mixture effects of hepatotoxic pesticides in vitro. *Food Chem Toxicol*. 139:111283.
- Lin CY, Lin LY, Chiang CK, Wang WJ, Su YN, Hung KY, Chen PC. 2010. Investigation of the associations between low-dose serum perfluorinated chemicals and liver enzymes in us adults. *Am J Gastroenterol*. 105(6):1354-1363.
- Liss KH, Finck BN. 2017. Ppars and nonalcoholic fatty liver disease. *Biochimie*. 136:65-74.
- Liu F, Soares MJ, Audus KL. 1997. Permeability properties of monolayers of the human trophoblast cell line bewo. *Am J Physiol*. 273(5):C1596-1604.
- Loccisano AE, Campbell JL, Jr., Andersen ME, Clewell HJ, 3rd. 2011. Evaluation and prediction of pharmacokinetics of pfoa and pfos in the monkey and human using a pbpk model. *Regulatory toxicology and pharmacology* : RTP. 59(1):157-175.
- Louisse J, Alewijn M, Peijnenburg A, Cnubben NHP, Heringa MB, Coecke S, Punt A. 2020a. Towards harmonization of test methods for in vitro hepatic clearance studies. *Toxicol In Vitro*. 63:104722.
- Louisse J, Beekmann K, Rietjens IM. 2017. Use of physiologically based kinetic modeling-based reverse dosimetry to predict in vivo toxicity from in vitro data. *Chem Res Toxicol*. 30(1):114-125.
- Louisse J, Bosgra S, Blaauboer BJ, Rietjens IM, Verwei M. 2015. Prediction of in vivo developmental toxicity of all-trans-retinoic acid based on in vitro toxicity data and in silico physiologically based kinetic modeling. *Archives of toxicology*. 89(7):1135-1148.
- Louisse J, de Jong E, van de Sandt JJ, Blaauboer BJ, Woutersen RA, Piersma AH, Rietjens IM, Verwei M. 2010. The use of in vitro toxicity data and physiologically based kinetic modeling to predict dose-response curves for in vivo developmental toxicity of glycol ethers in rat and man. *Toxicological sciences : an official journal of the Society of Toxicology*. 118(2):470-484.
- Louisse J, Dellafiora L, van den Heuvel J, Rijkers D, Leenders L, Dorne J, Punt A, Russel F, Koenderink J. 2022. Perfluoroalkyl substances (pfass) are substrates of the renal human organic anion transporter 4 (oat4). *Arch Toxicol*; in press.
- Louisse J, Rijkers D, Stoopen G, Janssen A, Staats M, Hoogenboom R, Kersten S, Peijnenburg A. 2020b. Perfluorooctanoic acid (pfoa), perfluorooctane sulfonic acid (pfos), and perfluorononanoic acid (pfna) increase triglyceride levels and decrease cholesterogenic gene expression in human heparg liver cells. *Arch Toxicol*. 94(9):3137-3155.
- Louisse J, Rijkers D, Stoopen G, Janssen A, Staats M, Hoogenboom R, Kersten S, Peijnenburg A. 2020c. Perfluorooctanoic acid (pfoa), perfluorooctane sulfonic acid (pfos), and perfluorononanoic acid (pfna) increase triglyceride levels and decrease cholesterogenic gene expression in human heparg liver cells. *Arch Toxicol*.
- Loveless SE, Finlay C, Everds NE, Frame SR, Gillies PJ, O'Connor JC, Powley CR, Kennedy GL. 2006. Comparative responses of rats and mice exposed to linear/branched, linear, or branched ammonium perfluorooctanoate (apfo). *Toxicology*. 220(2-3):203-217.
- Lu H. 2016. Crosstalk of hnf4 α with extracellular and intracellular signaling pathways in the regulation of hepatic metabolism of drugs and lipids. *Acta Pharm Sin B*. 6(5):393-408.
- Lu J, Goldsmith MR, Grulke CM, Chang DT, Brooks RD, Leonard JA, Phillips MB, Hypes ED, Fair MJ, Tornero-Velez R et al. 2016a. Developing a physiologically-based pharmacokinetic model knowledgebase in support of provisional model construction. *PLoS Comput Biol*. 12(2):e1004495.

- Lu JT, Cai Y, Chen F, Jia WW, Hu ZY, Zhao YS. 2016b. A physiologically based pharmacokinetic model of amiodarone and its metabolite desethylamiodarone in rats: Pooled analysis of published data. *European journal of drug metabolism and pharmacokinetics*. 41(6):689-703.
- Luebker DJ, Hansen KJ, Bass NM, Butenhoff JL, Seacat AM. 2002a. Interactions of fluorochemicals with rat liver fatty acid-binding protein. *Toxicology*. 176(3):175-185.
- Luebker DJ, Hansen KJ, Bass NM, Butenhoff JL, Seacat AM. 2002b. Interactions of fluorochemicals with rat liver fatty acid-binding protein. *Toxicology*. 176(3):175-185.
- Luz AL, Tokar EJ. 2018. Pluripotent stem cells in developmental toxicity testing: A review of methodological advances. *Toxicol Sci*. 165(1):31-39.
- Ly Pham L, Watford S, Pradeep P, Martin MT, Thomas R, Judson R, Setzer RW, Paul Friedman K. 2020. Variability in in vivo studies: Defining the upper limit of performance for predictions of systemic effect levels. *Comput Toxicol*. 15(August 2020):1-100126.
- Macko P, Palosaari T, Whelan M. 2021. Extrapolating from acute to chronic toxicity in vitro. *Toxicology in Vitro*. 76:105206.
- Magnarin M, Rosati A, De Iudicibus S, Bartoli F, Decorti G. 2008. Role of abc transporters in the bewo trophoblast cell line. *Toxicol Mech Methods*. 18(9):763-769.
- Marques LR, Diniz TA, Antunes BM, Rossi FE, Caperuto EC, Lira FS, Gonçalves DC. 2018. Reverse cholesterol transport: Molecular mechanisms and the non-medical approach to enhance hdl cholesterol. *Front Physiol*. 9:526.
- Martin L, Gardner LB. 2015. Stress-induced inhibition of nonsense-mediated rna decay regulates intracellular cystine transport and intracellular glutathione through regulation of the cystine/glutamate exchanger slc7a11. *Oncogene*. 34(32):4211-4218.
- Martin SA, McLanahan ED, Bushnell PJ, Hunter ES, 3rd, El-Masri H. 2015. Species extrapolation of life-stage physiologically-based pharmacokinetic (pbpk) models to investigate the developmental toxicology of ethanol using in vitro to in vivo (ivive) methods. *Toxicological sciences : an official journal of the Society of Toxicology*. 143(2):512-535.
- Mathiesen L, Mørck TA, Zuri G, Andersen MH, Pehrson C, Frederiksen M, Mose T, Rytting E, Poulsen MS, Nielsen JK et al. 2014. Modelling of human transplacental transport as performed in copenhagen, denmark. *Basic Clin Pharmacol Toxicol*. 115(1):93-100.
- Matsuzaki T, Scotcher D, Darwich AS, Galetin A, Rostami-Hodjegan A. 2019. Towards further verification of physiologically-based kidney models: Predictability of the effects of urine-flow and urine-ph on renal clearance. *The Journal of pharmacology and experimental therapeutics*. 368(2):157-168.
- McGill MR, Yan HM, Ramachandran A, Murray GJ, Rollins DE, Jaeschke H. 2011. Heparg cells: A human model to study mechanisms of acetaminophen hepatotoxicity. *Hepatology*. 53(3):974-982.
- McMullen PD, Bhattacharya S, Woods CG, Pendse SN, McBride MT, Soldatow VY, Deisenroth C, LeCluyse EL, Clewell RA, Andersen ME. 2020. Identifying qualitative differences in ppar α signaling networks in human and rat hepatocytes and their significance for next generation chemical risk assessment methods. *Toxicol In Vitro*. 64:104463.
- Miao J, Fang S, Bae Y, Kemper JK. 2006. Functional inhibitory cross-talk between constitutive androstane receptor and hepatic nuclear factor-4 in hepatic lipid/glucose metabolism is mediated by competition for binding to the dr1 motif and to the common coactivators, grip-1 and pgc-1alpha. *J Biol Chem*. 281(21):14537-14546.
- Minata M, Harada KH, Kärrman A, Hitomi T, Hirosawa M, Murata M, Gonzalez FJ, Koizumi A. 2010. Role of peroxisome proliferator-activated receptor-alpha in hepatobiliary injury induced by ammonium perfluorooctanoate in mouse liver. *Ind Health*. 48(1):96-107.
- Morton RE, Izem L. 2014. Cholesteryl ester transfer proteins from different species do not have equivalent activities. *Journal of lipid research*. 55(2):258-265.
- Munley. 2000. S.M. (2000) flusilazole technical: Developmental toxicity study in rats. Unpublished report no. Dupont-2287 from haskell laboratory for toxicology and industrial medicine, de, USA. Submitted to who by e.I. Du pont de nemours & co., inc., de, USA.
- Mutlib AE, Goosen TC, Bauman JN, Williams JA, Kulkarni S, Kostrubsky S. 2006. Kinetics of acetaminophen glucuronidation by udp-glucuronosyltransferases 1a1, 1a6, 1a9 and 2b15. Potential implications in acetaminophen-induced hepatotoxicity. *Chemical research in toxicology*. 19(5):701-709.

- Myatt GJ, Ahlberg E, Akahori Y, Allen D, Amberg A, Anger LT, Aptula A, Auerbach S, Beilke L, Bellion P et al. 2018. In silico toxicology protocols. *Regulatory Toxicology and Pharmacology*. 96:1-17.
- Najjar A, Punt A, Wambaugh J, Paini A, Ellison C, Fragki S, Bianchi E, Zhang F, Westerhout J, Mueller D et al. 2022. Towards best use and regulatory acceptance of generic physiologically based kinetic (pbk) models for in vitro-to-in vivo extrapolation (ivive) in chemical risk assessment. *Archives of toxicology*.
- Nakagawa H, Terada T, Harada KH, Hitomi T, Inoue K, Inui K, Koizumi A. 2009. Human organic anion transporter hoat4 is a transporter of perfluorooctanoic acid. *Basic & clinical pharmacology & toxicology*. 105(2):136-138.
- Nakagawa T, Ramdhan DH, Tanaka N, Naito H, Tamada H, Ito Y, Li Y, Hayashi Y, Yamagishi N, Yanagiba Y et al. 2012. Modulation of ammonium perfluorooctanoate-induced hepatic damage by genetically different ppar α in mice. *Arch Toxicol*. 86(1):63-74.
- Nakamura T, Ito Y, Yanagiba Y, Ramdhan DH, Kono Y, Naito H, Hayashi Y, Li Y, Aoyama T, Gonzalez FJ et al. 2009. Microgram-order ammonium perfluorooctanoate may activate mouse peroxisome proliferator-activated receptor alpha, but not human pparalpha. *Toxicology*. 265(1-2):27-33.
- National Research Council Committee on the Institutional Means for Assessment of Risks to Public H. 1983. Risk assessment in the federal government: Managing the process. Washington (DC): National Academies Press (US) Copyright © National Academy of Sciences.
- Nelson JW, Hatch EE, Webster TF. 2010. Exposure to polyfluoroalkyl chemicals and cholesterol, body weight, and insulin resistance in the general U.S. Population. *Environmental health perspectives*. 118(2):197-202.
- Neville LF, Mathiak G, Bagasra O. 1997. The immunobiology of interferon-gamma inducible protein 10 kd (ip-10): A novel, pleiotropic member of the c-x-c chemokine superfamily. *Cytokine Growth Factor Rev*. 8(3):207-219.
- Nian M, Li QQ, Bloom M, Qian ZM, Syberg KM, Vaughn MG, Wang SQ, Wei Q, Zeeshan M, Gurrin N et al. 2019. Liver function biomarkers disorder is associated with exposure to perfluoroalkyl acids in adults: Isomers of c8 health project in china. *Environmental research*. 172:81-88.
- Ning J, Chen L, Rietjens I. 2019a. Role of toxicokinetics and alternative testing strategies in pyrrolizidine alkaloid toxicity and risk assessment; state-of-the-art and future perspectives. *Food and chemical toxicology : an international journal published for the British Industrial Biological Research Association*. 131:110572.
- Ning J, Chen L, Strikwold M, Lousse J, Wesseling S, Rietjens I. 2019b. Use of an in vitro-in silico testing strategy to predict inter-species and inter-ethnic human differences in liver toxicity of the pyrrolizidine alkaloids lasiocarpine and riddelliine. *Archives of toxicology*. 93(3):801-818.
- Noorlander A, Zhang M, van Ravenzwaay B, Rietjens I. 2022. Use of physiologically based kinetic modeling-facilitated reverse dosimetry to predict in vivo acute toxicity of tetrodotoxin in rodents. *Toxicological sciences : an official journal of the Society of Toxicology*. 187(1):127-138.
- Nordestgaard BG, Varbo A. 2014. Triglycerides and cardiovascular disease. *Lancet*. 384(9943):626-635.
- NTP. 2019. Toxicity studies of perfluoroalkyl carboxylates administered by gavage to sprague dawley (hsd:Sprague dawley sd) rats. *Toxic Rep Ser*. (97).
- NTP. 2019a. Ntp technical report on the toxicity studies of perfluoroalkyl sulfonates (perfluorobutane sulfonic acid, perfluorohexane sulfonate potassium salt, and perfluorooctane sulfonic acid) administered by gavage to sprague dawley (hsd:Sprague dawley sd) rats. Research triangle park, nc: National toxicology program. Toxicity report 96.
- NTP. 2019b. Ntp technical report on the toxicity studies of perfluoroalkyl carboxylates (perfluorohexanoic acid, perfluorooctanoic acid, perfluorononanoic acid, and perfluorodecanoic acid) administered by gavage to sprague dawley (hsd:Sprague dawley sd) rats. Research triangle park, nc: National toxicology program. Toxicity report 97.
- Numata J, Kowalczyk J, Adolphs J, Ehlers S, Schafft H, Fuerst P, Muller-Graf C, Lahrssen-Wiederholt M, Greiner M. 2014. Toxicokinetics of seven perfluoroalkyl sulfonic and carboxylic acids in pigs fed a contaminated diet. *Journal of agricultural and food chemistry*. 62(28):6861-6870.
- O'Flaherty EJ. 1994. Physiologically based pharmacokinetic models in developmental toxicology. *Risk Anal*. 14(4):605-611.
- OECD. 2012. Proposal for a template, and guidance on developing and assessing the completeness of adverse outcome pathways. OECD Publishing Paris.
- OECD. 2015. Risk reduction approaches for ppass – a crosscountry analysis.

- OECD. 2018. Toward a new comprehensive global database of per- and polyfluoroalkyl substances (pfass): Summary on updating the oecd 2007 list of per-and polyfluoroalkyl substances (pfass). .
- OECD. 2021a.
- OECD. 2021b. Guidance document on the characterisation, validation and reporting of physiologically based kinetic (pbk) models for regulatory purposes, oecd series on testing and assessment, no. 331, environment,health and safety,environment directorate, oecd.
- Ogiso T, Ito Y, Iwaki M, Yamahata T. 1986. Disposition and pharmacokinetics of valproic acid in rats. *Chem Pharm Bull (Tokyo)*. 34(7):2950-2956.
- Okyere J, Oppon E, Dzidzienyo D, Sharma L, Ball G. 2014. Cross-species gene expression analysis of species specific differences in the preclinical assessment of pharmaceutical compounds. *PLoS one*. 9(5):e96853-e96853.
- Olsen GW, Burris JM, Burlew MM, Mandel JH. 2003a. Epidemiologic assessment of worker serum perfluorooctanesulfonate (pfos) and perfluorooctanoate (pfoa) concentrations and medical surveillance examinations. *J Occup Environ Med*. 45(3):260-270.
- Olsen GW, Burris JM, Ehresman DJ, Froehlich JW, Seacat AM, Butenhoff JL, Zobel LR. 2007. Half-life of serum elimination of perfluorooctanesulfonate,perfluorohexanesulfonate, and perfluorooctanoate in retired fluorochemical production workers. *Environ Health Perspect*. 115(9):1298-1305.
- Olsen GW, Hansen KJ, Stevenson LA, Burris JM, Mandel JH. 2003b. Human donor liver and serum concentrations of perfluorooctanesulfonate and other perfluorochemicals. *Environmental science & technology*. 37(5):888-891.
- Olsen GW, Zobel LR. 2007. Assessment of lipid, hepatic, and thyroid parameters with serum perfluorooctanoate (pfoa) concentrations in fluorochemical production workers. *International archives of occupational and environmental health*. 81(2):231-246.
- Olson H, Betton G, Robinson D, Thomas K, Monro A, Kolaja G, Lilly P, Sanders J, Sipes G, Bracken W et al. 2000. Concordance of the toxicity of pharmaceuticals in humans and in animals. *Regulatory toxicology and pharmacology* : RTP. 32(1):56-67.
- Orlando R, Piccoli P, De Martin S, Padrini R, Floreani M, Palatini P. 2004. Cytochrome p450 1a2 is a major determinant of lidocaine metabolism in vivo: Effects of liver function. *Clinical pharmacology and therapeutics*. 75(1):80-88.
- Ory DS. 2004. Nuclear receptor signaling in the control of cholesterol homeostasis: Have the orphans found a home? *Circ Res*. 95(7):660-670.
- Pacifici GM, Nottoli R. 1995. Placental transfer of drugs administered to the mother. *Clin Pharmacokinet*. 28(3):235-269.
- Paini A, Leonard JA, Joossens E, Bessems JGM, Desalegn A, Dorne JL, Gosling JP, Heringa MB, Klaric M, Kliment T et al. 2019. Next generation physiologically based kinetic (ng-pbk) models in support of regulatory decision making. *Comput Toxicol*. 9:61-72.
- Paini A, Sala Benito JV, Bessems J, Worth AP. 2017. From in vitro to in vivo: Integration of the virtual cell based assay with physiologically based kinetic modelling. *Toxicol In Vitro*. 45(Pt 2):241-248.
- Paini A, Tan Y-M, Sachana M, Worth A. 2021a. Gaining acceptance in next generation pbk modelling approaches for regulatory assessments - an oecd international effort. *Computational Toxicology*. 18:100163.
- Paini A, Tan YM, Sachana M, Worth A. 2021b. Gaining acceptance in next generation pbk modelling approaches for regulatory assessments - an oecd international effort. *Comput Toxicol*. 18:100163.
- Paini A, Worth A, Kulkarni S, Ebbrell D, Madden J. 2021c. Assessment of the predictive capacity of a physiologically based kinetic model using a read-across approach. *Computational Toxicology*. 18:100159.
- Paixão P, Gouveia LF, Morais JA. 2012. Prediction of the human oral bioavailability by using in vitro and in silico drug related parameters in a physiologically based absorption model. *Int J Pharm*. 429(1-2):84-98.
- Palmer CN, Hsu MH, Griffin KJ, Raucy JL, Johnson EF. 1998. Peroxisome proliferator activated receptor-alpha expression in human liver. *Mol Pharmacol*. 53(1):14-22.
- Pang KS, Han YR, Noh K, Lee PI, Rowland M. 2019. Hepatic clearance concepts and misconceptions: Why the well-stirred model is still used even though it is not physiologic reality? *Biochem Pharmacol*. 169:113596.
- Papazyan R, Liu X, Liu J, Dong B, Plummer EM, Lewis RD, 2nd, Roth JD, Young MA. 2018. Fxr activation by obeticholic acid or nonsteroidal agonists induces a human-like lipoprotein cholesterol change in mice with humanized chimeric liver. *J Lipid Res*. 59(6):982-993.

- Parish ST, Aschner M, Casey W, Corvaro M, Embry MR, Fitzpatrick S, Kidd D, Kleinstreuer NC, Lima BS, Settivari RS et al. 2020. An evaluation framework for new approach methodologies (nams) for human health safety assessment. *Regulatory Toxicology and Pharmacology*. 112:104592.
- Parry S, Zhang J. 2007. Multidrug resistance proteins affect drug transmission across the placenta. *Am J Obstet Gynecol*. 196(5):476.e471-476.
- Pattillo RA, Gey GO. 1968. The establishment of a cell line of human hormone-synthesizing trophoblastic cells in vitro. *Cancer Res*. 28(7):1231-1236.
- Pawar G, Madden JC, Ebbrell D, Firman JW, Cronin MTD. 2019. In silico toxicology data resources to support read-across and (q)sar. *Frontiers in Pharmacology*. 10.
- Pawlak M, Lefebvre P, Staels B. 2015. Molecular mechanism of ppara action and its impact on lipid metabolism, inflammation and fibrosis in non-alcoholic fatty liver disease. *J Hepatol*. 62(3):720-733.
- Pearce RG, Setzer RW, Strobe CL, Wambaugh JF, Sipes NS. 2017. Httk: R package for high-throughput toxicokinetics. *J Stat Softw*. 79(4):1-26.
- Pemathilaka RL, Reynolds DE, Hashemi NN. 2019. Drug transport across the human placenta: Review of placenta-on-a-chip and previous approaches. *Interface Focus*. 9(5):20190031.
- Pendse SN, Efremenko A, Hack CE, Moreau M, Mallick P, Dzierlenga M, Nicolas CI, Yoon M, Clewell HJ, McMullen PD. 2020. Population life-course exposure to health effects model (plethem): An r package for pbpk modeling. *Computational Toxicology*. 13:100115.
- Peng S, Yan L, Zhang J, Wang Z, Tian M, Shen H. 2013. An integrated metabolomics and transcriptomics approach to understanding metabolic pathway disturbance induced by perfluorooctanoic acid. *J Pharm Biomed Anal*. 86:56-64.
- Pennanen S, Tuovinen K, Huuskonen H, Komulainen H. 1992. The developmental toxicity of 2-ethylhexanoic acid in wistar rats. *Fundam Appl Toxicol*. 19(4):505-511.
- Perez F, Nadal M, Navarro-Ortega A, Fabrega F, Domingo JL, Barcelo D, Farre M. 2013. Accumulation of perfluoroalkyl substances in human tissues. *Environment international*. 59:354-362.
- Perkins RG, Butenhoff JL, Kennedy GL, Jr., Palazzolo MJ. 2004. 13-week dietary toxicity study of ammonium perfluorooctanoate (apfo) in male rats. *Drug Chem Toxicol*. 27(4):361-378.
- Pery AR, Brochot C, Zeman FA, Mombelli E, Desmots S, Pavan M, Fioravanzo E, Zaldivar JM. 2013. Prediction of dose-hepatotoxic response in humans based on toxicokinetic/toxicodynamic modeling with or without in vivo data: A case study with acetaminophen. *Toxicology letters*. 220(1):26-34.
- Peyret T, Krishnan K. 2011. Qsars for pbpk modelling of environmental contaminants. *SAR QSAR Environ Res*. 22(1-2):129-169.
- Peyret T, Poulin P, Krishnan K. 2010. A unified algorithm for predicting partition coefficients for pbpk modeling of drugs and environmental chemicals. *Toxicol Appl Pharmacol*. 249(3):197-207.
- Pichard L, Domergue J, Fourtanier G, Koch P, Schran HF, Maurel P. 1996. Metabolism of the new immunosuppressor cyclosporin g by human liver cytochromes p450. *Biochem Pharmacol*. 51(5):591-598.
- Piepoli MF, Hoes AW, Agewall S, Albus C, Brotons C, Catapano AL, Cooney M-T, Corrà U, Cosyns B, Deaton C et al. 2016. 2016 european guidelines on cardiovascular disease prevention in clinical practice: The sixth joint task force of the european society of cardiology and other societies on cardiovascular disease prevention in clinical practice (constituted by representatives of 10 societies and by invited experts)/developed with the special contribution of the european association for cardiovascular prevention & rehabilitation (eacpr). *European Heart Journal*. 37(29):2315-2381.
- Piersma AH. 2006. Alternative methods for developmental toxicity testing. *Basic Clin Pharmacol Toxicol*. 98(5):427-431.
- Piersma AH, Baker NC, Daston GP, Flick B, Fujiwara M, Knudsen TB, Spielmann H, Suzuki N, Tsaioun K, Kojima H. 2022. Pluripotent stem cell assays: Modalities and applications for predictive developmental toxicity. *Current Research in Toxicology*. 3:100074.
- Piersma AH, Genschow E, Verhoef A, Spanjersberg MQ, Brown NA, Brady M, Burns A, Clemann N, Seiler A, Spielmann H. 2004. Validation of the postimplantation rat whole-embryo culture test in the international ecvam validation study on three in vitro embryotoxicity tests. *Altern Lab Anim*. 32(3):275-307.
- Pizzurro DM, Seeley M, Kerper LE, Beck BD. 2019. Interspecies differences in perfluoroalkyl substances (pfas) toxicokinetics and application to health-based criteria. *Regulatory toxicology and pharmacology : RTP*. 106:239-250.

- Pletz J, Blakeman S, Paini A, Parissis N, Worth A, Andersson AM, Frederiksen H, Sakhi AK, Thomsen C, Bopp SK. 2020. Physiologically based kinetic (pbk) modelling and human biomonitoring data for mixture risk assessment. *Environ Int.* 143:105978.
- Plomp TA, Wiersinga WM, Maes RA. 1985. Tissue distribution of amiodarone and desethylamiodarone in rats after repeated oral administration of various amiodarone dosages. *Arzneimittelforschung.* 35(12):1805-1810.
- Post SM, Duez H, Gervois PP, Staels B, Kuipers F, Princen HM. 2001. Fibrates suppress bile acid synthesis via peroxisome proliferator-activated receptor- α -mediated downregulation of cholesterol 7 α -hydroxylase and sterol 27-hydroxylase expression. *Arterioscler Thromb Vasc Biol.* 21(11):1840-1845.
- Poulin P, Krishnan K. 1995a. An algorithm for predicting tissue: Blood partition coefficients of organic chemicals from n-octanol: Water partition coefficient data. *J Toxicol Environ Health.* 46(1):117-129.
- Poulin P, Krishnan K. 1995b. A biologically-based algorithm for predicting human tissue: Blood partition coefficients of organic chemicals. *Hum Exp Toxicol.* 14(3):273-280.
- Poulin P, Krishnan K. 1996. A mechanistic algorithm for predicting blood:Air partition coefficients of organic chemicals with the consideration of reversible binding in hemoglobin. *Toxicol Appl Pharmacol.* 136(1):131-137.
- Poulin P, Theil FP. 2002. Prediction of pharmacokinetics prior to in vivo studies. 1. Mechanism-based prediction of volume of distribution. *J Pharm Sci.* 91(1):129-156.
- Poulsen MS, Rytting E, Mose T, Knudsen LE. 2009. Modeling placental transport: Correlation of in vitro bewo cell permeability and ex vivo human placental perfusion. *Toxicol In Vitro.* 23(7):1380-1386.
- Pouwer MG, Pieterman EJ, Chang SC, Olsen GW, Caspers MPM, Verschuren L, Jukema JW, Princen HMG. 2019. Dose effects of ammonium perfluorooctanoate on lipoprotein metabolism in apoe*3-leiden.Cetp mice. *Toxicological sciences : an official journal of the Society of Toxicology.* 168(2):519-534.
- Pouwer MG, Pieterman EJ, Worms N, Keijzer N, Jukema JW, Gromada J, Gusarova V, Princen HMG. 2020. Alirocumab, evinacumab, and atorvastatin triple therapy regresses plaque lesions and improves lesion composition in mice. *J Lipid Res.* 61(3):365-375.
- Prescott LF. 1980. Kinetics and metabolism of paracetamol and phenacetin. *British journal of clinical pharmacology.* 10 Suppl 2:291s-298s.
- Princen H, Post S, Twisk J. 1997. Regulation of bile acid biosynthesis. *Current Pharmaceutical Design.* 3:59-84.
- Princen HMG, Pouwer MG, Pieterman EJ. 2016. Comment on "hypercholesterolemia with consumption of pfoa-laced western diets is dependent on strain and sex of mice" by rebholz s.L. Et al. *Toxicol. Rep.* 2016 (3) 46-54. *Toxicology reports.* 3:306-309.
- Proença S, Escher BI, Fischer FC, Fisher C, Grégoire S, Hewitt NJ, Nicol B, Paini A, Kramer NI. 2021. Effective exposure of chemicals in in vitro cell systems: A review of chemical distribution models. *Toxicology in Vitro.* 73:105133.
- Prouillac C, Lecoecur S. 2010. The role of the placenta in fetal exposure to xenobiotics: Importance of membrane transporters and human models for transfer studies. *Drug Metab Dispos.* 38(10):1623-1635.
- Punt A, Bouwmeester H, Blaauboer BJ, Coecke S, Hakkert B, Hendriks DFG, Jennings P, Kramer NI, Neuhoff S, Masereeuw R et al. 2020. New approach methodologies (nams) for human-relevant biokinetics predictions. Meeting the paradigm shift in toxicology towards an animal-free chemical risk assessment. *Altex.* 37(4):607-622.
- Punt A, Bouwmeester H, Schiffelers MWA, Peijnenburg A. 2018. Expert opinions on the acceptance of alternative methods in food safety evaluations: Formulating recommendations to increase acceptance of non-animal methods for kinetics. *Regulatory toxicology and pharmacology : RTP.* 92:145-151.
- Punt A, Louisse J, Pinckaers N, Fabian E, van Ravenzwaay B. 2021a. Predictive performance of next generation physiologically based kinetic (pbk) model predictions in rats based on in vitro and in silico input data. *Toxicological Sciences.* 186(1):18-28.
- Punt A, Louisse J, Pinckaers N, Fabian E, van Ravenzwaay B. 2022. Predictive performance of next generation physiologically based kinetic (pbk) model predictions in rats based on in vitro and in silico input data. *Toxicol Sci.* 186(1):18-28.
- Punt A, Peijnenburg A, Hoogenboom R, Bouwmeester H. 2017. Non-animal approaches for toxicokinetics in risk evaluations of food chemicals. *Altex.* 34(4):501-514.
- Punt A, Pinckaers N, Peijnenburg A, Louisse J. 2021b. Development of a web-based toolbox to support quantitative in-vitro-to-in-vivo extrapolations (qivive) within nonanimal testing strategies. *Chemical research in toxicology.* 34(2):460-472.

- Punt A, Schiffelers MJ, Jean Horbach G, van de Sandt JJ, Groothuis GM, Rietjens IM, Blaauboer BJ. 2011. Evaluation of research activities and research needs to increase the impact and applicability of alternative testing strategies in risk assessment practice. *Regulatory toxicology and pharmacology* : RTP. 61(1):105-114.
- R Core Team. 2020. R: A language and environment for statistical computing. R foundation for statistical computing, vienna, austria url <https://www.R-project.Org/>. (version 4.0.2).
- RAC. 2012. Committee for risk assessment (rac). Committee for socio-economic analysis (seac). Background document to the opinion on the annex xv dossier proposing restrictions on four phthalates. Echa/rac/res-o-0000001412-86-07/s1. Echa/seac/res-o-0000001412-86-10/s2. 5 december 2012.
- RAC. 2018. Committee for risk assessment, rac. Annex 1 background document to the opinion proposing harmonised classification and labelling at eu level of 2-butoxyethanol; ethylene glycol monobutyl ether. Clh-o-0000001412-86-226/f. Adopted 14 september 2018.
- Raies AB, Bajic VB. 2016. In silico toxicology: Computational methods for the prediction of chemical toxicity. *Wiley Interdiscip Rev Comput Mol Sci*. 6(2):147-172.
- Ramsey JC, Andersen ME. 1984. A physiologically based description of the inhalation pharmacokinetics of styrene in rats and humans. *Toxicol Appl Pharmacol*. 73(1):159-175.
- Reardon AJF, Rowan-Carroll A, Ferguson SS, Leingartner K, Gagne R, Kuo B, Williams A, Lorusso L, Bourdon-Lacombe JA, Carrier R et al. 2021. Potency ranking of per- and polyfluoroalkyl substances using high-throughput transcriptomic analysis of human liver spheroids. *Toxicol Sci*. 184(1):154-169.
- Rebholz SL, Jones T, Herrick RL, Xie C, Calafat AM, Pinney SM, Woollett LA. 2016. Hypercholesterolemia with consumption of pfoa-laced western diets is dependent on strain and sex of mice. *Toxicology reports*. 3:46-54.
- Ren H, Vallanat B, Nelson DM, Yeung LWY, Guruge KS, Lam PKS, Lehman-McKeeman LD, Corton JC. 2009. Evidence for the involvement of xenobiotic-responsive nuclear receptors in transcriptional effects upon perfluoroalkyl acid exposure in diverse species. *Reproductive toxicology* (Elmsford, NY). 27(3-4):266-277.
- RenwickAG. 1993. Data-derived safety factors for the evaluation of food additives and environmental contaminants. *Food Addit Contam*. 10(3):275-305.
- Rietjens I, Ning J, Chen L, Wesseling S, Strikwold M, Louise J. 2019. Selecting the dose metric in reverse dosimetry based qivive : Reply to 'comment on 'use of an in vitro-in silico testing strategy to predict inter-species and inter-ethnic human differences in liver toxicity of the pyrrolizidine alkaloids lasiocarpine and riddelliine' by ning et al., arch toxicol doi: <https://doi.Org/10.1007/s00204-019-02397-7>, arch toxicol doi: <https://doi.Org/10.1007/s00204-019-02421-w>. *Archives of toxicology*. 93(5):1467-1469.
- Rim K-T. 2019. In vitro models for chemical toxicity: Review of their applications and prospects. *Toxicology and Environmental Health Sciences*. 11:94-103.
- RIVM. 2009. M. Luijten, a. De vries, a. Opperhuizen, a.H. Piersma. Alternative methods in reproductive toxicity testing: State of the art. RIVM report 340720002/2007: RIVM.
- RIVM. 2018. Mixture exposure to pfas: A relative potency factor approach. National institute for public health and the environment, the netherlands. Rivm report 2018-0070. M.J. Zeilmaker et al.
- Roberts MS, Rowland M. 1986. A dispersion model of hepatic elimination: 3. Application to metabolite formation and elimination kinetics. *Journal of pharmacokinetics and biopharmaceutics*. 14(3):289-308.
- Rodgers T, Leahy D, Rowland M. 2005. Physiologically based pharmacokinetic modeling I: Predicting the tissue distribution of moderate-to-strong bases. *J Pharm Sci*. 94(6):1259-1276.
- Rodgers T, Rowland M. 2006. Physiologically based pharmacokinetic modelling 2: Predicting the tissue distribution of acids, very weak bases, neutrals and zwitterions. *J Pharm Sci*. 95(6):1238-1257.
- Rodgers T, Rowland M. 2007. Mechanistic approaches to volume of distribution predictions: Understanding the processes. *Pharm Res*. 24(5):918-933.
- Rosen MB, Abbott BD, Wolf DC, Corton JC, Wood CR, Schmid JE, Das KP, Zehr RD, Blair ET, Lau C. 2008a. Gene profiling in the livers of wild-type and pparalpha-null mice exposed to perfluorooctanoic acid. *Toxicol Pathol*. 36(4):592-607.
- Rosen MB, Das KP, Rooney J, Abbott B, Lau C, Corton JC. 2017. Ppara-independent transcriptional targets of perfluoroalkyl acids revealed by transcript profiling. *Toxicology*. 387:95-107.
- Rosen MB, Lee JS, Ren H, Vallanat B, Liu J, Waalkes MP, Abbott BD, Lau C, Corton JC. 2008b. Toxicogenomic dissection of the perfluorooctanoic acid transcript profile in mouse liver: Evidence for the involvement of nuclear receptors ppar alpha and car. *Toxicological sciences : an official journal of the Society of Toxicology*. 103(1):46-56.

- Rosen MB, Schmid JR, Corton JC, Zehr RD, Das KP, Abbott BD, Lau C. 2010. Gene expression profiling in wild-type and ppar α -null mice exposed to perfluorooctane sulfonate reveals ppar α -independent effects. *PPAR Res.* 2010:794739.
- Rosenmai AK, Ahrens L, le Godec T, Lundqvist J, Oskarsson A. 2018. Relationship between peroxisome proliferator-activated receptor alpha activity and cellular concentration of 14 perfluoroalkyl substances in hepg2 cells. *J Appl Toxicol.* 38(2):219-226.
- Rotroff DM, Wetmore BA, Dix DJ, Ferguson SS, Clewell HJ, Houck KA, Lecluyse EL, Andersen ME, Judson RS, Smith CM et al. 2010. Incorporating human dosimetry and exposure into high-throughput in vitro toxicity screening. *Toxicological sciences : an official journal of the Society of Toxicology.* 117(2):348-358.
- Rovei V, Chanoine F, Strolin Benedetti M. 1982. Pharmacokinetics of theophylline: A dose-range study. *British journal of clinical pharmacology.* 14(6):769-778.
- Rovida C, Asakura S, Daneshian M, Hofman-Huether H, Leist M, Meunier L, Reif D, Rossi A, Schmutz M, Valentin JP et al. 2015. Toxicity testing in the 21st century beyond environmental chemicals. *Altex.* 32(3):171-181.
- Rowan-Carroll A, Reardon A, Leingartner K, Gagné R, Williams A, Meier MJ, Kuo B, Bourdon-Lacombe J, Moffat I, Carrier R et al. 2021. High-throughput transcriptomic analysis of human primary hepatocyte spheroids exposed to per- and polyfluoroalkyl substances as a platform for relative potency characterization. *Toxicol Sci.* 181(2):199-214.
- Rowland M, Benet LZ, Graham GG. 1973. Clearance concepts in pharmacokinetics. *Journal of pharmacokinetics and biopharmaceutics.* 1(2):123-136.
- Rozpedek W, Pytel D, Mucha B, Leszczynska H, Diehl JA, Majsterek I. 2016. The role of the perk/eif2 α /atf4/chop signaling pathway in tumor progression during endoplasmic reticulum stress. *Curr Mol Med.* 16(6):533-544.
- Ruggiero MJ, Miller H, Idowu JY, Zitzow JD, Chang S-C, Hagenbuch B. 2021. Perfluoroalkyl carboxylic acids interact with the human bile acid transporter ntcp. *Livers.* 1(4):221-229.
- Saillenfait AM, Langonné I, Leheup B. 2001. Effects of mono-n-butyl phthalate on the development of rat embryos: In vivo and in vitro observations. *Pharmacol Toxicol.* 89(2):104-112.
- Saillenfait AM, Payan JP, Fabry JP, Beydon D, Langonne I, Gallissot F, Sabate JP. 1998. Assessment of the developmental toxicity, metabolism, and placental transfer of di-n-butyl phthalate administered to pregnant rats. *Toxicol Sci.* 45(2):212-224.
- Sakr CJ, Kreckmann KH, Green JW, Gillies PJ, Reynolds JL, Leonard RC. 2007a. Cross-sectional study of lipids and liver enzymes related to a serum biomarker of exposure (ammonium perfluorooctanoate or apfo) as part of a general health survey in a cohort of occupationally exposed workers. *J Occup Environ Med.* 49(10):1086-1096.
- Sakr CJ, Leonard RC, Kreckmann KH, Slade MD, Cullen MR. 2007b. Longitudinal study of serum lipids and liver enzymes in workers with occupational exposure to ammonium perfluorooctanoate. *J Occup Environ Med.* 49(8):872-879.
- Salihovic S, Stubleski J, Kärrman A, Larsson A, Fall T, Lind L, Lind PM. 2018. Changes in markers of liver function in relation to changes in perfluoroalkyl substances - a longitudinal study. *Environment international.* 117:196-203.
- Sand S, Parham F, Portier CJ, Tice RR, Krewski D. 2017. Comparison of points of departure for health risk assessment based on high-throughput screening data. *Environ Health Perspect.* 125(4):623-633.
- Sandborgh-Englund G, Adolffson-Erici M, Odham G, Ekstrand J. 2006. Pharmacokinetics of triclosan following oral ingestion in humans. *Journal of Toxicology and Environmental Health, Part A.* 69(20):1861-1873.
- Sandesara PB, Virani SS, Fazio S, Shapiro MD. 2019. The forgotten lipids: Triglycerides, remnant cholesterol, and atherosclerotic cardiovascular disease risk. *Endocr Rev.* 40(2):537-557.
- Sauer UG, Deferme L, Gribaldo L, Hacker Müller J, Tralau T, van Ravenzwaay B, Yauk C, Poole A, Tong W, Gant TW. 2017. The challenge of the application of 'omics technologies in chemicals risk assessment: Background and outlook. *Regulatory Toxicology and Pharmacology.* 91:S14-S26.
- Sayre RR, Wambaugh JF, Grulke CM. 2020. Database of pharmacokinetic time-series data and parameters for 144 environmental chemicals. *Scientific Data.* 7(1):122.
- Scharmach E, Buhrke T, Lichtenstein D, Lampen A. 2012. Perfluorooctanoic acid affects the activity of the hepatocyte nuclear factor 4 alpha (hnf4alpha). *Toxicology letters.* 212(2):106-112.

- Schleizinger J, Puckett H, Oliver J, Nielsen G, Heiger-Bernays W, Webster T. 2020. Perfluorooctanoic acid activates multiple nuclear receptor pathways and skews expression of genes regulating cholesterol homeostasis in liver of humanized ppar α mice fed an american diet. *bioRxiv*.2020.2001.2030.926642.
- Schmitt W. 2008a. General approach for the calculation of tissue to plasma partition coefficients. *Toxicol In Vitro*. 22(2):457-467.
- Schmitt W. 2008b. General approach for the calculation of tissue to plasma partition coefficients. *Toxicology in Vitro*. 22(2):457-467.
- Scholz G, Genschow E, Pohl I, Bremer S, Paparella M, Raabe H, Southee J, Spielmann H. 1999. Prevalidation of the embryonic stem cell test (est)-a new in vitro embryotoxicity test. *Toxicol In Vitro*. 13(4-5):675-681.
- Scholze M, Taxvig C, Kortenkamp A, Boberg J, Christiansen S, Svungen T, Lauschke K, Frandsen H, Ermler S, Hermann SS et al. 2020. Quantitative in vitro to in vivo extrapolation (qivive) for predicting reduced anogenital distance produced by anti-androgenic pesticides in a rodent model for male reproductive disorders. *Environ Health Perspect*. 128(11):117005.
- Schoonjans K, Staels B, Auwerx J. 1996. Role of the peroxisome proliferator-activated receptor (ppar) in mediating the effects of fibrates and fatty acids on gene expression. *J Lipid Res*. 37(5):907-925.
- Schulpen SH, Robinson JF, Pennings JL, van Dartel DA, Piersma AH. 2013. Dose response analysis of monophthalates in the murine embryonic stem cell test assessed by cardiomyocyte differentiation and gene expression. *Reprod Toxicol*. 35:81-88.
- Schwartz GJ, Brion LP, Spitzer A. 1987. The use of plasma creatinine concentration for estimating glomerular filtration rate in infants, children, and adolescents. *Pediatr Clin North Am*. 34(3):571-590.
- Schwinghammer TL, Przepiorka D, Venkataramanan R, Wang CP, Burckart GJ, Rosenfeld CS, Shaddock RK. 1991. The kinetics of cyclosporine and its metabolites in bone marrow transplant patients. *British journal of clinical pharmacology*. 32(3):323-328.
- Scott WJ, Jr., Collins MD, Nau H. 1994. Pharmacokinetic determinants of embryotoxicity in rats associated with organic acids. *Environ Health Perspect*. 102 Suppl 11(Suppl 11):97-101.
- Seacat AM, Thomford PJ, Hansen KJ, Clemen LA, Eldridge SR, Elcombe CR, Butenhoff JL. 2003. Sub-chronic dietary toxicity of potassium perfluorooctanesulfonate in rats. *Toxicology*. 183(1-3):117-131.
- Seacat AM, Thomford PJ, Hansen KJ, Olsen GW, Case MT, Butenhoff JL. 2002. Subchronic toxicity studies on perfluorooctanesulfonate potassium salt in cynomolgus monkeys. *Toxicological sciences : an official journal of the Society of Toxicology*. 68(1):249-264.
- Seiler A, Visan A, Buesen R, Genschow E, Spielmann H. 2004. Improvement of an in vitro stem cell assay for developmental toxicity: The use of molecular endpoints in the embryonic stem cell test. *Reprod Toxicol*. 18(2):231-240.
- Seiler AE, Spielmann H. 2011. The validated embryonic stem cell test to predict embryotoxicity in vitro. *Nat Protoc*. 6(7):961-978.
- Sevin E, Dehouck L, Fabulas-da Costa A, Cecchelli R, Dehouck MP, Lundquist S, Culot M. 2013. Accelerated caco-2 cell permeability model for drug discovery. *J Pharmacol Toxicol Methods*. 68(3):334-339.
- Shao W, Espenshade PJ. 2012. Expanding roles for srebp in metabolism. *Cell Metab*. 16(4):414-419.
- Shebley M, Sandhu P, Emami Riedmaier A, Jamei M, Narayanan R, Patel A, Peters SA, Reddy VP, Zheng M, de Zwart L et al. 2018. Physiologically based pharmacokinetic model qualification and reporting procedures for regulatory submissions: A consortium perspective. *Clinical pharmacology and therapeutics*. 104(1):88-110.
- Sheng N, Li J, Liu H, Zhang A, Dai J. 2016. Interaction of perfluoroalkyl acids with human liver fatty acid-binding protein. *Arch Toxicol*. 90(1):217-227.
- Sleet. 1989. Teratologic evaluation of ethylene glycol monobutyl ether administered to fischer 344 rats on either gestational days 9-11 or days 11-13 [final report]. Public health service, u.S. Department of health and human services; ntp-cter-86-103. Available from the national institute of environmental health sciences, research triangle park, nc.
- Slob W. 1999. Thresholds in toxicology and risk assessment. *International Journal of Toxicology*. 18(4):259-268.
- Slob W. 2002. Dose-response modeling of continuous endpoints. *Toxicological Sciences*. 66(2):298-312.
- Smith BP, Auvil LS, Welge M, Bushell CB, Bhargava R, Elango N, Johnson K, Madak-Erdogan Z. 2020. Identification of early liver toxicity gene biomarkers using comparative supervised machine learning. *Scientific Reports*. 10(1):19128.

- Smith DA, Di L, Kerns EH. 2010. The effect of plasma protein binding on in vivo efficacy: Misconceptions in drug discovery. *Nature Reviews Drug Discovery*. 9(12):929-939.
- Sodhi JK, Wang HJ, Benet LZ. 2020. Are there any experimental perfusion data that preferentially support the dispersion and parallel-tube models over the well-stirred model of organ elimination? *Drug metabolism and disposition: the biological fate of chemicals*. 48(7):537-543.
- Sohlenius-Sternbeck AK, Jones C, Ferguson D, Middleton BJ, Projean D, Floby E, Bylund J, Afzelius L. 2012. Practical use of the regression offset approach for the prediction of in vivo intrinsic clearance from hepatocytes. *Xenobiotica*. 42(9):841-853.
- Son HY, Kim SH, Shin HI, Bae HI, Yang JH. 2008. Perfluorooctanoic acid-induced hepatic toxicity following 21-day oral exposure in mice. *Arch Toxicol*. 82(4):239-246.
- Spielmann H. 2009. The way forward in reproductive/developmental toxicity testing. *Altern Lab Anim*. 37(6):641-656.
- Starling AP, Engel SM, Whitworth KW, Richardson DB, Stuebe AM, Daniels JL, Haug LS, Eggesbo M, Becher G, Sabaredzovic A et al. 2014. Perfluoroalkyl substances and lipid concentrations in plasma during pregnancy among women in the norwegian mother and child cohort study. *Environment international*. 62:104-112.
- Stec J, Fomovska A, Afanador GA, Muench SP, Zhou Y, Lai BS, El Bissati K, Hickman MR, Lee PJ, Leed SE et al. 2013. Modification of triclosan scaffold in search of improved inhibitors for enoyl-acyl carrier protein (acp) reductase in *Toxoplasma gondii*. *ChemMedChem*. 8(7):1138-1160.
- Steenland K, Tinker S, Frisbee S, Ducatman A, Vaccarino V. 2009. Association of perfluorooctanoic acid and perfluorooctane sulfonate with serum lipids among adults living near a chemical plant. *Am J Epidemiol*. 170(10):1268-1278.
- Strikwold M, Spenkeliink B, de Haan LHJ, Woutersen RA, Punt A, Rietjens I. 2017. Integrating in vitro data and physiologically based kinetic (pbk) modelling to assess the in vivo potential developmental toxicity of a series of phenols. *Archives of toxicology*. 91(5):2119-2133.
- Strikwold M, Spenkeliink B, Woutersen RA, Rietjens IM, Punt A. 2013. Combining in vitro embryotoxicity data with physiologically based kinetic (pbk) modelling to define in vivo dose-response curves for developmental toxicity of phenol in rat and human. *Archives of toxicology*. 87(9):1709-1723.
- Syme MR, Paxton JW, Keelan JA. 2004. Drug transfer and metabolism by the human placenta. *Clin Pharmacokinet*. 43(8):487-514.
- Szabo M, Veres Z, Baranyai Z, Jakab F, Jemnitz K. 2013. Comparison of human hepatoma heparg cells with human and rat hepatocytes in uptake transport assays in order to predict a risk of drug induced hepatotoxicity. *PLoS One*. 8(3):e59432.
- . A method for calculating the pka values of small and large molecules. American Chemical Society Spring meeting; 2007.
- Szultka M, Krzeminski R, Jackowski M, Buszewski B. 2014. Identification of in vitro metabolites of amoxicillin in human liver microsomes by lc-esi/ms. *Chromatographia*. 77(15):1027-1035.
- Takacs ML, Abbott BD. 2007. Activation of mouse and human peroxisome proliferator-activated receptors (alpha, beta/delta, gamma) by perfluorooctanoic acid and perfluorooctane sulfonate. *Toxicological sciences : an official journal of the Society of Toxicology*. 95(1):108-117.
- Tan X, Xie G, Sun X, Li Q, Zhong W, Qiao P, Sun X, Jia W, Zhou Z. 2013. High fat diet feeding exaggerates perfluorooctanoic acid-induced liver injury in mice via modulating multiple metabolic pathways. *PLoS One*. 8(4):e61409.
- Tannenbaum J, Bennett BT. 2015. Russell and burch's 3rs then and now: The need for clarity in definition and purpose. *J Am Assoc Lab Anim Sci*. 54(2):120-132.
- Tateno C, Yoshizane Y, Saito N, Kataoka M, Utoh R, Yamasaki C, Tachibana A, Soeno Y, Asahina K, Hino H et al. 2004. Near completely humanized liver in mice shows human-type metabolic responses to drugs. *Am J Pathol*. 165(3):901-912.
- Tavares-Sanchez OL, Rodriguez C, Gortares-Moroyoqui P, Estrada MI. 2015. Hepatocyte nuclear factor-4 α , a multifunctional nuclear receptor associated with cardiovascular disease and cholesterol catabolism. *Int J Environ Health Res*. 25(2):126-139.
- Taylor RR, Hoffman KL, Schniedewind B, Clavijo C, Galinkin JL, Christians U. 2013. Comparison of the quantification of acetaminophen in plasma, cerebrospinal fluid and dried blood spots using high-performance liquid chromatography-tandem mass spectrometry. *J Pharm Biomed Anal*. 83:1-9.

- Tebby C, van der Voet H, de Sousa G, Rorije E, Kumar V, de Boer W, Kruisselbrink JW, Bois FY, Faniband M, Moretto A et al. 2020. A generic pbtk model implemented in the mcra platform: Predictive performance and uses in risk assessment of chemicals. *Food Chem Toxicol.* 142:111440.
- Thelen K, Coboeken K, Willmann S, Burghaus R, Dressman JB, Lippert J. 2011. Evolution of a detailed physiological model to simulate the gastrointestinal transit and absorption process in humans, part 1: Oral solutions. *J Pharm Sci.* 100(12):5324-5345.
- Thelen K, Coboeken K, Willmann S, Dressman JB, Lippert J. 2012. Evolution of a detailed physiological model to simulate the gastrointestinal transit and absorption process in humans, part ii: Extension to describe performance of solid dosage forms. *J Pharm Sci.* 101(3):1267-1280.
- Thompson MB. 1996. Bile acids in the assessment of hepatocellular function. *Toxicol Pathol.* 24(1):62-71.
- Thumser AE, Wilton DC. 1996. The binding of cholesterol and bile salts to recombinant rat liver fatty acid-binding protein. *Biochem J.* 320 (Pt 3)(Pt 3):729-733.
- Toro-Ramos T, Paley C, Pi-Sunyer FX, Gallagher D. 2015. Body composition during fetal development and infancy through the age of 5 years. *Eur J Clin Nutr.* 69(12):1279-1289.
- Trapani L, Segatto M, Pallottini V. 2012. Regulation and deregulation of cholesterol homeostasis: The liver as a metabolic "power station". *World J Hepatol.* 4(6):184-190.
- Trivier JM, Libersa C, Belloc C, Lhermitte M. 1993. Amiodarone n-deethylation in human liver microsomes: Involvement of cytochrome p450 3a enzymes (first report). *Life Sci.* 52(10):PL91-96.
- Tsaion K, Blaauboer BJ, Hartung T. 2016. Evidence-based absorption, distribution, metabolism, excretion (adme) and its interplay with alternative toxicity methods. *Altex.* 33(4):343-358.
- Tugwood JD, Aldridge TC, Lambe KG, Macdonald N, Woodyatt NJ. 1996. Peroxisome proliferator-activated receptors: Structures and function. *Ann N Y Acad Sci.* 804:252-265.
- UNEP/POPS/COP.4/17 SC. 2009. Recommendations of the persistent organic pollutants review committee of the stockholm convention to amend annexes a, b or c of the convention. Conference of the Parties of the Stockholm, Convention on Persistent Organic Pollutants. Fourth meeting, Geneva, 4-8 May 2009.
- US EPA. 2009. Us epa, november 2009. Toxicological review of ethylene glycol monobutyl ether (egbe). *Epa/635/r-08/006d.* In support of summary information on the integrated risk information system (iris).
- US EPA. 2016a. Drinking water health advisory for perfluorooctanoic acid (pfoa). In: US EPA Office of Water (4304T) Health and Ecological Criteria Division Washington D, EPA Document Number: 822-R-16-005, May 2016, editor.
- US EPA. 2016b. Drinking water health advisory for perfluorooctane sulfonate (pfos). In: US EPA Office of Water (4304T) Health and Ecological Criteria Division Washington D, EPA Document Number: 822-R-16-004, May 2016, editor.
- Utoguchi N, Audus KL. 2000. Carrier-mediated transport of valproic acid in bewo cells, a human trophoblast cell line. *Int J Pharm.* 195(1-2):115-124.
- Utoguchi N, Magnusson M, Audus KL. 1999. Carrier-mediated transport of monocarboxylic acids in bewo cell monolayers as a model of the human trophoblast. *J Pharm Sci.* 88(12):1288-1292.
- van der Voet H, Kruisselbrink JW, de Boer WJ, van Lenthe MS, van den Heuvel J, Crépet A, Kennedy MC, Zilliacus J, Beronius A, Tebby C et al. 2020. The mcra toolbox of models and data to support chemical mixture risk assessment. *Food and chemical toxicology : an international journal published for the British Industrial Biological Research Association.* 138:111185.
- van Leeuwen CJVT. 2007. Risk assessment of chemicals: An introduction. Second edition. European commission, joint research centre, ispra, italy. Netherlands organization for applied scientific research tno, zeist, the netherlands. National institute for public health and the environment, bilthoven, the netherlands. Isbn 978-1-4020-6102-8 (e-book).
- van Meer PJ, Kooijman M, Gispens-de Wied CC, Moors EH, Schellekens H. 2012. The ability of animal studies to detect serious post marketing adverse events is limited. *Regulatory toxicology and pharmacology : RTP.* 64(3):345-349.
- Van Norman GA. 2019a. Limitations of animal studies for predicting toxicity in clinical trials: Is it time to rethink our current approach? *JACC Basic Transl Sci.* 4(7):845-854.
- Van Norman GA. 2019b. Phase ii trials in drug development and adaptive trial design. *JACC Basic Transl Sci.* 4(3):428-437.

- Vanden Heuvel JP, Thompson JT, Frame SR, Gillies PJ. 2006. Differential activation of nuclear receptors by perfluorinated fatty acid analogs and natural fatty acids: A comparison of human, mouse, and rat peroxisome proliferator-activated receptor- α , - β , and - γ , liver x receptor- β , and retinoid x receptor- α . *Toxicological sciences : an official journal of the Society of Toxicology*. 92(2):476-489.
- Varga OE, Hansen AK, Sandøe P, Olsson IA. 2010. Validating animal models for preclinical research: A scientific and ethical discussion. *Altern Lab Anim*. 38(3):245-248.
- Varma DR, Ramakrishnan R. 1985. A rat model for the study of transplacental pharmacokinetics and its assessment with antipyrine and aminoisobutyric acid. *J Pharmacol Methods*. 14(1):61-74.
- Vasiliogianni AM, Achour B, Scotcher D, Peters SA, Al-Majdoub ZM, Barber J, Rostami-Hodjegan A. 2021. Hepatic scaling factors for in vitro-in vivo extrapolation of metabolic drug clearance in patients with colorectal cancer with liver metastasis. *Drug Metab Dispos*. 49(7):563-571.
- Vinken M. 2013. The adverse outcome pathway concept: A pragmatic tool in toxicology. *Toxicology*. 312:158-165.
- Volak LP, Hanley MJ, Masse G, Hazarika S, Harmatz JS, Badmaev V, Majeed M, Greenblatt DJ, Court MH. 2013. Effect of a herbal extract containing curcumin and piperine on midazolam, flurbiprofen and paracetamol (acetaminophen) pharmacokinetics in healthy volunteers. *British journal of clinical pharmacology*. 75(2):450-462.
- Wada Y, Kikuchi A, Kaga A, Shimizu N, Ito J, Onuma R, Fujishima F, Totsune E, Sato R, Niihori T et al. 2020. Metabolic and pathologic profiles of human Irs deficiency recapitulated in mice. *PLoS Genet*. 16(2):e1008628-e1008628.
- Wambaugh JF, Hughes MF, Ring CL, MacMillan DK, Ford J, Fennell TR, Black SR, Snyder RW, Sipes NS, Wetmore BA et al. 2018. Evaluating in vitro-in vivo extrapolation of toxicokinetics. *Toxicological sciences : an official journal of the Society of Toxicology*. 163(1):152-169.
- Wambaugh JF, Setzer RW, Pitruzzello AM, Liu J, Reif DM, Kleinstreuer NC, Wang NC, Sipes N, Martin M, Das K et al. 2013. Dosimetric anchoring of in vivo and in vitro studies for perfluorooctanoate and perfluorooctanesulfonate. *Toxicological sciences : an official journal of the Society of Toxicology*. 136(2):308-327.
- Wambaugh JF, Wetmore BA, Pearce R, Strobe C, Goldsmith R, Sluka JP, Sedykh A, Tropsha A, Bosgra S, Shah I et al. 2015. Toxicokinetic triage for environmental chemicals. *Toxicological sciences : an official journal of the Society of Toxicology*. 147(1):55-67.
- Wan HT, Zhao YG, Wei X, Hui KY, Giesy JP, Wong CK. 2012. Pfos-induced hepatic steatosis, the mechanistic actions on β -oxidation and lipid transport. *Biochim Biophys Acta*. 1820(7):1092-1101.
- Wang B, Gray G. 2015. Concordance of noncarcinogenic endpoints in rodent chemical bioassays. *Risk Anal*. 35(6):1154-1166.
- Wang L, Mao B, He H, Shang Y, Zhong Y, Yu Z, Yang Y, Li H, An J. 2019. Comparison of hepatotoxicity and mechanisms induced by triclosan (tcs) and methyl-triclosan (mtcs) in human liver hepatocellular hepg2 cells. *Toxicol Res (Camb)*. 8(1):38-45.
- Wang L, Wang Y, Liang Y, Li J, Liu Y, Zhang J, Zhang A, Fu J, Jiang G. 2013. Specific accumulation of lipid droplets in hepatocyte nuclei of pfoa-exposed balb/c mice. *Sci Rep*. 3:2174.
- Wang L, Wang Y, Liang Y, Li J, Liu Y, Zhang J, Zhang A, Fu J, Jiang G. 2014. Pfos induced lipid metabolism disturbances in balb/c mice through inhibition of low density lipoproteins excretion. *Sci Rep*. 4:4582.
- Westerterp M, van der Hoogt CC, de Haan W, Offerman EH, Dallinga-Thie GM, Jukema JW, Havekes LM, Rensen PC. 2006. Cholesteryl ester transfer protein decreases high-density lipoprotein and severely aggravates atherosclerosis in apoE3-leiden mice. *Arterioscler Thromb Vasc Biol*. 26(11):2552-2559.
- Wetmore BA, Wambaugh JF, Ferguson SS, Li L, Clewell HJ, 3rd, Judson RS, Freeman K, Bao W, Sochaski MA, Chu TM et al. 2013. Relative impact of incorporating pharmacokinetics on predicting in vivo hazard and mode of action from high-throughput in vitro toxicity assays. *Toxicological sciences : an official journal of the Society of Toxicology*. 132(2):327-346.
- Wetmore BA, Wambaugh JF, Ferguson SS, Sochaski MA, Retroff DM, Freeman K, Clewell HJ, 3rd, Dix DJ, Andersen ME, Houck KA et al. 2012. Integration of dosimetry, exposure, and high-throughput screening data in chemical toxicity assessment. *Toxicological sciences : an official journal of the Society of Toxicology*. 125(1):157-174.
- WHO. 1999. World health organization. Environmental health criteria 210. Principles for assessment of risks to human health from exposures to chemicals. Who, geneva.

- WHO. 2010. World health organization. International programme on chemical safety. Characterization and application of physiologically based pharmacokinetic models in risk assessment. Harmonization project document no. 9
- Wice B, Menton D, Geuze H, Schwartz AL. 1990. Modulators of cyclic amp metabolism induce syncytiotrophoblast formation in vitro. *Exp Cell Res*. 186(2):306-316.
- Wigger L, Casals-Casas C, Baruchet M, Trang KB, Pradervand S, Naldi A, Desvergne B. 2019. System analysis of cross-talk between nuclear receptors reveals an opposite regulation of the cell cycle by lxr and fxr in human heparg liver cells. *PLoS One*. 14(8):e0220894.
- Willmann S, Schmitt W, Keldenich J, Lippert J, Dressman JB. 2004. A physiological model for the estimation of the fraction dose absorbed in humans. *J Med Chem*. 47(16):4022-4031.
- Wilson JP. 1967. Surface area of the small intestine in man. *Gut*. 8(6):618-621.
- Winquist A, Steenland K. 2014. Modeled pfoa exposure and coronary artery disease, hypertension, and high cholesterol in community and worker cohorts. *Environmental health perspectives*. 122(12):1299-1305.
- Wolf CJ, Rider CV, Lau C, Abbott BD. 2014. Evaluating the additivity of perfluoroalkyl acids in binary combinations on peroxisome proliferator-activated receptor- α activation. *Toxicology*. 316:43-54.
- Wolf CJ, Schmid JE, Lau C, Abbott BD. 2012. Activation of mouse and human peroxisome proliferator-activated receptor-alpha (ppar α) by perfluoroalkyl acids (pfaas): Further investigation of c4-cl2 compounds. *Reproductive toxicology* (Elmsford, NY). 33(4):546-551.
- Wolf CJ, Takacs ML, Schmid JE, Lau C, Abbott BD. 2008. Activation of mouse and human peroxisome proliferator-activated receptor alpha by perfluoroalkyl acids of different functional groups and chain lengths. *Toxicological sciences : an official journal of the Society of Toxicology*. 106(1):162-171.
- Woodcroft MW, Ellis DA, Rafferty SP, Burns DC, March RE, Stock NL, Trumpour KS, Yee J, Munro K. 2010. Experimental characterization of the mechanism of perfluorocarboxylic acids' liver protein bioaccumulation: The key role of the neutral species. *Environ Toxicol Chem*. 29(8):1669-1677.
- Wu X, Xie G, Xu X, Wu W, Yang B. 2018. Adverse bioeffect of perfluorooctanoic acid on liver metabolic function in mice. *Environ Sci Pollut Res Int*. 25(5):4787-4793.
- Yan J, Chen B, Lu J, Xie W. 2015a. Deciphering the roles of the constitutive androstane receptor in energy metabolism. *Acta Pharmacologica Sinica*. 36(1):62-70.
- Yan S, Wang J, Dai J. 2015b. Activation of sterol regulatory element-binding proteins in mice exposed to perfluorooctanoic acid for 28 days. *Arch Toxicol*. 89(9):1569-1578.
- Yang CH, Glover KP, Han X. 2009. Organic anion transporting polypeptide (oatp)1a1-mediated perfluorooctanoate transport and evidence for a renal reabsorption mechanism of oatp1a1 in renal elimination of perfluorocarboxylates in rats. *Toxicology letters*. 190(2):163-171.
- Yang R. 2011. The application of physiologically based pharmacokinetic (pbpk) modeling to risk assessment.
- Yee S. 1997. In vitro permeability across caco-2 cells (colonic) can predict in vivo (small intestinal) absorption in man--fact or myth. *Pharm Res*. 14(6):763-766.
- Yeh MM, Bosch DE, Daoud SS. 2019. Role of hepatocyte nuclear factor 4-alpha in gastrointestinal and liver diseases. *World J Gastroenterol*. 25(30):4074-4091.
- Yin L, Ma H, Ge X, Edwards PA, Zhang Y. 2011. Hepatic hepatocyte nuclear factor 4 α is essential for maintaining triglyceride and cholesterol homeostasis. *Arterioscler Thromb Vasc Biol*. 31(2):328-336.
- Yoon M, Blaauboer BJ, Clewell HJ. 2015. Quantitative in vitro to in vivo extrapolation (qivive): An essential element for in vitro-based risk assessment. *Toxicology*. 332:1-3.
- Yoon M, Campbell JL, Andersen ME, Clewell HJ. 2012. Quantitative in vitro to in vivo extrapolation of cell-based toxicity assay results. *Critical reviews in toxicology*. 42(8):633-652.
- Yoon M, Nong A, Clewell HJ, 3rd, Taylor MD, Dorman DC, Andersen ME. 2009. Evaluating placental transfer and tissue concentrations of manganese in the pregnant rat and fetuses after inhalation exposures with a pbpk model. *Toxicol Sci*. 112(1):44-58.
- Yu L, Li H, Zhang C, Zhang Q, Guo J, Li J, Yuan H, Li L, Carmichael P, Peng S. 2020. Integrating in vitro testing and physiologically-based pharmacokinetic (pbpk) modelling for chemical liver toxicity assessment—a case study of roglitazone. *Environ Toxicol Pharmacol*. 74:103296.
- Yu WG, Liu W, Jin YH. 2009. Effects of perfluorooctane sulfonate on rat thyroid hormone biosynthesis and metabolism. *Environmental toxicology and chemistry*. 28(5):990-996.

- Yun YE, Edginton AN. 2013. Correlation-based prediction of tissue-to-plasma partition coefficients using readily available input parameters. *Xenobiotica*. 43(10):839-852.
- Zadelaar S, Kleemann R, Verschuren L, de Vries-Van der Weij J, van der Hoorn J, Princen HM, Kooistra T. 2007. Mouse models for atherosclerosis and pharmaceutical modifiers. *Arterioscler Thromb Vasc Biol*. 27(8):1706-1721.
- Zandvliet AS, Huijtema AD, de Jonge ME, den Hoed R, Sparidans RW, Hendriks VM, van den Brink W, van Ree JM, Beijnen JH. 2005. Population pharmacokinetics of caffeine and its metabolites theobromine, paraxanthine and theophylline after inhalation in combination with diacetylmorphine. *Basic Clin Pharmacol Toxicol*. 96(1):71-79.
- Zhang F, Bartels M, Clark A, Erskine T, Auernhammer T, Bhatarai B, Wilson D, Marty S. 2018a. Performance evaluation of the gastroplus(tm) software tool for prediction of the toxicokinetic parameters of chemicals. *SAR QSAR Environ Res*. 29(11):875-893.
- Zhang H, Temel RE, Martel C. 2014. Cholesterol and lipoprotein metabolism: Early career committee contribution. *Arterioscler Thromb Vasc Biol*. 34(9):1791-1794.
- Zhang L, Ren XM, Guo LH. 2013a. Structure-based investigation on the interaction of perfluorinated compounds with human liver fatty acid binding protein. *Environ Sci Technol*. 47(19):11293-11301.
- Zhang M, van Ravenzwaay B, Fabian E, Rietjens IMCM, Lousse J. 2018b. Towards a generic physiologically based kinetic model to predict in vivo uterotrophic responses in rats by reverse dosimetry of in vitro estrogenicity data. *Archives of toxicology*. 92(3):1075-1088.
- Zhang Q, Li J, Middleton A, Bhattacharya S, Conolly RB. 2018c. Bridging the data gap from in vitro toxicity testing to chemical safety assessment through computational modeling. *Front Public Health*. 6:261.
- Zhang Y, Beeson S, Zhu L, Martin JW. 2013b. Biomonitoring of perfluoroalkyl acids in human urine and estimates of biological half-life. *Environ Sci Technol*. 47(18):10619-10627.
- Zhang YM, Dong XY, Fan LJ, Zhang ZL, Wang Q, Jiang N, Yang XS. 2017. Poly- and perfluorinated compounds activate human pregnane x receptor. *Toxicology*. 380:23-29.
- Zhao S, Kamelia L, Boonpawa R, Wesseling S, Spenkelink B, Rietjens IMCM. 2019. Physiologically based kinetic modeling-facilitated reverse dosimetry to predict in vivo red blood cell acetylcholinesterase inhibition following exposure to chlorpyrifos in the caucasian and chinese population. *Toxicological Sciences*. 171(1):69-83.
- Zhao W, Zitzow JD, Ehresman DJ, Chang S-C, Butenhoff JL, Forster J, Hagenbuch B. 2015a. Na⁺/taurocholate cotransporting polypeptide and apical sodium-dependent bile acid transporter are involved in the disposition of perfluoroalkyl sulfonates in humans and rats. *Toxicological sciences : an official journal of the Society of Toxicology*. 146(2):363-373.
- Zhao W, Zitzow JD, Ehresman DJ, Chang SC, Butenhoff JL, Forster J, Hagenbuch B. 2015b. Na⁺/taurocholate cotransporting polypeptide and apical sodium-dependent bile acid transporter are involved in the disposition of perfluoroalkyl sulfonates in humans and rats. *Toxicological sciences : an official journal of the Society of Toxicology*. 146(2):363-373.
- Zhao W, Zitzow JD, Weaver Y, Ehresman DJ, Chang S-C, Butenhoff JL, Hagenbuch B. 2017a. Organic anion transporting polypeptides contribute to the disposition of perfluoroalkyl acids in humans and rats. *Toxicological sciences : an official journal of the Society of Toxicology*. 156(1):84-95.
- Zhao W, Zitzow JD, Weaver Y, Ehresman DJ, Chang SC, Butenhoff JL, Hagenbuch B. 2017b. Organic anion transporting polypeptides contribute to the disposition of perfluoroalkyl acids in humans and rats. *Toxicol Sci*. 156(1):84-95.

Appendix

Nederlandse samenvatting

Dit proefschrift bestaat uit drie verschillende onderdelen. Het eerste deel (Sectie I) evalueert twee generieke PBK-modellen met ingebouwde QSAR-modelparameterisering wat betreft de beschrijving van de toxicokinetiek van een breed scala aan chemicaliën met onderling sterk verschillende fysisch-chemische en biologische eigenschappen (Hoofdstuk 2). Dit hoofdstuk bouwt voort op een eerdere evaluatie van het toepassingsbereik (“applicability domain”) van het generieke PBK-model IndusChemFate (Fragki et al. 2017). Concreet is het IndusChemFate model vergeleken met een biologisch meer complex PBK model (“TNO Model”). Het TNO-model omvat meer gedetailleerde orgaan:bloedpartitie, levermetabolisme en absorptiekinetiek. Beide modellen werken met ingebouwde QSAR's voor orgaan: bloed verdeling, uitschieding via de nieren en vereisen minimale parametrisering. Het “eenvoudiger” IndusChemFate bleek beter te voldoen, illustrerend dat dit model geschikt is als screeningsmethode (“first tier”) voor het simuleren van toxicokinetiek op basis van QSAR's en *in vitro* metabolisme parameters.

In sectie II werd IndusChemFate geselecteerd voor het uitvoeren van een “Quantitative *in vitro* to *in vivo* extrapolation” (QIVIVE) voor het eindpunt van ontwikkelingstoxiciteit, op basis van beschikbare *in vitro* embryotoxiciteitstesten. Dit vereiste de schaling van *in vitro* waargenomen dosis-responskarakteristieken naar de *in vivo* foetale blootstelling. In Hoofdstuk 3 werden als modelverbindingen drie verschillende klassen van reproductie toxische chemicaliën gekozen: triazolen, alkoxyazijnzuur metabolieten van glycolethers en primaire ftalaatmetabolieten. Deze verbindingen werden eerder getest in drie *in vitro* toxiciteitsassays: embryocultuur (“Whole Embryo Culture”, WEC), de zebravis-embryotest (ZET) en de muizenembryonale stamceltest (EST). Als *in vivo* proxy voor foetale blootstelling werden hierbij PBK maternale bloedconcentraties gebruikt. Het IndusChemFate-model bleek in staat om de *in vivo* kinetiek van de drie gebruikte klassen van reproductie toxische stoffen te beschrijven, zij het ten koste van verschillende chemische specifieke aanpassingen. Verder werden voor alle drie assays vergelijkingen gemaakt van de PBK-gesimuleerde bloedspiegels bij toxische *in vivo* doses met de effectieve *in vitro* concentraties. De resultaten gaven aan dat een combinatie van testen de voorkeur heeft voor het voorspellen van het eindpunt van *in vivo* reproductietoxiciteit.

In Hoofdstuk 4 (Sectie II) werd de QIVIVE methode verfijnd door het PBK-model aan te passen met de fysiologische veranderingen in het lichaam van de moeder tijdens de zwangerschap, inclusief de hiermee overeenkomende placenta-overdracht en foetale groei. Placenta-overdracht werd *in vitro* nagebootst met behulp van de BeWo-cell assay voor selectief transplacentaal transport. In deze assay zijn zes reproductie toxische stoffen experimenteel onderzocht. De BeWo-resultaten lieten verschillende transplacentale transportprofielen zien, waarbij de stoffen in twee afzonderlijke groepen ingedeeld

konden worden: de ‘snel getransporteerden’ en de ‘langzaam getransporteerden’. De verschillende transportprofielen werden in het IndusChemFate PBK-model opgenomen. In de rat toonden PBK-simulaties waarin experimenteel gemeten maternale bloed- en foetale concentraties vergeleken werden bevredigende kinetische voorspellingen. Vervolgens werd PBK-modellering (“reverse dosimetry”) toegepast om *in vitro* concentratie-responscurven naar equivalente *in vivo* dosis-responscurven te schalen. Hier werd de foetale C_{max} genomen als de interne dosismaat voor de inductie van reproductietoxiciteit. Geselecteerde *in vitro* testen waren de WEC en de EST (cardiaal:ESTc en neuraal:ESTn). De op *in vitro* gebaseerde *in vivo* dosimetrie voorspellingen werden vergeleken met *in vivo* gegevens over reproductietoxiciteit bij de rat. Deze vergelijking resulteerde in een tamelijk goede voorspelling voor de WEC, gevolgd door de ESTc (voor drie van de vijf verbindingen), met onderlinge verschillen die binnen dezelfde orde van grootte liggen (<10-voudig). Hoewel er een duidelijk behoefte blijft aan verder validatie/optimalisatie van de toegepaste QIVIVE methodologie geven de *in vitro* met *in vivo* vergelijkingen aan dat deze methodologie van duidelijke meerwaarde kan zijn bij de screening/prioritering en veiligheidsbeoordeling van reproductietoxische stoffen.

In het laatste deel (Sectie III) wordt een “New Approach Methodology” (NAM)-case study gepresenteerd voor per- en polyfluoralkylstoffen (PFAS’s). Het aantal bestaande PFAS’s wordt geschat op enkele duizenden, waarvoor voor velen *in vivo* toxiciteit ontbreken gegevens. Om deze reden kan de toepassing van NAM’s nuttig zijn voor de screening van PFAS’s en de identificatie van verbindingen die prioriteit moeten krijgen voor een uitgebreidere risicokarakterisering. Het hier geselecteerde eindpunt was hepatotoxiciteit en verstoringen in de homeostase van lipiden. In Hoofdstuk 5 wordt op basis van literatuuronderzoek de huidige stand van zaken besproken met betrekking tot verstoring van de homeostase van lipiden door de twee meest voorkomende congenere PFOA en PFOS, met de nadruk op voor de mens relevante onderliggende mechanismen. Verschillende bevolkingsonderzoeken hebben herhaaldelijk correlaties gevonden tussen verhoogde bloedspiegels van PFOS/PFOA en verhoogd totaal cholesterol en LDL-C in het bloed (en in mindere mate TG’s). Desalniettemin zijn deze bevindingen niet in verband gebracht met een overeenkomstig nadelig gezondheidseffect en zijn ze niet consistent met toxicologische dierstudies, waar hoge doses PFOS/PFOA het serumcholesterol en TG’s juist verlagen en leverlipiden verhogen. Deze ogenschijnlijk uiteenlopende bevindingen stellen gezondheidsrisicobeoordelaars voor een raadsel. Deze tegenstrijdigheid kan een gevolg zijn van verschillen in de blootstelling van de mens en die in dierstudies, of voortkomen uit wezenlijke verschillen in toxicodynamie tussen mens en dier met betrekking tot lipidehomeostase, en/of PFAS-soortverschillen in toxicokinetiek, als ook verschillen in voedingspatroon. Op basis van de literatuur kon er geen eenduidige mechanistische verklaring voor het genoemde interspecies verschil gegeven worden. Deze studie benadrukt derhalve de behoefte aan studies met humane *in vitro* testsystemen die een goed beeld geven van voor de mens relevante mechanistische PFAS toxiciteit routes.

In Hoofdstuk 6 werden de effecten van 18 PFAS's op cellulaire triglyceridenaccumulatie (AdipoRed assay) en genexpressie (DNA microarray voor PFOS en RT-qPCR voor alle 18 PFAS's) in humane HepaRG-cellen bestudeerd. BMDExpress-analyse van de PFOS-microarraygegevens werd gebruikt als leidraad voor het selecteren van tien genen om de concentratie-effect relatie van alle 18 PFAS's met qRT-PCR-analyse te beoordelen. De AdipoRed-gegevens en de qRT-PCR-gegevens werden gebruikt voor het afleiden van *in vitro* relatieve potenties. *In vitro* relatieve potentiefactoren (RPF's) konden worden verkregen voor 8 PFAS's op basis van de AdipoRed-gegevens, terwijl voor de geselecteerde genen *in vitro* RPF's konden worden verkregen voor 11-18 PFAS's. Voor de uitlezing van OAT5-expressie werden *in vitro* RPF's verkregen voor alle PFAS's, wat suggereert dat OAT5-genexpressie, samen met enkele van de andere genen, een geschikte uitlezing kan zijn om de relatieve *in vitro* levertoxiciteitspotentie van PFAS's te bepalen. Voor 7 van de 10 gekozen genen waren de *in vitro* gebaseerde RPF's in overeenstemming met de gerapporteerde gegevens voor PFAS-geïnduceerde levertoxiciteit bij ratten. In combinatie met informatie over de toxicokinetiek van de PFAS's bij mensen, kunnen deze *in vitro* gegevens worden gebruikt om potentieverschillen van PFAS's bij mensen *in vivo* te schatten.

Als vervolgstap laat Hoofdstuk 7 een PFAS QIVIVE case studie voor PFOA, PFNA, PFHxS en PFOS zien. *In vitro* concentratie-responsgegevens (TG-accumulatie en genexpressieveranderingen van 12 geselecteerde genen) verkregen in HepaRG-cellen werden met PBK-model-gefaciliteerde omgekeerde dosimetrie omgezet in *in vivo* dosis-responscurven. Voor deze studie werden *in vitro* cellulaire PFAS-niveaus bepaald in de HepaRG-cellen om *in vitro* blootstelling te koppelen aan *in vivo* blootstelling in de lever. Daarbij is rekening gehouden met een blootstellingsscenario van 50 jaar om de levenslange chronische humane blootstelling aan PFAS weer te geven. Ten slotte werden de voorspelde orale equivalente effect doses vergeleken met de chronische humane blootstelling via de voeding zoals recent door EFSA voor de Europese bevolking is vastgesteld. De orale equivalente effectdoses die in deze QIVIVE-analyse werden voorspeld, bleken binnen het bereik te liggen van de humane blootstelling. Deze case study illustreert hoe gegevens uit humane *in vitro* assays gebruikt kunnen worden voor het bepalen van uitgangspunten (POD's) voor screening, risico-identificatie en prioritering van PFAS's waarvoor in op dit moment *in vivo* toxiciteitsgegevens ontbreken.

List of publications

- Fragki S, Louisse J, Bokkers B, Luijten M, Peijnenburg A, Rijkers D, Piersma AH, Zeilmaker MJ, 2023. New approach methodologies: A quantitative *in vitro* to *in vivo* extrapolation case study with PFASs. *Food and Chemical Toxicology* 172: 113559. <https://doi.org/10.1016/j.fct.2022.113559>
- Louisse J, Fragki S, Rijkers D, Janssen A, Staats M, Bokkers B, Zeilmaker MJ, Piersma AH, Luijten M, Hoogenboom R, Peijnenburg A, 2023. Determination of *in vitro* hepatotoxic potencies of a series of perfluoroalkyl substances (PFASs) based on gene expression changes in HepaRG liver cells. Accepted for publication in *Archives of Toxicology*.
- Fragki S, Piersma AH, Marco JZ, Westerhout J, Kienhuis A, Kramer NI, Zeilmaker M, 2022. Applicability of generic PBK modelling in chemical hazard assessment: A case study with IndusChemFate. *Regulatory Toxicology and Pharmacology* 136:105267. <https://doi.org/10.1016/j.yrtph.2022.105267>
- Fragki S, Hoogenveen S, van Oostrom C, Schwillens P, Piersma AH, Zeilmaker M, 2022. Integrating *in vitro* chemical transplacental passage into a generic PBK model: A QIVIVE approach. *Toxicology* 465:153060. <https://doi.org/10.1016/j.tox.2021.153060>
- Fragki S, Dirven H, Fletcher T, Grasl-Kraupp B, Bjerve Gützkow K, Hoogenboom R, Kersten S, Lindeman B, Louisse J, Peijnenburg A, Piersma A, Princen HMG, Uhl M, Westerhout J, Zeilmaker MJ, Luijten M, 2021. Systemic PFOS and PFOA exposure and disturbed lipid homeostasis in humans: what do we know and what not? *Critical Reviews in Toxicology* 51(2): 141-164. <https://doi.org/10.1080/10408444.2021.1888073>
- Fragki S, Piersma AH, Rorije E, Zeilmaker M, 2017. *In vitro* to *in vivo* extrapolation of effective dosimetry in developmental toxicity testing: Application of a generic PBK modelling approach. *Toxicology and Applied Pharmacology* 332:109-120. <https://doi.org/10.1016/j.taap.2017.07.021>

Curriculum Vitae

Styliani (Stella) Fragki was born in Thessaloniki, Greece on 1st September 1983. She studied Biology (Aristotle University of Thessaloniki, Greece) and she has an MSc in Food Safety (Wageningen University, the Netherlands). During her MSc she specialized in food toxicology and completed her thesis on the safety evaluation of botanicals and botanical preparations. After completing her master (in 2009) she worked for several years as a consultant in toxicological risk assessment, providing support to the (agro)chemical industry with regard to their dossier preparation for plant protection products, biocides, and substances falling within the REACH Regulation. In 2016 she started working for the Dutch government (RIVM-National Institute for Public Health and the Environment) as a scientist in the safety of substances entering the food chain (food contaminants, food contact materials, botanicals, etc.), but also in the application of New Approach Methodologies (NAMs) in chemical risk assessment. She started her PhD Project at the Centre for Health Protection within RIVM, on the quantitative *in vitro* to *in vivo* extrapolations (QIVIVE) of alternative assays with physiologically based kinetic (PBK) models, parameterized with data based on *in vitro* and *in silico* tools. She has completed the full training for a European Registration as a Toxicologist. After her PhD contract she worked as a human toxicologist at Triskelion. Since 1st January 2023, Stella joined esqLABS as a Senior Scientist Systems Toxicology, where she works on QIVIVE and the application of PBK modelling in chemical safety.

Acknowledgements

This long journey is coming to an end. I wouldn't have come so far just by myself and therefore, I reckon it is time to thank the people standing next to me all these years assisting in the realization of this thesis.

I am very grateful to my promoter **Aldert Piersma** for giving me the opportunity to undertake this PhD thesis. As an unusual PhD student, being already in the working arena for many years prior to starting this thesis, he trusted that I will be able to take this through. Thank you for always being optimistic on my research and for giving me the freedom to follow my scientific curiosity and explore possibilities.

My deep gratitude to my co-promoter, daily supervisor, and by now also friend **Marco Zeilmaker**. Your faith and support have been priceless during all these adventurous years. Thank you for your meticulous guidance and for sharing your passion for science and PBK modelling with me. Your great knowledge and enthusiasm have been the foundation of this achievement. Next to these, I would like to thank you and your wife **Brigitte** for your sincere help and for standing next to my family during the difficult moments we have been through.

Mirjam Luijten, my co-promoter, thank you for accepting me for this PhD position. Thank you for the interesting scientific discussions and your help during these years, in particular in the PFAS review. I greatly appreciate you took so much of your time to assist me with this. I would also like to thank you for the moral support and for sending me home to rest when most needed. It was the wisest advice!

I would like to show my appreciation specifically to a number of people that took part in this work and played an important role in its completion: **Rudolf Hoogenven** (RIVM) for all the mathematical modelling, **Conny van Oostrom** and **Paul Schwillens** (RIVM) for the work on the BeWo transplacental assay, **Joost Westerhout** (TNO) the developer of the TNO model, **Emiel Rorije** (RIVM) for introducing me to the QSAR-world, **Bas Bokkers** (RIVM) for his support on the BMD modelling, **Anne Kienhuis** (RIVM) and **Nynke Kramer** (previously from IRAS, WUR) for their guidance and advice. Special thanks to **Jochem Louisse** (currently at EFSA) and **Ad Peijnenburg** from WFSR (Wageningen Food Safety Research) for the excellent collaboration and for generating the PFAS HepaRG data. To all the HBM4EU group PFAS experts that participated in the writing of the review (Chapter 5).

I would like to express my gratitude to **Bernadette Ossendorp** for opening the RIVM door to me. Her initiative gave me the opportunity to be introduced to PBK modelling and the sparkle to later jump on this PhD thesis.

I would like to thank **Janine Ezendam** and **Jan van Benthem** that made it possible this PhD project to take place in their Department (VTS-RIVM), as well as the whole **VTS group** for this nice period. I hope to have convinced you about the importance of QIVIVE for the future! Special thanks to the nice **PhD team**: Laura, Gina, Victoria, Astrid, Coen, Kim, Charlotte and Erna for the warm support all these years!

I want to thank all my friends that I met during these years in the Netherlands for being here for me, and for all the great times we shared. **Rahul, Victor, Marie, Rita, Carol, Isida, Roberto, Laura, Pedro, Maryna, Xe, Miguel, Bernice, Khadim, Laurens, Alex, Christina** I am so glad that we had the chance to get to know each other. I miss you and I hope to see you soon in Portugal (except for the Portuguese Rita of course)! My love to my **Wageningen group**, from different parts of the world, for sharing their culture, for the nice travelling and great times we had together. Soon more to come!

My dear paranymphs **Sarah** and **Ioanna**, you stood next to me all these years. I am grateful to have you in my life, you are both very special to me.

Giwta, childhood friend and companion on the Dutch trip, our friendship has grown even more these years. I am very happy for all these moments we have shared together. My friends from childhood **Anna M., Voula, Dimitra, and Anna K.**, we know each other since ever. I always feel connected to you although we are far apart and I gratefully thank you for your friendship.

My godmother **Filiw**, you are wise, witty, and as a real godmother should be. Thank you for always being there for me when I need your advice.

Above all, I want to dedicate this thesis to my family.

To my dear parents **Marianthi** and **Nikos**. I cannot describe how happy I am that you are here with me to celebrate this moment. Thank you for your unconditional love and for raising me with so much care.

To my siblings **Eleni** and **Giorgos**. Our bond is getting stronger with time; even if we live far away from each other we can conquer the distance. I can feel your support closer than ever.

To **Stefanos** and **Maaïke**, the partners and now dear friends, I see you really as part of my family.

To my beloved nephew **Swtiris** and my nieces **Marianthi, Mursini**, and little **Lina**. I will always be there for you.

To all my dear aunts, uncles and cousins that I deeply love. Special thanks to my youngest cousin **Giorgos** who supported me when I most needed.

To my **Portuguese family** for all the hearty support all these years and for the warm welcome to Portugal. My specific gratitude to Leonor who came several times to NL to help us!

To the little magician, the most fabulous girl in the world, my daughter **Matilda**, who brought the brightest light in my life. Who teaches me daily what is important in life and how to be a better person. To the small star that is growing inside me and will come to meet us in June. Looking forward to know you!

To my loving man **Duarte** who simply gave me the freedom to follow my path and put his own wishes aside for some time. Who didn't let me fall when I was falling. Thank you for choosing to stand next to me and for sharing all these meaningful moments with me. Thank you for being such a great father for our daughter. Thank you for being so extraordinary, for your kindness and for believing in people.

